Schwebstoff-Monitoring und Verschleiss an Peltonturbinen (Teile a und b)

SI/500638-01 und -02

Beilagen zum Schlussbericht (2016)

Projektbezogene Publikationen aus dem Jahr

2012

Felix D., Albayrak I., Boes R.M. (2012a). **Schwebstoff- und Verschleiss-Monitoring an Wasserkraft-Hochdruckanlagen: Laborversuche zu Partikelmessmethoden und Vorbereitung der Fallstudie Fieschertal**. *Berichte des Lehrstuhls und der Versuchsanstalt für Wasserbau und Wasserwirtschaft*, TU München, Nr. 125: 11-24.

Felix D., Albayrak I., Boes R.M. (2012b). **Schwebstoffmonitoring und Verschleiss an Pelton-turbinen am Fallbeispiel Fieschertal - Vorbereitende Laborversuche zu Partikelmessmethoden**. *Proc. Wasserbausymposium 2012*, ISBN 978-3-85125-230-9. Graz, Österreich: 117-124.

Felix D., Albayrak I., Abgottspon A., Boes R.M., Gruber P. (2012c). **Suspended Sediment and Pelton Turbine Wear Monitoring: Experimental Investigation of various Optical and Acoustic Devices and Begin of the Prototype Study Fieschertal**. *Proc. Vienna Hydro 2012*, 17th International Seminar on Hydropower Plants, Wien, Österreich: 483-494.

Technische Universität München

14. Treffen junger WissenschaftlerInnen an Wasserbauinstituten

Beiträge zum JuWi-Treffen am 25. und 26. Juni 2012
an der Technischen Universität München

Schwebstoff- und Verschleiss-Monitoring an Wasserkraft-Hochdruckanlagen: Laborversuche zu Partikelmessmethoden und Vorbereitung der Fallstudie Fieschertal

David Felix, Ismail Albayrak und Robert Boes

Zusammenfassung

Bei Wasserkraftwerken, insbesondere bei Hoch- und Mitteldruckanlagen, kann der Hydroabrasiv-Verschleiss an Turbinen und Stahlwasserbauteilen infolge schwebstoffhaltigen Triebwassers erhebliche Betriebskosten und Ertragseinbussen verursachen. Für einen wirtschaftlich optimierten Anlageentwurf und -betrieb besteht Bedarf an weiteren Bemessungsgrundlagen und an anwendungstauglichen Messverfahren.

Im Rahmen eines interdisziplinären Forschungsprojekts soll an einer bestehenden Hochdruck-Wasserkraftanlage (Kraftwerk Fieschertal, im Wallis, Schweiz), die über keinen Stausee verfügt, die Schwebstoffführung des Triebwassers (Konzentration und Partikelgrößenverteilung) mittels neuartiger Messtechnik kontinuierlich erfasst werden. Die Schädigung der Peltonturbine, d.h. der Materialabtrag an den Bechern und Düsennadeln, wird durch mehrere Inspektionen dokumentiert und mit der Einwirkung, d. h. der Schwebstoffführung des Triebwassers, korreliert, um Berechnungsansätze zur Prognose des Hydroabrasiv-Verschleisses und der Wirkungsgradabnahme zu überprüfen und zu erweitern.

Im Projekt werden verschiedene optische und akustische Messsysteme, die zur kontinuierlichen Überwachung des Schwebstoffaufkommens in Echtzeit eingesetzt werden können, untersucht und verglichen: *in-situ* Laserdiffraktometrie und Trübungs- bzw. Streulichtsonden sowie die Amplitudendämpfung von Ultraschallsignalen, wie sie bei akustischen Durchflussmessungen eingesetzt werden.

Der vorliegende Artikel beschreibt den ersten Teil eines mehrjährigen Forschungsprojekts, welches im August 2011 gestartet wurde. Zunächst werden die Problemstellung, das gewählte Vorgehen, die zu untersuchende Wasserkraftanlage und die gewählten Methoden zur Erfassung des Schwebstoffaufkommens beschrieben. Anschliessend wird auf die Versuche im hydraulischen Labor eingegangen, in welchen die Messeinrichtungen in einem Tank mit verschiedenen Wasser-Schwebstoff-Gemischen untersucht und kalibriert werden.

1 Einleitung

Sedimente an Wasserkraftanlagen und Verschleiss

Fliessgewässer können je nach Jahreszeit und Abfluss beträchtliche Mengen an Geschiebe und Schwebstoffen mit sich führen. Abb. 1 zeigt ein Beispiel eines stark geschiebe- und schwebstoffführenden Bergflusses. Für einen nachhaltigen Betrieb von Wasserkraftanlagen stellt der Umgang mit Feststoffen eine Herausforderung dar. Angesichts des im Alpenraum beobachteten Gletscherrückzugs gewinnt diese Thematik an Bedeutung, da zukünftig mehr (Fein-)Sedimente zu erwarten sind.

Abb. 1 Mündung des Wysswassers (von links im Bild) in die Rhone bei Fiesch (August 2010, Bild: VAW).

Bei Wasserkraftanlagen können die im Triebwasser enthaltenen mineralischen Partikel bei Fallhöhen von mehreren Hundert Metern und bei einem grossen Anteil harter kantiger Partikel (z.B. Quarz) zu beträchtlichen Abnutzungserscheinungen an den wasserführenden Bauteilen, besonders an den hydraulischen Maschinen (Turbinen und Pumpen) führen (z. B. Gummer 2009).

In Abb. 2 sind mineralische Partikel dargestellt, die welche in einem klassischen Sandfang nicht ausgeschieden werden und folglich mit dem Triebwasser die Turbine passieren und zu Hydroabrasiv-Verschliess führen. Abb. 3 zeigt ein Beispiel von Schäden an einem unbeschichteten Peltonlaufrad infolge Hydroabrasiv-Verschleiss.

Der Verschleiss an Turbinen kann erhebliche Betriebskosten (Revisionsarbeiten, Ersatz-anschaffungen) und Ertragseinbussen (Minderproduktion infolge Wirkungsgradabnahme und Betriebsunterbruch während Revisionen) verursachen.

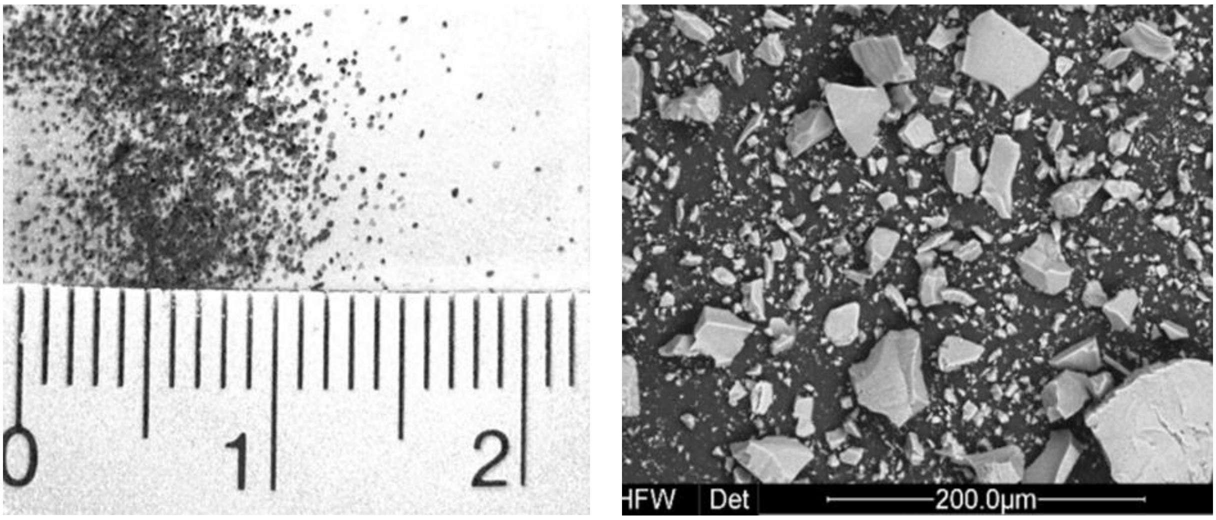

Abb. 2 Feinsand (links) sowie Quarzmehl unter dem Elektronenmikroskop (Bilder: VAW).

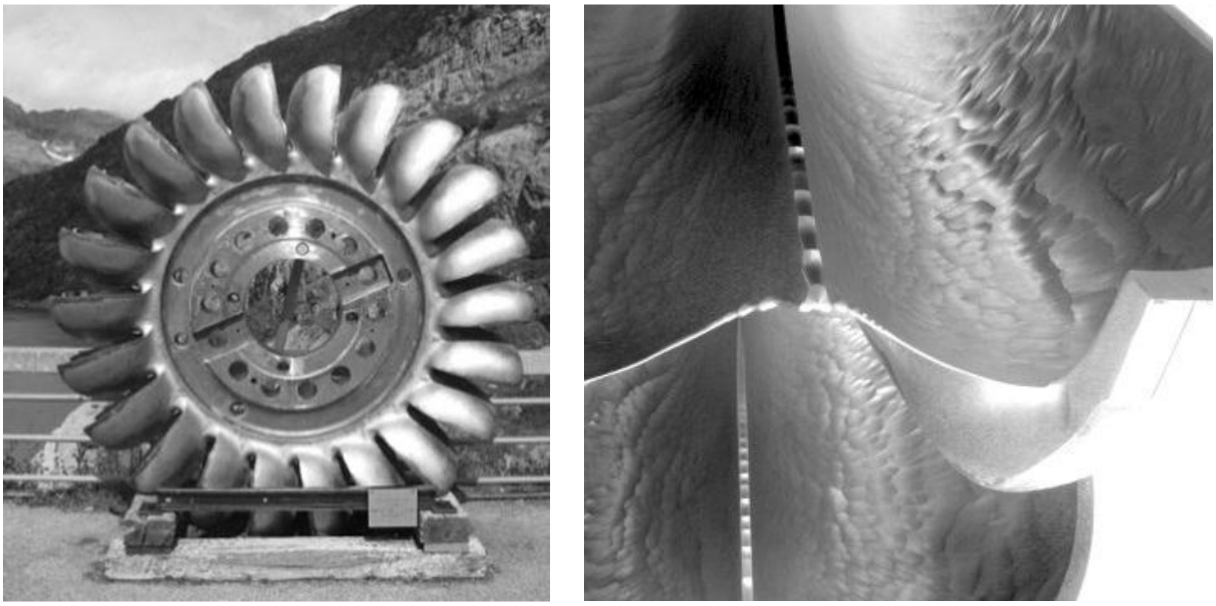

Abb. 3 Peltonturbine (links) und Schäden an den Bechern des Laufrads (Ausstellungsobjekt bei der Staumauer Emosson, Wallis, Schweiz; Bilder: VAW).

Bei Wasserspeichern können fortschreitende Sedimentablagerungen zu einer Reduktion des Nutzvolumens oder zur Beeinträchtigung der Betriebssicherheit führen. Massnahmen gegen die Speicherverlandung sind nicht Gegenstand dieses Artikels, es besteht jedoch eine Querverbindung: Heutzutage wird auch das gezielte Abführen von Feinsedimenten aus Stauseen über den Triebwasserweg (Jenzer Althaus 2011) vermehrt geprüft, wobei das Ausmass der je nach Fallhöhe, Partikelgrösse und Gesteinshärte zu erwartenden Hydroabrasiv-Verschleissschäden für die wirtschaftliche Abwägung von Interesse ist.

Gegenmaßnahmen

Bei Triebwassersystemen von Hoch- und Mitteldruckwasserkraftanlagen, welche keinen Stausee aufweisen (Laufkraftwerke), wird nach Möglichkeit grobes Geschiebe (in der Regel Steine und Kies) an der Fassung oder in Entkiesern abgewiesen, während Sand (über 0.3 bis 0.5 mm) in Entsandungsanlagen ausgeschieden und in das Gewässer zurück gespült wird. Aus wirtschaftlichen und praktischen Gründen ist eine vollständige Entfernung der im Triebwasser enthaltenen mineralischen Partikel jedoch nicht möglich.

Mit hartmetallischen, keramischen oder polymeren Beschichtungen von Turbinen kann die Einsatzzeit von Laufrädern in gewissem Masse verlängert werden. Von der Werkstofftechnologie her lässt sich allerdings der Abrasionswiderstand von Turbinen nicht beliebig steigern.

Da die Schwebstoffführung zeitlich meist sehr variabel ist, kann es wirtschaftlich sein - falls von den übergeordneten Bedingungen her möglich, das Turbinieren während kurzzeitig auftretenden Konzentrationsspitzen, beispielsweise nach einem Sommergewitter, vorübergehend für wenige Stunden einzustellen.

Forschungsbedarf und Zielsetzung

Bei zahlreichen bestehenden Hochdruck-Wasserkraftanlagen ist das Problem des Hydroabrasiv-Verschleisses qualitativ bekannt und es bestehen gewisse Berechnungsansätze zur Abschätzung des Materialabtrags (z.B. in DWA 2006). Da über die Schwebstoff-Führung des Triebwassers in der Regel jedoch kaum detaillierte Informationen zur Verfügung stehen, fällt es schwer, den Hydroabrasiv-Verschleiss zu prognostizieren und eine bezüglich Verschleiss optimierte Betriebs- und Unterhaltsweise zu finden. Weiter besteht Bedarf an Messsystemen, die für den Einsatz an Wasserkraftanlagen geeignet sind (z. B. Bishwakarma & Stole 2008).

Bei Neubauprojekten besteht auch ein Interesse an verbesserten Bemessungsgrundlagen für einen bezüglich Sedimentmanagement und Hydroabrasiv-Verschleiss wirtschaftlich optimierten Anlagenentwurf und -betrieb.

Das von der VAW der ETH Zürich initiierte und nachfolgend beschriebene Forschungsprojekt soll einen Beitrag zur Verbesserung der Kenntnisse betreffend des Schwebstoffaufkommens, der Schwebstoffmessung und des Hydroabrasiv-Verschleisses leisten.

2 Beschreibung des Forschungsprojekts

Methode und Projektbeteiligte

Der Schwerpunkt der Untersuchung liegt auf einer Prototypstudie an einer bestehenden Hochdruckwasserkraftanlage. Vorgängig werden im hydraulischen Labor Versuche zu optischen und akustischen Partikelmessmethoden durchgeführt.

Folgende Hochschul- und Industriepartner wirken an diesem interdisziplinären Forschungsprojekt mit:

- Hochschule Luzern, Kompetenzzentrum für Fluidmechanik und Hydromaschinen
- Kraftwerksbetreiber (Gommerkraftwerke AG)
- Engineering-Abteilung des Kraftwerksmiteigentümers (BKW FMB Energie AG, Bern)
- Turbinenhersteller (Andritz Hydro, Kriens/Luzern)
- Hersteller von akustischen Durchflussmessungen (Rittmeyer AG, CH-Baar)

- Trübungsmessgeräte Sigrist Photometer, CH-Ennetbürgen
- Laboranalysen von Schwebstoffproben: Institut für Geotechnik, ETH Zürich

Im Folgenden wird ein erster Teil des Forschungsprojekts, welches im August 2011 gestartet wurde und über mehrere Jahre laufen wird, beschrieben.

Beschreibung der Prototyp-Wasserkraftanlage

Als geeignete Wasserkraftanlage für dieses Forschungsprojekt konnte das Kraftwerk Fieschertal (im Kanton Wallis, Schweiz) identifiziert werden. Es handelt sich um eine Hochdruckwasserkraftanlage mit Fallrechenfassung, deren Einzugsgebiet stark vergletschert ist.

Nach der Fassung folgen ein unterirdischer Entkieser, ein Entsander und ein 2 km langer Freispiegelstollen (Abb. 4), der in Zeiten ohne Volllastbetrieb als Tagesspeicher eingesetzt wird. Vom Freispiegelstollen gelangt das Triebwasser durch eine erdverlegte Druckleitung zum Maschinenhaus beim Dorf Fieschertal, von wo das Triebwasser in den Vorfluter, das Wysswasser, zurückfliesst. Das Kraftwerk Fieschertal weist folgende technische Daten auf:

- Bruttofallhöhe 520 m
- Ausbauwassermenge 15 m^3/s
- Turbinen: 2 horizontalachsige, zweidüsige Pelton
- Nennleistung 2 x 32 MW = 64 MW

Es sind Laufräder mit Wolframkarbid-Beschichtung im Einsatz. Die mittlere Schwebstoffkonzentration am Kraftwerk Fieschertal wird bei weniger als 1 g/l erwartet. Es wurden aber schon Spitzen bis 90 g/l gemessen.

Untersuchungsprogramm

An der Kraftwerksanlage sind folgende Erhebungen vorgesehen:

- kontinuierliche Erfassung der Schwebstoffführung des Triebwassers bei der Fassung, beim Einlauf in die Druckleitung und in den Unterwasserkanälen der beiden Maschinen (Messmethoden und Messeinrichtungen gemäss folgendem Abschnitt)
- periodische Inspektion bzw. Vermessung der Laufräder und Düsen bzw. deren Beschichtungen an beiden Maschinen
- periodische Messung des Wirkungsgrads der beiden Maschinen (Index-Wirkungsgrad)

Die Messungen an der Kraftwerksanlage sind hauptsächlich in zwei Schwebstoffsaisons, d.h. in den Sommermonaten der Jahre 2012 und 2013, geplant.

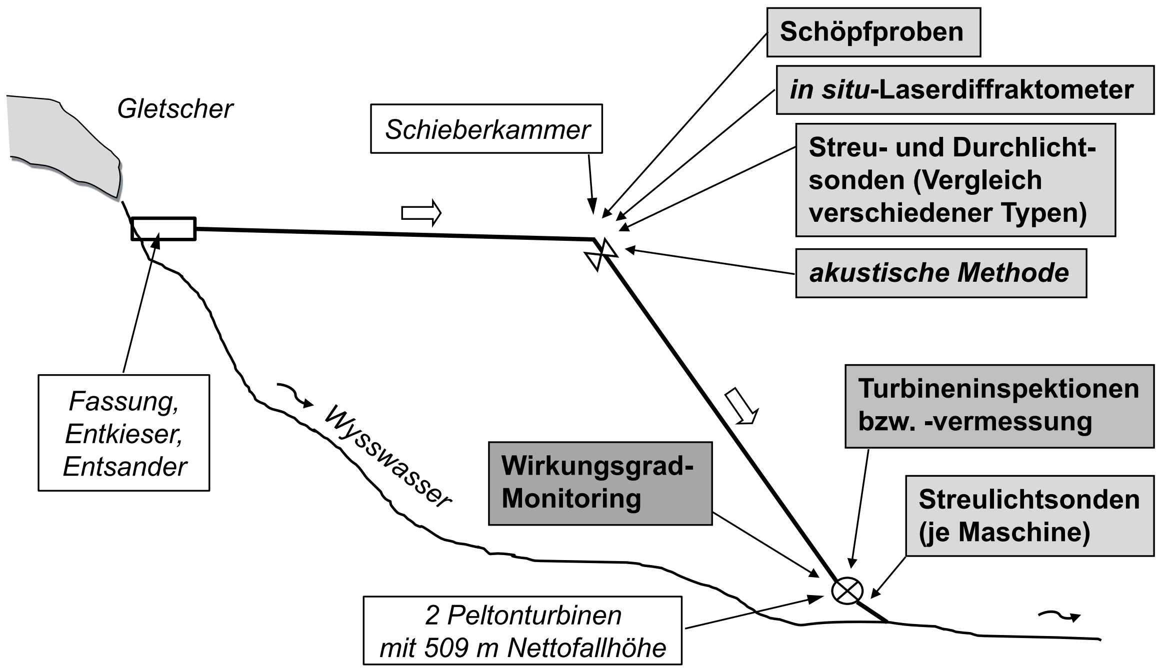

Abb. 4 Schematisches Längsprofil der Kraftwerksanlage Fieschertal mit Darstellung der vorgesehenen Untersuchungen

3 Schwebstoff-Monitoring

Streulicht- und Durchlichtsonden

Zur Überwachung von Flüssigkeiten bzw. Suspensionen in industriellen Prozessen, in der Trinkwasserversorgung, in der Abwassertechnik oder an einigen Abflussmessstationen an Fliessgewässern werden „Trübungssonden" eingesetzt. Bei diesen wird die Absorption und/oder die Streuung von Licht, typischerweise im nahen Infrarotbereich (NIR), nach dem Durchgang durch das Messmedium gemessen.

Beim Einsatz von Trübungssonden zur Bestimmung der Massenkonzentration von Feststoff-Partikeln in einer Flüssigkeit ist ein Zusammenhang (Kalibrierung) zwischen dem in optischen Einheiten gemessenen Wert (in der Regel mit der Einheit FNU) und der Massenkonzentration zu finden. Eine solche Kalibrierung kann im Labor für eine bestimmte Partikelart und für einen bestimmten Messbereich ermittelt werden.

Wenn nun aber, wie in der vorliegenden Anwendung, die Partikelzusammensetzung zeitlich veränderlich ist, kann die Umrechnung mit erheblichen Unsicherheiten behaftet sein. Einflussfaktoren für die Kalibrierung sind: Partikelgrösse, Partikelform und Partikelfarbe (und andere optische Eigenschaften).

In den Vorversuchen im hydraulischen Labor werden die in Tab. 1 aufgeführten Trübungsmessgeräte untersucht. Es ist vorgesehen, anschliessend eine Auswahl von Trübungssonden im zu untersuchenden Kraftwerk zu installieren.

Tab. 1 Untersuchte Trübungsmessgeräte

Messgerät	Hersteller	Einbauart
Solitax ts-line sc	Hach-Lange	eingetaucht
Turbimax W CUS41	Endress-Hauser	eingetaucht
TurbiScat (90° und 25°)	Sigrist Photometer	im Strang (unter Druck)
TF16-N mit Messzelle F20	Optek Danulat	im Strang (unter Druck)
AquaScat	Sigrist Photometer	im Strang (Freifall)

In-situ Laserdiffraktometrie und -transmissiometrie

Da die Grösse von mineralischen Partikeln für den Hydroabrasiv-Verschleiss eine entscheidende Grösse ist und zeitlich stark variieren kann, ist für den Einsatz an Wasserkraftanlagen ein Messgerät gefragt, welches nebst der Schwebstoffkonzentration auch die Partikelgrössenverteilung kontinuierlich erfassen kann.

Dies ist mit Geräten möglich, welche auf dem Messprinzip der Laserbeugung (Diffraktion) beruhen. Bis vor einigen Jahren wurden solche Geräte ausschliesslich im Labor eingesetzt. Nun sind tragbare Laserbeugungs-Geräte verfügbar, welche auch für Feldstudien eingesetzt werden können (Agrawal et al. 2011, Boes 2009). Von den derzeit angebotenen Geräten (Sequoia Scientific 2010), wurde das vielseitig einsetzbare Modell *LISST-100X*, Typ C, ausgewählt.

Ein Laserstrahl verläuft in der Längsachse des Geräts (Abb. 5): Der Laserstahl tritt aus der Optik im Messkopf (L) durch die zu untersuchende Suspension (Pfeil in Abbildung 5) in die Optik (R) im Hauptteil des Instruments, wo die Intensität des unter verschiedenen, kleinen Winkeln gestreuten Laserstrahls auf 32 ringförmigen Detektoren (D) aufgenommen wird. Weiter wird die Intensität des nicht gestreuten Laserstrahls, d.h. die Transmission registriert (P). Mittels einer mathematischen Umkehrung (Inversion) werden die Volumenkonzentrationen in 32 logarithmisch verteilten Partikelgrössenklassen berechnet. Mit einer anzunehmenden Sedimentdichte kann die totale Massenkonzentration berechnet werden. Das Messgerät bzw. die Software erlauben, jede Sekunde eine Partikelgrössenverteilung zu bestimmen.

Mit diesem Gerät können Partikelgrössen zwischen 2.5 und 500 Mikrometer erfasst werden, vorausgesetzt, dass die Suspension nicht zu trübe ist bzw. eine zu hohe Partikelkonzentration aufweist. Um den Bereich messbarer Konzentrationen zu vergrössern, wurde die optische Pfadlänge, d.h. die Strecke, auf welcher der Laserstrahl durch die Suspension geführt wird, mittels eines einsetzbaren Glaskörpers von standardmässig 50 mm auf 5 mm verkürzt.

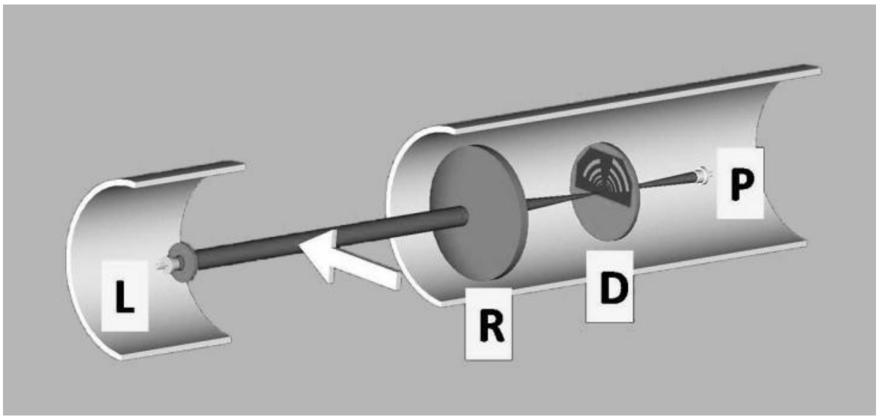

Abb. 5 Schematische Darstellung des Messprinzips des in-situ Laser-Diffraktometers (Sequoia 2010)

Akustische Messungen

Bei zahlreichen Wasserkraftanlagen wird der Durchfluss im Triebwassersystem laufend mittels Fliessgeschwindigkeitsmessungen berechnet, welche auf dem akustischen Laufzeitverfahren beruhen. Dabei wird beispielsweise zwischen baugleichen *Transducern*, die abwechslungsweise als Sender oder Empfänger dienen, ein Ultraschallpuls einmal in Fliessrichtung und einmal gegen die Fliessrichtung durch die Strömung gesendet, womit die Laufzeitdifferenz bestimmt wird. Diese wird in eine über den Pfad gemittelte Strömungsgeschwindigkeit umgerechnet.

Bei solchen akustischen Durchflussmessungen können mineralische Partikel im Wasser die Messung beeinflussen (Costa et al. 2010) oder bei hohen Konzentrationen unter Umständen verunmöglichen.

Es soll nun versucht werden, die zusätzliche Amplitudendämpfung des Ultraschallsignals infolge von mineralischen Partikeln für das Schwebstoff-Monitoring zu nutzen. Dabei ist eine Schwierigkeit, dass es verschiedene Kombinationen von Partikelgrössen und Konzentrationen gibt, welche die gleiche Dämpfung zur Folge haben. Wird ein bestimmter Partikeldurchmesser vorausgesetzt, kann eine Konzentration berechnet werden. Eine solche Annahme ist jedoch für die Anwendung im Bereich des Monitorings von Schwebstoffen ungeeignet, da Partikelgrössen *und* Konzentrationen überwacht werden sollen.

Akustische Methoden, welche mit mehreren Frequenzen arbeiten, haben das Potenzial, Informationen bezüglich Partikelgrössen zu liefern. Es wird nun geprüft, wie sich Ultraschallmessungen mit mehr als einer Frequenz im Zusammenhang mit bei Kraftwerken üblichen akustischen Durchflussmessungen realisieren lassen.

Wasserproben und Laboranalysen

Die Messgeräte sind durch Einzelproben, die im Labor bezüglich Schwebstoffkonzentration und Partikelgrössenverteilung untersucht werden, zu überprüfen.

Da bei der Prototyp-Untersuchung Schwebstoffproben bei hoher Schwebstoffführung besonders interessieren und keine dauernde Personalpräsenz bei der Fassung und in der Schieberkammer möglich ist, werden automatische Wasserprobenehmer installiert. Die Probennehmer werden so programmiert, dass in regelmässigen Intervallen und beim Überschreiten gewisser Trübungswerte Proben abgefüllt werden. So können auch während Phasen, in welchen das Schwebstoffaufkommen den Messbereich der Messgeräte überschreitet, Informationen über die Schwebstoffführung gewonnen werden.

Das Material von Schöpfproben wird für weitere Laboruntersuchungen verwendet: Bestimmung der mineralogischen Zusammensetzung (Gehalt an harten Mineralien mit Mohshärten ≥ 6, d.h. hier Quarz und Feldspat) und der Kornform.

4 Versuche im hydraulischen Labor

Zielsetzung

Vor dem Einsatz am zu untersuchenden Kraftwerk sollen die optischen und akustischen Messverfahren unter kontrollierten Bedingungen im hydraulischen Labor untersucht werden, um Kalibrierungen, Einsatzgrenzen und Messunsicherheit der Messgeräte in unterschiedlichen Suspensionen festzustellen. Gegenüber früheren Untersuchungen (z. B. Bittner 2008) soll hier auf den Einsatz eines in-situ Laserdiffraktometers *LISST-100X* in Verbindung mit Partikelsorten, die bezogen auf die Prototypstudie gewählt wurden, eingegangen werden.

Versuchseinrichtung und Methode

An der Hochschule Luzern, am Kompetenzzentrum für Fluidmechanik und Hydromaschinen in Horw, besteht eine Versuchseinrichtung, an welcher Versuche zu Partikelmessmethoden durchgeführt werden. In einem Tank mit Rührwerk (Abb. 6) werden unterschiedliche Partikelsorten mit Wasser gemischt. Der Tank hat eine Länge von 2.12 m und eine Breite von 1.13 m. Bei einer Füllhöhe von 0.5 m ergibt sich ein Volumen von 1.2 m^3.

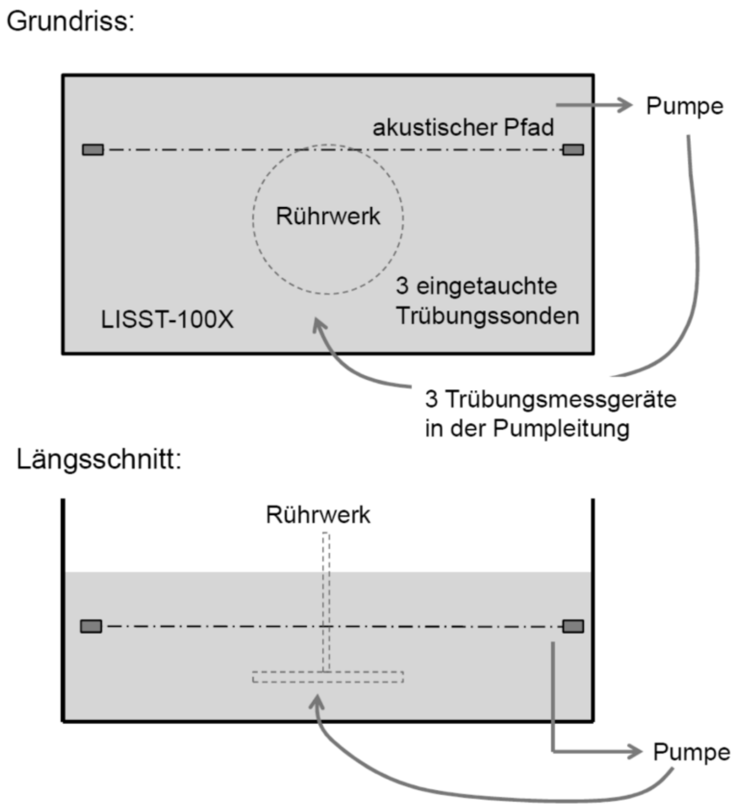

Abb. 6 Mischtank mit optischen und akustischen Messgeräten für Schwebstoffmessungen.

Ausgehend von einer „Nullmessung“ in Trinkwasser wird für jede Partikelsorte die Konzentration stufenweise gesteigert und mit allen am Mischtank installierten Geräten werden jeweils Messungen durchgeführt. Die Konzentration der Suspensionen wird nach Möglichkeit bis zum Erreichen der Messbereichsgrenzen der einzelnen Instrumente gesteigert.

Verwendete mineralische Partikel

Von früheren Untersuchungen am Kraftwerk Fieschertal ist bekannt, dass die dortigen Schwebstoffe zur Hauptsache aus Quarz, Feldspat und Glimmer bestehen, also den Hauptbestandteilen von Granitgestein.

Für die Schwebstoff-Messversuche im hydraulischen Labor wurden mineralische Partikel gesucht, welche mit den Schwebstoffpartikeln in der Natur vergleichbar und von industriellen Anwendungen her kommerziell erhältlich sind. Es wurden auch kugelförmige Partikel (Sandstrahlmittel aus Glas) in das Versuchsprogramm aufgenommen, da diese idealen Partikel oft den Messsystemen bzw. den Auswertungsalgorithmen zugrunde gelegt werden.

Aus dem Unterwasser der Turbinen des Kraftwerks Fieschertal, genauer gesagt aus dem Pumpensumpf des Turbinenkühlsystems, wurden während Revisionsarbeiten einige Eimer der abgelagerten Feinsedimente für die Laborversuche entnommen.

Von den im hydraulischen Labor verwendeten mineralischen Partikeln sind die Partikelgrössenverteilungen in Abb. 7 dargestellt. Diese wurden am Institut für Geotechnik der ETH Zürich mit dem stationären Laserdiffraktometer *Horiba* gemessen und als Referenz verwendet.

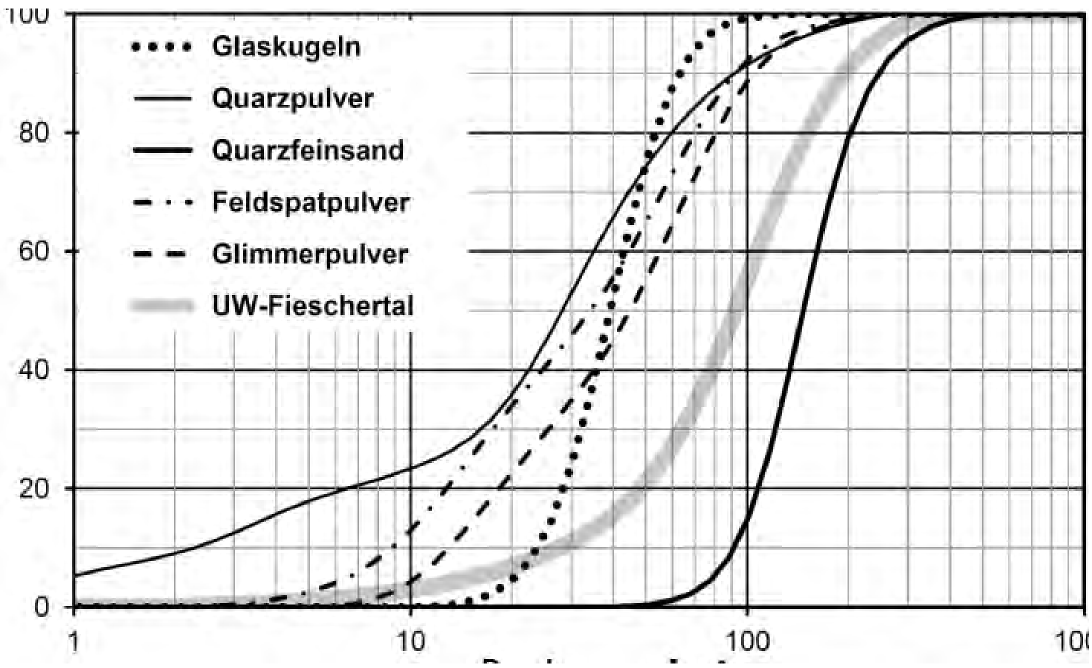

Abb. 7 Korngrössenverteilungen der untersuchten Partikel (mit Labor-Laserdiffraktometer gemessen)

Erste Versuchsresultate

Beispiele erster Resultate der Laborversuche sind in Abb. 8 und Abb. 9 dargestellt.

In Abb. 8 sind Partikelgrössenverteilungen von Quarzfeinsand, welche mit dem in-situ Laserdiffraktometer (*LISST-100X*) im Mischtank bei einer Schwebstoffkonzentration von 1 g/l gemessen und unter Annahme einer runden Kornform mithilfe der zughörigen Software berechnet wurden, in schwarz dargestellt. Aufgrund der turbulenten Verhältnisse im Mischtank mit Rührwerk variieren die gemessenen Kornverteilungen. Die dünnen Linien zeigen die Bandbreite von 100 Kornverteilungen, die mit einer Frequenz von 1 Hz gemessen wurden; die dicke schwarze Linie zeigt deren Mittelwert. Zum Vergleich ist die Referenzmessung (graue gestrichelte Linie) dargestellt. Der Mittelwert stimmt – vor allem im Bereich kleiner als etwa 120 µm – gut mit der Referenzmessung überein. Die Streuung ist bei kleineren Partikeln geringer.

In Abb. 9 ist eine erste Auswahl von in den Laborversuchen bestimmten Kalibrierkurven am Beispiel von Quarzfeinsand dargestellt. Die mit unterschiedlichen Geräten gemessenen Trübungswerte wurden in Funktion der Schwebstoffkonzentration aufgetragen, welche mit dem in-situ-Laserdiffraktometer (*LISST-100X)* gemessen wurde. Es wurde wieder mit einer Frequenz von 1 Hz gemessen und die Mittelwerte über jeweils 100 Werte gebildet. Die Schwebstoffkonzentrationen, welche mit dem LISST gemessen wurden, wurden mit Schöpfproben (Ofentrocknung) validiert. Der Zusammenhang zwischen Schwebstoffkonzentration und Trübung ist wie erwartet nahezu linear. Für die verschiedenen Sonden sind gerätespezifische Kalibrierkurven zu verwenden.

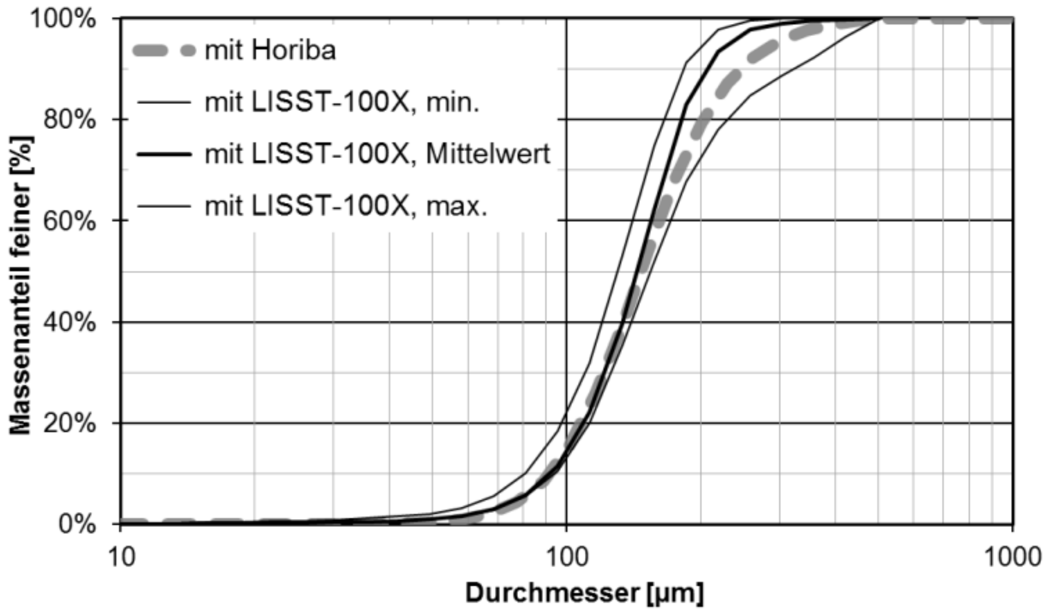

Abb. 8 Vergleich von gemessenen Partikelgrössenverteilungen (Beispiel Quarzfeinsand)

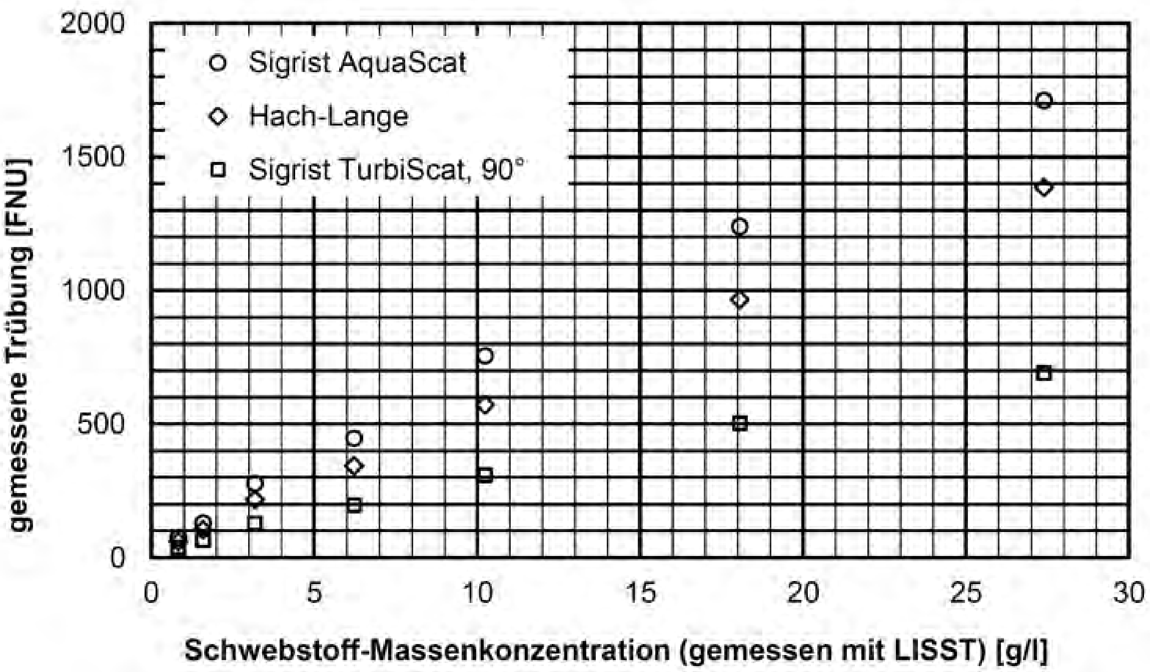

Abb. 9 Trübungswerte, welche mit drei Turbidimetern gemessen wurden, in Funktion der mittels in-situ-Laserdiffraktometer (LISST-100X) gemessenen Schwebstoffkonzentration, am Beispiel von Quarzfeinsand.

Schluss

Nach intensiven Vorbereitungen und ersten Versuchsreihen werden die Laborversuche mit den verschiedenen Partikelsorten weitergeführt und weiter ausgewertet. Für die Untersuchungen am Prototypen werden Messeinrichtungen installiert, so dass während der kommenden zwei Schwebstoffsaisons Felddaten erhoben werden können.

Basierend auf der Laboruntersuchung der Partikelmessgeräte und der Erfahrung beim Einsatz am Prototypen werden Empfehlungen bezüglich Messgeräten für Schwebstoff-Monitoring an Wasserkraftanlagen formuliert.

Ein möglichst vollständiger Datensatz über das Schwebstoffaufkommen, den Materialabtrag an den Turbinen und den zugehörigen Wirkungsgradverlust kann dazu genutzt werden, Berechnungsansätze zur Vorhersage des Turbinenverschleisses weiterzuentwickeln und zu verifizieren.

Dank

Das Forschungsprojekt wird durch swisselectric research, das Schweizer Bundesamt für Energie (BFE) und die Gommerkraftwerke sowie durch die eingangs genannten weiteren Projektpartner unterstützt. Die Autoren bedanken sich bei allen Projektpartnern für ihr Engagement.

Ein weiterer Dank geht an Prof. Dr. T. Staubli, Prof. Dr. P. Gruber, A. Abgottspon und M. Duss von der Hochschule Luzern, Kompetenzzentrum für Fluidmechanik und Hydromaschinen, welche als Forschungspartner für die Laborversuche und die Untersuchung an der Prototypanlage mitwirken.

Literatur

[01] Agrawal Y., Mikkelsen O.A. & Pottsmith H.C. (2011). Sediment monitoring technology for turbine erosion and reservoir siltation applications. Proc. HYDRO 2011 Conference, Prague, Czech Republic.

[02] Bishwakarma M.B. & Støle H. (2008). Realtime sediment monitoring in hydropower plants. J. Hydr. Res. 46(2): 282–288.

[03] Bittner G. (2008). Vergleich von Trübungssonden bei der Schwebstoffmessung unter definierten Laborbedingungen. Diplomarbeit, Universität für Bodenkultur, Wien, Österreich.

[04] Boes R. (2009). Real-time monitoring of suspended sediment concentration and particle size distribution in the headwater way of a high-head hydropower plant. Proc. 33rd IAHR Congress, Vancouver, Canada: 4037–4044.

[05] Costa I., Storti G., Lüscher B., Gruber P. & Staubli Th. (2010). Influence of solid particle parameters on the sound speed and attenuation of pulses in acoustic discharge measurements (ADM), Switzerland. Journal of Hydrologic Engineering (accepted for publication).

[06] DWA (2006). Entlandung von Stauräumen. DWA-Themen, Deutsche Vereinigung für Wasserwirtschaft, Abwasser und Abfall, Hennef (Hrsg.), ISBN 978-3-937758-33-6.

[07] Gummer J. H. (2009). Combating Silt Erosion in Hydraulic Turbines. Hydro Review Wordwide, 17(1).

[08] Jenzer Althaus J. (2011). Sediment evacuation from reservoirs through intakes by jet induced flow. Dissertation Thesis, Communication Nr. 45 (A. Schleiss, ed.), LCH, EPF Lausanne.

[09] Sequoia Scientific (2010). Broschüren über das in-situ-Laser-diffraktometer LISST-100X, LISST-Hydro und LISST-Infinite, Sequoia Scientific, Inc., USA, http://www.sequoiasci.com.

Anschrift der Verfasser

David Felix
Versuchsanstalt für Wasserbau, Hydrologie und Glaziologie
ETH Zürich
Gloriastr. 37/39
CH-8092 Zürich
E-mail: david.felix@vaw.baug.ethz.

Dr. Ismail Albayrak
Versuchsanstalt für Wasserbau, Hydrologie und Glaziologie
ETH Zürich
Gloriastr. 37/39
CH-8092 Zürich

Prof. Dr. Robert M. Boes
Versuchsanstalt für Wasserbau, Hydrologie und Glaziologie
ETH Zürich
Gloriastr. 37/39
CH-8092 Zürich

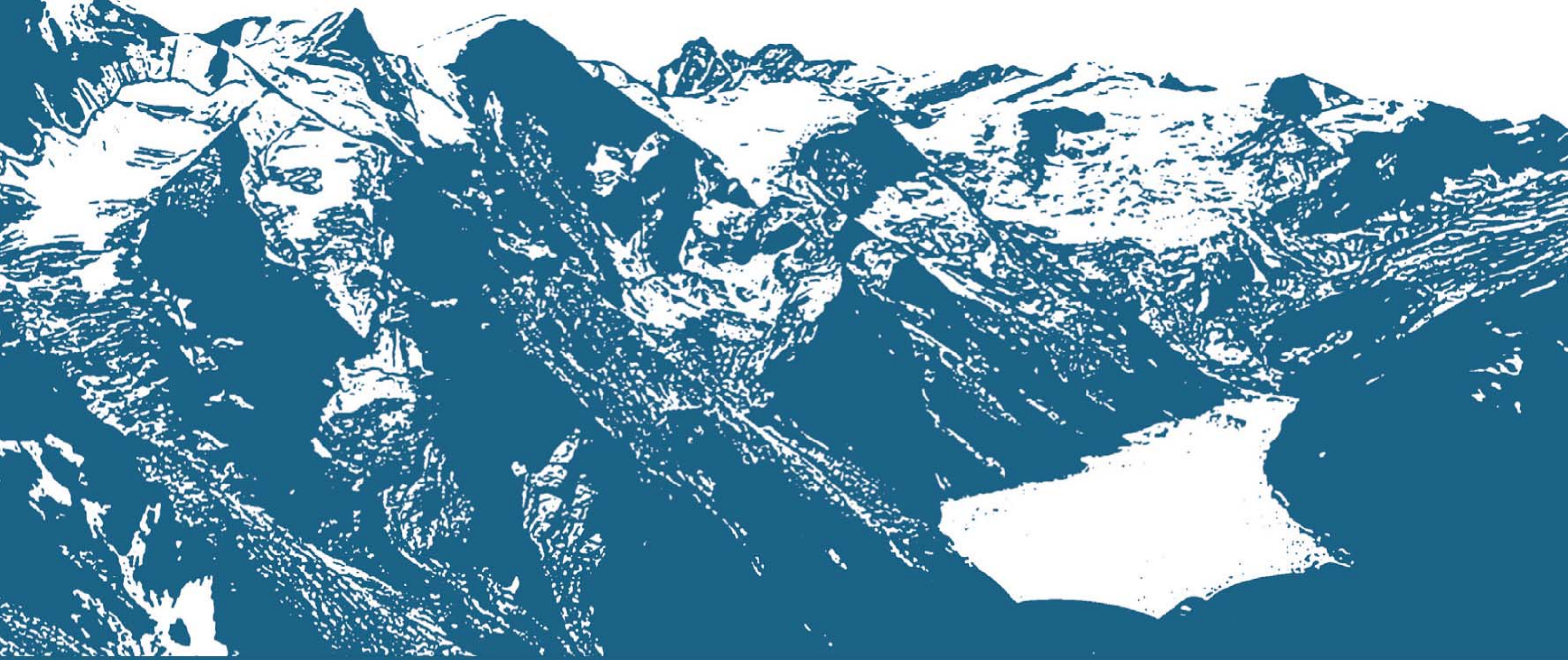

Wasserbau Symposium 2012

Wasser - Energie
Global denken - lokal handeln

12. - 15. September 2012, Graz, Österreich

Tagungsband

Herausgeber: Gerald Zenz

TU Graz

Technische Universität München

ETH Eidgenössische Technische Hochschule Zürich
Swiss Federal Institute of Technology Zurich

Arbeitsgemeinschaft Alpine Wasserkraft

Das Land Steiermark

→ Wissenschaft und Forschung

Verlag der Technischen Universität Graz
www.ub.tugraz.at/Verlag
ISBN 978-3-85125-230-9

Die Autoren sind für den Inhalt ihrer Beiträge verantwortlich. Die Texte der verschiedenen Beiträge des Bandes wurden unter der Aufsicht von jedem der betroffenen Autoren gesetzt.

Titelbilder Copyright bei
Graz Tourismus GmbH
Technische Universität Graz
Layout und Design - Technische Universität Graz
Gedruckt von der Medienfabrik Graz GmbH, Graz, Austria – www.mfg.at

Schwebstoffmonitoring und Verschleiß an Peltonturbinen am Fallbeispiel Fieschertal
Vorbereitende Laborversuche zu Partikelmessmethoden

D. Felix[1], I. Albayrak[1] und R. Boes[1]

[1] ETH Zürich, Versuchsanstalt für Wasserbau, Hydrologie und Glaziologie, Gloriastr. 37/39, CH-8092 Zürich, SWITERLAND

E-Mail: felix@vaw.baug.ethz.ch

Kurzfassung

Bei Wasserkraftwerken, insbesondere bei Hoch- und Mitteldruckanlagen mit vergletscherten Einzugsgebieten und ohne Speicherseen, kann der Hydroabrasiv-Verschleiß an Turbinen und Stahlwasserbauteilen infolge schwebstoffhaltigen Triebwassers erhebliche Betriebskosten und Ertragseinbußen verursachen. Für einen wirtschaftlich optimierten Anlagenentwurf und -betrieb sollen die Bemessungsgrundlagen verbessert und anwendungstaugliche Messverfahren erprobt werden.

Im Rahmen eines interdisziplinären Forschungsprojekts soll am Kraftwerk Fieschertal im Wallis (Schweiz) die Schwebstoffführung des Triebwassers (Konzentration und Partikelgrößenverteilung) mittels neuartiger Messtechnik kontinuierlich erfasst werden. Die Schädigung der Peltonturbine, d.h. der Materialabtrag an den Bechern und Düsennadeln, und die Wirkungsgradabnahme werden am Prototypen mehrmals erhoben und mit der Einwirkung, d. h. der Schwebstoffführung des Triebwassers, korreliert, um Berechnungsansätze zu überprüfen und zu erweitern. Im Projekt werden optische und akustische Messsysteme zur Echtzeit-Überwachung des Schwebstoffaufkommens eingesetzt: in-situ Laserdiffraktometrie, verschiedene „Trübungssonden“ sowie Ultraschallpulse.

Vorgängig zur Messkampagne an der Prototypanlage wurden diese Messeinrichtungen im Labor in einem Tank mit verschiedenen Wasser-Schwebstoffgemischen untersucht. Erste Auswertungen bestätigen, dass instrumentenspezifische Kalibrierungen erforderlich sind und diese stark von der Partikelgröße und –form abhängen. Mittels in-situ Laserdiffraktometrie konnten Partikelgrößenverteilungen in einer Feldspatpulver-Suspension gemessen werden, die gut mit einer anerkannten Referenzmethode übereinstimmen. Es wird erwartet, dass die kontinuierliche Messung von Partikelgrößen „im Feld“ zur besseren quantitativen Beschreibung des Hydroabrasiv-Verschleißes beiträgt.

Einleitung

Sedimente an Wasserkraftanlagen und Verschleiß

Bei Wasserkraftanlagen können die im Triebwasser enthaltenen mineralischen Partikel bei Fallhöhen von mehreren Hundert Metern und bei einem großen Anteil harter kantiger Partikel (z.B. Quarz und Feldspat) bekanntlich zu beträchtlichen Abnutzungserscheinungen an den wasserführenden Bauteilen, besonders an den hydraulischen Maschinen führen (z. B. [1]). Der Verschleiß an Turbinen kann erhebliche Betriebskosten und Ertragseinbußen verursachen.

Abbildung 1a zeigt ein Beispiel von Schäden an einem Peltonlaufrad infolge Hydroabrasiv-Verschleiß, welche durch feine mineralische Partikel (Abbildung 1b) im Triebwasser verursacht werden.

a) 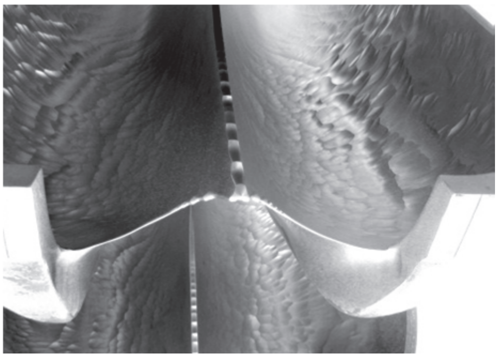

b) 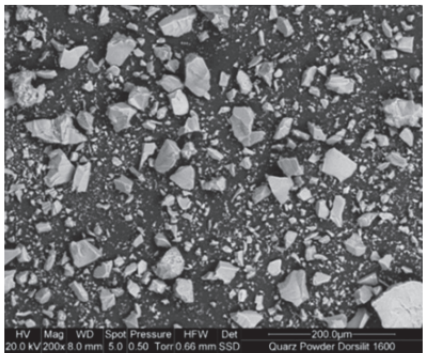

Abbildung 1: (a) Schäden an den Bechern eines unbeschichteten Pelton-Laufrades (Ausstellungsobjekt bei der Staumauer Emosson, Schweiz) und (b) feine Quarzpartikel, wie sie in sog. „Gletschermilch“ vorkommen, unter dem Elektronenmikroskop (Bilder: VAW).

Forschungsbedarf und Zielsetzung

Bei zahlreichen bestehenden Hochdruck-Wasserkraftanlagen ist das Problem des Hydroabrasiv-Verschleißes qualitativ bekannt und es bestehen gewisse Berechnungsansätze zur Abschätzung des Materialabtrags (z.B. [2]). Um Kenntnis über die vorhandene Schwebstoff-Führung des Triebwassers zu haben, besteht Bedarf an Messsystemen, die für den Einsatz an Wasserkraftanlagen geeignet sind [3].

Es besteht auch Interesse an verbesserten Bemessungsgrundlagen für einen bezüglich Sedimentmanagement und Hydroabrasiv-Verschleiß wirtschaftlich optimierten Anlagenentwurf und –betrieb, namentlich zur Bestimmung des Bemessungskorns für Entsandungsanlagen, für die Wahl von Turbinenbeschichtungen, die Auslegung von Pumpen, zur Prüfung der Option des gezielten Abführens von Feinsedimenten aus Stauseen über den Triebwasserweg oder zur Abschätzung eines Grenzwertes für vorübergehende Kraftwerksabschaltungen während kurzzeitig starkem Schwebstoffaufkommen.

Das von der VAW der ETH Zürich initiierte und nachfolgend beschriebene Forschungsprojekt soll einen Beitrag zur Verbesserung der Kenntnisse betreffend des Schwebstoffaufkommens, der Schwebstoffmessung und des Hydroabrasiv-Verschleißes leisten.

Im Folgenden wird ein erster Teil des mehrjährigen Forschungsprojekts, welches im August 2011 begonnen wurde, beschrieben.

Beschreibung des gesamten Forschungsprojekts

Methode und Projektbeteiligte

Der Schwerpunkt der Untersuchung liegt auf einer Prototypstudie an einer bestehenden Hochdruck-Wasserkraftanlage. Vorgängig werden im hydraulischen Labor Versuche zu optischen und akustischen Partikelmessmethoden durchgeführt. Folgende Hochschul- und Industriepartner wirken an diesem interdisziplinären Forschungsprojekt mit:

- Hochschule Luzern, Kompetenzzentrum für Fluidmechanik und Hydromaschinen
- Kraftwerksbetreiber (Gommerkraftwerke AG, Ernen, Schweiz)
- Engineering-Abteilung eines KW-Miteigentümers (BKW FMB Energie AG, Bern)
- Turbinenhersteller (Andritz Hydro, Kriens/Luzern)
- Hersteller von akustischen Durchflussmessungen (Rittmeyer AG, Baar, Schweiz)

Beschreibung der Prototyp-Wasserkraftanlage

Als geeignetes Fallbeispiel konnte das Wasserkraftwerk Fieschertal (Wallis, Schweiz) identifiziert werden. Es handelt sich um eine Hochdruckanlage mit Fallrechenfassung, deren

Einzugsgebiet stark vergletschert ist und bei welcher seit der Inbetriebnahme im Jahr 1976 starker Hydroabrasiv-Verschleiß beobachtet wurde.
Nach der Fassung folgen ein unterirdischer Entkieser, ein Entsander und ein 2 km langer Freispiegelstollen (Abbildung 2), der in Zeiten mit Teillastbetrieb als Tagesspeicher eingesetzt wird. Über eine Druckleitung gelangt das Triebwasser (Ausbauabfluss 15 m^3/s) auf zwei zweidüsige horizontalachsige Peltonturbinen mit einer Nennleistung von total 64 MW. Es sind Laufräder mit Wolframkarbid-Beschichtung im Einsatz. Die mittlere Schwebstoffkonzentration am Kraftwerk Fieschertal wird bei weniger als 1 g/l erwartet, es wurden aber schon Spitzen bis 90 g/l gemessen.

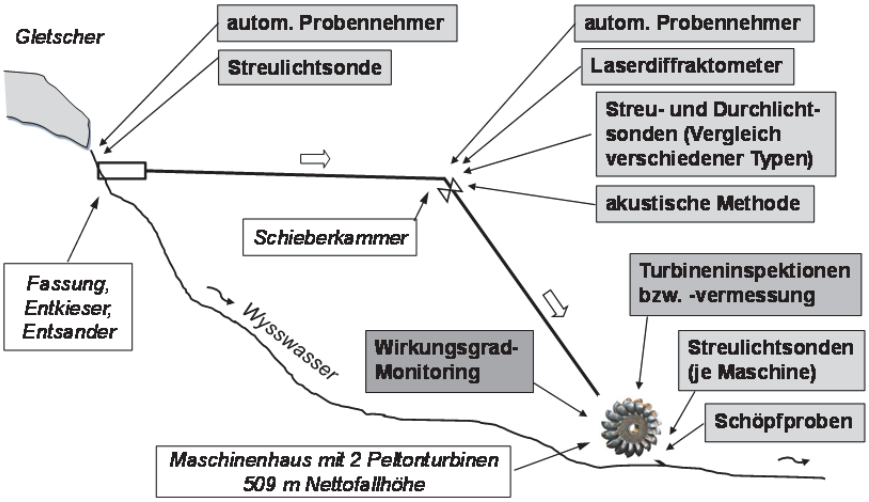

Abbildung 2: Schematisches Längsprofil der Kraftwerksanlage Fieschertal mit Darstellung der vorgesehenen Untersuchungen

Untersuchungsprogramm
An der Kraftwerksanlage sind folgende Erhebungen vorgesehen:

- kontinuierliche Erfassung der Schwebstofffführung des Triebwassers bei der Fassung, beim Einlauf in die Druckleitung und in den Unterwasserkanälen der beiden Maschinen (Messeinrichtungen gemäß folgender Beschreibung); Kalibrierung bzw. Überprüfung der Messeinrichtungen durch manuell oder automatisch zu entnehmende Schöpfproben mit Konzentrationsbestimmung und Laboruntersuchungen (Partikelgrößenverteilung; mineralogische Zusammensetzung und Kornform) ausgewählter Proben.
- periodische Inspektion bzw. Vermessung der Laufräder und Düsen bzw. deren Beschichtungen an beiden Turbinen
- periodische Messung des Wirkungsgrads der beiden Maschinen (Index-Wirkungsgrad)

Die Messungen an der Kraftwerksanlage sind hauptsächlich in zwei Schwebstoffsaisons, d.h. in den Sommermonaten der Jahre 2012 und 2013, geplant.

Versuche zu Partikelmessmethoden

Zielsetzung
Vor dem Einsatz am zu untersuchenden Kraftwerk sollen die optischen und akustischen Messverfahren unter kontrollierten Bedingungen im hydraulischen Labor untersucht werden, um Kalibrierungen, Einsatzgrenzen und Messunsicherheit der Messgeräte in unterschied-

lichen Suspensionen festzustellen. Gegenüber früheren Untersuchungen (z. B. [4]) soll hier auf den Einsatz eines in-situ Laserdiffraktometers LISST-100X in Verbindung mit Partikelsorten, die bezogen auf die Prototypstudie gewählt wurden, eingegangen werden.

Versuchseinrichtung und Methode

An der Hochschule Luzern, am Kompetenzzentrum für Fluidmechanik und Hydromaschinen in Horw, besteht eine Versuchseinrichtung, an welcher Versuche zu Partikelmessmethoden durchgeführt werden. In einem Tank mit Rührwerk (Abbildung 3) werden unterschiedliche Partikelsorten mit Wasser gemischt.

Ausgehend von einer „Nullmessung" in Trinkwasser wird für jede Partikelsorte die Konzentration stufenweise gesteigert und mit allen am Mischtank installierten Geräten werden jeweils gleichzeitig Messungen durchgeführt. Die Messgeräte sind alle auf demselben Horizont bei 60% der Wassertiefe montiert (Abbildung 3, rechts).

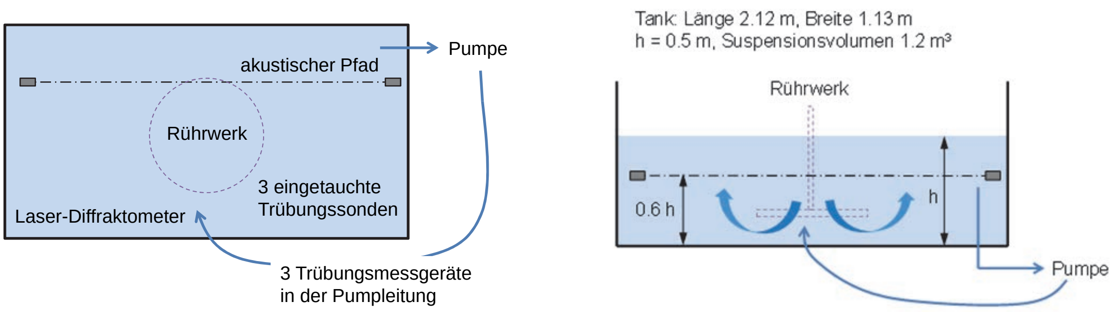

Abbildung 3: Mischtank mit optischen und akustischen Messgeräten für Schwebstoffmessungen im hydraulischen Labor, links im Grundriss und rechts im Vertikalschnitt

Streulicht- und Durchlichtsonden

Zur Überwachung von Suspensionen in der Prozessindustrie, der Wasserversorgung und der Abwassertechnik werden Streu- bzw. Durchlicht-Messgeräte, welche oft als „Trübungssonden" bezeichnet werden, eingesetzt. Bei Streulichtsonden wird in der Regel die Einheit FNU (formazine nephtolometric unit) verwendet. Mittels einer Kalibrierung wird von dem in optischen Einheiten gemessenen Wert auf die Massenkonzentration der Feststoff-Partikel in der Flüssigkeit umgerechnet. In den Versuchen im hydraulischen Labor wurden die in Tabelle 1 aufgeführten Trübungsmessgeräte untersucht.

Tabelle 1: Untersuchte Trübungsmessgeräte

Messgerät	Hersteller	Einbauart
Solitax ts-line sc	Hach-Lange	eingetaucht
Turbimax W CUS41	Endress-Hauser	eingetaucht
TurbiScat (90° und 25°)	Sigrist Photometer	im Strang (unter Druck)
TF16-N mit Messzelle F20	Optek Danulat	im Strang (unter Druck)
AquaScat	Sigrist Photometer	im Strang (Freifall)

In-situ Laserdiffraktometrie und –transmissiometrie (LISST)

Da die Größe der mineralischen Partikeln für den Hydroabrasiv-Verschleiß ein entscheidender Parameter ist und zeitlich stark variieren kann, ist für den Einsatz an Wasserkraftanlagen ein Messgerät gefragt, welches nebst der Schwebstoffkonzentration auch die Partikelgrößenverteilung kontinuierlich in Echtzeit erfassen kann.

Dies ist mit Messgeräten möglich, welche auf der Beugung (Diffraktion) und Dämpfung

(Transmission) von Laserstrahlen beruhen. Seit einigen Jahren sind tragbare Laserbeugungs-Geräte verfügbar, welche auch für Feldstudien eingesetzt werden können ([5], [6]). Von den derzeit angebotenen Geräten [7], wurde das vielseitig einsetzbare Modell LISST-100X, Typ C, ausgewählt. Mittels einer mathematischen Umkehrung (Inversion) der gemessenen Laser-Intensitäten werden die Volumenkonzentrationen in 32 logarithmisch verteilten Partikelgrößenklassen berechnet. Mit einer anzunehmenden Sedimentdichte kann die totale Massenkonzentration berechnet werden.
Mit diesem Gerät können Partikelgrößen zwischen 2.5 und 500 Mikrometer erfasst werden, vorausgesetzt, dass die Suspension nicht zu trübe ist bzw. eine zu hohe Partikelkonzentration aufweist. Um den Bereich messbarer Konzentrationen zu vergrößern, wurde die optische Pfadlänge, d.h. die Strecke, auf welcher der Laserstrahl durch die Suspension geführt wird, mittels eines einsetzbaren Glaskörpers von standardmäßig 50 mm auf 5 mm verkürzt.

Akustische Messungen
Bei zahlreichen Wasserkraftanlagen werden Durchflüsse mit dem akustischen Laufzeitdifferenzverfahren gemessen. Dabei wird zwischen zwei schräg zur Fließrichtung an den Rohr- oder Kanalwänden angeordneten Transducern ein Ultraschallpuls in die eine Richtung und anschließend ein weiterer in entgegengesetzter Richtung durch die Strömung gesendet, womit die Laufzeitdifferenz und die Fließgeschwindigkeit bestimmt wird. Bei solchen akustischen Durchflussmessungen (ADM) können mineralische Partikel im Wasser die Messung beeinflussen [8] oder bei hohen Konzentrationen unter Umständen verunmöglichen.
Es wird nun untersucht, wie sich die Beeinflussung des Ultraschallsignals durch die suspendierten mineralischen Partikel für das Schwebstoff-Monitoring nutzen lässt.

Verwendete mineralische Partikel
Von früheren Untersuchungen am Kraftwerk Fieschertal ist bekannt, dass die dortigen Schwebstoffe zur Hauptsache aus Quarz, Feldspat und Glimmer bestehen, also den Hauptbestandteilen von Granitgestein. Für die Schwebstoff-Messversuche im hydraulischen Labor wurden zum einen mineralische Partikel ausgesucht, welche mit den Schwebstoffpartikeln in der Natur vergleichbar und von industriellen Anwendungen her kommerziell erhältlich sind. Aus dem Unterwasser der Turbinen des Kraftwerks Fieschertal, genauer gesagt aus dem Pumpensumpf des Turbinenkühlsystems, wurden zum anderen während Revisionsarbeiten einige Eimer der abgelagerten Feinsedimente für die Laborversuche entnommen.
Von den im hydraulischen Labor verwendeten mineralischen Partikeln sind die Partikelgrößenverteilungen in Abbildung 4 dargestellt. Diese wurden am Institut für Geotechnik der ETH Zürich mit dem stationären Laserdiffraktometer Horiba gemessen und als Referenz verwendet.

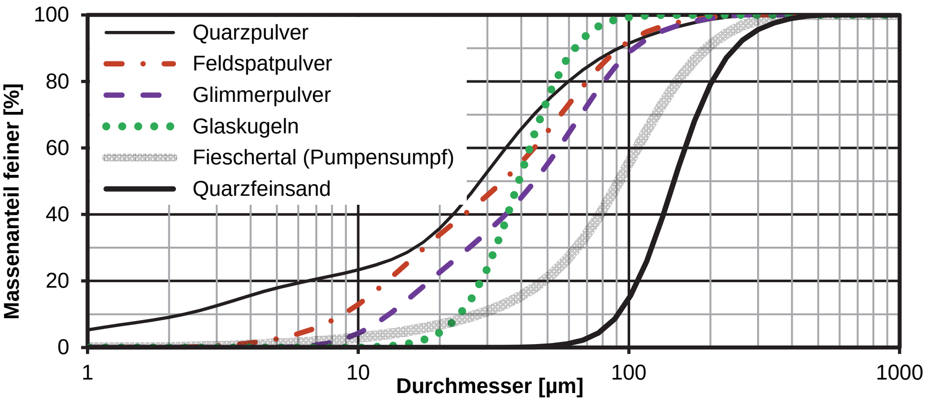

Abbildung 4: Korngrößenverteilungen der verwendeten Partikel

Erste Versuchsresultate und Diskussion

In den folgenden drei Abbildungen sind Resultate von ersten Auswertungen der Laborversuche bezüglich Partikelmessmethoden dargestellt.

Abbildung 5 zeigt Partikelgrößenverteilungen von Feldspatpulver, welche mit dem Laserdiffraktometer im Mischtank bei einer nominellen Schwebstoffkonzentration von 1 g/l gemessen und mithilfe der zugehörigen Software unter Annahme einer unregelmäßigen Partikelform berechnet wurden. Die gemessenen Partikelverteilungen variieren u.a. aufgrund der Turbulenz im Mischtank. Die gestrichelten schwarzen Linien zeigen die 5% bzw. 95%-Fraktilen von 100 Kornverteilungen, die mit einer Frequenz von 1 Hz gemessen wurden; die ausgezogene schwarze Linie zeigt den Median. Zum Vergleich ist die Referenzmessung (aus Abbildung 4) als graue Linie dargestellt. Die Messung der Partikelgrößenverteilung mit dem LISST-100X stimmt generell recht gut mit der Referenzmessung überein.

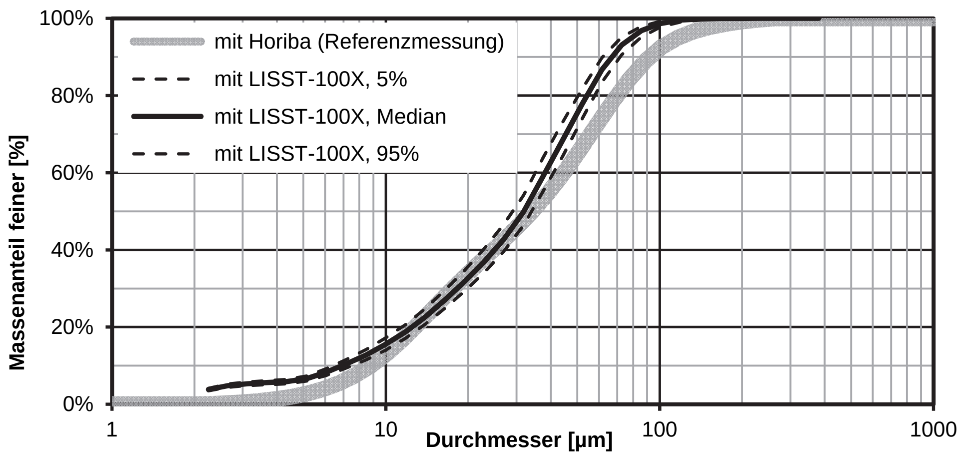

Abbildung 5: Vergleich von gemessenen Partikelgrößenverteilungen (Feldspatpulver)

Abbildung 6 zeigt ausgewählte Messresultate am Beispiel von Feldspatpulver in Funktion der Referenz-Schwebstoffkonzentration. Diese wurde mittels Schöpfproben, die aus dem Tank auf dem Horizont der Messgeräte entnommen und im Ofen getrocknet wurden, unter Berücksichtigung der im verwendeten Trinkwasser gelösten Mineralien ermittelt.

An der linken Ordinate ist die mit dem Laserdiffraktometer ermittelte Massenkonzentration der Schwebstoffe im Mischtank abzulesen. Dabei wurde pro Konzentrationsstufe die Volumenkonzentration über 100 Messwerte gemittelt und mit einer angenommenen Dichte von 2.65 g/l (wie Quarz) multipliziert. Die so mit der Werkskalibrierung ermittelten Schwebstoffkonzentrationen liegen bei dieser Partikelsorte ca. 20% bis 60% über den Referenzkonzentrationen.

An der rechten Ordinate sind die Messresultate von vier Streulichtsonden dargestellt. Es wurden jeweils die Mittelwerte über 500 Messungen, die im Sekundentakt aufgezeichnet wurden, gebildet. Der Zusammenhang zwischen Schwebstoffkonzentration und Trübung ist - wie in diesem Konzentrationsbereich erwartet - nahezu linear. Obwohl bei allen vier Geräten die Einheit FNU verwendet wird, weichen die Messwerte der unterschiedlichen Geräte bei gleichen Bedingungen bei dieser Partikelsorte im dargestellten Konzentrationsbereich um ca. 40% voneinander ab.

In Abbildung 7 sind wiederum Kalibriergeraden dargestellt, nun aber für Suspensionen mit verschiedenen Partikelsorten, am Beispiel der Trübungssonde Solitax ts-line sc (Hach-Lange). Für die Partikelsorten sind die Durchmesser bei 50% Massenanteil (d_{50}) gemäß Referenzmessung der Partikelgrößenverteilungen (Abbildung 4) angegeben. Wie aus der Literatur (z.B. [9]) bekannt, ist eine starke Abhängigkeit der Trübung vom Partikeldurchmesser zu erkennen. Die Lage der Geraden des Glimmerpulvers (plättchenförmige Partikel) und der

Glaskugeln zeigt weiter im Vergleich zu den gebrochenen Partikeln trotz ähnlichen d_{50} einen deutlichen Einfluss der Partikelform.

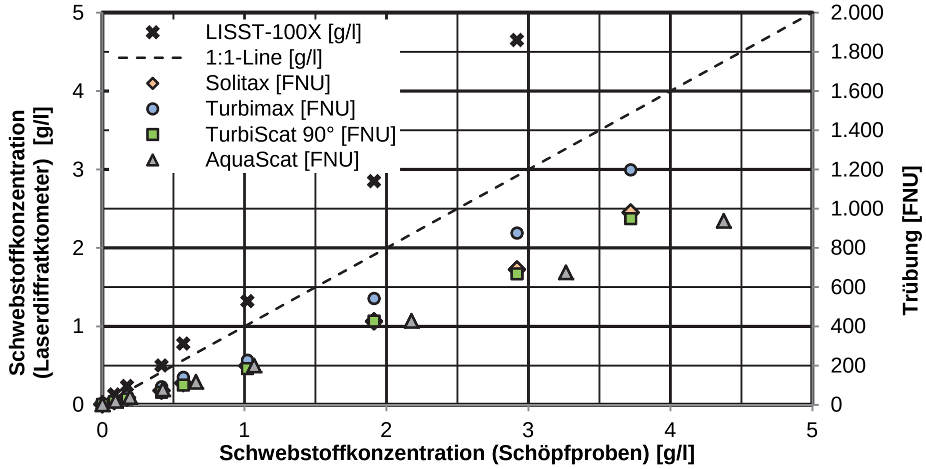

Abbildung 6: Messresultate des Laserdiffraktometers und ausgewählter Trübungssonden in Funktion der Referenz-Konzentrationsmessungen mittels Schöpfproben (Feldspatpulver)

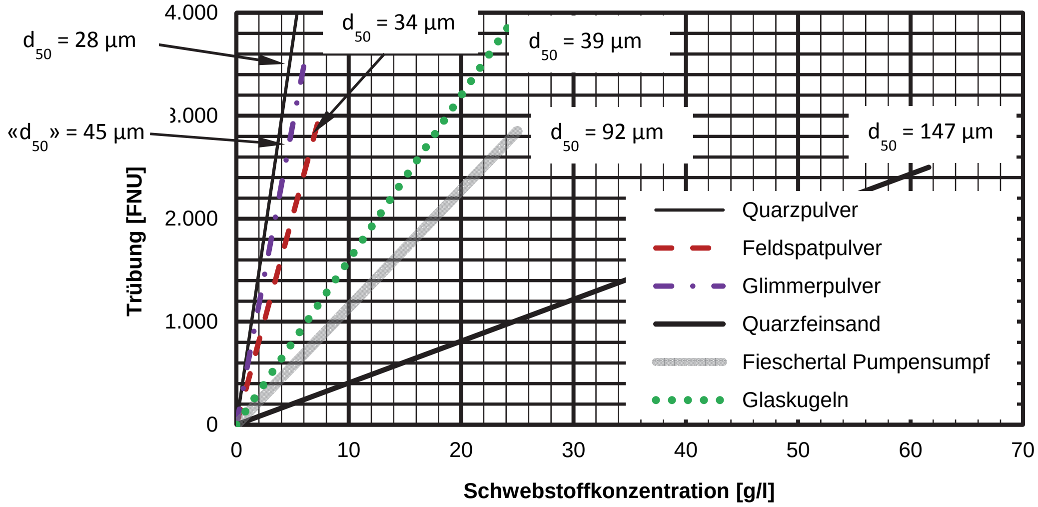

Abbildung 7: Trübungswerte, welche mit einer Trübungssonde (Hach-Lange Solitax ts-line sc) in Suspensionen mit sechs verschiedenen Partikelsorten gemessen wurden

Schlussfolgerungen und Ausblick

In Laborversuchen wurden verschiedene Partikelmessgeräte und -methoden an Suspensionen aus mineralischen Partikeln untersucht. Als Partikel kamen kommerziell erhältliche Gesteinspulver, Feinsand, Glaskugeln sowie ein Schluff-Feinsand-Gemisch aus einer alpinen Wasserkraftanlage zum Einsatz.

Die Kalibrierkurven von Trübungssonden können je nach Messgerät und Partikeleigenschaften, insbesondere der Partikelgröße, stark unterschiedlich sein. Für die Messgeräte sind Kalibrierkurven zu verwenden, die mit dem jeweiligen Messgerät und einer bestimmten Partikelsorte im interessierenden Messbereich durch Vergleich mit Schöpfproben ermittelt wurden. Für den Einsatz in der Praxis bringt dies einen gewissen Aufwand mit sich.

In Wasserkraftanlagen können sich die Größe und allenfalls die Form und Farbe der im Triebwasser mitgeführten Partikel im Lauf der Zeit ändern, was bei der Umrechnung von Trübungs- auf Konzentrationsganglinien eine beträchtliche Unsicherheit mit sich bringen

kann . Die Anwendung des in-situ Laserdiffraktometers für das Schwebstoffmonitoring an Wasserkraftanlagen wird weiter untersucht, da dies nebst der Konzentrationsmessung eine Messung der Partikelgrößen erlaubt.
Für die Untersuchungen am Prototypen werden Messeinrichtungen installiert, so dass während der kommenden zwei Schwebstoffsaisons Felddaten erhoben werden können. Basierend auf der Laboruntersuchung der Partikelmessgeräte und der Erfahrung beim Einsatz am Prototypen werden Empfehlungen bezüglich Messgeräten für das Schwebstoff-Monitoring an Wasserkraftanlagen formuliert.
Ein möglichst vollständiger Datensatz über das Schwebstoffaufkommen, den Materialabtrag an den Turbinen und den zugehörigen Wirkungsgradverlust kann dazu genutzt werden, Berechnungsansätze zur Vorhersage des Turbinenverschleißes weiterzuentwickeln und zu verifizieren.

Danksagung

Das Forschungsprojekt wird durch swisselectric research, das Schweizer Bundesamt für Energie (BFE) und die Gommerkraftwerke sowie durch die eingangs genannten weiteren Projektpartner unterstützt. Die Autoren bedanken sich bei allen Projektpartnern für ihr Engagement und besonders bei Prof. Dr. T. Staubli, Prof. Dr. P. Gruber, A. Abgottspon und M. Duss von der Hochschule Luzern, Kompetenzzentrum für Fluidmechanik und Hydromaschinen, für die Unterstützung bei der Durchführung der beschriebenen Laborversuche. Ein weiterer Dank geht an die Firma Sigrist Photometer, Ennetbürgen, welche ein Trübungsmessgerät für die Laboruntersuchungen zur Verfügung gestellt hat.

Quellenverzeichnis

[1] Gummer J. H. (2009). Combating Silt Erosion in Hydraulic Turbines. Hydro Review Wordwide, 17(1).
[2] DWA (2006). Entlandung von Stauräumen. DWA-Themen, Deutsche Vereinigung für Wasserwirtschaft, Abwasser und Abfall e.V., Hennef (Hrsg.), ISBN 978-3-937758-33-6.
[3] Bishwakarma M.B., Støle H. (2008). Realtime sediment monitoring in hydropower plants. J. Hydr. Res. 46(2): 282–288.
[4] Bittner G. (2008). Vergleich von Trübungssonden bei der Schwebstoffmessung unter definierten Laborbedingungen. Diplomarbeit, Universität für Bodenkultur, Wien, Österreich.
[5] Agrawal Y., Mikkelsen O.A., Pottsmith H.C. (2011). Sediment monitoring technology for turbine erosion and reservoir siltation applications. Proc. HYDRO 2011 Conference, Prague, Czech Republic.
[6] Boes R. (2009). Real-time monitoring of suspended sediment concentration and particle size distribution in the headwater way of a high-head hydropower plant. Proc. 33rd IAHR Congress, Vancouver, Canada: 4037–4044.
[7] Sequoia Scientific (2010). Broschüren über das in-situ-Laserdiffraktometer LISST-100X, LISST-Hydro und LISST-Infinite, Sequoia Scientific, Inc., USA, www.sequoiasci.com.
[8] Costa I., Storti G., Lüscher B., Gruber P., Staubli Th. (2010). Influence of solid particle parameters on the sound speed and attenuation of pulses in acoustic discharge measurements (ADM), Switzerland. Journal of Hydrologic Engineering (accepted for publication).
[9] Gippel, C. J. (1995). Potential of turbidity monitoring for measuring the transport of suspended solids in streams. Hydrological Processes 9: 83-97.

SUSPENDED SEDIMENT AND PELTON TURBINE WEAR MONITORING: EXPERIMENTAL INVESTIGATION OF VARIOUS OPTICAL AND ACOUSTIC DEVICES AND BEGIN OF THE CASE STUDY FIESCHERTAL

D. Felix, I. Albayrak, A. Abgottspon, R. Boes, P. Gruber

Abstract: Considerable hydro-abrasive wear may occur at turbines of hydroelectric power plants particularly at high-head run-of-river schemes in glaciated catchment areas.
In order to optimize the operation of such power plants, real-time information on suspended sediment is required. Optical and acoustic devices for suspended sediment monitoring were calibrated in the laboratory and installed at a case study site in the Swiss Alps, delivering first results. Furthermore, the 3D-geometry of the turbine buckets was digitalized with high accuracy to quantify changes in geometry and material loss.

1 Introduction

Hydro-abrasive wear at turbines and steel hydraulics parts due to suspended mineral particles in the water can lead to substantial maintenance costs and significant negative impacts on power generation and revenue at hydroelectric power plants (HPP), particularly at high-head run-of-river type plants in glaciated catchment areas with igneous rocks such as granite. For well-balanced plant design and operation there is still a need for improved design knowledge and adequate real-time measuring systems to monitor suspended sediment load at prototype conditions [1].
In order to advance in the understanding and addressing of this problem VAW of ETH Zurich initiated an interdisciplinary project in cooperation with Hochschule Luzern and supported by swisselectric research, the Swiss Federal Office of Energy, the power plant operator (Gommerkraftwerke) and co-owner (Bernische Kraftwerke) as well as industry partners (Andritz Hydro and Rittmeyer). This project focusses on the investigation of hydro-abrasive wear at the existing high-head HPP Fieschertal, in Upper Valais, Switzerland. Since the plant was built in 1976 severe hydro-abrasive wear at needles, nozzles and runners of the two 32 MW-Pelton units has been observed. Although coating of turbines and other hydraulics parts reduced the extent of the damages, sediment handling as well as optimized operation and maintenance of the HPP remain an important economic issue. Increased yield of fine sediment is expected in the Alps due to the glacier retreat.
In this project, suspended sediment in the turbine water is continuously monitored during two or three summer seasons using various measuring techniques. In parallel material loss on turbines and efficiency reduction are measured. Suspended sediment load, material loss on turbines and efficiency reduction shall be correlated in order to verify and improve forecasting of hydro-abrasive wear.

This paper focuses on suspended sediment monitoring (preliminary laboratory tests and first case study results) and the selected method for quantifying geometry changes at turbine runners.

2 Suspended sediment monitoring techniques

2.1 Overview

For the investigation of hyro-abrasive wear the following parameters are of interest:

- Suspended sediment (mass) concentration (SSC)
- Particles size distribution (PSD)
- Hardness (mineralogical composition) and shape of the mineral particles

Hardness and shape of the particles are assumed to be relatively constant and can be determined by laboratory analysis of a few periodically taken samples.
SSC and PSD however may vary considerably in time. Thus a continuous monitoring of these parameters is required. Various devices to monitor SSC are currently available or under development. The following optical and acoustic devices were selected for this study:

(a) Turbidimeters (attenuation and/or scattering of near infrared or laser light),
(b) Portable laser transmissiometry and diffraction (LD) and
(c) Acoustic transducers as used in acoustic discharge measurement (ADM) devices.

From literature (e.g. [2]) it is known that the particle size has a significant effect on hydro-abrasive wear. As to our knowledge the portable laser diffraction device is the only instrument that provides in-situ real-time particles size distributions in addition to information on SSC.

2.2 Turbidimeters

For monitoring of suspensions in industrial processes, water and wastewater plants optical probes - called “turbidimeters” - are used. The readings (displayed in optical units) delivered by such probes are converted to SSC using a calibration curve which has to be obtained by the user for the prevailing type of particles. The devices listed in Tab. 1 were tested in the lab prior to the installation at the case study site.

Product	Manufacturer	Measuring principle	Installation	Nom. range
Solitax ts-line sc	Hach-Lange	Combined scattering at 90° and 140°	submerged	0…4000 [FNU]
Turbimax W CUS41	Endress-Hauser	Scattering at 90° multiple channels	submerged	0…9999 [FNU]
TurbiScat	Sigrist Photometer	Scattering at 90° and 25°, in combination with transmission	in-line (pressure flow)	2 channels 0…4000 [FNU]
AquaScat	Sigrist Photometer	Scattering at 90°	in-line (free falling jet)	0…4000 [FNU]
TF16-N with flow cell F20	Optek Danulat	Transmission (0°)	in-line (pressure flow)	0...5 [CU]

Table 1. Tested optical probes

2.3 Portable laser transmissiometry and diffraction (LD)

Among the available portable laser diffraction devices a LISST-100X, Typ C (from Sequoia Scientific) was selected. This submersible instrument can also be used for investigations of suspended sediment in reservoirs and desilting facilities. A similar LD instrument is in use at a high-head HPP on a mountain stream in Austria [3]. The use of LD instruments at HPPs is discussed in [4]. By means of a mathematical inversion of the measured laser intensities the volume concentrations of 32 log-spaced particle size bins are calculated. The total mass concentration (SSC) can be calculated using an estimated sediment density. The nominal size range of measureable particles is 2.5 to 500 micrometers for the selected type of instrument. In order to extend the range of measurable SSC the optical path length was reduced from 50 mm to 5 mm by using a 90%-path reduction module.

2.4 Acoustic measurements at ADM-installations

In many HPPs worldwide discharges are measured using the acoustic transit time method (acoustic discharge measurement ADM). Ultrasonic pulses are subsequently sent through the flow on several paths, which are arranged oblique to the main flow direction. Between two identical transducers that are installed at the penstock or channel walls ultrasonic pulses are sent and received once forward and then backwards. From the difference in the measured “time of flight” between both directions the average flow velocity and discharge are calculated. Acoustic discharge measurement can be influenced or possibly disrupted in case of high SSCs [5]. On the other hand, the alteration of the received signals due to the presence of mineral particles can be used for (at least qualitative) suspended sediment monitoring.

3 Laboratory investigation on suspended sediment monitoring

3.1 Experimental set-up and methodology

Prior to the field study the devices for suspended sediment monitoring were tested in in the hydraulic laboratory of Hochschule Luzern, at an existing facility of the Competence Centre for Fluid Mechanics and Hydro Machines [6]. In a tank equipped with a stirrer (Fig. 1) various suspensions of water and mineral particles with SSC from 0.1 g/l up to 50 g/l (depending on the type of particles) were prepared. Starting from a zero measurement in drinking water the concentration was increased step-wise and measurements were done simultaneously with all devices involved. All devices were placed at the same level.

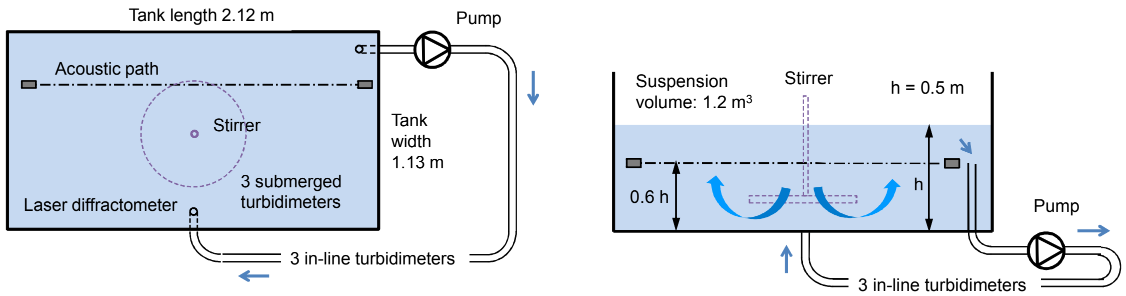

Fig. 1. Mixing tank in the hydraulic laboratory with optical and acoustic devices for measuring suspended sediment, left plan view and right vertical section.

3.2 Materials

According to previous investigations [6] the suspended sediment at the case study site consists of approximately 20 % quartz, 50 % feldspar and 30 % mica, i.e. the main components of granite rock. The mineral particles used in the laboratory tests were selected considering the similarity to natural conditions at the case study site. Most of the particles were bought from industrial applications. In addition, natural particles taken from the turbine's tailwater channel during revision works (deposit in the pump sump of the turbine cooling system) were included in the tests. Glass beads were used as a reference (spherical shape). Quartz and feldspar powder particles have angular shape (from grinding) while quartz fine sand and mica powder have rounded (natural sand) and flaky shape, respectively.

3.3 Results

First results of the measurements made with a turbidimeter, the LISST and the acoustic method are presented in this section.
The measured values (except for PSD) are plotted against the reference SSC, which was determined by samples taken from the tank at the instrument's elevation (three samples per concentration level). By weighing the samples before and after drying in the oven, the effectively prevailing SSC was determined, deducting the dissolved minerals from the residue. Reference measurements of PSD were obtained from the samples analysed by a non-portable laser diffractometer (Horiba) at the Geotechnical Institute of ETH Zurich.
Fig. 2 shows turbidity measured by the optical transmission probe (Optek) as a function of the reference SSC for four kinds of particles and d_{50}, which is the particle diameter of 50 % finer, according to the PSD reference measurement. The plotted values are averages of 500 measurements per concentration level, recorded at 1 Hz.

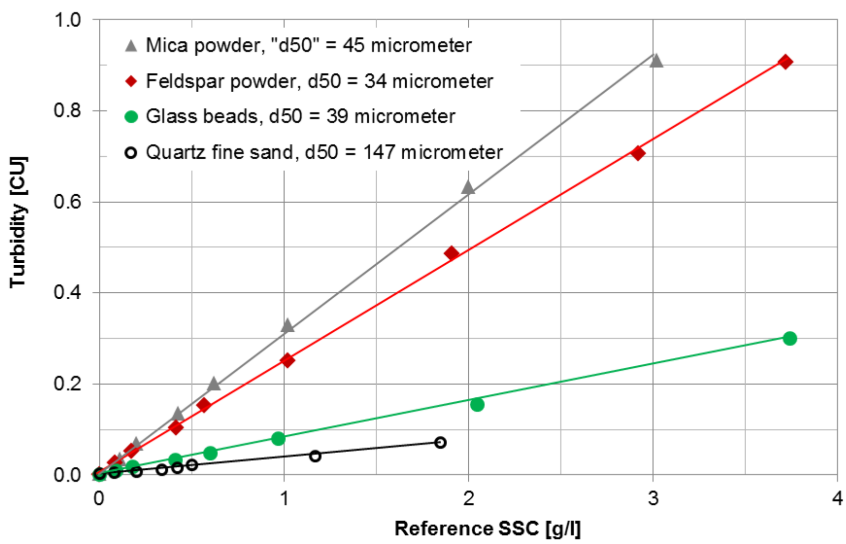

Fig. 2. Turbidity measured by optical transmission as a function of reference SSC

In the displayed range of SSC there is a linear relationship between turbidity and the reference SSC for each type of particle. However, turbidity is not only function of SCC but also of particle type with effects of particle size, shape and optical properties.
Fig. 3 shows the damping of the amplitude of the received ultrasonic pulses (forward scattering) normalized with the amplitude measured in drinking water (SSC = 0) as a function of the reference concentration for various kind of particles in the mixing tank. The amplitudes were measured at a distance of 1.73 m away from the sender and the sent pulses have a frequency of 1 MHz. The plotted values are averages over 60 values per concentration level, recorded at 1 Hz. The amplitude of the received signal decreases almost linearly as SSC increases. The damping depends on particle material, size and shape. Previous investigations [6] indicate that the calibration curves for the acoustic method vary less with particle size than those of turbidimeters.

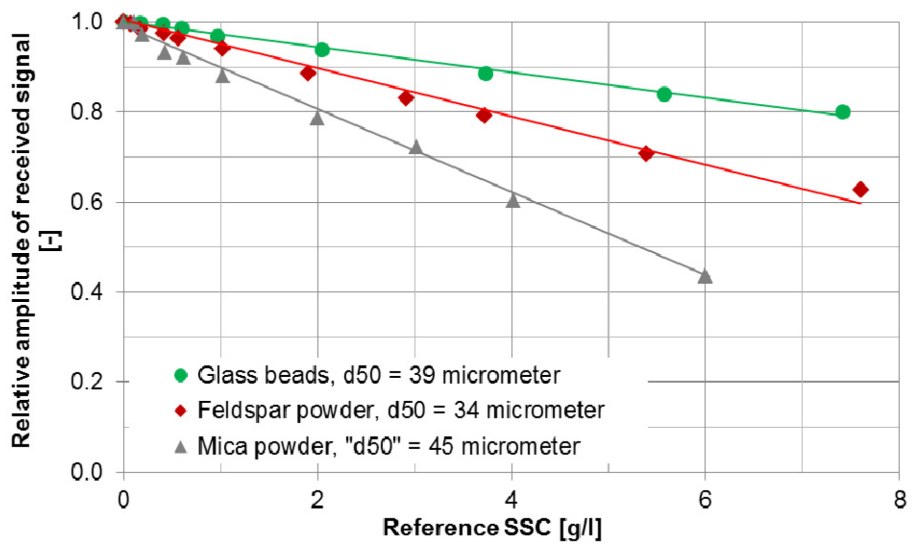

Fig. 3. Relative amplitude of received ultrasonic pulses as a function of reference SSC

Fig. 4 shows a comparison of the time-averaged PSDs measured by LISST at 1Hz for 100s at a nominal SSC of 1 g/l and the reference PSDs for feldspar and quartz fine sand. In LISST PSD calculations, particle shape was assumed to be “irregular”.
The PSDs measured by LISST match approximately with the reference PSDs, e.g. with respect to the range of d_{50} and the general shape of the PSD (narrow or wide distribution), for fine sand as well as coarse silt. The PSD of feldspar powder, whose left end touches the lower limit of measureable sizes, is biased by “fine out of range particles” [7]. The LISST underestimates the proportion of coarser particles within the PSDs; this is more pronounced for fine quartz sand. It should be noted that for the flaky shape of mica powder the definition of the particle diameter is not obvious and it was not possible to check the accuracy of the reference PSDs, since in contrast to SSC no primary measuring method is available. The deviations between LISST and the reference measurements will be further analyzed.
The relationship between the SSC measured by LISST and the reference SSC is presented in Fig. 5. Plotted values are again the time-averages of 100 measurements per concentration level at 1 Hz. For the conversion of volume concentration to mass concentration (SSC) a density of 2.65 kg/l (standard value for

quartz) was assumed for all materials, leading to an error of presumably less than 5%.
For fine quartz sand, which is the coarsest particle among the other particles, SSC measured by LISST correspond generally well to the expected SSCs (1:1-line). It should be noted that no custom calibration was applied. For feldspar powder, the LISST SSCs correspond to the reference SSCs at lower concentrations, but LISST increasingly overestimates SSCs at higher concentrations. This can be related to the effect of “fine out of range particles”, which may bias the inversion and becomes more pronounced as the SSC approaches the upper measurement limit of the LISST. For the mica powder however, the LISST significantly overestimates the SSC (factor of 6), what can be attributed to the flaky shape of these particles producing over-proportional scattering.

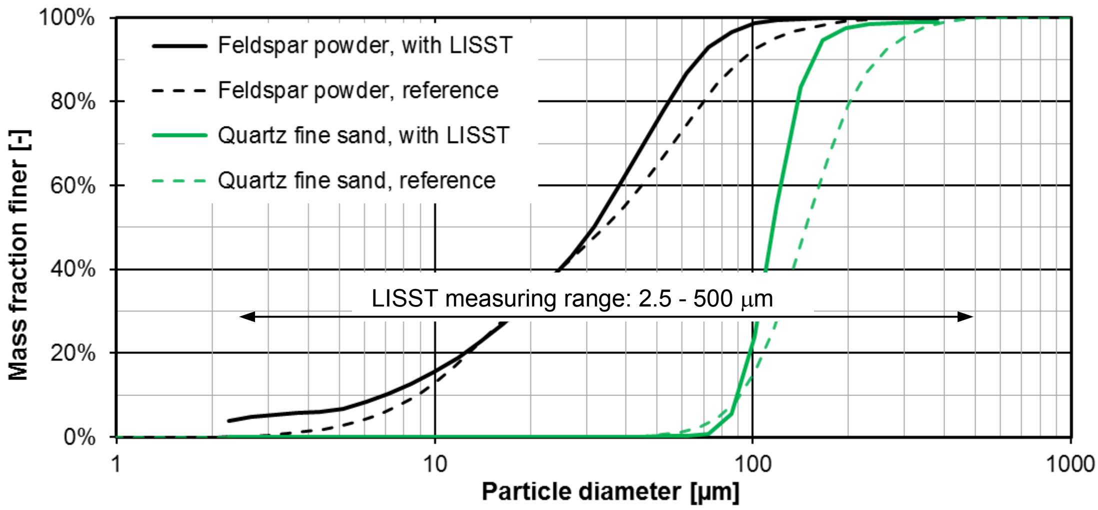

Fig. 4. PSDs measured in by portable laser diffraction (LISST) and by the reference method

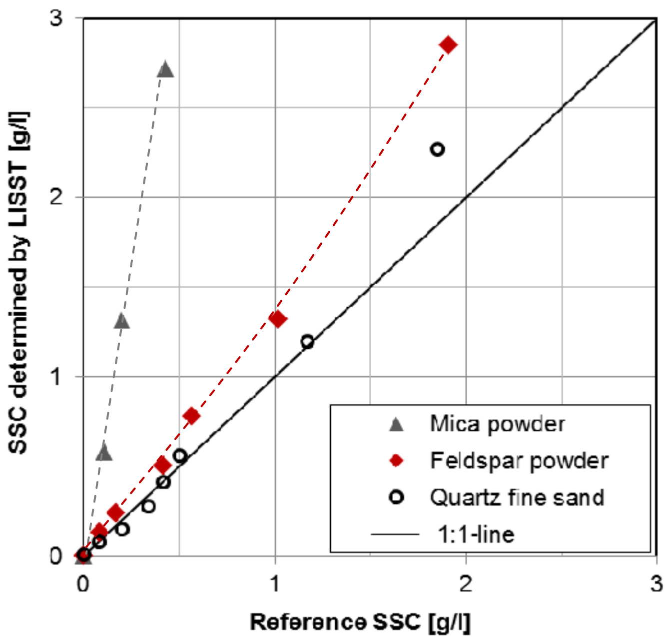

Fig. 4. SSCs determined by LISST as a function of reference SSC

4 Field investigations on suspended sediment and turbine wear

4.1 Installation of suspended sediment monitoring devices

After the tests were completed in the laboratory, the devices for real-time monitoring of suspended sediment were installed in the HPP of Fieschertal (see Fig. 6). Most devices were placed in the valve chamber at the top of the penstock and fed by a sampling pipe with sediment-laden water taken from the axis of the penstock. In addition, two turbidimeters were installed and turbined water is pumped up to them from each turbine unit's tailrace channel.
An automatic water sampler with 24 bottles in the valve chamber was installed to collect samples of the turbined sediment-laden water. SSC is determined from the water samples and used to calibrate the instruments with respect to the particles of the study site. The water sampler is triggered by a turbidimeter in order to take more samples during sediment peaks.

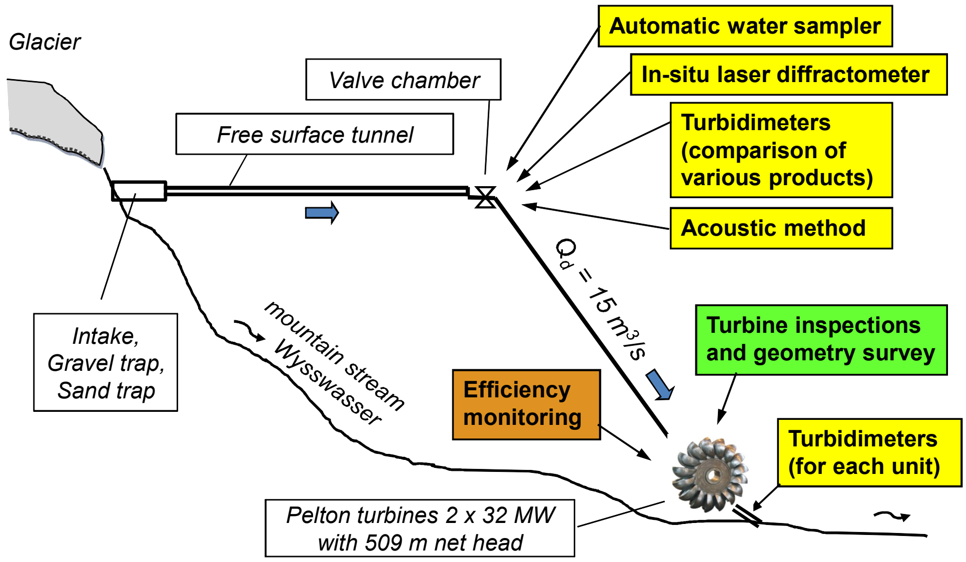

Fig. 5. Schematic longitudinal profile of the Fieschertal hydroelectric power plant showing the investigation program.

4.2 First results on suspended sediment monitoring

On July 2 and 3, 2012, a major thunderstorm occurred in Fieschertal, which produced a flood discharge with an estimated return period between 10 and 30 years. Fig. 7 shows the time series of turbidity measured by optical transmission (Optek) and the scaled relative amplitude of the received ultrasonic pulses at one path of the acoustic discharge measurement installation. The scaled relative amplitude of the received ultrasonic pulses is well in line with the turbidity time series, except for the highest peak that was only recorded by optical transmission. This means that the sampling pipe was not clogged during the event and that at least qualitative information on suspended sediment, measured directly in the power waterway, can be retrieved from ADM-systems existing in many HPPs. The results

are promising to develop a method to estimate real-time SCC using the amplitude of received acoustic signals available as an auxiliary parameter in ADM-systems.
Since the prevailing particles in Fieschertal consist of mostly feldspar and mica particles and the calibration curves of the optical transmission probe for powders of these materials are similar (Fig. 2), the calibration curve of feldspar powder was used to estimate the SSC. Based on the assumption, that the suspended sediment during the thunderstorm was similar to the feldspar and mica particles used in the laboratory, the turbidity peak of almost 5 CU (Fig.6) corresponds to approximately 20 g/l, what is relatively high. Water samples taken during the thunderstorm will be analysed to obtain more precise SSCs by weighing of dried samples.

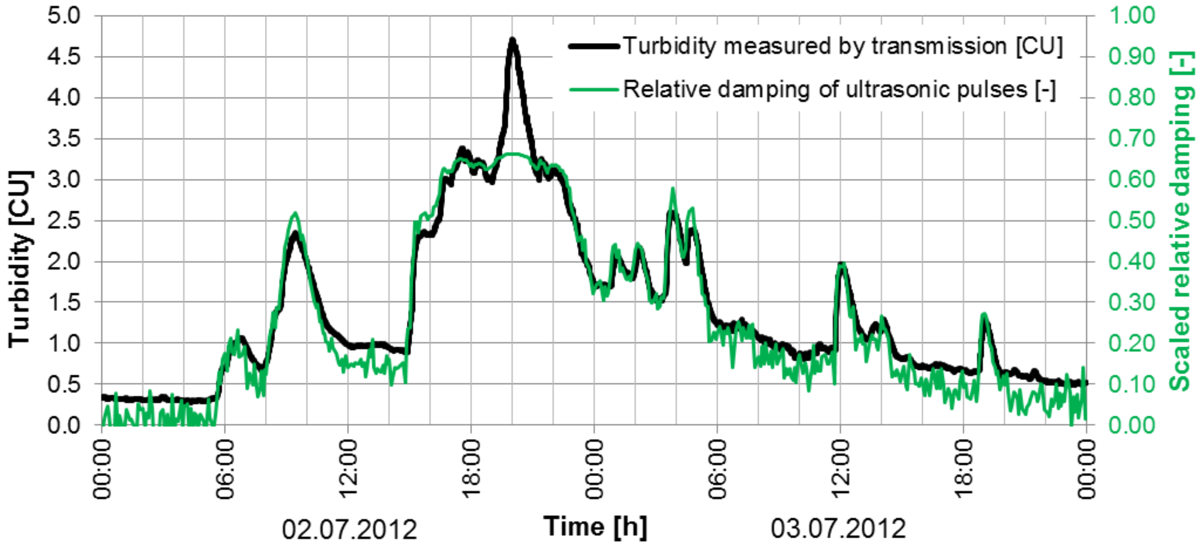

Fig. 6. Time series of measured turbidity (left vertical axis) and scaled relative amplitude of received ultrasonic pulses (right vertical axis) during the thunderstorm of July 2 and 3, 2012.

Besides sediment peaks due to weather phenomena, there are sediment peaks which depend on the power plant's operation and on the hydraulic conditions in the free surface tunnel, which serves as a daily storage reservoir. Low water levels in the free surface tunnel may cause re-suspension of settled particles and may thus lead to relatively high SSCs [6].

4.3 Turbine inspections and 3D-digitalization of bucket geometry

Besides monitoring of suspended sediment the turbines are inspected in the on-going project at least before and after the sediment season and occasionally during the sediment season, e.g. during flushing of the free surface tunnel. The local coating thicknesses in selected buckets are measured with a thickness meter based on magnetic induction.
Erosion damages on the turbine buckets are documented with photographs and their current geometries are measured with an optical scanner (Fig. 7). The working principle of the optical scanner is based triangulation and it has a resolution of five megapixels in a measurement volume of 480 x 400 x 250 mm. The 3D point distance is 190 μm and the accuracy of the system is within 25 μm. The optical measurements focus on the monitoring of the abrasion of the main splitter in selected buckets.

Fig. 7. Digitizing of Pelton buckets geometry in the power plant: Special camera mounted on a tripod below the buckets of the runner with stick-on reference points.

Fig. 8 shows the results of the geometric analysis. The mid-plane cut through the bucket in the axis of the main splitter is displayed with a solid black line. This cut is extracted from the point cloud of the 3D-digitization of bucket no. 1. The initial (theoretical) splitter profile is shown as a dotted black line. A serious abrasion of the main splitter can be observed from the difference of the two splitter contours.
The grey lines with the vertical axis on the right hand side show the abrasion (in mm) at the top of the main splitters of two digitized buckets. The abrasion processes on both splitters are comparable with respect to the affected parts of the splitters and the magnitude of the abrasion depth of approximately 8 mm.
Further scans after the sediment season will allow to obtain quantitative data on geometry changes and to relate the material loss to the suspended sediment load.
The second turbine inspection made in August 2012 after the thunderstorm described above revealed considerable wear on the runners of both turbines.

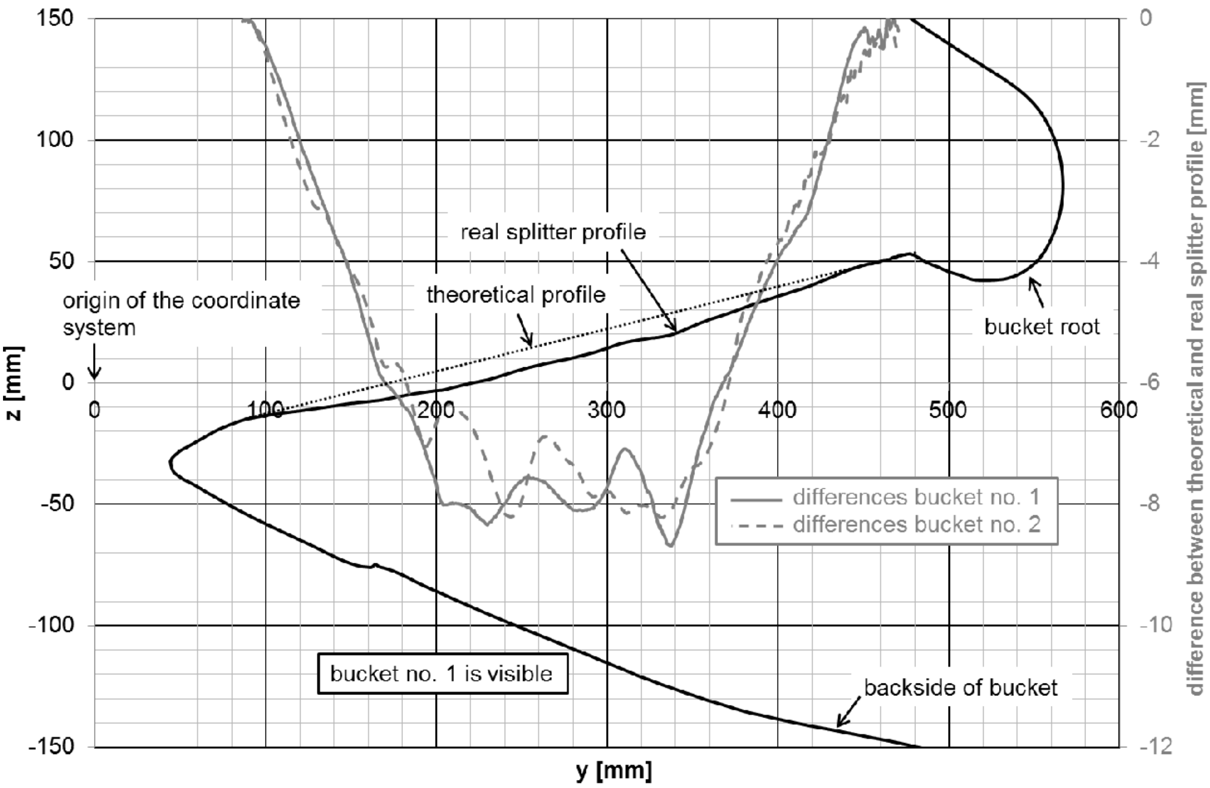

Fig. 8. Profile of main splitter (side view): Comparison of theoretical and real geometry

5 Conclusions

Regarding suspended sediment monitoring, various devices were investigated in the laboratory to assess the measuring range, measuring uncertainty and calibration parameters. Custom calibrations depending on the type of particles prevailing in the turbine water are required for turbidimeters and the acoustic method. As a drawback, temporal variation of the properties of the prevailing suspended sediment particles may lead to significant uncertainty when estimating SSC from turbidimeters or acoustic signals obtained from sensors used in ADMs.

First results show that LISST allows capturing PSDs and SSCs for particles in the range of silt to fine sand at concentrations up to a few g/l. Existence of particles smaller than the lower limit of the measurement range of the LISST may bias PSD and thus cause an overestimation of SSC. First results further indicate that coarser fractions within the PSDs are underestimated by the LISST. Concerning the particle shape effect, mica in suspended sediment may lead to a considerable overestimation of SSC. This is related to the fact that the flaky shape of mica differs greatly from the rounded or angular shape of the other investigated particles and from the currently assumed particle shape in the calculation model.

First evaluation of field data showed that during a major thunderstorm two devices (optical transmission probe and ADM) were able to record the time series on turbidity and amplitude, respectively. The good correlation between acoustic amplitude damping and optical transmission is promising to develop a real-time suspended sediment monitoring based on ADM devices. Devices for suspended sediment

monitoring based on optical methods are suitable at lower concentrations while the use of ADM signals is advantageous at higher concentrations.
Regarding monitoring of turbine wear, digitalization of the 3D-geometry of Pelton buckets by the means of an optical scanner offers the possibility to quantify geometry changes and thus material loss at turbine runners.

6 Outlook

The data from the laboratory measurements and the field will be further evaluated. The combination of acoustic and optical methods and the use of existing ADM-devices will be pursued. After the first sediment season the data from the turbine inspections and turbine efficiency measurements will be evaluated.
In view of the damages observed on the turbine runners after the thunderstorm, the option of temporary turbine shutdowns for some hours during extreme sediment peaks shall be further investigated towards the determination of economically balanced switch-off criteria based on SSC and possibly particle size.

Acknowledgements

The authors gratefully acknowledge the support by *Swisselectric Research,* the Swiss Federal Office of Energy and Gommerkraftwerke AG (the case study power plant operator) and further thank to all project partners mentioned in the text.

References

[1] Bishwakarma M.B. & Støle H. (2008). Realtime sediment monitoring in hydro-power plants. *J. Hydr. Res.* 46(2): 282–288.
[2] Gummer J. H. (2009). Combating Silt Erosion in Hydraulic Turbines. *Hydro Review Wordwide*, 17(1).
[3] Boes R. (2009). Real-time monitoring of SSC and PSD in the headwater way of a high-head hydropower plant. *Proc. 33rd IAHR Congress*, Vancouver, Canada: 4037–4044.
[4] Agrawal Y., Mikkelsen O.A. & Pottsmith H.C. (2011). Sediment monitoring technology for turbine erosion and reservoir siltation applications. *Proc. HYDRO 2011 Conference*, Prague, Czech Republic.
[5] Costa I., Storti G., Lüscher B., Gruber P. & Staubli Th. (2010). Influence of solid particle parameters on the sound speed and attenuation of pulses in acoustic discharge measurements (ADM). *Journal of Hydrologic Engineering* (accepted for publication in October 2012).
[6] Abgottspon A. (2011): Messung abrasiver Partikel in Wasserkraftanlagen. *Masterthesis* (unpublished), Hochschule Luzern, CC Fluid Mechanics and Hydro Machines, Lucerne, Switzerland
[7] Andrews S. W., Nover D. M., Reuter J. E. & Schladow S. G. (2011). Limitations of laser diffraction for measuring fine particles in oligotropic systems: Pitfalls and potential solutions. *Water Resour. Res., 47*

Author(s)

David Felix graduated in Civil Engineering (M.Sc.) from the Federal Institute of Technology (ETH) in Zurich in 2005. He worked for five years with Pöyry Energy Ltd., Zurich, in the field of hydropower plant design and dam safety. Since 2010, he is a Ph.D.-student and teaching assistant at the Laboratory of Hydraulics, Hydrology and Glaciology (VAW) of ETH Zurich.
felix@vaw.baug.ethz.ch; phone +41 44 632 59 31, fax +41 44 632 11 92

Dr. Ismail Albayrak received his M.Sc. in Hydraulic Engineering from Istanbul Technical University in 2003 and obtained his Ph.D. in the field of environmental hydraulics at the Federal Institute of Technology in Lausanne (EPFL) in 2008. He worked for three years as a research fellow in the University of Aberdeen in the project of 'Biophysics of flow-plant interactions in aquatic systems'. Since 2011 he has been working as a scientist and research engineer at the Laboratory of Hydraulics, Hydrology and Glaciology (VAW) of ETH Zurich.
albayrak@vaw.baug.ethz.ch; phone +41 44 632 97 44, fax +41 44 632 11 92

André Abgottspon graduated in Mechanical Engineering (B.Sc.) from the Hochschule Luzern in 2005 and completed his Master's degree in Engineering (M.Sc.) in 2011. Since 2006 he works as a research assistant in the university's Competence Centre for Fluid Mechanics and Hydro Machines, e.g. in the fields of Pelton jet quality and thermodynamic efficiency measurements. In 2009 he co-founded etaeval GmbH, a company specialized in measurements and simulations at hydro power plants.
andre.abgottspon@hslu.ch; phone + 41 41 349 35 49, fax +41 41 349 39 60

Prof. Dr. Robert M. Boes graduated in 1996 in Civil Engineering from Technical University of Munich. In 2000 he completed his Ph.D. in the field of hydraulic structures at ETH Zurich. At TIWAG-Tiroler Wasserkraft AG, an Austrian utility, he was responsible for dam and hydropower as well as flood protection projects. Since 2009 he is Professor for hydraulic structures and Director of the Laboratory of Hydraulics, Hydrology and Glaciology (VAW) at ETH Zurich.
boes@vaw.baug.ethz.ch; phone +41 44 632 40 90, fax +41 44 632 11 92

Prof. Dr. Peter Gruber completed both his graduate and Ph.D. studies in Electrical Engineering at the Federal Institute of Technology (ETH) in Zurich. After 20 years of applied research work with Landis & Gyr and Siemens in the field of instrumentation, signal processing and control he was head of the development of ultrasonic flow meters with Rittmeyer, Baar, Switzerland from 2002 to 2007. Since 2007 he is professor at the Hochschule Luzern where he was already part-time lecturer for many years.
peter.gruber@hslu.ch; phone +41 41 349 32 53, fax +41 41 349 39 60

Schwebstoff-Monitoring und Verschleiss an Peltonturbinen (Teile a und b)

SI/500638-01 und -02

Beilagen zum Schlussbericht (2016)

Projektbezogene Publikationen aus dem Jahr

2013

Abgottspon A., Staubli T., Felix D., Albayrak I., Boes R.M. (2013a). **Hydro-abrasive Erosion of Pelton buckets and Suspended Sediment Monitoring**. *Proc. Hydrovision International 2013*, Denver, USA.

Abgottspon A., Stern P., Staubli T., Felix D., Winkler K. (2013b). **Measuring Turbine Abrasion and Efficiency Decrease: First Results of the Case Study at HPP Fieschertal**. **Proc. Hydro 2013 Conference**, Innsbruck, Österreich: paper no. 18.05.

Boes R. M., Felix D., Albayrak I. (2013). **Schwebstoffmonitoring zum verschleissoptimierten Betrieb von Hochdruck-Wasserkraftanlagen**. ***Wasser Energie Luft*** 105(1): 35-42; schriftliche Fassung zum Vortrag vom 08.11.2012 von Prof. Dr. R. Boes in Horw an der Fachtagung Wasserkraft des Schweizerischen Wasserwirtschaftsverbands (SWV).

Felix D., Albayrak I., Boes R.M (2013a). **Monitoring Suspended Sediment Concentration and Particle size using Optical and Acoustic Methods – Laboratory tests and Case study in the Swiss Alps**. ***Advances in River Sediment Research***, Fukuoka S., Nakagawa H., Sumi T., Zhang H. (eds), Taylor & Francis Group, London: 1757-1766

Felix D., Albayrak I., Boes R.M., Abgottspon A., Deschwanden F., Gruber P. (2013b). **Measuring Suspended Sediment: Results of the first Year of the Case Study at HPP Fieschertal in the Swiss Alps**. ***Proc. Hydro 2013 Conference***, Innsbruck, Österreich: paper no. 18.03.

Felix D., Albayrak I., Boes R.M. (2013c). **Laboratory Investigation on measuring Suspended Sediment by portable Laser Diffractometer (LISST) focusing on Particle Shape**. *Geo-marine Letters* 33(6): 485-498.

HYDRO-ABRASIVE EROSION OF PELTON BUCKETS AND SUSPENDED SEDIMENT MONITORING

André Abgottspon[1], Thomas Staubli[1], David Felix[2], Ismail Albayrak[2], Robert M. Boes[2]

[1] Hochschule Luzern, Competence Centre Fluid Mechanics and Hydro Machines, Technikumstrasse 21, 6048 Horw, SWITZERLAND

[2] Swiss Federal Institute of Technology (ETH) Zurich, Laboratory of Hydraulics, Hydrology and Glaciology (VAW), Gloriastrasse 37/39, 8092 Zurich, SWITZERLAND

ABSTRACT

Wear of turbine parts due to abrasive particles in the water of hydroelectric power plants (HPP) is of special importance for Pelton turbines where extreme redirection and deceleration of the flow occurs. In an on-going research project at HPP Fieschertal, Switzerland, wear on coated runner buckets is measured with a 3D optical scanner and a thickness gauge, turbine efficiency is periodically evaluated by "sliding needle" index tests and suspended sediment is monitored using various devices.

3D digitizations (measurements) of selected Pelton buckets allow quantifying material losses of the main splitter or of the cut-out section due to turbine operation during a sediment season. In the sediment season 2012 the splitter height decreased in the range of 3 to 5 mm, i.e. approximately 0.5 to 0.8 percent of the inner bucket width of 650 mm. The erosion on the splitter is influenced by the initial geometric condition of the splitter, the particle load and the operating hours.

The history of the index efficiency permits to identify relevant efficiency variations due to hydro-abrasive erosion or due to mechanical works on the turbine runner (e.g. grinding of the splitters). Measurements before and after mechanical works and during the sediment season (with no mechanical works) allow to separate both effects. For one runner the efficiency decrease was 0.9 percent for more than the half sediment season 2012.

Turbidimeters, an acoustic method and a laser diffractometer (LISST) were site-specifically calibrated based on automatically taken water samples. The measurements confirm that suspended sediment concentration (SSC) and particle size distribution (PSD) in turbine water may vary strongly in time. The LISST provides not only SSC but also PSD which is important in the context of hydro-abrasive erosion. All devices yielded similar SSC at low to moderate levels while the LISST measured SSC more accurately during periods of increased SSC with transport of coarser particles. Accepting a temporary bias, turbidimeters and the acoustic method can be used as pragmatic contributions to a real-time decision making system for the operation and maintenance of HPPs.

1. INTRODUCTION

The complications associated with wear due to abrasive particles in the water of hydropower plants (HPPs), so called hydro-abrasive wear or hydro-abrasive erosion, are not new, but the issue is increasingly emphasized because of the worldwide growing energy demand. Hydro-abrasive erosion has a detrimental effect on efficiency, leads to significant maintenance costs and may cause downtime of turbines with corresponding production losses.

To take adequate measures in design, operation and maintenance of HPPs, the knowledge on turbine wear needs to be improved and relevant parameters have to be quantified. The relevant parameters for hydro-abrasive erosion, such as suspended sediment concentration, size, hardness and shape of particles as well as relative velocity between the flow and turbine parts, turbine geometry and turbine material, have been identified (e.g. Gummer 2009, Winkler et al. 2011). But it is still not fully understood to which extent these parameters contribute to the dominant damages. Monitoring suspended sediment concentrations (SSC) and size distributions (PSD) throughout the year is still not common and the effect of hydro-abrasive erosion on efficiency is only qualitatively known.

In an interdisciplinary project initiated by VAW of ETH Zurich and Hochschule Luzern, the problem of hydro-abrasive erosion is investigated mainly by means of a case study at the existing HPP Fieschertal. The goal of the project is to contribute to a better understanding of interactions between suspended sediment load, turbine wear and efficiency as a basis for economic and environmental optimization (Fig. 1):

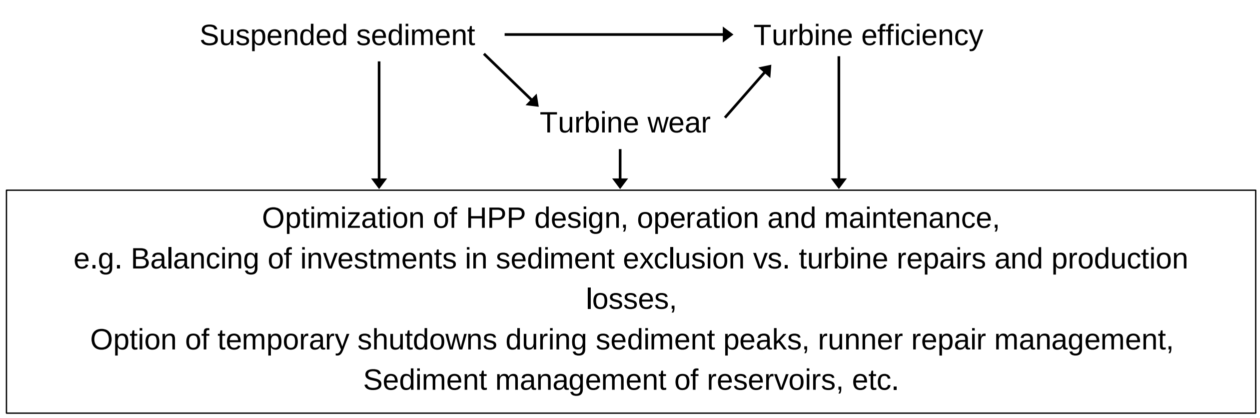

Fig. 1: Knowledge on turbine wear as a basis for optimization of HPPs

The HPP Fieschertal (Fig. 2) is a 509 m net head run-of-river type scheme located in the Canton of Valais in the Swiss Alps. Since the HPP was brought into service in 1976 severe hydro-abrasive erosion at needles, nozzles and runners of the two 32 MW Pelton units has been observed. Although coating of turbines and other hydraulics parts reduced the extent of the damages, sediment handling as well as optimized operation and maintenance of the HPP remain an important economic issue.

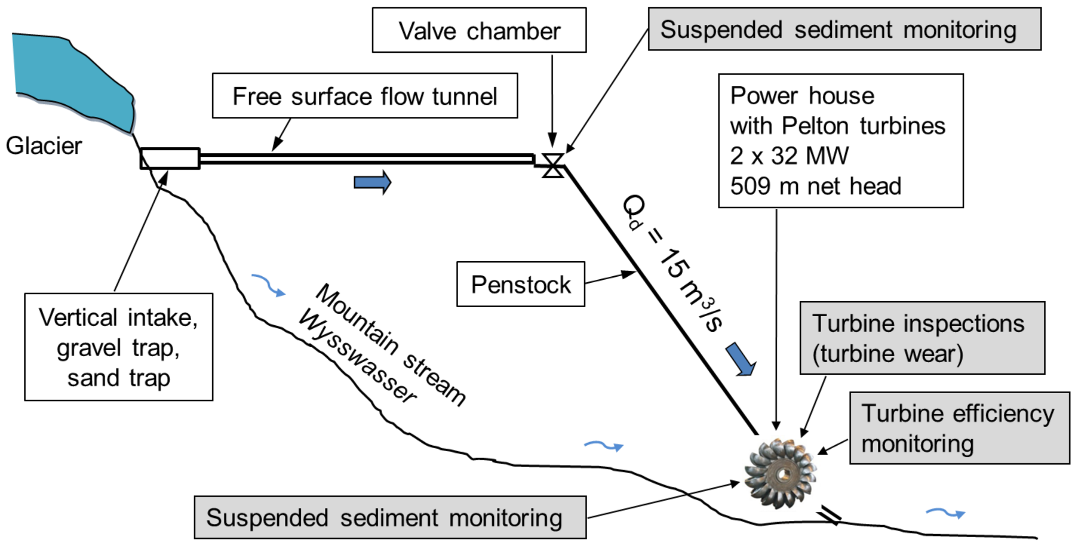

Fig. 2: Schematic overview of the HPP Fieschertal with the investigation program (grey).

This paper presents results from the on-going research project on turbine wear, efficiency and suspended sediment monitoring. Turbine inspections giving indications on turbine wear are documented with photographs, surface mapping using a 3D optical scanner and coating thickness measurements inside selected runner buckets before and after the sediment season. The evolution of turbine efficiency over time is measured by periodical efficiency index tests. Suspended sediment in the turbine water is monitored using various optical and acoustic devices, such as turbidimeters, a laser diffractometer and a method based on acoustic discharge measurement installation (see Felix et al. 2012). In the following sections, the measurement devices, the experimental procedure and the results are presented and discussed.

2. TURBINE WEAR MEASUREMENTS

2.1. 3D digitization

The geometries of selected buckets of Pelton runners were measured with a 3D optical scanning camera (Steinbichler Comet L3D) directly inside the turbine casing (Fig. 3). The working principle of the scanner is based on triangulation. It has a resolution of five megapixels in a measurement volume of 480 x 400 x 250 mm. The 3D point distance is 190 µm and the accuracy of the system is within 25 µm.

Since the surfaces of the buckets (stainless steel) are light reflecting a whitening spray has to be applied prior to the scanning. Furthermore, reference markers are used to improve the matching of point clouds and the measuring accuracy. One full day with a two-men team is required to digitize two buckets including calibration of the sensor before the digitizing.

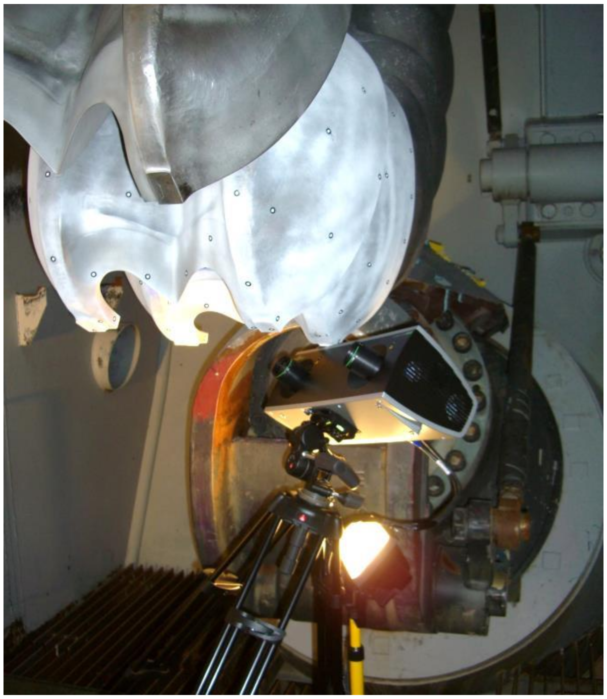

Fig. 3: 3D optical scanning camera used to digitize two selected buckets with reference points.

With regard to wear and efficiency of Pelton turbines the splitters and cut-outs of the buckets are of special importance. Brekke et al. (2002) formulated as a rule of thumb: When the thickness of the splitter has increased to 1 percent of the bucket width, the efficiency drops by 1 percent at full load. The maximum splitter width is practical to measure at turbine inspections. Boes (2009) related the evolution of splitter width with cumulated suspended sediment load.

In Figures 4 to 6, geometrical changes due to hydro-abrasive erosion at splitters and cut-outs, obtained from comparisons of digital geometric models taken before and after the sediment season, are shown.

At the beginning of the sediment season 2012 the runner installed in machine group 1 was fully reconditioned (welding, grinding and complete coating; with geometry close to planned geometry) whereas the runner in machine group 2 has been in use for several seasons after the last factory overhaul and was repaired on site (grinding and local re-coating).

The hydro-abrasive erosion at the splitter (analysed here as height differences along the splitter's longitudinal profile) for the bucket no. 1 of the runners of the machine group 1 and 2 is displayed in Fig. 4. During the sediment season 2012 the splitter height was reduced by about 3 mm after 3426 operating hours at machine group 1 and by 5 mm after 1430 operating hours at machine group 2. In summer 2012 a major flood event with SSC ranging up to approx. 50 g/l occurred when both turbines were running.

The erosion rates indicate that hydro-abrasive erosion does not mainly depend on operating hours but rather on suspended sediment transport events, e.g. during floods, and on the geometry of the splitters at the beginning of the sediment season (Fig. 5).

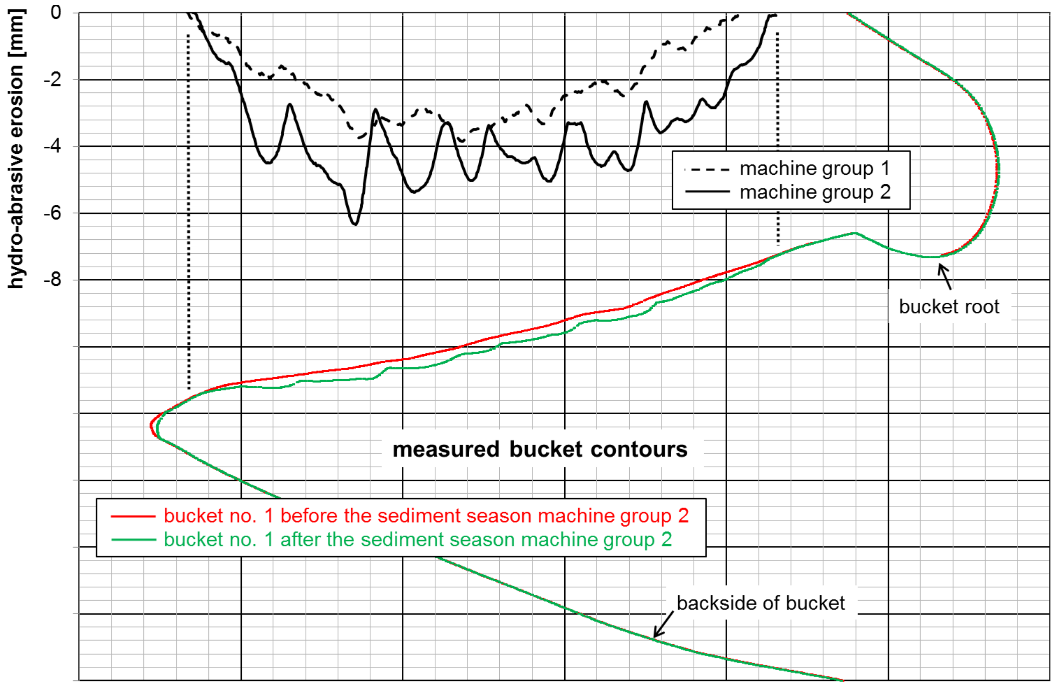

Fig. 4: Side view of the digitized main splitter: Comparison (black) between the splitter geometries of buckets no. 1 of the machine groups 1 and 2 before (red) and after (green) the sediment season.

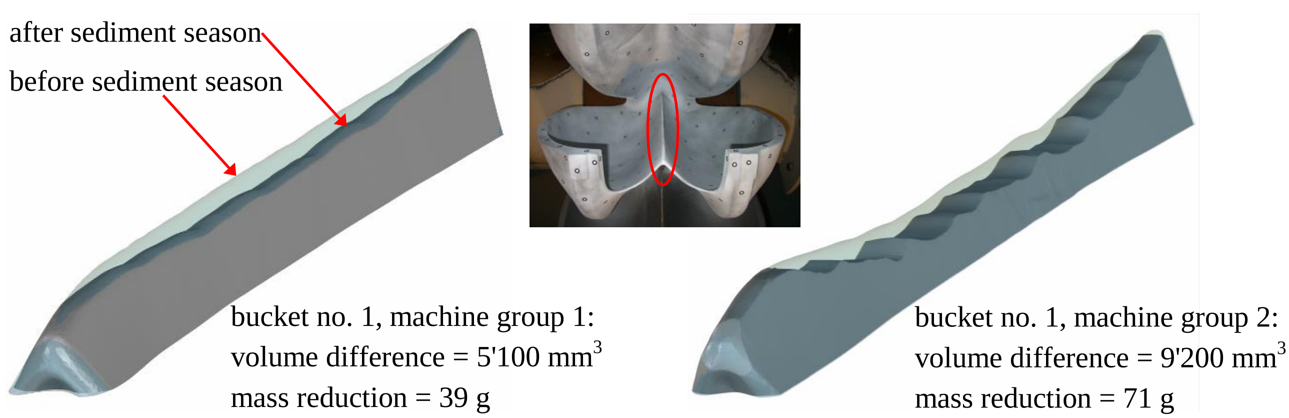

Fig. 5: 3D views of the digitized main splitters (red ellipse): Comparison between the splitter geometries before (transparent) and after the sediment season (grey) of buckets no. 1 of machine groups 1 and 2. The mass reduction is calculated with a density of 7.7 g/cm^3 for the base material.

Further damages occur at the cut-out section of the bucket. The digitized edges of the cut-outs of bucket no. 1 of machine group 1 before and after the sediment season are shown in the lower part of Fig. 6 (top view). The differences in geometry of the cut-outs before and after the sediment season are plotted in the upper part of Fig. 6 for both machine groups. The cut-outs were abraded by up to 9 mm towards the turbine axis at machine group 1 and by up to 6 mm at machine group 2. Interestingly, the erosion measured at the cut-outs exhibits an opposite behaviour compared to the erosion at the splitters.

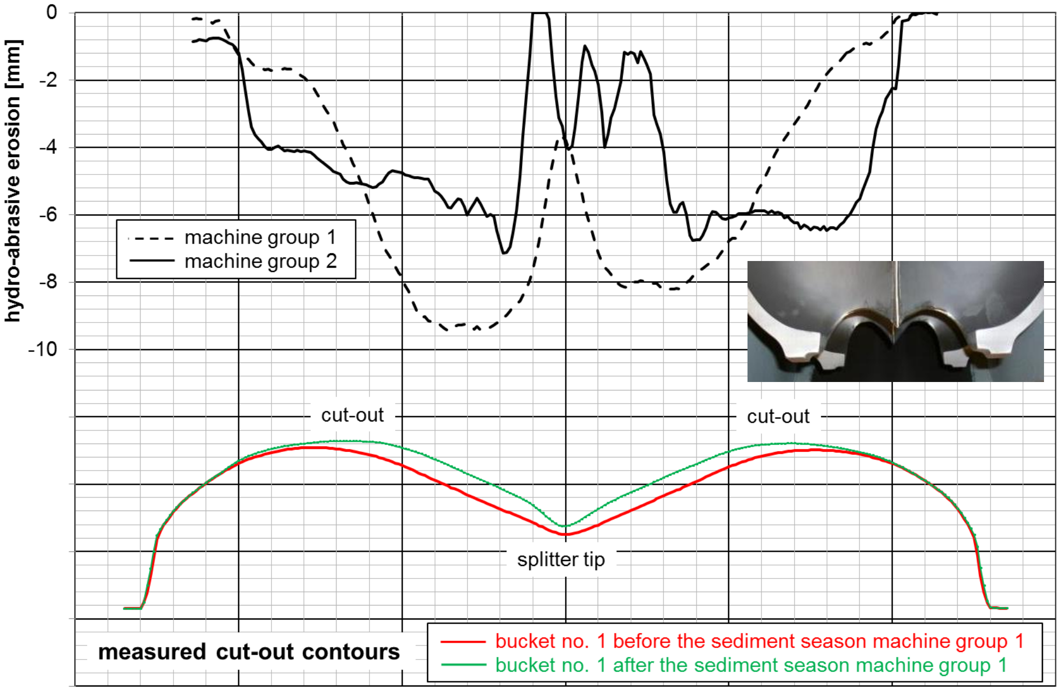

Fig. 6: Top view of the digitized cut-out (with the splitter tip in the centre): Comparison (black) of buckets no. 1 of machine groups 1 and 2 between the cut-out geometries before (red) and after (green) the sediment season.

2.2. Coating thickness measurements

To analyse turbine wear mechanisms and local damages in coated Pelton buckets as installed in the HPP Fieschertal, it is essential to quantify coating thicknesses. Since the coating material (approximate Mohs hardness 7.5) is much harder than the base material (approximate Mohs hardness 4.5) of the Pelton bucket, the erosion potential raises significantly when the coating material is removed locally. Reduced coating thicknesses can result from continuous silt and sand abrasion or from single grain or stone impacts, which may crack the coating surface.

In this on-going project the coating thickness distributions inside selected Pelton buckets before and after the sediment season are measured using a thickness gauge (Helmut Fischer Deltascope FMP30 with dual-tip probe) based on magnetic induction. First spatially distributed thickness measurements using a template that defines the measurement locations within the buckets were completed. An example of such a coating thickness distribution inside a bucket of the runner which has been fully reconditioned before the sediment season is shown in Fig. 7. The distribution was obtained from an interpolation between 153 measurement locations (black points in Fig. 7). At each location, ten repeated measurements were done to achieve a mean value with an expanded measurement uncertainty (at a confidence level of 95 percent) less than 3 percent (average over all measurement locations). As it can be seen from the colour bar, the coating thicknesses vary mainly between 200 and 400 µm with an approximate mean value of 300 µm.

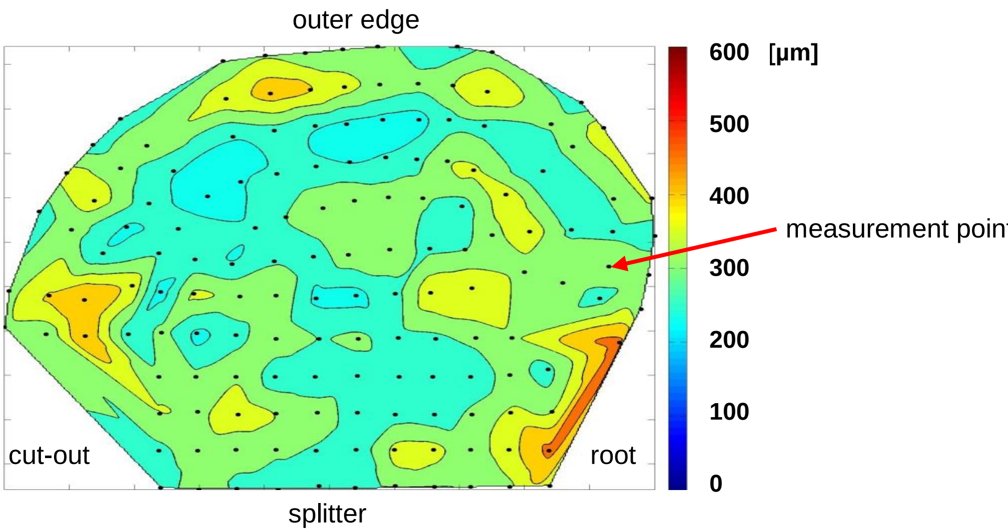

Fig. 7: Coating thickness distribution inside the left half of bucket no. 2 of machine group 1 after the sediment season.

3. EFFICIENCY MONITORING

Turbine wear leads to efficiency reduction. Only a few published data are available (e.g. Dahlhaug et al. 2010 or Bajracharya et al. 2008), describing quantitatively the efficiency decay in defined time intervals, correlated to different turbine damages. One main reason for this lack of published data is the effort associated with efficiency measurements with respect to direct costs and cost of eventual power losses during efficiency measurements.

With index efficiency measurements the efficiency changes between two tests can be determined, absolute efficiency data are not required. A periodical evaluation of the index efficiency allows thus to quantify the evolution in turbine efficiency. Classical index efficiency measurements encompass a series of measuring points (part load to full load) with constant operating conditions. Accordingly, such measurements are time-consuming. Almquist et al. (1995) introduced the so called "sliding gate method". In this method the guide vanes of a Kaplan turbine were continuously opened and closed while acquiring data for efficiency evaluation. This method can also be adapted to Pelton and Francis turbines, as discussed by Abgottspon and Staubli (2008). Necessary condition for good measurements is that they are performed under quasi-steady conditions. The closing and opening ramps must accordingly be slow enough to fulfil this condition. An example of such a "sliding needle" procedure in the HPP Fieschertal is shown in Fig. 8. The main advantages of this kind of index efficiency method are:

- feasible for Kaplan, Francis and Pelton turbines,
- reduced time required to perform efficiency tests, and
- continuous efficiency curves over the entire operating range, instead of discrete points.

A further advantage of such index tests is that in most cases the instrumentation of the HPP can be used or data can be extracted from the control system. To do so, an adequate data acquisition algorithm has to be implemented in the control system. At HPP Fieschertal three principal possibilities to calculate the index efficiency are available:

- acoustic discharge measurements at the upper and lower end of the pressure shaft,
- pressure difference measurements in a Venturi pipe section upstream of each machine group, and
- needle stroke measurements.

Redundantly performed measurements and evaluation allow cross-checks and contribute to an increase of the reliability of the evaluated differences in efficiency.

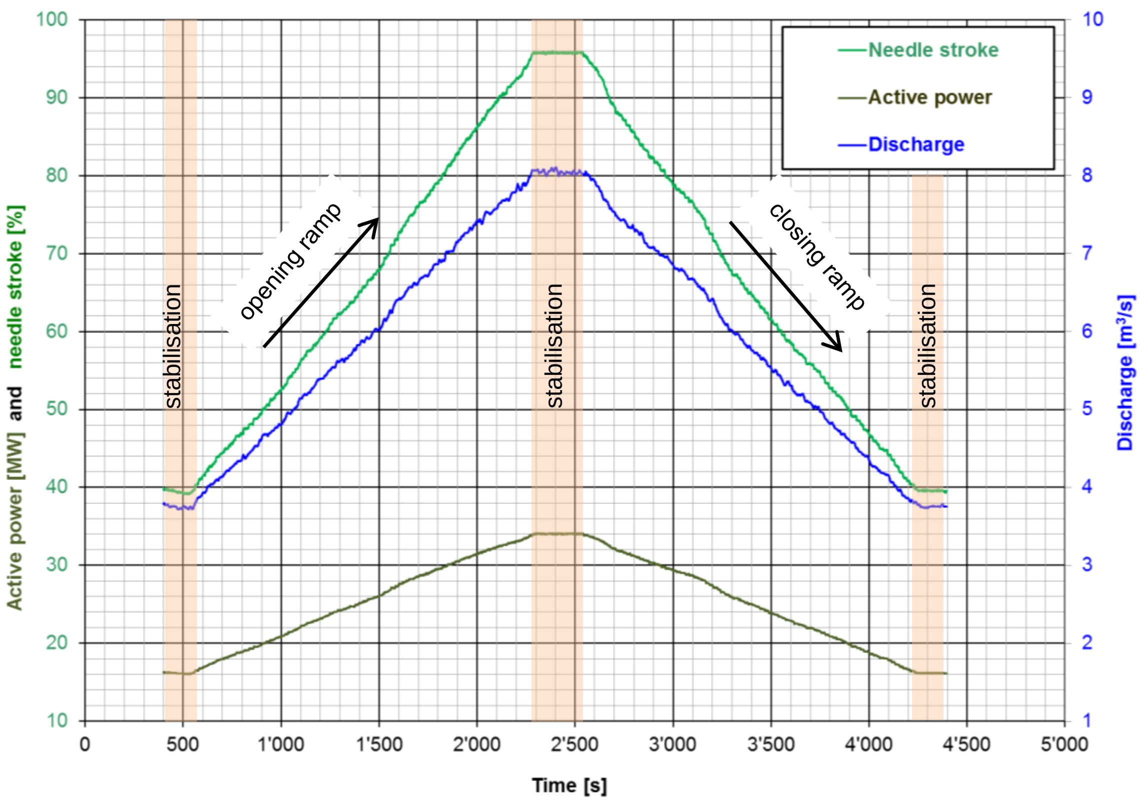

Fig. 8: Active power (dark green, lowest curve), needle stroke (green, highest curve) and discharge (blue, curve in the middle) variation during a sliding needle index efficiency measurement.

Fig. 9 shows the efficiency history of machine group 1, calculated twice (independently) based on the two available acoustic discharge measurements. The differences between the instruments indicate reproducibility within 0.2 percent.

Between the reference measurements of July 4, 2012 and the second measurements of Sept. 27, 2012 more than half of the sediment season passed. An index efficiency decrease of 0.9 percent is obtained. This decrease is attributed to hydro-abrasive erosion. On Nov. 5, 2012 none or only a minor rise in the index efficiency level is found compared to the previous measurement, i.e. the index efficiency level remained constant. This agrees with the suspended sediment load which is measured to be low during this period. In the period until the next measurement of March 8, 2013 very low suspended sediment concentrations were measured. The observed index efficiency level rise of up to 0.5 percent can be explained with maintenance works carried out at the main splitters of the Pelton buckets during winter.

In order to distinguish the effects of hydro-abrasive erosion or of maintenance works at relevant turbine parts on turbine efficiency, index tests are required as close as possible before and after such works.

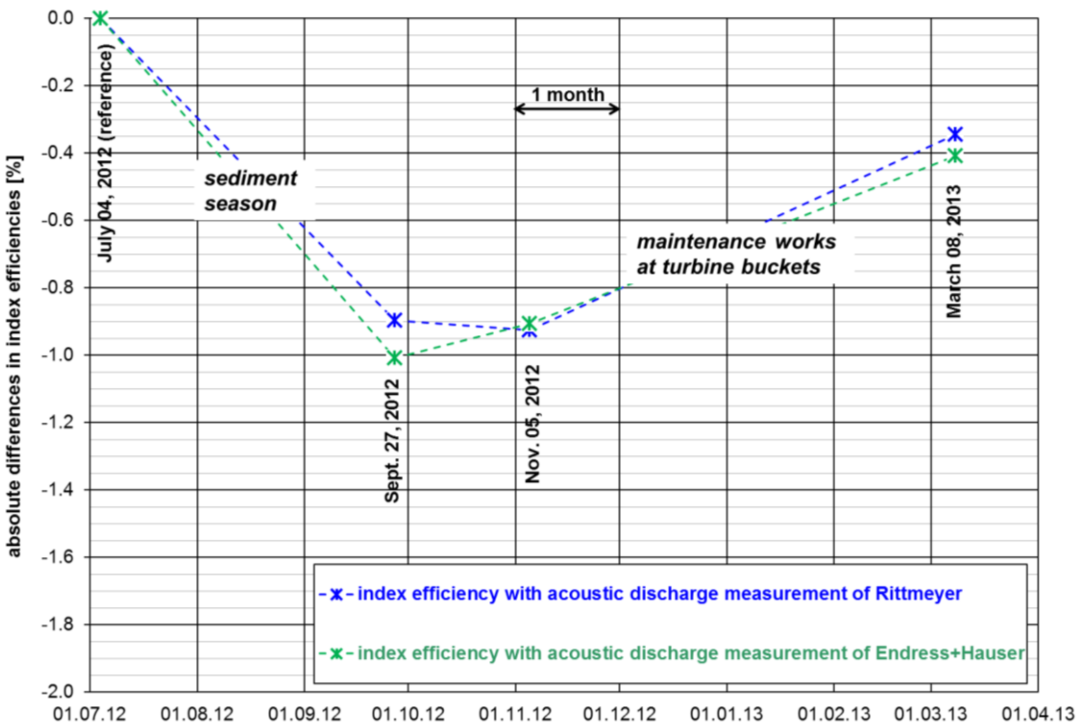

Fig. 9: History of the index efficiency for machine group 1: Absolute differences from weighted index efficiency levels with two different acoustic discharge measurement devices (blue: Rittmeyer crossed 4-path inside mount, green: Endress + Hauser 1-path clamp-on outside mount)

4. SUSPENDED SEDIMENT MONITORING

Among the available techniques for suspended sediment monitoring (SSM) turbidimeters are most popular, despite the fact that their calibration is strongly particle-size dependant and the calibration needs generally to be established by the user (Wren et al. 2000). Various kinds of turbidimeters (measuring optical transmission or scattering) have been used in the present study. An acoustic method for SSM based on installations for acoustic discharge measurement (ADM) is also applied (single frequency attenuation, see also Costa et al. 2012). Furthermore, a portable laser diffractometer (LISST) is used (Agrawal and Pottsmith 2000). The latter yields not only estimates of SSC, but also of PSD. Particle size is an important parameter in the context of turbine wear.

The devices for SSM used in this study are summarized in Table 1. In a first phase of the project, these devices were tested in the mixing tank in the hydraulic laboratory at Hochschule Luzern, Competence Centre for Fluid Mechanics and Hydro Machines. In summer 2012 they were installed at the study HPP (locations see Tab. 1 and Fig. 2). Most devices are installed in the valve chamber, at the inlet to the penstock. Further information on these devices, the laboratory tests as well as the installation at the study HPP and previous results are described by Felix et al. (2012) and Abgottspon (2011).

In addition to the devices for continuous real-time SSM, an automatic water sampler was installed in the valve chamber and the obtained samples are analysed in the laboratory as a reference for the other devices. Reference SSCs are determined by weighing of the solid residues (primary method). The sampler is programmed to take one sample every 2 days and is additionally triggered by the signal of a turbidimeter to increase the sampling rate during relatively high SSC.

<table>
<tr><th>Device type</th><th>Device model and manufacturer</th><th>Device output and measuring principle</th><th>Derived parameters</th><th>Installed in HPP Fieschertal at</th></tr>
<tr><td rowspan="2">Turbidimeter, submerged</td><td>Turbimax W CUS41
Endress-Hauser</td><td>Turbidity [FNU]
from backscatter</td><td>SSC</td><td>Intake
(starting 2013)</td></tr>
<tr><td>Solitax ts-line sc
Hach-Lange</td><td>Turbidity [FNU]
from backscatter</td><td>SSC</td><td>Tailrace channels of each unit</td></tr>
<tr><td rowspan="2">Turbidimeter, in-line</td><td>TurbiScat (90°, 25°)
Sigrist Photometer</td><td>Turbidity [FNU]
from backscatter</td><td>SSC</td><td rowspan="4">Valve chamber, at the inlet to the penstock</td></tr>
<tr><td>TF16-N with F20
Optek Danulat</td><td>Turbidity [CU]
from transmission</td><td>SSC</td></tr>
<tr><td>Acoustic method</td><td>Risonic Modular
Rittmeyer</td><td>Received amplitude [V]
forward scattering</td><td>SSC</td></tr>
<tr><td>Portable laser diffractometer</td><td>LISST-100X, Type C
Sequoia Scientific</td><td>Volume concentrations in 32 size classes [ppm]</td><td>SSC and PSD</td></tr>
</table>

Table 1: Devices used for continuous suspended sediment monitoring.

The time series of SSC in the turbine water obtained from the devices installed in the valve chamber are shown in Fig. 10 for the period from July 2012 to the end of the sediment transport season. The conversion (calibration) from original units of the devices (e.g. FNU) to SSC is based on the reference SSCs collected so far at the study site.

The time series of the in-line turbidimeter (optical backscatter and optical transmission) models used here show considerable drift. Their signals are increasingly biased by particles that accumulated on the optics in the flow-through cells and by bio-fouling. Flushing of the flow cells by increasing the discharge of the sampling line for some minutes was not sufficient to clean the optics. Only manual cleaning (at day 303) brought the signals back to the low level expected for the relatively clear water in late autumn. In the sediment season 2013 another turbidimeter model, measuring the turbidity at a free falling jet (*AquaScat* from Sigrist Photometer), will be installed at the sampling line in order to avoid signal drift and frequent manual cleaning. At the two turbidimeters installed at the tailrace channels no problem of signal drift occurred since those submerged turbidimeters are equipped with a wiper that keeps their optics clean.

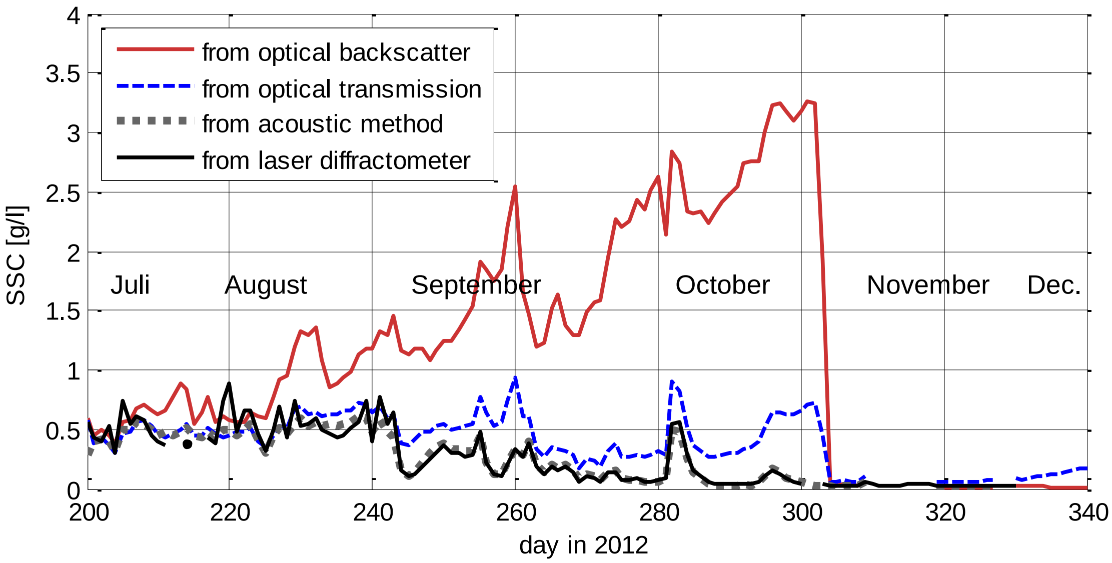

Fig. 10: Time series of daily averaged SSC in the turbine water, obtained from various devices installed in the valve chamber, from July, 19 (day 200) to December, 6 (day 340) in year 2012.

Figure 11 shows a close caption of Figure 10 as an example of suspended sediment transport during three summer days. In addition, three of the reference SSCs from laboratory analysis of bottled samples and the time series of the median size of the particles in the turbine water (d_{50}, i.e. the median diameter by mass) obtained from the LISST (right axis) are also shown in Fig. 11. Data were recorded every second for turbidimeters and the acoustic method and every minute for the LISST. The time series were smoothed by moving average over 20 minutes and implausible data were discarded. Trends and offsets visible in Fig. 10 were removed from the turbidimeter data.

During summer days SSC was approx. 0.5 g/l and the time series from all devices (turbidmeters, laser diffractometer and acoustics) show similar behaviour, except for a sediment transport peak in the early morning hours of day 239. During this event the LISST yields a higher SSC compared to the other continuous measuring methods. The LISST measurement is supported by the reference measurement taken during the rising limb of the SSC peak. From Figure 11 it can be seen that the median size of the particles in the turbine water is approximately 15 microns, except for the phase of increased sediment transport. During this phase, about three times coarser particles (d_{50} approximately 45 microns for some hours) were transported. The maximum of d_{50} occurred approximately one hour after the maximum in SSC.

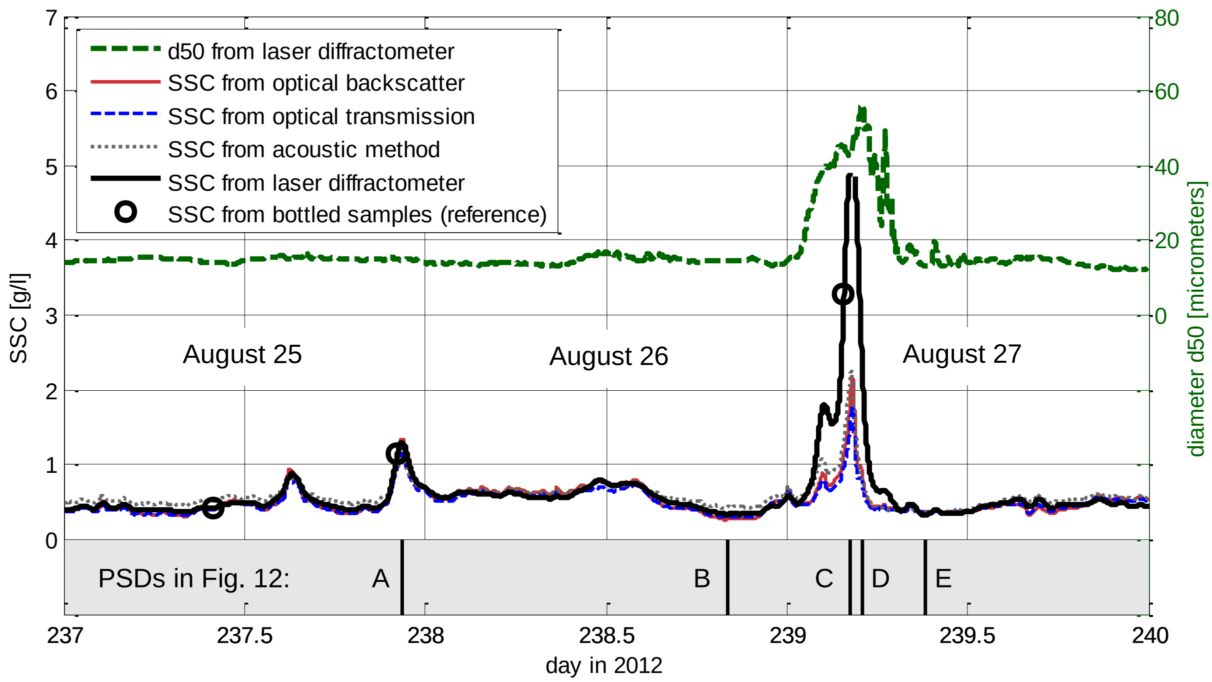

Fig. 11: Time series of SSC in the turbine water, from devices as in Figure 10, reference SSCs from bottled samples, and time series of d_{50} obtained from LISST; example of three summer days (August 25 to 27, 2012).

In Figure 12 selected PSDs obtained from the LISST are displayed. The times at which these PSDs were measured are indicated in Fig. 11 with capital letters. The PSDs measured before (B) and after (E) the SSC peak as well as during a minor SSC peak (A) are similar. The PSDs recorded at maximum SSC (C) and at maximum d_{50} (D) are considerably coarser.

The underestimation of SSC by the turbidimeters and the acoustic method (single frequency forward scattering) in times with transport of coarser particles is related to their physical operating principle. Coarser particles do not cause as much turbidity or scattering as finer ones (at same SSC). The calibration of those devices depends strongly on particle size, for which in practice a constant time-averaged value has to be adopted. As it can be seen from Figures 10 and 11, the deviation in SSC estimates of those devices with respect to SSC from the LISST and reference SSCs may be significant during phases of increased suspended sediment transport. In the rest of the time, however, those devices provide quite accurate SSC estimates.

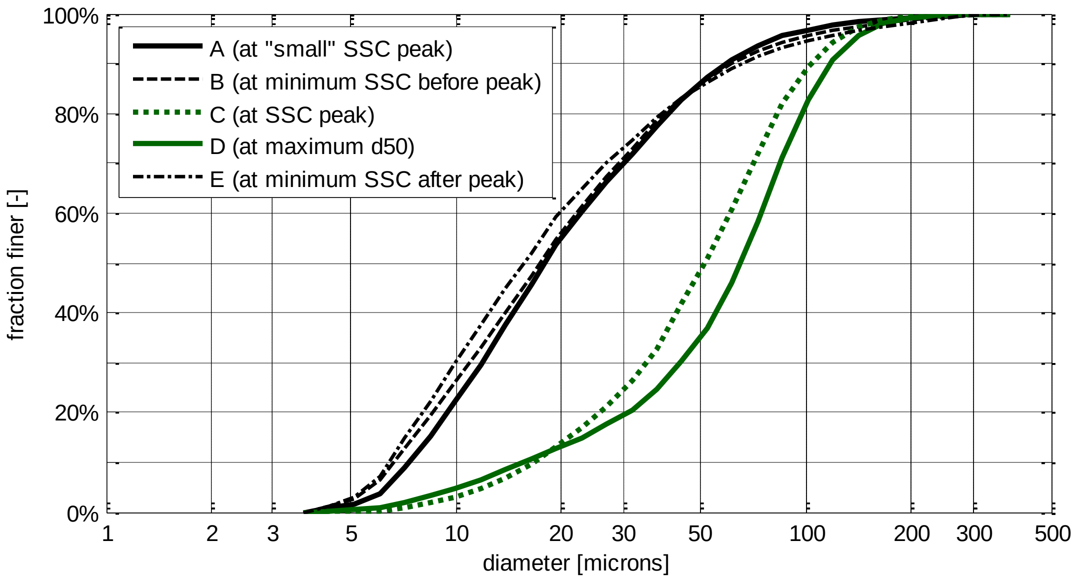

Fig. 12: Selected PSDs obtained from LISST, measured in the turbine water at times indicated in Fig. 11.

5. CONCLUSIONS

First analyses of the hydro-abrasive erosion rates for both machine groups in the HPP Fieschertal, Switzerland, showed that single events such as heavy rains lead to major material loss at Pelton buckets. Therefore, temporary shutdowns of the HPP would help to prevent excessive hydro-abrasive erosion during such events. To do so, a reliable method for continuous real-time measurement of suspended sediment load is needed.

Using several devices for SSM based on different physical principles allows for a cross-comparison of their measuring capabilities under field conditions and leads to higher reliability. The combination of devices for continuous SSM with an automatic water sampler allows calibrating the devices based on the site-specific conditions, e.g. with respect to typically prevailing particle sizes and mineralogical composition (particle shape, optical properties). The calibration of the devices will be improved based on the increasing data set of reference SSC from the study site.

Since frequent manual cleaning of measuring devices is not practical, turbidimeters with an automatic cleaning system (wiper or pressurized air) or turbidimeters with optics not in contact with the sediment-laden flow (free falling jet type) are recommended, even in cold and relatively nutrient-poor water of mountain streams. The acoustic method based on ADM installations existing in many HPPs offers the advantage of monitoring suspended sediment directly in the penstock. Among the devices used here, LISST offers new possibilities for SSM, since it provides not only information on SSC, but also on PSD. In environments with variable particle sizes LISST measures SSC more accurately than devices with a fixed calibration depending on particle size. For a better understanding of hydro-abrasive erosion, measuring PSD is important since coarser particles have higher abrasion potential (for a given SSC) and are therefore particularly harmful to turbines. Devices with particle size-dependant calibration may be used as pragmatic contributions to a real-time decision making system for the operation and maintenance of HPPs, especially for smaller schemes.

In summer 2012 SSC of approximately 0.5 g/l with d_{50} of normally 15 microns was observed in the turbine water of HPP Fieschertal. The measurements confirmed that SSC and PSD may vary strongly within short time, e.g. due to precipitation events, to SSC of up to approximately 50 g/l and d_{50} of e.g. 45 microns.

Wear at coated Pelton runner buckets was measured with a 3D optical scanner and a thickness gauge. Digital models of selected Pelton buckets allowed quantifying material losses at the main splitter and at the cut-outs due to turbine operation over a sediment season. The analysis showed that the splitter height decreased 3 to 5 mm during the sediment season 2012, this corresponds to approximately 0.5 to 0.8 percent of the inner bucket width of 650 mm. The hydro-abrasive erosion at the splitter is influenced by the splitter geometry at the beginning of the sediment season, particle load and the operating hours. Local coating thicknesses in the bucket of a Pelton runner were measured with a thickness gauge based on magnetic induction.

Turbine efficiency was periodically evaluated by "sliding needle" index measurements. The history of the index efficiency permits to identify relevant efficiency variations due to hydro-abrasive erosion. For one of the investigated turbines the efficiency decrease was 0.9 percent for half of the sediment season 2012. In order to distinguish the effects of hydro-abrasive erosion and the effects of maintenance works at relevant turbine parts (e.g. grinding of the splitter) on turbine efficiency, index tests should be performed before and after such works. Redundantly performed index measurements and evaluation allows cross-checking and increasing the reliability of the evaluated differences in efficiency.

ACKNOWLEDGEMENTS

The authors gratefully acknowledge the financial support by *swisselectric research*, the Swiss Federal Office of Energy and Gommerkraftwerke AG (HPP Fieschertal) and measuring equipment support by Rittmeyer and Sigrist Photometer. Further thanks go to the members of the project team, including collaborators from Hochschule Luzern and HPP Fieschertal, U. Aebi (BKW FMB Energy) and Dr. K. Winkler (Andritz Hydro).

REFERENCES

Abgottspon A. (2011). Messung abrasiver Partikel in Wasserkraftanlagen. *Master Thesis* (un-published, in German), Hochschule Luzern, CC Fluid Mechanics and Hydro Machines, Lucerne, Switzerland.

Abgottspon A., Staubli T. (2008). Index Tests of a Francis Unit using the Sliding Gate Method. *Proc.* 7th Intl. conference on Hydraulic Efficiency Measurements, IGHEM, Milan, Italy.

Agrawal Y.C., Pottsmith H.C. (2000): Instruments for particles size and settling velocity observations in sediment transport, *Mar. Geol.* 168:89-114.

Almquist C. W., March P. A., Pearson H. S., Fransen H. W., Whitehead B. H. (1995). The Sliding Gate Method for Hydroturbine Efficiency Testing. *Proc.* WaterPower '95, American Society of Civil Engineers, New York, 793-801.

Bajracharya T. R., Acharya B., Joshi C. B., Saini R. P., Dahlhaug O. G. (2008). Sand erosion of Pelton turbine nozzles and buckets: A case study of Chilime hydropower plant. *Wear* 264(3-4):177-184.

Boes R. (2009). Real-time monitoring of SSC and PSD in the headwater way of a high-head hydropower plant. *Proc.* 33rd IAHR Concress, Vancouver, Canada, 4037-4044.

Brekke H., Wu Y. L., Cai B. Y. (2002). Design of hydraulic machinery working in sand laden water, in *Abrasive Erosion & Corrosion of Hydraulic Machinery*, Book series on Hydraulic machinery, Vol. 2, edited by Duan C. G. and Karelin V. Y., ISBN 1-86094-335-7, Imperial College Press, London, 155-233.

Costa L.I., Storti G., Lüscher B., Gruber P., Staubli T. (2012): Influence of solid particle parameters on the sound speed and attenuation of pulses in ADM, *J. of Hydrologic Eng.*, 17(10):1084-1092.

Dahlhaug O. G., Skåre P. E., Mossing V., Gutierrez A. (2010). Erosion resistant coatings for Francis runners and guidevanes, *Intl. J. on Hydropower & Dams*, 17(2):109-112.

Felix D., Albayrak I., Abgottspon A., Boes R., Gruber P. (2012). Suspended Sediment and Pelton Turbine Wear Monitoring: Experimental Investigation of various Optical and Acoustic Devices and Beginning of the Case Study at HPP Fieschertal. *Proc.* 17th Intl. Seminar on Hydropower Plants (*Viennahydro*), Vienna, 483-494.

Gummer J. H. (2009): Combating Silt Erosion in Hydraulic Turbines. *Hydro Review Worldwide*, 17(1).

Winkler K., Dekumbis R., Rentschler M., Parkinson E. & Garcin H. (2011): Understanding hydro-abrasive erosion, *Proc.* Hydro 2011, Aqua-Media International Ltd., Prague, Czech Republic.

Wren D., Barkdoll B., Kuhnle R., & Derrow R. (2000): Field Techniques for Suspended Sediment Measurement. *J. of Hydraulic Eng.*, 126(2):97-104.

AUTHORS

André Abgottspon graduated in Mechanical Engineering (M.Sc.) from the Hochschule Luzern (HSLU) in Horw, Switzerland. Since 2006 he works as a research assistant at the Competence Centre Fluid Mechanis and Hydro Machines of HSLU in the fields of hydropower plant efficiency measurements, Pelton jet quality and hydro-abrasive erosion. In 2009 he co-founded etaeval GmbH, a company specialized in measurements and simulations on hydropower plants.
andre.abgottspon@hslu.ch

Thomas Staubli graduated in Mechanical Engineering from the Swiss Federal Institute of Technology (ETH) in Zurich. After two years of post-doctoral research in the field of flow induced vibration at Lehigh University, Pennsylvania, he worked in experimental fluid mechanics at Sulzer Hydro (now Andritz Hydro) in Zurich. He then headed the Hydromachinery Laboratory at ETH Zurich. Since 1996 he is Professor in Fluid Mechanics and Hydro Machines at Hochschule Luzern. In 2009 he co-founded etaeval GmbH. thomas.staubli@hslu.ch

David Felix graduated in Civil Engineering (M.Sc.) from the Federal Institute of Technology (ETH) in Zurich in 2005. He worked for five years with Pöyry Energy Ltd., Zurich, in the field of hydropower plant design and dam safety. Since 2010, he is a Ph.D. student (ongoing thesis on suspended sediment and turbine wear) and teaching assistant at the Laboratory of Hydraulics, Hydrology and Glaciology (VAW) of ETH Zurich. felix@vaw.baug.ethz.ch

Dr. Ismail Albayrak received his M.Sc. in Hydraulic Engineering from Istanbul Technical University in 2003 and obtained a Ph.D. in the field of environmental hydraulics at the Federal Institute of Technology in Lausanne (EPFL), Switzerland, in 2008. He worked for three years in a project on flow-plant interactions at the University of Aberdeen. Since 2011 he has been working as a research scientist at VAW of ETH Zurich. albayrak@vaw.baug.ethz.ch

Prof. Dr. Robert M. Boes graduated in 1996 in Civil Engineering from the Technical University of Munich. In 2000 he completed a Ph.D. in the field of hydraulic structures at ETH Zurich. At TIWAG-Tiroler Wasser¬kraft AG, an Austrian utility, he was responsible for dam and hydro-power as well as flood protection projects from 2002 to 2009. He then became a Professor for Hydraulic Structures and Director of VAW at ETH Zurich. boes@vaw.baug.ethz.ch

Measuring turbine abrasion and efficiency decrease: First results of the case study at the Fieschertal project

A. Abgottspon, P. Stern and T. Staubli
Hochschule Luzern (HSLU)
Engineering and Architecture,
Competence Centre Fluid
Mechanics and Hydro Machines
Technikumstrasse 21
6048 Horw (Lucerne)
Switzerland

D. Felix
Swiss Federal Institute of
Technology (ETH)
Laboratory of Hydraulics,
Hydrology and Glaciology (VAW)
Wolfgang-Pauli-Str. 27
8093 Zurich
Switzerland

K. Winkler
Andritz Hydro AG
Center of Competence
Coating
Obernauerstrasse 4
6010 Kriens (Lucerne)
Switzerland

Besides siltation of reservoirs, wear on turbines of hydroelectric power plants (HPP) is an economically important issue related to sediment-laden natural waters. Hydro-abrasive erosion on turbines that is caused by suspended sediment may lead to considerable maintenance and repair costs as well as significant generation losses due to reduced turbine efficiency or downtimes.

For Pelton turbines, the efficiency decrease caused by hydro-abrasive erosion is mainly due to geometrical changes in the bucket profile. These geometrical changes can be local or extensive area damages due to abrasion or secondary cavitation. The location of such damages is influenced by the local flow field, which itself is affected by progressive wear. 3D digitizations (measurements) of selected Pelton buckets allow quantifying material losses at relevant parts like the main splitter and the cut-out section. The paper shows different possibilities to quantify such material losses, e.g. reduction of height, increase of width and volume differences at the main splitter, and geometrical changes at the cut-outs. Erosion rates determined over one sediment season at the HPP Fieschertal lie in the range of 4 to 5 mm for the main splitter height, 2 to 3 mm for the main splitter width and 7 to 9 mm for the cut-out section. The erosion is influenced by the initial geometry of the Pelton bucket and the sediment load (particle concentration, size distribution, mineral composition and particle shape) during the operating hours.

Changes in efficiency were evaluated based on periodical measurements with the sliding needle index measurement method. A decrease in efficiency of 0.9 percent for a little more than half of the sediment season 2012 was observed at one runner. Due to maintenance works on that runner during the winter the efficiency increased by 0.5 percent. The index efficiency was evaluated based on each of the different discharge measurement instruments installed at HPP Fieschertal. The results with acoustic discharge measurement indicate the best reproducibility being within 0.2 percent.

This paper focuses on wear at Pelton buckets and associated turbine efficiency decrease, whereas the corresponding paper by Felix et al. (2013) treats measurements of suspended sediment at the same HPP.

1 Introduction

Hydro-abrasive erosion has a detrimental effect on efficiency, leads to significant maintenance costs and may cause downtime of turbines with corresponding production losses. To take adequate measures in design, operation and maintenance of HPPs, the knowledge on turbine wear needs to be improved and relevant parameters have to be quantified. Few quantitative studies on the interrelations of suspended sediment, turbine wear and efficiency are available, especially for Pelton turbines. Laboratory tests of hydro-abrasive erosion on turbine parts (Winkler et al. 2011) contribute to a better understanding, e.g. of the influence of particle size. Complementary to this, measurements at full scale conditions are required.

For this reason, an interdisciplinary project by VAW of ETH Zurich and Hochschule Luzern was initiated in order to investigate hydro-abrasive erosion by means of a case study at the HPP Fieschertal. The HPP Fieschertal (Fig. 1) is a 509 m net head run-of-river type scheme located in the Canton of Valais in the Swiss Alps. From the time of first operation in 1976 till today severe hydro-abrasive erosion at needles, nozzles and runners of the two 32 MW Pelton units occurred. In the past decades an increase of fine sediments has been observed due to glacier retreat and increased variation in precipitation. Although coating of turbine parts increases the time between overhauls, sediment handling as well as optimized operation and maintenance of the HPP have remained important economic issues. One operational option studied in this project is to switch-off the turbines during suspended sediment peaks in case the costs caused by turbine wear exceed the benefits from power sales.

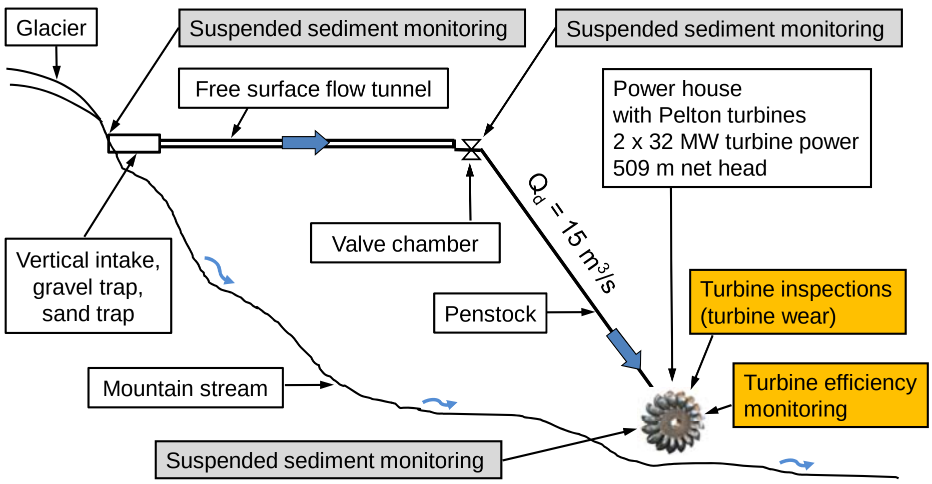

Fig. 1: Schematic longitudinal profile of the case study HPP Fieschertal.

In this paper, wear at buckets of Pelton turbines measured over the sediment season 2012 at this HPP and efficiency decreases measured until early summer 2013 are presented (components of the study highlighted in Fig. 1). The corresponding paper by Felix et al. (2013) describes methods and selected results of suspended sediment measurements at this HPP in the same period.

2 Turbine wear determination

2.1 Analysis method

Turbine wear was determined by comparing geometries of Pelton buckets measured before and after a period during which the turbines were operated with sediment-laden water. Geometrical models of Pelton buckets were determined using an optical digitizing system. The used system has a resolution of five megapixels in a measurement volume of 480 x 400 x 250 mm. The 3D point distance is 190 μm and the accuracy of the system is within 25 μm. Digitizing two buckets of an installed runner (in the turbine casing) requires one full working day of a two men team. Prior to digitizing, the system was calibrated to the prevailing temperature.
As the main splitter and the cut-outs of Pelton buckets are known to be relevant for turbine wear and performance, the focus of the analysis of turbine wear is set to these parts.

2.2 Definitions

2.2.1 Local coordinate system in the Pelton bucket

In order to compare the geometries of Pelton buckets measured in a series of turbine inspections, a consistent and reproducible geometrical reference has to be used for the positioning of the digital geometric models (3D point clouds) of the buckets. The surfaces A, B1, B2 and the outer radius ra in Fig. 2 are normally not affected by abrasion or by maintenance works at the runners. Based on these surfaces, a local Cartesian coordinate system was defined in the bucket. The coordinate system is placed using surface A as xy-plane. Surface B, which is the mid-plane of B1 and B2, sets the origin of the x-coordinate. The origin of the y-coordinate is set to the intersection of plane B with the outer radius ra (plane C).

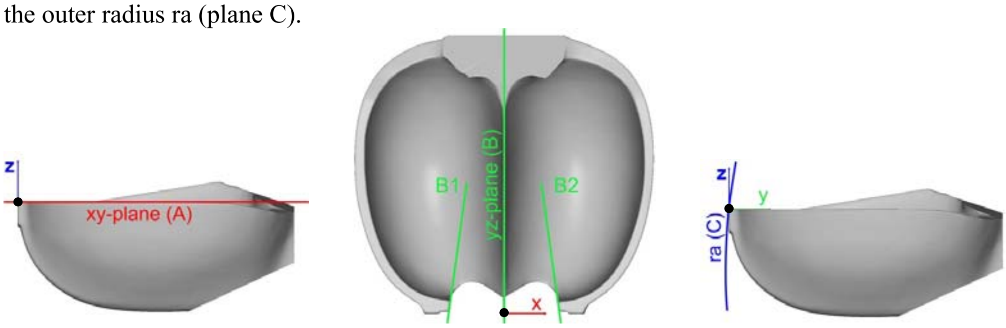

Fig. 2: Digitized Pelton buckets and definition of the coordinate system.

2.2.2 Main splitter height reduction *h*

One way to analyse the abrasion at the main splitter is to evaluate its height. The measured splitter profile was compared to a straight reference top line of the splitter (red line in Fig. 3). The angle and position of the reference splitter top line can be taken from construction drawings of the runner or from a measurement at a new runner. The distance from the actual splitter profile perpendicular to the reference splitter top line is defined as *h* (Fig. 3). Eroded splitter height *h* is evaluated along the splitter, not including the region of the splitter tip and the area of the transition to the bucket root. The boundaries, between the eroded splitter height was evaluated, are shown in Figure 3 and were used in all analysis related to the main splitter.

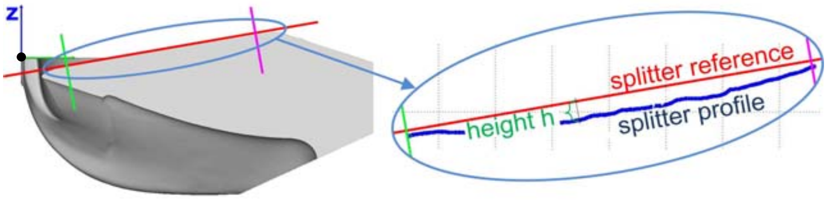

Fig. 3: Definition of eroded splitter height of a Pelton bucket.

2.2.3 Main splitter width *w*

Another way to monitor turbine wear is measuring the width of the main splitter. An increase of splitter width is known to be associated with efficiency decrease (e.g. Brekke et al. 2002). Boes (2009) considered the width of the main splitter as a key parameter describing hydro-abrasive erosion at a Pelton runner. If a coated splitter is eroded the splitter width is clearly visible because of its flat top surface and with sharp edges to the flanks of the splitter. In case of a splitter top with rounded cross section, however, the definition of splitter width is not obvious, also because the gradients of the splitter flanks vary along the splitter length.

Therefore, the splitter width was determined in cross sections of the splitter (normal to the y-axis). Figure 4 shows two examples of such cross sections in the region of the top of the splitter, one before and one after the sediment season. The dots represent the splitter geometries; the lines indicate the respective gradients from point to point. The splitter width *w* was defined as the distance (in x-direction) between points on both flanks of the splitter where the slope is 2:1 (z:x), see Figure 4. The plotted gradients were set to zero if the gradient was steeper than this limit.

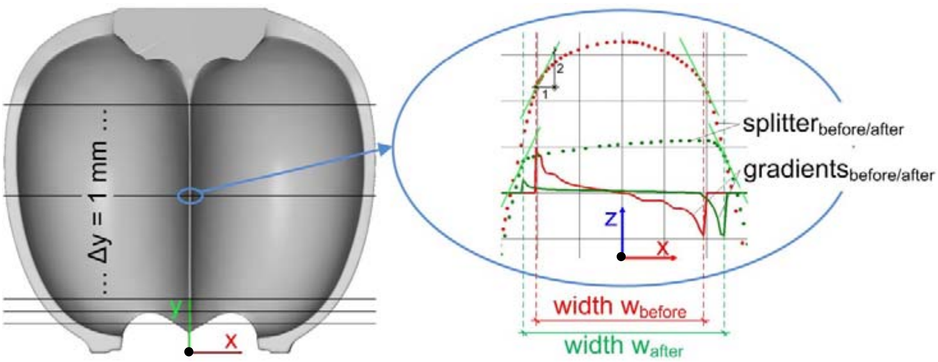

Fig. 4: Definition of the main splitter width of a Pelton bucket.

2.2.4 Cut-out depth *d*

The hydro-abrasive erosion at the cut-out section is determined as difference in the cut-out depths measured at various times. The cut-out depth *d* is measured in top view of a bucket from the outer radius of the runner (origin of local coordinate system) to the cut-out contour projected into the xy-plane (Fig. 5). Cut-out depth was evaluated in cutting planes normal to the x-axis at increments of 1 mm. Extracting the smallest y-values with their corresponding x-value yields the cut-out depths from left to right. This method is simple and easily reproducible. To calculate the differences in cut-out depths no interpolation is needed thanks to using the same locations of the cross sections.

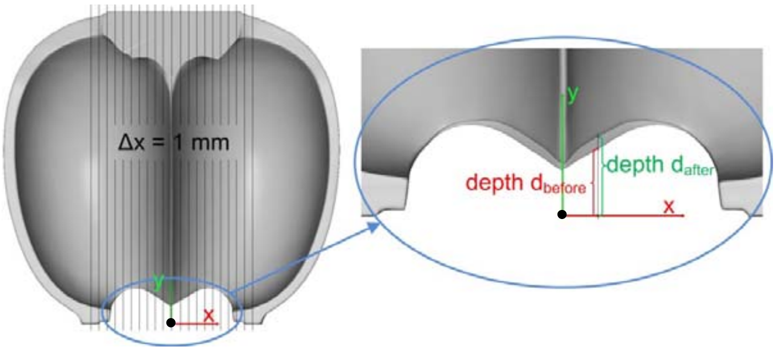

Fig. 5: Definition of the cut-out depth at a Pelton bucket.

2.3 Inspection dates and description of runner conditions

In the HPP Fieschertal two machine groups (1 and 2) with one Pelton runner each are installed. Turbine wear was determined at two buckets of each runner. Altogether four buckets were analysed by a comparison of measurements before and after the sediment season (see Table 1).

At HPP Fieschertal the sediment season, i.e. the period with increased suspended sediment concentration, is approximately between Mai and October. 50 percent of annual turbine discharge and power generation are normally in July and August, only 5 percent from November to April. On July 2 and 3, 2012, a major thunderstorm occurred in the region of Fieschertal, which produced a flood discharge with an estimated return period between 10 and 30 years (Felix et al. 2012). The turbines were running at suspended sediment concentration of up to approx. 50 g/l. After this event the runner in machine group 2 had to be replaced due to heavy damages. In the following, the second measurement of turbine geometry at this runner is also called "after sediment season", even though this runner was not in operation during the full sediment season. The runner in machine group 1, however, exhibited less damages after the flood event and could be operated until the end of the season, when it was revised on site.

	machine group 1	machine group 2
date of first measurement	Mai 2012 before sediment season	April 2012 before sediment season
number of sediment seasons in operation since last factory overhaul	0	3
actual runner condition	fully reconditioned at factory, including new coating	after annual on-site revision (grinding and local recoating)
date of second measurement	February 2013 after sediment season / before next sediment season	August 2012 during sediment season, taken out of operation
number of sediment seasons in operation since last factory overhaul	1	3.5
actual runner condition	"usual wear"	"heavy wear"

Table 1: Dates of turbine geometry measurements and respective runner conditions at HPP Fieschertal.

2.4 Results of Pelton turbine wear measurements

In this section, results of the bucket geometry measurements are given for the parameters as defined in section 2.2 (h, w and d). The following plots include geometrical properties measured before and after the sediment season as well as calculated differences (Δh, Δw and Δd). In addition, the volume differences, i.e. mass losses, were calculated at main splitters to give an example of further possibilities of the described method using digitized geometries.

Figure 6 shows the shapes of the four examined main splitters before and after the sediment season. Comparing the machine groups, a great difference in the initial conditions can be seen. With a similar splitter height reduction on both machines (see Fig. 7) the volume differences at machine group 2 are considerably greater since the width of the splitter increases as erosion progresses. The mean material loss observed at machine group 2 is almost twice that of machine group 1, what is attributed to the different initial conditions. The volume differences for the buckets 1 and 2 of the machine group 2 are very similar, but for the buckets of the machine group 1 they vary significantly. It is advisable to digitize at least two buckets per runner to get a reliable mean value.

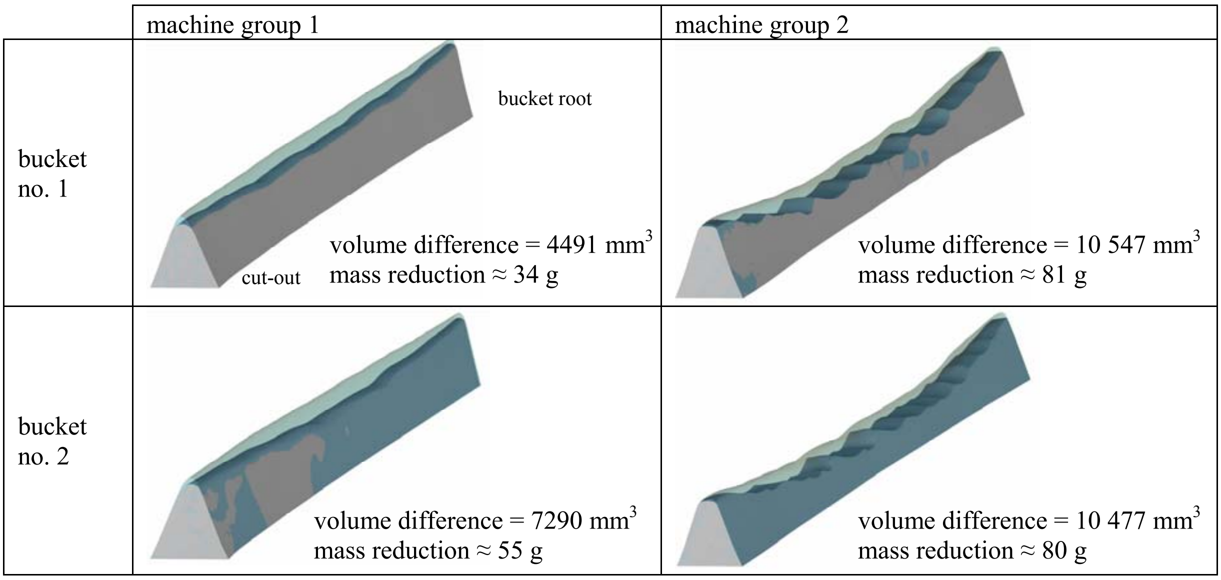

Fig. 6: 3D views of the digitized main splitters: Comparison between the splitter geometries before (transparent) and after the sediment season (grey).

During the sediment season 2012 the splitter height was reduced by about 4 mm for the machine group 1 and by 5 mm for the machine group 2 in the central part of the splitter length (Fig. 7). This corresponds to 0.6 to 0.8 percent of the Pelton bucket inner width of 650 mm at HPP Fieschertal. Dimensionless quantifications are used e.g. for correlating relative splitter width increase and efficiency decrease at different HPP with various bucket sizes. As mentioned before, the top of the splitters at machine group 1 was almost straight before the sediment season (red line).

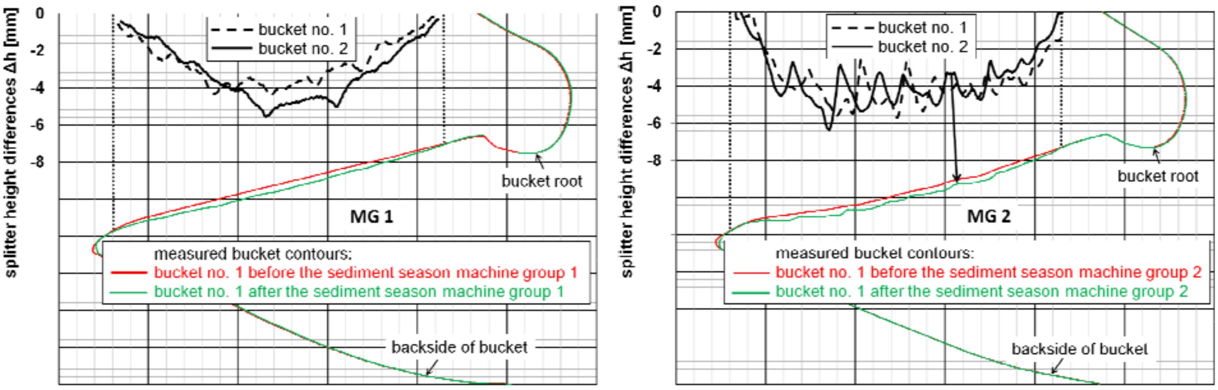

Fig. 7: Side view of the main splitter for machine group 1 (left) and 2 (right): Red and green lines show splitter profiles before and after the sediment season for bucket 1, black lines indicate the differences (erosion heights Δh) for buckets 1 and 2.

During the sediment season 2012 a splitter width increase of in maximum 3 mm for machine group 1 and 2 mm for machine group 2 were evaluated (Fig. 8). This is 0.3 to 0.5 percent of the inner bucket width. Similarly to the difference in splitter height, the difference in splitter width has its maximum approximately at half of the splitter length, where the splitter was hit most frequently by the jet of sediment-laden water.

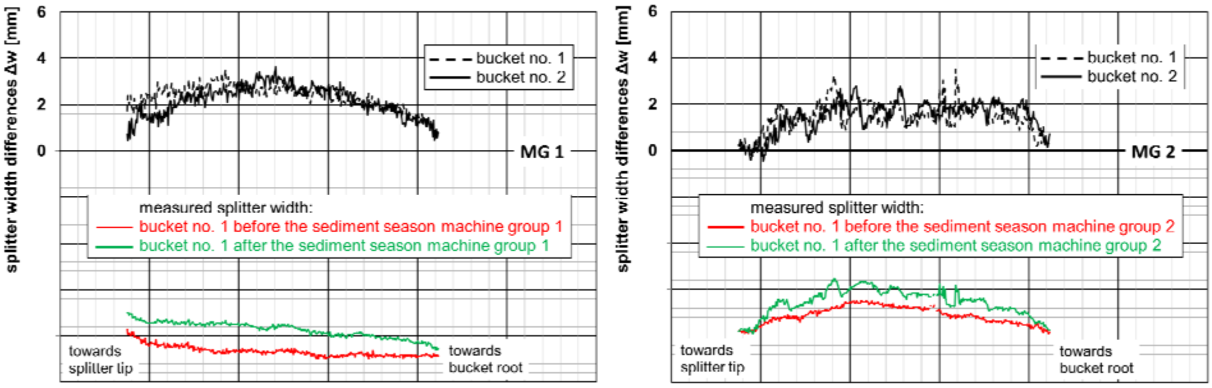

Fig. 8: Splitter widths along the main splitter for machine group 1 (left) and 2 (right): Red and green lines in the lower parts of the diagrams show splitter widths before and after the sediment season for bucket 1, black lines indicate the differences (Δw) for buckets 1 and 2

Further damages occur at the cut-out section of the Pelton bucket. The top views of bucket no. 1 for both machine groups are shown in Fig. 9. The shape of the cut-outs differs considerably between both units (compare the green and red lines left and right in Fig. 9). The shape of cut-outs is influenced by the different number and extent of revisions (grinding and welding) performed at the runners. The increase in cut-out depth *Δd* varies between the two machine groups. Cut-out depths increased by up to 10 mm towards the turbine axis at machine group 1 and by up to 7 mm at machine group 2. This corresponds to 1.0 to 1.5 percent of the inner bucket width.

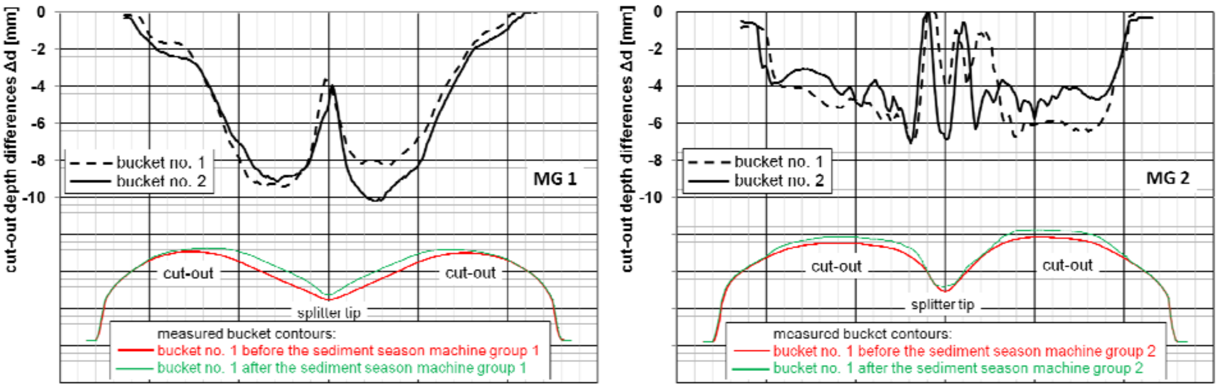

Fig. 9: Top view of the digitized cut-out for machine group 1 (left) and 2 (right): Red and green lines in the lower parts of the diagrams show the cut-out contours before and after the sediment season for bucket 1, black lines indicate the differences in cut-out depths (Δd) for buckets 1 and 2.

3 Index efficiency measurements

Turbine efficiency history at HPP Fieschertal is measured using the periodical sliding needle index measurement method (Abgottspon et al. 2013). "Sliding needle" stands for a gradual variation of turbine discharge between part load and full load during the measurement in case of Pelton turbines. In case of e.g. Francis turbines, the corresponding procedure is called "sliding gate" (Abgottspon & Staubli 2008, Almquist et al. 1995). Measurements involve basically the recording of electric power output, pressure upstream of the turbine and turbine discharge during a test, which takes slightly more than an hour for one machine group. For the determination of turbine discharge, acoustic discharge measurement installations at the top and the bottom of the penstock and two differential pressure sensors at a Venturi pipe section upstream of each machine group are available at HPP Fieschertal. The term "index efficiency" stands for the fact that no absolute efficiencies are measured. Measurements with this method are less laborious and less expensive than measuring absolute efficiency. The results allow establishing a history of efficiency changes, what is suitable for the present application.
In Figure 10 the efficiency histories of both machine groups are plotted since the sliding needle measurement program was implemented in the control system of the HPP Fieschertal. Plotted index efficiencies are a weighted average (according to the average load profile) of the index efficiencies determined between 40 and 100 percent of

installed power. At machine group 2 no measurements were possible for some months because one needle servomotor was not fully operational. Both histories begin with a reference index efficiency of 0 percent (at point A for machine group 1 and at point D for machine group 2). No absolute efficiency differences among both units can be analysed from the diagrams below.

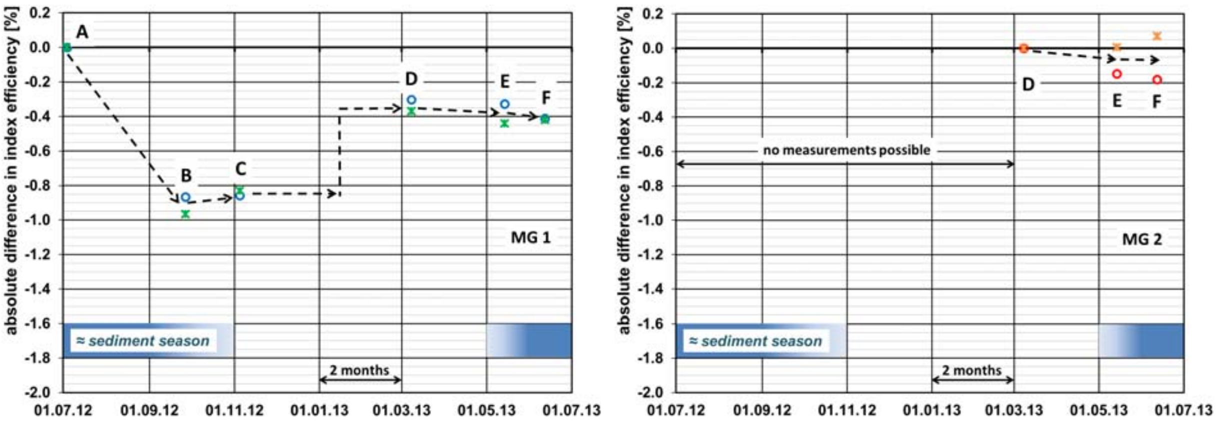

Fig. 10: History of index efficiency for machine group 1 (left) and 2 (right): Absolute differences from weighted index efficiency levels based on two different acoustic discharge measurement devices (circles: Rittmeyer crossed 4-path inside mount, crosses: Endress + Hauser 1-path clamp-on outside mount).

In Table 2 measured efficiency differences for both machine groups are given (mean values of both evaluations based on different discharge measurements). Furthermore, information on revision works at the Pelton buckets and qualitative information on sediment load is given for the respective periods. According to IEC Standard 62364 (2013), particle load is defined as the integral of the product of suspended sediment concentration and weighing factors for particle size, shape and hardness over time. Particle load will be quantified based on suspended sediment measurements.

	A → B	B → C	C → D	D → E	E → F
sediment load	high	low	very low	low	low to medium
works on buckets	-	-	grinding	local re-coating	-
efficiency difference machine group 1	-0.9 %	+0.05 %	+0.5 %	–0.05 %	–0.05 %
efficiency difference machine group 2	-	-	-	–0.1 %	0 %

Table 2: Differences in index efficiencies related to sediment load and mechanical works.

The index efficiency decrease of 0.9 percent for machine group 1 is attributed to hydro-abrasive erosion. As mentioned in section 2.3 a major sediment transport event occurred in Fieschertal on July 2 and 3, 2012. This was prior to the first index efficiency measurement on July 4, 2012. It is assumed that a considerable efficiency decrease has occurred in the first half of the sediment season 2012 including the flood event.
The observed index efficiency increase of 0.5 percent at machine group 1 can be explained with grinding works carried out at the main splitters and cut-out sections of the Pelton buckets during winter. Minor efficiency differences of less than 0.2 percent shall be interpreted with care, since they are of the same order of magnitude as the reproducibility of 0.2 percent which can be reached with the two available acoustic discharge measurements (except one measurement, point F for machine group 2 in Fig. 10).

4 Conclusion and outlook

Turbine wear was investigated on two buckets of two Pelton runners. Based on digital geometrical models measured before and after the sediment season, changes in geometry of areas that are most exposed to hydro-abrasive erosion were calculated. For the main splitter, the reduction in height, increase of width and lost material volume were defined and evaluated, for the cut-outs the increase of cut-out depth in radial direction were examined. Whereas an approximate value of the main splitter width can be quickly obtained with a ruler at a turbine inspection, the changes in cut-out geometry, the current shape of the main splitter's longitudinal profile or material loss cannot be quantified "by hand" and visual inspection in such accuracy as with the described method based on digitizing. In particular, a method for the evaluation of actual main splitter width, based on the gradient of the splitter flanks, was proposed. Digitizing of at least two buckets per runner is advisable to get reasonable average values.

A series of index efficiency measurements was performed by the sliding needle method. Among other parameters, the signals of four independent devices for the determination of turbine discharge were recorded. The evaluation of these measurements showed best results using acoustic discharge measurements. Besides efficiency reduction due to hydro-abrasive erosion, an increase of efficiency due to maintenance works (grinding of splitter and cut-out edges) was measured. The method is suitable for the determination of an index efficiency history since the reproducibility is 0.2 percent and relevant changes in efficiency over the sediment season or due to maintenance works in winter can be quantified.

Measurements of turbine wear and efficiency will be continued together with measurements of suspended sediment in the power waterway (see paper by Felix et al. 2013). It is planned to correlate the measurements of suspended sediment, turbine wear and turbine efficiency in order to contribute to the development of respective prediction formulas.

Acknowledgements

The authors gratefully acknowledge the financial support by swiss*electric* research, the Swiss Federal Office of Energy and Gommerkraftwerke AG (HPP Fieschertal) and technical support for using the digitizing system (Steinbichler Optotechnik). Further thanks go to the members of the project team, including collaborators from ETH Zurich (Prof. Dr. R. Boes, Dr. I. Albayrak), Hochschule Luzern (A. Schwery), BKW (U. Aebi) and HPP Fieschertal (B. Truffer and M. Perren).

References

1. **Abgottspon A., Staubli T., Felix D., Albayrak I., Boes R.M.** (2013). Hydro-abrasive Erosion of Pelton buckets and Suspended Sediment Monitoring. *Proc. HydroVision International* 2013, Denver, USA.
2. **Abgottspon A., Staubli T.** (2008). Index Tests of a Francis Unit using the Sliding Gate Method. *Proc. 7th Intl. conference on Hydraulic Efficiency Measurements*, IGHEM, Milan, Italy.
3. **Almquist C. W., March P. A., Pearson H. S., Fransen H. W., Whitehead B. H.** (1995). The Sliding Gate Method for Hydroturbine Efficiency Testing. *Proc. WaterPower '95*, American Society of Civil Engineers, New York, 793-801.
4. **Boes R.M.** (2009). Real-time monitoring of SSC and PSD in the headwater way of a high-head hydropower plant. *Proc. 33rd IAHR Congress*, Vancouver, Canada: 4037–4044.
5. **Brekke H., Wu Y. L., Cai B. Y.** (2002). Design of hydraulic machinery working in sand laden water, in *Abrasive Erosion & Corrosion of Hydraulic Machinery*, Book series on Hydraulic machinery, Vol. 2, edited by Duan C. G. and Karelin V. Y., ISBN 1-86094-335-7, Imperial College Press, London, 155-233.
6. **Felix D., Albayrak I., Abgottspon A., Boes R.M & Gruber P.** (2012). Suspended Sediment and Pelton Turbine Wear Monitoring: Experimental Investigation of various Optical and Acoustic Devices and Beginning of the Case Study at HPP Fieschertal. *Proc. 17th International Seminar on Hydropower Plants*. Vienna: 483-494.
7. **Felix D., Albayrak I., Boes R.M., Abgottspon A., Deschwanden F., Gruber P.** (2013). Measuring Suspended Sediment: Results of the first Year of the Case Study at HPP Fieschertal in the Swiss Alps. *Proc. Hydro 2013 Conference*, Innsbruck, Austria.
8. **IEC 62364** (2013): Hydraulic machines - Guide for dealing with hydro-abrasive erosion in Kaplan, Francis and Pelton turbines, Edition 1.0 (June 3013), *International Electrotechnical Commission*, Geneva, Switzerland
9. **Winkler K., Dekumbis R., Rentschler M., Parkinson E. & Garcin H.** (2011). Understanding hydro-abrasive erosion, *Proc. Hydro 2011 Conference*, Aqua-Media Intl. Ltd., Prague, Czech Republic.

The Authors

A. Abgottspon graduated in Mechanical Engineering (M.Sc.) from the Hochschule Luzern (HSLU) in Switzerland. Since 2006 he works as a research assistant at the Competence Centre Fluid Mechanics and Hydro Machines of the HSLU, in the fields of hydro power plant efficiency measurements, Pelton jet quality and hydro-abrasive erosion. In 2009 he co-founded etaeval, a company specialized in measurements and simulations on hydro power plants.

P. Stern graduated in Mechanical Engineering (B.Sc.) from the Hochschule Luzern (HSLU) in Switzerland. Since 2011 he works as a research assistant at the Competence Centre Fluid Mechanics and Hydro Machines of the HSLU, mainly in the fields of Computational Fluid Dynamics applications.

T. Staubli graduated in Mechanical Engineering from the Swiss Federal Institute of Technology (ETH) in Zurich. After two years of post-doctoral research in the field of flow induced vibration at Lehigh University, Pennsylvania, he worked in experimental fluid mechanics at Sulzer Hydro (now Andritz Hydro) in Zurich. He then headed the Hydromachinery Laboratory at

ETH Zurich. Since 1996 he is professor in Fluid Mechanics and Hydro Machines at Hochschule Luzern (HSLU). In 2009 he co-founded etaeval.

D. Felix graduated in Civil Engineering (M.Sc.) from the Federal Institute of Technology (ETH) in Zurich in 2005. He worked for five years with Pöyry Energy Ltd., Zurich, in the field of hydropower plant design and dam safety. Since 2010, he is a Ph.D. student (ongoing thesis on suspended sediment and turbine wear) and teaching assistant at the Laboratory of Hydraulics, Hydrology and Glaciology (VAW) of ETH Zurich.

Dr. K. Winkler graduated in Material Science in 1992 at University RWTH Aachen. She worked as a research scientist for five years in the material science department at the University Bremen (PhD in 1997). Then she was a senior scientist for five years for DeBeers Industrial Diamonds/Element Six in South Africa and England. In 2003 she moved into the hydro industry, working for Voith Siemens in the field of material science and coating and joined Andritz Hydro in 2009 first as associated head and since February 2011 as head of research & development for Coating.

Schwebstoffmonitoring zum verschleiss-optimierten Betrieb von Hochdruck-Wasserkraftanlagen

Robert M. Boes, David Felix, Ismail Albayrak

Zusammenfassung

Die Schädigung von Wasserkraftturbinen durch feinkörnige, harte mineralische Partikel im Wasser (Schwebstoffe) ist bei gewissen Hochdruck-Wasserkraftanlagen sowohl in der Schweiz als auch weltweit ein wirtschaftlich bedeutender Aspekt bei der Planung und im Betrieb. Durch die zunehmende Variabilität der Niederschläge und den Gletscherrückgang gewinnt diese Problematik an Bedeutung.

Für eine wirtschaftliche Optimierung ist es erforderlich, die Schwebstoffführung im Triebwasser, die Schädigung an den Turbinen (Hydroabrasivverschleiss) und die damit einhergehende Wirkungsgradabnahme zu quantifizieren. Als Grundlage für Verbesserungen des Betriebs und der Planung von Revisionsarbeiten ist eine Überwachung (Monitoring) der relevanten Parameter, möglichst in Echtzeit, wünschenswert.

Im vorliegenden Artikel werden Methoden des Schwebstoffmonitorings und die Notwendigkeit von Kalibrierungen der Messgeräte, vorzugsweise unter kontrollierten Laborbedingungen, aufgezeigt. Weiter werden Lösungsansätze zur Minderung der Hydroabrasion, insbesondere die Option eines wirtschaftlich auch bezüglich des aktuellen Verschleisses optimierten Anlagenmanagements, d.h. die Abschaltung von Turbinen während Schwebstoffkonzentrationsspitzen, diskutiert.

Résumé

Des dégâts aux turbines hydrauliques causés par des particules solides fines en suspension dans l'eau turbinée sont économiquement importants et doivent être pris en compte lors de la conception et l'exploitation de certains aménagements hydrauliques en Suisse et dans le monde. En raison de la variabilité croissante des précipitations et du recul des glaciers cette problématique ne cesse de prendre de l'ampleur.

Pour une optimisation économique il faut quantifier le transport solide en suspension dans l'eau turbinée, les dégâts aux turbines (l'usure par hydro-abrasion) ainsi que la réduction correspondante en rendement. Une surveillance des paramètres en jeu est désirable, si possible en temps réel, en tant que données de base pour l'exploitation et la planification des travaux de révision optimisées.

Le présent article décrit des méthodes actuelles pour la surveillance des solides en suspension et la nécessité d'étalonner les instruments, de préférence sous des conditions contrôlées en laboratoire. En plus, des approches pour diminuer l'hydro-abrasion, particulièrement l'option d'une exploitation économiquement optimisée entre autres par rapport à l'usure actuelle, c'est-à-dire l'arrêt des machines pendant des pointes de transport solide en suspension, sont discutées.

1. Einleitung

Der vorliegende Artikel bezieht sich auf einen am 8.11.2012 in Horw im Rahmen der Fachtagung Wasserkraft des Schweizerischen Wasserwirtschaftsverbands (SWV) gehaltenen Vortrag.

1.1 Hydroabrasion an Wasserkraftanlagen

Hydroabrasivverschleiss wird nach DIN 50320 (1979) definiert als Schaden an Oberflächen von Bau- und Anlagenteilen, der durch den Transport von Feststoffpartikeln in Flüssigkeiten auftritt. Verallgemeinert werden in diesem Zusammenhang oft die Begriffe der (Hydro-)Abrasion und der Erosion verwendet. Die Wasserkraft ist räumlich und zeitlich unterschiedlich stark von Hydroabrasivverschleiss betroffen. Bei Wasserkraftwerken an Gewässern mit hohem Feststoffgehalt, wie sie typischerweise im Gebirge dominant sind, tritt Hydroabrasion vor allem an Anlagen mit grossen Fallhöhen und ohne grösseren Kopfspeicher (Laufkraftwerke) auf, wo sich der Grossteil der als Schwebstoffe mittransportierten Feinanteile der Sedimente nicht in Speichern oder Entsandern absetzt und im Triebwasser mittransportiert wird. Zeitlich beschränkt sich der Verschleiss auf die sog. Schwebstoffsaison, also auf die Zeiten hohen Feststofftransportes während Schnee- und Gletscherschmelze bzw. während (oft nur kurz andauernden) Hochwassern, z.B. nach Gewitterereignissen. Peltonturbinen sind am meisten betroffen, da diese bei grossen Fallhöhen eingesetzt werden und die Beanspruchung der Turbinenbauteile infolge der hohen Strahlgeschwindigkeiten gross ist. Am meisten werden die Haupt- und Nebenschneiden der Peltonbecher beschädigt, an denen der eintretende Wasserstrahl aufgeteilt wird *(Bild 1)*. Die anfangs scharfen Mittelschneiden und Bechereintrittskanten werden im Lauf des Betriebs zunehmend breiter, was zu Sekundärströmungen führt, die Kavitationserosion zur Folge haben können. Bei unbeschichteten Laufrädern kommt es weiter zu flächigem Abtrag im Bechergrund. Die Auswirkungen werden schliesslich für den Betreiber anhand von Produktionsverlusten infolge Wirkungsgradabnahmen spürbar.

Die wesentlichen Faktoren für Hydroabrasionsschäden an Wasserturbinen (Sulzer Hydro 1996 in DWA 2006, Winkler et al. 2011) sind die

- Relativgeschwindigkeit u zwischen Strömung und Turbinenbauteil,
- in der Regel zeitlich sehr veränderliche Schwebstoffkonzentration C,
- zeitlich ebenfalls veränderliche Partikelgrösse,
- für ein gegebenes Einzugsgebiet eher

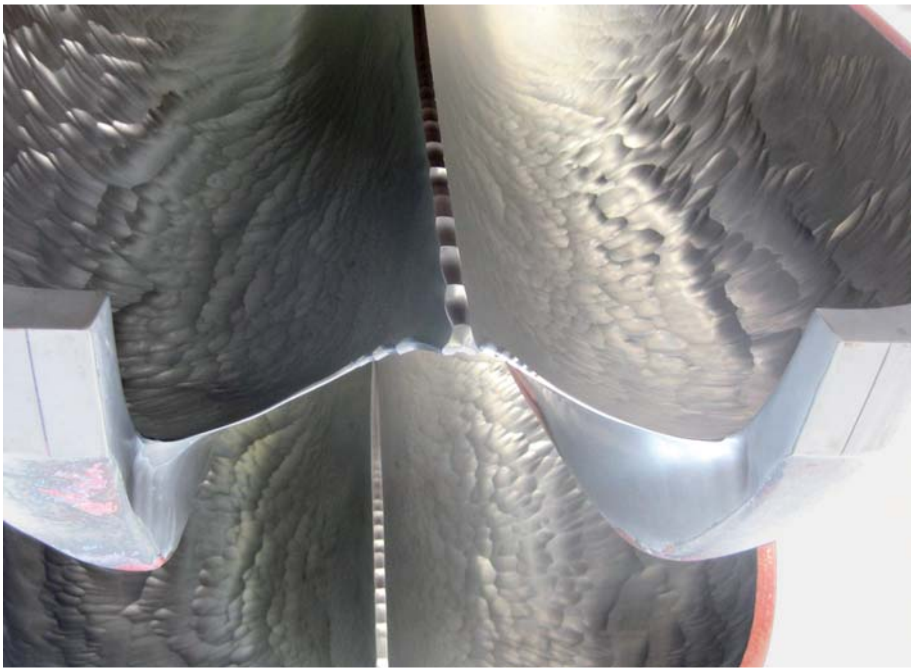

Bild 1. Becher eines unbeschichteten Pelton-Laufrads mit Verschleiss-Schäden (Ausstellungsobjekt bei der Staumauer Emosson, Foto: VAW).

konstante Partikelform (insbesondere kantige Partikel),
- Partikelhärte (vor allem Mohshärte grösser 6, d.h. Quarz- und Feldspatgehalt, da diese Minerale härter sind als das übliche Turbinengrundmaterial).

Um den Prozess des Hydroabrasivverschleisses besser zu verstehen, müssen die Schwebstoffeigenschaften im Triebwasser, der Materialverlust an den Turbinen und die Wirkungsgradreduktion quantifiziert werden. Solche Datensätze können zum Verifizieren und Weiterentwickeln von Prognosemodellen des Turbinenverschleisses (z.B. Nozaki 1990, Sulzer Hydro 1996 in DWA 2006) verwendet werden. Dazu wurde ein interdisziplinäres Forschungsprojekt von der Versuchsanstalt für Wasserbau, Hydrologie und Glaziologie (VAW) der ETH Zürich initiiert, im Rahmen dessen gemeinsam mit dem Kompetenzzentrum Fluidmechanik & Hydromaschinen der Hochschule Luzern sowie den Gommerkraftwerken (GKW), der BKW FMB Energie AG, Bern, und der Andritz Hydro AG, Kriens, u.a. Prototyp-Untersuchungen an einer bestehenden Kraftwerksanlage (KW Fieschertal, Wallis) durchgeführt werden. Die dabei verwendeten Messeinrichtungen für das Monitoring von Schwebstoffen wurden vorgängig im Labor in einem Mischtank mit verschiedenen Partikelsorten untersucht, bevor sie im Sommer 2012 an der Wasserkraftanlage Fieschertal im Wallis, einer stark von Hydroabrasivverschleiss betroffenen Hochdruckanlage mit stark vergletschertem Einzugsgebiet ohne Speichersee, basierend auf Vorarbeiten von Abgottspon (2011) eingebaut wurden. Die nachfolgend gezeigten ersten Resultate des laufenden Forschungsprojekts beziehen sich sowohl auf die Labor- als auch Prototypversuche (Felix et al. 2012a und b).

1.2 Lösungsansätze zur Minderung des Hydroabrasivverschleisses

Zur Verminderung des Hydroabrasivverschleisses gibt es verschiedene Ansätze, die entweder eine Verringerung der Beanspruchung oder eine Erhöhung des Widerstands bewirken:

a. Optimierung der Feststoffabscheidung (baulich) und des Turbinendesigns (elektromechanisch) (Verringerung der Einwirkungen),
b. Verbesserung der Turbinenmaterialien, z.B. mittels den heute üblichen rund 300 µm starken Wolframkarbid-Beschichtungen (Erhöhung des Widerstands),
c. Verschleissoptimierte Betriebsweise (Verringerung der Einwirkungen).

Die Schwebstoffbelastung (Konzentrationen und Partikelgrössen) kann bei Neuanlagen in einem gewissen Mass über die Absetzwirkung von Entsandern bzw. Kopfspeichern (Massnahmentyp a) beeinflusst werden (Ortmanns 2006). Solchen Anlagen zur Feststoffabscheidung sind aber wirtschaftliche, z.T. auch räumlich-topographische Grenzen gesetzt. Für bestehende Anlagen kann eine verbesserte Feststoffabscheidung in der Regel nur mit beträchtlichem bautechnischen Aufwand erreicht werden. Weitere Parameter wie Kornhärte, -form und Relativgeschwindigkeit zwischen Strömung und Laufrad spielen zwar, wie oben erwähnt, ebenfalls eine Rolle hinsichtlich Verschleiss, können aber praktisch nicht beeinflusst werden, da sie durch die Geologie des Einzugsgebiets bzw. die Fallhöhe (Lage von Fassungen und Maschinenhäusern) gegeben sind. Da der Massnahmentyp b trotz fallweise deutlicher Erhöhung der Turbinen-Standzeiten oft nicht allein das erhoffte Ergebnis bringt (und auch die Laufradrevisionen deutlich aufwändiger macht), soll der Fokus in diesem Beitrag auf einen verschleissoptimierten Anlagenbetrieb (Massnahmentyp c) gelegt werden. Als Voraussetzung dazu müssen die wichtigen Einflussgrössen des Hydroabrasivverschleisses, insbesondere die Partikelkonzentration und -grösse, in Echtzeit bekannt sein, was besondere Anforderungen an die Messtechnik stellt.

Ein kontinuierliches Schwebstoffmonitoring und vorübergehende Kraftwerksabstellungen aufgrund temporär hoher Stromgestehungskosten infolge starkem Hydroabrasivverschleiss sind bei Wasserkraftanlagen noch die Ausnahme. Temporäre Kraftwerksabschaltungen oder das vorübergehende Ausleiten von Fassungen werden bisher vor allem während starkem Geschiebetrieb, der den Betrieb der Wasserkraftanlage erschwert oder verunmöglicht, praktiziert (z.B. mit Geschiebe aufgefüllte oder überschüttete Fassungen).

2. Methoden des Schwebstoffmonitorings

Beim Schwebstoffmonitoring ist zunächst zwischen kontinuierlichen und diskontinuierlichen Messmethoden zu unterscheiden. Zu letzteren zählen klassische Schöpfproben, bei denen mit einem Schöpfgefäss von Hand ein Wasservolumen entnommen wird und entweder mittels Imhoff-Trichter oder im Nachgang im Labor mittels Filtrierung und/oder Ofentrocknung die Schwebstoffkonzentration und ggf. die Korngrössenverteilung bestimmt werden. Eine Weiterentwicklung sind automatische Probennahmegeräte, welche mittels einer Pumpe z.B. bis zu 24 Flaschen abfüllen *(Bild 2)*. Der Zeitpunkt der Entnahme kann durch einen Computer gesteuert werden, beispielsweise auch als Funktion der Trübung, die dann mit einem anderen Gerät in Echtzeit gemessen werden muss.

Kontinuierliche Schwebstoffmessungen sind im Wesentlichen auf optischem oder akustischem Weg durchführbar. Zu den optischen Geräten zählen die

Bild 2. Programmierbarer Wasserprobennehmer, im Bild mit abgehobenem Deckel, mit Pumpe und Vorrichtung zum Füllen von bis zu 24 Flaschen (Foto: VAW).

weithin eingesetzten Trübungssonden, sei es nach dem Streu- oder Durchlichtverfahren. Die Ausgabe der Messwerte erfolgt hierbei in Trübungseinheiten (z.B. FNU = Formazine Nephelometric Unit; CU = Concentration Unit). Bei konstanten und bekannten Partikeleigenschaften (insbesondere Grösse und Form) können die Messwerte von Trübungssonden in eine Schwebstoff-Massenkonzentrationen (z.B. [mg/l]) umgerechnet werden, bzw. diese Kalibrierung kann im zugehörigen Messumformer hinterlegt werden. In der Realität ist aber insbesondere die Partikelgrösse zeitlich oft sehr variabel, was ohne zusätzliche Informationen zu beträchtlichen Unsicherheiten bei der Bestimmung der Schwebstoffkonzentration führen kann. Anhand von Schöpfproben können die kontinuierlichen Messungen von Trübungssonden besser interpretiert werden.

Eine andere optische Messmethode, die Laserdiffraktometrie, ermöglicht neben der Konzentrationsmessung zusätzlich die Bestimmung von Partikelgrössen und deren Verteilung. Dabei wird ein Laserstrahl durch die Wasser-Sediment-Suspension gesendet und die an den Partikeln gestreute Strahlung auf verschiedenen Ringen detektiert. Über das gemessene Streuungsmuster lassen sich die Partikelgrössenverteilung und die Volumenkonzentration der Partikel bestimmen, welche das gemessene Streuungsmuster verursacht hätten (Agrawal et al. 2011). Das im KW Fieschertal – nach Wissen der Autoren erstmals an einer Schweizer Wasserkraftanlage – installierte in-situ Laserdiffraktometer (LISST-100X, Typ C) weist einen nominellen Korngrössenmessbereich von 2.5 bis 500 µm auf.

Bei Wasserkraftwerken wird der turbinierte Volumenstrom oft mit akustischer Durchflussmessung bestimmt. Dabei werden Ultraschallpulse diagonal durch die Druckleitung geschickt. Wenn das Wasser Schwebstoffe enthält, wird das Empfangssignal in Funktion der Schwebstoffkonzentration und der Partikelgrösse abgeschwächt. Da solche Einrichtungen für die akustische Durchflussmessung in vielen Kraftwerken vorhanden sind, ist – basierend auf der Amplitudendämpfung – zumindest ein qualitatives Schwebstoffmonitoring im Sinne von Warnungen für den Kraftwerksbetrieb denkbar. Diese Methode wird derzeit im Rahmen des Forschungsprojekts weiter untersucht.

3. Kalibrierung von Schwebstoffmessgeräten

Wie oben ausgeführt ist eine Kalibrierung von kontinuierlichen Schwebstoffmessgeräten unumgänglich, wenn eine der Realität nahe kommende Massenkonzentration C bestimmt werden soll. Die in der Regel gemessenen Trübungswerte müssen dazu zunächst in die Einheit einer Massenkonzentration umgerechnet werden, was besonders mit der Korngrösse und -form, aber auch mit den optischen Eigenschaften (z.B. Farbe) der Partikelminerale (Gippel 1995, Sutherland et al. 2000) variiert. Für die Laborversuche wurden mineralische Partikel *(Bild 3)*, die kommerziell erhältlich und mit den Partikeln in Fieschertal vergleichbar sind (Granitge-

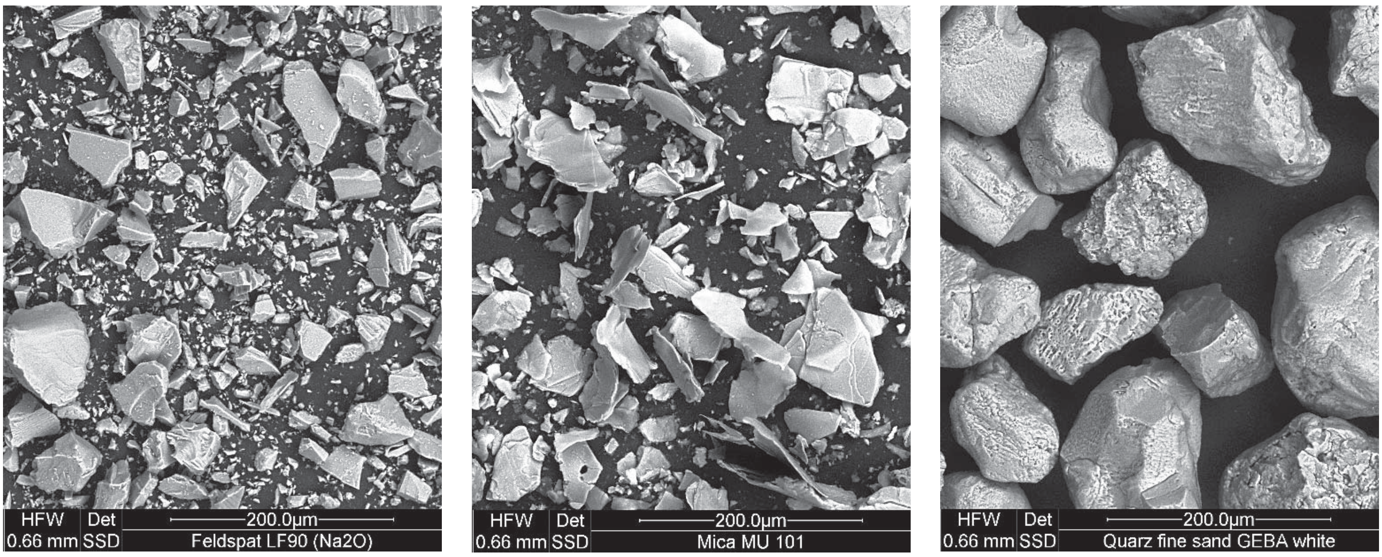

Bild 3. Mineralische Partikel, welche in den Laborversuchen betreffend Schwebstoffmessung verwendet wurden: Feldspatpulver (links, d_{50} = 34 µm), Glimmerpulver (Mitte, «d_{50}» = 45 µm) und Quarzfeinsand (rechts, d_{50} = 147 µm) (Bilder: VAW und IfB, ETH Zürich).

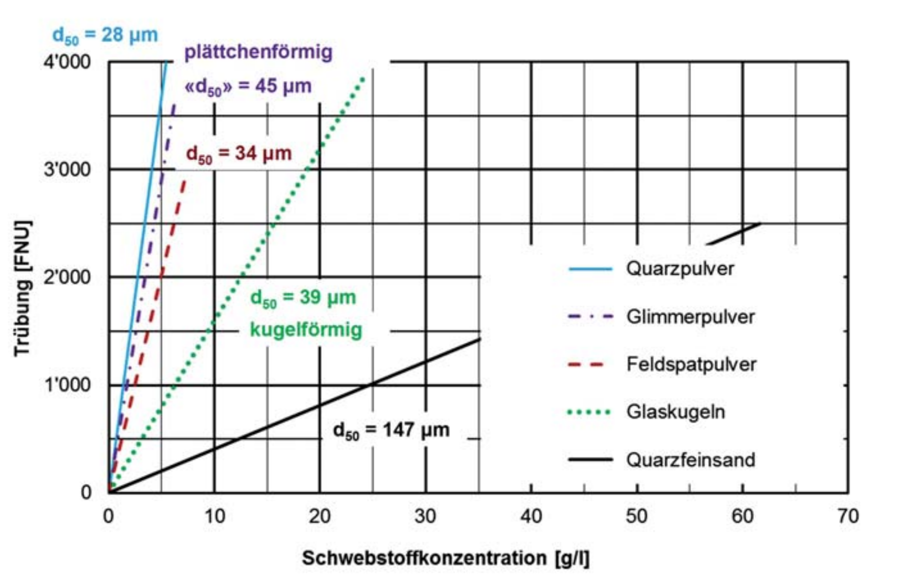

Bild 4. Trübungswerte, welche mit einer Trübungssonde (Hach-Lange Solitax ts-line sc) in Suspensionen mit verschiedenen Partikelsorten gemessen wurden (nach Felix et al. 2012a).

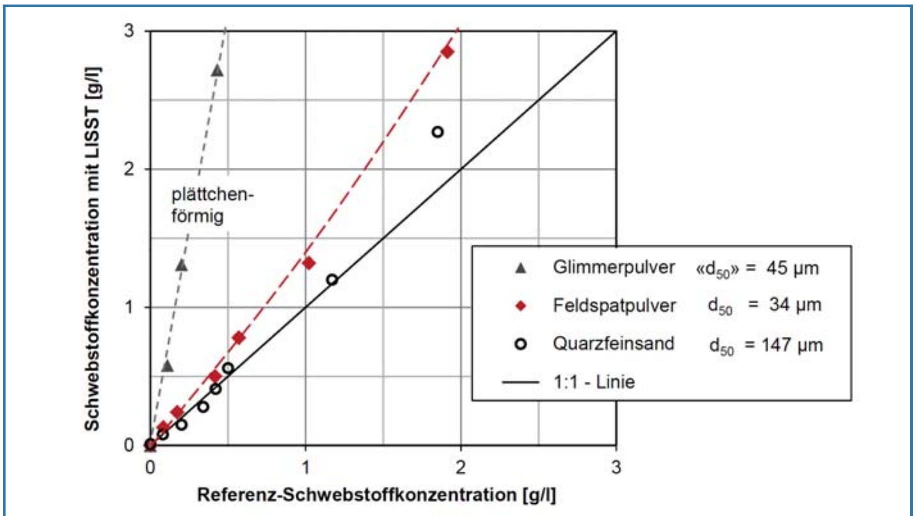

Bild 5. Mit einem tragbaren Laserdiffraktometer (Sequoia LISST-100X) bestimmte Schwebstoffkonzentrationen im Vergleich zur Referenz-Konzentration (nach Felix et al. 2012b).

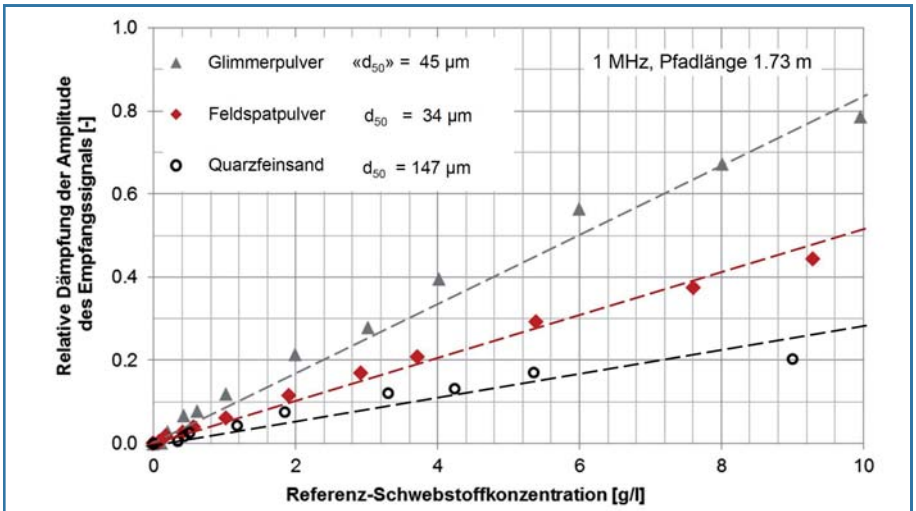

Bild 6. Relative Dämpfung von akustischen Ultraschallsignalen (akustische Durchflussmesseinrichtung, Rittmeyer) im Vergleich zur Referenz-Konzentration (nach Felix et al. 2012b).

biet mit Quarz, Feldspat und Glimmer), sowie Feinsedimente vom Unterwasserkanal des KW Fieschertal verwendet. Für Referenzzwecke kamen auch Glaskugeln zum Einsatz. Die bei *Bild 3* angegebenen Massen-Median-Korndurchmesser d_{50} stammen von Messungen mit einem nicht tragbaren Laserdiffraktometer am Institut für Geotechnik (IGT) der ETH Zürich, welche als Referenz verwendet wurden. *Bild 3* wurde mittels Rasterelektronenmikroskop am Institut für Baustoffe (IfB) der ETH Zürich aufgenommen. Weitere Angaben zu den durchgeführten Laborversuchen sind in Felix et al. (2012a und b) publiziert.

Bild 4 zeigt den deutlichen Einfluss der Korngrösse auf die Trübung. Die Korngrösse wird hier durch den Massen-Median-Durchmesser d_{50} ausgedrückt. Weiter sind in *Bild 4* Einflüsse der Partikelform zu erkennen, z.B. bei Vergleich der Linien für Glimmerpulver mit plättchenförmigen Partikeln und für Glaskugeln, die beide etwa denselben d_{50}-Wert aufweisen.

In *Bild 5* sind mit dem tragbaren Laserdiffraktometer gemessene Schwebstoffkonzentrationen im Vergleich zu den Referenz-Konzentrationen dargestellt. Letztere wurden durch Wägung von ofengetrockneten Schöpfproben, die auf der Höhe der Instrumente aus dem Mischtank bei den jeweiligen Konzentrationsstufen entnommen wurden, bestimmt. Beim Laserdiffraktometer ist die Bestimmung der Schwebstoffkonzentration theoretisch nicht von der Korngrösse abhängig. Dies wird durch die Punkte von Quarzfeinsand und Feldspatpulver, welche trotz unterschiedlichen Korndurchmessern in *Bild 5* relativ nahe beieinander liegen, bestätigt. Das Vorhandensein von feinen Partikeln, die kleiner sind als der Bereich der messbaren Partikel (< 2.5 µm), kann aber dazu führen, dass die Schwebstoffkonzentration überschätzt wird. Auch bei der Laserdiffraktometrie führt eine Kornform, welche stark von der in der Auswertungssoftware zugrunde gelegten abweicht, zu Fehlern bei der Bestimmung der Schwebstoffkonzentration. Die Streuung der Versuchsdaten, insbesondere bei gröberen Partikeln, kann den lokalen und zeitlichen Konzentrationsunterschieden in der turbulenten Suspension zugeschrieben werden. Es ist bemerkenswert, dass beim Laserdiffraktometer lediglich mit Verwendung der Werkkalibrierung, d.h. unter Annahme von unregelmässig geformten Partikeln mit einer Dichte von 2.65 t/m^3, die dargestellten Schwebstoffkonzentrationen resultierten, die mit Ausnahme des Glimmers relativ nahe an den erwarteten

Schwebstoffkonzentrationswerten liegen (1:1-Linie).

Auch die akustische Messmethode ist bei der Konzentrationsbestimmung nicht frei vom Effekt der genannten Partikeleigenschaften, was aus *Bild 6* hervorgeht, jedoch sind die Unterschiede zwischen den Kalibrierkurven geringer als bei Trübungssonden.

Bild 7 verdeutlicht, dass bei der Messung der Partikelgrössen mittels tragbarem Laserdiffraktometer die Breite der Korngrössenverteilung, d.h. die Stufung, gut erkannt wurde. Die Messwerte liegen sowohl für Feldspatpulver als auch für Quarzfeinsand in der richtigen Grössenordnung. Im Fall von Glimmerpulver mit der speziellen plattigen Partikelform gibt es eine systematische Abweichung von den Referenzmessungen, wobei zu bedenken ist, dass die Definition des «Durchmessers» eines plattigen Teilchens unklar ist. Zu den Referenzmessungen (durchgeführt mit nicht-tragbarem Laserdiffraktometer am IGT der ETH Zürich) ist zu bemerken, dass diese Proben zu Beginn der Versuchsreihen von den Behältern der Partikelsorten trocken entnommen wurden. Die Abweichungen zwischen den im Mischtank gemessenen Korngrössenverteilungen von den Referenzmessungen, insbesondere bei gröberen Fraktionen, sind vermutlich dem Phänomen zuzuschreiben, dass im Mischtank gröbere Partikel trotz Rührwerk tendenziell im unteren Bereich der Wassersäule, unterhalb des Messkopfs des Laserdiffraktometers, vorhanden waren (vertikales Konzentrationsprofil) oder nicht vollständig in Schwebe gehalten werden konnten.

4. Option temporärer Turbinenabschaltungen während Schwebstoffspitzen

Wie in Abschnitt 1 beschrieben, sind für den Hydroabrasivverschleiss von Turbinen insbesondere die Schwebstoffkonzentrationen (bzw. -frachten) und Partikelgrössen massgebend. Stark erhöhte Konzentrationen im Triebwasser kommen in der Regel bei grösseren Abflussereignissen vor, z.B. nach Starkregen wie Gewittern, und weisen meist eine kurze Dauer auf. Die in *Bild 8* und *Bild 9* zu erkennenden Konzentrationsspitzen am Kraftwerk Dorferbach in Tirol, Österreich, haben beispielsweise typische Dauern von wenigen Stunden, innerhalb derer eine vergleichbare Sedimentfracht über die Turbine abgeleitet wird wie bei Normalbetrieb während mehrerer Tage. Um diese Schweb-

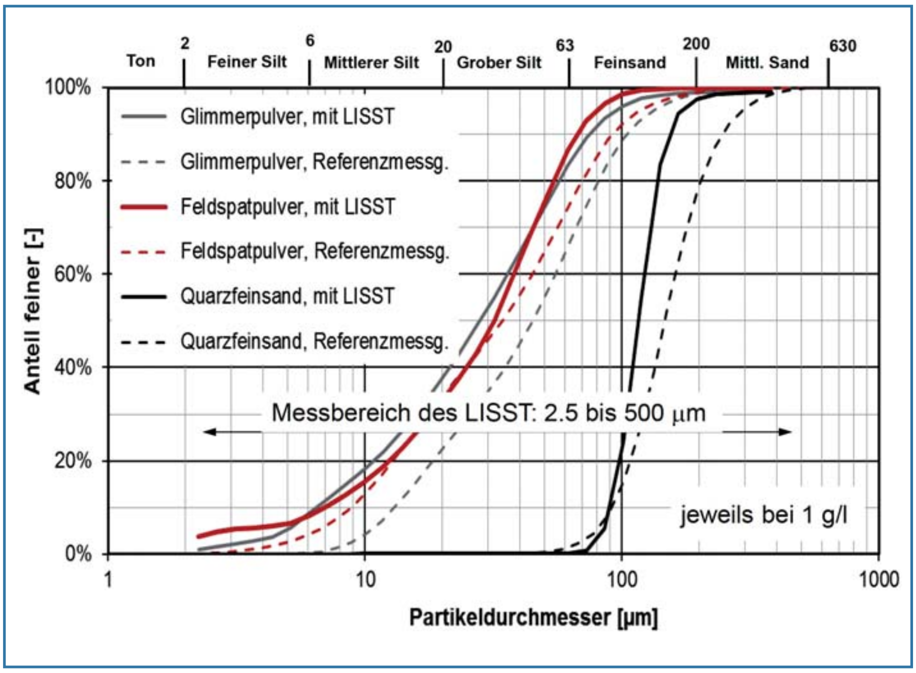

Bild 7. Mit tragbarem Laserdiffraktometer (Sequoia LISST-100X) ermittelte Korngrössenverteilung im Vergleich zu Referenz-Messungen (nach Felix et al. 2012b).

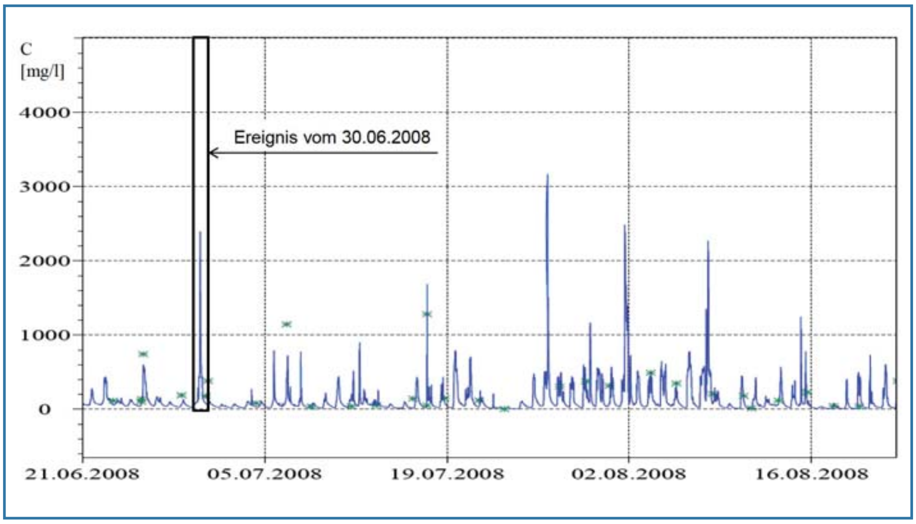

Bild 8. Verlauf der Schwebstoffkonzentration im Triebwasser des KW Dorferbach im Sommer 2008, (–) Daten der Trübungssonde nach Kalibrierung anhand von (*) Einzelproben (nach Boes 2010).

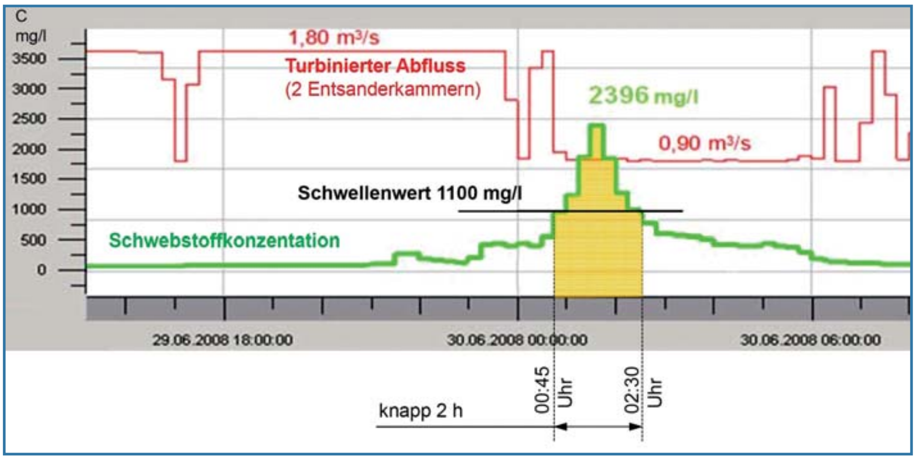

Bild 9. Verlauf der Schwebstoffkonzentration (linke Achse, gemessen mit kalibrierter Trübungssonde, Ausschnitt aus Bild 8) und des Turbinendurchflusses Ende Juni 2008 und Angabe des Schwellenwerts für die vorübergehende Ausserbetriebnahme des KW Dorferbach (Quelle: TIWAG).

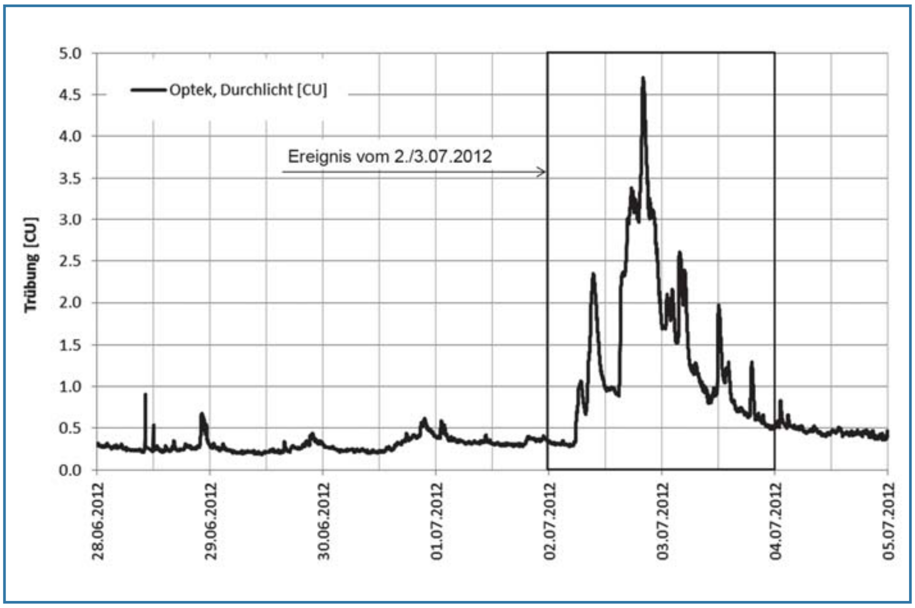

Bild 10. Verlauf der Trübung als Indikator für die Schwebstoffkonzentration im Triebwasser des KW Fieschertal Ende Juni/Anfang Juli 2012.

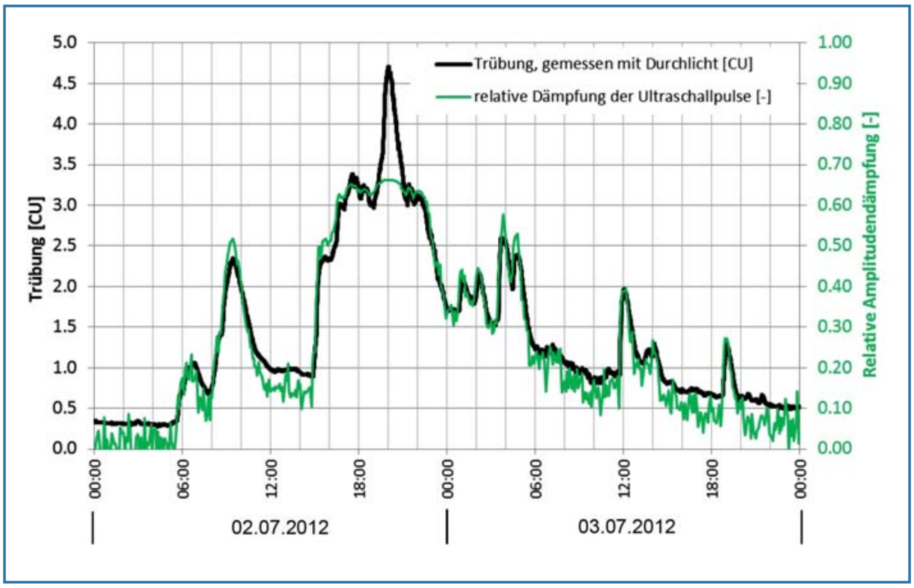

Bild 11. Verlauf der Trübung (linke Achse, Ausschnitt aus Bild 10) und der relativen Amplitudendämpfung von akustischen Ultraschallsignalen (rechte Achse) im Triebwasser des KW Fieschertal Anfang Juli 2012 (nach Felix et al. 2012b).

stoffbelastung zu reduzieren, liegt es daher nahe, eine von Hydroabrasion betroffene Wasserkraftanlage bei hoher Schwebstoffführung kurzzeitig ausser Betrieb zu nehmen, sofern dies von den übergeordneten Randbedingungen her möglich ist (Kraftwerkspark, Verbundnetz, Produktionsverpflichtungen, usw.). Dies bedingt jedoch einerseits ein verlässliches und kontinuierliches Schwebstoffmonitoring (Bishwakarma & Støle 2008), andererseits die Kenntnis von Grenzwerten bezüglich Konzentration und idealerweise auch der Korngrösse.

Die Grenz- oder Schwellenwerte sind eine Frage der betriebswirtschaftlichen Optimierung (vor allem Verlust an produzierter Energie während Turbinenabschaltungen vs. Einsparungen bei Laufradrevisionen), zu deren Beantwortung der quantitative Zusammenhang zwischen den oben erwähnten Parametern und dem Hydroabrasivverschleiss an Turbinen bzw. dessen Auswirkungen (Wirkungsgradminderung) bekannt sein muss, was – wie einleitend erwähnt – noch Gegenstand der Forschung ist. Auf Grundlage von kontinuierlichen Schwebstoffdaten sowie von Verschleissmessdaten, die in einem zeitlich engen Raster während der Sedimentsaison 2008 erhoben wurden, wurde für das KW Dorferbach ein Konzentrationsgrenzwert von 1100 mg/l im Triebwasser festgelegt, bei dessen Überschreiten das Kraftwerk ausser Betrieb genommen wird (Boes 2010). Mit dieser Massnahme konnten die Hydroabrasionsschäden markant reduziert werden (Götsch 2012). In diesem Fall erlaubte das umfangreiche Schwebstoff- und Verschleiss-Monitoring eine anlagenspezifische Kalibrierung eines Verschleiss-Prognosemodells und eine rechnerische Abschätzung der Entwicklung der Mittelschneidenbreiten des Peltonlaufrads in Abhängigkeit der Schwebstoffkonzentration. Dabei wurde ein empirisch gefundener Zusammenhang zwischen der Schwebstoffkonzentration und dem mittleren Partikeldurchmesser verwendet (Boes 2010).

Vom Triebwasser des KW Fieschertal liegen erste Schwebstoffdaten vor. Ein seltenes Hochwasserereignis (ca. 30- bis 50-Jährlichkeit im Goms) führte Anfang Juli 2012 zu extremen Schwebstoffkonzentrationen von mindestens 68 g/l in der Spitze (auf Grundlage von Schöpfproben ermittelt), was zu erheblichen Schädigungen der beschichteten, schon eine zeitlang in Betrieb stehenden Turbinenlaufräder führte. In *Bild 10* und *Bild 11* ist der zeitliche Verlauf der mittels Durchlichtverfahren gemessenen Trübung dargestellt. Es ist deutlich zu sehen, dass die Trübung von den üblichen rund 0.2 bis 0.5 CU während des Ereignisses bis auf 4.7 CU anstieg, also um das rund 10-Fache *(Bild 10)*. *Bild 11* lässt zudem die gute Übereinstimmung der Trübungswerte mit der relativen Amplitudendämpfung der Ultraschallpulse erkennen. Dass die absolute Spitze mittels der akustischen Methode nicht aufgezeichnet werden konnte, hängt mit der vorhandenen Pfadlänge und der verwendeten Sendefrequenz zusammen. Von Mitte April 2012 bis unmittelbar nach diesem Hochwasser hat der Turbinenwirkungsgrad gemäss Indexwirkungsgradmessungen, die noch ausgewertet werden, relativ stark abgenommen. Es ist zu vermuten, dass ein Grossteil der Wirkungsgradabnahme in dieser Periode allein durch dieses Ereignis verursacht wurde.

Für den Fall derartiger Schwebstofftransportereignisse sollen hier exemplarisch zwei denkbare Varianten einer auch hinsichtlich aktuellem Turbinenverschleiss optimierten Betriebsweise des KW Fieschertal aufgezeigt werden. Die in *Bild 12* angenommenen Grenzwerte bezüglich Schwebstoffführung des Triebwassers beruhen vorerst auf der Beobachtung des Schwebstoffaufkommens in «normalen Sommerverhältnissen» und darauf aufgesetzten ereignisbedingten Schwebstofftransportspitzen. Im ersten fiktiven Szenario mit einem Trübungs-Schwellenwert von 3.0 CU für das Abstel-

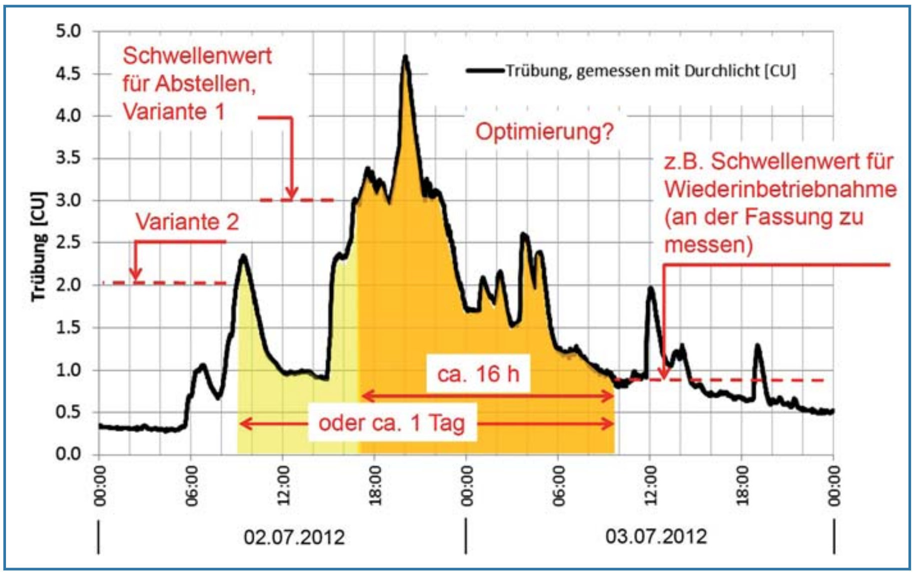

Bild 12. Verlauf der Trübung Anfang Juli 2012 (Ausschnitt aus Bild 10) und angenommene Schwellenwerte für die Ausser- und Wiederinbetriebnahme des KW Fieschertal in zwei fiktiven Szenarien.

len der beiden Maschinen, die nach dem Unterschreiten von 0.9 CU wieder in Betrieb genommen würden, würde die Anlage rund 16 h nicht produzieren. In einem zweiten Szenario würde die Anlage bereits b ei Überschreiten von 2.0 CU ausser Betrieb genommen, so dass die Turbinen mit weniger Schwebstoffen als bei Szenario 1 belastet würden. Mit demselben Grenzwert für die Wiederinbetriebnahme käme man auf einen Stillstand während rund eines Tages.

Die entsprechenden Produktionsausfälle würden sich bei einer Ausbauleistung des KW Fieschertal von 64 MW unter Ansatz eines Energiepreises von 60 CHF/MWh in den beiden oben genannten Szenarien auf gut 60 bzw. 90 kCHF belaufen. Obwohl dies zunächst hoch erscheinen mag, relativieren sich diese Werte bei einem Vergleich mit typischen Revisionskosten von mehreren 100 kCHF für derartige Pelton-Laufräder. Zudem verursacht ein Laufradwechsel, der infolge eines unvorhergesehenen Schwebstoffereignisses während der Volllastzeit erforderlich wird, bei einem Zeitbedarf von rund 16 h bei diesem Laufkraftwerk Produktionsausfallkosten von gut 30 kCHF. Laufradwechsel erfolgen normalerweise während der Niederwasserperiode, wenn eine Maschine ohne Produktionsausfall ausser Betrieb genommen werden kann.

Es sei darauf hingewiesen, dass die Schwebstoffe für eine solche Betriebsweise nicht nur im Triebwasser, sondern auch an der Wasserfassung gemessen werden müssen, um die Wiederinbetriebsetzung des Kraftwerks in Abhängigkeit des aktuellen Schwebstoffaufkommens im Gewässer zu ermöglichen, da ja nach dem Abstellen der Turbinen kein Wasser mehr im Triebwasserweg fliesst. Weiter sei erwähnt, dass die Wiederinbetriebnahme einer grösseren Kraftwerksanlage, die bei hoher Schwebstoffkonzentration ausser Betrieb genommen wurde, mit einigem Arbeitsaufwand verbunden sein kann (z.B. Entfernen von Ablagerungen in Hilfseinrichtungen). Der Aufwand für die Wiederinbetriebsetzung nach einer sedimentbedingten Abschaltung sollte aber gegenüber den vermiedenen Schäden in der Regel nicht ins Gewicht fallen.

5. Schlussfolgerungen und Ausblick

Es besteht ein zunehmender Bedarf an praxistauglichen Messeinrichtungen zur Echtzeit-Erfassung des Schwebstoffaufkommens (Konzentration und Korngrössenverteilung) nicht nur an Wasserkraftanlagen, sondern auch an Fliessgewässern und Seen. Die hier vorgestellten Schwebstoffmessmethoden lassen sich neben einer hinsichtlich dem aktuellen Turbinenverschleiss wirtschaftlich optimierten Betriebsweise von Hochdruck-Wasserkraftanlagen auch im Zusammenhang mit dem Sedimentmanagement an Stauanlagen und Seen sowie zur Untersuchung ökologischer Fragestellungen einsetzen. Die meisten der dabei zum Einsatz kommenden Messgeräte benötigen eine auf die am Einsatzort vorhandenen Schwebstoffe abgestimmte Kalibrierung, welche vorzugsweise vorgängig im Labor unter kontrollierten Bedingungen durchgeführt wird.

Die heutzutage auch für in-situ-Messungen verfügbare Methode der Laserdiffraktometrie ermöglicht es, die Schwebstoffkonzentration bei wechselnden Partikeleigenschaften genauer zu bestimmen und Informationen über die Korngrössen zu gewinnen, was für den Hydroabrasivverschleiss ein wichtiger Parameter ist. Weiter können akustische Durchflussmessungen, wie sie an zahlreichen Wasserkraftwerken vorhanden sind, durch geringfügige Anpassungen zumindest für ein qualitatives Schwebstoffmonitoring verwendet werden, was den Vorteil einer Messung direkt im Triebwasserweg mit sich bringt.

Die durchgeführten Laborversuche werden weiter ausgewertet und die Untersuchungen an der Kraftwerksanlage weitergeführt. Neben den Schwebstoffmessungen werden auch die Schädigung der Turbinen und die Wirkungsgradänderungen periodisch erfasst.

Ein verschleissoptimierter Betrieb von Wasserkraftanlagen erfordert eine langjährige Datengrundlage und eine anlagenspezifische Betrachtung des Gesamtsystems über den Lebenszyklus. Schlussendlich sollen die Forschungsergebnisse zur Effizienzsteigerung der Wasserkraft beitragen.

Verdankung

Das Forschungsprojekt wird durch swisselectric research, das Schweizer Bundesamt für Energie (BFE) und die Gommerkraftwerke (GKW) finanziell unterstützt. Die Autoren bedanken sich bei diesen sowie den weiteren eingangs genannten Projektpartnern für ihr Engagement und für die Unterstützung bei der Durchführung der Laborversuche und der Felddatenerhebung. Ein weiterer Dank geht an die Firma Sigrist Photometer, Ennetbürgen, welche ein Trübungsmessgerät für die Laboruntersuchungen zur Verfügung gestellt hat, sowie die Firma Rittmeyer, Baar, für die Unterstützung betreffend der akustischen Messmethode.

Literatur

Abgottspon, A. (2011): Messung abrasiver Partikel in Wasserkraftanlagen. Masterarbeit (unveröffentlicht), CC Fluidmechanik & Hydromaschinen, Hochschule Luzern.

Agrawal, Y., Mikkelsen, O.A., Pottsmith, H.C. (2011). Sediment monitoring technology for turbine erosion and reservoir siltation applications. Proc. Hydro 2011 Conference, Aqua-Media Intl. Ltd., Prague, Czech Republic.

Bishwakarma, M.B., Støle, H. (2008). Realtime sediment monitoring in hydropower plants. J. Hydr. Res. 46 (2): 282–288.

Boes, R. (2010). Kontinuierliche Messung von Schwebstoffkonzentration und -korngrössenverteilung im Triebwasser und Quantifizierung

der Hydroabrasion an einer Peltonturbine. «Wasser Energie Luft» 102 (2): 101–107.
DIN 50320 (1979). Verschleiss; Begriffe, Systemanalyse von Verschleissvorgängen, Gliederung des Verschleissgebietes. Deutsches Institut für Normung, Beuth-Verlag, Berlin.
DWA (2006). Entlandung von Stauräumen. DWA-Themen, Deutsche Vereinigung für Wasserwirtschaft, Abwasser und Abfall e.V., Hennef (Hrsg.).
Felix, D., Albayrak, I., Boes, R.M. (2012a). Schwebstoffmonitoring und Verschleiss an Peltonturbinen am Fallbeispiel Fieschertal – Vorbereitende Laborversuche zu Partikelmessmethoden. Proc. Wasserbausymposium, TU Graz (G. Zenz, ed.), A15: 117–124.
Felix D., Albayrak I., Abgottspon A., Boes R., Gruber P. (2012b). Suspended Sediment and Pelton Turbine Wear Monitoring: Experimental Investigation of various Optical and Acoustic Devices and Beginning of the Case Study at HPP Fieschertal. Proc. 17^{th} Intl. Seminar on Hydropower Plants (Viennahydro), ISBN 978-3-9501937-8-7. Wien, 483–494.
Gippel, C.J. (1995). Potential of turbidity monitoring for measuring the transport of suspended solids in streams. Hydrological Processes 9: 83–97.
Götsch, H. (2012). Private Kommunikation.
Nozaki, T. (1990). Estimation of repair cycle of turbine due to abrasion caused by suspended sand and determination of desilting basin capacity. Report Japan International Cooperation Agency, Tokyo.
Ortmanns, C. (2006). Entsander von Wasserkraftanlagen. Mitteilung 193, Versuchsanstalt für Wasserbau, Hydrologie und Glaziologie (H.-E. Minor, ed.), ETH Zürich.
Sutherland, T.F., Lane, P.M., Amos, C.L., Downing, J. (2000). The calibration of optical backscatter sensors for suspended sediment of varying darkness levels. Marine Geology 162: 587–597.
Winkler, K., Dekumbis, R., Rentschler, M., Parkinson, E., Garcin, H. (2011). Understanding hydro-abrasive erosion, Proc. Hydro 2011 Conference, Aqua-Media Intl. Ltd., Prague, Czech Republic.

Anschrift der Verfasser
Versuchsanstalt für Wasserbau, Hydrologie und Glaziologie (VAW), ETH Zürich, CH-8092 Zürich
Prof. Dr. *Robert M. Boes*
boes@vaw.baug.ethz.ch
David Felix, felix@vaw.baug.ethz.ch
Dr. *Ismail Albayrak*
albayrak@vaw.baug.ethz.ch

Advances in River Sediment Research – Fukuoka et al. (eds)

Monitoring of suspended sediment—laboratory tests and case study in the Swiss Alps

D. Felix, I. Albayrak & R.M. Boes
Laboratory of Hydraulics, Hydrology and Glaciology (VAW), Swiss Federal Institute of Technology (ETH), Zurich, Switzerland

ABSTRACT: There is an increasing demand for continuous real-time monitoring of Suspended Sediment Concentration (SSC) and Particle Size Distribution (PSD), e.g. for sustainable operation of hydraulic schemes. Most optical and acoustic devices need to be calibrated with respect to the properties of the suspended particles. Prior to a field study in the Swiss Alps, various turbidimeters, a portable laser diffractometer (LISST) and an ultrasonic system were tested in suspensions made of various mineral particles in a mixing tank. Significant influences of particle size and shape on the SSC estimation were observed and quantified. The data from the devices that have subsequently been installed in the headwater of a hydropower plant confirm temporal variation of PSD and allow cross-comparing the measuring capabilities of the devices under field conditions. LISST has the advantage to provide not only SSC but also PSD, and SSC data is less or not affected by varying size of suspended particles.

1 INTRODUCTION

Sediment transport in rivers and waterways is an important issue when planning and operating hydraulic schemes. Particularly, hydro-abrasive wear at turbines due to hard suspended mineral particles in the water or reservoir siltation may cause substantial maintenance costs and significant negative impact on power generation and revenue at Hydroelectric Power Plants (HPP). For optimized design and operation of hydraulic structures as well as for environmental concerns, there is an increasing need for real-time monitoring of Suspended Sediment Concentration (SSC) and Particle Size Distribution (PSD) in rivers, lakes and seas.

Such data can be used for a better design of desilting facilities or sand traps at hydraulic schemes, conveying or removing sediments from reservoirs by evacuating suspended sediment through outlets of dams or power waterways (e.g. Jenzer Althaus 2011), and for estimates of hydro-abrasive wear at turbines (e.g. Winkler et al. 2011). Real-time data on SSC and PSD from streams at intakes and/or waterways of HPPs can be used as a basis for economically optimized operation in which actual wear of hydraulic turbines is considered with the option of temporary switch-offs of HPPs during suspended sediment peaks.

Thus, the Laboratory of Hydraulics, Hydrology and Glaciology (VAW) of the Swiss Federal Institute of Technology, ETH Zurich, initiated an interdisciplinary research project in collaboration with Hochschule Lucerne, supported by swisselectric research, the Swiss Federal Office of Energy, a HPP operator (Gommerkraftwerke) and co-owner (Bernische Kraftwerke) as well as industry partners (Andritz Hydro and Rittmeyer). As an initial part of this project various devices for Suspended Sediment Monitoring (SSM) were investigated in the first half of 2012. As a second and main part of this project, these devices were installed in the existing HPP Fieschertal located at a tributary of the upper Rhone River in the Swiss Alps for continuous real-time in-situ SSM.

This paper presents selected results of the laboratory investigation and exemplary field data from a suspended sediment transport event that occurred at the study HPP in late summer 2012. The presented event may occur several times a year and gives thus an impression of the measuring capabilities of the devices during the sediment season.

Information on parts of this laboratory investigation as well as a preliminary analysis of suspended sediment data during a major flood event in July 2012 are given by Felix et al. (2012). In the following section, an overview of measuring techniques for SSC and PSD is given. Thereafter, the experimental setup and methodology, and the results and discussion for the laboratory and field investigations are presented, followed by conclusions and outlook.

2 MEASURING TECHNIQUES

2.1 *Suspended sediment concentration (SSC)*

Suspended Sediment Concentration (SSC, in g/l) of mineral particles can be determined by laboratory analysis of bottle samples (discontinuous) or using mainly acoustic or optical instruments (continuous). Bottle sampling can be made manually or automatically and is a direct, widely used and reliable technique. However, it has many disadvantages such as time consuming laboratory analysis of the samples, effort of transporting bottles from the study sites to the laboratory, being flow intrusive, having a poor temporal resolution and giving results not in real-time (Wren et al. 2000).

As an optical technique, turbidimeters are popular and widely used for SSM at rivers and lakes (e.g. Spraefico et al. 2005, Habersack et al. 2008). These devices measure either the scattering (at one or several angles, then they are also called optical backscatter probes) or the absorption (transmission) of near infrared or laser light. Output values are given in optical units (e.g. Formazine Nephelometric Unit, FNU) and have to be converted to SSC. Therefore, a custom calibration based on the particle properties (particle size, shape, colour or composition) is required (e.g. Gippel 1995). A main disadvantage of turbidimeters is the problem of the dependency on particle size and shape.

Recently, portable laser diffractometers (Laser in-situ Scattering and Transmissiometry, LISST) have become available for in-situ SSM (e.g. Boes 2009, Agrawal et al. 2011, Agrawal et al. 2012). SSC estimates made by LISST have the advantage of being not or less dependent from particle size since particle size is considered in the design of the instrument and its software. The use of in-situ laser diffractometers for SSM at rivers and lakes is not yet widespread, because it is relatively expensive and its SSC measuring range (without dilution) is limited.

Acoustic methods are another approach to monitor SSC. Among many possibilities (backscatter as used in ADCP etc.) the method of measuring the attenuation of ultrasonic pulses sent through the sediment-laden water in tunnels, penstocks or channels is of particular interest for HPP operators since installations for Acoustic Discharge Measurement (ADM) existing at many HPPs can be upgraded to be used for SSM. This method of single frequency acoustic forward scattering (e.g. investigated by Costa et al. 2012) can be calibrated for constant particle properties. In order to determine SSC at variable particle sizes the use of multi-frequency-acoustics is required. Such methods are currently under development (e.g. Skripalle et al. 2012).

Lastly, the SSC of sediment-laden flow can be determined by measuring its density with a precise, temperature compensated Coriolis mass flow meter (Biswakarma & Støle 2008) if SSC is above approximately 0.5 g/l. This mass-based method has the advantage of being not sensitive to particle properties.

2.2 *Particle size distribution (PSD)*

Besides SSC, PSD of mineral particles in the water is an important parameter for sediment dynamics (transport, deposition and re-suspension) and hydro-abrasive wear of turbines.

The primary method to obtain PSDs is by sieve analysis of collected particles. Especially for smaller fractions, laser diffraction has been used in laboratories for decades. However, as mentioned above, analysing collected sediment in the laboratory has many disadvantages. Therefore, portable laser diffractometers are recently used as a practical real-time monitoring system of both SSC and PSD in field studies.

3 EXPERIMENTAL SET-UP AND METHODOLOGY

3.1 *Laboratory investigation*

3.1.1 *Experimental set-up*

Prior to the field study the devices for SSM were tested in the hydraulic laboratory of Hochschule Lucerne at the facility of the Competence Centre for Fluid Mechanics and Hydro Machines. Experiments were carried out in an existing mixing tank (Abgottspon 2011) equipped with a stirrer (Fig. 1). All devices were placed in the tank at

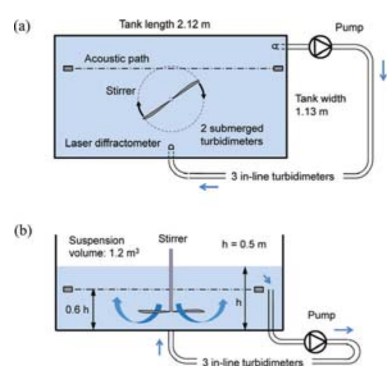

Figure 1. Mixing tank in the hydraulic laboratory with optical and acoustic devices for measuring suspended sediment, (a) plan view and (b) vertical section (Felix et al. 2012).

the same level in order to reduce effects of possible vertical SSC gradients.

3.1.2 *Tested devices*

The devices used for SSM are listed in Table 1. Two different submersible turbidimeters with wipers were installed in the tank. Two in-line type turbidimeters were installed in the pump line connected to the tank. Another turbidimeter, which measures scattering of light at a free falling jet, was mounted above the tank and fed from the pump line, letting the water fall back into the tank.

Among the available portable laser diffraction devices a *LISST-100X*, Type C with a nominal particle size measuring range from 2.5 to 500 microns (10^{-6} m) was selected. These size limits apply to spherical particles; for random shaped particles the size range is 2 to 380 microns. In contrast to a stream-side type model, this submersible instrument can be used for investigations of SSM in reservoirs (down to 300 m water depth) and desilting facilities, too. In order to extend the range of measurable concentrations the optical path length was reduced from 50 mm to 5 mm by insertion of a 90%-path reduction module (glass cylinder).

As far as acoustics are concerned, ultrasonic transducers operating at 1 MHz at a path length of 1.73 m were used in the experiments (Fig. 1a & b). The signal sent by the emitter, i.e. by one of the ultrasonic transducers, is attenuated (damped) when travelling through the water or the suspension to the receiver. The attenuation due to the existence of suspended particles in the water (excess attenuation) is examined. The difference between the received signal's amplitudes in clear water A_c and in the suspension A_s gives the amplitude of attenuation due to suspended sediments A_a (Equation 1). The relative attenuation A_r due to suspended sediment is obtained by normalizing A_a with A_c (clear water). Thus $A_r = 0$ in clear water, increasing with SSC (up to 1).

$$A_a = A_c - A_s \qquad (1)$$

$$A_r = A_a / A_c \qquad (2)$$

3.1.3 *Tested mineral particles*

The previous studies at HPP Fieschertal show that the mineral particles prevailing in the turbined water are mainly quartz, feldspar and mica, i.e. the components of Granite rock, and the size of the mineral particles in normal summer conditions (with glacier melt) was estimated to be d_{50} = 20 to 40 microns (d_{50} stands for the diameter of graded particles of which 50% by mass is finer). During flood events bigger particles up to 0.3 or 0.5 mm corresponding to the design grain size of sand traps of HPPs may be transported in the turbine water.

In the mixing tank experiments feldspar powder, mica powder, fine quartz sand and natural sediment of the study HPP were used. The latter was taken from deposits in the tailrace channel whereas the other three types of particles were bought from commercial applications. It should be noted that the natural sediment taken from the tailrace channel is coarser than the sediment normally found in the turbine water since these particles settled while finer ones were transported downstream.

The size distributions of the particles used in the experiments are shown in Figure 2. These results were obtained from the measurements performed by a non-portable laser diffraction instrument (*Horiba*) in the geotechnical laboratory of ETH Zürich. Note that particle samples for the sieve analysis were taken from the boxes in which

Table 1. Tested devices for suspended sediment monitoring.

Type	Model	Manufacturer
T (submerged)	*Solitax ts-line sc*	Hach-Lange
T (submerged)	*Turbimax W CUS41*	Endress-Hauser
T (in-line)	*TurbiScat (90°, 25°)*	Sigrist Photometer
T (in-line)	*TF16-N with F20*	Optek Danulat
T (free fall)	*AquaScat*	Sigrist Photometer
LD	*LISST-100X, Type C*	Sequoia Scientific
ADM	*Risonic Modular*	Rittmeyer

Legend: T = Turbidimeter, LD = Laser diffractometer and ADM = acoustic system as used in acoustic discharge measurement.

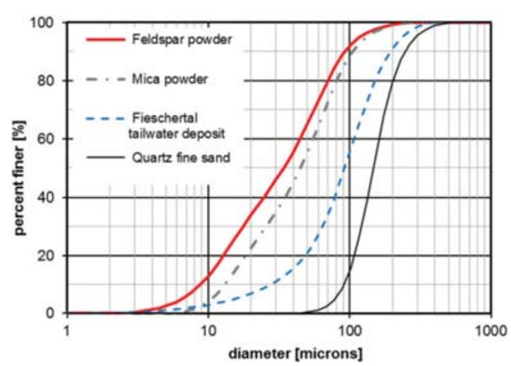

Figure 2. PSDs of selected mineral particles used in the laboratory tests of suspended sediment measuring devices.

the particles were kept prior to the mixing tank experiments. The grading of the natural particles collected from the tailrace channel may not be homogeneous throughout the whole lot.

Based on the images from a scanning electron microscope (Fig. 3) feldspar powder, mica powder and fine quartz sand particles have angular (from grinding), flaky (corresponding to the mechanical properties of mica) and rounded (natural sand) shapes, respectively. The natural sediment from the study site is expected to be composed of particles of these shapes. The size information on the mica particles have to be interpreted with precaution since it is not clear how laser diffraction determines the diameter of flaky particles.

Furthermore, fine glass spheres and quartz powder were used in the experiments. Glass spheres were included in the test program to allow a later comparison with theoretical models of attenuation and scattering of light or sound, in which particles are assumed to be spherical.

3.1.4 *Methodology*

Firstly, a zero measurement of all devices was done in still drinking water. Then the SSC was step-wise increased and the measurements at each step were simultaneously done with all devices until the SSC-measuring range of most devices was exceeded. SSC was increased up to 50 g/l for coarser particles (fine sand).

For the turbidimeters and the acoustic system 500 data points were recorded at a frequency of 1 Hz at each nominal SSC level. For LISST, 100 values were recorded at the frequency of about 2 Hz at each nominal SSC level. Finally, the data obtained from each device were time-averaged for each SSC-level.

Reference SSCs were determined by weighing of suspension samples before and after drying in an oven. The weight of minerals that were dissolved in the drinking water before drying of the sample was deducted from the residue. Three samples per nominal SSC-level were taken from the tank at the same vertical position as the instruments were placed.

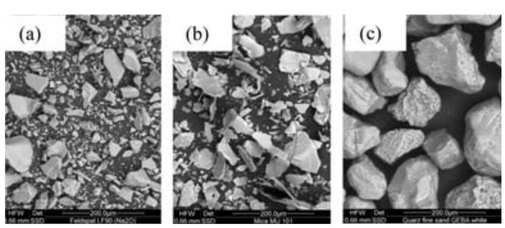

Figure 3. Selected mineral particles used for laboratory tests, (a) feldspar powder, (b) mica powder and (c) quartz fine sand.

For feldspar and mica powders the reference SSCs agreed well with nominal SSCs that were calculated from the amount of water and particles added to the tank. With coarser particles, such as fine quartz sand and the particles from the tailrace channel of the study site, however, SSCs determined in the tank at the level of the instruments were lower than nominal SSCs. This can be attributed to settling of coarser fractions due to insufficient mixing.

The LISST records the intensity of scattered laser light at 32 ring detectors and the attenuation in the axis of the laser beam. From these values the volume concentrations in 32 log-spaced size classes can be calculated, using the corresponding software (inversion algorithm) from the instrument manufacturer. The inversion mode assuming "irregular shaped" particles (Agrawal et al. 2008) was used for the calculation of the results presented here (no spherical particles). The total volume concentration of suspended sediment results from summing up the volume concentrations of all 32 size bins.

For the conversion of volume concentration to mass concentration (SSC) a density of 2.65 kg/l (standard value for quartz) was assumed for all materials, leading to an error of presumably less than 10%.

3.2 *Field investigation*

3.2.1 *Installations at the study HPP*

After the laboratory tests were completed in June 2012 two turbidimeters and the LISST have been installed at the waterway of the high-head HPP Fieschertal (Fig. 4), a run-of-river type HPP located in the Canton of Valais, in the Alps of Switzerland.

Water used in the HPP comes from a mountain stream emerging from a glacier, which is on retreat. This glacier leaves an abundance of easily erodible sediments of all sizes in the lower part of the barely vegetated catchment area.

At this HPP, there is no storage lake in which fine particles could settle. In the free surface flow tunnel, partial settling and also re-suspension of

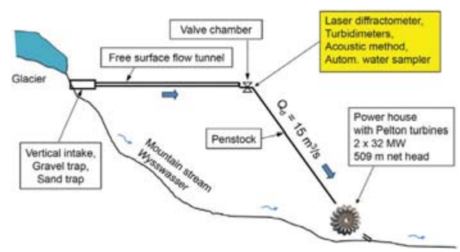

Figure 4. Schematic longitudinal profile of Fieschertal HPP at which suspended sediment is monitored.

particles occur according to the operation conditions (in- and outflowing discharge, water level). Since the commissioning of the HPP in 1976 relatively high SSC have been observed in the turbine water during the summer season.

In the valve chamber, two turbidimeters (*TF16-N* and *TurbiScat*) as well as the LISST are fed through a pipe (DN 40 mm) with sediment-laden water taken from the axis of the penstock (Abgottspon 2011). The measuring end of the LISST device is inserted laterally into a bucket with an overflow and a flushing outlet. An automatic water sampler (*Isco 3700*) with 24 bottles was installed with a suction line from the LISST bucket.

As far as the acoustic method is concerned, no modification of the existing ADM installation was required. The ADM is a four path arrangement on two horizontal layers in the penstock, with 1 MHz and path lengths of 2.27 m. At the controller of the ADM the amplitudes of the received signals at the four paths were defined as additional output signals.

The output signals of all instruments were connected to a data acquisition board running with an industrial computer which can work under tough field conditions.

3.2.2 *Methodology*

Data from the turbidimeters and the acoustic method were recorded at 1 Hz; LISST-measurements were performed and saved every minute. The time series in Figures 9, 10 and 12 were obtained by plotting one-minute values, smoothed with moving average.

The automatic water sampler was set to take water samples every two days and more frequently in case of increased SSC. The water sampler is controlled by a custom-made software that is triggered by a turbidimeter. Sampling rules depend on several turbidity levels, which can be adjusted depending on the season.

4 RESULTS AND DISCUSSION

4.1 *Laboratory investigation*

4.1.1 *Turbidimeters*

The calibration curves of a submersible and an in-line optical backscatter probe obtained from the laboratory measurements are presented in Figures 5 & 6, respectively. The values of d_{50} for the four types of particles indicated in the legends of Figures 5 and 6 were obtained from the reference laser diffraction measurements (Fig. 2).

The relationships between reference SSC and turbidity can be approximated with linear functions for both turbidimeters (Figs. 5 & 6). As known from literature, turbidity is not only a function of SSC but also of particle size, shape and optical properties.

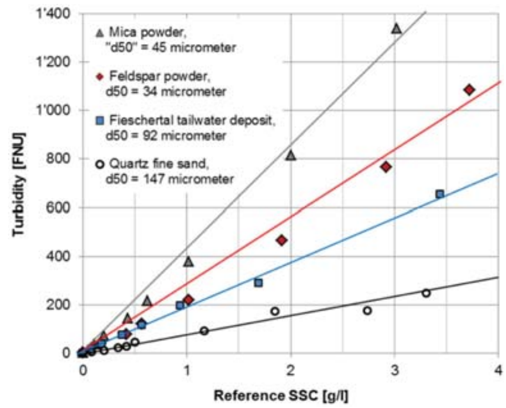

Figure 5. Turbidity measured with a submerged optical backscatter probe (*Solitax ts-line sc*) as a function of reference SSC.

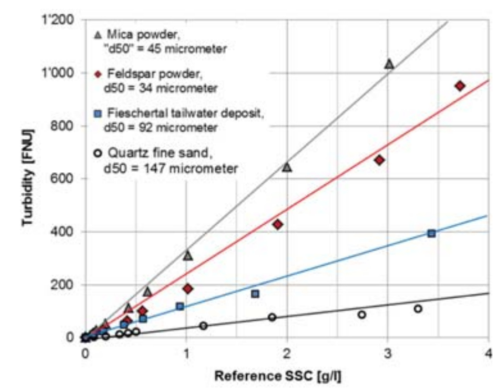

Figure 6. Turbidity measured with an in-line optical backscatter probe (*TurbiScat, 90°*) as a function of reference SSC.

The calibration curves of both devices are qualitatively similar. The *Solitax ts-line sc* yields higher values than the 90° channel of the *TurbiScat* although both devices measure turbidity in the same physical unit (FNU). This means that for accurate SSC estimates not only particle-specific but also instrument-specific calibrations are required.

4.1.2 *Acoustic system*

Figure 7 shows the relationship between the relative attenuation A_r due to suspended sediment and the reference SSC for each type of particles. Up to about 6 g/l the relationships can be approximated with linear functions. At higher SSC a non-linear fitting is required.

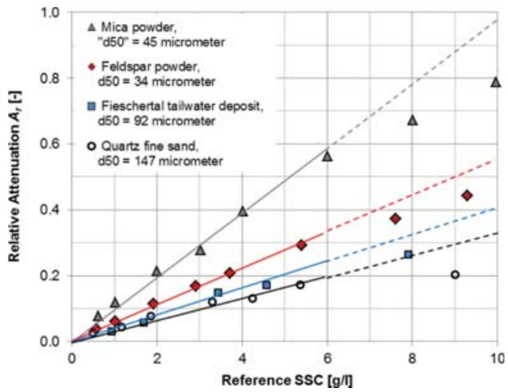

Figure 7. Relative attenuation A_r of ultrasonic pulses due to suspended sediment particles as a function of reference SSC.

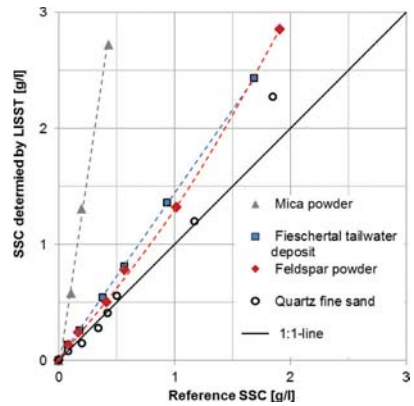

Figure 8. SSCs determined by LISST as a function of reference SSCs.

Comparable to optical backscatter, the damping due to the particles is not only a function of SSC, but also of particle size and shape. The curves of the four types of particles in Figure 7 are in the same sequence as those of turbidity (Figs. 5 & 6).

Compared to Figures 5 & 6, the range between the curves of the finest to the coarsest type of particles is smaller in Figure 7. This is a sign for a less pronounced effect of particle properties in the acoustic method compared to optical backscatter (turbidimeters), indicating a reduction in possible errors in SSC estimates when using a fixed calibration in case of variable particle properties.

The acoustic method with the frequency and path length used here is not well adapted to measure SSCs below 0.5 g/l, but allows measuring up to higher SSCs in comparison to the turbidimeters.

4.1.3 *Laser diffraction*

The relationships between SSCs measured by LISST and the reference SSCs are shown in Figure 8 for the four types of particles.

The measured data for fine quartz sand are generally in good agreement with the 1:1-line. It should be noted that no custom calibration was applied and the SSC in the tank was subject to possibly imperfect mixing.

For feldspar powder, the LISST increasingly overestimates SSC as SSC increases, mainly due to relatively high contributions in the lowest size classes. This effect becomes more pronounced as the SSC approaches the upper measurement limit of the LISST. Possible reasons for overestimation at lower size bins can be multiple scattering, strongly non-spherical particle shape or refractive index (Agrawal & Pottsmith 2000, Agrawal et al. 2008, Andrews et al. 2011).

For the mica powder LISST SCCs are about 6 times higher than reference SSCs. This can be attributed to the flaky shape of these particles that produces over-proportional scattering compared to particles with a more compact shape at given SSC.

For the natural sediment particles from Fieschertal, which are coarser than the feldspar and the mica powders, the LISST overestimates SSC by about 40%. It is assumed that this approximately constant deviation can be attributed to particle shape as the Fieschertal sediments contain mica and angular particles.

Furthermore, PSDs can be calculated from the volume concentrations in the 32 size classes. PSD data from LISST experiments are currently being evaluated. When comparing LISST PSDs measured in the tank to reference PSDs (from non-portable laser diffraction) the effect of possibly imperfect mixing in the tank and uncertainty in true PSDs of non-spherical particles have to be taken into account.

4.2 *Field investigation*

4.2.1 *Laser diffraction*

Figure 9 shows—as an example—the time series of SSC measured by LISST during two weeks in late summer 2012. Time is indicated in days from the beginning of the year 2012. As in the data analysis of the laboratory experiments, the “random shaped” inversion mode was used and a density of 2.65 kg/l as for quartz was assumed. No corrections for effects of particle shape or for overestimations at lower size bins (possibly due to fine out-of-size-range particles, as e.g. described by Andrews et al. 2011) were applied yet. The bold dots in Figure 9 indicate the reference SSCs obtained from

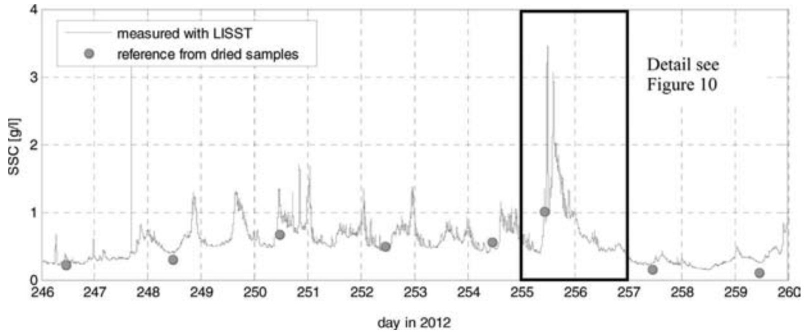

Figure 9. SSC obtained from LISST-measurements in comparison to laboratory results of water samples (September 3 to 17, 2012).

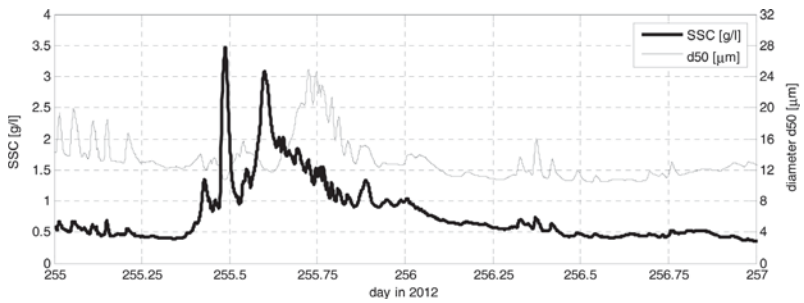

Figure 10. SSC and diameter d_{50} from LISST during a minor suspended sediment transport event (September 12 and 13, 2012). A, B, C and D indicate times at which selected PSDs are plotted in Figure 11.

laboratory analysis of the bottle samples taken by the automatic sampler.

The LISST SSCs lie in reasonable agreement with the reference SSCs in most cases displayed in Figure 9. The LISST SSC tends to be higher than the reference SSC. This can be attributed to the shape effect or overestimations at lower size bins. Deviations between the LISST and the reference SSCs will be further analyzed. Typical daily patterns of SSC (from glacier melt), SSC peaks induced by precipitation events and periods of relatively low SSC are seen in Figure 9.

Figure 10 shows a detail of two selected days of the SSC time series from Figure 9, corresponding to September 12 and 13, 2012. During approximately one day, the SSC rose from 0.5 to 3.5 g/l and fell back to the initial level. The thin line in Figure 10 shows the time-series of the d_{50} of the particles measured by LISST (right axis).

The d_{50} increased from about 12 to 24 microns and fell back to the initial level. Interestingly, the peak in d_{50} occurred some six hours after the SSC peak. A physical reason for this could be that finer particles are transported before coarser ones. Before and after the period of increased SSC,

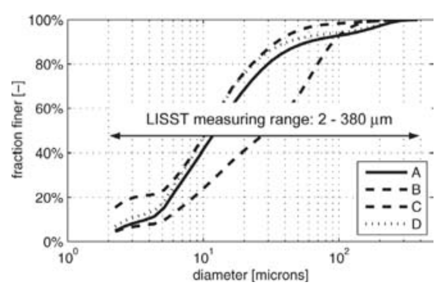

Figure 11. Selected PSDs obtained from LISST, at times specified in Figure 10.

however, peaks of SSC and d_{50} occurred simultaneously (in the time range of Fig. 10). The sediment dynamics in the free surface tunnel including in- and outflowing discharge and water level will be further analysed.

In the rising limb of the SSC curve the d_{50} curve dips during SSC peaks. This can be partly real and partly an effect of overestimation at lower size bins (see curve B in Fig. 11). The cross-correlation between d_{50} and SSC will be further analysed.

Figure 11 shows four selected PSDs measured by LISST; (A) and (D) before and after the SSC peak, (B) at the SSC peak and (C) at the d_{50} peak. Whereas curves A, B and D are comparable, curve C indicates a considerably coarser particle distribution (in the range below 100 microns). Overestimation at lower size bins can lead to PSDs which do not depart from zero at the lower end of the size measuring range (especially curve B). Corrections to reduce overestimation of concentrations at lower size bins in LISST measurements will have to be further studied.

4.2.2 *Turbidimeters*

Figure 12a shows the time series of turbidity measured by *TurbiScat* at 90° in comparison to SSC measured by LISST (as in Fig. 10). This in-line turbidimeter (without wiper) was affected by biofouling and deposition of particles on the window of the flow-through cell even though the water temperature did never exceed 2°C. The raw data recorded at this device show a general temporal increase (trend) of turbidity from the installation in early summer (correct measurement with clean window) to the beginning of the winter season (increasingly biased measurement). This trend, however, is not continuous since manual flushing of the sampling pipe was done occasionally, leading to offsets in the recordings. The turbidity time series shown in Figure 12a was de-trended (by 40 FNU per day). The unknown offset in the turbidity time series could not be removed. With the selected scaling of the turbidity axis in Figure 12a a relative comparison with the LISST SSC is however possible.

The turbidity time series matches reasonably with that of LISST SSC until September 12 at 6 p.m. (day 255.75). Then, the turbidimeter data deviate from the LISST data as the first do not fall back completely to the level before the sediment transport peak. This remaining offset is attributed to the deposition of particles and bio-fouling on the window in the flow-through cell of the in-line turbidimeter.

4.2.3 *Acoustic system*

Figure 12b shows the time-series of the relative attenuation A_r from the acoustic method again in comparison to SSC measured by LISST (as in Fig. 10). A_r can be used to derive an SSC-estimate. With an appropriate scaling A_r is generally well in line with the LISST data. Peaks measured by the acoustic method are less pronounced compared to the LISST measurement. LISST SSC peaks may be overestimated due to overestimation at lower size bins.

In Figure 12b, during some hours around September 12, 6 p.m. (day 255.75), the offset between the two curves is slightly different compared to the rest of the time. This is attributed

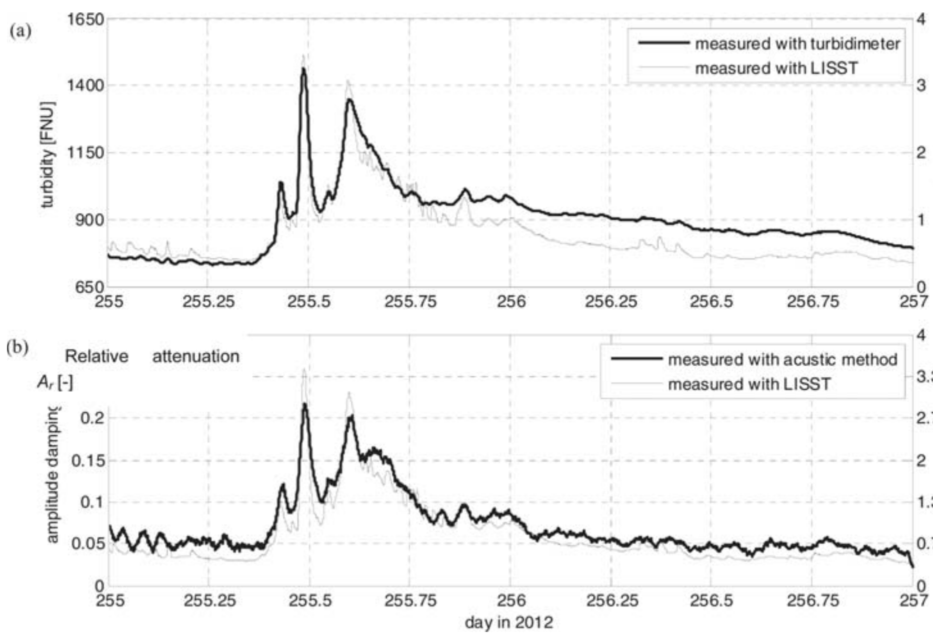

Figure 12. Measurements of (a) in-line turbidimeter (*TurbiScat, 90°)* and (b) relative attenuation A_r obtained from acoustic method, both in comparison to SSC measured by LISST (right axes), from September 12 to 13, 2012.

to effects of varying particle size (compare d_{50} in Fig. 10) and can be observed accordingly for the turbidimeter in Figure 12a.

The good temporal correlation between A_r and LISST data also indicates that the sampling pipe was not clogged and the sediment-laden water measured at the end of the sampling pipe differs not much from the water in the penstock.

The field data on acoustics (Fig. 12b) cannot directly be compared to the laboratory data (Fig. 7), since the path lengths are different. The attenuation of ultrasonic pulses due to the particles shall be normalized considering the length of the acoustic path.

5 CONCLUSIONS

The calibration and measuring range of various optical and acoustic devices for SSM were assessed in the laboratory using different types of mineral particles in a range of concentrations and selected results were presented in the first part of this paper.

It was found that turbidimeters have to be calibrated for each device and each type of particles. This requires quite an effort. Such fixed calibrations may lead to considerable uncertainties in SSC measurements if the particle properties vary in time. The acoustic method seems to be less sensitive to particle size and shape.

The LISST allows measuring SSC and PSD of particles in the range of medium silt to fine sand. SSCs obtained from LISST showed generally good agreement with reference SSCs if the particle shape does not differ considerably from the rounded or slightly angular particle shape assumed in the current inversion procedure. The existence of mica with a flaky shape or strongly angular particles may lead to a considerable overestimation of SSC.

The operating range of the used *LISST-100X* with the strongest available 90% path reduction module is limited to a few g/l of the used mineral powders with d_{50} in the range of coarse silt. Another model of in-situ laser diffractometers with automatic dilution (*LISST-Infinite*) would allow measuring up to 90 g/l according to the supplier's specifications.

In the second part of this paper the installation of the devices for SSM at the study HPP in the Swiss Alps was described and examples of the field data on SSM were given. The presented data from late summer 2012 cover "normal" suspended sediment transport conditions with glacier melt and an example of a suspended sediment transport event.

In the presented period the LISST provides reasonable estimates of SSC when compared to reference SSCs obtained from bottle samples. SSM based on laboratory analysis of occasionally taken bottle samples would not be sufficient to capture the SSC dynamics in this environment. In the example data, coarser particles were observed in conjunction to an SSC peak. A time shift between the peaks in SSC and d_{50} was observed. In the present research project information on PSD is important as it is a decisive parameter for turbine wear. LISST offers the great advantage to collect information on PSD with high temporal resolution directly at the study site.

For turbidimeters, models with a wiper or no window in contact to the sediment-laden water are advisable to use, even in cold and nutrient-poor water, in order to avoid effects of bio-fouling and deposition of particles in the instrument optics. Frequent manual cleaning (with opening of the flow cell) is not practical and flushing with temporarily increased discharge is not sufficient. With the relatively moderate variation in average particle size during the presented suspended sediment event of small extent, a turbidimeter with a fixed custom calibration is able to provide reasonable estimates of SSC. With stronger variations of particle size, however, larger errors in SSC estimates have to be expected according to the laboratory investigations.

Using ADM systems for SSM is an interesting option for operators of hydraulic schemes at which relatively high SSC occur. No requirement for additional hardware and sampling pipes and the direct measurement of path-averaged values in the waterway are practical advantages of SSM monitoring based on ADM installations. However, with the current state of research, a site-specific calibration for time-averaged particle properties is required in order to convert the measured values in g/l (as for turbidimeters). For qualitative warnings of high SSC events to operators of hydraulic schemes no conversion to g/l is required. Since this acoustic method is not suitable to measure SSC below approx. 0.5 g/l a combination with an optical device can be advantageous.

6 OUTLOOK

The measurements at the study HPP will be continued and the installations will be extended (e.g. turbidimeter and automatic water sampler at the intake) and modified based on the first year's experiences.

The data from the laboratory measurements and the field including a major flood event with measured SSC in the range of 50 g/l in July 2012 will be further evaluated. The laboratory analysis of on-going water sample collection will be used for the interpretation and calibration of the recorded data in order to estimate the sediment flux in the penstock and the abrasion potential (considering particle size and particle hardness based on mineralogical composition).

In view of the damages observed on the turbine runners after a major flood event the option of temporary turbine shutdowns for some hours during significant sediment peaks will be further investigated towards the determination of economically balanced switch-off criteria based on SSC and possibly PSD.

ACKNOWLEDGEMENTS

The authors gratefully acknowledge the support by Swisselectric Research, the Swiss Federal Office of Energy and Gommerkraftwerke AG. Thanks go to the project partners, especially to Prof. Dr. T. Staubli, Prof. Dr. P. Gruber, A. Abgottspon und M. Duss from Hochschule Lucerne, Competence Center for Fluid Mechanics and Hydro Machines. A further thank is to Rittmeyer and Sigrist Photometers for providing measuring equipment.

REFERENCES

Abgottspon, A. 2011. Messung abrasiver Partikel in Wasserkraftanlagen. *Master thesis* (unpublished, in German), Hochschule Luzern, CC Fluid Mechanics and Hydro Machines, Lucerne, Switzerland.

Agrawal, Y.C. & Pottsmith, H.C. 2000. Instruments for particle size and settling velocity observations in sediment transport, *Mar. Geol.* 168: 89–114.

Agrawal, Y.C., Whitmire, A., Mikkelsen, O.A. & Pottsmith H.C. 2008. Light scattering by random shaped particles and consequences on measuring suspended sediments by laser diffraction, *Journal of Geophysical Research* 113.

Agrawal Y., Mikkelsen, O.A. & Pottsmith, H.C. 2011. Sediment monitoring technology for turbine erosion and reservoir siltation applications. *Proc. Hydro 2011 Conference*, Aqua-Media Intl. Ltd., Prague, Czech Republic.

Agrawal, Y., Mikkelsen, O.A., Pottsmith, H.C. & Slade, W.H. 2012. Turbine abrasion: one year's experience in real-time sediment monitoring at Hidroagoyan HPP, Ecuador. *Proc. Hydro 2012 Conference*, Aqua-Media Intl. Ltd., Bilbao, Spain.

Andrews, S.W., Nover D.M., Reuter J.E. & Schladow S.G. 2011. Limitations of laser diffraction for measuring fine particles in oligotropic systems: Pitfalls and potential solutions. *Water Resources Research*, 47.

Bishwakarma, M.B. & Støle, H. 2008. Realtime sediment monitoring in hydro-power plants. *Journal of Hydraulic Research* 46(2): 282–288.

Boes, R. 2009. Real-time monitoring of SSC and PSD in the headwater way of a high-head hydropower plant. *Proc. 33rd IAHR Congress*, Vancouver, Canada: 4037–4044.

Costa, I., Storti, G., Lüscher, B., Gruber, P. & Staubli, T. 2012. Influence of solid particle parameters on the sound speed and attenuation of pulses in acoustic discharge measurements (ADM). *Journal of Hydrological Engineering,* 17(10): 1084–1092.

Felix, D., Albayrak, I., Abgottspon, A., Boes, R. & Gruber, P. 2012. Suspended Sediment and Pelton Turbine Wear Monitoring: Experimental Investigation of various Optical and Acoustic Devices and Beginning of the Case Study at HPP Fieschertal. *Proc. 17th International Seminar on Hydropower Plants*. Vienna: 483–494.

Gippel, C.J. 1995. Potential of turbidity monitoring for measuring the transport of suspended solids in streams. *Hydrological Processes* 9: 83–97.

Habersack, H., Haimann, M., Kerschbaumsteiner, W. & Lalk, P. 2008. Schwebstoffe im Fliessgewässer, *Leitfaden zur Erfassung des Schwebstofftransportes*. Bundesministerium für Land- und Forstwirtschaft, Umwelt und Wasserwirtschaft BLFUW (Hrsg.), Wien, Österreich (in German).

Jenzer Althaus, J. 2011. Sediment evacuation from reservoirs through intakes by jet induced flow. *Dissertation Thesis*, Communication Nr. 45 (A. Schleiss, ed.), LCH, EPF Lausanne, Switzerland.

Skripalle, J., Hies, T., Liu, Y. & Nguyen, H.H. 2012. Application of multi-frequency acoustics to estimate concentration of suspended sediments from Jurong Lake, Singapore. *Proc. 17th International Seminar on Hydropower Plants*. Vienna: 725–736.

Spraefico, M., Lehmann, C., Jakob, A. & Grasso, A. 2005. Feststoffbeobachtung in der Schweiz—Ein Tätigkeitsgebiet der Landeshydrologie. *Berichte des BWG*, Serie Wasser Nr. 8, Bern (in German).

Winkler, K., Dekumbis, R., Rentschler, M., Parkinson, E. & Garcin, H. 2011. Understanding hydro-abrasive erosion, *Proc. Hydro 2011 Conference*, Aqua-Media Intl. Ltd., Prague, Czech Republic.

Wren, D., Barkdoll, B., Kuhnle, R., & Derrow, R. 2000. Field Techniques for Suspended-Sediment Measurement. *Journal of Hydraulic Engineering*, 126(2): 97–104.

Measuring suspended sediment: results of the first year of the case study at Fieschertal in the Swiss Alps

D. Felix, I. Albayrak and R.M. Boes
Swiss Federal Institute of Technology (ETH)
Laboratory of Hydraulics, Hydrology and Glaciology (VAW)
Wolfgang-Pauli-Str. 27
8093 Zurich
Switzerland

A. Abgottspon, F. Deschwanden and P. Gruber
Hochschule Luzern (HSLU)
Engineering and Architecture, Competence Centre Fluid Mechanics and Hydro Machines
Technikumstrasse 21
6048 Horw (Lucerne)
Switzerland

Rivers and waterways may transport large quantities of suspended sediment that can cause severe damages to turbines of hydropower plants (HPP) and lead to reservoir sedimentation. To mitigate these negative effects, continuous and real-time suspended sediment monitoring (SSM) is required. In a research study at the HPP Fieschertal, a high-head scheme in the Swiss Alps with a strongly glaciated catchment area and without storage lake, suspended sediment mass concentration (SSC) and particle size distribution (PSD) are measured since summer 2012 using a portable laser diffractometer (LD). PSD is an important parameter for hydro-abrasive erosion and sediment transport or deposition. For comparison, also devices based in simpler measurement principles, such as turbidimeters and an acoustic method based on existing installations for acoustic discharge measurement (ADM) are employed to obtain SSC estimates.

Based on the data recorded at the study HPP, prior laboratory tests of the devices and site-specific time-invariant SSC-calibrations obtained from laboratory analysis of automatically taken bottle samples, time series of SSC and PSD in the turbine water were calculated. The calibration factor for SSC from LD accounts for strongly non-spherical shape of the particles. The results show that not only SSC but also PSD may vary considerably in time. In an example period of ten summer days, with SSC ranging between 0.2 and approx. 10 g/l, the median particle size d_{50} increased occasionally from 12 to approx. 100 μm. Although the transport of coarser particles was observed to be mostly associated with increased SSC, there is a wide scatter in the correlation between SSC and PSD due to a different temporal behavior of SSC and PSD. SSC and PSD depend on meteorological and hydrological processes and also on the operation of the free-surface-flow storage tunnel of HPP Fieschertal.

The turbidimeters, and to a smaller extent also the acoustic method, underestimate SSC if particles are greater than assumed in the time-averaged calibration. At HPPs with existing ADM installation, no additional hardware is required to get estimates of SSC in the penstock by means of the acoustic method. The accuracy of SSC estimates from the acoustic method and turbidimeters decreases as the variability in PSD increases and the PSD variations are not well correlated with SSC. In such environments, LD is recommended for SSM, since actual particle sizes are considered in SSC-estimates and information on PSD with high temporal resolution is provided. Further acoustic systems to measure SSC together with PSD are under development.

The measurements of suspended sediment at HPP Fieschertal will be continued and SSC and PSD data will be further evaluated. The particle load passing the turbines in time intervals between turbine inspections or efficiency measurements will be calculated in order to find correlations between particle load, turbine wear and efficiency which contribute to optimized design and operation of HPPs.

This paper focuses on measurements of suspended sediment, whereas the corresponding paper by Abgottspon et al. (2013b) treats measurements of wear at Pelton buckets and turbine efficiency changes at the same HPP.

1 Introduction

In the design and operation of hydropower plants (HPPs) handling of sediment transported in river water is a major challenge. Siltation of reservoirs and hydro-abrasive erosion at turbines can be economically important issues. In order to improve the understanding of the processes related to hydro-abrasive erosion and to contribute to an appropriate design and operation of HPPs, suspended sediment mass concentration (SSC) and particle size distribution (PSD) have to be measured continuously and in real-time at intakes and/or waterways of HPPs in combination with regular turbine inspections and monitoring of turbine efficiency decrease.

The Laboratory of Hydraulics, Hydrology and Glaciology (VAW) of ETH Zurich in cooperation with Hochschule Luzern (HSLU) initiated an interdisciplinary research project to investigate the problem of hydro-abrasive erosion on turbines mainly by means of a case study at the existing HPP Fieschertal. It is a high-head scheme located at a tributary of the upper Rhone River, in the Canton of Valais, in the Swiss Alps. Since the first operation in 1976 severe hydro-abrasive erosion at needles, nozzles and runners of the two 32 MW-Pelton units has been observed. Although coating of turbines parts reduced the extent of annual on-site revision works and increases the time between factory overhauls, sediment handling as well as optimized operation and maintenance of the HPP have remained important economic issues. In the past decades an increased yield of fine sediment has been observed due to glacier retreat and increased variation in precipitation. One operational option studied in this project is to systematically switch-off turbines during suspended sediment peaks if the costs caused by turbine wear exceed the benefits from power sales.

In a first part of this research project various devices for SSM as described in section 2 were tested in a mixing tank in the hydraulic laboratory of HSLU using suspensions made of mineral particles. This allowed establishing calibration curves for various types of particles and to investigate effects of particles size and shape (Felix et al. 2012). Particle size is a relevant parameter for turbine wear since the hydro-abrasive erosion potential is higher for coarser grains at given SSC (e.g. Winkler et al. 2011). In a second part of this on-going project, these devices were installed in the case study HPP (Fig. 1) for continuous SSM. In parallel periodical turbine inspections are made and turbine efficiency is monitored.

In this paper, methods and selected results of suspended sediment measurements of the year 2012 at this HPP are presented. Project components related to SSM are highlighted in Figure 1. The corresponding paper by Abgottspon et al. (2013b) describes methods to quantify wear at buckets of Pelton turbines and efficiency changes, and first results from the same case study HPP. Further results of this study were presented by Abgottspon et al. (2013a).

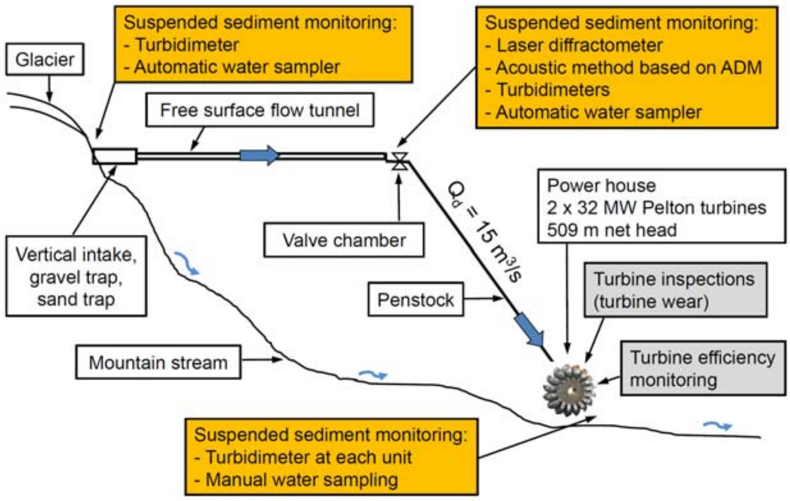

Fig. 1: Schematic longitudinal profile of the Case Study HPP Fieschertal

2 Devices used for suspended sediment monitoring

As particle size is an important parameter for turbine wear, a portable laser diffractometer (LD), which provides not only information on SSC but also on PSD was employed (item 6 in Table 1). For the use in HPPs specific models of LD devices were developed (Agrawal et al. 2012). In this project a multi-purpose model, as used in marine science and limnology, was used. In order to extend the range of measurable SSC the optical path length of the LD was reduced from 50 mm to 5 mm by insertion of a glass cylinder (90 percent path reduction module). The used LD has a nominal particle size measuring range from 2 to 380 µm in the calculation mode for so called ‘random shaped’ particles, which are according to Agrawal et al. (2008) particles with an irregular surface and no preferred axes (no elongated or platy particles). The working principle of LD is based on the inversion of a scattering pattern, which, in the portable LD device used here, is measured at small angles (up to approx. 10 degrees, Agrawal et al. 2008). Similar LD devices are used for SSM at a few HPPs so far (Boes 2009, Agrawal et al. 2012).

For comparison and in view of the acquisition costs, also devices for SSC estimates based on simpler measurement principles, such as tubidimeters and an acoustic system, were included in the study. Two models of submerged turbidimeter probes as mainly used in waste water treatment plants (items 1 and 2 in Table 1), two in-line turbidimeters measuring in flow-cells on a pipe as mainly used in the process industry (items 3 and 4 in Table 1) and one turbidimeter measuring at a free falling jet are employed (item 5 in Table 1). Turbidimeters measure either the back-scattering of light from suspended particles (e.g. at 90 degrees) or the attenuation of light through the suspension (optical transmission). Turbidimeter data are usually converted to SSC with a linear and time-invariant calibration curve. Turbidimeters are inexpensive and widely used. The major drawback thereby is that their calibration depends strongly on particle properties, mainly particle size (e.g. Gippel 1995, Wren et al. 2000).

The acoustic method for SSM used in this project (item 7 in Table 1) is based on existing acoustic discharge measurement (ADM) installations. ADM is widely used at waterways of HPPs. In ADM, ultrasonic pulses are sent from one transducer through the water and are received by a transducer at the other end of the path (Fig. 2). For the basic task of an ADM, i.e. the calculation of discharge based on flow velocity, differences in transit time of acoustic pulses travelling in and counter flow direction are measured. For SSM, one possibility is to use the additional attenuation of the received signals caused by suspended sediment particles. The correlation of attenuation of forward scattered ultrasonic signals and SSC has been investigated in recent laboratory tests at HSLU using transducers that are similar to those in ADM installations (Costa et al. 2012, Felix et al. 2012). At HPP Fieschertal a 4 path arrangement (2 crossed path of 2.27 m length in two horizontal layers) operated at 1 MHz is available at the top of the penstock. In the software of the ADM controller the amplitudes of the received signals at the four paths were defined as additional output parameters and no additional hardware had to be installed for SSM.

Table 1: Devices used for continuous suspended sediment monitoring (SSM)

Device type		Item No.	Device model and manufacturer	Device output and measuring principle	Derived parameters	Installed at
Turbidimeter, submerged, with wipers		1)	*Turbimax W CUS41* Endress-Hauser	Turbidity [FNU] from backscatter	SSC	Intake
		2)	*Solitax ts-line sc* Hach-Lange	Turbidity [FNU] from backscatter	SSC	Tailrace channels
Turbi-dimeter, in-line	Pressure flow (in flow-cells without wipers)	3)	*TurbiScat (90°, 25°)* Sigrist Photometer	Turbidity [FNU] from backscatter	SSC	Valve chamber, at the inlet to the penstock
		4)	*TF16-N with F20* Optek Danulat	Turbidity [CU] from transmission	SSC	
	Free falling jet	5)	*AquaScat* Sigrist Photometer	Turbidity [FNU] from backscatter	SSC	
Portable laser diffractometer (LD)		6)	*LISST-100X, Type C* Sequoia Scientific	Volume concentrations in 32 size classes [ppm]	SSC and PSD	
Acoustic method (based on existing ADM installation)		7)	*Risonic Modular* Rittmeyer	Received amplitude [V] forward scattering	SSC	

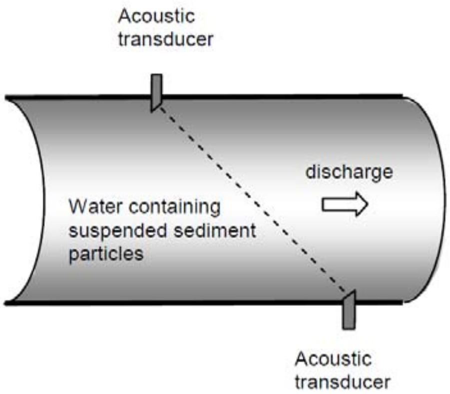

Fig. 2: Schematic of penstock with an acoustic path of an ADM installation, which can also be used for estimating suspended sediment concentration

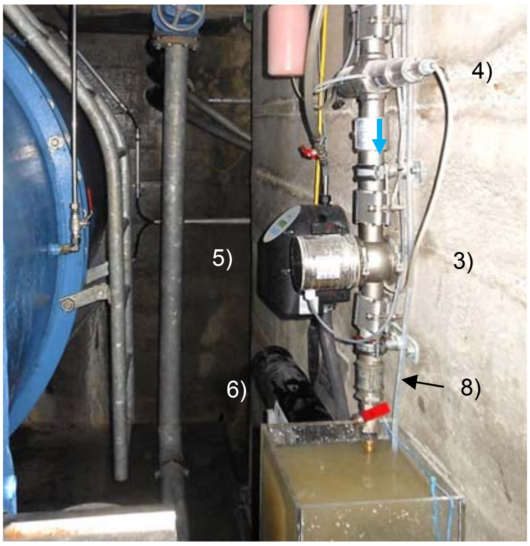

Fig. 3: Optical devices for continuous suspended sediment monitoring installed in the valve chamber of HPP Fieschertal; numbers 3 - 6 refer to items in Table 1

The devices for SSM were installed at the study HPP in summer 2012 (locations see Tab. 1 and Fig. 1), except items 1 and 5, which were added in 2013. Most of the devices are placed in the valve chamber at the top of the penstock (Fig. 3). The turbidimeters are installed at a sampling pipe fed from the penstock, which leads to a bucket with overfall and bottom outlet. The measuring head of the LD is inserted laterally into the bucket and the optical path of the LD is arranged below the end of the pipe. Further information on the devices, the laboratory tests as well as the installation at the study HPP and previous results are described by Felix et al. (2012) and Abgottspon (2011).

3 Method

The LD was programmed to take a measurement every minute whereas the signals of the other devices were recorded every second. The devices and the sampling pipes were checked and flushed regularly.

In addition to the devices for continuous SSM, automatic water samplers are operated in the valve chamber and at the intake, respectively. They are programmed to take samples every three days. In addition to that, the samplers are triggered by signals of turbidimeters at the respective sampler locations in order to increase sampling frequency in case of increased turbidity. The samplers contain each 24 one-litre bottles. The bottles are filled by means of a peristaltic pump. The transparent suction hose of the sampler in the valve chamber can be seen on Figure 3 (item 8). From each bottle sample the SSC (g/l) was determined in the laboratory by weighing before and after drying in an oven, deducting dissolved minerals.

From selected samples the quantitative mineralogical composition was determined using x-ray diffraction (XRD). The samples contain mainly quartz, feldspar and mica, i.e. the main components of granite rock. The solid density of selected samples of mineral particles was determined by means of a gas pycnometer and was found to be close to the density of quartz (2.65 g/cm^3).

The volume concentrations obtained from LD in the three smallest size classes (approx. 2-3 μm, not relevant for turbine wear) were discarded, since these contributions were considered to be overestimated with the prevailing particle mix (compare Andrews et al. 2011, Felix et al. 2013). Since the particle mix at the study site contains angular (not yet rounded by fluvial transport) and flaky (mica) particles, which differ considerably from the particle shape assumed in the LD inversion software (Agrawal et al. 2008), SSC obtained from LD was calibrated based on bottle samples using a constant factor.

The time series from turbidimeters and the acoustic method were also converted to SSC based on time-averaged calibrations from bottle samples. The calibration curves obtained from field data were compared to those from laboratory tests and were found to be within a plausible range.

4 Results and discussion

4.1 Time series of suspended sediment concentration and particle size

From the time series of SSC and median particle size d_{50} in the turbine water of HPP Fieschertal obtained from LD, an extract of ten days during the sediment season is presented in Figure 4. The median particle size d_{50} stands for the diameter of graded particles of which 50 percent by mass are smaller. Whereas the average SSC during this period was 0.5 g/l, periods of increased SSC ranging up to several g/l for some hours occurred (Fig. 4b). Strong SSC increases occur within less than a few hours, decreases however are generally slower; similarly to typical flood hydrographs. Calibrated SSC is in overall good agreement with reference SSCs (circular markers in Fig. 4b).

The median particle size d_{50} had a base level of 12 μm and rose occasionally up to approx. 100 μm (Fig 4a). Periods of increased SSC are mostly associated with the occurrence of coarser particles. The time series of SSC and d_{50} are, however, not synchronous and time shifts among peaks in SSC and d_{50} were observed.

Figure 5 shows a detail with one selected period of increased SSC (suspended sediment transport event), as indicated by the shaded areas in Figure 4. SSC obtained from LD rose from 0.2 g/l to several g/l and fell back to 0.4 g/l (Fig. 5b). The SSC-estimate from LD is supported by one bottle sample. With the particle sizes in this event, LD measurements were possible until approx. 10 g/l and resumed when SSC was falling below approx. 7 g/l.

In Figure 5a, d_{16} and d_{84}, i.e. the sizes of particles of which 16 or 84 percent by mass are smaller, are plotted in addition to d_{50}. The diameters d_{16} and d_{84} are often used in geotechnical and river engineering to characterize the “width”, i.e. the so called spreading, of a PSD. d_{84} of up to approx. 200 μm was measured, this is smaller than the classical design grain size for sand traps of 250 to 300 μm. Whereas SSC decayed rather continually after the peak, d_{50} remained at an elevated level until SSC fell back to the base level.

In addition to LD, SSC estimates from the other SSM devices in the valve chamber are displayed in Figure 5b. The turbidimeter signals were de-trended in order to compensate signal drift caused by accumulating contamination of the optical windows in the flow-cells. It turned out that the flow in the flow-cells is not strong enough for self-cleaning and that occasional flushing of the sampling pipe without manual cleaning of the windows in the flow-cells was insufficient to prevent signal drift (Abgottspon et al. 2013a).

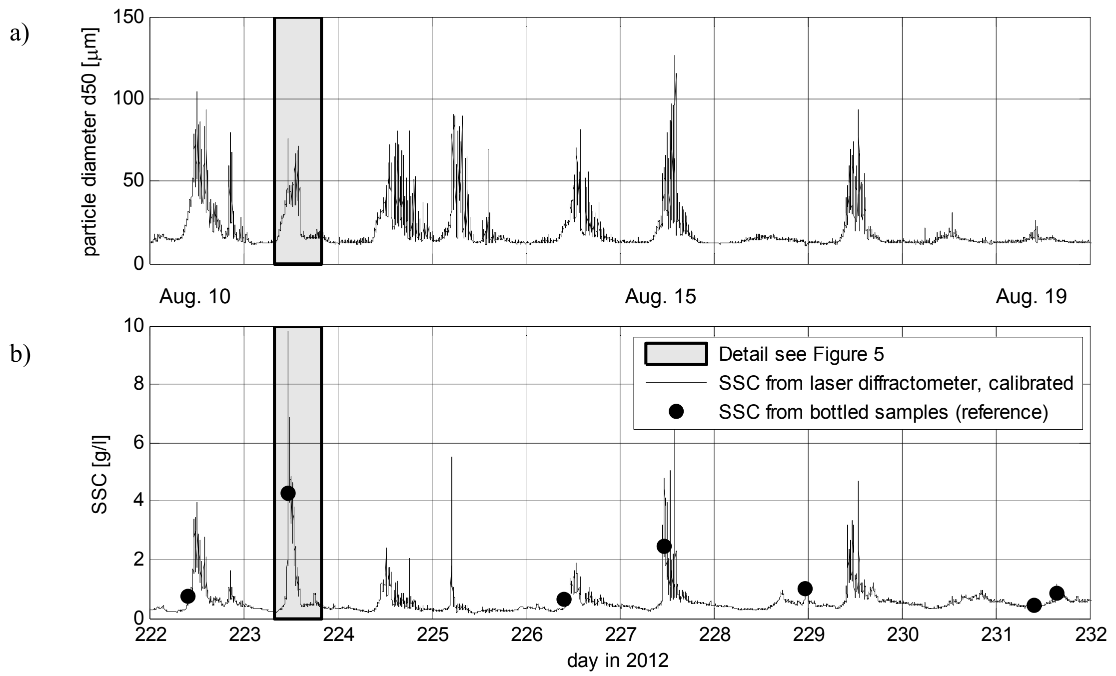

Fig. 4: Time series of (a) d_{50} and (b) SSC in the turbine water obtained from LD after calibration to reference SSCs from bottled samples (circular markers); example of ten days in summer (from August 10 to August 19, 2012)

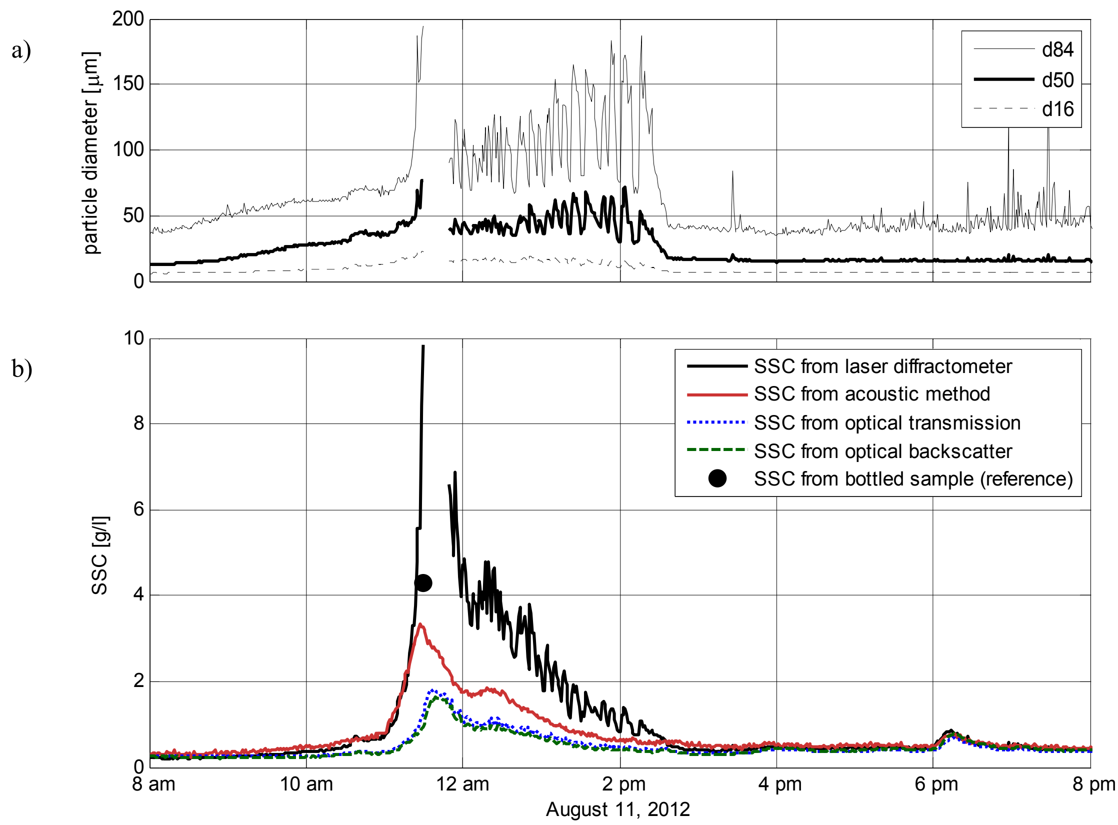

Fig. 5: Detail of half a day out of the time series in Figure 4, additionally including SSC-estimates from the other devices installed in the valve chamber and particle sizes d_{16} and d_{84} (from LD)

Before and after the period of increased SSC all devices yielded similar SSC estimates. During the period of increased SSC, however, the acoustic method and the turbidimeters underestimated SSC, because their calibration is based on the usually prevailing relatively fine particles ($d_{50} \approx 15$ μm) and these devices do not recognize the variation in particle size in contrast to LD. At given SSC, turbidity and attenuation are smaller with coarser particles. The acoustic method is less sensitive to changes in particle size than the used turbidimeters, what was also observed in laboratory experiments (Abgottspon 2011, Felix et al. 2012).

4.2 Correlation of suspended sediment concentration and particle size

As observed from Figures 4 and 5, coarser particles tend to be associated with higher SSC. Figure 6 shows an example of pairs of SSC and d_{50} values obtained from LD during ten summer days from August 10 to 19, 2012 (as in Fig. 4). A positive correlation with a wide scatter can be seen. In that period, SSC above approx. 1.5 g/l were associated with $d_{50} \geq 30$ μm. SSC and d_{50} may be quite independent variables, depending on sediment availability and the processes which govern suspended sediment transport in a specific system.

SSC and PSD depend generally on meteorological and hydrological factors, such as glacier melt, precipitation in form of rain or snow, extent of snow cover in the catchment area, changes of flow paths in the glacier, etc. In the present case, SSC and PSD depend also on the operation of the turbines and the free-surface-flow storage tunnel (Fig. 1) upstream of the measurement location; as observed earlier by the HPP operator and described by Abgottspon (2011). Depending on the turbine discharge and the water level in the storage tunnel, sediment particles settle or are re-suspended, according to the prevailing turbulence and bottom shear stress. If the river flow exceeds the design discharge of the HPP, turbines are run at full load with filled storage tunnel, whereas in other periods the water level and the discharge in the storage tunnel fluctuate due to intermittent part-load operation of the turbines.

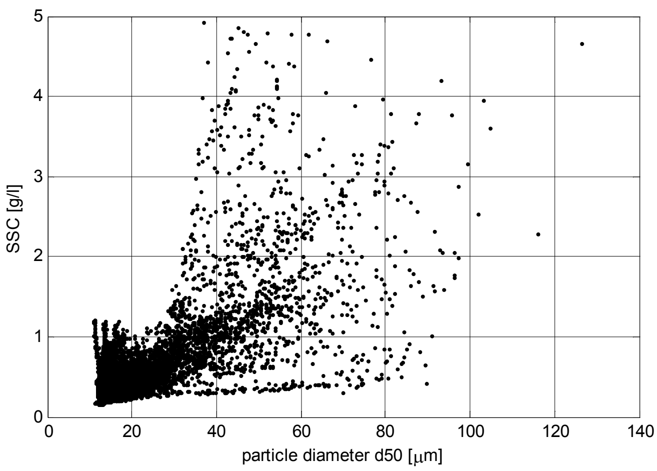

Fig. 6: Correlation of concentration (SSC) and median diameter (d_{50}) of suspended sediment in the turbine water of HPP Fieschertal, example from August 10 to 19, 2012, obtained from LD (SSC calibrated with bottle samples)

5 Conclusions and recommendations

Selected results of concentration and PSD of suspended sediment measured in summer 2012 in the power waterway of HPP Fieschertal, which has a strongly glaciated catchment area and no storage lake, were presented. This gives information on site-specific SSC and PSD ranges of an example period of 10 days in the sediment season (without rare events) and allows also a cross-comparison of the measuring capabilities of the instruments used for SSC-estimates.

The measurements confirm that not only SSC but also PSD can vary considerably in time. In periods of increased SSC coarser particles were transported compared to the conditions before and after such events (positive correlation of PSD and SSC). However, it was observed that peaks of SSC and PSD do not occur simultaneously and that after a SSC-peak particle size did not decrease as quickly as SSC. This different temporal behaviour of SSC and d_{50} contributes to a wide scatter in the correlation of SSC and PSD.

In dynamic sediment environments, where SSC and PSD are quite independent variables, the use of portable LD is recommended. With LD, actually prevailing particle size is considered in SSC measurements and PSDs with high temporal resolution can be obtained, what was previously not affordable with laboratory PSD analysis of bottled samples. The portable LD device is suitable for SSM in the power waterway of HPPs since particles greater than the upper limit of the size measuring range are usually excluded by sand traps. An option to extend the limited range of

measureable SSC is to perform LD measurements on suspension samples that are diluted with clear water at a known mixing ratio (Agrawal et al. 2012).
SSC estimates from methods that are based on simpler measurement principles, such as turbidimeters and the described acoustic system, are biased in periods in which the size of the transported particles differs from that assumed in the calibration. Such methods can be used with good accuracy for SSC estimates in situations where (i) particle size is almost constant over time or (ii) a strong correlation of SSC and PSD exists and is known. In the latter case, a calibration curve which accounts for changes in PSD with increasing SSC has to be used. Correlations between SSC and PSD can be investigated using portable LD for some period at a certain measurement location. If turbidimeters and the described acoustic system are used in situations with no clear correlation of SSC and PSD, temporarily biased SSC estimates and less accuracy have to be accepted.
If turbidimeters are used, it is highly recommended to select models which have an automatic cleaning system (wiper or pressurized air) or measure turbidity at a free falling jet, in order to prevent signal drift and the need of frequent manual cleaning, even in cold waters of mountain streams, were little bio-fouling may be expected. In contrast to the acoustic method, turbidimeters are suitable for measuring low SSCs (e.g. < 0.2 g/l).
The acoustic system described here showed less sensitivity to variations of particle size than the investigated turbidimeters. Since the measurements are performed directly in the penstock, no sampling pipe is required that could be clogged or lead to non-representative sampling. Measurements are averaged over the path length and several paths over the cross-section of the penstock can be considered. Using the existing installation at the study HPP measurements up to several 10 g/l were possible. No maintenance (cleaning of the sensors) is required. If no information on actually prevailing PSD is required, this method lends itself particularly for HPPs with an existing ADM installation, since in these cases no additional hardware is required for SSM. The obtainable accuracy in SSC estimates depends on the temporal variability of PSD or its correlation with SSC at a given site.

6 Outlook

The measurements of suspended sediment at HPP Fieschertal will be continued. SSC and PSD will be further evaluated seasonally and event-based. The correlation of SSC and PSD time series will be further investigated and duration curves will be produced.
SSC and PSD time series based on LD will be used to calculate the so called ‘particle load’ that was passing the turbines in time intervals between turbine inspections or efficiency measurements. According to IEC Standard 62364 (2013), particle load is defined as the integral of the product of SSC and weighting factors for particle size, shape and hardness over time.
Regarding SSM using acoustics, methods and systems that allow estimating both SSC and PSD are being investigated and various attempts have been made (e.g. Thorne et al. 2007, Moore 2011, Skripalle et al. 2012). The joint determination of SSC and PSD is physically not possible using one frequency. Therefore, multi-frequency approaches are investigated. With forward scattering (as described above), the use of multiple frequencies is limited due to the small frequency sensitivity of the damping in the particle size and concentration range of interest. If however backscattered signals are used a stronger frequency dependency can be observed, which can be exploited for estimating particle size and SSC simultaneously, although one has to deal with much lower signal levels. The low signal-to-noise ratio of the backscattered signals poses a big challenge for estimating PSD and SSC from the recorded signals (inversion of the backscattering process). HSLU in collaboration with ETH Zurich is currently analysing various analytical models predicting backscattered signals. Having once identified the best suited model for the application range, the ill-posed inversion problem in a noisy environment will be tackled. It is planned to verify the applicability and accuracy of such an approach by experimental investigations at HSLU.
Besides SSM, measurements of turbine wear and efficiency (see Abgottspon et al. 2013b) will be continued. Data on suspended sediment, turbine wear and turbine efficiency will be evaluated to find correlations which contribute to the development of respective prediction formulas and to determine economically balanced criteria for temporary turbine switch-offs during suspended sediment peaks.

Acknowledgements
The authors gratefully acknowledge the support by swiss*electric* research, the Swiss Federal Office of Energy and Gommerkraftwerke AG. Thanks go to the project partners, especially to Prof. Dr. T. Staubli from Hochschule Luzern, Competence Center for Fluid Mechanics and Hydro Machines, and to Gommerkraftwerke, the operator of the study HPP. A further thank is to Rittmeyer, Sigrist Photometers and Endress+Hauser for measuring equipment support. The work of Philipp Grüninger, who contributed with his Master thesis to the evaluation of the suspended sediment data collected in 2012, is acknowledged.

References

1. **Abgottspon A.** 2011. Messung abrasiver Partikel in Wasserkraftanlagen. *Master thesis* (unpublished, in German), Hochschule Luzern, CC Fluid Mechanics and Hydro Machines, Lucerne, Switzerland.
2. **Abgottspon A., Staubli T., Felix D., Albayrak I., Boes R.M.** (2013a). Hydro-abrasive Erosion of Pelton buckets and Suspended Sediment Monitoring. *Proc. Hydrovision International* 2013, Denver, USA.
3. **Abgottspon A., Stern P., Staubli T., Felix D., Winkler K.** (2013b). Measuring Turbine Abrasion and Efficiency Decrease: first Results of the Case Study at HPP Fieschertal. *Proc. Hydro 2013 Conference*, Innsbruck, Austria.
4. **Agrawal, Y.C., Whitmire, A., Mikkelsen, O.A. & Pottsmith H.C.** 2008. Light scattering by random shaped particles and consequences on measuring suspended sediments by laser diffraction, *Journal of Geophysical Research* 113, C04023.
5. **Agrawal Y., Mikkelsen O.A., Pottsmith H.C. & Slade W.H.** 2012. Turbine abrasion: one year's experience in real-time sediment monitoring at Hidroagoyan HPP, Ecuador. *Proc. Hydro 2012 Conference*, Aqua-Media Intl. Ltd., Bilbao, Spain.
6. **Andrews S.W., Nover D.M., Reuter J.E. & Schladow S.G.** 2011. Limitations of laser diffraction for measuring fine particles in oligotropic systems: Pitfalls and potential solutions. *Water Resources Research*, 47, W05523.
7. **Boes R.M.** 2009. Real-time monitoring of SSC and PSD in the headwater way of a high-head hydropower plant. *Proc. 33rd IAHR Congress*, Vancouver, Canada: 4037–4044.
8. **Costa I., Storti G., Lüscher B., Gruber P. & Staubli T.** 2012. Influence of solid particle parameters on the sound speed and attenuation of pulses in acoustic discharge measurements (ADM). *Journal of Hydrological Eng.*, 17(10): 1084–1092.
9. **Felix D., Albayrak I., Abgottspon A., Boes R.M & Gruber P.** 2012. Suspended Sediment and Pelton Turbine Wear Monitoring: Experimental Investigation of various Optical and Acoustic Devices and Beginning of the Case Study at HPP Fieschertal. *Proc. 17th International Seminar on Hydropower Plants*. Vienna: 483-494.
10. **Felix D., Albayrak I., Boes R.M.** 2013. Laboratory Investigation on measuring Suspended Sediment by portable Laser Diffractometer (LISST) focussing on Particle Shape. *Geo-marine Letters*: accepted.
11. **Gippel C.J.** 1995. Potential of turbidity monitoring for measuring the transport of suspended solids in streams. *Hydrological Processes 9*: 83–97.
12. **IEC 62364**. 2013. Hydraulic machines - Guide for dealing with hydro-abrasive erosion in Kaplan, Francis and Pelton turbines, Edition 1.0 (June 2013), *International Electrotechnical Commission*, Geneva, Switzerland.
13. **Moore S.A.** 2011. Monitoring flow and fluxes of suspended sediment in rivers using side-looking acoustic Doppler current profilers. *Dissertation*, Université de Grenoble, France.
14. **Skripalle J., Hies T., Liu Y. & Nguyen H.H.** 2012. Application of multi-frequency acoustics to estimate concentration of suspended sediments from Jurong Lake, Singapore. *Proc. 17th International Seminar on Hydropower Plants*. Vienna: 725-736.
15. **Thorne P.D., Agrawal Y.C., Cacchione D.A.** 2007. A Comparison of Near-Bed Acoustic Backscatter and Laser Diffraction Measurements of Suspended Sediments, *IEEE Journal of Oceanic Eng.*, 32(1): 225-235.
16. **Winkler K., Dekumbis R., Rentschler M., Parkinson E. & Garcin H.** 2011. Understanding hydro-abrasive erosion, *Proc. Hydro 2011 Conference*, Aqua-Media Intl. Ltd., Prague, Czech Republic.
17. **Wren D., Barkdoll B., Kuhnle R., & Derrow R.** 2000. Field Techniques for Suspended-Sediment Measurement. *Journal of Hydraulic Eng.*, 126(2): 97–104.

The Authors

D. Felix graduated in Civil Engineering (M.Sc.) from the Federal Institute of Technology (ETH) in Zurich in 2005. He worked for five years with Pöyry Energy Ltd., Zurich, in the field of hydropower plant design and dam safety. Since 2010, he is a Ph.D. student (ongoing thesis on suspended sediment and turbine wear) and teaching assistant at the Laboratory of Hydraulics, Hydrology and Glaciology (VAW) of ETH Zurich.

Dr. I. Albayrak received his M.Sc. in Hydraulic Engineering from Istanbul Technical University in 2003 and obtained his Ph.D. in the field of environmental hydraulics at the Federal Institute of Technology in Lausanne (EPFL) in 2008. He worked for three years in a project on flow-plant interactions at the University of Aberdeen. Since 2011 he has been working as a scientist at the Laboratory of Hydraulics, Hydrology and Glaciology (VAW) of ETH Zurich.

Prof. Dr. R. M. Boes graduated in 1996 in Civil Engineering from Technical University of Munich. In 2000 he completed his Ph.D. in the field of hydraulic structures at ETH Zurich. At TIWAG-Tiroler Wasserkraft AG, an Austrian utility, he was responsible for dam and hydropower as well as flood protection projects from 2002 to 2009. Since then he is Professor for hydraulic structures and Director of the Laboratory of Hydraulics, Hydrology and Glaciology (VAW) at ETH Zurich.

A. Abgottspon graduated in Mechanical Engineering (M.Sc.) from Hochschule Luzern (HSLU) in Switzerland. Since 2006 he works as a research assistant at the Competence Centre Fluid Mechanics and Hydro Machines of HSLU, in the fields of hydropower plant efficiency measurements, Pelton jet quality and hydro-abrasive erosion. In 2009 he co-founded etaeval, a company specialized in measurements and simulations on hydropower plants.

F. Deschwanden graduated in Mechanical Engineering (B.Sc.) from Hochschule Luzern (HSLU) in Switzerland. Since summer 2012 he has been working as a research assistant at the Competence Centre Fluid Mechanics and Hydro Machines of HSLU, mainly in the fields of developing ADM devices in different hydraulic applications.

Prof. Dr. P. Gruber completed both his graduate and Ph.D. studies in Electrical Engineering at ETH Zurich. After 20 years of applied research work with Landis & Gyr and Siemens in the field of instrumentation, signal processing and control he was head of the development of ultrasonic flow meters with Rittmeyer, Switzerland from 2002 to 2007. Since 2007 he is Professor at Hochschule Luzern (HSLU), where he was already part-time lecturer for many years.

Geo-Mar Lett (2013) 33:485–498
DOI 10.1007/s00367-013-0343-1

ORIGINAL

Laboratory investigation on measuring suspended sediment by portable laser diffractometer (LISST) focusing on particle shape

David Felix · Ismail Albayrak · Robert M. Boes

Received: 1 April 2013 / Accepted: 8 October 2013 / Published online: 25 October 2013

Abstract This paper deals with a laboratory investigation on measuring suspended sediment volume and mass concentration (SSC) and particle size distribution (PSD) by a portable submersible laser diffractometer (*LISST-100X*) focusing on effects of particle shape and inversion modes on the results. Experiments were carried out in a mixing tank using suspensions of glass beads, fine quartz sand, feldspar and mica powder particles of spherical, rounded, angular and flaky shapes respectively, at various SSCs. SSCs and PSDs measured by LISST were compared to SSCs from gravimetric analysis and to PSDs obtained from image analysis of dry particles and from a non-portable laser diffractometer. Experiments using spherical and rounded particles showed that LISST with the corresponding inversion modes, i.e. spherical and 'random shaped', provides PSD and SSC values similar to reference methods. For angular and flaky particles, however, SSCs were found to be overestimated by factors of 1.5 and 8 respectively. Measurements in a mixture of 70% feldspar and 30% mica powders showed that the SSC overestimation factor for mixed particle-type suspensions can be predicted as the weighted sum of the SSC factors of the components and their mixing ratio. For known highly non-spherical particle types, LISST SSCs can be corrected by a gravimetrically determined or predicted overestimation factor. Moreover, correction of overestimated contributions of lower size bins, the range of measureable SSC and time averaging of LISST measurements are addressed. Further investigations are necessary to assess effects of non-spherical particles and mixtures of various particle types on LISST SSC and PSD estimates.

D. Felix (✉) · I. Albayrak · R. M. Boes
Laboratory of Hydraulics, Hydrology and Glaciology (VAW), ETH Zurich, Swiss Federal Institute of Technology, Wolfgang-Pauli-Str. 27, 8093 Zurich, Switzerland
e-mail: felix@vaw.baug.ethz.ch

Introduction

Monitoring of suspended sediment mass concentration (SSC) and particle size distribution (PSD) is important for improved understanding and management of sediment-related processes in natural aquatic systems such as rivers, lakes, estuaries and seas, and at hydraulic schemes for hydropower, irrigation or flood protection. An overview of methods for measuring suspended sediment is given by Wren et al. (2000). Pumped or manual bottle sampling is a discontinuous technique with poor temporal resolution. Samples have to be transported to a laboratory, where SSC is determined by weighing of oven-dried residues (gravimetric analysis) and PSD by sieving, hydrometer or pipette analysis (Konert and Vandenberghe 1997), image analysis or laser diffraction (LD). Such sampling is costly, not practical and insufficient to capture the dynamic processes of sediment mobilization, transport, deposition and re-suspension in field conditions. Hence, practical systems for continuous measurements, preferably in real time, are required.

Among the techniques employed for such measurements, turbidimeters are the most common with the drawback of a particle size-dependent calibration leading to significant errors in SSC estimates in environments where PSD considerably varies in time and is not well correlated with SSC. Similarly, acoustic systems using one frequency are also affected by particle size. Multi-frequency acoustic devices to determine SSC and PSD are under development (e.g. Thorne et al. 2007; Skripalle et al. 2012). Since 1995, portable and submersible LD devices, from which both SSC and PSD estimates can be obtained, are available for field studies (known as 'laser in-situ scattering and transmissiometry', LISST). Such devices are mainly used in marine research (e.g. Bowers and Braithwaite 2012; Fettweis et al. 2012). Since a few years, their use has been extended to suspended sediment measurements in the context of turbine wear (e.g. Boes 2009, Agrawal et al. 2012) and reservoir sedimentation (e.g. Haun et al. 2013). LISST has the advantages of yielding particle volume concentration (PVC), which is converted to SSC using particle density, theoretically without effect of particle size, and PSDs with high temporal resolution (approx. 1 Hz).

LD has been used for decades and is widely accepted in industry and research for particle size analysis in laboratories. In the technique of LD, measured data on scattering and transmission are inverted to obtain PSD and PVC by an algorithm (kernel matrix), which is usually based on the assumption that particles have spherical shape (Mie solution to Maxwell equations). More recently, an additional inversion mode for so-called random shaped particles was developed by Agrawal et al. (2008) and added to the LISST software for data analysis. Agrawal et al. (2008) stated that the term 'random' refers to particles with no preferred axes, and clarified that elongated and platy particles were not considered. Although the latter particle types exist in natural environments, no specific inversion mode is available yet to the knowledge of the present authors. The literature review given in Agrawal et al. (2008) indicates a lack of experimental investigations on effects of highly non-spherical particle shapes on PSD and especially on SSC estimates from LD.

In the study reported here, effects of particle shape, inversion modes and mixture of particle types on LISST SSC and PSD estimates and on the SSC-measuring range are addressed by an experimental investigation using a *LISST-100X*. A series of experiments with suspensions made of water and four types of mineral particles varying in shape (glass beads, fine quartz sand, feldspar and mica powder) was carried out in a mixing tank. This laboratory investigation was an initial part of a research project on suspended sediment monitoring in the context of hydro-abrasive wear at turbines in hydropower plants (Felix et al. 2012, 2013) initiated by the Laboratory of Hydraulics, Hydrology and Glaciology (VAW) of the Swiss Federal Institute of Technology, ETH Zurich in collaboration with Hochschule Luzern, Competence Centre for Fluid Mechanics and Hydro Machines.

Materials and methods

Mineral particles

The mineral particles used in this laboratory investigation were selected with reference to a case study site in the Swiss Alps, where suspended sediment consists of mainly quartz, feldspar and mica particles, i.e. the main components of granite rock. In the upper reaches of mountain streams, especially from glaciated catchment areas, suspended mineral particles have typically angular shape, as opposed to downstream sites where particles tend to be more rounded due to fluvial transport. The basic particle shape depends on mineral properties, such as the characteristic layer structure of mica that generates platy particles.

This paper covers investigations using four types of particles listed in Table 1 and shown in Fig. 1. The particles were purchased from commercial applications. Glass beads were chosen as a reference due to their ideal shape. Since the water at the study site comes from a highly glaciated catchment area and has a temperature of less than 5 °C throughout the year, no organic particles were studied. The density of the selected particle types was measured using a gas expansion pycnometer. Particle shapes are seen from Fig. 1. All four types of particles have whitish color.

Definitions of particle sizes and shape

When considering non-spherical particles, the parameterization of particle size and shape in three-dimensional space is not evident. An approach described by Nichols (2009) is adopted here. A particle is characterized firstly by the three dimensions of an enveloping cuboid and secondly by the degree of rounding of its primary shape. The longest, the intermediate and the shortest diameter of a particle are denoted by a, b and c respectively, where c is measured perpendicular to the longest diameter and b is measured perpendicular to a and c. The aspect ratios b/a and c/b (ranging between 0 and 1) indicate the basic particle shape, which can be cubic (equant), platy (discoid, flaky), blade- or rod-like. The volume-equivalent sphere diameter d_{es} serves as a simple and comparable parameter for the size of non-spherical particles.

Additionally, the Sauter mean diameter (SMD), defined as 6 times the volume divided by the surface area of an ensemble of particles, is used when the specific area of graded, especially non-spherical particles is relevant. For non-graded spheres SMD corresponds to the sphere diameter.

Instrumentation and experimental setup

A portable submersible LD device, a *LISST-100X*, Type C (from Sequoia Scientific, Inc., Bellevue, WA) was used. Its optical path length was reduced from 50 mm to 5 mm by insertion of a 90% path-reduction module (glass cylinder) to extend the range of measurable SSC. The principles of LD, the construction of LISST instruments, and the mathematical approach used in the data treatment and analysis are described in Agrawal and Pottsmith (2000). In the present study the two inversion modes available with LISST are referred to as IMS for spherical and IMR for 'random shaped' particles. The nominal range of measurable particle sizes of this device is 2.5 to 500 µm for IMS, and 1.9 to 381 µm for IMR (Sequoia

Table 1 Properties of mineral particles

Particle type (material and grading)	Shape (qualitative)	Description	Density (g/cm^3)
Glass beads	Spherical, smooth		2.423
Quartz fine sand	Irregular, rounded	Natural, washed (no fines)	2.658
Feldspar powder (Na-plagioclase)	Elongated, angular	Milled	2.648
Mica powder (muscovite)	Flaky, not rounded	Milled, typical mica structure	2.856

2011). LISST yields PVCs in 32 log-spaced size bins. Cumulative PSD is calculated from the contribution of each size bin. SSC is obtained by multiplying the sum of the PVCs with the particle density, which has to be either known a priori or measured by another device.

Measurements were carried out on suspensions prepared in a mixing tank shown in Fig. 2 as used previously by, for example, Abgottspon (2011) and Costa et al. (2012). The tank (2.12 m long and 1.13 m wide) is equipped with a central stirrer running at about 300 revolutions per minute, resulting in highly turbulent flow conditions to prevent particles from settling. This relatively big tank allowed accommodating a set of instruments. The LISST was mounted horizontally at 60% of the water depth above the tank invert, with the laser beam approx. 0.2 m off the wall. A pump line, connected to the tank for simultaneous testing of in-line turbidimeters, contributed to mixing in the tank.

Experimental procedure

Five series of measurements were carried out at increasing SSCs. While in four series single types of particles as listed in Table 1 were used, 70% feldspar and 30% mica powders were mixed for the last series (mixing ratio according to mass). From many possibilities of mixed particle-type experiments, a mixture of feldspar and mica was chosen with regard to the study site, where mainly angular particles (quartz and feldspar) and up to 30% by mass of platy particles (mica) are expected (Abgottspon 2011).

Suspensions were prepared with clear drinking water and mineral particles (no dispersant agent added). As a preparation of each series, the tank was filled to a water depth of h=0.5 m (Fig. 2), corresponding to a volume of 1.2 m^3. In each series, SSC was increased stepwise until the SSC-measuring range of the LISST was exceeded. SSC was increased to the next level by adding a portion of particles with weights calculated to

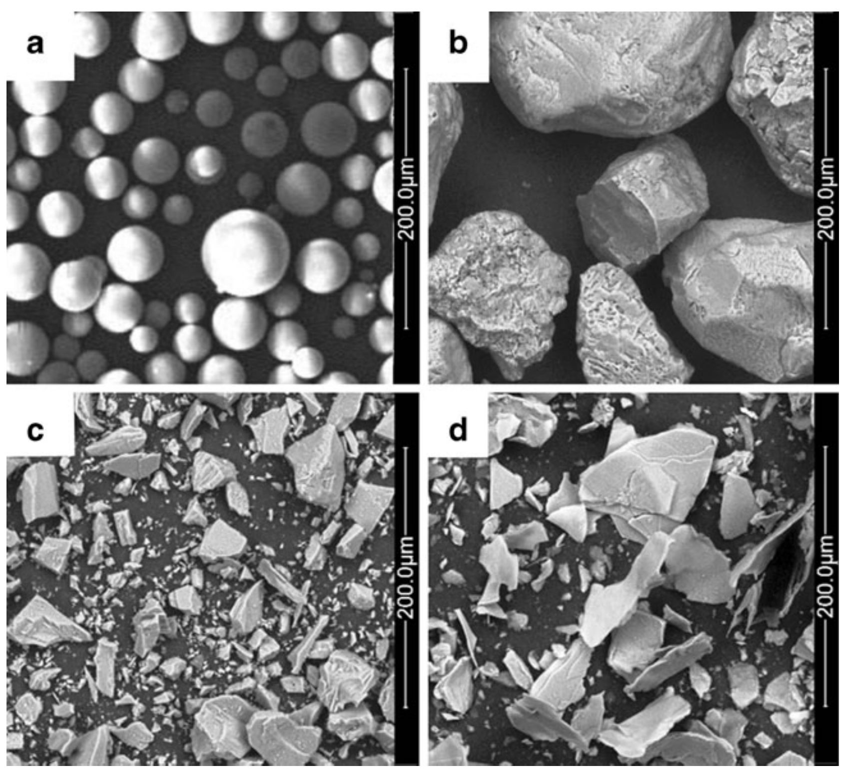

Fig. 1 Particles used in the experiments: **a** glass beads, **b** quartz fine sand, **c** feldspar powder and **d** mica powder (SEM images **a** courtesy of Hochschule Luzern, **b**–**d** ETH Zurich)

reach the next nominal SSC level. Nominal SSC is the total weight of added particles divided by the volume of suspension in the tank. At the beginning of each test series, the so-called background scatter in the water (with no added particles) was recorded by LISST. This allows also checking whether the path reduction module has been installed properly (no air between the receiving window and the module).

At each nominal SSC, after a mixing time of at least 10 minutes, a LISST measurement consisting of 100 single measurements was performed in real-time mode using the LISST SOP (v5) software. The measuring frequency in this mode was between 0.4 and 0.6 Hz, corresponding to a measuring duration of approx. 3 to 4 minutes at each nominal concentration level. From the raw data of each single measurement, PVCs were processed with both IMS and IMR using the recorded background scatter of the respective test series. SSCs were calculated from the PVCs using the densities listed in Table 1.

SSC reference measurements

In order to have a reference for LISST SSCs, two suspension samples per nominal SSC in each test series were taken from the tank at the level of the LISST's laser beam. SSCs of these samples were calculated based on the weight of the samples before and after evaporating the water in an oven (primary method for SSC). The sample volume was normally 0.1 l, and was increased to 0.5 l at low SSCs to achieve sufficient precision in weighing of residues for all samples. Since dried residues contained not only particles but also minerals that had been dissolved in the drinking water, the dissolved solids concentration was deducted from the total mass concentration. The concentration of dissolved solids in the drinking water was measured at the beginning of each series and was found to be approx. 0.15 g/l. SSCs from the bottle samples were averaged for each nominal concentration level. In the following, these are referred to as 'reference SSCs'.

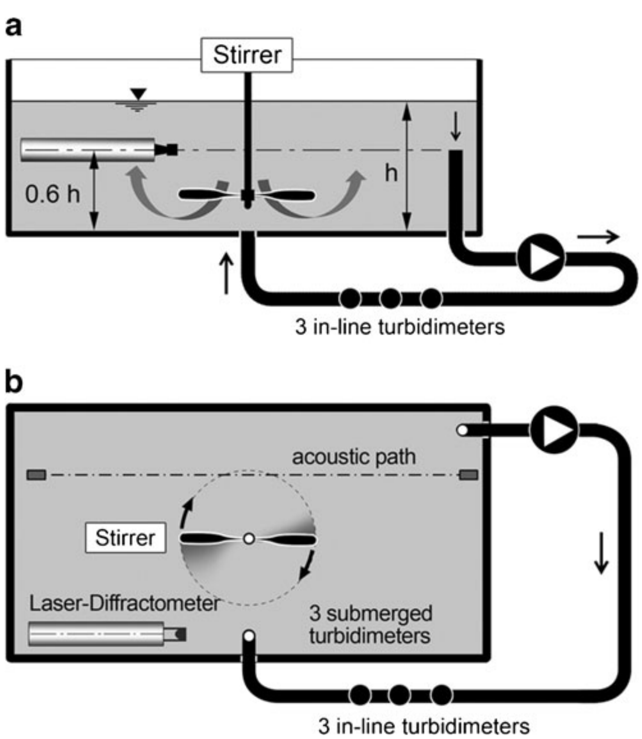

Fig. 2 Mixing tank with LISST device: **a** vertical section and **b** plan view (modified from Felix et al. 2012)

PSD reference measurements

For comparison with LISST PSD estimates, PSDs for each particle type were obtained from both the analyses of scanning electron microscope (SEM) images and a non-portable LD device. The samples for the reference PSD measurements were taken from the dry particle material prior to the LISST measurements.

Image analysis

Information on PSD and particle shape of the four particle types was obtained from geometric measurements on microscope images shown with scaling bars in Fig. 1. The two dimensions of particles visible in the plane of the image, i.e. usually a and b, were measured for each particle type for approx. 100 selected particles. For mica, with some upright-standing flakes visible in the image (Fig. 1d), the flake thickness c was measured and correlated with a. The correlation between c and a was used to estimate the flake thickness when it was not visible in the image. For the other particle types, c was estimated from the image assuming a typical shape. For mica and feldspar powders containing particles with a<5 μm, which could not be individually counted, the fraction of finer particles was estimated (<10%). From the listed a, b and c values, the volume and surface area of each particle were calculated assuming spheres, ellipsoids or cuboids, depending on the particle type. The sorted volume values were used to obtain distributions of the particle sizes a, b, c and d_{es} according to the mass fraction, similar to classical sieve curves. The total volume and surface area of the measured particles served to estimate SMD. In this study, image analysis is used as primary method for particle size and shape.

Non-portable laser diffractometer

Additional PSD measurements were performed with a *LA-950* from *Horiba*, which was available for this study at the Geotechnical Institute of ETH Zurich. This device is a non-portable laboratory LD with a nominal size-measuring range of 0.01 μm to 3 mm. In addition to forward scattering at small angles, it measures and evaluates side- and backward scattering as well, which allows assessing particle sizes below the wavelength (sub-micron range). Calculation of PSDs is based on the assumption of spherical particles. The PSDs were measured in suspensions of adequate concentrations in a small stirring chamber (SSC was not measured).

Results

Particle size and shape based on image analysis

The particle sizes obtained from image analysis are summarized in Table 2 using the definitions given above. To describe sizes of graded particles, a subscript serves to denote the percentage of finer particles (by mass). In addition, the aspect ratios b/a and c/b, which give quantitative information on the basic particle shapes, are presented in Table 3. Qualitative information on the degree of rounding is found in Table 1. Feldspar and mica powders include more elongated particles compared to quartz fine sand (low b/a values at 90% fractile). Whereas the particle shapes of glass beads, quartz fine sand and feldspar powder are approx. independent of particle size (self-similarity), the shape of mica particles varies strongly with size. Since the flake thickness c of mica is almost constant at about 2 µm, the aspect ratio c/b decreases with increasing particle size (b and a).

Effects of particle shapes and LISST inversion modes on SSC estimates

SSCs obtained using IMS and IMR are shown as a function of reference SSCs in Fig. 3 for each particle type. Each point represents one LISST measurement at a nominal SSC, i.e. the time average of 100 single measurements. The effect of inversion mode is quite small with all four investigated particle types. For glass beads, SSC obtained by IMS was found to be generally closer to reference SSC than by IMR, as expected for this particle shape. For the highly non-spherical particles (feldspar and mica), IMR yields slightly smaller SSC estimates than IMS, closer to reference SSCs.

For quartz fine sand and glass beads, LISST SSCs are in good agreement with reference SSCs (generally close to 1:1 lines). For feldspar powder, however, LISST overestimates SSC by a factor of 1.53 and for mica by a factor of about 8. Note that for quartz fine sand LISST measurements were possible beyond the range plotted in Fig. 3b. The SSC-measuring range of the LISST is treated below in the section 'Upper limit of measureable SSC'.

Effects of particle shapes and LISST inversion modes on PSD estimates

Figure 4 shows the PSDs obtained from LISST using IMS and IMR, as well as PSDs obtained from the non-portable LD and information on particle sizes from image analysis (Table 2) for the four particle types. LISST PSDs are the results of the measurements taken at a nominal SSC of 1 g/l, i.e. the averages of 100 single measurements each. Selected results from LISST measurements shown in Fig. 4 and the so-called spreading, $\sigma=(d_{84}/d_{16})^{0.5}$, which describes the 'width' of a PSD, are given in Table 4 for each particle type.

As expected for glass beads, the PSD obtained from LISST with IMS (broken line in Fig. 4a) matches well with the PSD from non-portable LD (grey line), and the median particle size d_{50} from LISST with IMS (40 µm, Table 4) corresponds well to the value obtained from image analysis (39 µm, Table 2). Using IMR instead of IMS produces smaller sizes at the coarse fractions within the PSD.

For quartz fine sand, PSDs from LISST IMS and non-portable LD are similar again, and using IMR instead of IMS has a similar effect as observed with glass beads. The intermediate and the equivalent sphere diameter at 50% by mass obtained from image analysis ($b_{50} \approx d_{es,50}$ = 130 µm, Table 2) are within the d_{50} values from LISST IMR and IMS (116 and 141 µm respectively, Table 4).

For feldspar powder, the PSD obtained with LISST IMS is well in line with that from non-portable LD, except for finer particles, where LISST shows more fine particles towards the lower end of its size-measuring range. With IMR the deviation at fine particles is less pronounced. Although

Table 2 Particle sizes obtained from image analysis

Particle type	Particle size (µm)												
	Longest diam.			Intermediate diam.			Shortest diam.			Equiv. sphere diam.			Sauter
	a_{10}	a_{50}	a_{90}	b_{10}	b_{50}	b_{90}	c_{10}	c_{50}	c_{90}	$d_{es,10}$	$d_{es,50}$	$d_{es,90}$	SMD
Glass beads	24	39	~55	≈a			≈a			≈a			37
Quartz fine sand	130	200	~270	80	130	~190	~45	~70	~140	87	130	~190	110
Feldspar powder	10	40	~80	6	23	~45	~4	~11	~20	7	25	~50	13
Mica powder	16	55	~90	9	24	~48	1	2	3	7	15	~25	4

Table 3 Quantification of basic particle shapes based on image analysis

Particle type	Aspect ratios (-)					
	b/*a*			*c*/*b*		
% finer by no. of particles	10	50	90	10	50	90
Glass beads	~1					
Quartz fine sand	0.82	0.63	0.50	No data available		
Feldspar powder	0.86	0.60	0.31	No data available		
Mica powder	0.80	0.60	0.33	0.21	0.11	0.06

the measurement with non-portable LD indicates that the feldspar powder contains no particles smaller than the lower limit of the size-measuring range of the LISST (approx. 2 μm), the LISST PSDs using both IMS and IMR do not set in at 0% at the lower limit of the size-measuring range. This means that, in the LISST measurements of feldspar powder, a considerable proportion of PVC is detected in the lowest size bin. Similar to glass beads and fine quartz sand, IMR yields smaller sizes in the coarse fractions within the PSD compared to those obtained with IMS or non-portable LD. The d_{50} values of the feldspar particles (with angular and elongated shapes) obtained from LISST IMR and IMS (32 and 34 μm respectively, Table 4) are greater than the corresponding intermediate and equivalent sphere diameters obtained from image analysis (b_{50}≈23 μm, $d_{es,50}$=25 μm, Table 2).

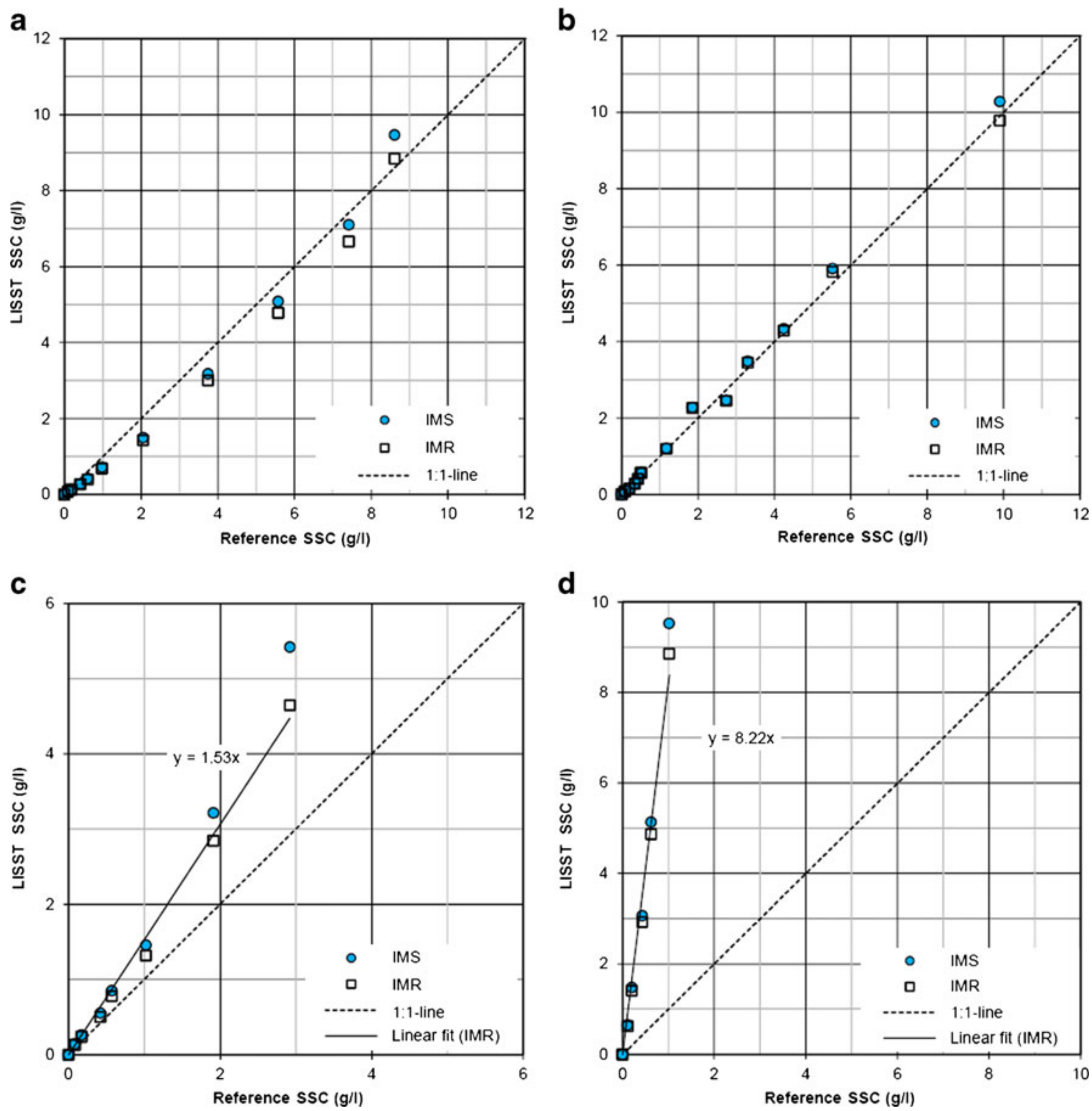

Fig. 3 SSCs obtained from LISST using both inversion modes compared to reference SSCs: **a** glass beads, **b** quartz fine sand, **c** feldspar powder and **d** mica powder

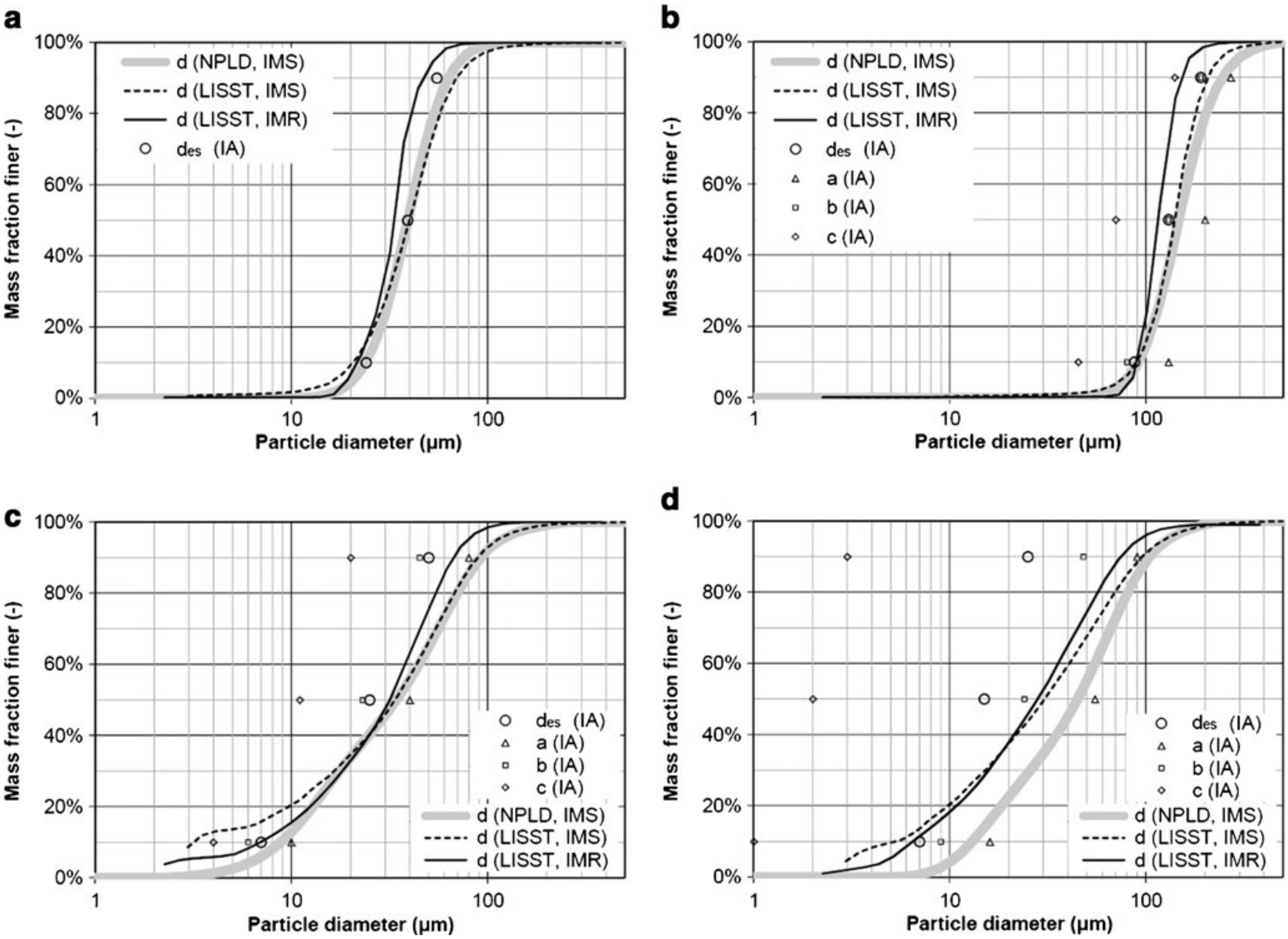

Fig. 4 PSDs obtained from LISST (using both inversion modes, at nominal SSC=1 g/l) and from the non-portable LD device (NPLD) in comparison to particle sizes from image analysis (IA): **a** glass beads, **b** quartz fine sand, **c** feldspar powder and **d** mica powder

For mica powder, LISST yields with both inversion modes smaller particle sizes than the non-portable LD. The particle size d_{50} with IMR (28 µm) is slightly greater than the intermediate diameter of the mica flakes (b_{50}≈24 µm) and considerably greater than the equivalent sphere diameter ($d_{es,50}$=15 µm), which were obtained from image analysis. IMR yields less fine and coarse particles within PSDs compared to IMS, i.e. the spreading of the PSD obtained by IMR is smaller, which is qualitatively similar to the results for feldspar powder.

Table 4 Particle sizes and spreading obtained from LISST (at nominal SSC=1 g/l)

Particle type	Particle size (µm)						Spreading σ of PSDs (-)	
	IMS			IMR				
	d_{10}	d_{50}	d_{90}	d_{10}	d_{50}	d_{90}	IMS	IMR
Glass beads	20	40	69	22	33	47	1.59	1.33
Quartz fine sand	89	141	208	89	116	154	1.37	1.22
Feldspar powder	3	34	89	7	32	67	3.23	2.40
Mica powder	5	30	95	6	28	75	3.15	2.65

Effects of SSC on LISST PSD estimates

Ideally, PSD should not depend on SSC for a given particle type. However, in the experiments shifts in PSDs were observed with increasing SSC, especially with SSC approaching the upper limit of the SSC-measuring range of LISST. The PSDs using IMR for a range of SSC are shown in Fig. 5 for the four particle types. For glass beads and quartz fine sand, the PSDs up to a few g/l are quite constant with increasing SSC and slightly deviate to finer sizes at higher SSCs such as 10 or 20 g/l. The proportion of fine particles within the measured PSDs of mica and feldspar powders increases with increasing SSC. For feldspar powder the proportion of PVC obtained in the lowest size bin increases at higher SSC (growing offset at the fine end of PSDs in Fig. 5c). This effect is also visible in Fig. 6 in which the contributions of the size bins to total PVC are shown. Similarly, SSC overestimation slightly increasing with SSC is seen at the individual

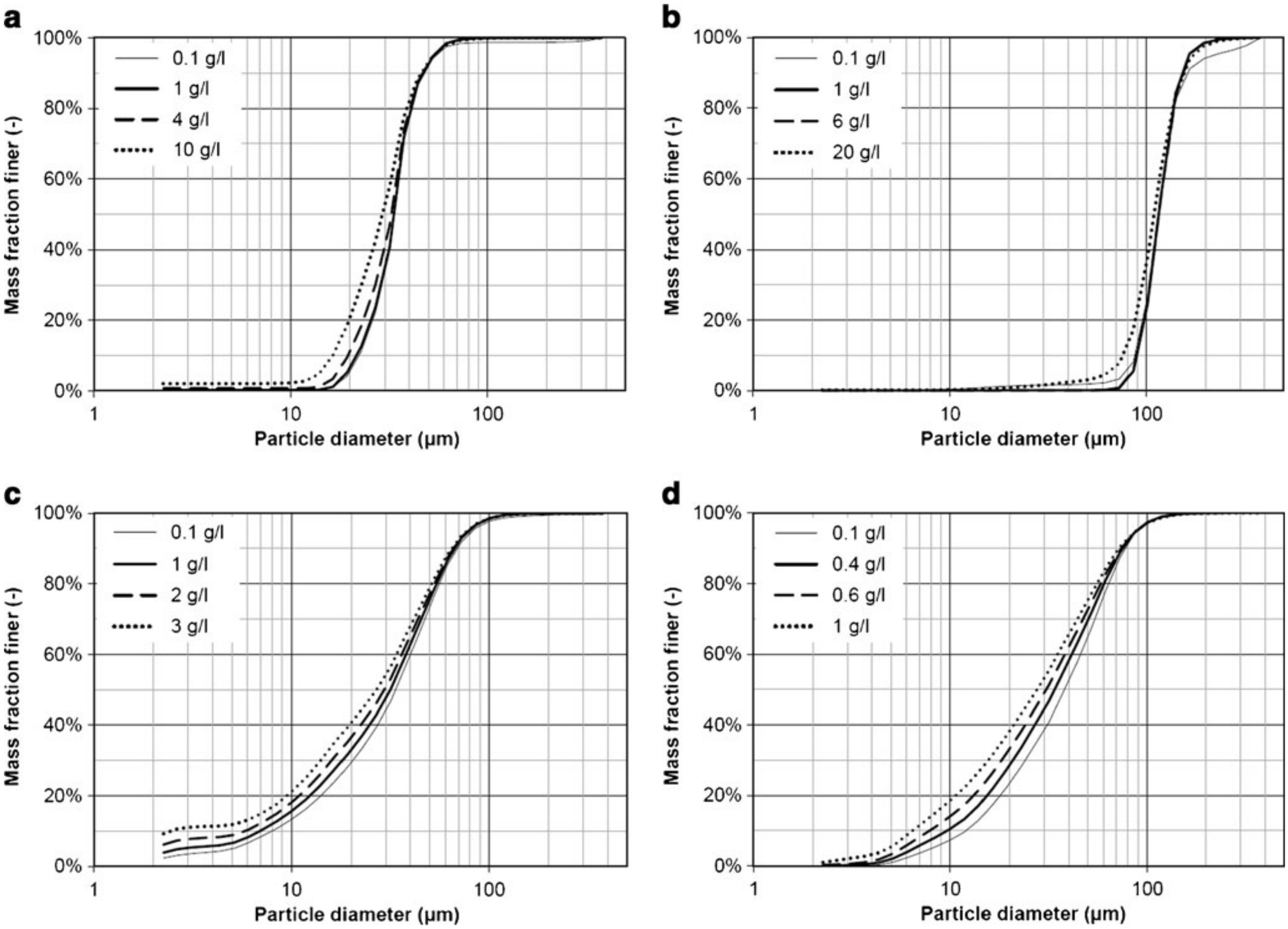

Fig. 5 PSDs obtained from LISST using IMR at increasing SSCs: **a** glass beads, **b** quartz fine sand, **c** feldspar powder and **d** mica powder

IMR points in Fig. 3c. On the contrary, for mica powder there are no offsets at the fine end of the measured PSDs.

Mixed particle-type effects on SSC and PSD

Figure 7 shows IMR SSCs of feldspar and mica suspensions (as in Fig. 3c and d) and of a suspension made of 70% feldspar and 30% mica as a function of reference SSC with linear fits

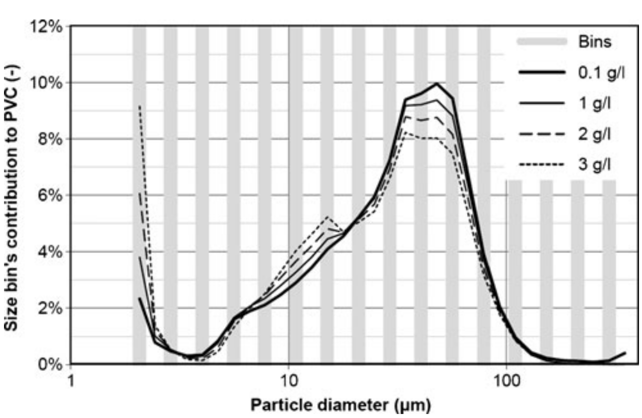

Fig. 6 Contribution of each of the 32 size bins to total PVC measured in feldspar powder suspension at increasing SSC using IMR

(calibration curves) and equations (SSC overestimation factors). LISST overestimates SSC of this mixture by a factor of

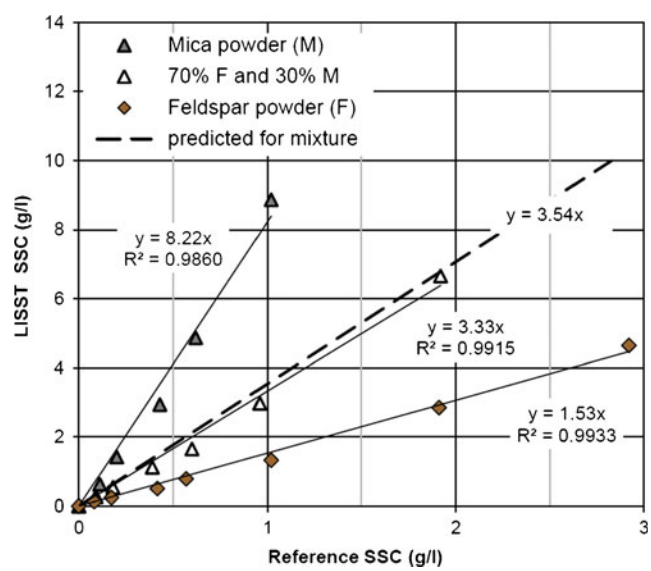

Fig. 7 LISST SSCs of feldspar and mica powders and a 7:3 mixture of these components as a function of reference SSC using IMR, in comparison to the predicted curve for the mixture

3.33. Assuming that the SSC overestimation factor for a mixed particle-type suspension can be calculated as the weighted sum of the SSC overestimation factors of the components and their mass fractions, the predicted calibration curve for the mixture was plotted, too. The slope of this curve, i.e. the predicted overestimation factor, is 70% × 1.53 + 30% × 8.22 = 3.54, which is in a good agreement with the experimentally determined value of 3.33, justifying the assumption of linear superposition.

Figure 8 shows the PSDs for the mixture and its two components individually (Fig. 4c and d). Again, the curves are the averages of 100 single measurements taken at a nominal SSC of 1 g/l, processed with IMR. By coincidence, the LISST PSDs of the feldspar and mica particles are similar even though their particle sizes and shapes are different according to image analysis. For the mixture, no considerable shift in PSD was observed.

Upper limit of measureable SSC

The nominal range of SSC that can be measured with LISST according to the instrument manufacturer (Sequoia 2008) is plotted in Fig. 9 (shaded area) as a function of SMD. The upper limit of the nominal SSC-measuring range scales linearly with SMD and is based on the recommended value of optical transmission $\tau \geq 0.3$ and a particle density of 2.65 g/cm^3 (Sequoia 2008). Below this limit, measurements may still be possible, but reportedly with less accuracy due to multiple scattering.

With τ decreasing below 0.3, some or eventually all of the single measurements performed at one nominal SSC result in zero values for PVCs when the data are processed using the LISST software. In other words, data in some or all rows of the raw data file may be non-invertible as SSC reaches or exceeds the upper limit of measurable SSC. In the present study, the ratio k of the number of invertible to the total number of single measurements at each nominal SCC was calculated. The highest reference SSC with k=1 and the reference SSC of

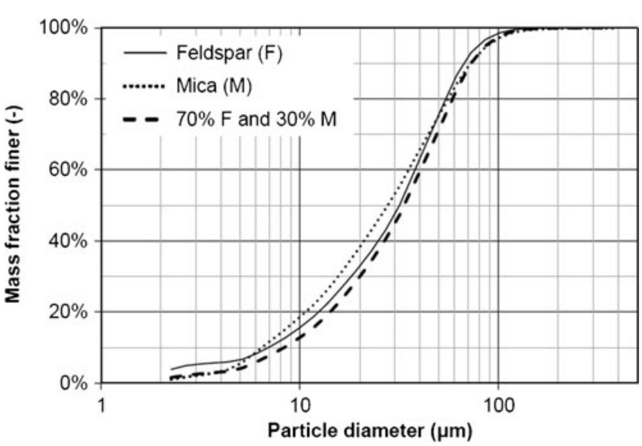

Fig. 8 LISST PSDs of feldspar and mica powders, and a 7:3 mixture of these components (using IMR at nominal SSC=1 g/l)

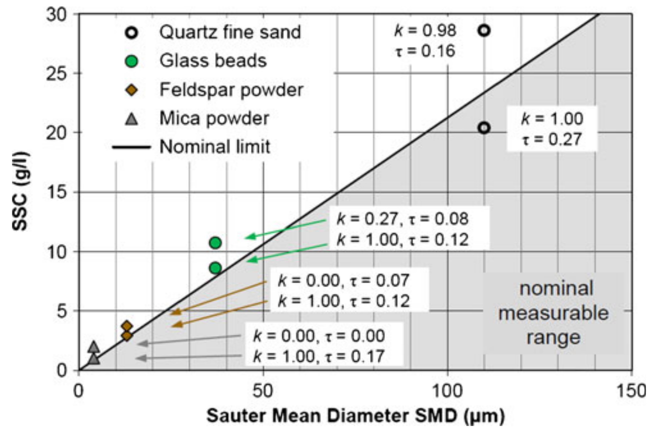

Fig. 9 SSC range that can be measured by LISST as a function of SMD: experimental results (with rate of invertible measurements k and optical transmission τ) in comparison to nominal range (*shaded area*)

the next higher nominal SSC level (with k<1) are plotted in Fig. 9 for each particle type, as a function of SMD obtained from image analysis (Table 2). The values of k and τ are also indicated in the figure. The latter were obtained from LISST and averaged over the invertible measurements. The inversion of all single measurements (k=1) at each nominal SSC was possible down to τ values between 0.12 and 0.27. As the SSC was increased stepwise in the experiments, the highest SSCs with k=1 are not exactly known; nevertheless, it is known that the upper limit of the SSC-measuring range lies between each pair of points (with τ<0.3). Note that the information shown in Fig. 9 refers to a *LISST-100X* with a 90% path reduction module inserted (without path reduction module, the upper limit of measurable SSC would be 10 times lower).

Fluctuations of SSC and PSD

SSC and PSD data obtained from measurements at each nominal SSC level exhibit temporal variations (fluctuations). Figure 10 shows two examples of SSC time series (extract of 2 minutes) measured in suspensions of quartz fine sand or

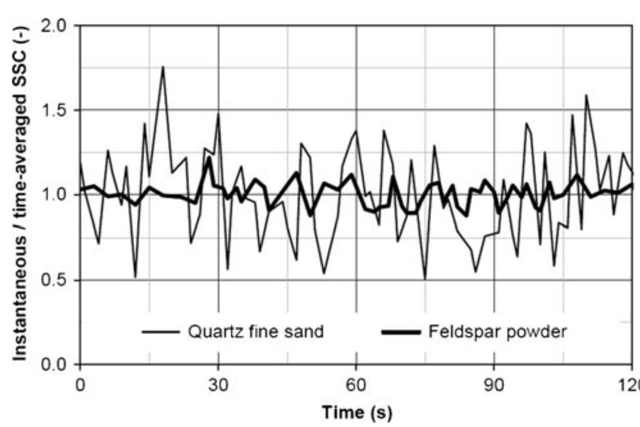

Fig. 10 Normalized time series of LISST SSC for feldspar powder and quartz fine sand at nominal SSC=1 g/l

feldspar powder, both at nominal SSC=1 g/l using IMR. The instantaneous SSC values of each series are normalized by their time averages. SSC fluctuations for quartz fine sand are greater than for feldspar powder.

Table 5 summarizes the coefficients of variation (CV) of LISST SSCs, i.e. the standard deviation of 100 single measurements divided by their time average, for the four particle types with increasing SSCs. The CV is a measure of relative deviations of instantaneous SSC from its mean value and allows a comparison across measurements at various SSCs. It was found that the CVs of quartz fine sand are about 3 to 6 times higher than those of the other particle types. Moreover, for quartz fine sand the CV decreases with increasing SSC while for the other particle types less dependence on SSC was observed.

Characteristic ranges of PSDs obtained from LISST again using IMR for quartz fine sand or feldspar powder at nominal SSC=1 g/l are shown in Fig. 11. For both particle types the time-averaged PSD (thick lines) are plotted together with the 5% and 95% fractiles (thinner lines). The fractile values were obtained by taking the 5th and the 95th value out of 100 sorted values in the respective size classes. Absolute PSD fluctuations (in μm) are greater with coarser particles. The relative fluctuation of, for example, d_{50} is similar for both particle types.

Discussion

Accuracy and experimental errors

For the relatively fine particles (feldspar and mica powders, as well as glass beads), the determined reference SSCs were not more than 10% below nominal SSCs, indicating a satisfactory mixing in the tank. For coarser particles (quartz fine sand), however, SSCs of individual bottle samples fluctuated considerably and average reference SSCs per concentration level were generally some 40% below nominal SSCs due to incomplete mixing. Besides incomplete mixing, deviations between

Table 5 Coefficients of variation (CVs) of LISST SSCs

Nominal SSC (g/l)	Quartz fine sand (-)	Glass beads (-)	Feldspar powder (-)	Mica powder (-)
0.1	0.45	0.15	0.10	0.07
0.2	0.35	0.07	0.08	0.07
0.4	0.30	0.06	0.07	0.06
1	0.27	0.06	0.08	0.07
2	0.30	0.05	0.07	-
4	0.28	0.06	-	-
10	0.26	0.07	-	-

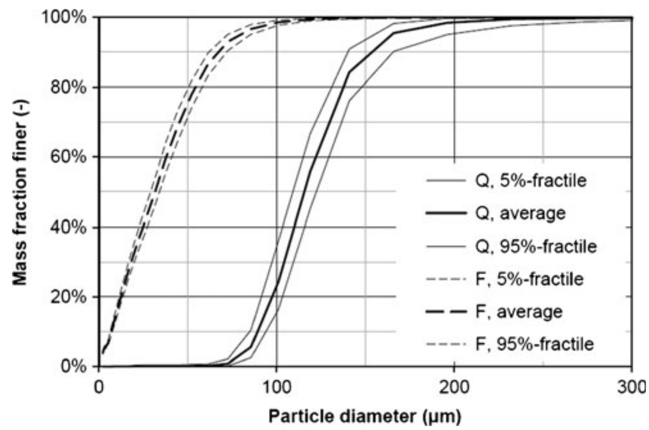

Fig. 11 Fluctuations of LISST PSDs for feldspar powder (F) and quartz fine sand (Q) at nominal SSC=1 g/l

reference and nominal SSCs can be attributed partly to instantaneous local SSC variations and partly to imperfections when taking or treating the samples. The SSC data points in Fig. 3 indicate that the experimental setup and procedure allowed getting systematic results, although the SSC data show some scatter around the average for each particle type. An independent second measurement performed with quartz fine sand at reference SSC of 0.5 g/l showed a good reproducibility (5% deviation among repeated reference SSC measurements and less than 1% deviation among repeated time-averaged LISST SSCs).

Reference PSDs were not determined from the samples taken from the mixing tank but from the dry material prior to the experiments, which potentially lead to non-representative sampling. With respect to image analysis, coarser fractions within PSDs are subject to uncertainty depending on the selected investigation area and due to the small number of coarser particles. PSDs from non-portable LD are, as LISST, subject to effects of particle shape and should thus not be considered as results of a primary method for the non-spherical particle types but rather as an additional independent measurement from an LD device with a wider size-measuring range. For future laboratory investigations, analyses of a high number of microscope images based on automatic object detection and/or using certified particles are recommended to increase the accuracy of reference PSDs.

The effect of incomplete mixing in the tank is not relevant with regard to SSC since the SSC prevailing in the tank at the instrument's level was taken as reference. With regard to PSDs, however, incomplete mixing occurring especially at high SSC and with coarser particles may cause deviations from reference PSDs because the samples were not directly taken from the tank in which coarser particles may settle or preferentially stay below the instrument's level (vertical SSC gradient). Effects of potential flocculation were neglected, since it was assumed that the particle densities correspond to the solid densities of the minerals.

Particle shape and inversion mode

The biases on LISST measurements due to particle shape are discussed first with respect to SSC and secondly with respect to PSD. It was found that non-spherical particles cause stronger biases on SSC than on PSD.

For glass beads and quartz fine sand with spherical and rounded shapes, and with d_{50} in the size range of coarse silt to fine sand, the LISST yields SSC estimates with reasonable accuracy (Fig. 3a, b). Note that this is based on the factory calibration (instrument-specific volume conversion constant). With respect to SSC, the selection of inversion mode plays a minor role for these particle shapes. However, the measurements in suspensions of feldspar and mica powders showed that LISST considerably overestimates SSCs (Fig. 3c, d). The elongated and partly very angular or flaky shapes of these particles (Fig. 1c, d) differ considerably from those of the natural sediment grains depicted in Agrawal et al. (2008) and used in the development of IMR. Using IMR instead of IMS only slightly reduces the overestimation of SSCs for strongly non-spherical particles (Fig. 3c, d).

The considerable SSC overestimation measured with mica and feldspar powders can be explained by the deviation between the particle sizes d obtained from LISST and the equivalent sphere diameters d_{es} from image analysis. For mica, the ratio of the median diameters obtained by the two methods is $d_{50}/d_{es,50} = 28/15 = 1.87$ (using IMR). A factor of 1.87 in particle diameter causes a change in volume and thus SSC of $1.87^3 = 6.5$. Considering the ratio of particle diameters obtained by the two methods not only for the median diameters but also for the whole PSD, an SSC overestimation of 9.6 was calculated (based on diameter ratios in steps of 10% by weight). For feldspar powder an SSC overestimation of 1.8 was calculated with the same procedure. The measured SSC overestimations by a factor of 8 for mica and by a factor of 1.53 for feldspar powders are thus not surprising and are mainly attributed to non-spherical particle shapes. Further investigations on this aspect are recommended, considering also the light scattering of angular particles.

LISST measurements in glass beads suspension, for which IMS is applicable by definition, yield PSD similar to those obtained from image analysis and non-portable LD (Fig. 4a) as expected. For quartz fine sand, at which IMR is applicable, IMR yields particle sizes that are comparable to intermediate (b-axis) and volume-equivalent sphere diameters from image analysis (Fig. 4b). From the LISST PSDs using both inversion modes and the analysis of only one microscope image, it cannot be concluded whether IMR is an improvement over IMS with respect to PSD for this particle type. For feldspar and mica powder, i.e. highly non-spherical particles, the use of IMR reduces the spreading of PSDs and the overestimation at small particle sizes, which is discussed in the next section.

Overestimation at small particle sizes

In feldspar powder suspension, especially at SSC approaching the upper limit of measureable SSC, the LISST yielded relatively high PVCs at the lower end of its size-measuring range, i.e. in the lower size bins (Figs. 5c and 6). Previous studies (Agrawal and Pottsmith 2000; Agrawal et al. 2008; Andrews et al. 2011) report that LISST may overestimate PVCs mainly in lower size bins contributing to the overestimation of SSC. This can be due to one or several of the following reasons: (1) presence of fine out-of-range particles, (2) multiple scattering at low optical transmission, (3) effects of refractive index and (4) effects of particle shape.

With respect to *out-of-range particles*, i.e. particles smaller or larger than the nominal sizes measurable with a given LD model, Agrawal and Pottsmith (2000) describe that such particles may affect LISST results since part of the scattering they cause is recorded at the most inner or most outer rings ('leakage' of out-of-range particles into the measuring range). The size-measuring range of a LD device is related to the range of angles at which scattering can be recorded. Andrews et al. (2011) describe that fine out-of-range particles have a stronger effect on LISST measurements than coarse out-of-range particles. As mentioned in the Results section above, there were no out-of-range particles based on the PSDs from the non-portable LD device with a measuring range down to 0.01 μm (grey lines in Fig. 4). The relatively high PVCs at lower size bins obtained by LISST in feldspar powder suspension are thus unrealistic and are not explained by fine out-of-range particles.

With respect to *multiple scattering*, Agrawal and Pottsmith (2000) reported that PSD may be biased to small sizes at optical transmission $\tau<0.3$ (high turbidity). In the present study, in feldspar powder suspension at nominal SSCs of 0.1, 1, 2 and 3 g/l (see Fig. 5c), the corresponding optical transmissions τ were 0.93, 0.50, 0.24 and 0.12 respectively. Multiple scattering may thus be an issue at higher SSCs. However, since unrealistically high PVCs in lower size bins were also obtained at $\tau>0.3$, these cannot be attributed to solely multiple scattering.

As far as the *refractive index* is concerned, Andrews et al. (2011) reported a reduction of unrealistically high PVCs in lower size bins as a result of an alternative inversion procedure with a different refractive index. The refractive indices of glass, quartz and feldspar in water are quite similar; for mica it may vary according to the orientation of the particle. As the optical properties of the particles were not measured and custom inversion procedures were not treated in this study, effects of refractive indices cannot be addressed in detail but are considered to be unimportant except for mica. Since the highest overestimation of PVCs at small particle sizes was observed for feldspar powder, it is concluded that this effect is not to be explained by refractive index.

With respect to *particle shape*, Agrawal et al. (2008) showed that relatively high PVCs obtained in lower size bins can be associated with particle shape. By developing IMR, unrealistic contributions of lower size bins were reduced in comparison to IMS. Based on the measurements in this study, however, it is concluded that a non-negligible overestimation at lower size bins remains with feldspar powder suspension when using IMR. It appears that this effect is mainly associated with very angular particle shape and, possibly, to a smaller extent with multiple scattering.

Omitting contributions of three lowest size bins

Since PVCs measured in the lower size bins in feldspar powder suspension are not realistic, a simple correction method was applied to the data. Expecting a unimodal PSD in Fig. 6, it was decided to discard the PVCs of the three lowest size bins (1.9 to 3.1 μm) in the calculation of SSC and PSD. In other words, the 'raising tail' at the fine end of the non-cumulative size distribution (Fig. 6) is omitted. Figure 12 shows the effect of this correction on LISST SSCs for feldspar powder. These are reduced, but do not reach reference SSCs. With the correction the SSC overestimation depends less on SSC (better linear fit in Fig. 12 compared to Fig. 7) and is reduced from 1.53 to 1.38. When the three lowest size bins are omitted, the corresponding PSDs in Fig. 13 are almost not affected by increasing SSC, in contrast to those before the correction shown in Fig. 5c. Further experiments including angular particles are recommended to investigate the causes of unrealistically high PVCs at lower size bins and PSD variations due to increasing SSC in order to find and validate correction methods with higher accuracy.

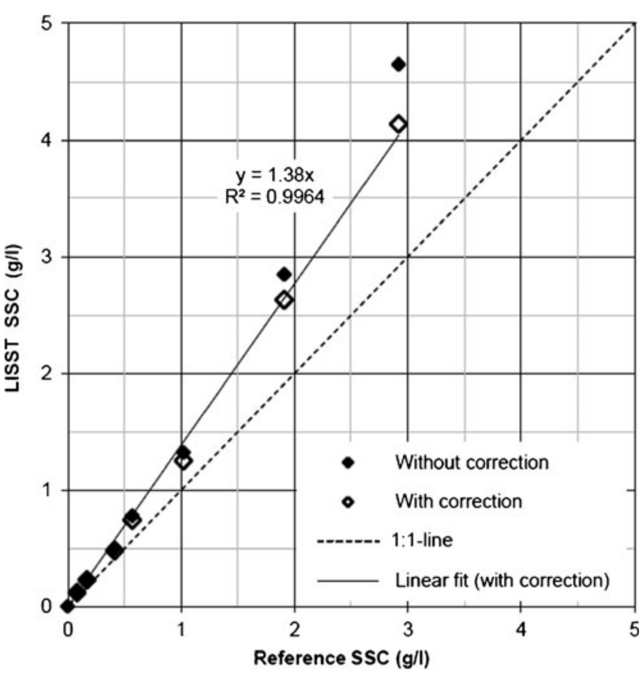

Fig. 12 Effect on LISST SSC estimate if contributions of three lowest size bins are omitted (feldspar powder)

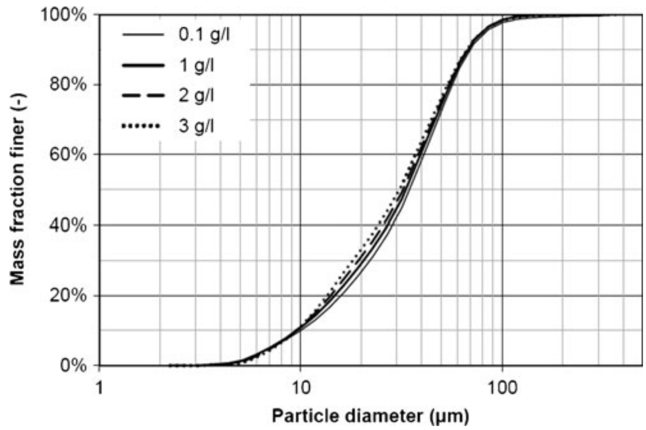

Fig. 13 LISST PSDs at increasing SSC without contributions of three lowest size bins (feldspar powder)

Particle shape-dependent SSC correction factors

LISST raw data are recorded on detector rings in a plane and are related to the average projected area of particles. For the calculation of PVC, information on the ratio of average projected area to particle volume is required. Such information comes from the selection of the inversion mode (according to particle shape) and the device-specific volume conversion constant—e.g. for mica flakes the ratio of average projected area to particle volume differs strongly from that of spheres.

The experiments showed that LISST IMR does not provide PVCs and SSCs with good accuracy for highly non-spherical particles. SCCs can be corrected using the overestimation factor, i.e. the slope of the calibration curve for a known particle type. For a known suspension made with particles of different shapes and known overestimation factors for the involved particle types, SSC can be corrected by the weighed sum of these factors and the mass fraction of the components, as found in one example (see Results section, 'Mixed particle-type effects on SSC and PSD'). Further investigations are suggested to support the generalization of this approach. The prediction of the overestimation factor in the example is improved when unrealistic contributions of the three lowest size bins, which occurred with feldspar powder, are omitted (cf. above; Fig. 12): then, the predicted overestimation factor is 70% × 1.38 + 30% × 8.22 = 3.43, which is closer to the experimentally determined slope (3.33) than before.

The magnitudes of the correction factors found in this study for feldspar or mica powders should not be taken as fixed values since there are many different types and sub-types of minerals and particle shapes differing from those investigated in this study. In field studies, flaky or very angular particles usually make up just a fraction of the particle mix and therefore it is suggested to determine a time-averaged SSC correction factor specifically for such a particle mixture prevailing at a measuring location. This can be done by a comparison of LISST and reference SSCs obtained from laboratory analysis of manually or automatically taken bottled samples at corresponding times. In addition, microscope images of the particles prevailing at the study site may be useful to characterize the geometrical properties of the particles.

Range of measureable SSC

The SSC-measuring range of the LISST determined in this study is in good agreement with the nominal range given by the manufacturer as a function of SMD (Sequoia 2008), although optical transmissions slightly below τ=0.3 were measured at the nominal upper limit of the SSC-measuring range. For many LISST applications the upper limit of measurable SSC is important. In order to estimate it realistically, SMD has to be used for graded particles rather than d_{50}, as recommended by Sequoia (2008). This is particularly important for elongated and platy particles, for which SMD is usually considerably smaller than d_{50}. If higher SSCs are to be measured, a further reduction of the optical path length can be considered, or an in-line LISST device with a mixing chamber in which pumped samples are diluted with clear water at a known mixing ratio (Agrawal et al. 2011). The lower limit of measurable SSC (detection limit), however, was not relevant in the context of this study.

Time averaging

As seen from Table 5, the CV values of LISST SSCs for glass beads, feldspar or mica powders are considerably smaller than those for fine quartz sand. This difference in the CVs can be attributed (1) to the interaction between the particles and the turbulent flow and (2) to the measurement method. Particle size has an influence on the particle behavior in the flow field because smaller particles (powder) mostly follow the local flow like a passive tracer, whereas larger particles (fine sand) show different behavior resulting in a less homogenous distribution. With respect to the measurement method, it has to be considered that the number of particles in the relatively small measurement volume (thickness of the laser beam over an optical path length of 5 mm) decreases strongly with increasing particle size: at identical SSC the number of fine sand particles (e.g. 150 μm) is about 1,000 times lower than the number of silt particles (e.g. 15 μm), leading to phenomena well known in the statistical description of small populations. Therefore, time averaging of repeated single LISST measurements is particularly important for coarser particles, especially at low concentrations. The measuring frequency and the period over which measurements are averaged have to be selected in accordance to the time scale of the process, the PSD and SSC of the expected particles, as well as the desired accuracy.

Conclusions

The results convincingly demonstrate that the LISST yields reasonable PSD estimates in the range of coarse silt to fine sand. With respect to SSC, the factory calibration of the instrument was found to be satisfactory for spherical and rounded particles using IMS and IMR respectively. However, when IMR is used with very angular, elongated or flaky particles, PSDs are biased, for feldspar mainly at lower size bins, and SSCs are considerably overestimated. For highly non-spherical particles, SSC estimates can be corrected by the overestimation factor of a given particle type. For suspensions containing various particle types, the SSC estimate can be corrected by the weighted sum of the overestimation factors of the components and their mass fractions. If these are not known, then gravimetrical analyses of samples with a specific particle mix are required for calibration of SSC. In addition to applying factors on SSC, SSC and PSD can be corrected by omitting overestimated contributions of lower size bins if applicable.

With an optical path length of 5 mm, SSCs can be measured up to a few g/l in a suspension of angular silt particles and up to approx. 25 g/l for rounded fine sand. Measurement accuracy can be improved by time averaging over a higher number of individually inverted single measurements, especially for coarser particles at low SSC.

The intermediate diameter b was found to be similar to d_{es} for all particle types except for mica, which has a flake thickness that is an order of magnitude smaller than the length or width of the particles. Further investigations are necessary to assess effects of non-spherical particles and mixtures of various types of particles on LISST SSC and PSD estimates.

Prior to field deployments, testing and calibrating of measuring devices under controlled laboratory conditions with respect to the specific application are important and strongly recommended. Compared to other available instruments for continuous real-time in-situ suspended sediment monitoring, LISST offers the great advantage of providing not only SCC but also PSD data at high temporal resolution, and the provided SSC estimates are not, or less, affected by particle size changing in time.

Acknowledgements The authors gratefully acknowledge the financial support for this study by swisselectric research, the Swiss Federal Office of Energy and Gommerkraftwerke (the operator of the case study hydropower plant). We thank Prof. Dr. T. Staubli, A. Abgottspon, Prof. Dr. P. Gruber, and M. Duss from Hochschule Luzern, Competence Centre Fluid Mechanics and Hydro Machines, for their valuable contributions to the laboratory investigations. Further thanks go to the Geotechnical Laboratory and the Institute for Building Materials of ETH Zurich for the measurements of particle density and PSDs with non-portable LD, as well as the scanning electron microscope images of the particles. The efforts from Sequoia Scientific's team for promoting knowledge exchange in the domain of in-situ suspended sediment monitoring and contributions to measure other than smooth spherical particles by LD are acknowledged. We thank Sequoia Scientific and the local partners for organizing the conference 'Particles in Europe' held in October 2012 in Barcelona, where parts of this paper were presented. The constructive comments of three reviewers of this paper are acknowledged.

References

Abgottspon A (2011) Messung abrasiver Partikel in Wasserkraftanlagen. MSc Thesis, Hochschule Luzern, Switzerland

Agrawal YC, Pottsmith HC (2000) Instruments for particle size and settling velocity observations in sediment transport. Mar Geol 168: 89–114. doi:10.1016/S0025-3227(00)00044-X

Agrawal YC, Whitmire A, Mikkelsen OA, Pottsmith HC (2008) Light scattering by random shaped particles and consequences on measuring suspended sediments by laser diffraction. J Geophys Res 113, C04023. doi:10.1029/2007JC004403

Agrawal YC, Mikkelsen OA, Pottsmith HC (2011) Sediment monitoring technology for turbine erosion and reservoir siltation applications. In: Proc Hydro 2011 Conf, Aqua-Media Int Ltd, Prague, Czech Republic

Agrawal YC, Mikkelsen OA, Pottsmith HC, Slade WH (2012) Turbine abrasion: one year's experience in real-time sediment monitoring at Hidroagoyan HPP, Ecuador. In: Proc Hydro 2012 Conf, Aqua-Media Int Ltd, Bilbao, Spain

Andrews SW, Nover DM, Reuter JE, Schladow SG (2011) Limitations of laser diffraction for measuring fine particles in oligotropic systems: pitfalls and potential solutions. Water Resour Res 47, W05523. doi: 10.1029/2010WR009837

Boes RM (2009) Real-time monitoring of suspended sediment concentration and particle size distribution in the headwater way of a high-head hydropower plant. In: Proc 33rd IAHR Congr, Vancouver, Canada, pp 4037–4044

Bowers DG, Braithwaite KM (2012) Evidence that satellites sense the cross-sectional area of suspended particles in shelf seas and estuaries better than their mass. Geo-Mar Lett 32(2):165–171. doi:10.1007/s00367-011-0259-6

Costa LI, Storti G, Lüscher B, Gruber P, Staubli T (2012) Influence of solid particle parameters on the sound speed and attenuation of pulses in ADM. J Hydrol Eng 17(10):1084–1092. doi:10.1061/(ASCE)HE.1943-5584.0000555

Felix D, Albayrak I, Abgottspon A, Boes RM, Gruber P (2012) Suspended sediment and Pelton turbine wear monitoring: experimental investigation of various optical and acoustic devices and beginning of the case study at HPP Fieschertal. In: Proc 17th Int Seminar Hydropower Plants, Vienna, Austria, pp 483–494

Felix D, Albayrak I, Boes RM (2013) Monitoring of suspended sediment - laboratory tests and case study in the Swiss Alps. In: Fukuoka S, Nakagawa H, Sumi T, Zhang H (eds) Advances in river sediment research. Taylor & Francis Group, London, pp 1757–1766

Fettweis M, Baeye M, Lee BJ, Chen P, Yu JCS (2012) Hydro-meteorological influences and multimodal suspended particle size distributions in the Belgian nearshore area (southern North Sea). Geo-Mar Lett 32(2):123–137. doi:10.1007/s00367-011-0266-7

Haun S, Kjærås H, Løvfall S, Olsen NRB (2013) Three-dimensional measurements and numerical modelling of suspended sediments in a hydropower reservoir. J Hydrol 479:180–188. doi:10.1016/j.jhydrol.2012.11.060

Konert M, Vandenberghe J (1997) Comparison of laser grain size analysis with pipette and sieve analysis: a solution for the underestimation of the clay fraction. Sedimentology 44:523–535. doi:10.1046/j.1365-3091.1997.d01-38.x

Nichols G (2009) Sedimentology and stratigraphy, 2nd edn. Wiley-Blackwell, Chichester

Sequoia (2008) LISST concentration limits. Article dated 29 August 2008, accessed 27 September 2013. Sequoia Scientific, Inc, Bellevue, WA, http://www.sequoiasci.com/article/lisst-concentration-limits/

Sequoia (2011) LISST bin sizes for inversions based on randomly shaped grains. Article dated 18 March 2011, accessed 27 September 2013. Sequoia Scientific, Inc, Bellevue, WA, http://www.sequoiasci.com/article/lisst-bin-sizes-for-inversions-based-on-randomly-shaped-grains/

Skripalle J, Hies T, Liu Y, Nguyen HH (2012) Application of multi-frequency acoustics to estimate concentration of suspended sediments from Jurong Lake, Singapore. In: Proc 17th Int Seminar Hydropower Plants, Vienna, Austria, pp 725–736

Thorne PD, Agrawal YC, Cacchione DA (2007) A comparison of near-bed acoustic backscatter and laser diffraction measurements of suspended sediments. IEEE J Oceanic Eng 32(1):225–235. doi:10.1109/JOE.2007.890978

Wren D, Barkdoll B, Kuhnle R, Derrow R (2000) Field techniques for suspended-sediment measurement. J Hydraul Eng 126(2):97–104. doi:10.1061/(ASCE)0733-9429(2000)126:2(97)

Schwebstoff-Monitoring und Verschleiss an Peltonturbinen (Teile a und b)

SI/500638-01 und -02

Beilagen zum Schlussbericht (2016)

Projektbezogene Publikationen aus dem Jahr

2014

Abgottspon A., Staubli T., Felix D., Albayrak I., Boes R.M. (2014). **Monitoring Suspended Sediment and Turbine Efficiency**. *Hydro Review Worldwide*, 22(4): 28-36.

Felix D., Albayrak I., Boes R.M. (2014a). **Variation des Feinsedimentgehalts im Triebwasser infolge Speicherstollen-bewirtschaftung**. *Proc. Wasserbausymposium 2014,* VAW-Mitteilung 227, Boes R.M. (ed.), ETH Zürich: 183-193.

Felix D., Albayrak I., Boes R.M. (2014b). **Site-specific Conversion of Laser Diffractometer (LISST) Data to Suspended Sediment Mass Concentration (SSC)**. *Proc. Conference "Particles in Europe"*, Esbjerg, Denmark.

HRW®
Hydro Review Worldwide
www.hydroworld.com
July-August 2014
PennWell®

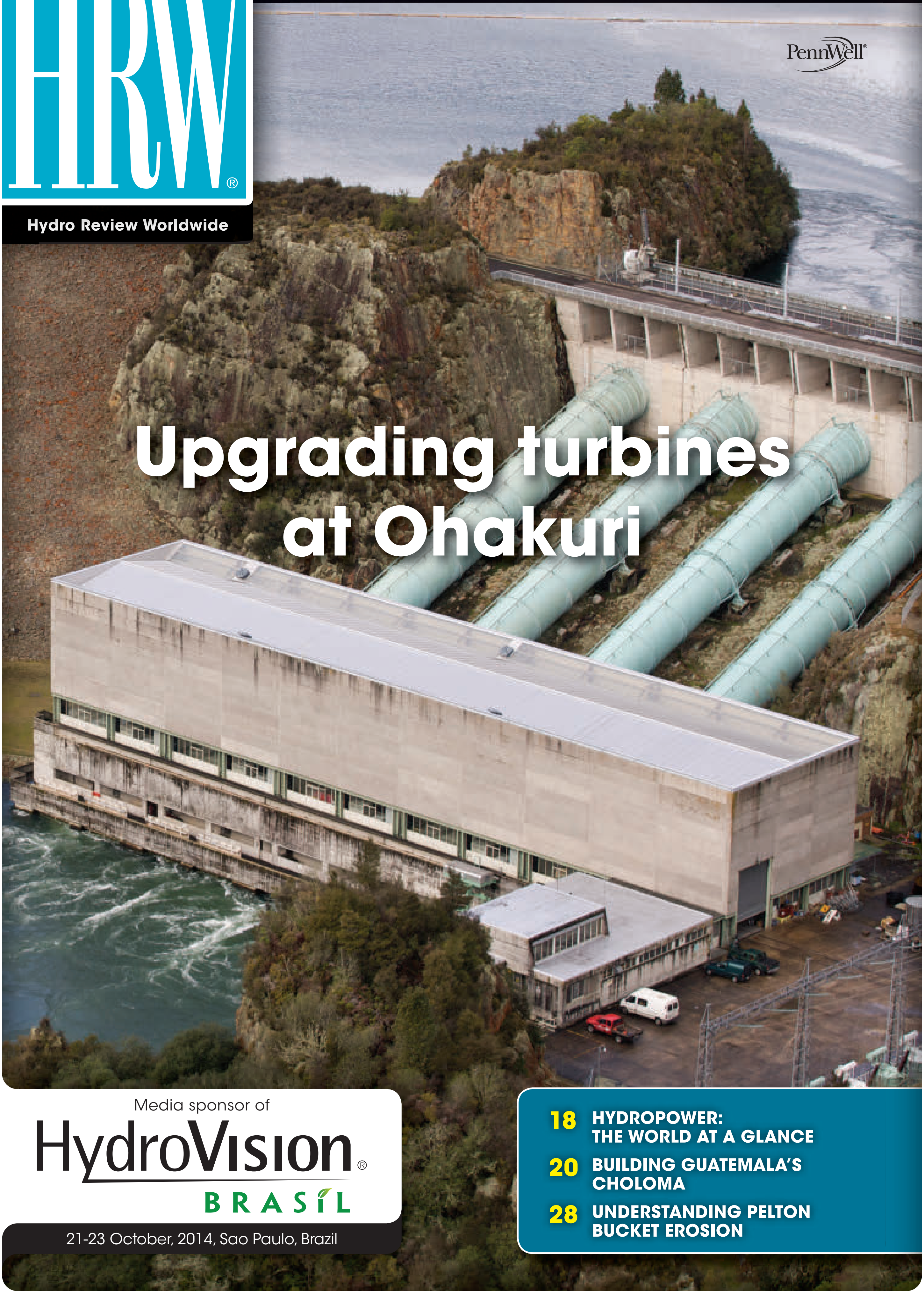

Upgrading turbines at Ohakuri

Monitoring Suspended Sediment and Turbine Efficiency

Sediment in the water passing through hydro turbines can have a significant effect on unit efficiency. The authors undertook a research project to better understand the interactions between suspended sediment, turbine wear and unit efficiency.

By André Abgottspon, Thomas Staubli, David Felix, Ismail Albayrak and Robert M. Boes

Andre Abgottspon is a research assistant and Thomas Staubli is a professor of fluid mechanics and hydro machines with the Competence Centre Fluid Mechanics and Hydro Machines at Hochschule Luzern. David Felix is a PhD student, Ismail Albayrak, PhD, is a research scientist and Robert Boes is a professor of hydraulic structures and director of the Laboratory of Hydraulics, Hydrology and Glaciology at the Swiss Federal Institute of Technology Zurich.

This article has been evaluated and edited in accordance with reviews conducted by two or more professionals who have relevant expertise. These peer reviewers judge manuscripts for technical accuracy, usefulness, and overall importance within the hydroelectric industry.

Abrasive particles in the water powering hydroelectric plants reduce unit efficiency, increase maintenance costs and may cause turbine downtime and associated production losses. To deal with this situation (called hydro-abrasive wear or hydro-abrasive erosion) during the design, operation and maintenance of hydro plants, knowledge of turbine wear needs to be improved and relevant parameters — i.e., suspended sediment concentration (SSC); size, hardness and shape of particles; relative velocity between the flow and turbine parts; turbine geometry and turbine material[1] — need to be quantified. It is not fully understood to what extent these parameters contribute to the dominant damages. Monitoring SSC and particle size distribution (PSD) is still not common, and the effect of hydro-abrasive erosion on efficiency is only qualitatively known.

In a project initiated by the Laboratory of Hydraulics, Hydrology and Glaciology (VAW) at the Swiss Federal Institute of Technology Zurich and Hochschule Luzern in Switzerland, hydro-abrasive erosion has been investigated by means of a case study at the Fieschertal hydro plant. The goal is to advance in a better understanding of interactions between suspended sediment load, turbine wear and efficiency as a basis for economic and environmental optimization.

Fieschertal is a run-of-river scheme in the Swiss Alps, with a net head of 509 m. Since the plant began operating in 1976, severe hydro-abrasive erosion has been observed at the needles, nozzles and runners of the two 32 MW Pelton units. Coating of turbines and other hydraulic parts reduced the extent of damage, but sediment handling and optimized operation and maintenance of the plant remain important economic issues.

This article presents the results on suspended sediment, turbine wear and efficiency monitoring. SSC in the water passing through the turbines is monitored using optical and acoustic devices, such as turbidimeters, a laser diffractometer and a method based on acoustic signal attenuation.[2] The inspections giving indications of wear are documented with photographs. Turbine wear is quantified by surface mapping using a three-dimensional optical scanner. The evolution of turbine efficiency is measured by periodic index tests.

Suspended sediment monitoring

The sediment load passing through the turbines can be quantified as described in the literature.[3] The so-called particle load is calculated from SSC, operating hours and weighting factors for particle size, shape and hardness.

SSC and PSD are continuously measured as they may vary considerably over time. Particle shape and hardness, however, are assumed to be constant properties of the catchment area. According to X-ray diffraction analysis, the sediments at the Fieschertal plant consist mainly of quartz and feldspar and about 20% mica. Quartz and feldspar with Mohs hardness of 6 to 7 are particularly abrasive, whereas Mica is not harmful to turbines. Microscope images reveal that the hard particles are very angular, which adds to their abrasion potential.

Among the techniques for suspended sediment monitoring (SSM), turbidimeters are most popular, despite the fact that their calibration is strongly particle-size dependent and needs generally to be established by the user.[4] Various kinds of turbidimeters (measuring optical transmission or scattering) have been used in this study. An acoustic method for SSM based on installations for acoustic discharge measurement is also applied (single frequency attenuation).[5] Furthermore, a portable laser diffractometer (LISST) is used[6] to estimate SSC and PSD. Particle size is an important parameter in the context of turbine wear.

In a first phase of the project, the SSM devices

Figure 1 — Time Series of SSC in Turbine Water

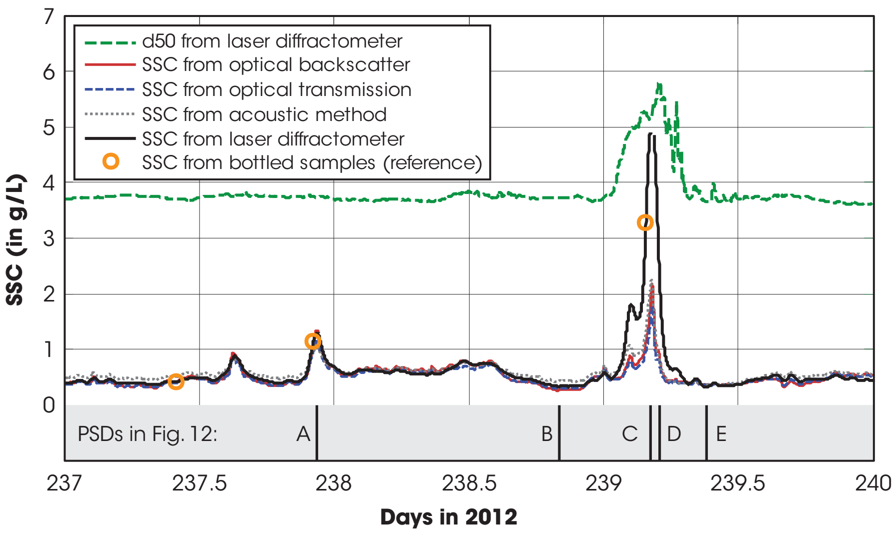

This time series of suspended sediment concentration in the water running through the turbines at the Fieschertal plant provides an example of suspended sediment transport during three summer days in 2012.

were tested in the mixing tank in the hydraulic laboratory at Hochschule Luzern, Competence Centre for Fluid Mechanics and Hydro Machines. In summer 2012, they were installed at Fieschertal. Most devices are installed in the valve chamber, at the inlet to the penstock. Information on these devices, laboratory tests, installation at the plant and previous results is available.[2,7]

An automatic water sampler was installed in the valve chamber and the samples are analyzed in the laboratory as a reference for the other devices. Reference SSCs are determined by weighing the solid residues. The sampler is programmed to take a sample every two days and is triggered by the signal of a turbidimeter to increase the sampling rate during relatively high SSC.

Figure 1 shows an example of suspended sediment transport during three summer days. In addition to SSCs determined by various methods, the figure also shows three of the reference SSCs from laboratory analysis of bottled samples and the time series of the median size of the particles in the turbine water (d50, i.e. the median diameter by mass) obtained from the LISST.

During the summer, SSC was about 0.5 g/l. The time series from all devices show similar behavior, except for a sediment transport peak early on Aug. 27. During this event, the LISST yields a higher SSC compared to the other measuring methods. The LISST measurement is supported by the reference measurement taken during the rising limb of the SSC peak. The median size of the particles in the turbine water is about 15 microns, except for the phase of increased sediment transport. During this phase, about three times coarser particles (d50 about 45 microns for some hours) were transported. The maximum d50 occurred about one hour after the maximum SSC was reached.

Figure 2 shows PSDs obtained from the LISST. The times at which these PSDs were measured are indicated in Figure 1. The PSDs measured before (B) and after (E) the SSC peak, as well as during a minor SSC peak (A), are similar. The PSDs recorded at maximum SSC (C) and at maximum d50 (D) are considerably coarser.

The underestimation of SSC by the turbidimeters and the acoustic method in the times with transport of coarser particles is related to their physical operating principles. Coarser particles do not cause as much turbidity or scattering as finer ones (at the same SSC). The calibration of those devices depends strongly on particle size, for which a constant value has to be adopted. As Figure 1 shows, the deviation in SSC estimates of those devices with respect to SSC from the LISST and reference SSCs may be significant during phases of increased suspended sediment transport.

Figure 2 — PSDs Obtained from Laser Diffractometer

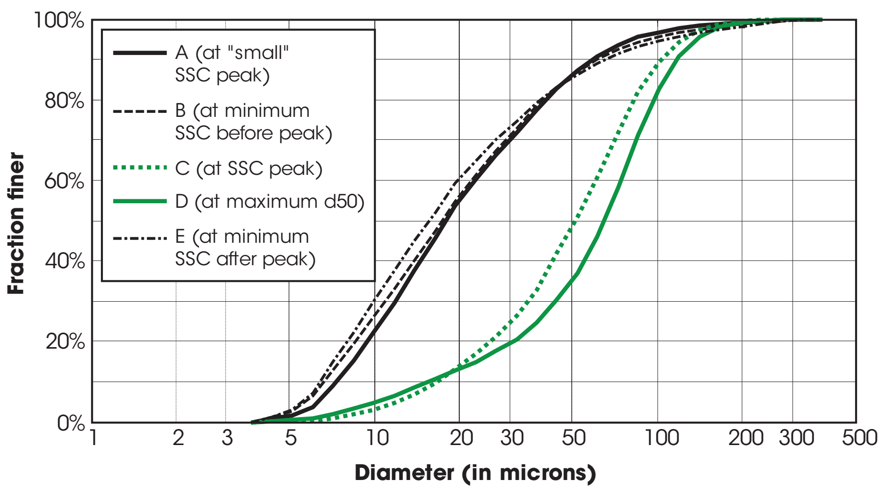

Selected particle size distributions measured in the turbine water at times indicated in Figure 1 show that particle size varied significantly over time.

Turbine wear measurements

Erosion of coated Pelton buckets is mainly observed at the splitter and the cut-out of the buckets. The widening of the splitter is of special importance: if the splitter width increases to 1% of the bucket width, efficiency drops by about the same amount at full load.[8] The increase of splitter width has been related to suspended sediment load.[9]

The geometries of selected buckets of the runners at Fieschertal were measured using a 3D optical scanning camera inside the turbine casing. Because the stainless steel buckets reflect light, a whitening spray was applied prior to scanning. Reference

Figure 3 — Side View of Digitized Main Splitter

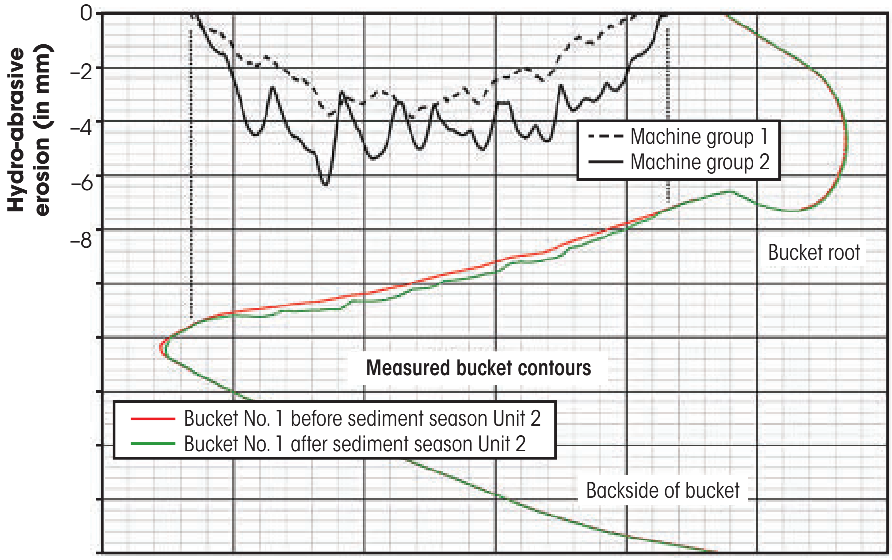

Comparison (black) between the splitter geometries of Bucket 1 of Units 1 and 2 before (red) and after (green) the sediment season reveal a reduction in splitter height on both units.

markers were used to improve the matching of point clouds and the measuring accuracy.

Figures 3 and 4 show the geometric changes due to hydro-abrasive erosion at splitters, obtained from comparisons of digital geometric models taken before and after the sediment season. At the beginning of sediment season 2012, the Unit 1 runner was fully reconditioned (welding, grinding and complete coating, with geometry close to planned geometry). The Unit 2 runner, however, has been in use for several seasons after the last factory overhaul and was repaired on site (grinding and local re-coating).

Figure 3 shows hydro-abrasive erosion at the splitter (analyzed as height differences along its longitudinal profile) for Bucket 1 of both runners. In summer 2012, a major flood event with SSC up to about 50 g/l occurred when both turbines were running. During sediment season 2012, splitter height was reduced by about 3 mm after 3,426 operating hours for Unit 1 and by 5 mm after 1,430 operating hours for Unit 2. These numbers indicate that hydro-abrasive erosion does not mainly depend on operating hours but rather on suspended sediment transport events (e.g. during floods) and on the geometry of the splitters at the beginning of the sediment season (see Figure 4).

The cut-outs were abraded by up to 9 mm toward the turbine axis in Unit 1 and by up to 6 mm in Unit 2.

Efficiency monitoring

Turbine wear reduces efficiency. Little published data is available[10] describing quantitatively the efficiency decay, correlated to various types of minor turbine damages and long-term exposure to suspended sediment load. One main reason for this lack of data is the effort associated with efficiency measurements with respect to direct costs and cost of eventual power losses during efficiency measurements.

With index efficiency measurements, the efficiency changes between two tests can be determined; absolute efficiency data are not required. Classical index efficiency measurements encompass a series of measuring points (part load to full load) with constant operating conditions. Such measurements are time-consuming. In the “sliding gate” method, the guide vanes of a Kaplan turbine were continuously opened and closed while acquiring data for efficiency evaluation.[11] This method has been adapted to Pelton and Francis turbines.[12] The main advantages of this kind of index efficiency method are:

— Feasible for Kaplan, Francis and Pelton turbines;

— Reduced time required to perform efficiency tests; and

— Continuous efficiency curves over the entire operating range, instead of discrete points.

A further advantage is that in most cases the instrumentation of the hydro plant can be used or data can be extracted from the control system. To do so, an adequate data acquisition algorithm has to be implemented in the control system. At Fieschertal, three possibilities to calculate the index efficiency are available:

— Acoustic discharge measurements at the upper and lower ends of the pressure shaft;

— Pressure difference measurements in a Venturi pipe section upstream of each machine group; and

— Needle stroke measurements.

Figure 5 on page 34 shows the efficiency history of Unit 1, calculated twice (independently) based on the two available acoustic discharge measurements. The differences between the instruments indicate reproducibility within 0.2%.

Between the measurements of July 4, 2012, and Sept. 27, 2012, more than half of the sediment season passed. An index efficiency decrease of 0.9% was obtained, attributed to hydro-abrasive erosion. On Nov. 5, 2012, none or only a minor rise in

Figure 4 — 3D views of Digitized Main Splitters

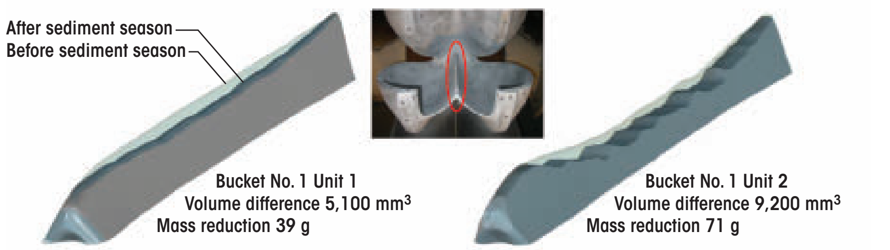

This three-dimensional comparison between the splitter geometries before (transparent) and after (gray) the sediment season for Bucket 1 of Units 1 and 2 shows the change in volume and mass.

Figure 5 — Index Efficiency History for Unit 1

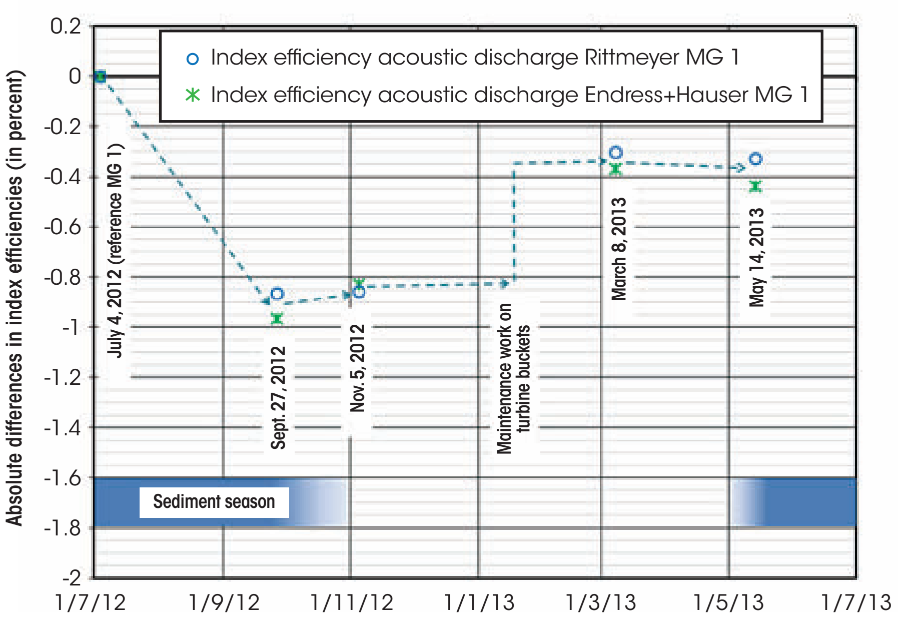

The index efficiency decreased due to hydro-abrasive erosion and increased due to turbine maintenance. Index efficiencies were calculated twice, based on the two available discharge measurements.

the index efficiency level was found. This agrees with the low SSC during this period. Until the next measurement of March 8, 2013, very low SSC was measured. The observed index efficiency level rise of up to 0.5% can be explained with maintenance work carried out at the main splitters of the Pelton buckets during winter and is confirmed by further measurement.

Conclusions

Using several devices for SSM based on different physical principles allows for a comparison of their measuring capabilities and leads to higher reliability. Combining devices for continuous SSM with an automatic water sampler allows calibrating the devices based on site-specific conditions with respect to typically prevailing particle sizes and mineralogical composition. The calibration of the devices will be improved based on the increasing data set of reference SSC from the study site.

> To deal with hydro-abrasive wear during the design, operation and maintenance of hydro plants, knowledge of turbine wear needs to be improved and relevant parameters need to be quantified.

For turbidimeters it is recommended to use the specific models with an automatic cleaning system (wiper or pressurized air) or with optics not in contact with the sediment-laden flow (free falling jet type). The acoustic method based on acoustic discharge measurement installations existing in many hydro plants offers the advantage of monitoring suspended sediment directly in the penstock. Among the devices used, LISST offers new possibilities for SSM because it provides information on both SSC and PSD. In environments with variable particle sizes, LISST measures SSC more accurately than devices with a fixed calibration depending on particle size. Measuring PSD is important because coarser particles have higher abrasion potential (for a given SSC) and are therefore particularly harmful to turbines. Devices with particle size-dependent calibration may be used as pragmatic contributions to a real-time decision making system for the operation and maintenance of hydro plants.

In summer 2012, SSC of about 0.5 g/l with d50 of normally 15 microns was observed in the turbine water of Fieschertal. The measurements confirmed that SSC and PSD may vary strongly within a short time, e.g., due to precipitation events. The wear at coated runner buckets was measured with a 3D optical scanner. Digital models of selected Pelton buckets allowed quantifying material losses at the main splitter and at the cut-outs due to turbine operation over a sediment season. The splitter height decreased 3 to 5 mm during the sediment season 2012, corresponding to about 0.5% to 0.8% of the inner bucket width. Hydro-abrasive erosion at the splitter was influenced by the splitter geometry at the beginning of the sediment season, particle load and the operating hours.

Turbine efficiency was periodically evaluated by "sliding needle" index measurements. The history of the index efficiency permits to identify relevant efficiency variations due to hydro-abrasive erosion. For one investigated turbine, the efficiency decrease was 0.9% for half of the sediment season 2012. To distinguish the effects of hydro-abrasive erosion and the effects of maintenance works at relevant turbine parts (e.g. grinding of the splitter) on efficiency, index tests should be performed before and after such works.

First analyses of the hydro-abrasive erosion rates for both units at Fieschertal showed that single events such as heavy rains lead to major material loss at Pelton buckets and significant efficiency drops. Plant shutdowns during such events would help to prevent excessive hydro-abrasive erosion.

Acknowledgments

The authors gratefully acknowledge financial support by *swisselectric research*, the Swiss Federal Office of Energy and

Gommerkraftwerke AG (Fieschertal) and measuring equipment support by Rittmeyer and Sigrist Photometer. Further thanks go to the members of the project team, including collaborators from Hochschule Luzern and Fieschertal, U. Aebi (BKW FMB Energy) and Dr. K. Winkler (Andritz Hydro).

Notes

[1]Gummer, J.H., "Combating Silt Erosion in Hydraulic Turbines," *HRW-Hydro Review Worldwide*, Volume 17, No. 1, March 2009, pages 28-34.

[2]Felix D., et al., "Suspended Sediment and Pelton Turbine Wear Monitoring: Experimental Investigation of various Optical and Acoustic Devices and Beginning of the Case Study at HPP Fieschertal," *Proceedings of the 17th International Seminar on Hydropower Plants*, University of Technology, Vienna, 2012.

[3]"Hydraulic Machines – Guide for Dealing with Hydro-abrasive Erosion in Kaplan, Francis and Pelton Turbines," Edition 1.0, IEC 62364, International Electrotechnical Commission, Geneva, Switzerland, 2013.

[4]Wren, D., B. Barkdoll, R. Kuhnle and R. Derrow, "Field Techniques for Suspended Sediment Measurement," *Journal of Hydraulic Engineering*, Volume 126, No. 2, 2000, pages 97-104.

[5]Costa, L.I., et al., "Influence of Solid Particle Parameters on the Sound Speed and Attenuation of Pulses in ADM," *Journal of Hydrologic Engineering*, Volume 17, No. 10, 2012, pages 1084-1092.

[6]Agrawal, Y.C., and H.C. Pottsmith, "Instruments for Particles Size and Settling Velocity Observations in Sediment Transport," *Marine Geology*, Volume 168, 2000, pages 89-114.

[7]Abgottspon, A., "Messung abrasiver Partikel in Wasserkraftanlagen," Master Thesis (unpublished, in German), Hochschule Luzern, Lucerne, Switzerland, 2011.

[8]Brekke, H., Y.L. Wu, and B.Y. Cai, "Design of Hydraulic Machinery Working in Sand Laden Water," in *Abrasive Erosion & Corrosion of Hydraulic Machinery*, Vol. 2, Imperial College Press, London, 2002.

[9]Boes, R., "Real-time Monitoring of SSC and PSD in the Headwater Way of a High-head Hydropower Plant," *Proceedings of the 33rd IAHR Congress*, International Association for Hydro-Environment Engineering and Research, 2009.

[10]Bajracharya, T.R., et al., "Sand Erosion of Pelton Turbine Nozzles and Buckets: A Case Study of Chilime hydropower plant," *Wear*, Volume 264, No. 3-4, 2008, pages 177-184.

[11]Almquist, C.W., et al., "The Sliding Gate Method for Hydroturbine Efficiency Testing," *Proceedings of WaterPower '95*, American Society of Civil Engineers, New York, 1995.

[12]Abgottspon, A., and T. Staubli, "Index Tests of a Francis Unit using the Sliding Gate Method," *Proceedings of 7th International Conference on Hydraulic Efficiency Measurements*, International Group for Hydraulic Efficiency Measurement, 2008.

Reference

Abgottspon, A., et al., "Hydro-Abrasive Erosion of Pelton Buckets and Suspended Sediment Monitoring," *Proceedings of HydroVision International 2013*, PennWell Corporation, Tulsa, Okla., 2013.

Versuchsanstalt für Wasserbau
Hydrologie und Glaziologie
der Eidgenössischen
Technischen Hochschule Zürich

Mitteilungen 227

Internationales Symposium

WASSER- UND FLUSSBAU IM ALPENRAUM

25.-27. Juni 2014 in Zürich

Band 1

Wasserkraft und Gewässerrenaturierung

Zürich, 2014

Herausgeber: Prof. Dr. Robert Boes

Variation des Feinsedimentgehalts im Triebwasser infolge Speicherstollen-bewirtschaftung

Variation of suspended sediment load in a penstock due to operation of a storage tunnel

David Felix, Ismail Albayrak, Robert M. Boes

Kurzfassung

Bei Wasserkraftanlagen, die keinen nennenswerten Kopfspeicher (See) aufweisen, kann ein im Oberwasser liegender Freispiegelstollen als (Tages-)Speicher bewirtschaftet werden, indem der Stollenwasserspiegel je nach Wasserdargebot und Produktionsplan vorübergehend abgesenkt wird. Feinsedimentpartikel, die auch nach Entsandungsanlagen noch im Triebwasser vorhanden sind, werden mehrheitlich durch den Speicherstollen transportiert und schliesslich turbiniert. Je nach Strömungsverhältnissen setzen sich im Speicherstollen Partikel ab oder werden resuspendiert.

In einem Forschungsprojekt über die Abnutzung und Wirkungsgradabnahme von Pelton-Turbinen infolge schwebstoffhaltigem Triebwasser werden am Kraftwerk Fieschertal (Wallis, Schweiz) die Schwebstoffkonzentration (SSC) und -partikelgrössenverteilung (PSD) im Triebwasser seit Sommer 2012 kontinuierlich gemessen. Dies erfolgt u.a. mit einem *in situ*-Laserdiffraktometer, welches mittels Laboranalyse von automatisch entnommenen Schöpfproben bezüglich SSC kalibriert wurde.

SSC und PSD sind üblicherweise durch meteorologisch-hydrologische Prozesse wie Schnee- und Gletscherschmelze sowie Regenereignisse geprägt. Die vorliegenden Messungen zeigen, dass die Bewirtschaftung eines Speicherstollens die SSC und PSD im Triebwasser einer Wasserkraftanlage zusätzlich stark beeinflussen kann. Wie aufgrund der Strömungsverhältnisse im Speicherstollen erwartet, werden bei tiefem Stollenpegel und Volllastbetrieb mehr und gröbere Feinsedimente turbiniert als in Phasen mit hohem Speicherfüllungsgrad und Teillastbetrieb. Durch die Messungen können Berechnungsansätze über das Absetz- und Resuspensionsverhalten von feinen mineralischen Partikeln verbessert oder validiert werden. Zusammen mit geeigneter Messtechnik für das Monitoring von SSC *und* PSD dient dies als Grundlage für betriebliche oder bauliche Anpassungen für ein optimiertes Feinsedimentmanagement von Wasserkraftanlagen.

Abstract

At hydropower plants (HPPs), which do not comprise a considerable headwater storage (lake), free-surface flow headrace tunnels may be operated as daily compensation reservoirs by temporary drawdown of the water level in the tunnel, depending on naturally varying inflow and demand-driven turbine discharge. Fine sediment particles which are not excluded by upstream sand traps are mostly transported through such storage tunnels and farther to the turbines. Particles may settle or be re-suspended depending on the actual flow conditions prevailing in the storage tunnel.

In a research project in which turbine wear and efficiency decrease due to hydro-abrasive erosion by fine sediment particles are investigated, suspended sediment concentration (SSC) and particle size distribution (PSD) have been continuously measured in the penstock of the high-head HPP of Fieschertal (Valais, Switzerland) since summer 2012. For these measurements an *in situ*-laser diffractometer is used, which has been calibrated with respect to SSC based on laboratory analysis of automatically taken bottled samples.

SSC and PSD usually depend on meteorological and hydrological processes such as snow and glacier melt or precipitation. In addition to this, the operation of a storage tunnel may strongly affect SSC and PSD in the power water of a HPP, as demonstrated by the presented measurements. According to the flow conditions in the storage tunnel, the turbine water contains more and coarser particles at low water level in the storage tunnel and design discharge than at high water level and part load operation of the turbines. The measurements can be used to improve or validate calculation models to predict settling and re-suspension of fine mineral particles. Together with suitable devices for monitoring of SSC *and* PSD, this serves as a basis for operational or structural adaptations for a well-balanced management of fine sediment at HPPs.

1 Einleitung

Zahlreiche Hoch- und Mitteldruckwasserkraftanlagen sind mit Saisonspeichern ausgerüstet, um die variabel anfallenden Wasserzuflüsse möglichst der Nachfrage entsprechend und effizient nutzen zu können. Einige Anlagen verfügen aber aus Gründen der Topografie, der Geologie, der Bauausführung, der Naturgefahren, des Landschaftsschutzes, der Ökologie oder der Wirtschaftlichkeit lediglich über kleinere Kopfspeicher, die auch unterirdisch angeordnet sein können. Bei gewissen Anlagen, wie in diesem Beitrag betrachtet, werden Freispiegelstollen als Speicher betrieben, indem der Stollenwasserspiegel vorübergehend abgesenkt wird.

Falls das Triebwasser Feinsedimente enthält, die von Entsandungsanlagen im Fassungsbereich nicht ausgeschieden werden, können sich in solchen Speicherstollen in Phasen mit geringer Fliessgeschwindigkeit Feinsedimente ablagern. Bei tiefem Stollenpegel und Volllastbetrieb, d.h. mit grösseren Fliessgeschwindigkeiten und Sohlschubspannungen, können abgelagerte Partikel resuspendiert werden. Der Schwebstoffgehalt im Triebwasser ist betreffend Turbinenabrasion und betrieblichem Unterhalt (Spülungen) der Triebwasserwege von Bedeutung.

Schwebstoffe werden üblicherweise durch ihre Massenkonzentration (*suspended sediment concentration SSC*) und Grössenverteilung (*particle size distribution PSD*) beschrieben. Die Grösse der Partikel ist insbesondere für die Feinsedimentabscheidung aus dem Triebwasser und die Turbinenabnutzung eine entscheidende Grösse (z. B. Winkler *et al.* 2011). Methoden und Geräte für die Messung von Schwebstoffen im Feld sind beispielsweise in Wren (2000) zusammengefasst.

Das Schwebstoffaufkommen in Fliessgewässern und im Triebwasser von Wasserkraftanlagen hängt normalerweise von meteorologischen Faktoren wie Lufttemperatur und Niederschlag ab und kann je nach Abfluss und Einzugsgebietseigenschaften saisonal oder ereignisbedingt (z. B. Gewitter) stark variieren (Boes *et al.* 2013). Gemäss Beobachtungen von Kraftwerksbetreibern und Messungen von Abgottspon (2011) kann sich nebst natürlichen Einflüssen auch der Kraftwerksbetrieb (Speicherstollenbewirtschaftung und Turbinierprogramm) stark auf das Schwebstoffaufkommen im Triebwasser auswirken.

Der in der Literatur kaum dokumentierte und bisher noch wenig quantifizierte Einfluss solcher betrieblicher Faktoren auf den Schwebstoffgehalt im Triebwasser wird im vorliegenden Artikel basierend auf *in situ*-Messungen aus dem Jahr 2012 beschrieben. Die Messungen wurden im Rahmen eines Forschungsprojekts zum Thema Hydroabrasiv-Verschleiss und Wirkungsgradabnahme von Peltonturbinen an der Hochdruckwasserkraftanlage Fieschertal durchgeführt (Abgottspon *et al.* 2013a und 2013b, Felix *et al.* 2013a).

2 Kraftwerksanlage und Messeinrichtungen

Die Kraftwerksanlage Fieschertal nutzt den Abfluss aus einem stark vergletscherten Einzugsgebiet und weist keinen Speichersee auf. Der ca. 2 km lange Freispiegelstollen (Abb. 1) mit einem 8 m breiten Torbogen-Querschnitt wird als Speicherstollen betrieben, wenn der Zufluss kleiner ist als der Ausbaudurchfluss (15 m^3/s). Mit einem Höhenunterschied von 4 m zwischen dem minimalen und dem maximalen nominalen Betriebswasserspiegel steht ein Speichervolumen von ca. 64'000 m^3 zur Verfügung. Es handelt sich um einen relativ kleinen Speicher, da die beiden Peltonturbinen ohne Zufluss zum Stollen nur während ca. einer Stunde mit Volllast betrieben werden könnten.

Auf halber Länge des Stollens ist ein Stollenfenster vorhanden, durch welches mittels einer tief liegenden Tafelschütze Feinsedimente aus der ersten Hälfte des Speicherstollens in den Vorfluter gespült werden können. Dabei wird der Stollenpegel kontrolliert abgesenkt und der Turbinierbetrieb für wenige Stunden unterbrochen.

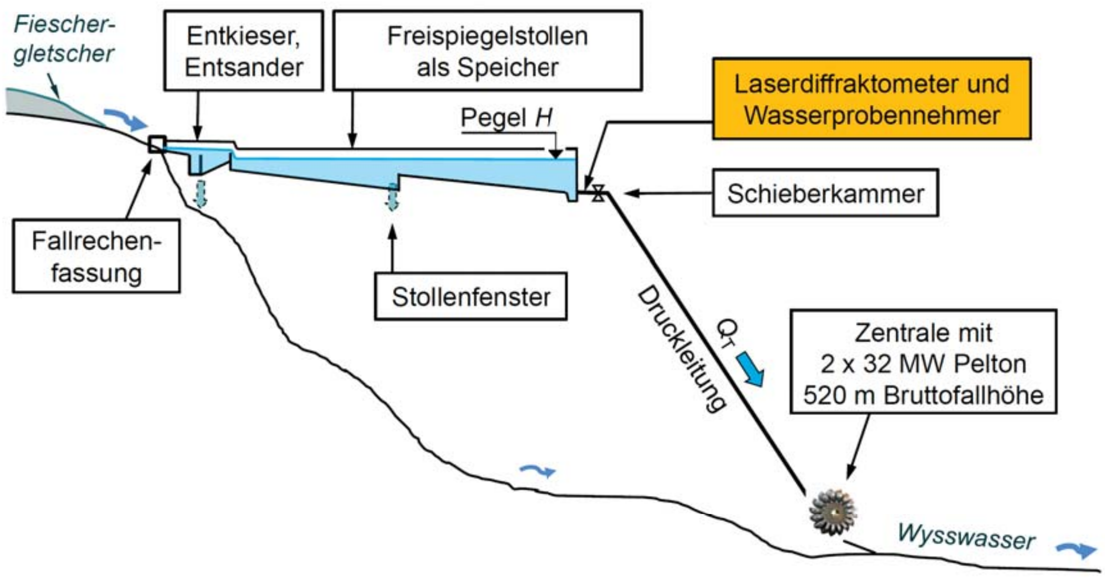

Abb. 1: Schematisches Längenprofil (überhöht) des Kraftwerks Fieschertal mit Speicherstollen und Instrumentierung für die Messung des Schwebstoffaufkommens im Triebwasser

Für die Messung des Schwebstoffaufkommens im Triebwasser wurde im Sommer 2012 in der Schieberkammer u.a. ein Laserdiffraktometer (LD) installiert. Das Funktionsprinzip und die Bauweise von solchen tragbaren LD sind beispielsweise in Agrawal *et al.* (2011) beschrieben, die Installation und die Probenahmeleitung in Felix *et al.* (2013a). Mit einem LD können PSD und SSC gemessen werden. Dabei wurde eine Partikeldichte von 2.65 kg/l (wie für Quarz) angenommen. Während der Schwebstoffsaison wurden minütlich je eine PSD und SSC gemessen. Zur SSC-Kalibrierung des LD auf die am Messort vorkommenden Partikeltypen (v. a. Einfluss der Partikelform, vgl. Felix *et al.* 2013b) wurden mit einem automatischen Probennehmer Flaschen abgefüllt und anschliessend im Labor mittels Ofentrocknung und Wägung die SSC bestimmt.

Weiter wurden an der Kraftwerksanlage Fieschertal u. a. der Pegel am unterstromigen Ende des Stollens (H in Abb. 1) sowie der Volumenstrom in der Druckleitung (Q_T) aufgezeichnet. Ergänzend wurden Niederschlagsdaten der Messstation Fieschertal (1095 m ü.M.) in die Auswertung miteinbezogen.

3 Resultate und Diskussion

3.1 Niederschlag und Schwebstoffkonzentration

Wie einleitend erwähnt, führen Niederschlagsereignisse in der Regel zu erhöhter SSC in Oberflächengewässern und im Triebwasser gewisser Wasserkraftanlagen. In Abb. 2 sind Ganglinien der am Kraftwerk Fieschertal im Triebwasser gemessenen SSC und die täglichen Niederschlagssummen in Fieschertal für zwei unterschiedliche Perioden von je zwei Wochen dargestellt: Während im Herbst (Abb. 2b) nach Regenereignissen erhöhte SSC auftreten, wurden im August (Abb. 2a) – in einer praktisch niederschlagsfreien Periode – markante tägliche SSC-Spitzen gemessen. Solche SSC-Spitzen werden im Folgenden am Beispiel der ersten vier Tage in Abb. 2a näher betrachtet.

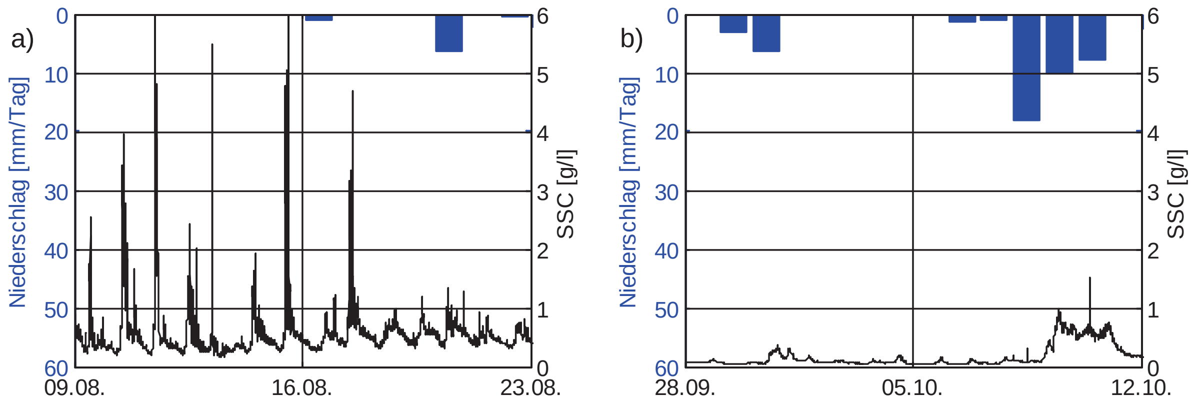

Abb. 2: Schwebstoffkonzentration *SSC* im Triebwasser des Kraftwerks Fieschertal (schwarze Linien) und tägliche Niederschlagssumme in Fieschertal (blaue Balken), a) im Hochsommer und b) im Herbst 2012

3.2 Schwebstoffeigenschaften im Triebwasser bei vorübergehenden Absenkungen des Stollenpegels

Abb. 3a zeigt die SSC-Ganglinie im Triebwasser für vier niederschlagsfreie Tage im August. Weiter sind die SSC-Laborresultate von zwei Schöpfproben dargestellt (Kreissymbole), die zur Kalibrierung der quasi-kontinuierlichen LD-Messung dienten. An der rechten Ordinate ist die Ganglinie der Median-Partikelgrösse (d_{50}), d. h. der Partikelgrösse, deren Masseanteil 50% beträgt, angegeben (dünne Linie). Die SSC steigt jeweils zur Mittagszeit von weniger als 0.5 g/l auf mehrere g/l an. Parallel dazu, leicht verzögert, nimmt auch d_{50} von normalerweise ca. 15 µm auf bis zu ca. 100 µm zu.

In Abb. 3b sind die Ganglinien des Stollenpegels H und des Turbinendurchflusses Q_T (dünne Linie) während derselben vier Tage dargestellt. Dem Tagesgang des glazial geprägten Zuflusses entsprechend, erreicht der Stollenpegel jeweils gegen Mitternacht den maximalen Betriebsspiegel (Überlaufkote beim

Stollenfenster) und um die Mittagszeit den Tiefststand. Während dieser Sommertage wurde meist etwa mit Ausbaudurchfluss turbiniert.

In Abb. 3c ist die Schwebstofffracht in der Druckleitung während dieser vier Sommertage dargestellt. Diese wurde durch Integration des Produkts von Q_T und SSC über die Zeit berechnet. Jeweils zur Mittagszeit, bei tiefem Stollenpegel und hoher SSC, nimmt die Schwebstofffracht stark zu. In diesem Beispiel von vier Tagen wurden in der Stunde mit dem grössten Schwebstofftransport (am 11.08. mittags) 253 t Schwebstoffe turbiniert, während der Mittelwert bei 31 t/h lag. Diese Werte entsprechen bei 15 m^3/s einer SSC von 4.7 g/l bzw. 0.6 g/l.

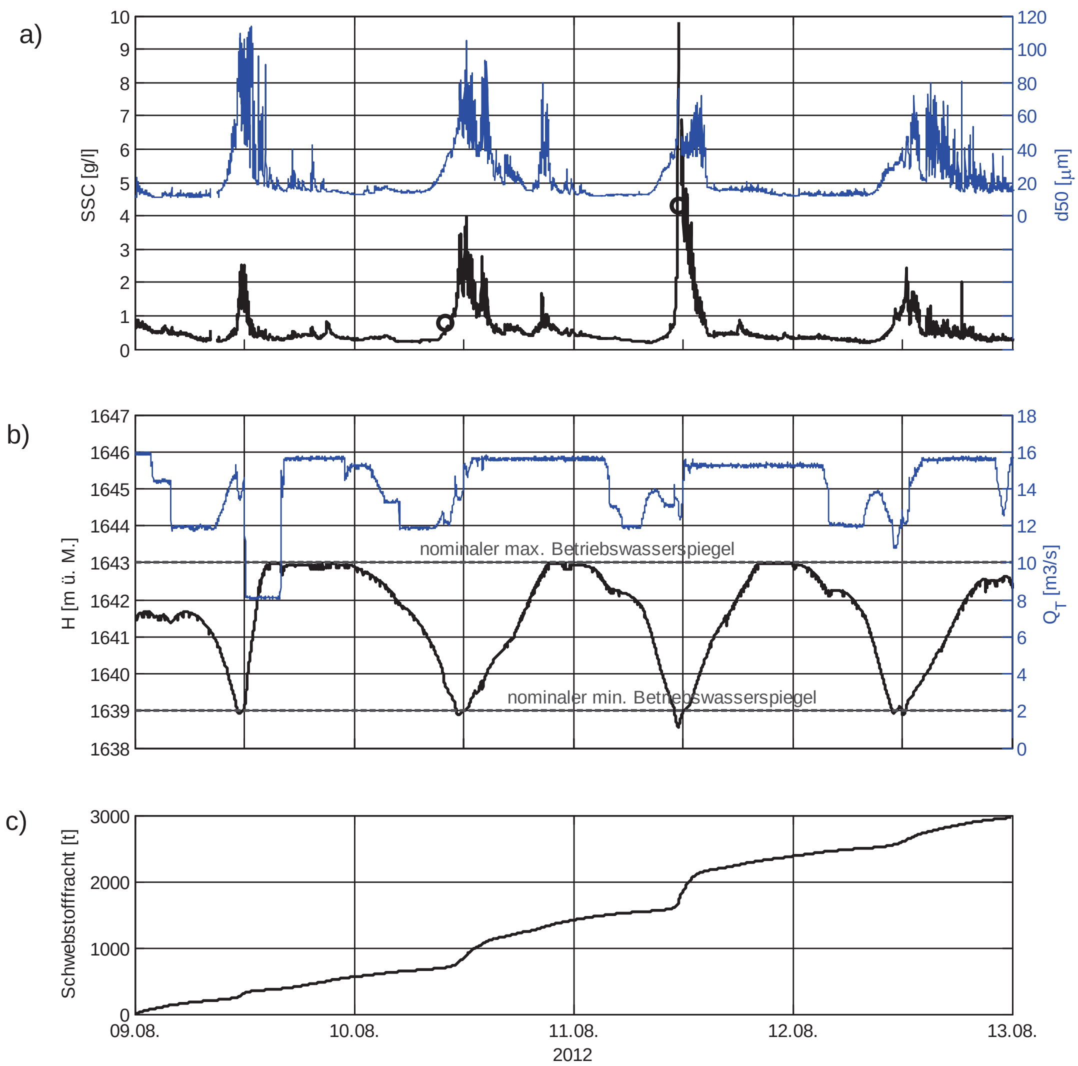

Abb. 3: Ganglinien a) der Schwebstoffkonzentration *SSC* und des Median-Partikeldurchmessers d_{50} im Triebwasser, b) des Stollenpegels H und des Turbinendurchflusses Q_T, sowie c) Schwebstofffracht im Triebwasser des Kraftwerks Fieschertal, über vier Sommertage ohne Regen

Gemäss IEC 62364 (2013) wird die Beanspruchung von Turbinen durch Feinsedimente mittels der so genannten *particle load* beschrieben, welche als Integral des Produkts von SSC und Gewichtungsfaktoren für Partikelgrösse, -form und -härte über die Zeit definiert ist. Diese Richtlinie enthält noch keine Werte für die Gewichtungsfaktoren der Partikelgrösse. Gemäss Winkler *et al.* (2011) und Sulzer Hydro (1996, publiziert in DWA 2006) verursachen gröbere Partikel mehr Hydroabrasiv-Verschleiss als feinere Partikel bei gleicher SSC. Da die SSC-Spitzen in Abb. 3 mit gröberen Partikeln und somit grösserem relativem Abrasionspotential einhergehen, weist die *particle load* noch stärker variierende Zunahmen auf als die Schwebstofffracht (Abb. 3c). Die Beanspruchung von Turbinen durch Feinsedimente kann also auch im Lauf eines Tages stark variieren.

In Abb. 4a ist der Zusammenhang zwischen gemessener *SSC* und dem Stollenpegel am Beispiel eines Sommertages (10.08.2012) dargestellt. Abb. 4b zeigt den Zusammenhang zwischen d_{50} und dem Stollenpegel am gleichen Tag. *SSC* und d_{50} nehmen während des Absenkens des Stollenpegels (violette bzw. dunklere Punkte) insbesondere im Bereich des minimalen Betriebsspiegels stark zu, was als Resuspension von früher abgelagerten Partikeln gedeutet wird. Bei ansteigendem Stollenpegel (grüne bzw. hellere Punkte) wurden grössere *SSC* und d_{50} gemessen als bei sinkendem Pegel (Hysterese). Dies hängt auch mit der Fliesszeit zwischen dem für die Resuspension massgebenden Stollenquerschnitt (Sohlhochpunkt beim Stollenfenster) und der Messstelle zusammen.

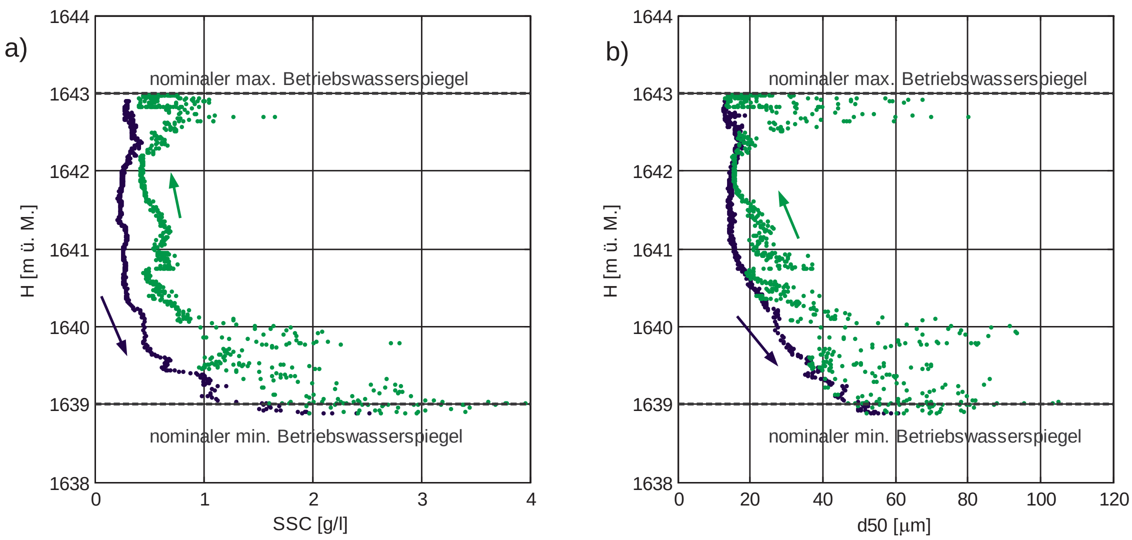

Abb. 4: a) Schwebstoffkonzentration *SSC* und b) Median-Partikeldurchmesser d_{50} im Triebwasser des Kraftwerks Fieschertal in Abhängigkeit des Stollenpegels H, Beispiel des 10.08.2012; violette (dunklere) Punkte mit sinkendem Stollenpegel, grüne (hellere) mit steigendem Stollenpegel

3.3 Zusammenhang zwischen Schwebstoffkonzentration und -partikelgrösse

Hinsichtlich der Turbinenabrasion und für die Auswahl geeigneter Schwebstoff-Messmethoden ist von Interesse, ob und wie *SSC* und *PSD* korrelieren. In Abb. 5a ist d_{50} im Triebwasser des Kraftwerks Fieschertal in Funktion der *SSC* dargestellt, wie in Abb. 4 am Beispiel des 10.08.2012 mit derselben farblichen Unterscheidung der Phasen der Stollenpegelabsenkung bzw. des -anstiegs. Gröbere Partikel treten bei höheren SSC auf, wobei bei hohen SSC die Streuung zunimmt. Abb. 5b zeigt die aufgetretenen Kombinationen von *SSC* und d_{50}, wenn nicht einzelne Ereignisse, sondern längere Zeiträume von zwei mal zwei Wochen, wie in Abb. 2, betrachtet werden: Im Sommer (09.–23.08.2012, hellbraune Punkte) ist eine positive Korrelation von d_{50} und *SSC* mit starker Streuung zu erkennen; im Herbst (28.09.–12.10.2012, schwarze Punkte) eher konstante Partikelgrössen von $d_{50} \approx 15$ µm.

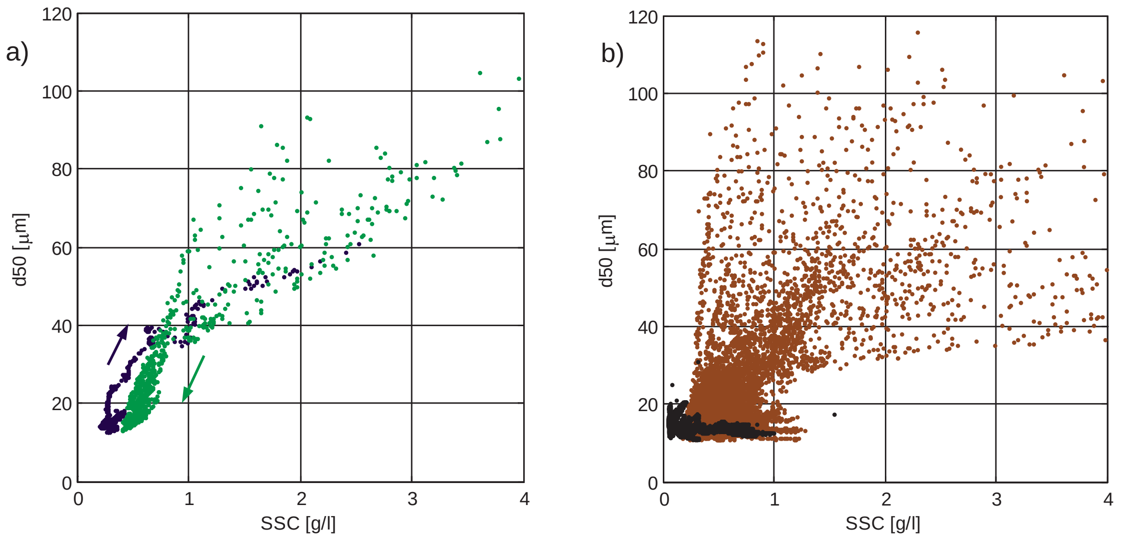

Abb. 5: Median-Partikeldurchmesser d_{50} im Triebwasser des Kraftwerks Fieschertal in Funktion der Schwebstoffkonzentration *SSC*, a) Beispiel des 10.08.2012 (Farben wie in Abb. 4) und b) für je zwei Wochen im Hochsommer (hellbraun) und im Herbst (schwarz) 2012

4 Ausblick

Die Messdaten über das Schwebstoffaufkommen in der Druckleitung werden zusammen mit Daten aus dem Kraftwerksleitsystem und regionalen Meteodaten weiter ausgewertet. Im Forschungsprojekt ist vorgesehen, das Schwebstoffaufkommen, die Turbinenabrasion und die Wirkungsgradabnahme miteinander in Beziehung zu setzen, um bestehende Berechnungsansätze zu überprüfen bzw. anzupassen. Die Untersuchungen können auch als Grundlage für betriebliche oder bauliche Anpassungen für den Umgang mit Sedimenten (Turbinierbetrieb, Spülregime, Spüleinrichtungen) dienen. Weiter können mit solchen Messdaten Kenntnisse über das Absetz- und Resuspensionsverhalten von Feinsedimenten verbessert und numerische Modelle validiert werden.

5 Schlussfolgerungen

Bei Wasserkraftanlagen ist das Schwebstoffaufkommen im Triebwasser in der Regel durch das Wettergeschehen geprägt. Bei der Bewirtschaftung von kleineren Speichern können abgelagerte Feinsedimente infolge Wasserspiegelabsenkungen resuspendiert werden, was zu beträchtlichen Schwebstoffkonzentrationen und zum Transport gröberer Partikel im Triebwasser führen kann, wodurch an den Turbinen entsprechend stärkerer Hydroabrasiv-Verschleiss auftritt.

Besonders bei solch dynamischen Verhältnissen ist ein kontinuierliches Schwebstoffmonitoring betreffend Konzentration *und* Partikelgrössenverteilung empfehlenswert, um den Betrieb von Wasserkraftanlagen auch hinsichtlich des zeitlich stark variablen Feststofftransports und seiner Auswirkungen wirtschaftlich optimieren zu können.

Danksagung

Wir danken für die Unterstützung des Forschungsprojekts durch swisselectric research, das Bundesamt für Energie und die Gommerkraftwerke (Betreiberin des KW Fieschertal) sowie durch die weiteren Projektpartner (BKW, Andritz Hydro, Rittmeyer, Sigrist Photometer, Endress+Hauser). Ein weiterer Dank geht an A. Abgottspon, Prof. Dr. T. Staubli und Prof. Dr. P. Gruber von der Hochschule Luzern (Kompetenzzentrum für Fluidmechanik und Strömungsmaschinen) für die gute Zusammenarbeit sowie an P. Grüninger und T. Humbel, welche zur Auswertung der Messdaten beigetragen haben (Grüninger 2013, Humbel 2013), und an MeteoSchweiz für das zur Verfügung stellen von Meteodaten.

Referenzen

Abgottspon, A. (2011). Messung abrasiver Partikel in Wasserkraftanlagen. *Masterarbeit* (unveröffentlicht), Hochschule Luzern.

Abgottspon, A., Staubli, T., Felix, D., Albayrak, I., Boes, R.M. (2013a). Hydro-abrasive Erosion of Pelton buckets and Suspended Sediment Monitoring. *Proc. Hydrovision International*, Denver, USA.

Abgottspon, A., Stern, P., Staubli, T., Felix, D., Winkler, K. (2013b). Measuring Turbine Abrasion and Efficiency Decrease: First Results of the Case Study at HPP Fieschertal. *Proc. Hydro 2013 Conference*, Innsbruck, Austria, 18.05.

Agrawal, Y., Mikkelsen, O.A., Pottsmith, H.C. (2011). Sediment monitoring technology for turbine erosion and reservoir siltation applications, *Proc. Hydro 2011 Conference*, Prague, Czech Republic, 29.09.

Boes, R. M., Felix, D., Albayrak, I. (2013). Schwebstoffmonitoring zum verschleissoptimierten Betrieb von Hochdruck-Wasserkraftanlagen. *Wasser Energie Luft* 105(1), 35–42.

DWA (2006). Entlandung von Stauräumen, Deutsche Vereinigung für Wasserwirtschaft, Abwasser und Abfall e.V., Hennef.

Felix, D., Albayrak, I., Boes, R.M., Abgottspon, A., Deschwanden, F., Gruber, P. (2013a). Measuring Suspended Sediment: Results of the first Year of the Case Study at HPP Fieschertal in the Swiss Alps. *Proc. Hydro 2013 Conference*, Innsbruck, Austria, 18.03.

Felix, D., Albayrak, I., Boes, R.M. (2013b). Laboratory Investigation on measuring Suspended Sediment by portable Laser Diffractometer (LISST) focusing on Particle Shape. *Geo-marine Letters* 33(6), 485–498.

Grüninger, P. (2013). Schwebstofftransport im Jahr 2012 am Wasserkraftwerk Fieschertal, *Masterarbeit* (unveröffentlicht), VAW, ETH Zürich.

Humbel, T. (2013). Variation des Schwebstoffgehalts im Triebwasser des KW Fieschertal infolge Speicherstollenbewirtschaftung, *Projektarbeit* (unveröffentlicht), VAW, ETH Zürich.

IEC 62364 (2013). Hydraulic machines - Guide for dealing with hydro-abrasive erosion in Kaplan, Francis and Pelton turbines, Edition 1.0 (June 2013), International Electrotechnical Commission, Geneva, Switzerland.

Winkler, K., Dekumbis, R., Rentschler, M., Parkinson, E., Garcin, H. (2011). Understanding hydro-abrasive erosion, *Proc. Hydro 2011 Conference*, Prague, Czech Republic, 2.05.

Wren, D., Barkdoll, B., Kuhnle, R., Derrow, R. (2000). Field Techniques for Suspended-Sediment Measurement. *J. of Hydraul. Eng.*, 126(2), 97–104.

Adresse der Autoren

David Felix (korrespondierender Autor)
Email: felix@vaw.baug.ethz.ch
Dr. Ismail Albayrak
Prof. Dr. Robert M. Boes
Versuchsanstalt für Wasserbau, Hydrologie und Glaziologie, ETH Zürich
Wolfgang-Pauli-Str. 27
CH-8093 Zürich

Particles in Europe (PiE)
7-9 October 2014
Esbjerg, Denmark

Organized by
Sequoia Scientific, Inc.,
MacArtney A/S,
University of Copenhagen

Program and Abstracts

Site-specific Conversion of Laser Diffractometer (LISST) Data to Suspended Sediment Mass Concentration (SSC)

David Felix[1], Ismail Albayrak[1], Robert M. Boes[1]

[1] ETH Zurich, Laboratory of Hydraulics, Hydrology and Glaciology (VAW), Switzerland

Abstract

This paper deals with a field investigation on measuring suspended sediment mass concentration (SSC) and particle size distribution (PSD) using a Laser In-Situ Scattering and Transmissiometry (LISST) device and bottle samples. The flowing water at the study site in a granite rock region in the Swiss Alps carries angular, elongated and flaky particles, as expected from the mineralogical composition and confirmed by microscope pictures. With such highly non-spherical particles, particle volume concentrations (PVCs) measured by LISST, and consequently SSCs, are overestimated (Felix *et. al.* 2013). For the particle mix at the study site, the overestimation was quantified by comparing SSCs calculated from (i) LISST measurements using a particle density of 2.77 g/cm^3 obtained by pycnometer and from (ii) gravimetrical analysis of bottle samples up to 2 g/l. The LISST-based SSCs over four months in 2013 were found to be on average 68% higher than the gravimetrical SSCs (R^2=0.89). If SSCs are to be calculated from LISST measurements, a site-specific calibration or validation by a mass-based measuring technique is recommended to account for effects of particle shape and density.

Introduction

Measuring concentration and size of suspended sediment particles is important for a better understanding and management of fine-sediment related processes in rivers, lakes, estuaries and seas and at hydraulic schemes for hydropower, irrigation and flood protection. Various direct and indirect measuring techniques are available (Wren *et al.* 2000). When quasi-continuous and real-time measurements of SSC and PSD are required, LISST devices are increasingly used. In such devices, the small-angle forward scattering and attenuation of light caused by suspended particles are measured and converted to particle volume concentrations (PVCs) in certain size classes using a mathematical inversion algorithm (Agrawal & Pottsmith 2000). This inversion is based on the assumption of spherical or relatively compact particle shapes. If the shapes of natural particles differ widely from spheres, PSDs and PVCs measured by LISST, and consequently SSCs, are biased. This is a physically-based general feature of laser diffraction instruments. Felix *et al.* (2013b) experimentally quantified the bias for selected particle types and reported that PVCs or SSCs of highly non-spherical particles can be approximately corrected by applying particle type-specific factors.

For the conversion of PVC to SSC, the particle density has to be known, which can be assumed or measured with another device, typically a pycnometer. The particle density may deviate from the solid density of the particle material due to conglomerated particles (flocks) and may also change in time, e.g. due to variations in the mineralogical composition of the particle mix caused by particle sorting during sedimentation or re-suspension.

In a present research project on monitoring of suspended sediment and hydro-abrasive wear at turbines of hydroelectric power plants (HPPs), an *in-situ* laser diffractometer *LISST-100X*, Type C, has been used to measure SSC and PSD of the mineral particles in the power waterway of HPP Fieschertal in the canton of Valais, Switzerland. The SSCs (i) calculated from LISST measurements using a particle density determined by pycnometer and (ii) from gravimetrical analysis of periodically taken bottle samples were compared in order to quantify the particle shape effect on SSCs calculated from LISST measurements.

Set-up, devices and methods

Among other devices, the LISST was installed in July 2012 in a flow-through bucket at the top of the penstock at the study HPP (Fig. 1). A sampling pipe feeds the bucket with sediment-laden water drawn from the level of the penstock axis. An automatic water sampler was used to collect bottle samples (0.5 l). The sampler was programmed to take a sample every 3 days or more frequently if certain turbidity thresholds were exceeded. From the bottle samples, SSCs were gravimetrically measured in the laboratory (weighing of dried residues).

In order to extend the range of measurable SSCs the optical path length of the LISST was reduced from 50 mm to 5 mm by insertion of a 90%-path reduction module. Since 2013 the LISST was programmed to run in burst mode: 10 measurements at 1 Hz are followed by a break of 50 seconds.

The LISST with the corresponding software provides PVCs in 32 log-spaced size classes called bins 1 to 32. The inversion mode for so called ‘random’ shaped particles (Agrawal *et al.* 2008) was employed. Using this mode termed IMR in this paper, the nominal range of measurable particle sizes is approx. 2 to 380 µm (Sequoia 2011). As reported by Andrews *et al.* (2011) and Felix *et al.* (2013b), PVCs measured by LISST in bins of small particle sizes may be unrealistically high in some cases ('raising tail' in the PSD, e.g. due to 'fine out of range particles' or particle shape effects). This was also observed in most LISST measurements in the present study. Thus, the PVCs of bins 1 to 3 were omitted in the calculations of the PSDs and SSCs, as described in Felix *et al.* (2013b). The lower limit of the range of measurable particle sizes is slightly shifted from approx. 2 to 3 µm.

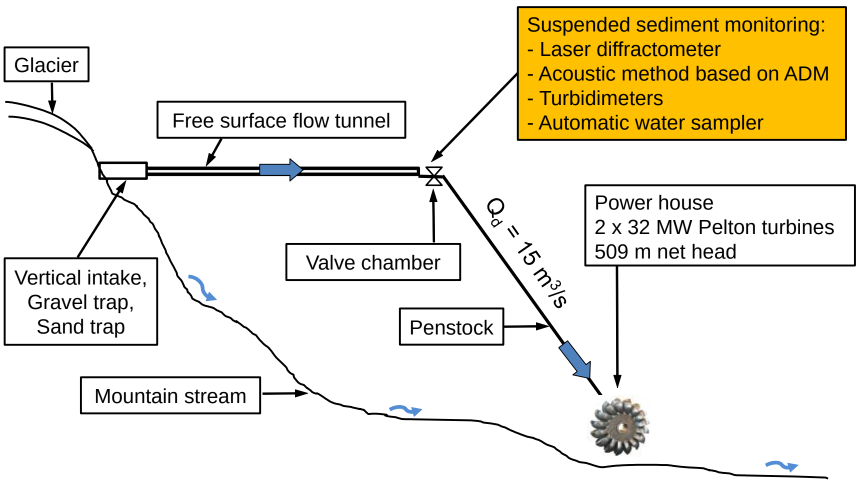

Fig. 1: Schematic longitudinal profile of the HPP Fieschertal, Switzerland, showing the measuring location at the power waterway (modified from Felix *et al.* 2013a)

Results and Discussion

Mineralogical composition and particle shapes

Rietveld X-ray diffraction analysis of three bottle samples taken in August, 2012 showed that the suspended sediments at the study site were composed of the following minerals:

- 65 to 80% of quartz, feldspars and epidote (Mohs hardness: 6 to 7), and
- 20 to 35% of muscovite, biotite, chlorite and smectite (Mohs hardness: 1 to 3).

Muscovite and biotite are typical mica minerals and belong together with the other soft minerals to the group of sheet silicates. According to their crystallographic structure, 20 to 35 mass percent of the particles at the study site are expected to have a flaky shape. The scanning electron microscope picture in Figure 2a confirms that flakes are not dominant among the particles at the study site. The picture shows that most of the particles are angular and some are elongated. Evidently, a considerable fraction of the particles at the study site has highly non-spherical shapes.

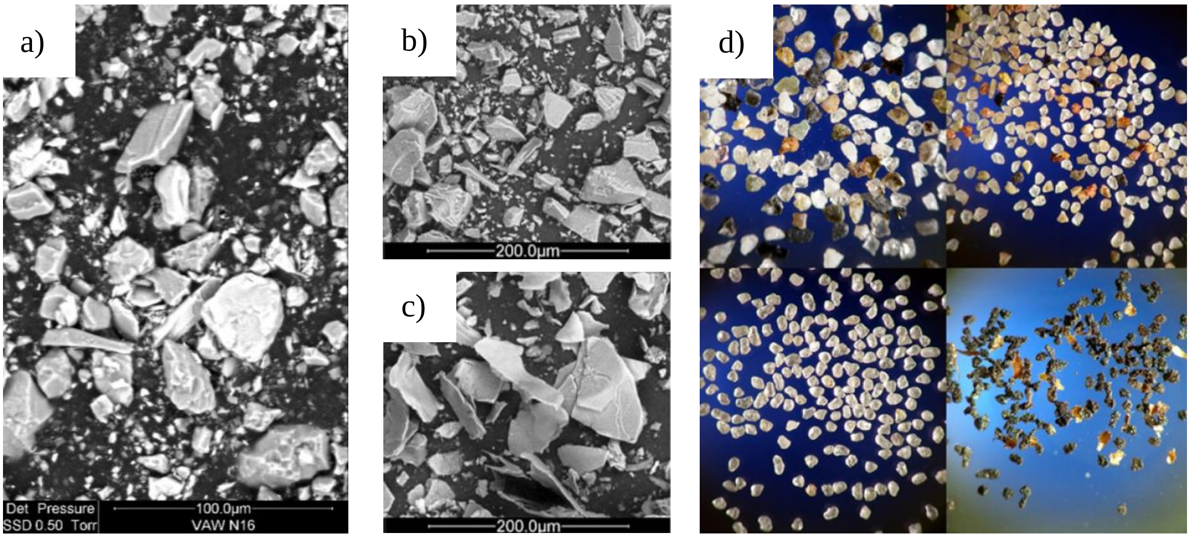

Fig. 2: Microscope pictures of the particles a) from the Fieschertal study site (picture: ETH Zurich), b) feldspar and c) mica powders used in laboratory tests by Felix *et al.* (2013b), and d) particles used for the development of IMR by Agrawal *et al.* (2008); for comparison of shapes (at different scales)

Particle density

The density of the particle mix at the study site was measured with a Helium pycnometer. A solid density of 2.77 g/cm^3 was obtained from dried and ground particle material. As expected, this value lies between the densities of quartz and muscovite. This value was used for the conversion of PVCs to SSCs.

Particle shape effect on SSCs calculated from LISST data

The SSCs obtained from gravimetrical analysis, SSC(G), and from LISST and pycnometer, SSC(L) at corresponding times are shown in Figure 3. A linear fit through the origin yields that the SSC(L)s are on average 68% higher than the SSC(G)s. Possible reasons for the scatter in Fig. 3 are: (i) temporal variations in particle density and shape, and (ii) less importantly measurement errors in SSC(L)s and SSC(G)s. The overestimation is mainly attributed to effects of highly non-spherical particle shapes. Many particles from the study site (Fig. 2a) deviate more from spheres than those used for the development of IMR (Fig. 2d), in which according to Agrawal *et al.* (2008) no elongated or platy particles were considered. In the laboratory investigation by Felix *et al.* (2013b) SSC(L)s were also found to be overestimated with factors of 1.38 for angular feldspar and approximately 8 for flaky mica (muscovite) particles (Figs. 2b and 2c), using also the PVCs in size bins 4 to 32. For a mixture of 70% feldspar and 30% mica powders an overestimation factor of 3.3 was found in the laboratory tests.

Since the flaky particles have a strong effect on the overestimation, it is concluded that mainly the shapes of flaky particles at the study site differ from the shapes of the mica particles used in the laboratory. The smaller overestimation in the present field study fits to the comparison of flake shapes: the sheet silicate particles at the study site (flaky particles in Fig. 2a) are thicker in relation to their size than the mica particles used in the laboratory (Fig. 2c). As reported by Felix *et al.* (2013b), the shape of mica particles depends on their size, since their thickness tends to vary less than their size. Overestimation factors of flaky particles are thus not easily transferable among various studies and sites, unless the size-dependent shape of flaky particles would be parameterized and known.

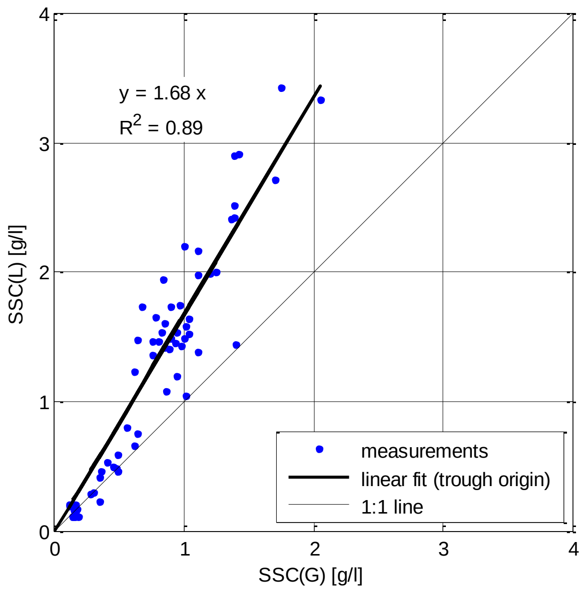

Fig. 3: SSCs calculated from LISST PVCs (in bins 4 to 32) with a particle density of 2.77 g/cm^3 in comparison to gravimetrical SSCs at HPP Fieschertal from June 3 to October 10, 2013 (65 samples)

Conclusions and Recommendations

The present study deals with the application of a LISST for suspended sediment monitoring in a granite rock environment. The comparison between the data obtained from (i) LISST and pycnometer and (ii) gravimetrical analysis of bottle samples indicates that the LISST over-estimated PVCs and consequently SSCs by 68%, which is attributed to flaky, elongated and angular particle shapes.

If SSCs are to be calculated based on LISST measurements, we recommend accompanying measurements of SSC by a mass-based method, i.e. gravimetrical analysis of bottle samples, to determine a site- and possibly time-specific conversion factor from LISST PVCs to SSCs accounting for both particle shape and density. Even if this factor is found to correspond to the assumed particle density, i.e. showing no bias by highly non-spherical particles, such measurements are still valuable to validate the assumptions on particle shapes and density.

Outlook

The data on suspended sediment at the study site obtained in the years 2012 to 2014 will be further evaluated to investigate the characteristics of the various measuring devices, to further examine the LISST PVC to SSC conversion factor described above and to quantify the sediment mass flux and PSD in the turbine water.

Acknowledgements

The authors gratefully acknowledge the support by Swisselectric Research, the Swiss Federal Office of Energy and Gommerkraftwerke AG (the operator of the study HPP) and other project partners, as well as the good research collaboration with Hochschule Luzern.

References

Agrawal Y. C. & Pottsmith H. C. (2000). Instruments for particle size and settling velocity observations in sediment transport, *Mar. Geol*. 168: 89-114, doi:10.1016/S0025-3227(00)00044-X

Agrawal Y. C., Whitmire A., Mikkelsen O. A., Pottsmith H. C. (2008). Light scattering by random shaped particles and consequences on measuring suspended sediments by laser diffraction, *J. Geophys. Res.*, 113, C04023, doi:10.1029/2007JC004403

Andrews S. W., Nover D. M., Reuter J. E., Schladow S. G. (2011). Limitations of laser diffraction for measuring fine particles in oligotropic systems: Pitfalls and potential solutions. *Water Resour. Res., 47,* W05523, doi:10.1029/2010WR009837

Felix D., Albayrak I., Boes R. M. (2013a). Monitoring of suspended sediment - laboratory tests and case study in the Swiss Alps, *Advances in River Sediment Research*, Fukuoka et al. (eds), ISBN 978-1-138-00062-9, Taylor & Francis Group, London: 1757-1766

Felix D., Albayrak I., Boes R. M. (2013b). Laboratory investigation on measuring suspended sediment by portable laser diffractometer (LISST) focusing on particle shape. *Geo-marine Letters* 33(6): 485-498, doi:10.1007/s00367-013-0343-1

Sequoia (2011). LISST bin sizes for inversions based on randomly shaped grains, article dated March 18, 2011; last visited on June 12, 2014; *Sequoia Scientific Inc*., www.sequoiasci.com/article/lisst-bin-sizes-for-inversions-based-on-randomly-shaped-grains

Wren D., Barkdoll B., Kuhnle R., Derrow R. (2000). Field Techniques for Suspended-Sediment Measurement. *J. of Hydraul. Eng.,* 126(2): 97-104, doi:10.1061/(ASCE)0733-9429(2000)126:2(97)

Schwebstoff-Monitoring und Verschleiss an Peltonturbinen (Teile a und b)

SI/500638-01 und -02

Beilagen zum Schlussbericht (2016)

Projektbezogene Publikationen aus dem Jahr

2015

Albayrak I., Felix D., Hagmann M., Boes R.M. (2015). **Suspended Sediment and Bed Load Transport Monitoring Techniques**. ***38. Dresdner Wasserbaukolloquium***, *Dresdner Wasserbauliche Mitteilungen Heft 53*, ISBN 978-3-86780-420-2: 405-414.

Felix D., Albayrak I., Boes R.M. (2015). **Field measurements of suspended sediment using several methods**. *36th IAHR World Congress*, Den Haag, Niederlande.

Suspended Sediment and Bed Load Transport Monitoring Techniques

Ismail Albayrak
David Felix
Michelle Hagmann
Robert M. Boes

ABSRACT Continuous monitoring of suspended sediment and bed load is important for a better understanding and management of sediment related processes in rivers and hydraulic facilities such as reservoirs and hydropower plants. Selected results from recent real-time in-situ measurements of bed load and suspended sediment at two sites in the Swiss Alps using geophones as well as turbidimeters, an acoustic method and a laser diffractometer, respectively, are presented and the measuring capabilities of these techniques are evaluated.

Keywords: Bed load, suspended sediment, real-time monitoring, geophone, laser diffractometer, LISST, turbidimeter, acoustic

1 Introduction

Sediment yield in the Alpine region tends to increase due to glacier retreat under the strong impact of climate change. With respect to the sustainable use of hydropower, this adds to the challenges in terms of reservoir sedimentation and wear of turbines and steel hydraulics parts of hydropower plants (HPPs) and other hydraulic structures.

As an effective and sustainable measure against reservoir sedimentation, sediment bypass tunnels (SBTs) also restore the natural sediment continuity in the river system by diverting sediment-laden discharges (Sumi *et al.* 2012, Facchini *et al.* 2015). A major problem affecting nearly all SBTs is severe hydro-abrasion on tunnel inverts due to the high flow velocities and the large amount of coarse sediment transport (Auel and Boes 2011). Depending on site-specific operating conditions and sediment properties, i.e. size, hardness and shape, invert abrasion can cause considerable refurbishment costs.

Even with well-designed sand traps, desilting facilities or flushable reservoirs, mineral particles cannot be completely removed from the water which passes the turbines. At high- and medium-head HPPs substantial turbine wear may occur which leads to significant maintenance cost and negative impact on power generation and revenues (Felix *et al*. 2013b).

For optimized design and operation of HPPs with respect to sustainable sediment management and cost efficiency, there is an increasing need for continuous real-time monitoring of both suspended sediment and bed load transport.

This paper presents measuring techniques employed in two on-going sediment transport monitoring studies at HPPs in the Swiss Alps. One study deals with suspended sediment in the penstock of a high-head HPP and the other focusses on bed load transport in a SBT. From the studies, the experimental set-ups and selected recent results are presented and the measuring capabilities of the techniques are evaluated.

2 Measuring techniques and devices

2.1 Suspended sediment concentration

Overview

Suspended sediment mass concentration (SSC, in g/l) of mineral particles can be determined by gravimetric laboratory analysis of bottle samples (discontinuous, non-real-time) or using mainly acoustic or optical instruments (continuous, real or non-real-time). A general overview on suspended sediment measurements for field applications is given by Wren *et al.* (2000).

Bottle samples

Bottle sampling can be manually or automatically made and is a direct, widely used and reliable technique. However, it has many disadvantages such as time-consuming laboratory analysis of the samples, effort of transporting bottles from the study sites to the laboratory, having poor temporal resolution and giving results not in real-time (Wren *et al.* 2000).

Turbidimeters

As an optical technique, turbidimeters are relatively inexpensive and widely used for suspended sediment monitoring (SSM) at rivers (e.g. Spraefico *et al.* 2005). These devices measure either the scattering (also called optical backscatter probes) or the absorption (transmission) of near infrared or laser light. Output values are given in optical units (e.g. Formazine Nephelometric Unit, FNU). For conversion to SSC, a calibration based on the particle properties (size, shape, colour and composition) is required. In general, a linear calibration curve (conversion factor) is assumed.

Laser Diffractometers

Devices based on laser diffraction such as Laser in-situ Scattering and Transmissiometry (LISST, Sequoia Scientific, USA) have become available for SSM (Agrawal and Pottsmith 2000). The working principle of a LISST is based on the mathematical inversion of the measured scattering pattern and transmission. SSC obtained from LISST have the advantage of being not or less dependent from temporally variable particle size, since particle size is considered. However, with highly non-spherical particles, a site-specific SSC-correction factor should be applied (Felix *et al.* 2013c).

Acoustic techniques

Furthermore, acoustic techniques can be employed for SSM. Among many possibilities such as using active sensors like Acoustic Doppler Current Profiler (ADCP, e.g. Haught *et al.* 2014) the method of measuring the attenuation of ultrasonic pulses sent through the sediment-laden water in penstocks or channels lends itself particularly in cases where installations for acoustic discharge measurement (ADM) already exist. Such facilities can be upgraded to be used for SSM. Similar to turbidimeters, the attenuation of the ultrasonic signal is correlated with SSC (Costa *et al.* 2012, Felix *et al.* 2013a).

2.2 Suspended sediment particle size distribution

Besides SSC, particle size distribution (PSD) is an important parameter for sediment dynamics and hydro-abrasive wear. The primary method to obtain PSDs is by sieve analysis of dried particles. Especially for smaller particles, laser diffraction has been used in laboratories for decades. However, as mentioned above, analysing collected samples in the laboratory has many disadvantages and limitations. With LISST, practical real-time monitoring devices for both SSC and PSD in field studies have become available.

2.3 Bed load transport monitoring

Overview

Bed load transport can be monitored either directly by sediment trapping, collecting moving particles and using tracer particles or indirectly by active and passive sensors. Active sensors are typically ADCP, radar and sonar. Passive sensors do not emit any signal but only register acoustic, magnetic or seismic signals (Bogen and Møen 2001, Gottesfeld and Tunnicliffe 2003, Møen *et al.* 2010). Such techniques are hydrophone, geophone or vibrational sensors (Rickenmann and McArdell 2007). Direct methods can provide accurate data during the sampling time but are often laborious and risky, whereas indirect methods allow continuous and real-time monitoring but require calibration.

Swiss plate geophone system

An indirect method using a passive sensor is implemented in the so called Swiss plate geophone (Rickenmann and McArdell 2007, Rickenmann *et al.* 2012, & 2014). It is a robust, submersible device developed at the Swiss Federal Institute for Forest, Snow and Landscape Research (WSL). The device consists of an elastically bedded steel plate installed flush to the channel bottom. A geophone sensor (GS-*20DX*) is mounted beneath the plate in a waterproof aluminium casing and registers the oscillations caused by gravel grains and stones impinging on the plate (Figure 1).

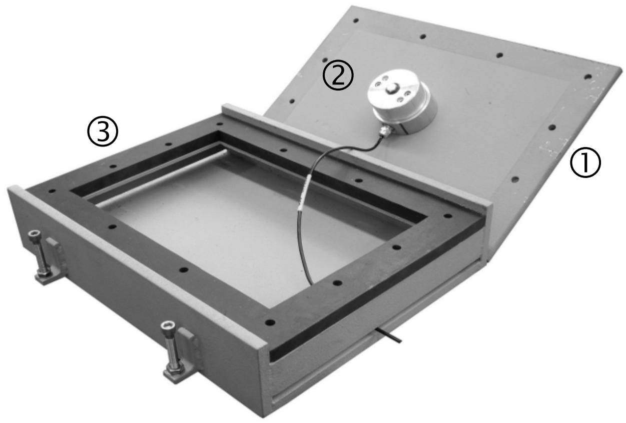

Figure 1: Swiss plate geophone system with steel plate ① (before assembly), geophone sensor ② and elastomer bearing ③ on the aluminum casing (VAW)

The number of impulses, defined as the signal exceeding a threshold, correlates linearly with the bed load volume (Rickenmann 1997, Rickenmann *et al.* 2012). The relation between impulses and bed load volume depends on site specific conditions like flow velocity, grain size and shape. A laboratory study demonstrated that smaller and a larger number of grains can be detected by inclining the geophone plate by 10 °against the bottom slope (Morach 2011). Recent investigations reveal that also the grain size distribution can be estimated based on the amplitude of the geophone signal (Wyss *et al.* 2014).

3 Methodology and set-up of field investigations

3.1 HPP Fieschertal

HPP Fieschertal is a high-head scheme located in Valais, Switzerland, at a tributary of the upper Rhone river in a highly glaciated area with relatively high yield of fine sediments. The HPP is equipped with gravel and sand traps at the intake to remove particles > 0.3 mm.

In this study, two in-line turbidimeters are used and relevant with respect to the results shown in this paper: (1) *AquaScat* from Sigrist Photometer, Switzerland, measuring light scattering at an angle of 90° at a free-falling jet and (2) *TF16-N* from Optek Danulat, Germany, measuring light attenuation over a path length of 10 mm in pressurized flow. The turbidimeters were installed in a valve chamber at the upstream end of the penstock in summer 2012 to quantify the suspended sediment load. They are fed from the penstock by a sampling pipe (d_i = 20 mm). The *LISST-100X* was installed in a bucket at the end of the sampling pipe. It has a nominal particle size measuring range from 2 to 380 µm in the calculation mode for so called ‘random shaped’ particles (Agrawal *et al.* 2008). Practically, particle sizes ≥ 5 µm can be measured. Furthermore, to extend the range of SSC, its optical path length was reduced from 50 to 5 mm with a glass cylinder.

Bottle samples were pumped from the bucket using an automatic sampler *Isco 3700*. The sampler was controlled by a program developed at VAW to take 0.5 liter samples every three days and more frequently if turbidity exceeded predefined threshold values.

Additionally, the existing ADM (from Rittmeyer) at the top of the penstock with four acoustic paths (each 2.27 m long) operating at 1 MHz was used for SSM.

Data from the turbidimeters and the acoustic method were recorded at 1 Hz, while the LISST was set to work at 1/60 Hz. The SSC time series in Figure 2 were obtained by calibrating the devices’ output signals to the gravimetrically determined SSC from bottle samples.

3.2 SBT Solis

The Solis reservoir located in Grisons in the Swiss Alps lies in a gorge and has a length of about 2.7 km. To maintain the active storage, a SBT was constructed and has been commissioned in 2012. Its intake is located 500 m upstream of the dam. The design discharge of the SBT is 170 m^3/s, corresponding to a 5-year-flood.

As part of a research study dealing with the abrasion resistance of various invert materials, suspended sediment and bed load transport in Solis SBT are monitored using two submersible turbidimeter probes *TurbiMax W CUS41* (Endress+Hauser) installed in the right and left tunnel walls 0.22 m above the invert, and eight Swiss plate geophones installed at the outlet of the SBT, respectively. The geophones are placed across the whole tunnel width of 4.40 m and have an inclination of 10° against the invert slope. Furthermore, the water levels in the reservoir and in the tunnel as well as the tunnel intake gate position are monitored. Data recording is triggered by the opening of the intake gate. The sampling rates are 1/60 Hz in general and 10 kHz for the geophone system.

The turbidimeter data were converted to SSC based on gravimetrically determined SSCs of bottle samples taken from the river at an existing gauging station1 km upstream of the reservoir. The geophone system was calibrated in the laboratory using natural stones with grain sizes similar to the field conditions.

4 Results and Discussion

4.1 HPP Fieschertal

From the suspended sediment measurements in the turbine water of HPP Fieschertal recorded from 2012 to 2014, an extract of four days is presented in Figure 2. The median particle size d_{50} stands for the diameter of graded particles, of which 50% by mass are smaller.

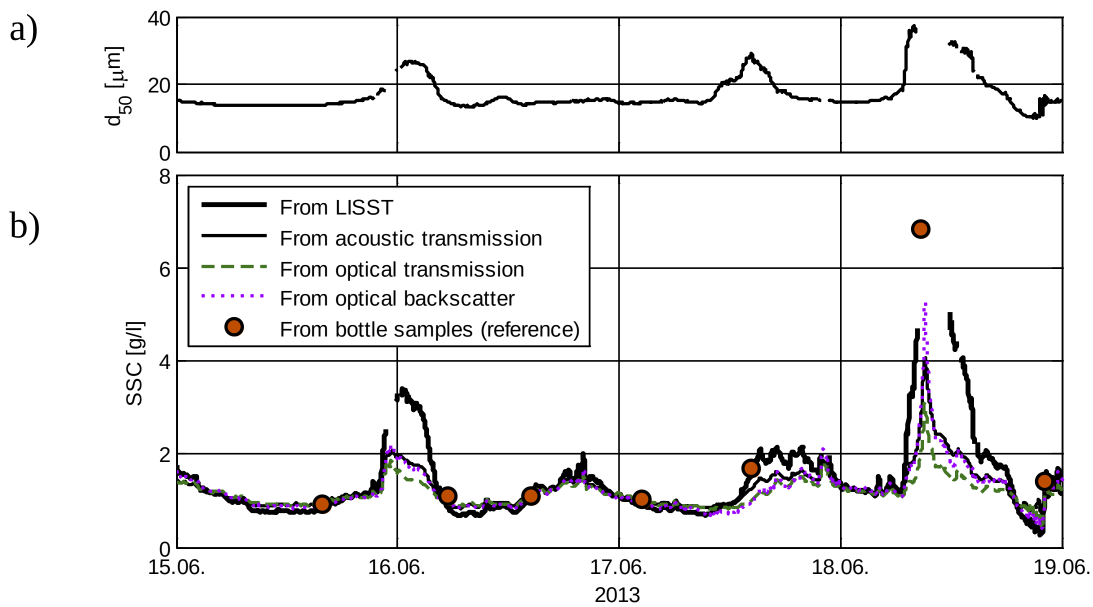

Figure 2: Time series of a) d_{50} from LISST and b) SSCs obtained from various methods after calibrating to bottle samples, measured in the turbine water of HPP Fieschertal

During these days in early summer 2013, the SSC occasionally rose to several g/l within a few hours. When the SSC was above 5 g/l, as captured by a bottle sample, no LISST results were available as the optical transmission was too low. The median particle size d_{50} had a base level of about 15 µm and rose up to approx. 35 µm at high SSCs. In many such events, the maximum d_{50} occurred after the SSC peak (time lag).

In periods of usual SSCs all devices yielded similar SSC values. During high SSCs, however, the acoustic method and the turbidimeters underestimated the

SSCs. This is attributed to temporal changes in particle size. When particles are coarser than the normally prevailing ones, less damping or scattering occurs. This was also observed in laboratory investigations prior to the field study by Felix *et al.* (2013c).

4.2 SBT Solis

Since its commissioning in 2012, the Solis SBT was in operation four times during 11 hours on average and diverted sediment volumes between 20’000 and 80’000 m^3. The operating conditions varied from event to event and within one single run. Figure 3 shows the normalized spanwise distribution of bed load transport across the eight geophones. It is seen that bed load transport was concentrated on the orographic right side of the tunnel. This is related to a horizontal curve in the tunnel layout located 100 m upstream of the geophones. The bend induces secondary currents transporting bed load at the inner side.

Figure 4 shows time series of volumetric suspended and bed load transport rates in the tunnel and the reservoir level during the largest flood event since the commissioning of the SBT. Monitoring data show that the lower the reservoir level, the coarser sediment material is transported into and through the tunnel. The geophone data revealed that during the drawdown, three peaks in bed load transport occurred at certain reservoir elevations (see arrows in Fig.4).Turbidity data showed a similar behavior for the suspended sediment transport rate, but the peaks occurred before those of the bed load (Fig. 4). In addition, suspended sediment transport in the tunnel occurred prior to the drawdown of the reservoir level.

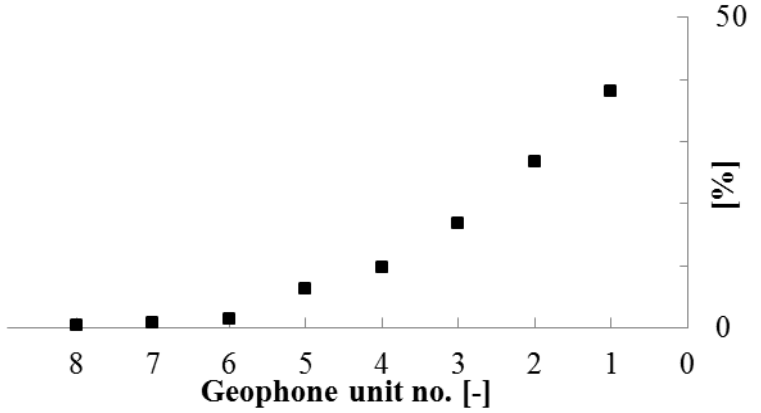

Figure 3: Distribution of the bed load transport in Solis SBT across the tunnel width, registered by the geophone units 1 to 8 at the outlet on 13th of August 2014

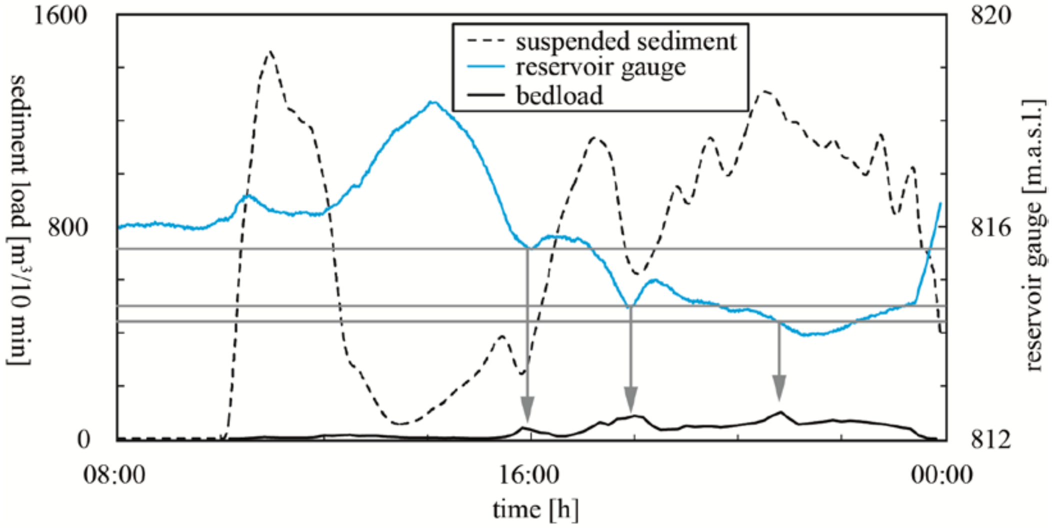

Figure 4: Time series of suspended and bed load transport in the Solis SBT as well as the reservoir level during the flood event on 13th of August 2014

5 Conclusion and Outlook

Selected state-of-the-art monitoring techniques and exemplary field data on suspended and bed load transport measurements were presented. The measuring capabilities of the devices during sediment transport events were evaluated.

In case of temporal variations in PSD, SSCs obtained from turbidimeters or single-frequency acoustic methods are less accurate than those from a calibrated LISST. In dynamic environments it is recommended to measure both SSC and PSD, and to combine continuous indirect measurements with automatic bottle sampling for calibration. In order to extend the SSC measuring range of LISST, devices with automatic dilution are an option (Agrawal *et al.* 2012).

As bed load transport may vary significantly in spanwise channel direction due to secondary currents, it is recommended to measure bed load across the channel width in such situations. Since suspended and bed load transports exhibit different temporal behaviors, it is recommended to measure both suspended and bed load to quantify total sediment transport in rivers and hydraulic schemes.

Measurements and data evaluation at both study sites are continued.

6 References

Agrawal Y.C., Pottsmith H.C. (2000). Instruments for particle size and settling velocity observations in sediment transport, Mar. Geol. 168: 89-114.

Agrawal Y.C., Whitmire A., Mikkelsen O.A., Pottsmith H.C. (2008). Light scattering by random shaped particles and consequences on measuring suspended sediments by laser diffraction, J. Geophys. Res., 113, C04023.

Agrawal Y. C., Mikkelsen O.A., Pottsmith H.C., Slade W.H. (2012). Turbine abrasion: one year’s experience in real-time sediment monitoring at Hidroagoyan HPP, Ecuador. *Proc. Hydro 2012 Conference*, Bilbao, Spain: Paper 14.08.

Auel C., Boes R. M. (2011). Sediment bypass tunnel design - review and outlook. Proc. ICOLD Symposium "Dams under changing challanges", (A. J. Schleiss & R. M. Boes, eds.), 79th Annual Meeting, Lucerne. Taylor & Francis, London, 403-412.

Bogen J., Møen K. (2001). Bed load measurements with a new passive ultrasonic sensor. Erosion and Sediment Transport Measurement: Technological and Methodological Advances, International Association of Hydrological Sciences: 19-21.

Costa L.I., Storti G., Lüscher B., Gruber P., Staubli T. (2012). Influence of solid particle parameters on the sound speed and attenuation of pulses in ADM, J. of Hydrologic Eng., 17(10): 1084-1092.

Facchini M., Siviglia A., Boes R.M. (2015). Downstream morphological impact of a sediment bypass tunnel – preliminary results and forthcoming actions. Proc. Intl. Workshop on Sediment Bypass Tunnels, Mitteilungen 232 (R.M. Boes, ed), VAW, ETH Zurich: in press.

Felix D., Albayrak I., Boes R.M. (2013a). Monitoring of Suspended Sediment – Laboratory Tests and Case Study in the Swiss Alps. Advances in River Sediment Research, Fukuoka S., Nakagawa H., Sumi T., Zhang H. (eds), Taylor & Francis, London: 1757-1766.

Felix D., Albayrak I., Boes R.M., Abgottspon A., Deschwanden F., Gruber P. (2013b). Measuring Suspended Sediment: Results of the first Year of the Case Study at HPP Fieschertal in the Swiss Alps. Proc. Hydro 2013 Conference, Innsbruck, Austria: paper 18.03.

Felix D., Albayrak I., Boes R.M. (2013c). Laboratory investigation on measuring suspended sediment by portable laser diffractometer (LISST) focusing on particle shape. Geo-marine Letters 33(6): 485-498.

Gottesfeld A. S., Tunnicliffe J. (2003). Bed load measurements with a passive magnetic induction device. IAHS Publication: 211-221.

Haught D.W., Venditti J.G., Church M. (2014). Acoustic sediment flux observations on the Fraser River, Canada. Proc. River Flow 2014 (A. Schleiss et al., eds.), Lausanne: 1943-1950.

Møen K., Bogen J., Zuta J., Ade P., Esbensen K. (2010). Bedload measurement in rivers using passive acoustic sensors. US Geological Survey Scientific Investigations Report 5091: 336-351.

Morach S. (2011). Geschiebemessung mittels Geophonen bei hohen Fliessgeschwindigkeiten - Hydraulische Modellversuche. Masterarbeit, VAW, ETH Zurich (unpublished).

Rickenmann D. (1997). Sediment transport in Swiss torrents. Earth Surface Processes and Landforms 22(10): 937-951.

Rickenmann D., McArdell B. W. (2007). Continuous measurement of sediment transport in the Erlenbach stream using piezoelectric bedload impact sensors. Earth Surface Processes and Landforms 32(9): 1362-1378.

Rickenmann D., Turowski J. M., Fritschi B., Klaiber A., Ludwig A. (2012). Bedload transport measurements at the Erlenbach stream with geophones and automated basket samplers. Earth Surface Processes and Landforms 37(9): 1000-1011.

Rickenmann D., Turowski J. M., Fritschi B., Wyss C., Laronne J., Barzilai R., Reid I., Kreisler A., Aigner J., Seitz H., Habersack H. (2014). Bedload transport measurements with impact plate geophones: comparison of sensor calibration in different gravel-bed streams. Earth Surface Processes and Landforms 39(7): 928-942.

Spreafico, M., Lehmann, C., Jakob, A., Grasso, A. (2005). Feststoffbeobachtung in der Schweiz – Ein Tätigkeitsgebiet der Landeshydrologie. Berichte des BWG, Serie Wasser Nr. 8, Bern.

Sumi T., Kantoush S., Suzuki S. (2012). Performance of Miwa dam sediment bypass tunnel: Evaluation upstream and downstream state and bypass efficiency. Q92 R 38. Proc. 24th ICOLD Congress Kyoto. 576-596.

Wren D., Barkdoll B., Kuhnle R., Derrow R. (2000). Field Techniques for Suspended-Sediment Measurement. J. of Hydraul. Eng., 126(2): 97-104.

Wyss C. R., Rickenmann D., Fritschi B., Weitbrecht V., Boes R. M. (2014). Bedload grain size estimation from the indirect monitoring of bedload transport with Swiss plate geophones at the Erlenbach stream. Proc. River Flow 2014 (A. Schleiss et al., eds.), Lausanne: 1907-1912.

Authors:

Dr.-sc. techn. Ismail Albayrak
Dipl.-Bauing. ETH David Felix
MSc ETH Bau-Ing. Michelle Hagmann
Prof. Dr sc. techn. Robert M. Boes

ETH Zürich
Versuchsanstalt für Wasserbau, Hydrologie und Glaziologie (VAW)
HIT F23
Wolfgang-Pauli-Str. 27
8093 Zürich

Tel.: +41 44 632 97 44
Fax: +41 44 632 11 92
E-Mail: albayrak@vaw.baug.ethz.ch
felix@vaw.baug.ethz.ch
hagmann@vaw.baug.ethz.ch
boes@vaw.baug.ethz.ch

E-proceedings of the 36th IAHR World Congress
28 June – 3 July, 2015, The Hague, the Netherlands

FIELD MEASUREMENTS OF SUSPENDED SEDIMENT USING SEVERAL METHODS

DAVID FELIX(1), ISMAIL ALBAYRAK(2) & ROBERT M. BOES(3)

(1) PhD student, Laboratory of Hydraulics, Hydrology and Glaciology (VAW), ETH Zurich, CH-8093 Zurich, Switzerland, felix@vaw.baug.ethz.ch

(2) Dr., Research Scientist, Laboratory of Hydraulics, Hydrology and Glaciology (VAW), ETH Zurich, CH-8093 Zurich, Switzerland, albayrak@vaw.baug.ethz.ch

(3) Prof. Dr., Director, Laboratory of Hydraulics, Hydrology and Glaciology (VAW), ETH Zurich, CH-8093 Zurich, Switzerland, boes@vaw.baug.ethz.ch

ABSTRACT

Field measurements of suspended sediment mass concentration (SSC) and particle size distribution (PSD) with high temporal resolution and good accuracy are required for a better understanding and management of many fine-sediment related processes. This paper deals with the recent field study on SSC and PSD in the turbine water at the high-head hydropower plant (HPP) Fieschertal in the Swiss Alps. Various types of turbidimeters, a 'Laser in-situ Scattering and Transmissiometry' (LISST) device and a single-frequency acoustic attenuation method were used for continuous suspended sediment measurements (SSM). The obtained data were converted to SSC based on reference SSCs gravimetrically determined from bottle samples. Furthermore, PSDs were obtained by LISST every minute. The results showed a high temporal variability of SSC and PSD as well as a weak correlation between them. During a sediment transport event with a SSC peak of almost 12 g/l, the particles were temporarily coarser than usual and the turbidimeters as well as the acoustic method underestimated SSC by up to 80%. However, the SSCs obtained by LISST agreed reasonably well with the reference SSCs despite occasional PSD variations. Based on these findings, the LISST technique in combination with automatic bottle sampling is recommended among the tested methods for SSM in sediment environments where PSD varies independently of SSC.

Keywords: Suspended sediment, turbidimeter, LISST, acoustic, gravimetric

1. INTRODUCTION

In rivers, lakes and seas as well as in hydraulic schemes for hydropower, irrigation and flood protection, sediment particles contained in the water may settle, be transported or be re-suspended. Fine-sediment related processes such as reservoir sedimentation, turbine wear or river bed colmatation can be economically and environmentally important. To better understand and manage such processes, measurements of SSC and PSD with high temporal resolution and good accuracy are required. For short-term decision making related to highly dynamic processes such as flushing of reservoirs or shutdowns of hydropower plants (HPPs) during floods, real-time data are required.

The primary method to determine SSC is gravimetric analysis of **bottle samples** in a laboratory. This discontinuous method is reliable but has many disadvantages such as relatively high effort for collection, transport and analysis of the samples, poor temporal resolution and long processing time. For continuous indirect measurements of SSC with the possibility of providing results in real-time, mainly optical and acoustic techniques are employed (Wren et al., 2000).

Turbidimeters are widely used since they are relatively inexpensive and easy to handle. They measure either the scattering at one or several angles or the absorption (transmission) of near infrared or laser light. The outputs depend not only on SSC, but also on PSD, shape and color (reflectivity) of the particles (e.g. Downing, 2006). The conversion between turbidimeter output and SSC (also called calibration) is usually made based on gravimetrically determined SSCs of bottle samples (e.g. Haimann et al., 2014). Such a conversion involves less uncertainty if the particle properties are practically constant or well correlated with SSC, e.g. if coarser particles always occur at higher SSC.

A more advanced optical technique for SSM is 'Laser in-situ Scattering and Transmissiometry' (**LISST**). This technique has been mainly used in seas and estuaries, and more recently in rivers as well as in waterways (Boes, 2009; Agrawal et al., 2012) and reservoirs of HPPs (Haun et al., 2013). From the intensities of the scattered (diffracted) light and the transmission measured with a LISST device, the particle volume concentrations in 32 log-spaced size bins are computed with the corresponding software (Agrawal and Pottsmith, 2000). From these, the total particle volume concentration (PVC) and the PSD are calculated. PVCs should be converted to SSCs based on gravimetrically determined SSCs of bottle samples. The conversion factor accounts for possible deviations between (1) the solid density of the primary particles and the bulk density of flocculated particles and (2) between actual and assumed particle shapes (Felix et al., 2013b).

Further techniques are based on **acoustics**. Among many possibilities, the attenuation of ultrasonic pulses sent through sediment-laden water can be exploited. Similarly to the second type of turbidimeters, the attenuation caused by the sediment particles is correlated with SSC (Costa et al., 2012; Felix et al., 2013a). This method lends itself particularly in cases where installations for acoustic discharge measurement (ADM) exist in channels or penstocks (Fig. 1).

This paper deals with a field study on suspended sediment in the turbine water of the high-head HPP Fieschertal in the Swiss Alps. The HPP is located at a tributary of the upper Rhone River in an area with high yield of fine sediment due to glacial erosion. The study aims at quantifying SSC and PSD in the penstock and to evaluate various methods for SSM. Several types of turbidimeters, a LISST device, an acoustic system as mentioned above and an automatic bottle sampler were used. In this paper, the setup and methods are described, selected results on SSC and PSD are presented, and the measuring performance of the devices is evaluated based on exemplary field data.

2. EXPERIMENTAL SETUP AND METHODS

Table 1 shows the devices for SSM installed in the valve chamber of HPP Fieschertal. The chamber is located 2 km downstream of the intake at the end of a free surface flow tunnel which serves as a daily reservoir. The turbine water in the penstock downstream of the chamber should contain only particles with less than 0.3 mm diameter, since coarser material is removed by the gravel and sand traps at the intake.

The three in-line turbidimeters (items no. 1 to 3 in Tab. 1) were fed with water from the penstock by a sampling pipe. Regarding LISST, a submersible multi-purpose model, *LISST-100X,* was installed at the end of the sampling pipe, looking laterally into a flushable bucket with an overflow (Fig. 2). To extend the range of measurable SSC, its optical path length was reduced from 50 mm to 5 mm by inserting a glass cylinder. The device has a nominal particle size measuring range from 2 to 380 µm in the mode for so-called 'random shaped' particles (Agrawal et al., 2008). Bottle samples were pumped from the bucket using an automatic sampler (item no. 6). The sampler was controlled by a computer to take 0.5 liter samples every three days and more frequently when turbidity exceeded predefined threshold values. Furthermore, an already existing ADM installation (item no. 4) was used for SSM. Only the software of its controller needed to be updated to yield the actual amplitudes of the received ultrasonic pulses as additional output signals. The ADM has four paths of 2.27 m length and operates at 1 MHz.

From 2012 to 2014, data on suspended sediment, penstock discharge, tunnel water level and other variables from the HPP's control system were recorded every minute. The devices for SSM were regularly cleaned. From the collected water samples, SSCs were determined in the laboratory by gravimetrical analysis. Linear relations between these SSCs and the outputs of each of the continuous SSM devices at corresponding times were established over a year. These relations (calibration factors) were used to convert the devices' outputs to SSC time series. Furthermore, daily precipitation data from a rain gauge close to the HPP was analyzed to investigate the correlation between precipitation and high SSCs.

Table 1. Devices for SSM in the valve chamber of HPP Fieschertal.

Item No.	Device Type	Subtype	Model	Manufacturer	Derived Parameters
1	Turbidimeter	in-line, pressure flow	*TF16-N*	Optek Danulat (Germany)	SSC
2	Turbidimeter	in-line, pressure flow	*TurbiScat*	Sigrist Photometer (Switzerland)	SSC
3	Turbidimeter	in-line, free falling jet	*AquaScat*	"	SSC
4	Acoustic	based on ADM installation	*Risonic*	Rittmeyer (Switzerland)	SSC
5	LISST	submersible; Type C	*LISST-100X*	Sequoia Scientific (USA)	SSC, PSD
6	Bottle sampler	24 bottles of 1 liter	*Isco 3700*	Teledyne Isco (USA)	SSC

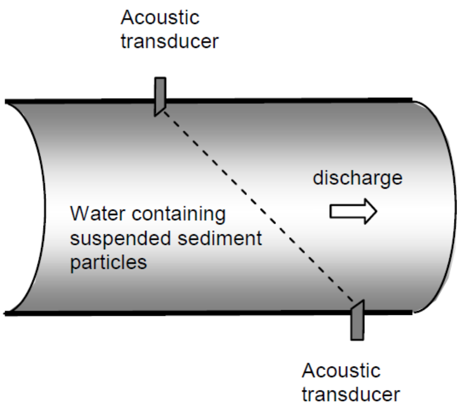

Figure 1. Schematic of a penstock with one path of an ADM installation which can also serve to monitor SSC, as item (4) in Table 1 (Felix et al. 2013c).

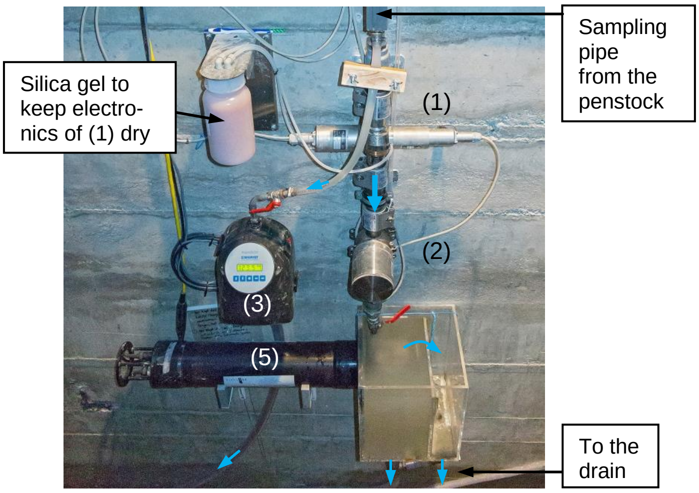

Figure 2. Optical devices for SSM in the valve chamber of HPP Fieschertal; numbers refer to items in Table 1.

3. RESULTS AND DISCUSSION

Figure 3 shows the time series of SSC and the median particle diameter, d_{50} obtained from LISST and the SSCs from bottle samples for the first two weeks in September 2013. The particle size d_x stands for the diameter of graded particles, of which *x* % by mass are smaller. During these days in late summer, the SSC was on average 0.23 g/l. Among smaller daily SSC peaks, a major peak of almost 12 g/l occurred in a short sediment transport event on September 9. The d_{50} had a base level of 10 μm and rose up to approx. 80 μm at some days (Fig. 3). Often, but not always, coarser particles were transported at higher SSCs. The largest particles tended to be transported after the SSC-peaks (time lag), as observed earlier by Felix et al. (2013a, c).

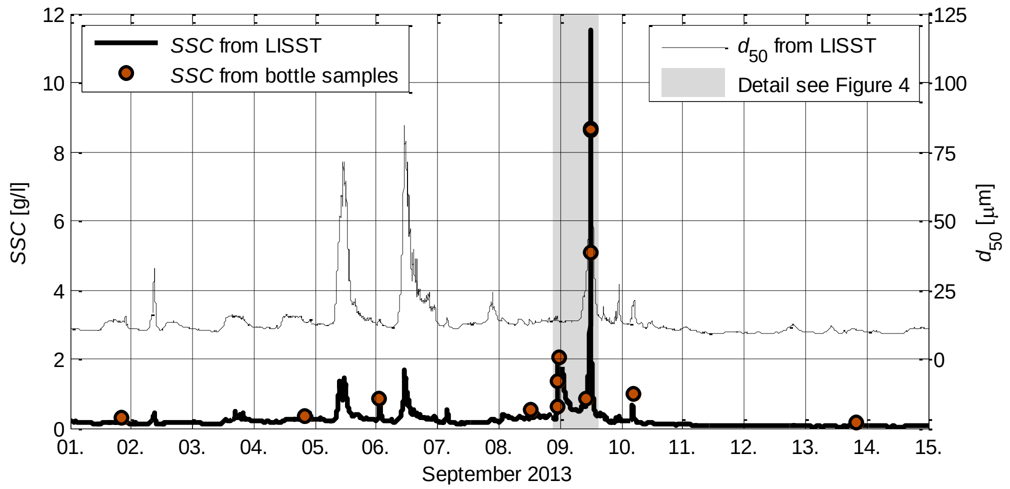

Figure 3. Time series of SSC and d_{50} obtained from LISST and SSCs from bottle samples in the turbine water of HPP Fieschertal during two weeks.

A detail of 18 hours including the major SSC peak is shown in Figure 4. Additionally, the time series of the particle sizes d_{16} and d_{84}, as well as the SSCs obtained from two turbidimeters and the acoustic method, are displayed. No data from the third turbidimeter was available because its small feeding pipe, branching off the main pipe (Fig. 2), was clogged in this period. A small SSC peak occurred some 12 hours before the major peak. In the following, these suspended sediment transport events are referred to as the first and the second event.

In the first event, no LISST results were available when SSC was above approx. 2 g/l (Fig. 4). According to the available LISST data, the particles were small as usual while the SSC was above its base level. It is assumed that the PSD did not change throughout the first event. However, during the second event particle sizes gradually increased and decreased. All methods provided similar SSCs except during the second event. During this event, the turbidimeters and the acoustic method yielded up to 80% lower SSCs than those from LISST and bottle samples (reference method). This is mainly attributed to the temporal variation in PSD. As coarser particles produce less attenuation and scattering at a given SSC, the turbidimeters and the acoustic method underestimate SSC when coarser particles are present. The coarser particles are furthermore the reason why results from LISST were available in the second event despite the higher SSC.

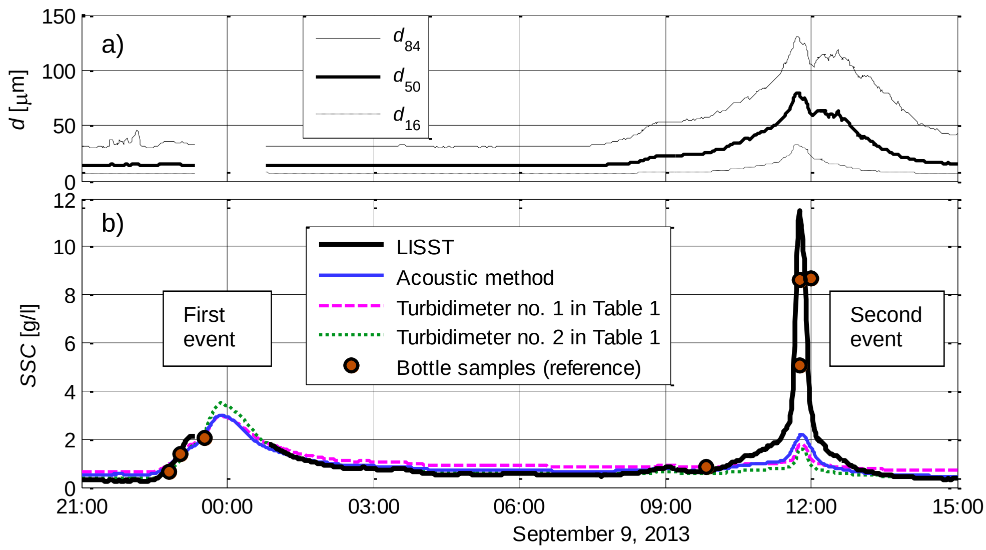

Figure 4. a) Time series of selected particle sizes obtained by LISST and b) SSC time series obtained by various devices for SSM based on gravimetrical analysis of bottle samples, detail of 18 hours.

The time shifts of several minutes between the LISST and the bottle sample SSCs during the second event (Fig. 4) are attributed to the setup in this study. Whereas the LISST device's optical path was placed directly beneath the outlet of the sampling pipe, the bottle samples were pumped from the bucket. The gradual mixing in the bucket caused a damping and delay of the gravimetric SSCs when the SSC in the sampling pipe rapidly changed.

The different character of the two events is explained as follows: In the first event, precipitation induced a higher SSC of relatively fine particles, as usually prevailing in the turbine water. In the second event, the operation of the HPP produced gradual changes of flow conditions in the reservoir tunnel upstream of the SSM location. The water level in the tunnel was drawn down to the minimum operation level while the turbines were running almost at design discharge. The drawdown caused higher flow velocity and bottom shear stress, which led to re-suspension and transport of increasingly coarser particles and significantly increased SSC in the penstock. After the turbine discharge was reduced, the tunnel water level rose and SSC and PSD fell back to the usual levels.

4. CONCLUSIONS AND OUTLOOK

Selected results of SSM in the waterway of an alpine HPP were presented. They show a high temporal variability of SSC and PSD as well as a weak correlation between them. In such conditions, SSCs obtained using LISST are more accurate than those from turbidimeters or the single-frequency acoustic method, since the latters can be biased by effects of PSD variations. In addition to SSC, the LISST also provides PSDs at high temporal resolution, e.g. every minute; which has been previously not affordable with laboratory PSD analyses. Automatic bottle sampling is highly recommended as a basis for adequate conversion of PVCs to SSCs. The combination of various SSM devices increases data availability and allows for quality checking by comparison of results.

The LISST used in this study provided SSCs up to 2 g/l at d_{50} = 15 µm (medium to coarse silt) and up to almost 12 g/l at $d_{50} \approx$ 80 µm (coarse silt and fine sand) with the shapes of the particles prevailing at the study site. The upper SSC-limit of the operation range of a LISST can be predicted as a function of its optical path length and the particles' Sauter mean diameter, which depends on the PSD and particle shapes (Felix et al., 2013b). To further extend the upper limit of the SSC-measuring range, using a LISST device with automatic clear-water dilution in a mixing chamber is an option (Agrawal et al., 2012). Other options for continuous indirect measurements of higher SSC encompass the use of alternative measuring principles, e.g. in-line density measurements at a vibrating tube bend as in Coriolis flow and density meters (Bishwakarma and Støle, 2008) or other acoustic systems using backscatter and multi-frequency, which are under development.

ACKNOWLEDGMENTS

The authors gratefully acknowledge the support by swisselectric research, the Swiss Federal Office of Energy and the HPP operator Gommerkraftwerke AG. Thanks go to the project partners, especially to Prof. Dr. T. Staubli, Prof. Dr. P. Gruber and A. Abgottspon from Hochschule Luzern, Competence Center for Fluid Mechanics and Hydro Machines. Further thanks go to Endress+Hauser, Sigrist Photometers and Rittmeyer for measuring equipment support.

REFERENCES

Agrawal YC. and Pottsmith HC. (2000). Instruments for particle size and settling velocity observations in sediment transport, *Mar. Geol.* 168, 89-114.

Agrawal YC., Mikkelsen OA., Pottsmith HC., and Slade WH. (2012). Turbine abrasion: one year's experience in real-time sediment monitoring at Hidroagoyan HPP, Ecuador. *Proc. Hydro 2012 Conference*, Bilbao, Spain, paper no. 14.08.

Agrawal YC., Whitmire A., Mikkelsen OA., and Pottsmith HC. (2008). Light scattering by random shaped particles and consequences on measuring suspended sediments by laser diffraction, *J. Geophys. Res.*, 113, C04023.

Bishwakarma MB. and Støle H. (2008). Realtime sediment monitoring in hydropower plants. *J. Hydr. Res.* 46(2), 282-288.

Boes RM. (2009). Real-time monitoring of SSC and PSD in the headwater way of a high-head hydropower plant. *Proc. 33rd IAHR Congress*, Vancouver, Canada, 4037-4044.

Costa LI., Storti G., Lüscher B., Gruber P., and Staubli T. (2012). Influence of solid particle parameters on the sound speed and attenuation of pulses in ADM, *J. of Hydrologic Eng.*, 17(10), 1084-1092.

Downing J. (2006). Twenty-five years with OBS sensors: The good, the bad, and the ugly. *Continental Shelf Research*, 26(17–18), 2299-2318.

Felix D., Albayrak I., and Boes RM. (2013a). Monitoring of Suspended Sediment – Laboratory Tests and Case Study in the Swiss Alps. *Advances in River Sediment Research*, Fukuoka S., Nakagawa H., Sumi T., Zhang H. (eds), Taylor & Francis, London, 1757-1766.

Felix D., Albayrak I., and Boes RM. (2013b). Laboratory investigation on measuring suspended sediment by portable laser diffractometer (LISST) focusing on particle shape. *Geo-marine Letters* 33(6), 485-498.

Felix D., Albayrak I., Boes RM., Abgottspon A., Deschwanden F., and Gruber P. (2013c). Measuring Suspended Sediment: Results of the first Year of the Case Study at HPP Fieschertal in the Swiss Alps. *Proc. Hydro 2013 Conference*, Innsbruck, Austria, paper no. 18.03.

Haimann, M., Liedermann, M., Lalk, P., and Habersack, H. (2014). An integrated suspended sediment transport monitoring and analysis concept. *J. of Sediment Research* 29(2), 135-148.

Haun S., Kjærås H., Løvfall S., and Olsen NRB. (2013). Three-dimensional measurements and numerical modelling of suspended sediments in a hydropower reservoir. *J. of Hydrology (479)*, 180-188.

Wren D., Barkdoll B., Kuhnle R., and Derrow R. (2000). Field Techniques for Suspended-Sediment Measurement. *J. of Hydraul. Eng.,* 126(2), 97-104.

Schwebstoff-Monitoring und Verschleiss an Peltonturbinen (Teile a und b)

SI/500638-01 und -02

Beilagen zum Schlussbericht (2016)

Projektbezogene Publikationen aus dem Jahr

2016

Abgottspon A., Felix D., Boes R., Staubli T. (2016a). **Schwebstoffe, hydro-abrasiver Verschleiss und Wirkungsgrad-änderungen an Peltonturbinen - Ein Forschungsprojekt am KW Fieschertal**. *Wasser Energie Luft* 108(1): 9-24.

Abgottspon A., Staubli T., Felix D. (2016b). **Erosion of Pelton buckets and changes in turbine efficiency measured in the HPP Fieschertal**. *Proc. 28th IAHR-Symposium on Hydraulic Machinery and Systems*, Grenoble, Frankreich: 1181-1190.

Felix D., Albayrak I., Abgottspon A., Boes R.M. (2016a). **Hydro-abrasive erosion of hydraulic turbines caused by sediment – a century of research and development**. *Proc. 28th IAHR-Symposium on Hydraulic Machinery and Systems*, Grenoble, Frankreich: 907-916.

Felix D., Albayrak I., Abgottspon A., Boes R.M. (2016b). **Real-time measurements of suspended sediment concentration and particle size using five techniques**. *Proc. 28th IAHR-Symposium on Hydraulic Machinery and Systems,* Grenoble, Frankreich: 1057-1066.

Felix D., Albayrak I., Abgottspon A., Boes R.M. (2016c). **Suspended sediment measurements and calculation of the particle load at HPP Fieschertal**. *Proc. 28th IAHR-Symposium on Hydraulic Machinery and Systems,* Grenoble, Frankreich: 1067-1076.

Felix D., Abgottspon A., Albayrak I., Boes R.M. (2016d). **Hydro-abrasive erosion on coated Pelton runners: Partial calibration of the IEC model based on measurements in HPP Fieschertal**. *Proc. 28th IAHR-Symposium on Hydraulic Machinery and Systems,* Grenoble, Frankreich: 1191-1200.

Felix D., Albayrak I., Abgottspon A., Boes R.M. (2016e). **Optimization of hydropower plants with respect to fine sediment focusing on turbine switch-offs during floods**. *Proc. 28th IAHR-Symposium on Hydraulic Machinery and Systems,* Grenoble, Frankreich: 1211-1220.

Felix D., Albayrak I., Boes R.M. (2016f). **Continuous measurement of suspended sediment concentration: Discussion of four techniques**. *Measurement* 89: 44-47.

Felix D., Albayrak I., Boes R.M. (2016g). **Combining in-situ laser diffraction (LISST) and vibrating tube densimetry to measure low and high suspended sediment concentrations**. *Proc. 13th Int. Symposium on River Sedimentation*, Stuttgart, Deutschland: 1264-1271.

Gruber P., Felix D., Storti G., Lattuada M., Fleckenstein P., Deschwanden F. (2016). **Acoustic measuring techniques for suspended sediment**. *Proc. 28th IAHR-Symposium on Hydraulic Machinery and Systems,* Grenoble, Frankreich: 927-936.

Schwebstoffe, hydro-abrasiver Verschleiss und Wirkungsgradänderungen an Peltonturbinen

Ein Forschungsprojekt am KW Fieschertal

André Abgottspon, David Felix, Robert Boes, Thomas Staubli

Zusammenfassung

Durch schwebstoffhaltiges Wasser kommt es insbesondere bei Hoch- und Mitteldruckwasserkraftanlagen zu hydro-abrasivem Verschleiss an Turbinen und Pumpen mit entsprechenden Wirkungsgradreduktionen. Die Folgen sind erhöhte Unterhaltskosten und Ertragseinbussen.

Im Rahmen eines Forschungsprojekts wurden die Schwebstoffbelastung, die Abrasion an Peltonlaufrädern und die dadurch verursachten Wirkungsgradänderungen am KW Fieschertal während dreier Jahre detailliert gemessen und untersucht. Mit den Messungen konnten die Variation der Schwebstoffbelastung mit der Zeit, die Abhängigkeit von der Gletscherschmelze, von Regenereignissen und auch vom Betrieb der Anlage aufgezeigt werden. Die untersuchten, praxistauglichen Messmethoden erlaubten ein kontinuierliches Monitoring der Schwebstoffbelastung und lieferten somit eine Grundlage für die wirtschaftliche Optimierung des Anlagenbetriebs, beispielsweise für das vorübergehende Ausleiten von Fassungen und den Betriebsunterbruch während eines Hochwassers.

Die Abrasion der Laufradbecher wurde mit detaillierten Messungen bestimmt. Um die Auswirkungen der Abrasion auf den Wirkungsgrad zu quantifizieren, wurde eine Methode des Wirkungsgradmonitorings entwickelt, die den Anlagebetrieb möglichst wenig beeinträchtigt. Darauf basierend kann die Wirtschaftlichkeit von Revisionsarbeiten (Nachschleifen, Nachbeschichten) und Ersatzinvestitionen beurteilt werden.

Résumé

Les turbines et les pompes des aménagements hydroélectriques à haute ou moyenne chute peuvent subir de l'usure par abrasion causée par des particules minérales contenues dans l'eau. L'usure engendre une diminution des rendements hydrauliques, une augmentation des coûts d'entretien et des pertes de revenu.

Dans le cadre d'un projet de recherche, la charge des sédiments en suspension, l'abrasion des roues Pelton ainsi que les différences de rendements hydrauliques en resultant ont été mesurées et analysées à l'aménagement de Fieschertal pendant trois ans. Les mesures ont montré la variation temporelle de la charge en sédiments ainsi que les effets de la fonte glaciaire, des pluies, et de l'exploitation de l'aménagement. Les techniques de mesure investiguées et éprouvées permettent une surveillance en continu de la charge des sédiments en suspension. Ceci fournit une base pour une opération économiquement optimisée, comme par exemple, d'interrompre le captage d'eau et le turbinage pendant les crues.

L'abrasion des augets des roues Pelton a été quantifiée par des mesurages détaillés. Pour quantifier l'effet de l'abrasion sur les rendements hydrauliques, une méthode de surveillance a été développée en prenant compte de ne pas entraver l'exploitation. La surveillance des rendements sert de base pour juger la rentabilité des travaux de maintenance (meulage et revêtement sur site) et des investissements de remplacement.

1. Einleitung

Dieser Artikel bezieht sich auf die am 30. September 2015 an der Hochschule Luzern während der Tagung «Schwebstoffe, hydro-abrasiver Verschleiss und Wirkungsgradänderungen an Peltonturbinen» in Horw gehaltenen Präsentationen.

1.1 Hydro-abrasiver Verschleiss

Eine beträchtliche Anzahl hydroelektrischer Anlagen im Alpenraum und weltweit (vor allem im Himalaya und in den Anden) sind jahreszeit– aber auch ereignisabhängig mit stark schwebstoffhaltigem Wasser belastet. Die betroffenen Wasserkraftanlagen befinden sich meist unterhalb von Einzugsgebieten mit aktueller oder ehemaliger, starker Vergletscherung. Sie weisen keinen grösseren Stauraum auf, oder es werden Gebirgsbäche direkt in das Triebwassersystem eingeleitet.

Hohes Schwebstoffaufkommen wird durch Schnee- und Gletscherschmelze, Starkniederschläge *(Bild 1)* oder auch durch die Speicherbewirtschaftung (z. B. bei gezieltem Turbinieren von schwebstoffhaltigem Wasser) verursacht. Die Turbinen und Pumpen betroffener Wasserkraftanlagen sind hydro-abrasivem Verschleiss («Silt- oder Sandabrasion») ausgesetzt. Abhilfe wird teilweise mit Entsandern (z.B. *Ortmanns* 2006) und Beschichtung der Maschinenteile (z. B. *Gummer* 2009) gefunden. Die Abscheidung der kleineren Partikel (Silt und Feinsand) ist jedoch oft nicht mit wirtschaftlich vertretbarem Aufwand möglich. Auch bei kleinen Partikeln treten bei hohen Fliessgeschwindigkeiten und starken Umlenkungen der Strömung rasch Abrasionsschäden an wasserberührten Turbinen- oder Pumpenbauteilen auf. Dies trifft auch bei beschichteten Oberflächen *(Bild 2)* zu. Der hydro-abrasive Verschleiss ist von folgenden Faktoren abhängig (*Winkler et al*. 2011, *IEC 62364* 2013):

Partikel
- Konzentration (Suspended Sediment Concentration, SSC)
- Grösse (Particle Size Distribution, PSD)
- Form
- Härte

Turbine und Strömung
- Turbinentyp, Bauteil
- Geometrie, Strömungsmuster

- Relativgeschwindigkeit
- Härte der Beschichtung und des Grundmaterials

Gemäss Erfahrung und in der Literatur beschriebenen Berechnungsansätzen (z. B. Sulzer Hydro 1996 in DWA 2006, *Winkler et al*. 2010) nimmt der hydro-abrasive Verschleiss in Funktion der Relativgeschwindigkeit der Partikel gegenüber den bewegten Turbinenteilen stark zu (v^2 bis v^4). Bei grossen Nettofallhöhen H_N und den damit verbundenen hohen Strömungsgeschwindigkeiten bei Peltonturbinen ($v \approx [2gH_N]^{0.5}$) ist mit grösseren Abrasionsschäden zu rechnen (z. B. *Bajracharya et al*. 2008). Aufgrund des Rückgangs der Gletscher und des Permafrosts gelangen von unbewachsenen Flächen tendenziell mehr Sedimente in Fliessgewässer. Mit zusätzlichen ökologischen Bestimmungen (z. B. betreffend Stauraumspülungen) rücken die Thematik des hydro-abrasiven Verschleisses und der Umgang mit Feinsedimenten weiter in den Vordergrund.

1.2 Auswirkungen des hydro-abrasiven Verschleisses

Durch die Abrasion der Turbinenteile weicht deren Geometrie zunehmend vom ursprünglichen hydraulischen Profil ab. Dies führt zu einer Verschlechterung der Strömungsbedingungen und zu einer Wirkungsgradabnahme (*Cateni et al*. 2008). Bei unbeschichteten Peltonturbinen werden die Mittelschneiden stumpf und die Becherinnenseite wellig; die bewirkte Wirkungsgradreduktion nach einer Schwebstoffsaison kann mehrere Prozente betragen (*Strübin* und *Bussy* 1988, *Thomann* 1988). Bei beschichteten Peltonturbinen treten grosse Wirkungsgradreduktionen erst auf, wenn die Beschichtung mindestens lokal abgetragen ist und das Grundmaterial erodiert wird. Von besonderer Bedeutung für die Wirkungsgradreduktion sind die Geometrie der Mittelschneiden und der Bechereintrittskanten. Aus der Literatur (*Brekke et al*. 2002, *Maldet* 2008) ist bekannt, dass der Wirkungsgrad um einige Prozent abfallen kann, wenn die Mittelschneidenbreite einige Prozent der Becherbreite erreicht. Die Mittelschneidenbreite wird in der Praxis oft als Indikator für die Abnutzung verwendet (*Boes* 2010). Die Mittelschneidenbreite ist aber nicht die einzige relevante Grösse für die Beschreibung des Verschleisses und seiner Auswirkungen. Die Wirkungsgradreduktion kann auch mit einer Vertiefung der Becherausschnitte in Verbindung gebracht werden (*Hassler* und *Schnablegger* 2006). Hydro-abrasiver Verschleiss kann beträchtliche Kosten für die Instandhaltung und den Ersatz von Turbinenbauteilen verursachen. Weiter können Laufradwechsel zu Produktionsausfällen führen, wenn diese während der Volllastzeit durchgeführt werden müssen. Liegt für das KW Fieschertal (64 MW, 144 GWh/a) beispielsweise eine Wirkungsgradabnahme von 1 % vor, beträgt die Minderproduktion ca. 1 GWh/a, was dem Jahresverbrauch von ca. 200 typischen Schweizer Haushalten entspricht. *Kalberer* (1988) schätzte die Produktionsverluste infolge Wirkungsgradreduktion bei Peltonanlagen im zeitlichen Mittel auf 0.5 %. Dies ergab bei einer wohl noch heute annähernd gültigen Produktionserwartung mit Peltonturbinen von 13 TWh/a in der Schweiz Produktionsverluste von 65 GWh/a.

1.3 Notwendigkeit kontinuierlicher Messmethoden

Wenn Laufräder beschichtet und in der Formgebung speziell für hohe Schwebstoffbelastung ausgelegt werden, ist meistens eine Wirkungsgradeinbusse in Kauf zu nehmen. Der Unterschied in der Wirtschaftlichkeit zwischen der verlängerten Einsatzzeit gegenüber dem Produktionsverlust infolge der Wirkungsgradeinbusse muss für jede Anlage individuell betrachtet werden. Diese Beurteilung der Wirtschaftlichkeit sollte aber nicht nur statisch vor der Errichtung einer neuen Anlage oder bei einer grösseren Revision (Laufradersatz) durchgeführt werden, sondern basierend auf Messdaten fortlaufend erfolgen.

Für ein wirksames Monitoring sind kontinuierliche Messmethoden erforderlich. Diese sollten insbesondere die Schwebstoffkonzentration und den Turbinenwirkungsgrad erfassen, welche die wichtigsten Einfluss- und Auswirkungsgrössen des hydro-abrasiven Verschleisses sind. Gemäss Laboruntersuchungen (*Sulzer Hydro* 1996 in DWA 2006, *Winkler et al*. 2011) verursachen gröbere Partikel bei gleicher Schwebstoffkonzentration (SSC) mehr Abrasion als feine Partikel. Deshalb ist zu empfehlen, bei umfassenden Monitorings ebenfalls die Partikelgrössenverteilung (PSD) zu messen. Dabei sollten Messwerte mindestens minütlich erfasst werden, da starke Schwebstoffereignisse zu raschen Anstiegen in der SSC führen können.

1.4 Ausgangslage und Forschungsprojekt

Das Problem des hydro-abrasiven Verschleisses ist qualitativ bekannt und es bestehen gewisse Berechnungsansätze zur Abschätzung des Materialabtrags an unbeschichteten Turbinenbauteilen (*Sulzer Hydro* 1996 in DWA 2006). Es sind aber praktisch keine vollständigen Prototyp-Messdatensätze bezüglich Schwebstoffbelastung, Abrasion und Wirkungsgradänderungen verfügbar. Physikalische Modellversuche zu Abrasion (*Grein* und *Krause* 1994, *Winkler et al*. 2011) tragen zur Verbesserung des Prozessverständnisses und der Grundlagenkenntnisse bei; aus Gründen der Durchführbarkeit weichen aber die Strömungsverhältnisse zum Teil stark von Prototyp-Bedingungen ab (Massstabseffekte). Es besteht also Bedarf an Messsystemen,

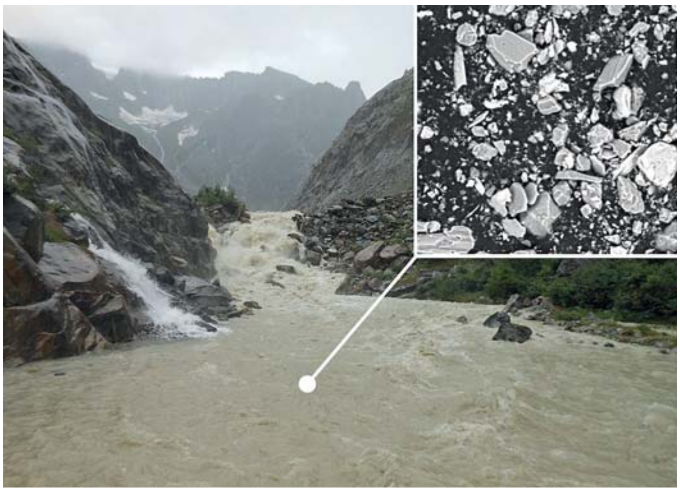

Bild 1. Stark schwebstoffhaltiger Gebirgsfluss Wysswasser am 08. August 2013 wenig oberhalb der Wasserfassung des KW Fieschertal und Mikroskopbild der Partikel (Fotos: VAW).

Bild 2. Hydro-abrasiver Verschleiss an Laufrädern im KW Fieschertal nach einer schwebstoffreichen Saison. Die Beschichtung wird meist zuerst auf der Mittelschneide und im Ausschnitt abgetragen (Foto: VAW).

die für den Einsatz an Wasserkraftanlagen geeignet sind, um die Schwebstoffführung des Triebwassers quantifizieren zu können. Neben dem Wunsch nach verbesserten Abrasionsmodellen besteht auch ein Interesse an verbesserten Bemessungsgrundlagen für den Anlagenentwurf und -betrieb. Diese sollten für das Sedimentmanagement und den hydro-abrasiven Verschleiss unter folgenden Gesichtspunkten optimiert werden:

- Bestimmung der Bemessungskorngrösse für Entsandungsanlagen
- Auswahl von Turbinenbeschichtungen
- Auslegung der hydraulischen Maschinen in Bezug auf die Formgebung
- Prüfung der Option des gezielten Weiterleitens von Feinsedimenten in Stauseen über den Triebwasserweg
- Abschätzung eines Grenzwertes für vorübergehende Kraftwerksabschaltungen während eines kurzzeitigen, starken Schwebstoffaufkommens

Zur Verbesserung der Kenntnisse über den hydro-abrasiven Verschleiss an Hochdruckwasserkraftanlagen und geeigneter Gegenmassnahmen haben die Versuchsanstalt für Wasserbau, Hydrologie und Glaziologie (VAW) der ETH Zürich und das Kompetenzzentrum für Fluidmechanik und Hydromaschinen (CC FMHM) der Hochschule Luzern im Jahr 2011 ein Forschungsprojekt initiiert. Das Ziel des Projekts war, die Zusammenhänge zwischen Schwebstoffbelastung, Abrasion und Wirkungsgradänderungen weiter zu untersuchen. Das Projekt wurde, gemeinsam mit Industriepartnern, mit Hauptgewicht auf einer Fallstudie am KW Fieschertal durchgeführt. Im Rahmen dieses interdisziplinären Forschungsprojekts wurde unter realen Betriebsbedingungen die Schwebstoffführung des Triebwassers (SSC und PSD) mittels neuartiger Messtechnik kontinuierlich erfasst. Der Verschleiss an den Laufrädern der Peltonturbinen und die Wirkungsgradveränderungen wurden mehrfach gemessen. Der Wirkungsgrad wurde unter anderem auch kontinuierlich gemessen, um ihn der Schwebstoffführung des Triebwassers gegenüberstellen zu können.

1.5 Das Kraftwerk Fieschertal

Das KW Fieschertal (schematischer Längsschnitt in *Bild 3*) ist eine Hochdruck-Wasserkraftanlage mit Tirolerfassung am Bergbach Wysswasser, dessen Einzugsgebiet zu 57 % vergletschert ist (Stand 2009). Es ist kein Stausee vorhanden. Die Fassung wurde in den 1970er-Jahren direkt an der Zunge des Fieschergletschers gebaut. Inzwischen hat sich der Gletscher um ca. 500 m zurückgezogen, wodurch ein Gletschervorfeld entstand. Bei geringem Abfluss lagern sich Sedimente ab, welche dann bei grossem Abfluss wieder erodiert werden. Weiter fallen Sedimente in verschiedenen Korngrössen von unbewachsenen, leicht erodierbaren Hängen und vor allem von der Erosion unter dem Gletscher an. Das Wasser fliesst von der Fassung durch einen Kies- und einen Sandfang in einen 2 km langen Freispiegelstollen, der als Tagesspeicher (64 000 m^3) dient. Vom Freispiegelstollen gelangt das Triebwasser durch eine erdverlegte Druckleitung zu den zwei Maschinengruppen (MG) im Dorf Fieschertal. In der Zentrale sind zwei horizontalachsige, zweidüsige Peltonturbinen mit einer Nennleistung von je 32 MW installiert. Die Fallhöhe beträgt 509 m und der Ausbauvolumenstrom der Anlage beträgt 15 m^3/s. Im *Bild 3* sind die im Monitoring des Forschungsprojekts erfassten Informationen dargestellt. Die Farben beziehen sich auf die drei Teilbereiche des Monitorings: (i) Schwebstoffe (gelb), (ii) Verschleiss (grün) und (iii) Turbinenwirkungsgrad (rosa).

2. Messtechniken und Vorgehen

2.1 Schwebstoffmessungen

2.1.1 Gravimetrische SSC mittels Flaschenproben

Schwebstoffkonzentrationen (SSC) können am zuverlässigsten durch Wägung des getrockneten Rückstands im Labor bestimmt werden (gravimetrische Methode). Dafür sind im Feld möglichst repräsentative Proben des sedimenthaltigen Wassers zu entnehmen. Wenn Proben in regelmässigen Intervallen von beispielsweise einigen Tagen entnommen werden, werden in der Regel die SSC-Spitzen schlecht erfasst. Deshalb wurden an der Wasserfassung und in der Schieberkammer des KW Fieschertal automatische Probenehmer eingesetzt, die von Messrechnern gesteuert wurden (*Boes et al*. 2013). So konnten auch Proben zu Zeitpunkten mit erhöhter SSC gewonnen werden. Über drei Jahre wurden von 285 Flaschenproben aus der Schieberkammer die SSC gravimetrisch bestimmt. Da die gravimetrische Methode aufwendig ist und die Messresultate nicht in Echtzeit zur Verfügung stehen, sind verschiedene indirekte Methoden entwickelt worden (*Wren et al*. 2000). Im vorliegenden Forschungsprojekt wurden die folgenden fünf Methoden für das Echtzeit-Monitoring des Schwebstoffaufkommens angewendet, untersucht und weiterentwickelt.

2.1.2 SSC mittels Trübungsmessungen

Bei Trübungssonden wird die Dämpfung oder die Rückstreuung von Licht infolge der Schwebstoffe im Wasser gemessen. Viele Streulicht-Trübungssonden haben einen Messbereich von 4000 FNU (Formazine Nephelometric Unit), einige bis 9999 FNU. Trübungsmesswerte hängen von der SSC sowie der Grösse, Form und Farbe der Partikel ab (*Sutherland et al*. 2000, *Boes et al*. 2013). Die Umrechnung von Trübungsmesswerten in SSC basiert auf Korrelationen, die durch Vergleich von Trübungsmesswerten und gravimetrischen SSC ermittelt werden. Im Langzeitbetrieb sind automatische Einrichtungen für die Reinigung der Sensorenoptik erforderlich, um Messwertverfälschungen zu vermeiden und den Unterhaltsaufwand gering zu halten. Dafür können Wischer oder Druckluftreinigung eingesetzt werden.

Im Wysswasser bei der Wasserfassung des KW Fieschertal und am Ende des Entsanders wurden Eintauch-Trübungs-

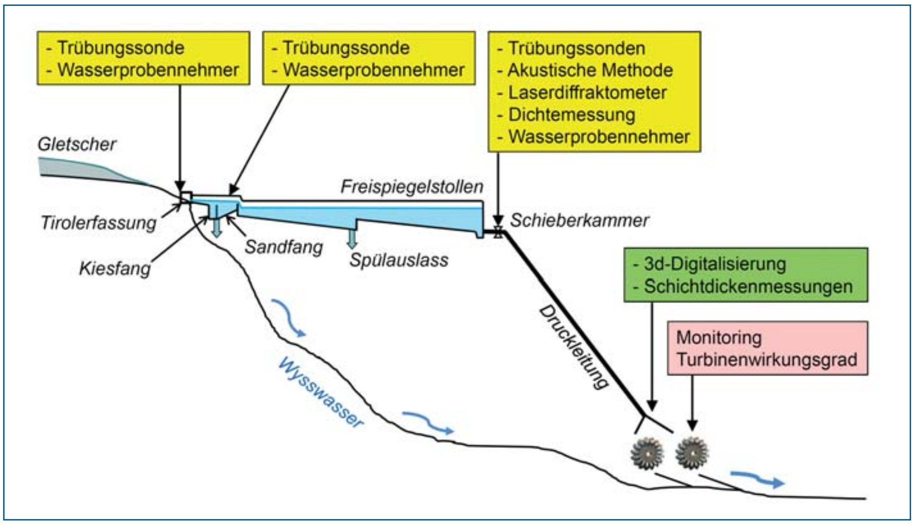

Bild 3. Schematisches Längenprofil des KW Fieschertal mit den drei Teilbereichen des Monitorings.

sonden installiert. Die Sonde im Wysswasser wurde zum Schutz vor Geschiebe und Eisstücken in einem massiven, gelochten Stahlrohr montiert. Diese Sonde hat die Aufgabe, auch aktuelle Trübungswerte zu liefern, wenn die Wasserfassung bei einem Unwetter geschlossen wird. Die Sonde im Entsander ist vor Naturgefahren besser geschützt und erhöht die Zuverlässigkeit des Schwebstoffmonitorings im Fassungsbereich (Redundanz). Von diesen Trübungssonden können hohe SSC aufgrund der Fliesszeit des Wassers im Triebwassersystem mit einer Vorwarnzeit von einer Stunde erkannt werden. In der Schieberkammer des KW Fieschertal wurden versuchsweise drei Trübungssonden an einer Probeentnahmeleitung installiert, die von der Druckleitung gespeist wird *(Bild 4)*. Bei zwei dieser Sonden wird die Trübung an der leicht unter Druck stehenden Entnahmeleitung gemessen, bei der dritten an einem frei fallenden Wasserstrahl am Austritt einer kleinen abzweigenden Leitung. Die Bauweise dieser Trübungssonde hat den Vorteil, dass keine Reinigung erforderlich ist, weil die Sensorenoptik nicht mit schwebstoffhaltigem Wasser in Kontakt kommt.

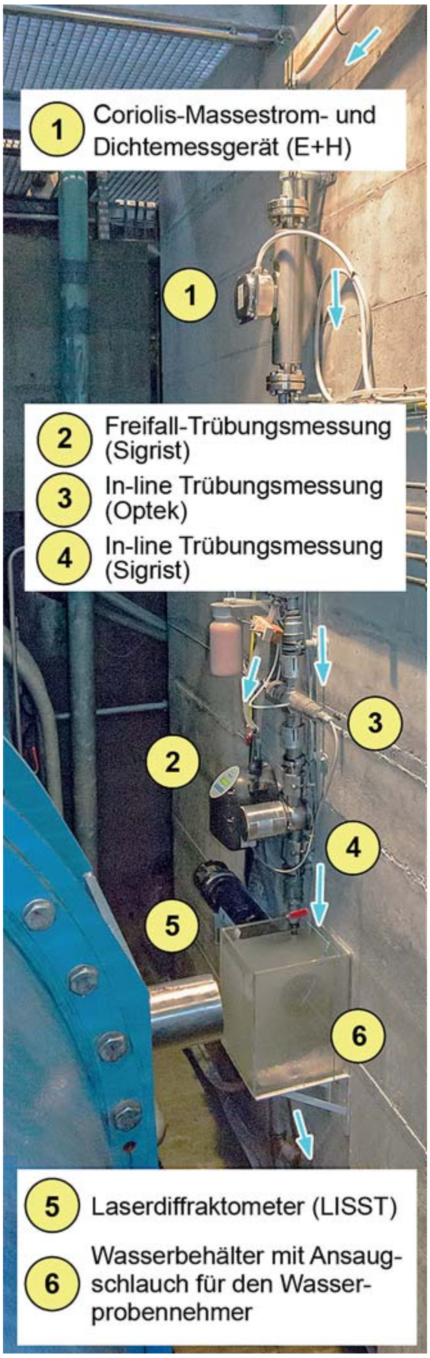

Bild 4. Schwebstoffmessgeräte in der Schieberkammer des KW Fieschertal (Foto: VAW).

2.1.3 SSC mittels akustischer Methode

Akustische Signale im Ultraschallbereich können auf verschiedene Arten für das Schwebstoffmonitoring genutzt werden (Stichworte: forward und/oder backscatter sowie multi-frequency). In diesem Projekt wurde eine akustische Methode eingesetzt, mit der das Schwebstoffaufkommen in einer Druckleitung ohne zusätzliche Sensoren überwacht werden kann, da unterstrom der Schieberkammer eine akustische Durchflussmessung (ADM) installiert ist (vier Pfade, $d_i = 1.95$ m, 1 MHz). Bei einer ADM werden Ultraschallpulse von einer Rohrwand zur anderen gesendet. Wenn das Wasser Schwebstoffe enthält, wird das empfangene Signal abgeschwächt. Das Ausmass dieser Dämpfung hängt – ähnlich wie bei Trübungsmessungen – von der SSC und der Partikelsorte ab *(Bild 5)*. Dies wurde vor den Messungen im KW Fieschertal mittels Versuchen im hydraulischen Labor an der Hochschule Luzern in Horw untersucht (*Costa et al*. 2012, *Boes et al*. 2013). Die im KW Fieschertal gemessenen Dämpfungen wurden wie bei den Trübungssonden mit den gravimetrischen SSC korreliert. Im Bereich höherer SSC wurden für die Korrelation auch Daten der im Folgenden erläuterten CMD- und der Druckmessmethode beigezogen. So wurden die über die Zeit gemittelten Eigenschaften der am Einsatzort vorhandenen Partikel berücksichtigt. Um die ADM für das Schwebstoffmonitoring nutzen zu können, war es mit dem verwendeten Modell (Rittmeyer Risonic) lediglich erforderlich, die Amplituden der empfangenen Ultraschallpulse auf dem Gerät als zusätzliche digitale Ausgangssignale zu definieren und diese dem Messcomputer zuzuführen.

2.1.4 SSC mittels Dichtemessung mit Coriolis-Messgerät

Die SSC kann auch mit einem Coriolis Massestrom- und Dichtemessgerät (CMD) indirekt gemessen werden (*Bishwakarma* und *Støle* 2008). Ein solches Gerät wurde ebenfalls in die Probenahmeleitung eingebaut *(Bild 4)*. Im verwendeten Gerät sind zwei parallele, gebogene Rohre vorhanden, die elektronisch gesteuert, zu feinen Schwingungen angeregt werden. In einem CMD wird der Coriolis-Effekt genutzt, um den Massestrom zu bestimmen. Die Dichte der Flüssigkeit wird über die Veränderung der Eigenfrequenz der durchflossenen Rohrbögen bestimmt. Gemäss Spezifikation des verwendeten CMDs kann die Dichte auf 0.5 g/l genau gemessen werden. Für die Umrechnung von der gemessenen Gemischdichte auf die SSC müssen die Dichte des Klarwassers und die Dichte des Partikelmaterials bekannt sein.

Die Dichte des Klarwassers wurde aufgrund von Literaturwerten und der Wassertemperatur, die ebenfalls im CMD gemessen wird, berechnet. Die Dichte des Partikelmaterials wurde im Labor des Geo-

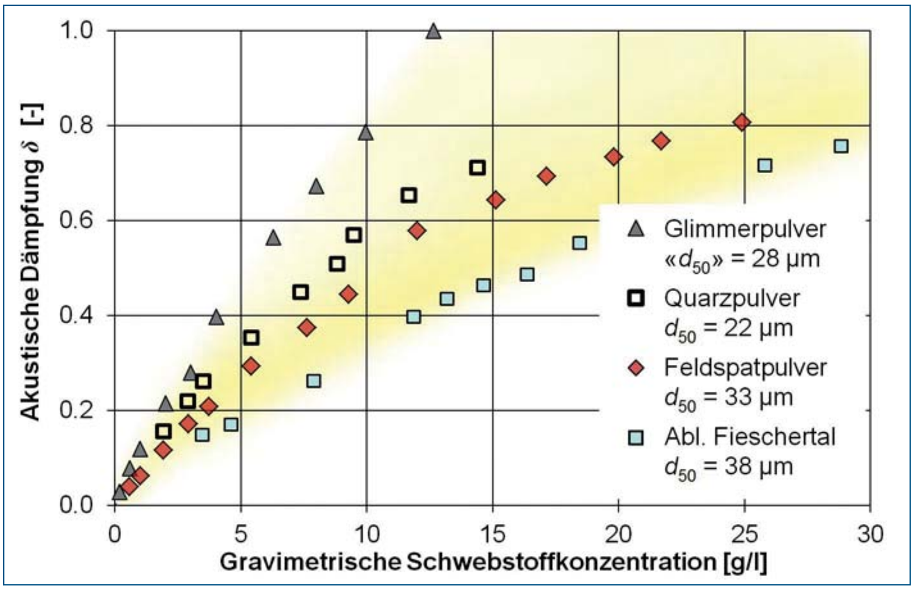

Bild 5. Dämpfung der Ultraschallsignale in Abhängigkeit der SSC für verschiedene Partikelsorten mit unterschiedlichen mittleren Durchmessern.

technischen Instituts der ETH Zürich an einigen getrockneten Proben mit einem Pyknometer bestimmt (ρ_s= 2730 kg/m^3) und als konstant angenommen. Bei der Berechnung der SSC wurde weiter ein periodischer Dichteabgleich berücksichtigt (< 0.6 g/l). Der Dichteabgleich trägt unter anderem der Konzentration gelöster Stoffe Rechnung und kompensiert die saisonal aufgetretene leichte Biofilmbildung in den Messrohren.

2.1.5 SSC und PSD mittels Laserdiffraktometrie

Laserdiffraktometer werden seit einigen Jahrzehnten in Labors für die Messung von Partikelgrössenverteilungen (PSD) verwendet. Seit dem Jahr 2000 sind auch tragbare bzw. eintauchbare Geräte für Messungen vor Ort unter dem Namen «Laser in-situ Scattering and Transmissiometry» (LISST) erhältlich (*Agrawal* und *Pottsmith* 2000), mit welchen sowohl die PSD als auch die Konzentration gemessen werden können. In LISST-Geräten werden die Streuung bzw. Beugung (diffraction) und die Dämpfung von Laserlicht gemessen, die von den Partikeln verursacht werden. Mit der mitgelieferten Software werden die Volumenkonzentration der Partikel in 32 logarithmisch verteilten Grössenklassen (nominal von 2 bis 380 µm) berechnet (*Agrawal et al*. 2008). Daraus können die PSD und die totale Volumenkonzentration ermittelt werden. Die Volumenkonzentrationen wurden mit den Laborresultaten der Flaschenproben auf Massekonzentrationen (SSC) umgerechnet. Mit diesem Vorgehen werden Effekte der Partikelform und allfälliger Flockenbildung auf die SSC berücksichtigt (*Felix et al.* 2013b). Mit LISST können also die SSC und die PSD im Minutentakt vor Ort gemessen werden. In früheren Studien wurden PSD-Messungen aus Kostengründen nur an wenigen Flaschenproben im Labor durchgeführt. Im Gegensatz zu Trübungssonden und der erwähnten akustischen Methode werden beim LISST die aktuellen Partikelgrössen für die Berechnung der SSC berücksichtigt.

In der Schieberkammer des KW Fieschertal wurde ein vielseitig einsetzbares, wasserdichtes LISST-Modell (LISST-100X) verwendet. Bei diesem Modell wird der Laserstrahl standardmässig auf einer Strecke von 50 mm durch die Wasserprobe gesendet. Um den Bereich messbarer SSC zu erhöhen, wurde die optische Pfadlänge durch Einsetzen des stärksten erhältlichen Pfadreduktionsmoduls (Glaskörper) auf 5 mm reduziert. Das LISST-Gerät wurde in der Schieberkammer des KW Fieschertal so montiert, dass dessen Messkopf seitwärts in einen spülbaren Behälter mit Überlauf ragte (*Bild 4*). Der optische Pfad des Geräts befand sich unmittelbar unter dem Auslauf der Probenahmeleitung.

2.1.6 SSC mittels Druckmessungen

Eine weitere Möglichkeit für die Überwachung der SSC im Triebwasser von Hoch- und Mitteldruckwasserkraftanlagen besteht in der Auswertung von statischen Druckmessungen. Wenn das Triebwasser viel Schwebstoffe enthält, sind die Gemischdichte und somit der Druck am unteren Ende der Druckleitung grösser als bei Klarwasserverhältnissen. Am KW Fieschertal werden u. a. der Oberwasserpegel, der Volumenstrom in der Druckleitung und die Drücke jeweils vor den Turbinen gemessen. Aus den Messdaten in stationären Klarwasserverhältnissen konnten die Druckverluste zwischen dem Oberwasserpegel und den Druckmessstellen in der Zentrale für verschiedene Betriebszustände in Funktion des Volumenstroms berechnet werden. Mit diesen Kennlinien sowie mit aktuellen Druck-, Pegel- und Volumenstromdaten konnte die Dichte des schwebstoffhaltigen Wassers in der Druckleitung in stationären Zuständen berechnet werden. Schliesslich wurde von der Gemischdichte, wie im Abschnitt 2.1.4 erwähnt, auf die SSC umgerechnet. Die mit dieser Methode ermittelte SSC bezieht sich im Gegensatz zu den anderen Methoden nicht auf eine Punkt- oder Querschnittsmessung, sondern auf den ganzen Inhalt der Druckleitung. Ein Vorteil dieser Methode ist, dass höhere SSC ohne zusätzliche Sensoren gemessen werden können. Ein Nachteil ist, dass keine Vorwarnzeit für allfällige Turbinenabschaltungen vorhanden ist.

Zu den Schwebstoffmessungen ist generell anzumerken, dass die Messunsicherheiten im Vergleich zu anderen Fachgebieten relativ hoch sind. Bei in-situ SSC- und PSD-Messungen gelten derzeit Messunsicherheiten von ± 20 % als realistisch.

2.2 Verschleissmessungen

Die Abrasion an den Bechern der Peltonlaufräder des KW Fieschertal wurde mit den folgenden zwei Methoden im Turbinengehäuse gemessen:

2.2.1 Beschichtungsdicke

Die lokalen Beschichtungsdicken wurden mit einem Schichtdickenmessgerät und Schablonen *(Bild 6)* gemessen. Letztere dienten zur Definition der Lage der Messpunkte innerhalb des Bechers und zum Wiederauffinden der Punkte bei Folgemessungen. Das Schichtdickenmessgerät (Deltascope FMP30 der Helmut Fischer AG mit Zweipolsonde V7FKB4) beruht auf dem Prinzip der magnetischen Induktion und wurde in Bezug auf das vorhandene Grundmaterial wie folgt kalibriert: An einer unbeschichteten, möglichst ebenen und glatten Stelle eines Bechers wurde der Nullpunkt eingestellt. Dann wurde eine Kunststofffolie bekannter Dicke aufgelegt und der zweite Kalibrierpunkt gemessen. Die Abnutzung der Sondenpole wurde kompensiert.

Für die rechte und die linke Becherhälfte wurden je eine Schablone aus Pappmaché durch Abformen an einem Becher erstellt. Beim wiederholten Einsetzen der Schablonen in die Becher der verschiedenen Laufräder mit unterschiedlicher Revisionsgeschichte wurde beobachtet, dass die Lage der Messpunkte auf ca. ±5 mm genau definiert ist. In jeder Messkampagne wurde die Schichtdicke an jedem Messpunkt n = 10 Mal gemessen. Die erweiterte Messunsicherheit (95 %-Vertrauensintervall) des Mittelwerts von n = 10 Schichtdickenmessungen an einem Messpunkt betrug bei der Hälfte der Messungen weniger als 2.5 µm und bei allen als gültig eingestuften Messwerten weniger als 5 µm. Bei einer nominalen Beschichtungsdicke von 300 µm entspricht dies einer relativen Abweichung von 0.8 % bzw. 1.6 %. Aufgrund der Auswertungen wurde weiter abgeschätzt, dass die Reproduzierbarkeit einer über einen Becher gemittelten Schichtdickendifferenz besser als ±5 µm ist.

2.2.2 3D-Digitalisierung

Für die wiederholte Vermessung der aktuellen Geometrie der durch Abrasion beanspruchten Becher wurde ein optischer 3D-Scanner (Comet L3D 5M von Steinbichler bzw. Carl Zeiss Optotechnik) im Turbinen-

Bild 6. Anwendung einer Schablone für die Messung der Schichtdicken in einem Peltonbecher in der Zentrale des KW Fieschertal (Foto: VAW).

gehäuse eingesetzt. Das Messsystem hat eine Auflösung von 5 Mio. Punkten pro Aufnahme. Mit einem Messvolumen von 480 × 400 × 250 mm beträgt der Abstand der Messpunkte auf der Objektoberfläche im Mittel 190 µm. Das System basiert auf den Methoden der Streifenlichtprojektion und der räumlichen Triangulation. Der Projektor und die Kamera sind in einem Gerät kombiniert, das auf einem Stativ frei platziert wird *(Bild 7)*. Das Messsystem wurde im Werk kalibriert. Die Abweichungen zum Soll und zwischen zwei Validierungsmessungen betrugen lediglich ca. 10 µm; Abweichungen bis 40 µm werden vom Hersteller als zulässig erachtet. Nach dem Transport des optischen Messsystems zur Kraftwerksanlage wurde jeweils die Kalibrierung des Messsystems mit einer Referenzplatte überprüft.

Zur Reduktion von Lichtspiegelungen wurden die zu vermessenden Becher vor dem Digitalisieren mit einer weissen Substanz eingesprüht (Entwicklerspray). Dann wurden Markierpunkte, die zum Zusammenfügen mehrerer Einzelaufnahmen dienen, in einem unregelmässigen Muster aufgeklebt. Aufgrund der gegebenen geometrischen Verhältnisse (Sichteinschränkungen durch benachbarte Becher bzw. durch Becherrand und Mittelschneide) und der Grösse der Peltonbecher im vorliegenden Fall (Becherbreite ≈ 65 cm) kann ein Becher nicht mit einer einzelnen Aufnahme vermessen werden, sondern es sind pro Becher ca. 75 Aufnahmen aus verschiedenen Blickwinkeln und geeigneter Distanz erforderlich. Die Einzelaufnahmen werden mithilfe der Markierpunkte und aufgrund der Oberflächengeometrie zu einem Gesamtmodell zusammengefügt (sogenanntes

Bild 7. 3D-Digitalisierung im Turbinengehäuse des KW Fieschertal. Das optische Messgerät ist auf einem fahrbaren Stativ aufgebaut (Foto: HSLU).

Matching). Es wurde ein Vorgehen entwickelt, mit welchem die Teilaufnahmen, beginnend von der Becheraussenseite, möglichst gut zusammengefügt werden können.

Die konsolidierten geometrischen Modelle der Oberflächengeometrien (3D-Punktewolken) wurden nachträglich auf dem Bildschirm an Referenzflächen ausgerichtet, um die zu verschiedenen Zeitpunkten aufgenommenen Geometriemodelle zu vergleichen. Als Referenzflächen wurden der Becherrand und die seitlichen Partien der Becherausschnitte verwendet, da diese eben und nicht von hydro-abrasivem Verschleiss betroffen sind. Aus den 3D-Modellen wurden diverse Schnitte erzeugt, in welchen unter anderem die Mittelschneidenbreite bestimmt wurde. Um diese Breite auch bei gerundeten oder unregelmässig abgetragenen Mittelschneiden zu bestimmen, wurden die Tangentensteigungen an den Schneidenseiten bestimmt. Durch den Vergleich der geometrischen Modelle beziehungsweise der Schnitte, die zu verschiedenen Zeitpunkten aufgenommen worden waren, wurden folgende Grössen bestimmt (*Abgottspon et al*. 2013):

- Abnahme der Mittelschneidenhöhe
- Zunahme der Mittelschneidenbreite
- Zunahme der Becherausschnittstiefe
- Volumenabnahme an den Mittelschneiden
- Volumenabnahme im Bereich der Becherausschnitte

Die Volumenunterschiede wurden mit einer Dichte von 7.7 g/cm^3 für das übliche Turbinengrundmaterial in einen Masseverlust umgerechnet. Die Reproduzierbarkeit der ermittelten geometrischen Differenzen wurde untersucht, indem jeweils zwei Geometriemodelle, die in Perioden mit vernachlässigbarer Schwebstoffbelastung aufgenommen worden waren, verglichen wurden. Die Abweichungen betrugen oft weniger als ±0.3 mm, in einem Fall bis ±0.7 mm auf der Innenseite einer Becheraussenwand. Es wurde festgestellt, dass in diesem Bereich und im Bechergrund die Messunsicherheit grösser ist als an den übrigen Partien des Bechers, vermutlich wegen ungünstigeren Bedingungen bei den Aufnahmen (Sichtverhältnisse) und beim Zusammenfügen der Aufnahmen (Anschlusspunkte und Überlappungsflächen). In der vorliegenden Anwendung ist die Geometrie im Bereich der Mittelschneiden und der Bechereintrittskanten relevant. In diesen Bereichen eines Peltonbechers in der untersuchten Grösse wird die Reproduzierbarkeit auf ±0.2 mm geschätzt. Bei einer Abtragstiefe von beispielsweise 1 mm beträgt der relative Fehler 20 %. Für kleinere Peltonbecher oder Teilbereiche von grösseren Bechern, die mit einer oder wenigen Einzelaufnahmen erfasst werden können, ist die Messunsicherheit geringer und dürfte gegen ±0.01 bis ±0.04 mm tendieren.

2.3 Wirkungsgradmonitoring

Um die Änderungen der Wirkungsgrade der beiden Turbinen im Lauf der Zeit zu bestimmen, wurden einerseits regelmässig Indexwirkungsgradmessungen mit dem sog. Sliding-Needle-Verfahren durchgeführt und andererseits eine Auswertemethode für ein kontinuierliches Wirkungsgradmonitoring entwickelt.

2.3.1 Sliding-Needle-Messungen

Mit Indexwirkungsgradmessungen werden Vergleichsmessungen durchgeführt. Diese dienen dazu, Wirkungsgradunterschiede zwischen zwei Messkampagnen quantitativ zu bestimmen. Die absoluten Wirkungsgradunterschiede werden bezüglich einer gleichbleibenden Referenzmessung ausgewiesen. Die periodisch wiederholte Bestimmung von Indexwirkungsgraden erlaubt, den Wirkungsgradverlauf einer Turbine über die Zeit zu überwachen (Wirkungsgradhistorie). Für Indexwirkungsgradmessungen sind langzeitstabile Messwertaufnehmer erforderlich, und die Messung des Volumenstromes ist von zentraler Bedeutung. Dabei ist nicht die Messunsicherheit, sondern die Reproduzierbarkeit relevant. Akustische oder magnetisch-induktive Volumenstrommessungen sind besonders geeignet, da das anspruchsvolle Spülen von Druckaufnehmern, beispielsweise bei Venturi-Messungen, nicht erforderlich ist.

Das Sliding-Needle-Verfahren erlaubt, während möglichst kurzer Zeit (etwa 1 Stunde) den Wirkungsgrad einer Peltonturbine über ihren relevanten Betriebsbereich aufzunehmen. Bei Francis- und Kaplanturbinen wird das entsprechende Messverfahren als Sliding Gate bezeichnet; es wurde erstmals von *Almquist et al*. (1995) erwähnt. Eine Übersicht zu diesem Messverfahren ist in *Abgottspon* und *Staubli* (2008) aufgeführt. Grundsätzlich wird das Stellorgan (Düse oder Leitapparat) bei quasi-stationären Bedingungen kontinuierlich geöffnet und wieder geschlossen *(Bild 8)*. Es werden alle Messgrössen, die für die Wirkungsgradberechnung relevant sind, mit einer Abtastrate von 1 Hz gespeichert. Klassische Indexwirkungsgradmessungen beinhalten im Gegensatz zu den Sliding-Needle- oder -Gate-Messungen eine Reihe von Messpunkten von Teil- bis Überlast, während deren Erfassung die Betriebsbedingungen konstant gehalten werden. Aus den während einer Sliding-Needle-Messung aufgezeichneten

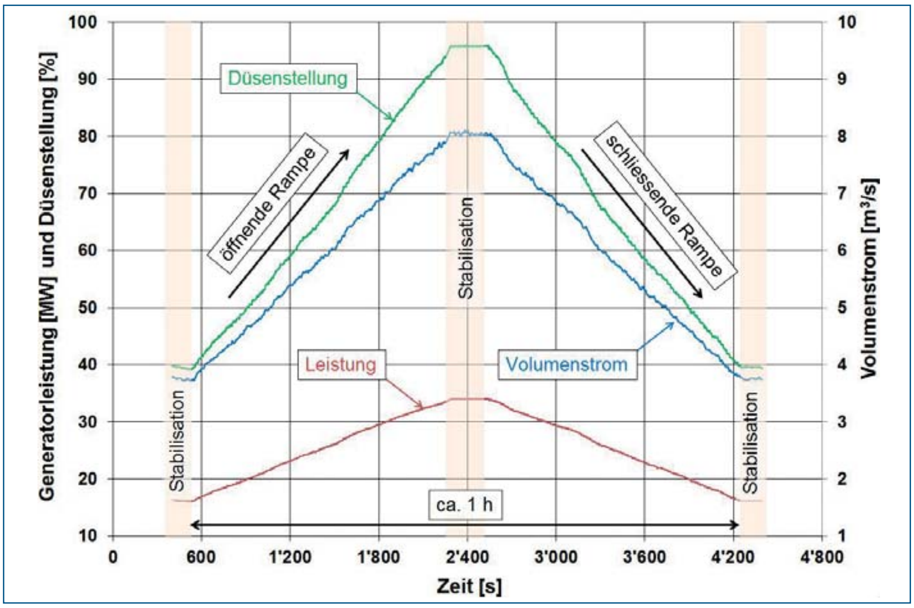

Bild 8. Ganglinien einiger aufgezeichneter Signale während eines Sliding-Needle-Tests.

Daten kann der Wirkungsgrad in Funktion der Leistung berechnet werden. Für jedes Messdatum wurde daraus ein gewichteter Indexwirkungsgrad berechnet und die gewichteten Indexwirkungsgrade in Funktion der Zeit aufgetragen (Wirkungsgradhistorie).

2.3.2 Kontinuierliches Wirkungsgradmonitoring

Für einen optimierten Betrieb einer stark von hydro-abrasivem Verschleiss betroffenen Anlage ist es wichtig, den Verlauf der Wirkungsgradreduktion mit einer guten zeitlichen Auflösung zu kennen. Obwohl das Sliding-Needle- bzw. -Gate-Messverfahren darauf optimiert wurde, den normalen Anlagenbetrieb möglichst wenig zu beeinträchtigen (Messdauer etwa 1 Stunde), ist es insbesondere in der Volllastzeit in der Praxis oft nicht gut möglich, z. B. monatliche Indexwirkungsgradmessungen durchzuführen. Daher wurde eine Methode für ein kontinuierliches Wirkungsgradmonitoring entwickelt, welche Daten mit einer hohen zeitlichen Auflösung liefert. Dafür werden die Messdaten idealerweise direkt von den Signalwandlern mit einer Abtastrate von 1 Hz von einem Messrechner gespeichert. Zu jedem Zeitpunkt wird ein Indexwirkungsgrad und bei der Tagesauswertung eine gewichtete Wirkungsgraddifferenz zu einer gleichbleibenden Referenzkurve berechnet. Die Wirkungsgraddifferenzen werden dann in der Wirkungsgradhistorie dargestellt. Beim jetzigen Entwicklungstand der Methode ist es möglich, den Indexwirkungsgrad im Einmaschinenbetrieb auszuwerten. Der Grund hierfür liegt darin, dass beim KW Fieschertal die zuverlässigste Volumenstrommessung in der Druckleitung, oberhalb der Aufteilung auf die einzelnen Turbinen, installiert ist. Im Zweimaschinenbetrieb kann die Aufteilung des Volumenstroms auf die einzelnen MG nicht genügend genau berechnet werden (erforderliche Unsicherheit kleiner 0.2 %).

Das kontinuierliche Wirkungsgradmonitoring erfordert anspruchsvolle Signalverarbeitung und Plausibilitätsüberprüfungen zwischen den Signalen in Echtzeit. Um die Messwerte und die Langzeitstabilität der Messwertaufnehmer zu kontrollieren, wurde ein System von Kontrollen, ähnlich eines Expertensystems, aufgebaut. Dabei werden unter anderem die vor den Turbinen gemessenen Drücke mit der Oberwasserpegelmessung unter Berücksichtigung der hydraulischen Verluste in der Triebwasserleitung verglichen. Weiter werden z. B. die Volumenstrommessungen am oberen und am unteren Ende der Druckleitung miteinander verglichen und die Abweichungen ebenfalls kontinuierlich analysiert.

3. Resultate der Schwebstoffmessungen

3.1 Allgemeine Partikeleigenschaften

Wie erwähnt, beträgt die Dichte des Partikelmaterials im Triebwasser des KW Fieschertal im Mittel 2730 kg/m^3. Gemäss weiteren Laboruntersuchungen an einigen getrockneten Proben mit der Rietveld-Röntgenbeugungsanalyse besteht die Partikelmasse zu 65–80 % aus Mineralien mit einer Mohshärte $\geq$ 6 (Quarz, Feldspat und Epidot), welche mindestens so hart sind wie das Turbinengrundmaterial. Der Rest sind weichere Mineralien (Mohshärte $\leq$ 3), vorwiegend Glimmer (Muskovit und Biotit). Die mineralogische Zusammensetzung der Partikel in Fieschertal ist mit anderen Anlagen im Wallis vergleichbar (vgl. *Ortmanns* 2006). Gemäss Mikroskopbildern *(Bild 1)* sind die Partikel vorwiegend kantig, einige sind plättchenförmig (Glimmer).

3.2 Verhalten der Schwebstoffmessgeräte allgemein

Die mit den verschiedenen Methoden ermittelten SSC-Ganglinien wurden miteinander verglichen, um Erkenntnisse über das Verhalten der Messgeräte unter verschiedenen Bedingungen zu gewinnen. In *Bild 9* ist ein Ausschnitt der Ganglinien während zweieinhalb Sommertagen dargestellt. Weiter ist der Medianpartikeldurchmesser d_{50} dargestellt, d. h. der Durchmesser, der von 50 % der Partikelmasse nicht überschritten wird.

Meist lagen die SSC unter 2 g/l, die Partikel waren relativ klein ($d_{50} \approx$ 15 µm) und die verschiedenen Messmethoden lieferten ähnliche SSC. In Perioden mit höheren SSC wurden tendenziell gröbere Partikel transportiert. Es wurde jedoch nur eine geringe Korrelation zwischen SSC und PSD festgestellt (*Felix et al*. 2013a). Dies kann von dynamischen Prozessen wie dem Abflussgeschehen im Einzugsgebiet und unter dem Gletscher herrühren. Weiter variiert die Strömung im Speicherstollen, weshalb es Änderungen der PSD infolge Absetzen und Resuspension von Schwebstoffpartikeln gibt. In Perioden höherer SSC wichen die SSC der verschiedenen Messmethoden bei einigen Ereignissen deutlich voneinander ab. Die SSC der CMD-Methode stimmte auch bei mehreren g/l gut mit den gravimetrischen Referenz-SSC überein; ähnlich wie die SSC des LISST (sofern vorhanden). Die Trübungssonden und die verwendete akustische Methode unterschätzten im Schwebstofftransportereignis von *Bild 9* die SSC, weil gröbere Partikel vorhanden waren als bei dieser SCC im zeitlichen Mittel üblich. Wie in den Abschnitten 2.1.2 und 2.1.3 erwähnt sowie in den *Bildern 5* und *10* ersichtlich, werden die SSCs von Trübungssonden und der akustische Methode von Veränderungen der Partikelgrösse beeinflusst. In Ereignissen, in denen die Partikelgrösse nicht mit der SSC korreliert, weisen diese beiden Methoden eine erhöhte Messunsicherheit auf. Umgekehrt kann die Tatsache, dass SSC von Trübungsmessungen und der akustischen Methode von der Partikelgrösse abhängen, in Kombination mit einem CMD genutzt werden, um ohne permanenten Einsatz eines LISST mittlere Grössen von aktuell vorhandenen Partikeln zu ermitteln.

Das LISST ermöglichte, SSC bis zu einigen g/l von vorwiegend Grobsilt (20–63 µm) zu messen; bei höheren SSC war das Wasser zu trübe. Die obere Grenze des SSC-Messbereichs hängt stark von der Partikelgrösse und der Partikelform ab. Die Messbereichsgrenze liegt tiefer, wenn feine und deutlich nicht kugelförmige Partikel vorhanden sind. Es gibt LISST-Modelle, die dank automatischer Verdünnung mit Klarwasser in einer Mischkammer gemäss Hersteller bis zu 10-mal höhere SSC messen können. Ein solches Gerät war jedoch im Rahmen des vorliegenden Forschungsprojekts nicht erschwinglich.

Mit einem CMD kann der Messbereich höherer SSC relativ kostengünstig abgedeckt werden, wobei keine PSD-Informationen vorliegen. Für die CMD-Methode mit dem periodischen Dichteabgleich wurde aus den Messungen eine erweiterte Messunsicherheit von ±0.3 g/l ermittelt. Die CMD-Methode wird für SSC über 1 g/l als geeignet angesehen (relativer Fehler ≤ 30 %). Die Auswertungen zeigten weiter, dass die akustische Methode für SSC über ca. 0.5 g/l geeignet ist, die Druckmethode für SSC über ca. 2 g/l. Mit optischen Messtechniken wie LISST und Trübungssonden können auch tiefe SSC gemessen werden, die aber bezüglich hydro-abrasivem Verschleiss weniger relevant sind.

3.3 Verhalten der Schwebstoffmessgeräte bei Hochwasser

Anfang Juli 2012 trat das grösste Hochwasserereignis in den drei Messjahren 2012–2014 auf. Dabei wurden auch am meisten Schwebstoffe transportiert. Das Ereignis gab Aufschluss über das Verhalten der Schwebstoffmessgeräte bei ausserordentlich hohen SSC. Da das CMD während dieses Hochwassers noch nicht installiert und hohe SSC mit den optischen und akustischen Messgeräten nicht durchgehend messbar waren, wurde die SSC-Ganglinie während des Hochwassers mit der Druckmethode berechnet. Beide Turbinen wurden während des Ereignisses durchgehend mit dem Ausbauvolumenstrom betrieben, und der Oberwasserpegel entsprach dem maximalen Betriebsspiegel. Gemäss zwei unabhängigen Druckmessungen (eine an jeder MG) war der Druck vor den Turbinen vorübergehend um bis zu 3.5 % grösser als vor und nach dem Hochwasserereignis. Auch die elektrische Leistung nahm während des Hochwassers im selben Ausmass zu. Daraus wurde geschlossen, dass die Dichte des schwebstoffhaltigen Wassers in der Druckleitung vorübergehend auf ca. 1035 kg/m^3 angestiegen sein musste. Dies entspricht einem SSC-Spitzenwert von ca. 50 g/l. Die berechnete SSC-Ganglinie während des Hochwasserereignisses ist in *Bild 22* dargestellt. Die Grössenordnung von 50 g/l wurde weiter durch eine Flaschenprobe aus der Schieberkammer sowie mehrere Imhoff-Trichtermessungen mit schwebstoffhaltigem Wasser aus dem Unterwasserkanal bestätigt.

Die akustische Signaldämpfung während des Hochwassers wurde mit der SSC auf Grundlage der Druckmethode verglichen. Dabei zeigte sich, dass die akustische Methode bis gut 15 g/l funktionierte. Bei höheren SSC wurde das Signal im schwebstoffhaltigen Wasser so stark gedämpft, dass es den Empfänger an der gegenüberliegenden Wand der Druckleitung nicht mehr erreichte. Die ermittelte Messbereichsgrenze von ca. 15 g/l ist kein allgemeingültiger Wert, sondern hängt u.a. von der Partikelgrösse, der Schallfrequenz, der Stärke und Art des gesendeten Signals sowie der Pfadlänge (Leitungsdurchmesser) ab.

Während des Hochwassers überstieg die Trübung während mehrerer Stunden den Messbereich des Streulicht-Trübungsmessgeräts (4000 FNU). Gemäss Druckmethode entsprach dies mit den bei diesem Ereignis vorhandenen Partikeln (d_{50} ≈ 20 µm) einer SSC-Messbereichsgrenze von ca. 6 g/l. Mit dem Durchlicht-Trübungsmessgerät (Optek) konnte eine durchgehende Trübungsganglinie aufgezeichnet werden. Durch Vergleich mit der Druckmethode wurde festgestellt, dass das Signal dieses Trübungsmessgeräts über ca. 5 g/l nicht mehr linear mit der SSC zunahm. Vom LISST waren keine Messdaten verfügbar, weil der Messbehälter mit Feinsand gefüllt wurde und das verwendete LISST für Messungen von SSC über einigen g/l nicht geeignet ist.

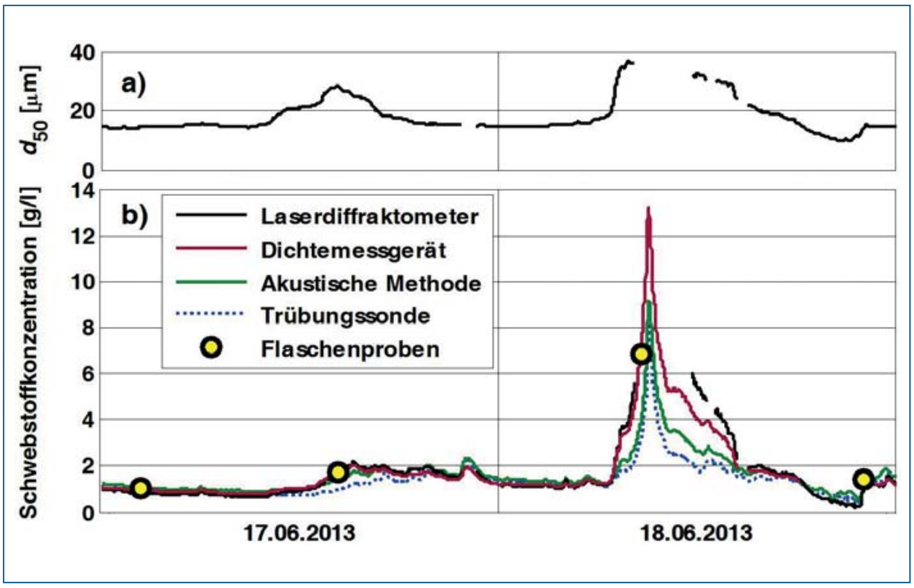

Bild 9. Ausschnitte aus den Ganglinien der a) Medianpartikelgrösse und b) SSC von verschiedenen Messmethoden im Triebwasser des KW Fieschertal.

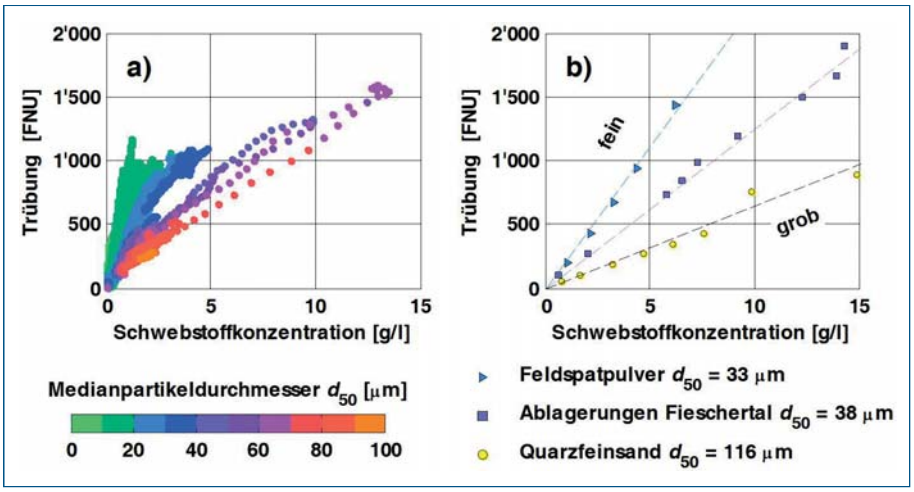

Bild 10 a.) Trübungswerte in Funktion der SSC im Triebwasser des KW Fieschertal, wobei die Farben die Partikelgrössen angeben, und b) entsprechende Messdaten von den Laborversuchen mit verschiedenen Partikelsorten.

3.4 Schwebstoffkonzentrationen und -frachten

Aus den SSC-Ganglinien der verschiedenen Messmethoden wurde eine durchgehende Ganglinie zusammengestellt. Bei SSC über 1 g/l wurde dem Messwert der Dichtemessmethode der Vorzug gegeben. Bei kleineren SSC wurden Messwerte des Laserdiffraktometers verwendet, und falls keine solchen vorhanden waren, wurden Messwerte von Trübungssonden und der akustischen Methode verwendet.

In *Bild 11* sind die SSC-Ganglinien für die Jahre 2012–2014 dargestellt. Im Mittel über die drei Jahre betrug die SSC 0.52 g/l. In der Schwebstoffsaison (ca. April bis Oktober) erreichte die SSC oft mehrere g/l, einige Male überschritt sie 10 g/l und während des Hochwasserereignisses Anfang Juli 2012 erreichte sie wie erwähnt 50 g/l. Aufgrund von Abflussmessungen in der Region wurde die Wiederkehrperiode dieses Hochwasserereignisses auf ca. 20 Jahre geschätzt.

Aus den Zeitreihen der SSC und des Volumenstroms in der Druckleitung wurde die Schwebstofftransportrate in jeder Minute berechnet und über die Zeit integriert. Die Schwebstofffracht in der Druckleitung im Laufe der drei untersuchten Jahre ist ebenfalls in *Bild 11* dargestellt. Die jährlichen Schwebstofffrachten (107 000, 61 000 und 43 000 t) variieren deutlich stärker als die Volumina des turbinierten Wassers (143, 130 und 128 Mio. m^3). Das heisst, die Unterschiede in den jährlichen Schwebstofffrachten kamen vorwiegend durch Variation der SSC zustande (SSC-Jahresmittel = 0.75, 0.47 und 0.34 g/l).

Die Schwebstofffracht in der Druckleitung von 61 000 t im Jahr 2013 beispielsweise entspricht, umgerechnet auf die Einzugsgebietsfläche (58 km^2), einem Abtrag von 0.4 mm pro Jahr. Gemäss *Wittmann et al*. (2007) beträgt die langfristige Denudationsrate in den kristallinen Schweizer Zentralalpen 0.9 ± 0.3 mm/a. Die Differenz kann damit erklärt werden, dass nicht das gesamte im Einzugsgebiet erodierte Sediment durch die Druckleitung transportiert wird. Dazu zählen Sedimente in Entkieser-, Entsander- und Stollenspülungen, der Sedimenttransport im nicht gefassten Wasser sowie Ablagerungen in einem neuen kleinen proglazialen See oberhalb der Wasserfassung.

In Bezug auf die Turbinenabrasion sind Phasen, in welchen die Schwebstofffracht in relativ kurzer Zeit stark zunimmt, von besonderem Interesse. Steile Abschnitte der Kurven in *Bild 11* stellen Schwebstofftransport-Ereignisse dar. Das relativ hohe Schwebstoffaufkommen im Frühsommer wird folgendem Vorgang im Einzugsgebiet zugeschrieben: Auch im Winterhalbjahr wird unter dem Gletscher Fels erodiert. Bei Beginn der Gletscherschmelze im Frühsommer werden die entstandenen Feinsedimentpartikel vermehrt abtransportiert und gelangen ins Triebwasser. Die Kurve der Schwebstofffracht des Jahres 2012 zeigt, dass während des Hochwassers Anfang Juli ein Grossteil der Jahresfracht transportiert wurde und dass die jährlichen Schwebstofffrachten stark von einzelnen Starkregenereignissen abhängen.

Aus den LISST-Messungen sind auch die Grössen der Schwebstoffpartikel bekannt. In Phasen, in denen vorübergehend keine LISST-Messungen vorhanden waren, wurden die Partikelgrössen aufgrund von verfügbaren Messdaten mehrerer anderer Methoden und mithilfe von Korrelationen, die in Phasen mit LISST-Daten ermittelt wurden, berechnet. In *Bild 12* sind die jährlichen Schwebstofffrachten in der Druckleitung in fünf Partikelgrössenklassen dargestellt. In allen drei Jahren waren etwa 55% der Schwebstoffe Fein- und Mittelsilt (<20 µm), etwa 30 % Grobsilt (20–63 µm) und ca. 15 % vorwiegend Feinsand. Im Jahr 2012 war der Anteil gröberer Partikel etwas grösser als in den anderen beiden Jahren, in denen es keine bedeutenden Hochwasser gab.

Nebst der Schwebstofffracht in der Druckleitung wurden auch die Schwebstofffrachten berechnet, welche durch die einzelnen Maschinengruppen gelangten. Dabei wurde angenommen, dass in beiden Turbinenzuläufen die gleiche SSC vorhanden war.

3.5 Gründe für Schwebstoffspitzen

Die SSC im Triebwasser variierte im Sommer bei Volllastbetrieb je nach Gletscherschmelze. Wie erwartet, traten erhöhte SSC nach Regenereignissen auf, siehe z. B. *Bild 13b*. Wie in *Bild 13a* ersichtlich, traten aber markante SSC-Spitzen auch in niederschlagsfreien Perioden auf. In *Bild 14* unten ist ein Detail der SCC-Ganglinie zusammen mit der Ganglinie des Medianpartikeldurchmessers d_{50} der Schwebstoffpartikel während der ersten drei Tage der in *Bild 13a* gezeigten Periode dargestellt. Der obere Teil des *Bilds 14* zeigt die zeitlich entsprechenden Ganglinien des Stollenpegels (gemessen bei der Schieberkammer) und des Volumenstroms in der Druckleitung. In diesen Augusttagen wurde der Speicherstollen zum Ausgleich tageszeitlicher Zuflussschwankungen genutzt. Der Pegel im Speicherstollen erreichte jeweils abends bzw. nachts den maximalen Betriebsspiegel (1643 m ü.M.) und zur Mittagszeit den minimalen Betriebsspiegel (1639 m ü.M.). Bei tiefem Stollenpegel traten höhere SSC und höhere d_{50} auf als bei vollem Speicher-

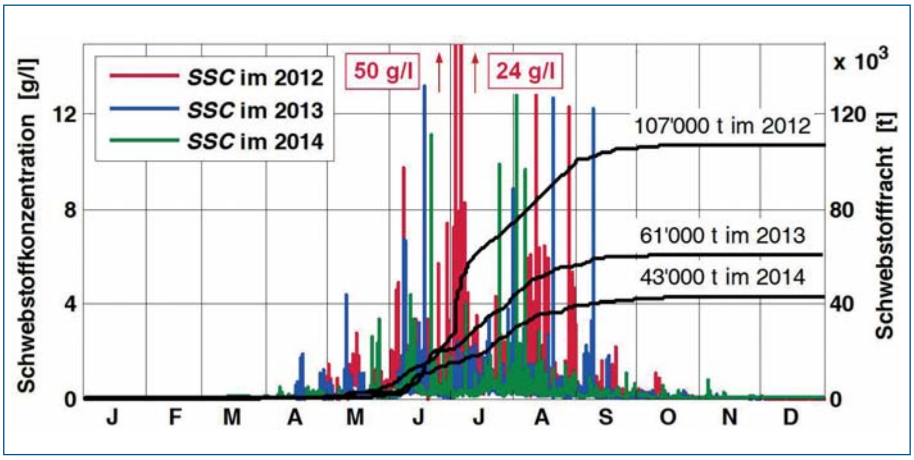

Bild 11. SSC-Ganglinien und Schwebstofffrachten für die Jahre 2012 bis 2014 im KW Fieschertal.

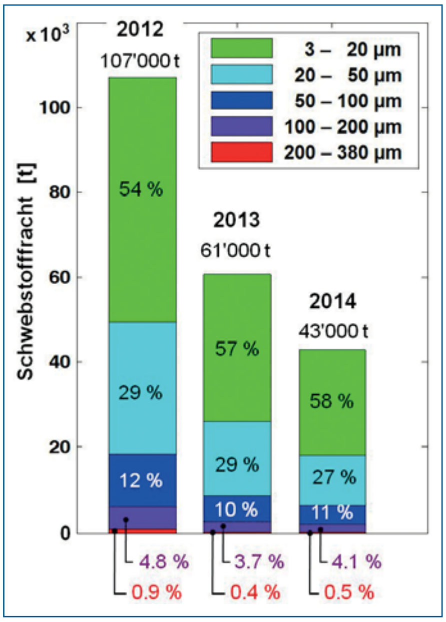

Bild 12. Schwebstofffrachten, aufgeteilt nach Grössenklassen.

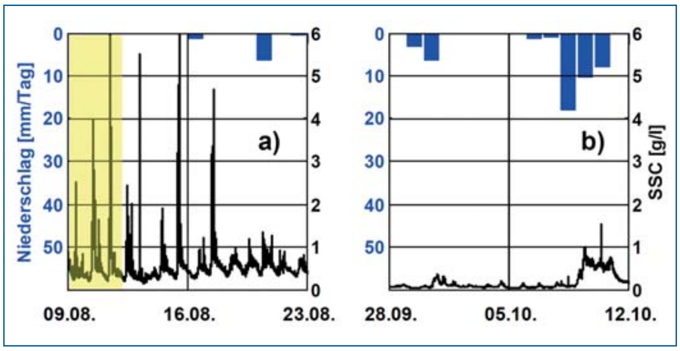

Bild 13. Schwebstoffspitzen, die a) nicht oder b) wesentlich von Regenereignissen abhängen (Felix et al. 2014).

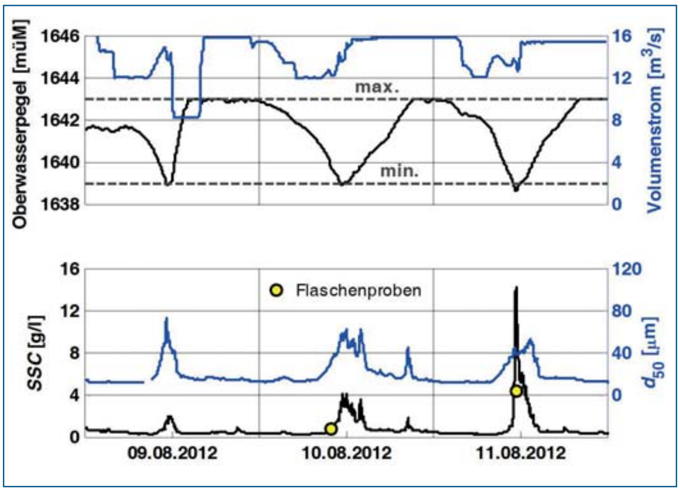

Bild 14. Spitzen der Schwebstoffbelastung bezüglich Konzentration (SSC) und Partikelgrösse infolge der Speicherstollen-Bewirtschaftung, gelb markierter Ausschnitt aus Bild 13.

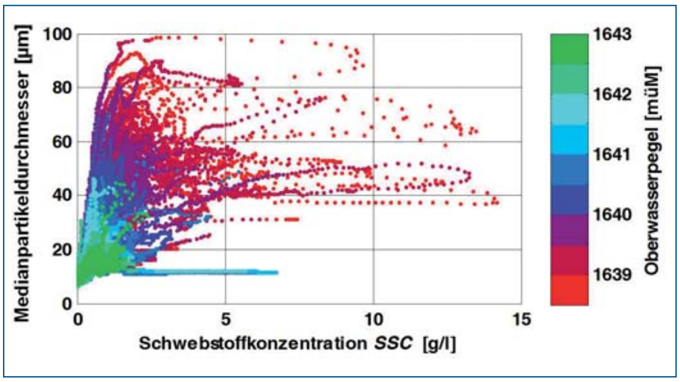

Bild 15. Medianpartikeldurchmesser bei verschiedenen Schwebstoffkonzentrationen infolge der Speicherstollen-Bewirtschaftung.

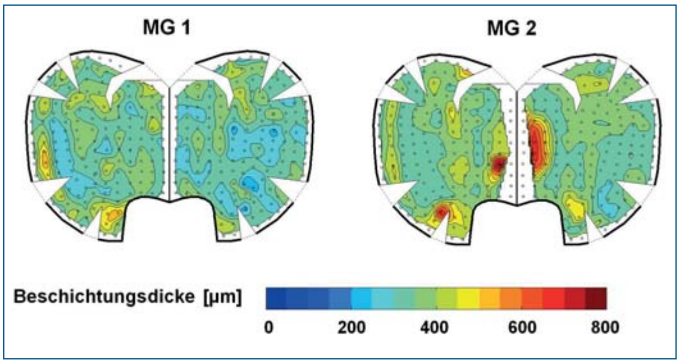

Bild 16. Schichtdickenverteilungen in Bechern des KW Fieschertal (Beispiele jeweils vom Becher Nr. 1 im April 2013).

stollen. Dies ist auch in *Bild 15* zu sehen, in welchem die Messdaten von niederschlagsarmen Perioden (<5 mm/Tag) in den Jahren 2012–2014 zusammengestellt sind.

Der verstärkte Transport gröberer Partikel bei tiefen Stollenpegeln kann mit den hydraulischen Verhältnissen im Speicherstollen erklärt werden: Gemäss Berechnungen betragen bei maximalem Stollenpegel die mittlere Fliessgeschwindigkeit im Stollen <0.5 m/s und die Sohlschubspannung <0.5 Pa. Bei tiefem Stollenpegel treten höhere Fliessgeschwindigkeiten (bis 2 m/s) und deutlich höhere Sohlschubspannungen (bis 20 Pa) auf, durch welche abgelagerte Partikel resuspendiert werden und ins Triebwasser gelangen können. Ein Teil der SSC-Spitzen im Triebwasser wird also durch den Betrieb des Speicherstollens verursacht.

Feinsedimentablagerungen in der ersten Hälfte des Speicherstollens können durch das Spülfenster ins Wysswasser zurückgegeben werden. Feinsedimente in der zweiten Hälfte des Speicherstollens werden aber früher oder später turbiniert. Mit einem Anheben des minimalen Betriebsspiegels im Speicherstollen könnten betriebsbedingte hohe SSC nur vorübergehend vermieden werden, da die Sedimentablagerungen im Stollen zunehmen würden.

4. Resultate der Verschleissmessungen

4.1 Verteilung und Abnahme der Beschichtungsdicken

Bild 16 zeigt Beispiele der räumlichen Verteilungen der Schichtdicken, die in Bechern von nicht fabrikneuen Peltonlaufrädern im April 2013 im KW Fieschertal gemessen wurden. Die Schichtdicken wurden zwischen den Messpunkten (schwarze Symbole) interpoliert und farblich auf einer ebenen Abwicklung der Becherinnenseite dargestellt.

Bei der MG 1 variierten die Beschichtungsdicken zwischen ca. 200 und 500 µm. Bei der MG 2 sind lokal Beschichtungsdicken von bis zu 800 µm vorhanden, da beim Nachbeschichten stellenweise Material auch auf die vorhandene Beschichtung aufgetragen wurde. Auch ohne lokales Nachbeschichten kann die Schichtdicke von benachbarten Messpunkten stark variieren: z. B. variiert die Schichtdicke am linken Rand des Bechers Nr. 1 der MG 1 auf einer Distanz von nur 4 cm um bis zu ca. 200 µm. Dies zeigt, wie wichtig die Lage der Messpunkte ist. An jeweils einem Laufrad haben die Schichtdickenverteilungen der Becher Nr. 1 und Nr. 2 einen ähnlichen Charakter aufgewiesen.

Über die Innenfläche der beiden Becher gemittelt, wurden an der MG 1 folgende Reduktionen der Schichtdicke berechnet: 10 µm während der Schwebstoffsaison 2013 (29 000 t Schwebstoffe) und 4 µm während der Schwebstoffsaison 2014 (22 000 t). Mit einer Reproduzierbarkeit der über einen Becher gemittelten Schichtdickendifferenz von ±5 µm wird die Schichtdickendifferenz von 2013 als signifikant eingestuft und als Abrasion interpretiert. Die Schichtdickendifferenz im Jahr 2014 hingegen liegt innerhalb der Messunsicherheit.

Die Beschichtung in den Bechern ist also für mehrere Jahre ausreichend, sofern keine grösseren Schwebstofftransportereignisse vorkommen. Am stark beschädigten Laufrad, das nach dem Hochwasser vom Juli 2012 ausgebaut werden musste, betrugen die Schichtdicken an 10 % der Messpunkte nur 50 bis 100 µm, u.a. im Bechergrund in der Nähe von Stellen, an denen die Beschichtung vollständig abgetragen wurde (vermutlich auch durch Sekundärschäden bedingt).

Relevant ist der Verschleiss bzw.

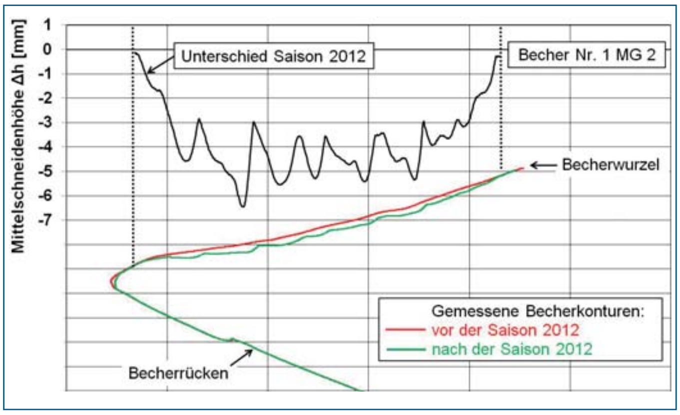

Bild 17. Reduktion der Mittelschneidenhöhe in einem Becher eines Laufrads des KW Fieschertal während der schwebstoffreichen Saison 2012.

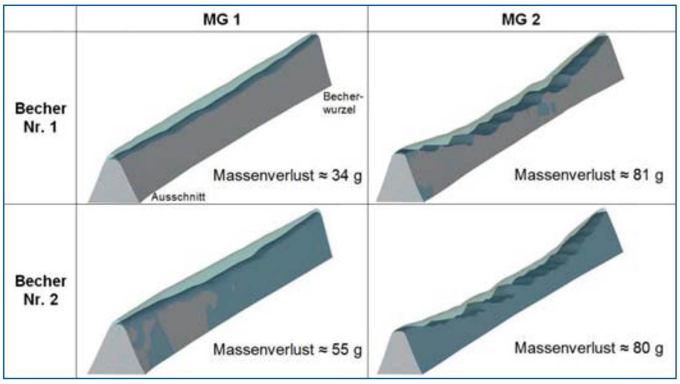

Bild 18. Quantifizierung des Materialverlusts an den Mittelschneiden im schwebstoffreichen Jahr 2012 (nach Abgottspon et al. 2014). Der Zustand vor der Saison ist halbtransparent dargestellt.

der lokale Verlust der Beschichtung auf den Mittelschneiden und an den Bechereintrittskanten am Ausschnitt, der im KW Fieschertal auch in Schwebstoffsaisons ohne grössere Hochwasser auftritt. Der vollständige lokale Verlust der Beschichtung ist von Bedeutung, da dort das weichere Grundmaterial oft tief ausgewaschen wird. Die Abnutzung der Beschichtung an den Mittelschneiden und Bechereintrittskanten kann aber mit der verwendeten Schichtdickenmesstechnik nicht oder nicht genügend genau erfasst werden.

4.2 Materialverlust an Mittelschneide und Becherausschnitt

Bild 17 zeigt ein Beispiel von zwei Längsschnitten durch die Mittelschneide des Bechers Nr. 1 des Peltonlaufrades der MG 2, welche vor (rot) und nach (grün) der Schwebstoffsaison 2012 gemessen wurden. Die Reduktion der Mittelschneidenhöhe ist als schwarze Linie eingetragen und bezieht sich auf die Achse am linken Rand des Diagramms. Die Mittelschneidenhöhe wurde in diesem Beispiel um bis zu 6.5 mm reduziert. Das Ausmass des hydro-abrasiven Verschleisses am Becher Nr. 2 hat einen ähnlichen Verlauf. Eine Reduktion um 6.5 mm entspricht im Fall des KW Fieschertal 1 % der Becherinnenbreite von 650 mm. In *Bild 18* sind die digitalen Geometriemodelle der Mittelschneiden der Becher Nr. 1 und 2 der beiden MG am Anfang und Ende der Beobachtungsperiode 2012, in der die Schwebstoffbelastung infolge des erwähnten Hochwasserereignisses relativ hoch war, dargestellt. Bei der MG 2 war die Mittelschneide infolge Betrieb während dreier vorangegangener Schwebstoffsaisons und vor Ort durchgeführten Revisionen schon vor der Schwebstoffsaison 2012 stark abgeflacht, was zu etwa doppelt so grossem Massenverlust als bei MG 1 führte. In der MG 1 war zu Beginn der Schwebstoffsaison 2012 ein neuwertiges Laufrad (nach Revision beim Turbinenhersteller) eingesetzt worden. Im mittleren Drittel der Länge der Mittelschneide, wo der Strahl am längsten einwirkt, wurde am meisten Material abgetragen. Aus den beträchtlichen Unterschieden der Masseverluste der Becher von MG 1 kann geschlossen werden, dass mindestens zwei Becher pro Laufrad digitalisiert werden sollten, um einen repräsentativen Mittelwert für ein Laufrad zu ermitteln.

Von den zwei vermessenen Bechern wurde ein mittlerer Massenverlust für das Laufrad der jeweiligen MG hochgerechnet. In der Schwebstoffsaison 2012 mit dem Hochwasserereignis betrug für die MG 1 der Massenverlust 0.9 kg an den Mittelschneiden und 1.5 kg an den Becherausschnitten. Bei der MG 2 betrug der Massenverlust 1.6 kg an den Mittelschneiden und ebenfalls 1.5 kg an den Ausschnitten. An den Ausschnitten kann also etwa gleich oder sogar mehr Material abgetragen werden als an den am meisten beachteten Mittelschneiden.

4.3 Vergleich mit der Schwebstoffbelastung

Die Höhen- und Breitenänderung der Mittelschneiden sind in *Bild 19* in Funktion der kumulierten Schwebstofffrachten für beide MG dargestellt (jeweils Mittelwerte der Becher Nr. 1 und 2). Bei der MG 1 war von 2012 bis 2014 dasselbe Laufrad installiert. Bei der MG 2 waren über denselben Zeitraum drei Laufräder installiert, weshalb nicht alle Datenpunkte miteinander verbunden sind. Ein erster Laufradwechsel war nach dem Hochwasserereignis im Jahr 2012 notwendig. Der zweite Laufradwechsel Ende 2013 war unabhängig von hydro-abrasiven Verschleiss wegen eines Risses nahe der Becherwurzel notwendig.

Bei der MG 1 wurde in der Schwebstoffsaison 2012 die Beschichtung an allen Mittelschneiden und Bechereintrittskanten vollständig abgetragen und die grossen Materialverluste entstanden durch Abtrag des Grundmaterials. Bei einer Schwebstofffracht von etwa 60 000 t wurde die Mittelschneidenhöhe um 6.5 mm reduziert, und die Mittelschneide wurde etwa 3 mm breiter. In den Schwebstoffsaisons 2013 und 2014 hingegen wurde bei der MG 1 die Beschichtung nur in einigen Bechern sehr lokal abgetragen, und die Mittelschneidenhöhen und -breiten änderten sich nicht.

Bei der MG 2 war die Mittelschneide

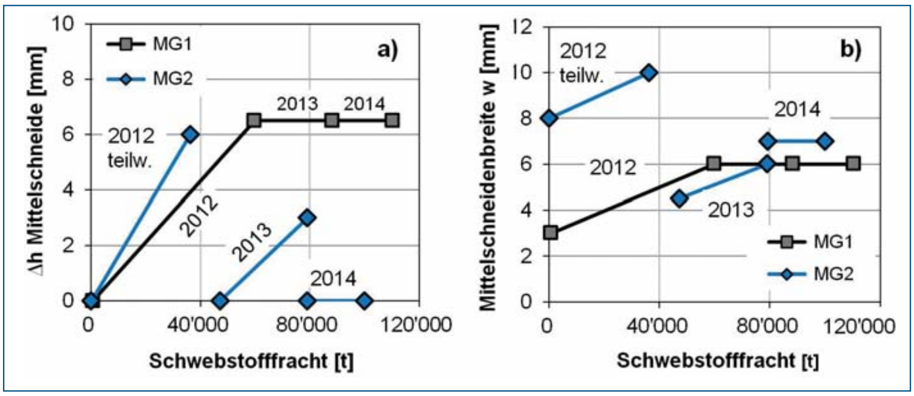

Bild 19. a) Reduktion der Mittelschneidenhöhe und b) Zunahme der Mittelschneidenbreite in Funktion der kumulierten Schwebstofffracht für beide MG des KW Fieschertal.

vor der Schwebstoffsaison 2012 mehr als doppelt so breit wie bei der MG 1. Dies hat dazu geführt, dass es mit der weiteren Verbreiterung der Mittelschneide während der Schwebstoffsaison zu weiteren Sekundärschäden kam, welche im Gegensatz zur MG 1 einen Laufradersatz erforderlich machten; dies trotz einer um ein Drittel kleineren Schwebstofffracht bei der MG 2 als bei der MG 1. Dies zeigt, dass der Zustand eines Turbinenlaufrades vor einer Belastungsperiode entscheidend für das Ausmass des Verschleisses ist.

5. Resultate der Wirkungsgradmessungen

5.1 Historie des Index-Turbinenwirkungsgrades

Bild 20 zeigt die Historie der Wirkungsgradveränderung der MG 1 im KW Fieschertal sowohl mittels der Sliding-Needle-Messungen als auch der kontinuierlichen Wirkungsgradauswertung. Die Wirkungsgradveränderung ist referenziert auf eine erste Messung vom Juli 2012. Die Werte der kontinuierlichen Auswertung streuen mehr als diejenigen der Sliding-Needle-Messungen. Durch Filterung und Mittelung der Messsignale des kontinuierlichen Monitorings konnte die Streuung so weit reduziert werden, dass eine verlässliche Wirkungsgradhistorie resultierte. Die Verläufe der beiden Methoden sind qualitativ und quantitativ ähnlich, sodass die Wirkungsgradhistorie als erhärtet betrachtet werden kann. Die Reproduzierbarkeit der gemessenen Wirkungsgradveränderung beträgt etwa 0.2 %.

In einem Teil der Schwebstoffsaison 2012 wurde bei der MG 1 während 1902 Betriebsstunden eine Wirkungsgradreduktion von 1 % gemessen. Diese Wirkungsgradreduktion ist hauptsächlich auf das im Abschnitt 3.3 erwähnte Hochwasserereignis und dessen Auswirkungen zurückzuführen. Im Jahr 2014 hingegen betrug die Wirkungsgradreduktion lediglich 0.14 % während 3048 Betriebsstunden. In *Bild 20* sind auch die jeweils im Winter durchgeführten Reparaturarbeiten an den Laufrädern eingetragen. Beim KW Fieschertal hat sich das Vorgehen bewährt, in jedem Winter ein Nachschleifen und Nachbeschichten vor Ort durchzuführen. Nach beträchtlichem hydro-abrasivem Verschleiss im Jahr 2012 resultierte durch das Nachschleifen der Mittelschneide und des Ausschnittes eine Wirkungsgradverbesserung von +0.56 %. Nach eher geringem hydro-abrasivem Verschleiss im Jahr 2013 resultierte durch das Nachschleifen keine signifikante Wirkungsgradänderung. Die Auswirkung des Nachbeschichtens der Mittelschneiden und der Becherausschnitte auf den Wirkungsgrad konnte zweimal untersucht werden. Diese lokalen Nachbeschichtungen bewirkten keine signifikanten Wirkungsgradänderungen. Im Lauf der Einsatzzeit eines Laufrads mit wiederholten Revisionen vor Ort sinkt sein Wirkungsgrad generell. Durch eine grosse Revision im Werk mit Materialauftragung kann das hydraulische Profil wiederhergestellt und der hydraulische Wirkungsgrad wieder deutlich erhöht werden.

Eine detaillierte Wirkungsgradhistorie, wie in *Bild 20* dargestellt, ist in der Literatur nicht zu finden. Meist werden zwei Einzelmessungen miteinander verglichen (*Lazzaro* und *Rossi* 1995, *Brekke et al*. 2002, *Singh et al*. 2013). Eine wichtige Erkenntnis aus dem vorliegenden Forschungsprojekt ist, dass Wirkungsgraddifferenzen infolge Abnutzungen oder Revisionsmassnahmen nur als Tendenz vorhersagbar sind. Ein Nachschleifen der Mittelschneiden beispielsweise hat nicht immer denselben Einfluss auf den Wirkungsgrad. Auch lassen sich die an einem Laufrad ermittelten Ergebnisse nicht einfach auf das andere übertragen. Es ist eine Wirkungsgradhistorie pro Laufrad zu erstellen.

Aufgrund der Messdaten mehrerer Jahre kann geprüft werden, ob in Jahren ohne signifikante Wirkungsgradreduktionen und mit wenig Verschleiss (vgl. *Bild 19*) ein jährliches Nachschleifen und Nachbeschichten notwendig und wirtschaftlich sinnvoll ist.

5.2 Vergleich mit der Schwebstoffbelastung

Die aus der Wirkungsgradhistorie in *Bild 20* resultierenden Wirkungsgraddifferenzen sind in *Bild 21* für die einzelnen Schwebstoffsaisons in Funktion der Schwebstofffrachten für beide MG dargestellt. Gelb markiert ist der Bereich der Reproduzierbarkeit der Messungen von ±0.2 %. In diesem Bereich sollten die Wirkungsgraddifferenzen nicht überinterpretiert werden, insbesondere ein geringer Wirkungsgradanstieg. Bei der MG 2 liegt für das Jahr 2012 keine Wirkungsgraddifferenz vor, da das Laufrad nach dem Hochwasserereignis ungeplant ausgewechselt werden musste. Bei etwa gleicher Schwebstofffracht von 30 000 t resultierten Wirkungsgraddifferenzen, die sich um einen Faktor 3 unterscheiden (-0.97 % bei MG 1 im 2012 im Vergleich zu -0.30 % bei MG 2 im 2013).

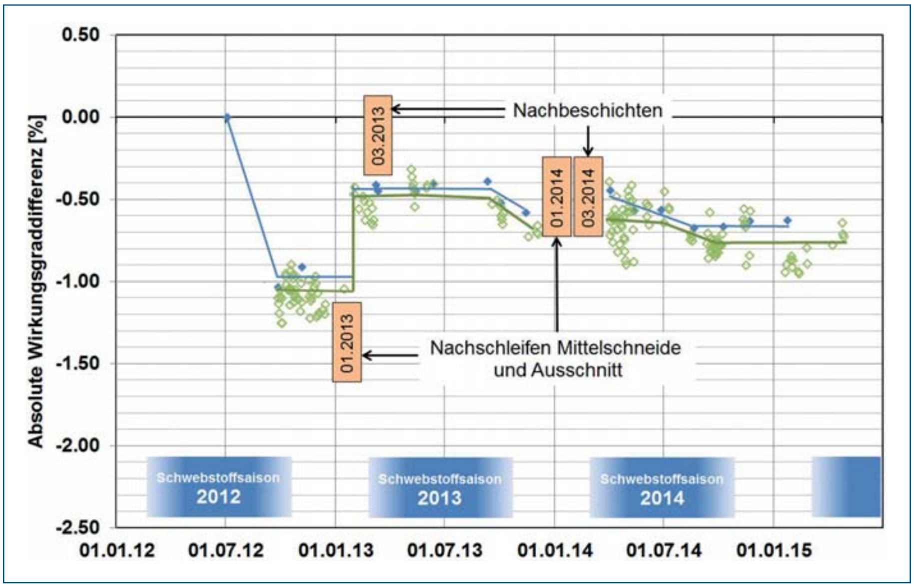

***Bild 20.** Verlauf der Wirkungsgradänderung der MG 1 im KW Fieschertal aus den Sliding-Needle-Messungen (blau) und aus dem kontinuierlichen Monitoring (grün).*

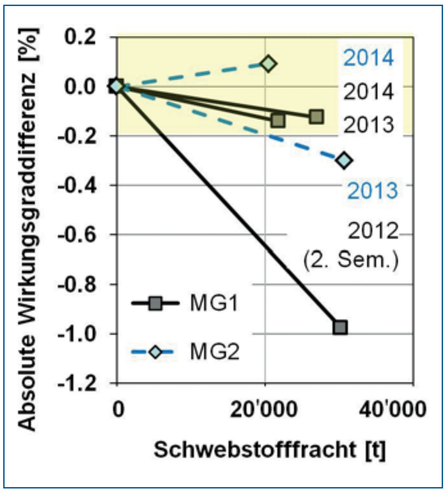

***Bild 21.** Vergleich der gemessenen Wirkungsgradänderungen an den MG des KW Fieschertal mit den entsprechenden Schwebstoffbelastungen.*

Durch Feinsedimente verursachte Kosten für zwei MG	kCHF/a	in % des Werts der Jahreserzeugung
Reparaturkosten	**300**	3.4 %
- an Laufrädern	200	
- an Düsen, Düsenschutzdächern	60	
- am Entsander (Anteil Spülsystem)	40	
Erzeugungsverluste	**30**	0.3 %
- infolge Wirkungsgradreduktion	10	
- infolge Stollenspülungen oder Laufradwechsel mit Wasserverlust	20	
Total Kosten für zwei MG	**330**	3.7 %

Tabelle 1. Erwartungswerte der durch Feinsedimente verur-sachten Kosten für zwei MG des KW Fieschertal im lang-jährigen Mittel, geschätzt auf Basis der Daten von 2012 bis 2014.

Spezifische Feinsedimentkosten	im Normalfall bei SSC = 0.5 g/l	bei SSC = 10 g/l
bezogen auf die Wassermenge	0.33 Rp/m^3	6.6 Rp/m^3
bezogen auf die Erzeugung	0.28 Rp/kWh	**5.5 Rp/kWh**

Tabelle 2. Spezifische Feinsedimentkosten im langjährigen Mittel, geschätzt auf Basis der Daten von 2012 bis 2014 für das KW Fieschertal.

Dies zeigt, dass die Schwebstofffracht alleine kein geeigneter Parameter für die Erklärung und Prognose der Wirkungsgradveränderungen ist.

6. Betriebsoptimierung

6.1 Warnungen vor hoher Schwebstoffbelastung

Da die Schwebstoffbelastung zeitlich stark variiert, kann es wirtschaftlicher sein, bei hoher Schwebstoffbelastung Fassungen vorübergehend auszuleiten und allenfalls das Turbinieren während eines Hochwassers zu unterbrechen. Dabei sind natürlich auch übergeordnete Randbedingungen wie Produktionsverpflichtungen und Produktionsausgleich durch andere Kraftwerke innerhalb einer Bilanzgruppe zu berücksichtigen. Um Situationen mit hoher Schwebstoffbelastung rechtzeitig und zuverlässig zu erkennen sowie vorübergehende Produktionsverluste wirtschaftlich begründen zu können, ist ein Schwebstoffmonitoring erforderlich, welches sich idealerweise nicht nur auf SSC, sondern auch auf die Partikelgrössen beziehen sollte.

Um eine Vorwarnzeit für eine Abschaltung zu erhalten, sind nicht nur Messungen im Triebwasser, sondern auch bereits im Fassungsbereich oder im Fluss oberhalb der Fassung empfehlenswert. Für Vorwarnungen sind auch Messgrössen wie Trübung, Abfluss im Oberlauf und Niederschlag verwendbar. Als zusätzliche Entscheidungsgrundlage können zudem Niederschlags- und Abflussprognosen berücksichtigt werden. Um nach einer Abschaltung zu entscheiden, wann die Anlage wieder in Betrieb genommen werden kann, ist es wichtig, mindestens eine Schwebstoffmessung im Fluss oberhalb bzw. ausserhalb der Wasserfassung zu haben.

Wenn die Signale der Schwebstoffmessungen auch im Kraftwerksleitsystem integriert werden, können Warnungen vor hohen Schwebstoffbelastungen wie andere Alarme an den Pikettdienst ausgegeben werden, welcher die Entscheidung einer Abschaltung zu treffen hat. Es sind keine automatischen Kraftwerksabstellungen aufgrund der Schwebstoffsituation vorgesehen. Bei einer Wasserkraftanlage mit Beileitungen aus anderen Tälern müssen in der Regel nicht alle Fassungen oder nicht alle gleichzeitig ausgeleitet werden, da Starkregenereignisse oft sehr lokal sind. Im Fall des KW Fieschertal ist bei grösseren Hochwassern ein Ausleiten der Fassung zu empfehlen, um starken Feinsedimenteintrag in den Speicherstollen und übermässige Turbinenabrasion zu vermeiden. Aufgrund des begrenzten Nutzvolumens des Speicherstollens ist spätestens eine Stunde nach dem Ausleiten der Fassung das Turbinieren vorübergehend einzustellen.

6.2 Berechnung der Abschaltkonzentration

Die Berechnung der Abschaltkonzentration basiert auf betriebswirtschaftlichen Überlegungen. Dafür sind Grundlagendaten über das Schwebstoffaufkommen, Wirkungsgradreduktionen, Unterhaltskosten und Strompreise erforderlich. Im Kraftwerk Fieschertal sind solche Daten über drei Jahre vorhanden. Von besonderer Bedeutung ist das Hochwasserereignis vom Juli 2012, bei dem ein Laufrad so stark beschädigt wurde, dass es während der Volllastzeit ausgetauscht werden musste, und am anderen Laufrad eine starke Wirkungsgradreduktion auftrat. Im Folgenden wird ein einfaches Vorgehen für die rechnerische Abschätzung der Abschaltkonzentration am Beispiel des KW Fieschertal aufgezeigt.

Die durch Feinsedimente verursachten Reparaturkosten an der Anlage wurden auf etwa 300 kCHF pro Jahr geschätzt *(Tabelle 1)*. Dies unter der Voraussetzung, dass das Kraftwerk bei grösseren Hochwassern nicht abgeschaltet wird und die entsprechenden Schäden auftreten. Dazu kommen Ertragsausfälle wegen Erzeugungsverlusten in der Grössenordnung von 30 kCHF pro Jahr. Für die Berechnung der im langfristigen Mittel erwarteten jährlichen Werte wurden verschiedene Kosten- und Minderertragspositionen mit deren Eintrittswahrscheinlichkeiten berücksichtigt.

Aufgrund der Daten von 2012 bis 2014 wurde geschätzt, dass die jährliche Schwebstofffracht im langjährigen Mittel 50 000 t beträgt. Mit der vereinfachenden Annahme, dass die durch Feinsedimente verursachten Kosten proportional zur Schwebstofffracht sind, ergeben sich damit spezifische Kosten pro Tonne Feinsediment von CHF 330 000 / 50 000 t / = 6.6 CHF/t (0.66 Rp/kg).

Im Normalfall mit SSC = 0.5 g/l während der Schwebstoffsaison sind in 1 m^3 Triebwasser 0.5 kg Schwebstoffe enthalten. Daraus resultieren durch Feinsedimente verursachte spezifische Kosten pro m^3 Wasser von 0.66 Rp/kg · 0.5 kg/m^3 = 0.33 Rp/m^3. Bei SSC = 10 g/l beispielsweise betragen diese 6.6 Rp/m^3 *(Tabelle 2)*. Im KW Fieschertal hat eine Maschinengruppe eine Nennleistung von 32 MW bei einem Nennvolumenstrom von 7.5 m^3/s. In einer Stunde Volllastbetrieb werden also mit 27 000 m^3 Wasser 32 000 kWh erzeugt. Das entspricht einem Arbeitswert von 1.2 kWh/m^3. Mit diesem Arbeitswert liegen die spezifischen Feinsedimentkosten im Normalfall bei 0.33 Rp/m3 / 1.2 kWh/m^3 = 0.28 Rp/kWh und bei hohen SSC von 10 g/l betragen diese 5.5 Rp/kWh. Bei einer SSC von ca. 10 g/l überschreiten die durch Feinsedimente verursachten Kosten den angenommenen Erlös, und es ist wirtschaftlicher, auf das Turbinieren zu verzichten. Es wird empfohlen, in einigen Jahren den Wert der Abschalt-SSC mit einer erweiterten Datenbasis erneut zu berechnen und gegebenenfalls anzupassen. Gemäss den wenigen auffindbaren Literaturangaben liegen Abschaltkonzentrationen bei andern Wasserkraftanlagen im Bereich von 1.1 g/l (Pelton-KW Dorferbach, *Boes* 2010) bis einige g/l (z. B. 3 g/l bei einem Kraftwerk in Indien, *Singh et al*. 2013). Die Abschaltkonzentration muss anlagespezifisch beurteilt werden, da sie von vielen Faktoren abhängt (Fallhöhe, spezifische Drehzahl, Abrasivität der Partikel, Beschichtung usw.).

Zusammen mit dem Betreiber des KW Fieschertal und dem für die Maschinen verantwortlichen Ingenieur (BKW Engineering) wurde festgelegt, die Fassung auszuleiten und den Turbinierbetrieb anschliessend zu unterbrechen, wenn die SSC in der Druckleitung während mehr als 15 Minuten 10 g/l überschreitet. Da die Wiederinbetriebnahme mit einem Aufwand verbunden ist, wird der Betrieb erst wieder aufgenommen, wenn die SSC unter 5 g/l gesunken ist und das Ende des Ereignisses absehbar wird. In *Bild 22* ist anhand des Verlaufs der SSC im Triebwasser dargestellt, wie dieses Szenario im Fall des Hochwassers vom Juli 2012 ausgesehen hätte. Es ist das einzige Hochwasserereignis während der Beobachtungsperiode von 2012 bis 2014, bei dem das Abstellkriterium erreicht worden wäre. Dies zeigt, dass die Anlage nur bei wirklich relevanten Schwebstoffereignissen ausser Betrieb ginge.

Während der Ausserbetriebnahme von 16 h wären 13 000 t Feinsedimente weniger über die Turbinen geleitet worden, das entspricht 12 % der Jahresfracht von 2012 oder etwa 25 % der Fracht in einem Jahr ohne grösseres Hochwasser. Wenn die Fassung während des Hochwasserereignisses ausgeleitet worden wäre, wären zudem deutlich weniger Feinsedimente in das System eingetragen worden. Dadurch wäre auch die Schwebstoffbelastung in den Wochen nach dem Hochwasserereignis geringer ausgefallen, da die während des Hochwassers im Speicherstollen abgelagerten Feinsedimente anschliessend infolge Resuspension turbiniert wurden.

6.3 Wirtschaftliche Aspekte

Die Wirtschaftlichkeit einer temporären Kraftwerksabschaltung wurde am Beispiel des Hochwasserereignisses vom Juli 2012 für das KW Fieschertal vereinfacht nachgerechnet *(Tabelle 3)*. Durch den vorübergehenden Stillstand beider Maschinengruppen ergeben sich Erzeugungsverluste und Ertragseinbussen. Weiter kann eine allfällige Strafgebühr für die Produktionsabweichung negativ zu Buche schlagen. Auf der anderen Seite würden durch die Abschaltung die Reparaturkosten und die Produktionsminderung infolge Wirkungsgradreduktion für beide MG geringer ausfallen, und es gäbe keinen Erzeugungsverlust infolge eines durch das Hochwasser erforderlich gewordenen Laufradtausches. In Summe wäre in diesem Ereignis ein vorübergehendes Einstellen des Turbinierens deutlich wirtschaftlich gewesen.

Diese wirtschaftliche Betrachtung im Nachhinein wurde durch Schwebstoff-, Turbineninspektions-, Wirkungsgrad- und Kostendaten ermöglicht. Mitte 2012 standen diese Grundlagen noch nicht alle zur Verfügung. Die Wirtschaftlichkeit von Betriebsunterbrechungen ist von Fall zu Fall verschieden, da die Dauer und Intensität eines Hochwassers bzw. der Sedimentbelastung und die Folgen für die Maschinen variieren können.

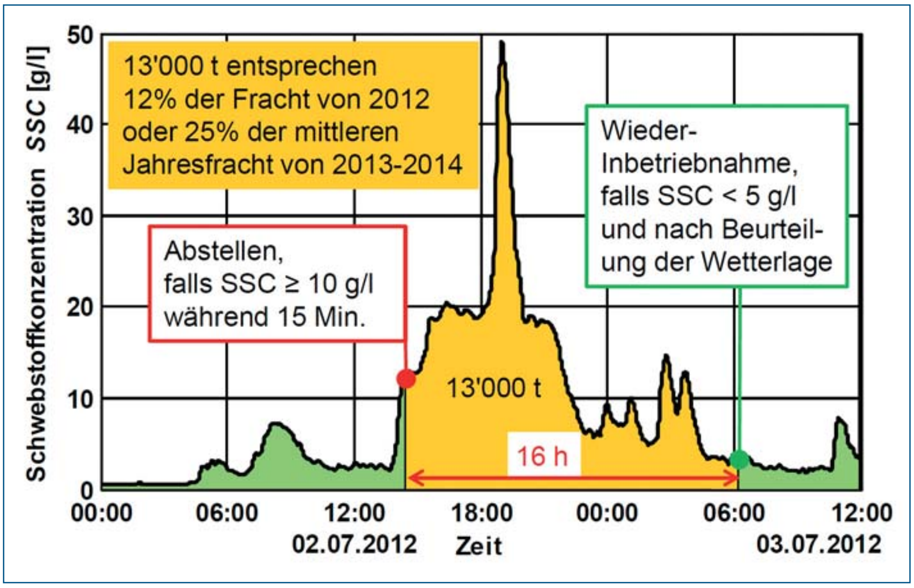

Bild 22. Verlauf der Schwebstoffkonzentration im Triebwasser des KW Fieschertal Anfang Juli 2012 mit Szenario für das vorübergehende Einstellen des Turbinierens.

7. Schlussfolgerungen

Um die Zusammenhänge zwischen der Schwebstoffbelastung, dem hydro-abrasiven Verschleiss und den Wirkungsgradänderungen an Peltonturbinen zu untersuchen, wurden umfangreiche Messungen und Analysen durchgeführt. In einer ersten Projektphase wurde das Verhalten von Schwebstoffmessgeräten unter kontrollierten Bedingungen im Labor erforscht. Anschliessend wurden am Prototyp im KW Fieschertal ein Schwebstoff- und Wirkungsgradmonitoring aufgebaut. Diese werden auch nach Projektende weitergeführt. Der Materialabtrag an den Mittelschneiden und Becherausschnitten wurde mit 3D-Digitalisierungen vor und nach den Schwebstoffsaisons quantifiziert, die Reduktion der Schichtdicke in den Bechern wurden mit Schichtdickenmessungen erfasst.

Die im Vergleich zu Trübungssonden kostspieligen LISST-Geräte sind derzeit die einzigen, die nebst der SSC auch die PSD messen können. Wenn die Messung hoher SSC im Vordergrund steht, kann die einfache und kostengünstigere Methode mit der Dichtemessung (CMD) empfohlen werden. Weiter bietet sich an, ADM-Messeinrichtungen, die in vielen grösseren Wasserkraftanlagen vorhanden sind, für das Schwebstoffmonitoring zu nutzen. Diese Methode bietet den Vorteil einer Messung direkt im Triebwasserweg und sie benötigt nahezu keinen Unterhalt. Eine interessante Möglichkeit ist die Kombination von CMD mit der akustischen Methode (oder Trübungsmessung), da so auch die mittlere Partikelgrösse abgeschätzt werden kann, wenn während einer Kalibrierungsphase zusätzlich ein LISST-Gerät verwendet wird. Das SSC-Monitoring mittels Druckmessungen kommt wie die akustische Methode ohne zusätzliche Sensoren aus, bietet aber keine Vorwarnzeit. Für Informationen über die SSC mit mehr Vorwarnzeit und auch im Fall von ausgeleiteten Fassungen sind Messungen oberhalb bzw. ausserhalb der Fassung erforderlich. Dafür eignen sich günstige Eintauch-Trübungssonden, wobei zeitweise ungenaue SSC-Werte zu tolerieren sind. Für ein verlässliches Schwebstoffmonitoring sind nach wie vor Schöpfproben erforderlich, die auch mit automatischen Probenehmern genommen werden können.

Die Schwebstoffmessungen zeigten, dass die SSC und die PSD nicht stark korrelieren. Sie variieren nicht nur aufgrund von Gletscherschmelze und Regen, sondern werden auch durch den Betrieb der Kraftwerksanlage beeinflusst. In Jahren mit nennenswerten Hochwasserereignissen kann die Schwebstofffracht deutlich über dem langjährigen Mittel liegen.

Die Schichtdickenmessungen zeigten, dass die Abrasion in den Bechern in Jahren ohne grössere Hochwasser, wie erwünscht, unwesentlich ist. Relevant ist der lokale Verlust der Beschichtungen an den Mittelschneiden und Bechereintrittskanten am Ausschnitt, infolgedessen das Grundmaterial abgetragen wird und Sekundärschäden entstehen. Der Materialabtrag an diesen relevanten Stellen konnte mit der optischen Vermessung (3D-Digitalisierung) erfasst werden.

Aufgrund der Variation der Schwebstoffbelastung korreliert der Verschleiss wenig mit den Betriebsstunden oder mit saisonal typischen SSC. Wie die Messungen zeigten, hängt der Verschleiss auch nicht nur von der Schwebstofffracht, sondern stark vom anfänglichen Zustand eines Laufrads (Geometrie der Mittelschneiden und Bechereintrittskanten vor einer Belastungsperiode) sowie vom Abtrag der Beschichtung ab.

Mit Sliding-Needle-Indexwirkungsgradmessungen konnten die Wirkungsgradänderungen quantifiziert werden. Um den Messaufwand und die Beeinträchtigung des Anlagenbetriebs weiter zu reduzieren, wurde eine Methode für das kontinuierliche Wirkungsgradmonitoring entwickelt, welche eine höhere zeitliche Auflösung aufweist. Nebst Wirkungsgradabnahmen um bis zu 1.0 % infolge des hydro-abrasiven Verschleisses wurde auch eine Zunahme von bis zu 0.5 % infolge Schleifens der Mittelschneiden gemessen. Wie der Verschleiss korrelieren die Wirkungsgradabnahmen wenig mit den Betriebsstunden oder der Schwebstofffracht. Vielmehr ist die anfängliche hydraulische Kontur des Laufrads wichtig. Da es kaum möglich ist, Wirkungsgradänderungen infolge Abnutzungen oder Revisionsmassnahmen quantitativ vorherzusagen, sind Messungen erforderlich, welche die Grundlage für Wirtschaftlichkeitsüberlegungen bilden. Die kontinuierliche Wirkungsgradüberwachung erlaubt es dem Betreiber, Revisionsarbeiten bezüglich deren Wirtschaftlichkeit zu bewerten.

Das Beispiel des Hochwassers vom Juli 2012 zeigte, dass es deutlich wirtschaftlich sein kann, das Turbinieren während starker Schwebstoffbelastung vorübergehend einzustellen. Mit einer vereinfachten Berechnung wurde am Beispiel des KW Fieschertal eine Abschaltkonzentration von rund 10 g/l ermittelt.

8. Ausblick

Das in diesem Artikel beschriebene Forschungsprojekt bildet den Schwerpunkt der Dissertation von *David Felix*, welche gegen Ende 2016 publiziert werden soll. Weitere Resultate aus diesem Projekt werden in einem Workshop im Rahmen des IAHR-Symposiums on Hydraulic Machinery and Systems am 06. Juli 2016 in Grenoble präsentiert.

Die in diesem Projekt gewonnenen Daten bezüglich Schwebstoffbelastung, Turbinenabrasion und Wirkungsgradveränderungen können genutzt werden, um Berechnungsansätze, insbesondere Abrasionsmodelle zur Vorhersage von Turbinenverschleiss, und numerische Modelle zu kalibrieren bzw. weiterzuentwickeln. Dabei sind der Turbinentyp, die beanspruchte Stelle innerhalb der Turbine und das Zusammenwirken von Beschichtung und Grundmaterial gegenüber früheren Untersuchungen stärker zu berücksichtigen. In Ergänzung zur Weiterführung der Untersuchungen am KW Fieschertal sind detaillierte Messkampagnen an weiteren von hydro-abrasivem Verschleiss betroffenen Anlagen wünschenswert. Da in Prototypuntersuchungen die Partikelparameter (v. a. die PSD) nicht kontrolliert und unabhängig variiert werden können und Verschleissmessungen mit hoher zeitlicher Auflösung vom Kraftwerksbetrieb her nicht möglich sind, sind nebst Messungen an Kraftwerksanlagen weitere, möglichst realitätsnahe Laboruntersuchungen zu Abrasion an Turbinenbauteilen erforderlich. Dabei sind nichtlineare Schadensverläufe und das mögliche Zusammenwirken von Abrasion und Kavitation eine besondere Herausforderung.

Die untersuchten und weiterentwickelten Messmethoden können in der Praxis eingesetzt werden. Aus einer Palette von Schwebstoffmessgeräten kann eine fallweise passende Kombination ausgewählt werden. Schwebstoffmessungen und das 3D-Digitalisieren können Kraftwerksbetreibern und Turbinenherstellern dazu dienen, Unterhaltsmassnahmen zu optimieren und festzustellen, ob Spezifikationen und Vertragsbestimmungen bezüglich hydro-abrasiven Verschleisses und Kavitation erfüllt wurden.

Verbesserte Kenntnisse über den hydro-abrasiven Verschleiss, dessen Ursachen und Auswirkungen sowie Gegenmassnahmen tragen dazu bei, den Entwurf, den Betrieb und den Unterhalt von Hoch- und Mitteldruckwasserkraftanlagen an sedimentreichen Gewässern zu optimieren. Dies trägt zur Steigerung der Wirtschaftlichkeit und der Effizienz der Wasserkraftnutzung bei.

Kosten- bzw. Ertragspositionen	**CHF**
Erzeugungsverlust während ca. 16 h Stillstand in Volllastzeit (64 MW, Annahme 55 CHF/MWh)	–60 000.–
Vermiedene Reparaturkosten für beide MG (Schätzung)	+200 000.–
Vermiedener Produktionsausfall infolge weniger reduziertem Wirkungsgrad (Schätzung)	+30 000.–
Vermiedener Erzeugungsverlust für Laufradtausch während Volllastzeit (1 MG, 17 h)	+30 000.–
Strafgebühr/Pönale für starke Abweichung der Produktion vom angemeldeten Sollwert	evtl.
Total (ohne allfällige Pönale)	**+200 000.–**

Tabelle 3. Das wirtschaftliche Potenzial einer vorübergehenden Ausserbetriebnahme des KW Fieschertal am Beispiel des Hochwasserereignisses vom Juli 2012.

Verdankung

Das Forschungsprojekt wurde bzw. wird durch *swisselectric research*, das *Schweizer Bundesamt für Energie (BFE)* und die *Gommerkraftwerke AG (gkw)* finanziell unterstützt. Von den Firmen *Sigrist Photometer, Endress+Hauser* und *Rittmeyer* wurden Schwebstoffmessgeräte leihweise zur Verfügung gestellt. Weiter wurde die Erarbeitung dieser Publikation durch den Forschungsfonds des *Schweizerischen Talsperrenkomitees* gefördert. Die Autoren bedanken sich bei allen Projektbeteiligten für ihr Engagement und für die Unterstützung bei der Durchführung der Labor- und Felduntersuchungen.

Literatur

Abgottspon, A., Staubli, T. (2008). Index Tests of a Francis Unit using the Sliding Gate Method. Proc. 7th Intl. Conf. on Hydraulic Efficiency Measurements, IGHEM, Milano.

Abgottspon, A., Stern, P., Staubli, T., Felix, D., Winkler, K. (2013). Measuring Turbine Abrasion and Efficiency Decrease: First Results of the Case Study at HPP Fieschertal. Proc. Hydro 2013, Innsbruck, Austria: paper no. 18.05.

Abgottspon, A., Staubli, T., Felix, D., Albayrak, I., Boes, R. M. (2014). Monitoring Suspended Se-

diment and Turbine Efficiency. Hydro Review Worldwide 22(4): 28–36.
Agrawal, Y. C., Pottsmith, H. C. (2000). Instruments for particle size and settling velocity observations in sediment transport. Mar. Geol. 168: 89–114.
Agrawal, Y. C., Whitmire, A., Mikkelsen, O. A., Pottsmith, H. C. (2008). Light scattering by random shaped particles and consequences on measuring suspended sediments by laser diffraction. J. Geophys. Res. 113, C04023.
Almquist, C. W., March, P. A., Pearson, H. S., Fransen, H. W., Whitehead, B.H. (1995). The Sliding Gate Method for Hydroturbine Efficiency Testing. Proc. WaterPower 95, American Society of Civil Engineers, New York: 793–801.
Bajracharya, T. R., Acharya, B., Joshi, C. B., Saini, R. P., Dahlhaug, O. G. (2008). Sand erosion of Pelton turbine nozzles and buckets: A case study of Chilime Hydropower Plant. Wear 264(3-4): 177–184.
Bishwakarma, M. B., Støle, H. (2008). Real-time sediment monitoring in hydropower plants. J. Hydr. Res. 46(2): 282–288.
Boes, R. (2010). Kontinuierliche Messung von Schwebstoffkonzentration und -korngrössenverteilung im Triebwasser und Quantifizierung der Hydroabrasion an einer Peltonturbine. «Wasser Energie Luft» 102(2): 101–107.
Boes, R. M., Felix, D., Albayrak, I. (2013). Schwebstoffmonitoring zum verschleissoptimierten Betrieb von Hochdruck-Wasserkraftanlagen. «Wasser Energie Luft» 105(1): 35–42.
Brekke, H., Wu, Y. L., Cai, B. Y. (2002). Design of Hydraulic Machinery Working in Sand Laden Water. In Duan C. G. und Karelin V. Y. (eds.), Abrasive Erosion & Corrosion of Hydraulic Machinery (pp. 155–233). London: Imperial College Press.
Cateni, A., Magri, L., Grego, G. (2008). Optimization of Hydro Power Plants Performance – Importance of rehabilitation and maintenance in particular for the runner profiles. Proc. 7th Intl. Conf. on Hydraulic Efficiency Measurements, IGHEM, Milano.
Costa, L. I., Storti, G., Lüscher, B., Gruber, P., Staubli, T. (2012). Influence of solid particle parameters on the sound speed and attenuation of pulses in ADM. J. of Hydrologic Eng. 17(10): 1084–1092.
DWA (2006). Entlandung von Stauräumen. Deutsche Vereinigung für Wasserwirtschaft, Abwasser und Abfall e.V., Hennef, Deutschland.
Felix, D., Albayrak, I., Boes, R.M., Abgottspon, A., Deschwanden, F., Gruber, P. (2013a). Measuring Suspended Sediment: Results of the first Year of the Case Study at HPP Fieschertal in the Swiss Alps. Proc. Hydro 2013, Innsbruck, Austria: paper no. 18.03.
Felix, D., Albayrak, I., Boes, R. M. (2013b). Laboratory investigation on measuring suspended sediment by portable laser diffractometer (LISST) focusing on particle shape. Geomarine Letters 33(6): 485–498.
Felix, D., Albayrak, I., Boes, R. M. (2014). Variation des Feinsedimentgehalts im Triebwasser infolge Speicherstollenbewirtschaftung. VAW-Mitteilungen 227, Boes R. (ed.), ETH Zürich: 183–193.
Grein, H., Krause, M. (1994). Research and Prevention of Hydroabrasive Wear. Proc. 17th IAHR Symposium on Hydraulic Machinery. Beijing, China.
Gummer, J. H. (2009). Combating Silt Erosion in Hydraulic Turbines. Hydro Review Worldwide 17(1).
Hassler, P., Schnablegger, W. (2006). Pelton runner maintenance and its results at Verbund-Austrian Hydro Power AG. Proc. 14th Intl. Seminar on Hydropower Plants, Doujak E. (ed.), Vienna, Austria: 445–454.
IEC 62364 (2013). Guide for dealing with hydro-abrasive erosion in Kaplan, Francis, and Pelton turbines. International Electrotechnical Commission, Geneva.
Kalberer, A. (1988). Erfahrungen mit neuartigen Beschichtungen im Wasserturbinenbau. Intl. Symposium über Erosion, Abrasion und Kavitation im Wasserbau. VAW-Mitteilungen 100, Vischer D. (ed.), ETH Zürich: 245–258.
Lazzaro, B., Rossi, G. (1995). Effetti del deterioramento sulle prestazioni delle macchine idrauliche. L'Energia elettrica. Associazione elettrotecnica ed elettronica italiana, Milano. 72(4): 49–52.
Maldet, R. (2008). Pelton runner with high erosion caused by glacier sediment: assessment and measures. Proc. 15th Intl. Seminar on Hydropower Plants, Doujak E. (ed.), Vienna, Austria: 639–646.
Ortmanns, C. (2006). Entsander von Wasserkraftanlagen. VAW-Mitteilungen 193, Minor H.-E. (ed.), Diss. ETH Zürich.
Singh, M., Banerjee, J., Patel, P. L., Tiwari, H. (2013). Effect of silt erosion on Francis turbine: a case study of Maneri Bhali Stage-II, Uttarakhand, India. ISH Journal of Hydraulic Engineering 19(1): 1–10.
Strübin, P., Bussy, M. (1988). Erosionserscheinungen im Kraftwerk Mörel der Aletsch AG aus Sicht der Betriebsleitung. VAW-Mitteilungen 100, Vischer D. (ed.), ETH Zürich: 95–123.
Sulzer Hydro (1996). Ein semi-empirisches Abrasionsmodell zur Vorhersage von hydro-abrasivem Verschleiss an X5 CrNi 13/4 Stahl. Report STT.TB94.020.
Sutherland, T. F., Lane, P. M., Amos, C. L., Downing, J. (2000). The calibration of optical backscatter sensors for suspended sediment of varying darkness levels. Marine Geology 162: 587–597.
Thomann, P. (1988). Erosion an den Pelton-Rädern der Zentrale Stalden der Kraftwerke Mattmark AG. VAW-Mitteilungen 100, Vischer D. (ed.), ETH Zürich: 151–160.
Winkler, K., Dekumbis, R., Wedmark, A. (2010). Finding a way to estimate the amount of abrasion. Proc. Hydro Conference, Lisbon, Portugal.
Winkler, K., Dekumbis, R., Rentschler, M., Parkinson, E., Garcin, H. (2011). Understanding hydro-abrasive erosion. Proc. Hydro Conference, Prague, Czech Republic.
Wittmann, H., von Blanckenburg, F., Kruesmann, T., Norton, K. P., Kubik, P. W. (2007). Relation between rock uplift and denudation from cosmogenic nuclides in river sediment in the Central Alps of Switzerland. J. Geophys. Res. 112: F04010.
Wren, D., Barkdoll, B., Kuhnle, R., Derrow, R. (2000). Field Techniques for Suspended-Sediment Measurement. J. of Hydraul. Eng. 126(2): 97–104.

Anschrift der Verfasser
André Abgottspon, Prof. Dr. *Thomas Staubli*, Hochschule Luzern Technik & Architektur, Kompetenzzentrum Fluidmechanik und Hydromaschinen, CH-6048 Horw
andre.abgottspon@hslu.ch
thomas.staubli@hslu.ch
David Felix, Prof. Dr. *Robert Boes*
ETH Zürich, Versuchsanstalt für Wasserbau, Hydrologie und Glaziologie (VAW)
CH-8093 Zürich
felix@vaw.baug.ethz.ch
boes@vaw.baug.ethz.ch

Erosion of Pelton buckets and changes in turbine efficiency measured in the HPP Fieschertal

A Abgottspon[1], T Staubli[1], D Felix[2]

[1] Competence Center for Fluid Mechanics and Hydro Machines (CC FMHM), Hochschule Luzern (HSLU), Technikumstrasse 21, CH-6048 Horw, Switzerland

[2] Laboratory of Hydraulics, Hydrology and Glaciology (VAW), ETH Zurich, Hönggerbergring 26, CH-8093 Zurich, Switzerland

andre.abgottspon@hslu.ch

Abstract. Geometrical changes and material loss of Pelton turbine runners as well as changes in turbine efficiency were measured at HPP Fieschertal in Valais, Switzerland. The HPP is equipped with two horizontal axis Pelton units, with each 32 MW nominal power, 7.5 m^3/s design discharge, 515 m head and two injectors. The injectors and the buckets are hard-coated. Hydro-abrasive erosion was quantified based on repeated measurements on two runner buckets using (i) 3d-scanning and (ii) a coating thickness gauge. Changes in efficiency were measured by applying the sliding needle procedure. In addition to these periodically performed measurements, efficiency was also continuously monitored.

The highest erosion rate was measured during the first half of the sediment season 2012 including a major sediment transport event. Because the runner was not fully reconditioned at the beginning of this season, progressive damages occurred. After the event, a splitter width of 10 mm was measured, corresponding to 1.5 % of the inner bucket width. The cut-outs were eroded by up to 9 mm towards the axis. The efficiency reductions ranged from 1 % in the year with the major sediment transport event to insignificant differences in 2014, when the sediment load was small and only little hydro-abrasive erosion occurred.

1. Introduction

Hydro-abrasive erosion increases the maintenance costs, affects the turbine efficiency and leads to production losses. As basis for adequate countermeasures in design, operation and maintenance of HPPs, the knowledge on hydro-abrasive erosion needs to be improved. Relevant parameters such as particle load, dimensions and velocities, as described in IEC 62364, have to be quantified.

In an interdisciplinary project initiated by VAW of ETH Zurich and Hochschule Luzern, the problem of hydro-abrasive erosion was investigated by a case study at the existing HPP Fieschertal. The goal of the project was to contribute to a better understanding of the relations between suspended sediment load, turbine wear and efficiency losses as a basis for economic and environmental optimization. A schematic overview of the HPP Fieschertal with the investigation program is shown in [1] and [2].

This paper presents results of on-going turbine wear and efficiency measurements. Regular inspections are carried out and turbine wear is documented in detail. During inspections before and after sediment seasons, photographs are taken, the actual bucket geometry is recorded using a 3D optical scanner and the coating thickness in selected buckets is measured. The changes in turbine efficiency over time (efficiency history) are measured periodically with the sliding needle procedure and continuously by efficiency monitoring.

2. Aspects of hydro-abrasive erosion

The amount of hydro-abrasive erosion in Pelton turbines is typically determined using a set of metallic 2D templates. With such templates the difference between the actual and the original design-geometry is visualized. This method is suitable to check the shape of the inner bucket contour. The actual splitter width and the cut-out depth can be measured e.g. with a ruler. With these simple methods it is not possible to determine the mass reduction or the areal variations at the cut-out and splitter profiles.

The total mass reduction of a runner can be determined by weighing. Such measurements are reported e.g. by [3] of an uncoated Francis turbine (75 MW, mass reduction of 1500 kg in a revision cycle), or by [4] of an uncoated Pelton runner (10 MW, mass reduction of 100 kg), or by [5] and [6] of model Pelton runners with removable buckets (mass reductions of some g per bucket). The weighing method is suitable for laboratory investigations and for HPPs where runners need to be replaced. For local wear measurements, some turbine manufacturers use 3D handheld laser scanner (e.g. ExoScan) or portable coordinate measuring devices (e.g. FaroArm).

With progressive hydro-abrasive erosion the actual geometries differ increasingly from the original. Reported changes of the geometry of Pelton buckets refer to either local changes at splitters and cut-outs or to global changes in uncoated buckets in form of rough, wavy or scaled surfaces. This leads to a deterioration of the flow conditions and to efficiency reductions ([7] and [8]). On an uncoated Pelton turbine, the efficiency reduction over a sediment season can reach several percent (e.g. [9]). On an uncoated Francis turbine with hydro-abrasive erosion on guide vanes, runner blades, sealing rings and facing plates, an efficiency reduction of 4 % at the best efficiency point and of 8 % at part load was reported by [10].

Since the degradation of splitters and cut-outs is important for Pelton turbines, attempts were made to relate these geometrical changes to efficiency reductions. According to [4] and [11] the efficiency reduction can reach several percent if the splitter width increases to a few percent of the inner bucket width. For practical purposes the splitter width was used e.g. by [12] as an indicator for turbine wear. However, other investigators [13] noticed that the splitter width is not always clearly defined. They decided to measure the radial erosion of the splitter tip and demonstrated its relationship with the efficiency reduction. The efficiency decrease at uncoated Pelton turbines is more pronounced with increasing erosion: according to [14] e.g. 1.2 % in the first year and 4 % after two years without intermediate maintenance works.

Hard coating greatly contributed to reduce hydro-abrasive erosion. Coated runners have generally a slightly lower efficiency than uncoated ones but longer time intervals between overhauls (e.g. [15] and [16]).

3. Hydro-abrasive erosion measured in the HPP Fieschertal

Hydro-abrasive erosion was measured on the mounted turbine runners inside the turbine housings with the instruments listed in table 1 and described in the sections 3.1. and 3.2.

Table 1. Instruments and parameters for turbine wear measurements at HPP Fieschertal.

No.	Measuring technique	Model	Manufacturer	Derived parameters		
1	Thickness gauge based on magnetic induction	*Deltascope FMP 30*	Helmut Fischer	Coating thickness		
2	3D-digitization with optical scanning camera	*Comet L3D 5M*	Steinbichler	Splitter height Δh	Splitter width s	Cut-out depth Δd

3.1. Coating thickness

The local thickness of the coating was measured using a handheld gauge based on electromagnetic induction. The use of this technique was possible since the base material, a martensitic chrome nickel steel, is magnetic while the coating is essentially non-magnetic. 3D templates were used for the positioning of the probe at 152 measuring points in each bucket half.

Figure 1 shows a map of the coating thickness in bucket no. 1 of each machine group (MG). The iso-color surfaces were interpolated from the measurements at the black dots. These measurements were taken in April 2013 on runners which have been in operation for at least one season since the last coating in the factory. The coating thickness varied between 200 and 500 µm for MG 1. At MG 2 local damages have been repaired by on-site re-coating, which explains local thicknesses of up to 800 µm. But also without re-coating the thickness may vary considerably, as e.g. in the bucket of MG 1, where the thickness changes by up to 200 µm within a distance of 40 mm close the left contour of the bucket. This emphasizes the importance of a good reproducibility of the measuring points. Measurements in a second bucket of both MGs showed similar patterns as in the first buckets.

From the successive measurements, an area-averaged reduction of the coating thickness was evaluated. This reduction amounted to 10 µm for the sediment season of 2013 with a sediment load of 29 000 tons and to 4 µm for 2014 with a sediment load of 22 000 tons (MG 1). The reproducibility of these coating thickness difference measurements was estimated to be ±5 µm. Thus the thickness reduction of 2013 is significant while the one of 2014 lies within the band of uncertainty.

It was concluded that in absence of a major sediment transport event as in 2012, the coating in the buckets lasts for several years. In the runner which had to be replaced after the sediment event in 2012, coating thicknesses of only 50 to 100 µm were measured in the bottom region of the bucket and in the neighborhood of areas where the coating was completely removed.

Most relevant for efficiency loss is the local erosion or the splintering due to stones at the cut-outs and the splitters of the bucket. Such local erosion occurred also in years without major sediment transport events. The complete removal of the coating in these zones leads to scouring of the less resistant base material. Since the magnetic induction method is not suited for coating thickness measurements at cut-outs or splitters, an optical method was applied to quantify the erosion in these zones.

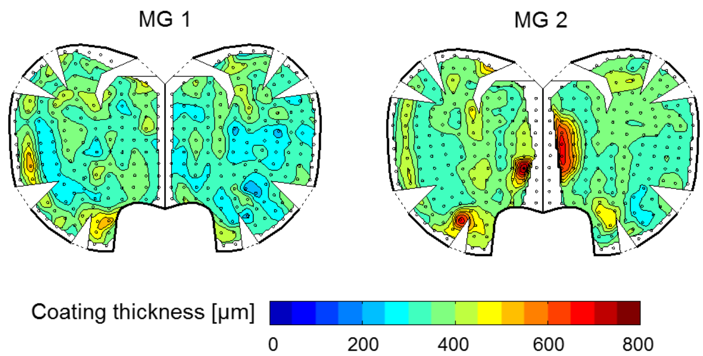

Figure 1. Maps of coating thickness in buckets no. 1 of MG 1 (left) and MG 2 (right).

3.2. 3D-digitization

Eroded or damaged splitters and cut-outs of Pelton buckets are not only relevant for efficiency, but also for secondary damages induced by local cavitation or droplet erosion. Cavitation damages are typically observed at the splitter sides or underneath the cut-out. High energy droplets arise when the jet impinges on a bluff splitter and also when the jet is interacting with an abraded cut-out. In the first case droplets hit the half buckets in their central part and in the second case droplets hit the precedent bucket [17].

The geometries of selected buckets were measured with a 3D optical scanning camera [18]. Its working principle is based on structured light projection and spatial triangulation. In order to compare the geometries of the successive measurements, a consistent and reproducible geometrical reference had to be used for the positioning of the digital geometric models (3D point clouds) of the buckets. Further information on this procedure and on the data treatment is given in [19]. Figure 2 shows an overlay of the measured geometries of two digitized buckets before and after the sediment season 2012 in topview in the zone of the cut-outs. Erosion occurred mainly in the centre part of the cut-outs and on the tips of the splitters. On the outer sides of the cut-outs the geometry is not altered with time.

The perfect overlay in the zones without erosion indicates a good reproducibility of the geometrical measurements with this method. The reproducibility was estimated to be better than ±0.2 mm in the zones of the splitters and the cut-outs.

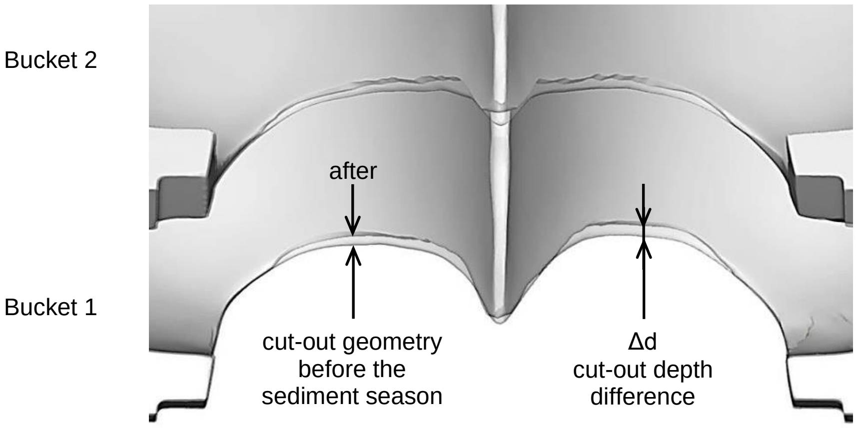

Figure 2. Overlay of the topview geometries of the cut-outs and splitter tips before and after the sediment season 2012 for MG 2.

In the lower part of figure 3 the measured contours for the cut-outs of buckets no. 1 of MG 1 are shown also in topview. In addition, the differences in cut-out depths are shown in the upper part of the figure for each sediment season. The results for the bucket no. 2 were similar.

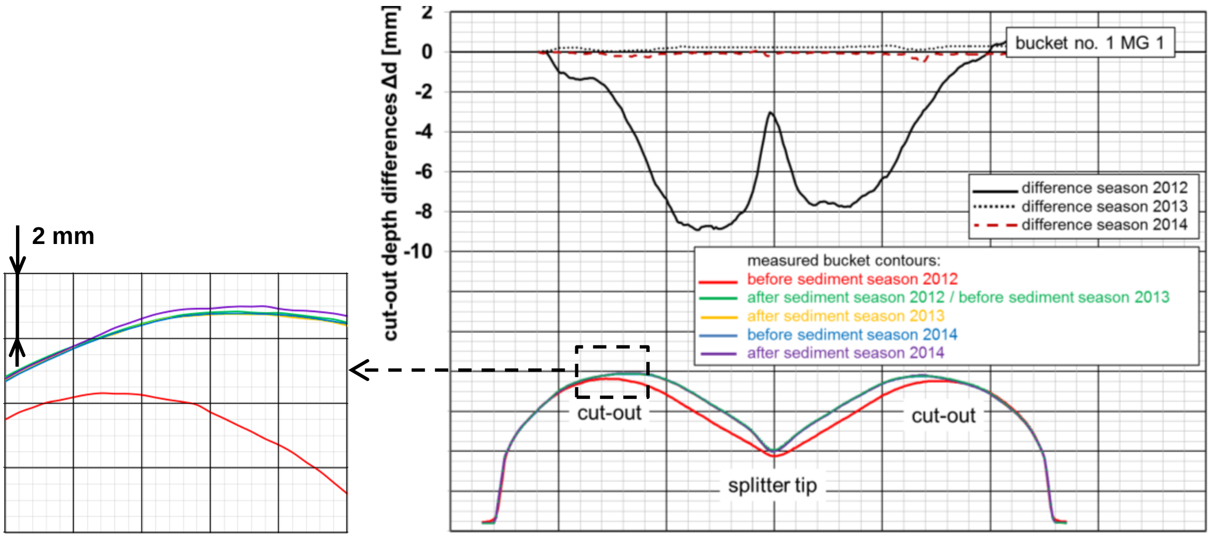

Figure 3. Topview of the cut-outs digitized at various times (with a zoom on the left) and differences (on the top) for each sediment season for bucket no. 1 of MG 1.

During the sediment season 2012 the cut-out depth increased for the bucket shown in figure 3 by up to 9 mm towards the turbine axis. This corresponds to 1.4 % of the inner bucket width (B=650 mm). Contrarily, no or very small hydro-abrasive erosion occurred in the other seasons (no detectable difference of the green, yellow, blue and purple lines). These findings are confirmed in figure 4 where for the same bucket the measured longitudinal profiles of the splitter are depicted. The resulting differences of the splitter heights for each sediment season are quantified. During the sediment season 2012 the splitter height was reduced by up to 6 mm in the middle part of the splitter. This corresponds to 0.9 % of the inner bucket width. The overlay of the lines in the zoomed details of figures 3 and 4 demonstrates the high resolution and the high degree of details of the measurement method used.

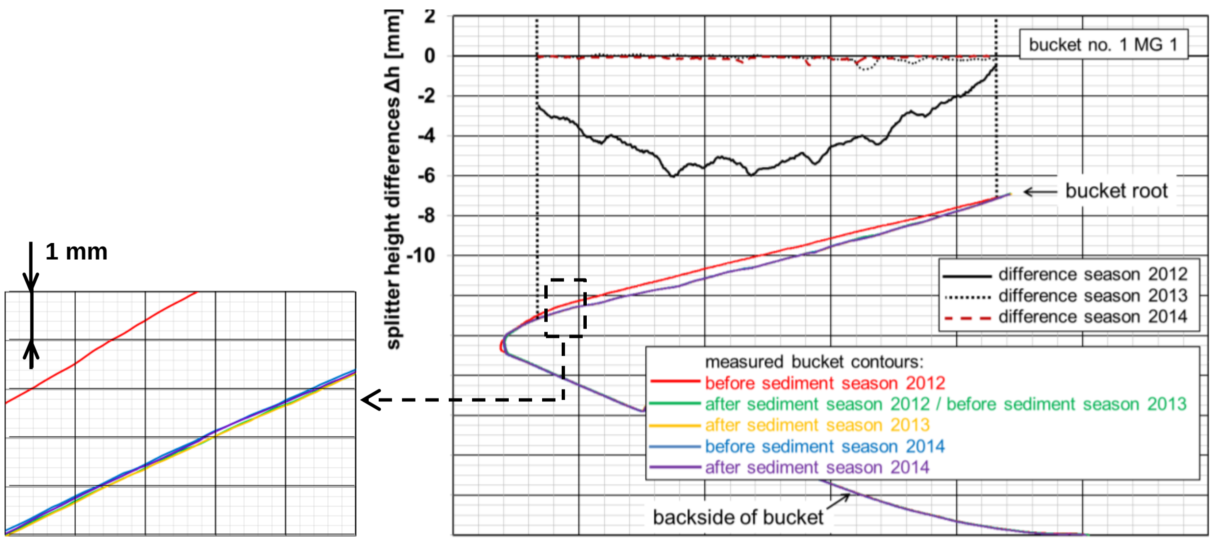

Figure 4. Side view of the splitters digitized at various times (with a zoom on the left) and differences (on the top) for each sediment season for bucket no. 1 of MG 1

Figure 5 shows the measured cross sections through the splitters of the buckets no. 1 of each MG. The sections are located at half of the splitter length. Always the same runner was installed in MG 1 in the years from 2012 to 2014. Due to heavy hydro-abrasive erosion in the year 2012 and the maintenance works afterwards, the splitter at MG 1 was widened and rounded. During the following two years it remained practically unchanged. At MG 2 the splitter was already relatively wide at the beginning of the sediment season 2012. The splitter was further widened in part of the year 2012. After the major sediment transport event the runner was taken out of operation in August 2012. Although the reductions of the splitter heights at MG 1 and 2 were similar, more material was eroded at MG 2 because of the wider splitter.

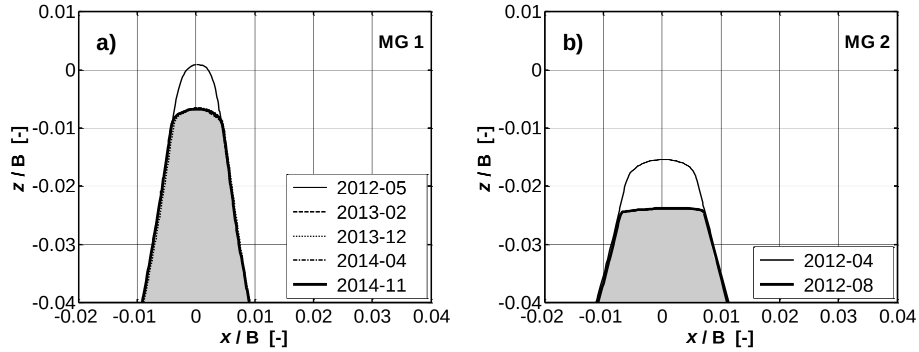

Figure 5. Splitter cross sections of buckets no. 1 at various stages of erosion and maintenance works: a) MG 1 and b) MG 2; coordinates are normalized by the inner bucket width B.

3.3. Correlation of turbine wear with sediment load

Figure 6 shows the variation of height and width of the splitter as well as the increase of the cut-out depth for both MGs as a function of their cumulated sediment loads. Displayed are the averaged values for bucket no. 1 and no. 2. As mentioned before, always the same runner was installed in MG 1 since 2012. In MG 2 three different runners were installed during the same period for which reason the lines are interrupted. A first runner exchange was necessary after the major sediment transport event of 2012. The second runner replacement became necessary due to a crack at the bucket root, unrelatedly to hydro-abrasive erosion.

In the course of the sediment season 2012 the coating in the zones of the splitters and the cut-outs of both MGs was completely removed by hydro-abrasive erosion. The successive erosion led to considerable loss of base material. At MG 1, the splitter was widened by about 3 mm and its height was reduced by 6.5 mm after a sediment load of 60 000 tons. In contrast, only very local removal of the coating was observed during the sediment seasons of 2013 and 2014 and no changes in splitter and cut-out geometries were measured. At MG 2, the initial splitter width was more than twice that of MG 1. This led to serious secondary damages and the runner had to be replaced after the major sediment transport event, in spite of a 30 % lower sediment load compared to MG 1, where no runner exchange was required. This demonstrates that the status of a runner before exposure to high sediment loads is essential for the arising amount of erosion.

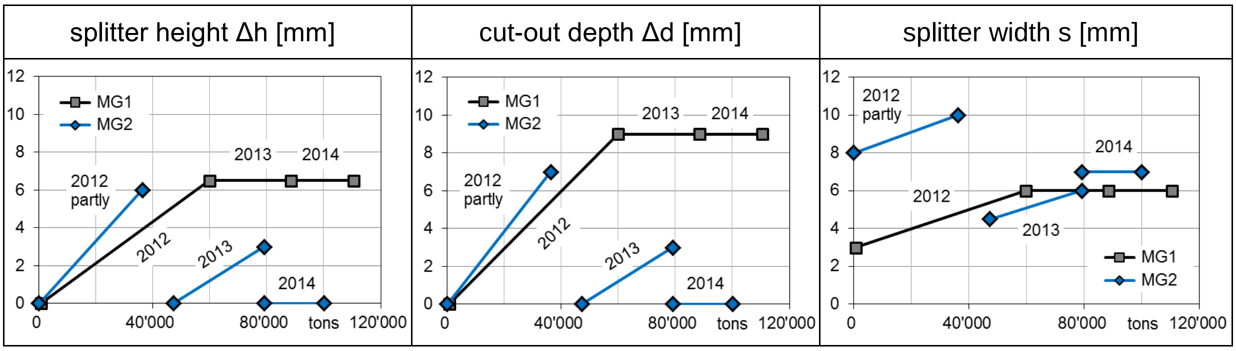

Figure 6. Histories of splitter and cut-out geometries as a function of the cumulated sediment load per MG in the HPP Fieschertal.

4. Monitoring turbine efficiency in the HPP Fieschertal

The quantities listed in table 2 were measured with a data acquisition system independently from the HPP's control system. These quantities were then used to calculate and monitor the turbine efficiency.

Table 2. Quantities and instruments for turbine efficiency measurements in the HPP Fieschertal.

No.	Measured quantities	Model	Manufacturer	Derived parameters
1	Static pressures	*gauge 2088*	Rosemount	Net heads
2	Head water level	*differential 1151*	Rosemount	Checking of pressure measurements
3	Discharge in the penstock	*Prosonic 93 PA2*	Endress+Hauser	Discharge of both MGs
4	Needle strokes	*Kinax WT707*	Camille Bauer	Discharge per MG
5	Generators active power	*Sineax M563*	Camille Bauer	Electric outputs

4.1. Sliding needle efficiency measurements

For comparative measurements of efficiency it is not necessary to know the absolute value of efficiency. Comparisons are possible based on index efficiency tests. The reference - a quantity proportional to the true discharge - must be well reproducible over time. A periodical determination of efficiency curves as a function of flow rate or power allows supervising the changes in efficiency. In the HPP Fieschertal only minor variations of head (less than 1 %) occur what facilitates such efficiency comparisons. In plants with high sediment loads, pressure taps have to be flushed on a regular basis. While this is less critical for head measurements, the measurements of an index flow rate based on pressure difference measurements, e.g. with a Venturi meter, becomes unfeasible in case of high sediment loads. Flow meters such as magnetic inductive meters or acoustic meters based on transit time measurements avoid such problems.

During the employed sliding needle procedure, the needle was opened continuously starting from a small opening – and after reaching full load – it was closed again continuously. The test duration was approximately one hour. The sliding needle procedure of Pelton turbines corresponds to the sliding gate procedure of Kaplan and Francis turbines first described by [20]. In both procedures an actuator increases and decreases the flow rate. Reliable measurements require quasi-steady conditions in the plant. An overview on this type of measurements is given by [21]. The sliding needle procedure can be performed in a much shorter time than a set of classical single point efficiency measurements. From the evaluated efficiency curve of each sliding needle measurement a weighted efficiency was calculated. The temporal evolution – the history – of this weighted efficiency shows the actual status of the runner as given in figure 7.

4.2. Continous efficiency monitoring

For an optimum operation of a plant with more than one MG it is important to monitor efficiency with good temporal resolution. Although the sliding needle procedure interferes during only one hour with the normal operation of the plant, such an operation constraint is undesirable especially during periods with full load operation. For this reason a procedure was developed to enable continuous evaluation of an averaged efficiency during normal operation.

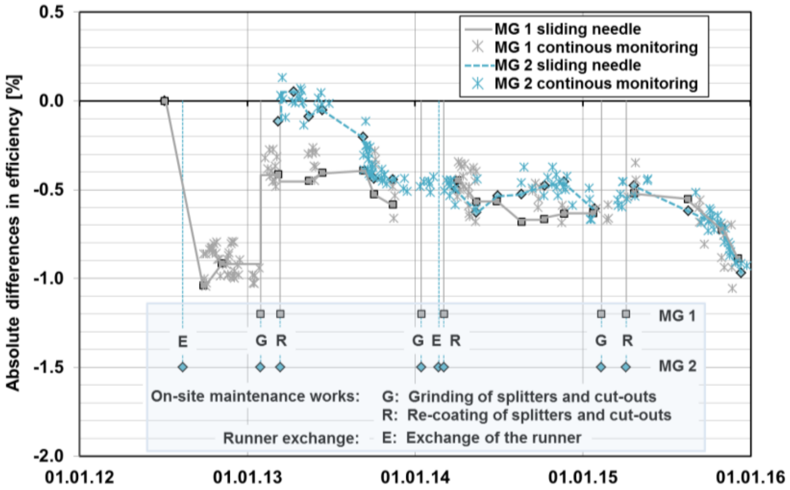

Figure 7. Efficiency history obtained from the sliding needle procedure compared with the continuous efficiency monitoring and remarks on maintenance works and runner exchanges.

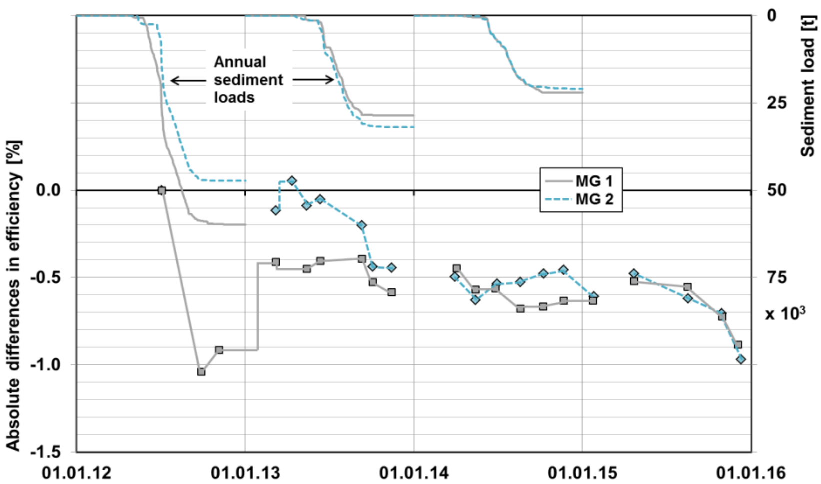

Figure 8. Comparison of the measured efficiency differences (primary axis) with the annual sediment loads (secondary axis) for MG 1 and 2.

For continuous monitoring, data are recorded at 1 Hz, as for the sliding needle measurements. For each set of sampled data efficiency is evaluated. The scatter of these efficiencies is relatively high and a daily averaged difference to a reference curve from a sliding needle measurement is evaluated in steady state conditions. The history of such data is displayed in figure 7 and the larger scatter compared to the sliding needle data is obvious. This scatter was reduced by sophisticated data processing, elimination of outliers and filtering. Further it was necessary to introduce plausibility tests to check the individual measuring quantities, especially the pressure measurements. Pressure data were compared to calculated pressures, evaluated from head water level measurements considering the head losses in the penstock. Figure 7 shows the index efficiency history for both MGs for a period of four

years from 2012 to 2015. The points which are connected by lines show the history evaluated from the sliding needle procedure. The crosses indicate the results from the continuous efficiency monitoring. The maintenance works carried out are marked as well.
In the second part of the sediment season 2012 an efficiency loss of 1 % was measured after 1902 operating hours at MG 1. The main cause for this efficiency loss is the major sediment transport event of July 2012. In the winter 2012 / 2013 the splitters and cut-outs were grinded and rounded. This led to a measured increase in efficiency of 0.56 %. In the year 2014 the measured efficiency reduction of MG 1 was only 0.14% after 3048 operating hours. Two further grinding and re-coating actions after the sediment seasons 2013 and 2014 did not lead to significant increases in efficiency. Efficiency benefits of on-site maintenance works depend on the erosion status of the runner.
Figure 8 shows the comparison of the efficiency histories and the sediment loads [22] for the three years from 2012 to 2014. The on-site grinding and re-coating for the MG 1 before the season 2013 led to slowed efficiency losses over the season. Although both MGs were exposed to a similar annual sediment load, MG 2 had a higher efficiency loss (-0.30 %) than MG 1 (-0.12 %). The initial status of a runner at the beginning of a sediment season is essential and this knowledge is most important for an estimated prediction of efficiency losses.

4.3. Correlation of turbine efficiency with sediment load

For each sediment season and each runner the efficiency changes are displayed in figure 9. The shown efficiency differences are taken from the efficiency data of figure 8. The estimated reproducibility is ±0.2 %. In this range the results should not be over-interpreted; especially the small increase of efficiency is questionable.
No efficiency difference is available for MG 2 in the year 2012, since the runner had to be replaced unexpectedly after the major sediment transport event. For MG 1 one observes for similar cumulated sediment loads of about 30 000 tons efficiency differences of -1.0 and -0.1 % in a part of the year 2012 and in the year 2014, respectively. This corresponds to a factor of ten, from what can be concluded that the sediment load alone is not suited for explanation and prediction of efficiency losses.

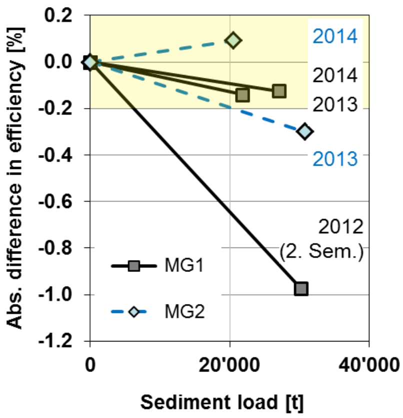

Figure 9. Comparison of the measured efficiency differences with the sediment loads per MG and year at HPP Fieschertal.

4.4. Correlation of turbine efficiency with turbine wear

As mentioned in section 2, the erosion at splitters and cut-outs is a main reason for efficiency reduction in a Pelton turbine. At HPP Fieschertal, with an inner bucket width of B=650 mm, the following values are available from the measurements:

- At MG 1, in part of the sediment season 2012: The splitter width increased from 3 to 6 mm, i.e. 0.5 % to 0.9 % of B, while the efficiency was reduced by 1.0 %.
- At MG 2, in the sediment season 2013: The splitter width increased from 4.5 to 6 mm, i.e. 0.7 % to 0.9 % of B, while the efficiency was reduced by 0.3 %.

The measurements confirm the positive correlation between increase of relative splitter width and turbine efficiency reduction. In contrast to smaller Pelton runners, the changes in relative splitter width and efficiency were relatively small in the present study. No quantitative correlation between splitter width and efficiency decrease can be determined, since the number of observations is yet too small and the splitter width is not the only influencing parameter. Although the measured efficiency reductions were in maximum 1 %, they are economically important. Since turbine wear cannot be monitored continuously and the amounts of related efficiency changes are not well predictable, efficiency monitoring is important for an economically optimized operation of HPPs.

5. Conclusions

Coating thickness reductions, material losses at splitters and cut-outs, as well as the associated efficiency losses were successfully measured in the HPP Fieschertal. From the coating thickness measurements in the buckets it was concluded that in years without a major sediment transport event the reduction of the coating thickness is immaterial. Relevant, however, is the coating removal on the splitters and the cut-outs and the successive scour of base material. In order to quantify this material removal, a 3D optical scanning camera was employed. From the geometrical 3D models dimensional changes and local mass losses were determined with sufficient accuracy.

From the sediment load measurements carried out in parallel it was concluded that the measured erosion correlates only to a minor degree with the sediment load. A higher degree of correlation is to be expected for new and uncoated runners. In the present study the erosion was highly dependent on the initial status of the splitters and cut-outs of each runner before the sediment season.

Efficiency changes were quantified using the sliding needle procedure. The results were confirmed by the continuous efficiency monitoring. The highest observed efficiency loss amounted to 1 % in the first part of the sediment season 2012 with the effects of a major sediment transport event. Besides efficiency reductions due to hydro-abrasive erosion, also effects of maintenance works were quantified. In one case an efficiency increase of 0.6 % due to grinding (rounding) of the splitters and the cut-outs was measured.

As was observed for the erosion, also the measured efficiency losses correlated only to a minor degree with the operating hours or the sediment load. The actual hydraulic contour at the beginning of each sediment season was again identified as the dominant influencing factor. Since no tools are available to estimate efficiency deficits of eroded buckets or the efficiency benefits of turbine maintenance works, periodically performed or continuous measurements of efficiency are needed.

The use of measurement techniques shown in this paper can provide a sound economic basis for HPP operators and turbine manufactures for an optimum planning of turbine maintenance works. The methods might also be useful to improve the formulation of specifications and for checking of guaranteed maximum mass losses due to hydro-abrasive erosion and cavitation. The correlations between sediment load, turbine wear and efficiency losses, however, are site-specific and depend on local conditions (e.g. particle properties), on the design characteristics and on the mode of operation of the turbines.

Acknowledgements

The support of this research project by swisselectric research, the Swiss Federal Office of Energy (SFOE) and the HPP operator Gommerkraftwerke AG is gratefully acknowledged. Further thanks go to Endress+Hauser, Sigrist Photometers and Rittmeyer for lending measuring equipment as well as to collaborators of VAW/ETH Zurich, Hochschule Luzern and the other project partners for the support.

References

[1] Felix D, Albayrak I, Boes R M, Abgottspon A, Deschwanden F and Gruber P 2013. Measuring Suspended Sediment: Results of the first Year of the Case Study at HPP Fieschertal in the Swiss Alps. *Proc.* Hydro 2013, Innsbruck, Austria: paper 18.03

[2] Felix D, Albayrak I, Abgottspon A and Boes R M 2016. Real-time measurements of suspended sediment concentration and particle size using five techniques. *Proc.* 28th IAHR Symposium on Hydraulic Machinery and Systems, Grenoble, France, IOP Conf. Series

[3] Singh M, Banerjee J, Patel P L and Tiwari H 2013. Effect of silt erosion on Francis turbine: a

case study of Maneri Bhali Stage-II, Uttarakhand, India. *ISH J. of Hydraul. Eng.* 19(1): 1-10
[4] Maldet R 2008. Pelton runner with high erosion caused by glacier sediment: assessment and measures. *Proc.* 15th Intl. Seminar on HPPs, Doujak E (ed.), Vienna, Austria: 639-646
[5] Rai A K, Kumar A and Staubli T 2015. Developing a test rig to measure hydro-abrasive erosion in Pelton turbine. *Proc.* Intl. Conf. on Hydropower for Sustainable Development, Dehradun, India: 535 - 547
[6] Padhy M K and Saini R P 2011. Study of silt erosion on performance of a Pelton turbine. *Energy*, 36(1): 141–147
[7] Cateni A, Magri L and Grego G 2008. Optimization of Hydro Power Plants Performance – Importance of rehabilitation and maintenance in particular for the runner profiles. *Proc.* 7th Intl. Conf. on Hydraulic Efficiency Measurements, IGHEM, Milano, Italy
[8] Lazzaro B and Rossi G 1995. Effetti del deterioramento sulle prestazioni delle macchine idrauliche (Effects of wear on the performance of hydraulic machines). *L' Energia elettrica*. Associazione elettrotecnica ed elettronica italiana, Milano: 72(4): 49-52 (in Italian)
[9] Strübin P and Bussy M 1988. Erosionserscheinungen im Kraftwerk Mörel der Aletsch AG aus Sicht der Betriebsleitung (Erosion in HPP Mörel, Switzerland). *VAW-Mitteilung* 100, Vischer D (ed.), ETH Zurich, Switzerland: 95-123 (in German)
[10] Pradhan P M S 2004. Improving Sediment Handling in the Himalayas. OSH Research, Nepal.
[11] Brekke H, Wu Y L and Cai B Y 2002. Design of Hydraulic Machinery Working in Sand Laden Water. In Duan C G und Karelin V Y (eds.), *Abrasive Erosion & Corrosion of Hydraulic Machinery* (pp. 155-233). London: Imperial College Press
[12] Boes R 2009. Real-time monitoring of SSC and PSD in the headwater way of a high-head hydropower plant. *Proc.* 33rd IAHR Concress, Vancouver, Canada, 4037-4044
[13] Hassler P and Schnablegger W 2006. Pelton runner maintenance and its results at Verbund-Austrian Hydro Power AG. *Proc.* 14th Intl. Seminar on Hydropower Plants, Doujak E (ed.), Vienna, Austria: 445-454
[14] Bajracharya T R, Acharya B, Joshi C B, Saini R P and Dahlhaug O G 2008. Sand erosion of Pelton turbine nozzles and buckets: A case study of Chilime hydropower plant. *Wear* 264(3-4):177-184
[15] Winkler K 2014. Hydro-abrasive erosion: problems and solutions. *Proc.* 27th IAHR Symposium on Hydraulic Machinery and Systems, Montreal, Canada. IOP Conf. Series 22 052022
[16] Dahlhaug O G, Skåre P E, Mossing V and Gutierrez A 2010. Erosion resistant coatings for Francis runners and guidevanes. *Intl. J. on Hydropower & Dams*, 17(2):109-112
[17] Bachmann P, Schärer C, Staubli T and Vullioud G 1990. Experimental Flow Studies on a 1-Jet Model Pelton Turbine. *Proc.* 15th IAHR Symposium on Hydraulic Machinery and Cavitation, Belgrade, Serbia
[18] Felix D, Albayrak I, Abgottspon A, Boes R M and Gruber P 2012. Suspended Sediment and Pelton Turbine Wear Monitoring: Experimental Investigation of various Optical and Acoustic Devices and Beginning of the Case Study at HPP Fieschertal. *Proc.* 17th Intl. Seminar on Hydropower Plants, Vienna, Austria: 483-494
[19] Abgottspon A, Stern P, Staubli T, Felix D and Winkler K 2013. Measuring Turbine Abrasion and Efficiency Decrease: First Results of the Case Study at HPP Fieschertal. *Proc.* Hydro 2013, Innsbruck, Austria: paper 18.05
[20] Almquist C W, March P A, Pearson H S, Fransen H W and Whitehead B H 1995. The Sliding Gate Method for Hydroturbine Efficiency Testing. *Proc.* WaterPower '95, American Society of Civil Engineers, New York: 793-801
[21] Abgottspon A and Staubli T 2008. Index Tests of a Francis Unit using the Sliding Gate Method. *Proc.* 7th Intl. Conf. on Hydraulic Efficiency Measurements, IGHEM, Milano, Italy
[22] Felix D, Albayrak I, Abgottspon A and Boes R M 2016. Suspended sediment measurements and calculation of the particle load at HPP Fieschertal. *Proc.* 28th IAHR Symposium on Hydraulic Machinery and Systems, Grenoble, France, IOP Conf. Series

Hydro-abrasive erosion of hydraulic turbines caused by sediment – a century of research and development

D Felix[1], I Albayrak[1], A Abgottspon[2] and R M Boes[1]

[1] Laboratory of Hydraulics, Hydrology and Glaciology (VAW), ETH Zürich, Hönggerbergring 26, CH-8093 Zurich, Switzerland

[2] Competence Center for Fluid Mechanics and Hydro Machines (CC FMHM), Hochschule Luzern (HSLU), Technikumstrasse 21, CH-6048 Horw, Switzerland

felix@vaw.baug.ethz.ch

Abstract. Hydro-abrasive erosion of hydraulic turbines is an economically important issue due to maintenance costs and production losses, in particular at high- and medium-head run-of-river hydropower plants (HPPs) on sediment laden rivers. In this paper, research and development in this field over the last century are reviewed. Facilities for sediment exclusion, typically sand traps, as well as turbine design and materials have been improved considerably. Since the 1980s, hard-coatings have been applied on Francis and Pelton turbine parts of erosion-prone HPPs and became state-of-the-art. These measures have led to increased times between overhauls and smaller efficiency reductions. Analytical, laboratory and field investigations have contributed to a better processes understanding and quantification of sediment-related effects on turbines. More recently, progress has been made in numerical modelling of turbine erosion. To calibrate, validate and further develop prediction models, more measurements from both physical model tests in laboratories and real-scale data from HPPs are required. Significant improvements to mitigate hydro-abrasive erosion have been achieved so far and development is ongoing. A good collaboration between turbine manufacturers, HPP operators, measuring equipment suppliers, engineering consultants, and research institutes is required. This contributes to the energy- and cost-efficient use of the worldwide hydropower potential.

1. Introduction

Since the inventions of Francis, Pelton and Kaplan turbines in the years 1848, 1880 and 1913, respectively, erosion of hydraulic machines due to cavitation and/or due to solid particles has been challenging engineers involved in the design, construction, operation and maintenance of hydropower plants (HPPs). Turbine erosion due to solid particles is also termed ‘sand erosion’, ‘silt erosion’, or ‘hydro-abrasive wear’. In this paper, the term ‘hydro-abrasive erosion’ [1] is adopted.

While improvements in turbine design have contributed to reduce erosion due to cavitation, hydro-abrasive erosion has remained an economically important aspect, particularly for medium and high-head run-of-river HPPs on sediment-laden rivers. High suspended sediment concentrations (SSC) and hard mineral particles causing significant hydro-abrasive erosion are typically found in rivers in the Himalayas, the European Alps, the Andes and the Pacific Coast ranges [2].

In the present paper, the problem of hydro-abrasive erosion in Francis and mainly Pelton turbines, related research, and countermeasures having been developed for about 100 years are reviewed based on selected literature in English, German, French and Italian language.

2. Turbine erosion and its consequences

2.1. Erosion damages

For the two types of turbines used in medium- and high-head HPPs, the following parts are mainly affected by hydro-abrasive erosion [1] [2] [3] [4] [5]:

- Francis: guide vanes, facing plates and labyrinths of head covers and bottom rings, runners;
- Pelton: needle tips (cones), seat rings and heads of injectors (nozzles); runner buckets, jet deflector, protection roof of injectors; casing, grating below runner.

Early examples of pictures from eroded turbine parts are shown in figure 1. Material losses lead to increased roughness and changes in hydraulic profiles, and may affect the mechanical stability and integrity of turbine parts, the HPPs' availability, electricity generation, and eventually safety [4].

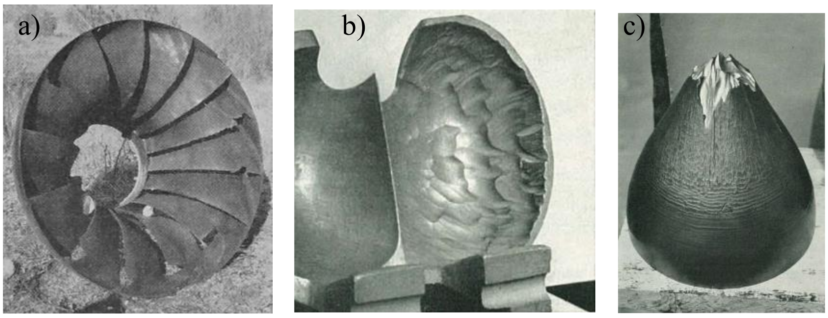

Figure 1. Examples of eroded turbine parts: **a)** Francis runner (with jammed stones) [6], **b)** Pelton bucket (left half of bucket reconstructed by welding) [7] and **c)** needle tip of a Pelton injector [7].

2.2. Efficiency reductions

An early study showing the reduction of turbine efficiency due to hydro-abrasive erosion was conducted by Dufour at HPP Klösterli, Switzerland [8] (figure 2). This HPP on a tributary of the upper Rhone

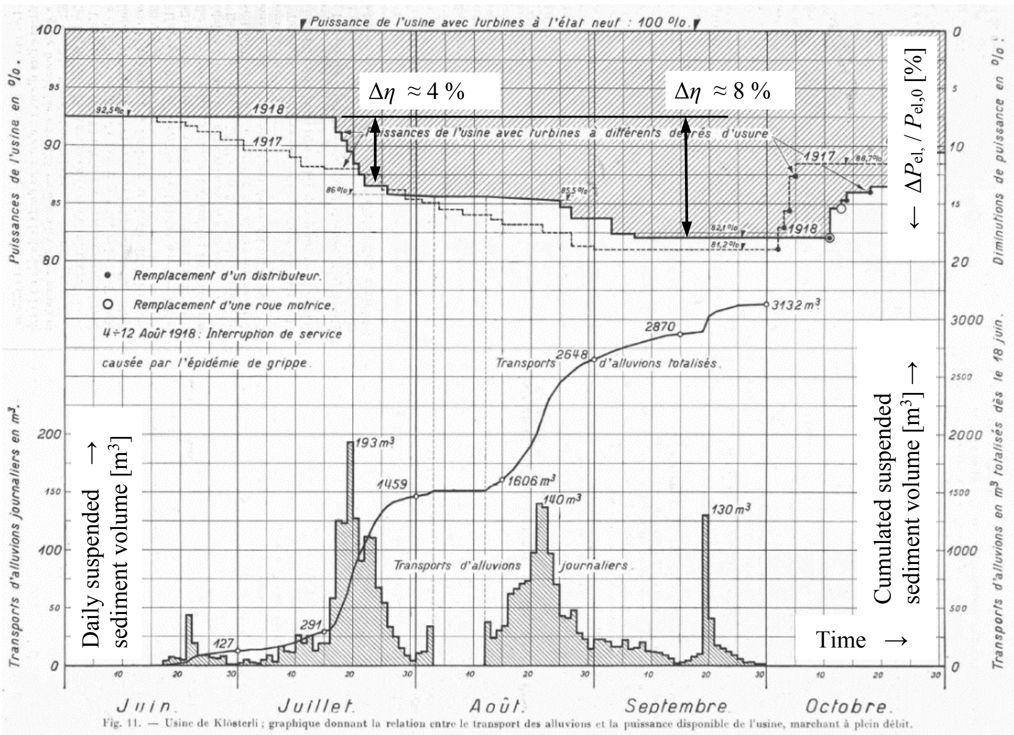

Figure 2. Time series of sediment load in the turbine water and relative changes in electric output (ΔP_{el} at design discharge compared to the output with new runners $P_{el,0}$) measured at HPP Klösterli, Switzerland, from June to October 1918 [8].

river with a design discharge of Q_d = 3 m^3/s and a head of H = 218 m, had one 2.6 MW-Pelton turbine and seven 0.4 MW-Girard turbines. Within one sediment season, the HPP's electric output at design discharge dropped by about 10 %, corresponding to an absolute efficiency reduction of about $\Delta\eta \approx 8$ % (figure 2). In particular, the efficiency dropped by about 4 % during only six days with increased sediment load. The SSC in the turbine water was on average 0.2 g/l during the observation period of 105 days and 1.3 g/l during the day with the maximum sediment transport (193 m^3 of unconsolidated sediment). Such SSC is not outstanding compared to other sediment-laden rivers, but from a today's perspective this efficiency decrease is quick and high.

3. Progress in reducing sediment load

3.1. Improving trapping efficiency and flushing systems

One of the measures to mitigate turbine erosion is to reduce the sediment load in the power waterway. To this end, facilities for partial sediment exclusion are built in the intake area at medium- and high-head HPPs with no or only small headwater storage, i.e. run-of-river HPPs.

Pioneering work in the design and improvement of sand traps was performed by Dufour [8]. He investigated the problem of turbine erosion and sediment handling at the HPP Florida-Alta (6 x 3 MW reaction turbines, H = 98 m, Q_d = 20 m^3/s) in Chile in 1911. The HPP was equipped with two upstream settling basins and manually operated flushing gates. The cross-section of the 85 m long basins increased in flow direction. Without sediment deposits, the theoretical average flow velocity in the cross section at the end of the basin was ≤ 0.08 m/s, which should allow for a reasonable settling performance. The measured SSC upstream of the basins were in the range of some g/l in the wet season, corresponding to several 1000 m^3 of sediment per day. Dufour found that the sediment evacuation from the basins was by far not sufficient and that the settling efficiency was reduced due to important sediment deposits. He proposed a new sand trap design with continuous automatic sediment evacuation and higher settling efficiency. With the new sand trap, the turbines needed revision every 8000 operating hours, whereas before they needed to be completely replaced after 2000 operating hours. Dufour's flushing system consists of a series of inclined slats between the bottom of a sand trap basin and a pressurized flushing channel below with an outlet valve.

Another early example of better sediment exclusion has been reported from the high-head HPP Ackersand (4 x 4.5 MW Pelton turbines, H = 700 m) in Switzerland [8]. With two parallel sand trap basins which were flushed intermittently, the efficiency of the turbines at design discharge dropped by 13 % during the sediment-rich year 1918. In winter, the sand trap was improved by implementing a continuous flushing system and tranquilizer racks at the inlets of the basins. After the modification of the sand trap, the efficiency drop of the turbines at design discharge was reduced to 6 % in 1919, the costs for turbine maintenance and spare parts were 70 % lower, and downtimes of the HPP were reduced by 95 %. With the improved sand trap, the turbine water contained only particles smaller than 0.5 mm (figure 3b) and the SSC in the turbine water was reduced accordingly. Before, particles up to 12 mm diameter (highlighted in figure 3a) passed the turbines, especially when the sand trap was temporarily operated at overload due to flushing of one basin with complete water level drawdown.

Further systems to evacuate sediment deposits from sand traps without water level drawdown have been developed since then, e.g. 'Bieri', '4S' (Serpent Sediment Sluicing System), 'SediCon Sluicer' and 'HSR (Hochschule Rapperswil)' [9] [10] [11]. The oldest sand trap flushing system, i.e. flushing with supercritical flow, is also still in use today. This simple system may have advantages when the water contains large quantities of fine driftwood, leaves or grass which might block advanced flushing systems. In rivers with high transport of coarse sediment, separate gravel traps upstream of sand traps may be advantageous. The following points remain important for sand trap design:

- Achieve a high trap efficiency by favorable hydraulic conditions at the inlet (geometry of the expansion, tranquilizer racks), flow guidance and avoiding of resuspension;
- Maintain a high trap efficiency by suitable flushing systems, i.e. preferably without interruption of operation, requiring only small volumes of flushing water and low maintenance.

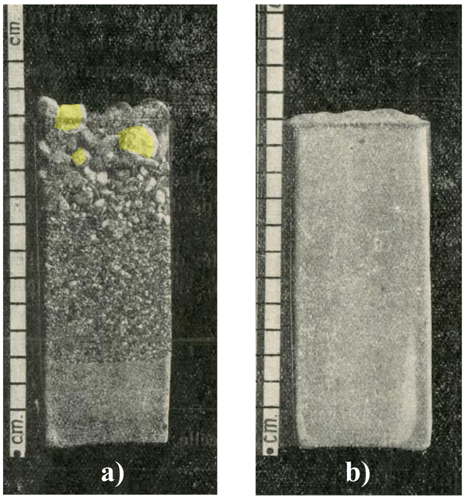

Figure 3.
Sediment sampled in the turbine water at the high-head Pelton HPP Ackersand, Switzerland in 1918/1919 [8]
a) before and
b) after improvement of the sand trap

3.2. Closing of intakes and turbine switch-offs

High sediment loads in the turbine water can be reduced not only by sediment exclusion facilities, but also with operational measures such as closing of intakes and pausing of turbine operation (switch-off) during floods or other events with high SSC and transport of larger particles. In the last decades, instruments for continuous real-time measurements of sediment levels, SSC and particle sizes have become available and have been installed in some HPPs [12] [13]. Such instruments allow for remote real-time monitoring with less effort. Decisions for HPP operation can be taken based on such sediment data, together with real-time (or forecast) weather and discharge data.

4. Progress in increasing turbine design and erosion resistance

4.1. General

In addition to reducing the sediment load, improved turbine design and increased resistance of turbine parts have contributed to mitigate turbine erosion. With well-designed geometries, cavitation is avoided for new turbine parts. Like this, not only damages due to cavitation, but also due to the synergy-effect of cavitation and hydro-abrasive erosion are avoided. However, cavitation may still occur on turbine parts with degraded hydraulic profiles.

The possibilities of increasing the erosion resistance of turbine parts are limited, because materials need to have not only high hardness, but also high toughness, resistance to fatigue and good machinability. Early turbine runners were made of cast iron. The advantages of using stainless steel were recognized and field-tested already in 1934 [4]. A martensitic stainless steel with 13 % chrome and 4 % nickel has become the standard material for hydraulic turbine parts [1]. Such steel has a Mohs hardness of 4.5 to 5. In many mountain ridges, igneous rocks are present which typically contain high percentages of harder minerals such as quartz and feldspar (Mohs hardness 7 and 6, respectively). Various surface treatments and e.g. chrome coatings were developed and tested over decades, but the progress was relatively small because the surface hardness of the turbine parts was not higher than the hardness of such mineral particles.

A significant step in the reduction of turbine erosion was the use of hard-coatings made of tungsten carbide, cobalt and chrome (WC-CoCr) [14]. This type of coating is particularly resistant to particles impinging at low angles or sliding on turbine parts [5]. Hard-coatings are applied by high velocity oxy fuel (HVOF). The quality of coatings may differ among suppliers because of the properties of the coating powder, the preparations and the spraying process. Hard-coatings have been increasingly used on Francis and Pelton turbine parts since the 1980s [15] [16] [17], and have become the state-of-the-art for Francis and Pelton turbine parts [2].

4.2. Coating of Francis turbines

In Francis turbines, coating can be applied on selected or all parts in contact with the water. An early example of a partly hard-coated Francis runner was in HPP Pradella (4 x 72 MW, H = 484 m) in Switzerland. Full coating was not possible on this medium-size high-head Francis runner, due to limited accessibility with the spray gun. Although the coating had been applied only partly, the efficiency drop was slowed down considerably.

Fully coated Francis turbines have been in operation for example at HPP Karcham Wangtoo (4 x 25 MW, H = 298 m) in India since 2011. After three monsoon seasons with SSC up to 8 g/l, the coating was removed from only about 5 % of the area [2]. Although the coating does not fully prevent erosion of the base material, the times between overhauls were extended. For relatively small coated Francis runners, whose blade surfaces are not fully accessible with the spray gun, a bolted construction is an option [18]. With this approach, the pieces of the runner are assembled after coating.

4.3. Coating of Pelton turbines

In Pelton turbines at sites with high erosion potential, hard-coating is typically applied in the buckets of runners as well as on cones and seat rings of injectors, if the injector parts are not made of other material with high resistance to erosion (e.g. steel-cobalt-alloys such as 'stellite').

Hard-coating contributed to reduce turbine erosion for example in HPP Fieschertal, Switzerland (2 x 32 MW, H = 520 m): In contrast to the earlier pronounced full-surface erosion with a scaly pattern inside uncoated buckets (similar to figure 4a), the coating inside the buckets prevented erosion of the base material (figure 4b). During a sediment season, the coating was only removed from the splitter crests and the entrance lips of the cut-outs [19]. The coating was repaired every winter directly in the turbine casing with a hand-held HVOF-spray gun, after rounding of bluntly eroded splitters and cut-out edges by grinding. Coatings sprayed on-site may have inferior quality compared to factory coatings, but runners do not need to be changed and transported. With on-site re-coating, frequent coating repairs are feasible, which contributes to limit the erosion propagation. With this maintenance strategy, measured reductions in turbine efficiencies were ≤ 1 % per sediment season in the years 2012-2014 [19].

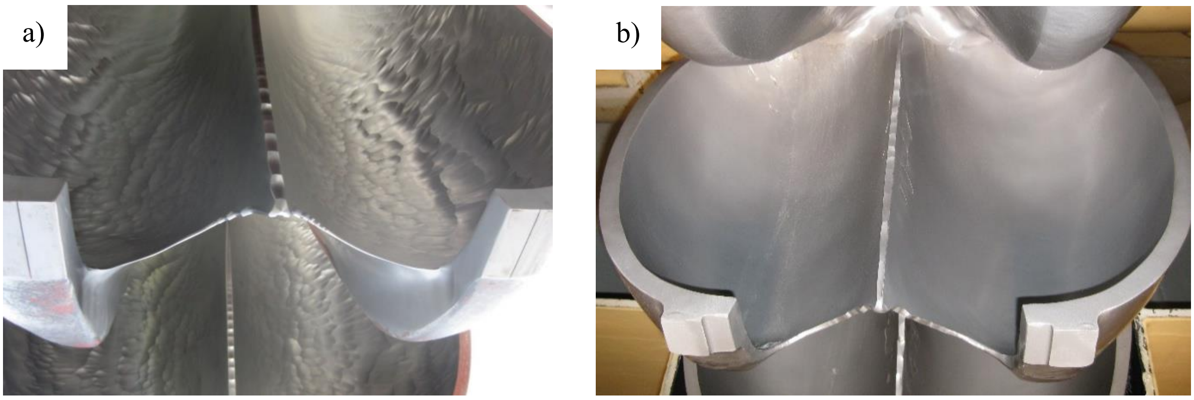

Figure 4. Pelton buckets with typical erosion: **a)** uncoated (HPP Emosson, Switzerland, runner out of service) and **b)** coated (HPP Fieschertal, Switzerland, 2012) (pictures: VAW, ETH Zürich).

In another example, at HPP Alfalfal, Chile (2 x 89 MW, H = 690 m), hard-coating also protected most of the bucket area from erosion and the coating was eroded from splitters and cut-outs. With an erosion potential higher than at HPP Fieschertal, the base material in these zones was considerably eroded and the turbine efficiency dropped by some percent during three months [2]. Although turbine erosion cannot fully be prevented in such severe conditions, hard-coating has led to tripling of the times between overhauls and the eroded steel mass has been reduced to one quarter [2].

5. Progress in research and modelling of hydro-abrasive erosion

5.1. Erosion mechanisms and analytical approaches

Bergeron (1950) [20] analytically studied hydro-abrasive erosion in centrifugal pumps and distinguished two modes of erosion by solid particles: (i) particle impact, and (ii) particle sliding along a curved wall. For (i) he postulated that the eroded mass is proportional to the difference in kinetic energy of a particle before and after the impact. For a single particle, the erosion is thus approximately proportional to the square of its relative velocity w before the impact. The number of impacts per unit time increases with w [21]. Thus, the eroded mass per unit time is approximately proportional to w^3.

For (ii), i.e. erosion due to sliding particles, Bergeron – and Bovet (1958) [7] – derived that the erosion rate is proportional to the friction power. The friction power is inversely proportional to the radius of curvature and again proportional to the third power of the relative velocity w^3.

Finnie (1960) and Bitter (1963) contributed to the theoretical understanding of these two types of erosion, which are also called erosion due to 'deformation' and due to 'cutting', respectively. Preece and Macmillan [22] reviewed the literature on erosion until 1977. An overview on erosion models has been given by Meng and Ludema (1995) [23]. Literature on erosion in hydraulic turbines has been reviewed by Truscott (1971) [24], as well as by Padhy and Saini (2008) [25].

5.2. Laboratory investigations

Several laboratory tests for the investigation of the erosion resistance of materials are described in [1]. Such tests yield the relative erosion resistance compared to a reference material. The erosion resistances obtained from various test methods may differ considerably among each other and from those in real-scale turbines. The type of erosion (angle of attack, etc.) depends also on the locations within Francis or Pelton turbines. Hence specific test setups are required to realistically investigate a certain type of turbine erosion in the laboratory. Several series of erosion tests have been conducted over decades (table 1). Such laboratory tests gave valuable insight into the effects of single parameters, e.g. SSC, relative velocity w, or angle of attack on the erosion rate. For example, velocity exponents were found to range between 2 and 4 [1] with a majority around 3 [24], which are similar to the analytical considerations mentioned above.

Table 1. Selected experimental laboratory investigations on hydro-abrasive erosion

Investigators and references	Type of test rig, velocity range	Remarks
Ilgaz 1952 [26]	Jet-type, 26 - 44 m/s	Tests on metal plates with varying angle; one of the first jet-type test rigs with sand in water found in the literature
Grein and Krause 1994 [27]	Rotating shaft, up to 80 m/s	Highly turbulent flow in gap between rotating shaft and specimens fixed on its housing; laboratory results were compared to field data (erosion depths on uncoated Pelton buckets)
Thapa 2004 [28]	Jet-type, up to 80 m/s	Tests on plates with varying angle and on specimens with a splitter and curvature, also with soft- and hard-coatings
Winkler et al. 2011 [29]	Jet-type, 40 - 85 m/s	Tests on plates and real-scale splitter specimens (with reduced jet diameter), also with hard-coatings
Grewal et al. 2013 [30]	Jet-type, 4 and 16 m/s	Tests on plates with varying angle; references given to ten other laboratory studies of erosion on 13Cr4Ni-steel

5.3. Empirical relations based on laboratory and field investigations

Nozaki (1990) [31] compiled field data on turbine erosion of HPPs in South America. He proposed a 'modified SSC' to consider the effects of particle size, shape (angularity), hardness, and the resistance of the turbine material on the erosion rate. Nozaki established outstanding diagrams from which the times between overhauls of uncoated Francis and Pelton turbine parts can be read as a function of the net head and the time-averaged modified SSC (figure 5a) [9] [32]. However, the application of the diagrams is limited because (i) it is not clear which extent of erosion or efficiency loss had been accepted until turbine overhauls, and (ii) coated turbine parts were not treated at that time.

Nozaki's diagrams have also been used to economically optimize the size of sand traps: In the example of HPP Kukule Ganga, Sri Lanka, the design particle size was varied between 0.2 mm and 0.5 mm, and the corresponding costs of (i) the construction of the sand trap and (ii) the maintenance/ replacement of the Francis turbines were estimated (figure 5b) [33]. With a moderate head of 185 m and a relatively low average SSC = 0.02 g/l, the minimum total cost was found with a design particle size of 0.3 mm, which is a typical value.

In 2013, a semi-empirical equation for prediction of erosion depths has been proposed in IEC 62364 [1] based on a literature review of various erosion models. Model parameters for uncoated Francis turbine parts were determined based on data obtained from seven HPPs mainly in China.

A few field investigations on turbine erosion in some HPPs worldwide are partly published, e.g. [12] [13] [15] [19] [34] [35] [36]. A systematic evaluation of the published data to determine parameters for erosion models is however difficult because (i) measured parameters and conditions are not always comparable, and (ii) not all required information is available.

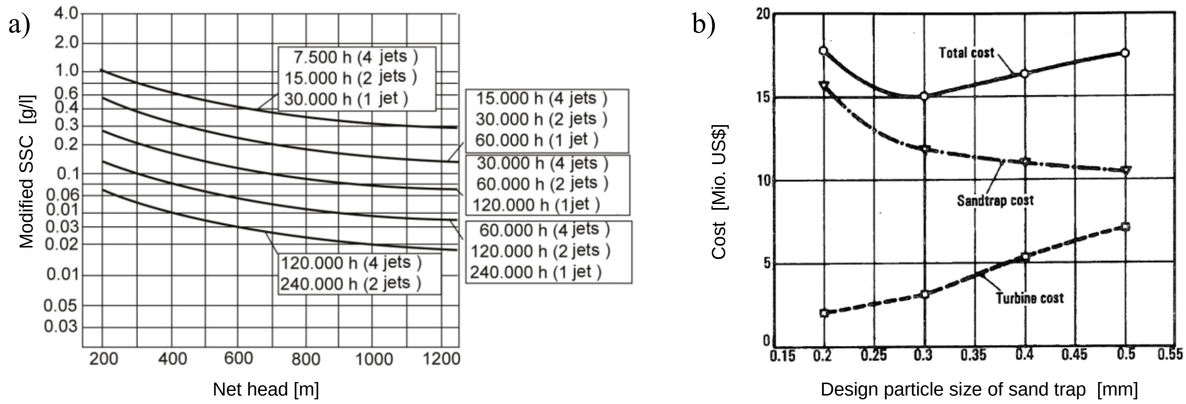

Figure 5. a) Operation hours between overhauls of uncoated Pelton runners according to Nozaki [31] (published in [32]) and **b)** Example of the determination of the limit particle size for a sand trap based on economic optimization [33].

5.4. Numerical simulations

More recently, mechanistic or semi-empirical erosion equations have been implemented in numerical simulation codes. The numerical simulation involves the determination of flow velocities (flow field) and SSC close to turbine parts. Depending on the implemented erosion model, the particle impingement rate and angle of attack, as well as the material removal are determined. This last step depends on the material properties and the behavior of the eroded material which is reflected by constitutive models.

For Francis turbines, spatially distributed relative erosion rates on runner blades have been simulated [37] [38], using the erosion model by Finnie (1960) which is summarized in [23]. In [38] the reduction of coating thickness on guide vanes and blades was also measured, but no quantitative comparison of numerically determined and measured erosion rates was presented. Numerical simulations of relative erosion rates were used to optimize the shapes of Francis runner blades [39].

For Pelton turbines, the simulation of the flow field is a particularly challenging task because of the 3d-free-surface flow (figure 6a). In addition to grid-based methods (e.g. Volume Of Fluid VOF), also mesh-free methods such as Smoothed Particle Hydrodynamics (SPH) or Finite Particle Volume Method (FPVM) have been further developed. They have been used to simulate the flow in Pelton buckets, as well as the particle movements and erosion under less complex conditions, e.g. for an inclined particle-laden jet on a stationary plate [40] [41]. The effect of particle size on the erosion of Pelton splitters was studied in [29]. Simulation showed that particles approaching directly above the splitter impinge on the splitter when they have a diameter of 80 µm (figure 6b), whereas smaller particles (20 µm) rather follow the streamlines around the splitter (figure 6c).

So far, not all processes can be simulated numerically, e.g. erosion on coated parts with local loss of coating and subsequent erosion of base material including secondary damages due to cavitation.

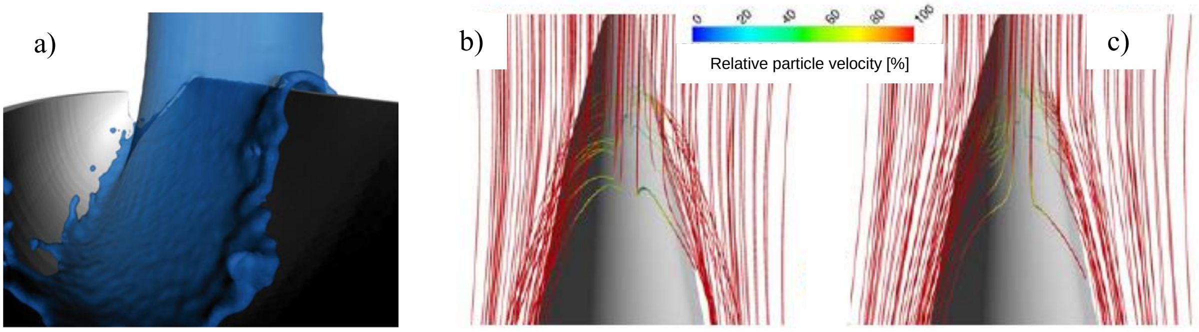

Figure 6. Examples of numerical simulation results at the splitter of a Pelton bucket: **a)** flow [40], and trajectories of particles with diameters of **b)** 80 µm and **c)** 20 µm [29].

6. Conclusions and Outlook

Hydro-abrasive erosion has been mitigated since the early 20th century by reducing the sediment load and improving turbine designs and materials, in particular by applying hard-coatings since the 1980s. Although it is not possible to fully prevent erosion damages, erosion-induced costs and electricity generation losses have been reduced.

Modelling and predicting hydro-abrasive erosion are challenging because of the many parameters involved and their complex interactions. Semi-empirical equations and numerical simulation models need calibration and validation based on data which have been and need to be acquired at HPPs and in laboratories. For the planning and design of HPPs with respect to sediment handling and mitigation of turbine erosion, operation experience remains an important source of information.

Proven measuring techniques are available for the real-time monitoring of SSC, particle sizes, turbine erosion and efficiency with high temporal resolution. Such monitoring data serve as a sound basis for decision making in operation and maintenance.

Significant improvements to mitigate hydro-abrasive erosion have been achieved so far. Further analytical, laboratory, field and numerical investigations are recommended to foster future development in this interdisciplinary field. A good collaboration between engineers and scientists working in the design and manufacturing of hydro-mechanical equipment and measuring systems, HPP operators, consultants and research institutes is required. This will contribute to further improve the energy- and cost-efficient use of the worldwide hydropower potential, also at medium- and high-head run-of-river HPPs on watercourses with high SSC and hard mineral particles.

Acknowledgements

The support of the research project [13] [19] by swisselectric research, the Swiss Federal Office of Energy (SFOE), the HPP operator Gommerkraftwerke AG as well as the Swiss Competence Center for Energy Research - Supply of Electricity (SCCER-SoE) and the Research Fund of the Swiss Committee on Dams are gratefully acknowledged. Further thanks go to Endress+Hauser, Sigrist Photometers and Rittmeyer for lending measuring equipment as well as to all members of the project team for their contributions.

References

[1] IEC 62364 2013. Guide for dealing with hydro-abrasive erosion in Kaplan, Francis, and Pelton turbines. Edition 1.0, *International Electrotechnical Commission* (IEC) Geneva, Switzerland

[2] Winkler K 2014. Hydro-abrasive erosion: problems and solutions. *Proc.* 27th IAHR Symposium on Hydraulic Machinery and Systems, Montreal, Canada. IOP Conf. Series 22 052022

[3] Neopane H P, Dahlhaug O G and Cervantes M 2011. Sediment Erosion in Hydraulic Turbines. *Global J. of researches in Engineering, Mechanical and Mechanics engineering* 11(6)

[4] Faletti N 1934. L'erosione e la corrosione delle turbine idrauliche (Erosion and corrosion of hydraulic turbines). *L'energia elettrica* 11 : 277-287 (in Italian)

[5] Gummer J H 2009. Combating Silt Erosion in Hydraulic Turbines. *Hydro Review Worldwide* 17(1)

[6] Dufour H 1936. Entkiesungs- und Entsandungsanlage der Kraftwerke Pont-de-Claix und Drac-Inférieur (Gravel and sand traps of HPPs Pont-de-Claix and Drac-Inférieur). *Schweizerische Bauzeitung* 108(12): 125-127 (in German)

[7] Bovet T 1958. Contribution à l'étude du phénomène d'érosion par frottement dans le domaine des turbines hydrauliques (Contribution to the study of abrasive erosion in hydraulic turbines). *Bulletin technique de la Suisse romande* 84(3): 37-49 (in French)

[8] Dufour H 1921. L'usure des turbines hydrauliques et ses conséquences et les moyens d'y parer (Wear of hydraulic turbines, consequences and countermeasures). Grenoble: J. Rey; also published in *La Houille Blanche* 1920(6): 233-237, 1921(1): 18-21, 1921(2): 53-56 and 1921(3): 97-104 (in French).

[9] Ortmanns C 2006. Entsander von Wasserkraftanlagen (Sand traps of HPPs). *PhD thesis*, *VAW-Mitteilung* 193 (Minor H E, ed.), ETH Zurich, Switzerland (in German)

[10] Jacobsen T and Jiménez A 2015. Recent experiences from sediment removal projects. *Proc.* Hydro Conf. Bordeaux, France

[11] Truffer B, Küttel M and Meier J 2009. Wasserfassung Titer der GKW – Entsanderabzüge System HSR in grossen Entsanderanlagen (Sand evacuation system HSR in large sand traps). *Wasser Energie Luft* 101(3): 207-208 (in German)

[12] Boes R 2009. Real-time monitoring of SSC and PSD in the headwater way of a high-head hydropower plant. *Proc.* 33rd IAHR Concress, Vancouver, Canada, 11026: 4037-4044

[13] Felix D, Albayrak I, Abgottspon A and Boes R M 2016. Real-time measurements of suspended sediment concentration and particle size using five techniques. *Proc.* 28th IAHR Symposium on Hydraulic Machinery and Systems, Grenoble, France, IOP Conf. Series

[14] Karimi A, Verdon C, Martin J L and Schmid R K 1995. Slurry erosion behaviour of thermally sprayed WC-M coatings. *Wear* 186-187: 480-486

[15] Kalberer A 1988. Erfahrungen mit neuartigen Beschichtungen im Wasserturbinenbau (experiences with new types of coatings for hydraulic turbines). In *VAW-Mitteilung* 100 (Vischer D, ed.), ETH Zürich, Switzerland: 245-258 (in German)

[16] Sidhu S S 1999. Experience of coating and successful field tests of coated guide vanes at Baira Siul HEP. In Varma C V J, Naidu B S K and Rao A R G (eds.), *Proc.* 1st Intl. Conf. on Silting Problems in Hydro Power Plants, New Delhi, India (paper no. 28). Rotterdam/ Brookfield: Balkema

[17] Engelhardt M, Schneider C and Oechsle D 2001. Real scale performance of advanced erosion protection techniques on water turbines. In Kaushish S P and Naidu B S K (eds.), *Proc. 2nd Intl. Conf. on Silting Problems in HPPs*, Bangkok, Thailand: 168-175

[18] Dahlhaug O G, Skåre P E, Mossing V and Gutierrez A 2010. Erosion resistant coatings for Francis runners and guidevanes. *Intl. J. on Hydropower & Dams*, 17(2):109-112

[19] Abgottspon A, Staubli T and Felix D 2016. Erosion of Pelton buckets and changes in turbine efficiency measured in the HPP Fieschertal. *Proc.* 28th IAHR Symposium on Hydraulic Machinery and Systems, Grenoble, France, IOP Conf. Series

[20] Bergeron P 1950. Similitude des usures causées par des mixtures liquide-solides (Similitude of wear caused by liquids carrying solids in suspension). *La Houille Blanche* (special issue B): 716-729 (in French)

[21] Brekke H, Wu Y L and Cai B Y 2002. Design of Hydraulic Machinery Working in Sand Laden Water. In Duan C G und Karelin V Y (eds.), *Abrasive Erosion & Corrosion of Hydraulic Machinery* (pp. 155-233). London: Imperial College Press

[22] Preece C and Macmillan N H 1977. Erosion. *Annual Review of Materials Science* 7: 95-121

[23] Meng H C and Ludema K C 1995. Wear models and predictive equations: their form and content. *Wear* 181-183: 443–457

[24] Truscott G F 1971. A literature survey on abrasive wear in hydraulic machinery. *Wear* 20: 29-50

[25] Padhy M K and Saini R P 2008. A review on silt erosion in hydro turbines. *Renewable and Sustainable Energy Reviews*, 12(7): 1974–1987

[26] Ilgaz C 1952. Etude de l'usure d'une surface plane par un jet d'eau chargé de sable (Study of the wear of a plane surface by a sand laden jet of water). *La Houille Blanche* (4): 554-566 (in French)

[27] Grein H and Krause M 1994. Research and Prevention of Hydroabrasive Wear. *Proc.* 17th IAHR Symposium on Hydraulic Machinery, Beijing, China

[28] Thapa B 2004. Sand Erosion in Hydraulic Machinery. *PhD thesis*, NTNU, Trondheim, Norway

[29] Winkler K, Dekumbis R, Rentschler M, Parkinson E and Garcin H 2011. Understanding hydro-abrasive erosion. *Proc*. Hydro Conference, Prague, Czech Republic

[30] Grewal H S, Agrawal A and Singh H 2013. Slurry erosion mechanism of hydroturbine steel: Effect of operating parameters. *Tribol Lett* 52: 287-303

[31] Nozaki T 1990. Estimation of repair cycle of turbine due to abrasion caused by suspended sand and determination of desilting basin capacity. Japan Intl. Cooperation Agency, Tokyo

[32] Ortmanns C 2006. A new design of desilting chambers of hydro power plants. *Proc.* Hydro Conf., Porto Carras, Greece

[33] Moric P 1996. Optimizing Desilting Facilities for Hydro Plants. *Intl. J. on Hydropower & Dams* 3(6): 31-35

[34] Singh M, Banerjee J, Patel P L and Tiwari H 2013. Effect of silt erosion on Francis turbine: a case study of Maneri Bhali Stage-II, Uttarakhand, India. *ISH J. of Hydr. Eng.* 19(1): 1-10

[35] Bajracharya T R, Acharya B, Joshi C B, Saini R P and Dahlhaug O G 2008. Sand erosion of Pelton turbine nozzles and buckets: A case study of Chilime hydropower plant. *Wear* 264 (3-4): 177-184

[36] Padhy M K and Saini R P 2011. Study of silt erosion on performance of a Pelton turbine. *Energy*, 36(1): 141–147

[37] Neopane H P 2010. Sediment Erosion in Hydro Turbines. *PhD thesis* NTNU, Trondheim, Norway

[38] Guangjie P, Zhengwei W, Yexiang X and Yongyao L 2013. Abrasion predictions for Francis turbines based on liquid-solid two-phase fluid simulations. *Engineering Failure Analysis* 33: 327-335

[39] Khanal K, Neopane H P, Rai S, Thapa M, Bhatt S and Shrestha R 2016. A methodology for designing Francis runner blade to find minimum sediment erosion using CFD. *Renewable Energy* 87(1): 307-316

[40] Vessaz C, Jahanbakhsh E and Avellan F 2015. Flow Simulation of Jet Deviation by Rotating Pelton Buckets Using Finite Volume Particle Method. *J. of Fluids Eng.* 137(7) 074501

[41] Jahanbakhsh E 2014. Simulation of Silt Erosion Using Particle-Based Methods. *PhD thesis* no. 6284. Laboratory for Hydraulic Machines, EPF Lausanne, Switzerland

Real-time measurements of suspended sediment concentration and particle size using five techniques

D Felix[1], I Albayrak[1], A Abgottspon[2] and R M Boes[1]

[1] Laboratory of Hydraulics, Hydrology and Glaciology (VAW), ETH Zürich, Hönggerbergring 26, CH-8093 Zurich, Switzerland

[2] Competence Center for Fluid Mechanics and Hydro Machines (CC FMHM), Hochschule Luzern (HSLU), Technikumstrasse 21, CH-6048 Horw, Switzerland

felix@vaw.baug.ethz.ch

Abstract. Fine sediments are important in the design and operation of hydropower plants (HPPs), in particular with respect to sediment management and hydro-abrasive erosion in hydraulic machines. Therefore, there is a need for reliable real-time measurements of suspended sediment mass concentration (*SSC*) and particle size distribution (PSD). The following instruments for *SSC* measurements were investigated in a field study during several years at the HPP Fieschertal in the Swiss Alps: (1) turbidimeters, (2) a Laser In-Situ Scattering and Transmissometry instrument (LISST), (3) a Coriolis Flow and Density Meter (CFDM), (4) acoustic transducers, and (5) pressure sensors. LISST provided PSDs in addition to concentrations. Reference *SSC*s were obtained by gravimetrical analysis of automatically taken water samples. In contrast to widely used turbidimeters and the single-frequency acoustic method, *SSC*s obtained from LISST, the CFDM or the pressure sensors were less or not affected by particle size variations. The CFDM and the pressure sensors allowed measuring higher *SSC* than the optical or the acoustic techniques (without dilution). The CFDM and the pressure sensors were found to be suitable to measure $SSC \geq 2$ g/l. In this paper, the measuring techniques, instruments, setup, methods for data treatment, and selected results are presented and discussed.

1. Introduction

In the design and operation of hydropower plants (HPPs), fine sediments are important with respect to reservoir sedimentation, hydro-abrasive erosion of hydraulic machines (pumps and turbines) and related countermeasures. The management of fine sediments, which make up the major part of the sediment yield, has economic and ecological implications. For a better understanding and management of sediment-related processes, *in-situ* measurements of suspended sediment mass concentration (*SSC*) and particle size distribution (PSD) with high temporal resolution are required. For many applications, continuous real-time measurements are an advantage or even a requirement to support short-term decision making, e.g. for temporary shut-downs of turbines during floods or the control of bottom outlet gates during reservoir flushing operations.

Many techniques for suspended sediment monitoring (SSM) in various application cases are available and described in literature [1] [2]. However, there are specific requirements for SSM systems at HPPs. For turbine erosion mitigation, reliable measurements of higher *SSC*s (up to e.g. 100 g/l), especially of coarser particles, are important – preferably with information in particle sizes.

This paper reports on the investigation of various measuring techniques for continuous SSM in a recent field study at the high-head HPP Fieschertal in the Canton of Valais, Switzerland. The study was conducted in the frame of a research project on hydro-abrasive erosion on Pelton turbines [3]. Other parts of the project are treated in companion papers, e.g. [4] and [5]. The HPP is situated downstream of a highly glaciated catchment. The water in the power waterway contains mainly silt particles with an average *SSC* of 0.5 g/l, rising several times a year above 5 g/l.

The following instruments have been used to continuously measure *SSC*: (1) turbidimeters, (2) a 'Laser In-Situ Scattering and Transmissometry' instrument (LISST) without dilution chamber, (3) a Coriolis Flow and Density Meter (CFDM), (4) acoustic transducers, and (5) pressure sensors. Reference *SSC*s were obtained by gravimetrical analysis of automatically taken bottled water samples. In addition, PSDs were obtained from LISST. The performance of the first four measuring techniques has been briefly discussed in [6]. To the knowledge of the authors, the LISST, the CFDM and the pressure-based technique have not been used in parallel for SSM at HPPs so far.

In the first part of this paper the measuring techniques are reviewed. Then the instruments, setup and methods for data treatment are described. Finally, selected results are presented and discussed with respect to the performance of the measuring techniques.

2. Measuring techniques

2.1. Turbidimeters
Turbidimeters are easy to handle, inexpensive and so far most popular for SSM. They measure either scattering or attenuation of emitted light. Measured turbidities are usually converted to *SSC*s based on the results of gravimetrical analysis of bottle samples (e.g. [7]). Turbidity does not only depend on *SSC*, but also on particle size, shape and color [8]. Hence, biases in SSCs obtained from turbidimeters are to be expected if these particle properties change over time and are not correlated with SSC.

2.2. Laser diffraction and LISST
Besides sieving, hydrometer and image analysis, laser diffraction is widely used for PSD analysis in laboratories. Portable laser diffraction instruments for *in-situ* PSD and *SSC* measurements have become available under the trademark 'LISST' since about 15 years [9]. In LISST instruments, the scattering (diffraction) of a laser beam at small angles (< 9°) and its attenuation, caused by suspended particles, are measured. From these light intensities, the particle volume concentrations in 32 logarithmically spaced size classes (also called size bins) are computed with the software provided by the manufacturer. From the volume concentrations of each size bin, the PSD and the total volume concentration (*TVC*) are determined. In a last step, the *TVC* is converted to *SSC* (concentration by mass).

LISST instruments allow measuring *SSC*s up to a limit which is given by a minimum optical transmittance. At high turbidity, *SSC*s in rivers and HPPs may temporarily exceed the measuring range of most LISST models. To measure also higher *SSC*s, a special type of LISST device with a dilution chamber is available [10].

2.3. Vibrating tube densimetry and CFDMs
Higher *SSC*s can be measured via the density of the water-particle mixture. In the process industry, continuous in-line density measurements are commonly done with 'Vibrating Tube Density Meters' (also called 'oscillating U-tubes') or 'Coriolis Flow and Density Meters' (CFDMs). In the first type of instruments, the density is measured based on the measuring tubes' natural frequency, which is reduced as the mass of the fluid in the tubes increases. In CFDMs, the Coriolis effect is exploited to measure the mass flow rate; the density measurement is also based on the tubes' natural frequency [11]. So far, CFDMs have been rarely used for SSM [12].

CFDMs overestimate the density and thus *SSC* if debris, sediment or biofilms accumulate inside the measuring tubes. The density and *SSC* may be underestimated if the measuring tubes are eroded or if so-called phase decoupling occurs in particulate fluids [13]. In the latter case, particles do not strictly follow the motion of the fluid in the oscillating tubes. This effect on the density measurement is known to be more important with larger particles.

2.4. Acoustic techniques

Ultrasonic signals are used for SSM in many ways, mostly with Acoustic Doppler Current Profilers (ADCPs). *SSC*s are estimated from acoustic backscatter intensities and reference *SSC*s (*in-situ* calibration) [14]. Acoustic discharge measurement installations (ADM), as existing in many larger HPPs, can also be used for SSM. This type of single-frequency acoustic attenuation technique and other acoustic approaches are treated more in detail in [4].

2.5. Differential pressure

Differential pressure is another SSM technique. The estimation of *SSC* is based on pressure measurements of two sensors installed at a fluid column at two levels with a known difference in elevation. In the application of this technique at the penstock of a HPP, the headwater level and the static pressure at the downstream end of the penstock (upstream of the turbines) are measured. If the water in the penstock contains suspended sediment, the pressure difference between the upper and the lower sensor is higher than in clear water conditions. Knowing the densities of the clear water and the particles, these pressure deviations are converted to *SSC*s in quasi-steady state conditions.

2.6. Automatic water sampling

Gravimetric analysis of bottled water samples in the laboratory is the reference for the indirect *SSC* measuring techniques described above. In field studies with manual bottle sampling, higher *SSC*s are likely to be missed because they rarely occur. This problem can be mitigated by using an automatic water sampler triggered by *SSC* (or indicators for high *SSC*).

3. Instruments and setup

3.1. Instruments

The instruments for SSM used in this study are listed in table 1. Further information on tested turbidimeter models are given in [15]. Prior to the field study, the measuring capabilities of the instruments (1), (2) and (4) were systematically investigated in a mixing tank in the laboratory [16] [17]. From this investigation, for instance, a good agreement between PSDs obtained from LISST and from image analysis was found for spherical and rounded particles [17].

Table 1. Measuring techniques and instruments for SSM used in the study.

Item no.	Measuring technique	Instrument description	Instrument model	Instrument manufacturer	Derived parameters
(1)	Turbidity	In-line turbidimeter, at free falling jet	*AquaScat*	Sigrist Photometer	*SSC*
(2)	Laser diffraction (LISST)	Type C, with 90% path reduction module	*LISST-100X*	Sequoia Scientific	*SSC*, PSD
(3)	Vibrating-tube densimetry	Coriolis Flow- and Density Meter (CFDM)	*Promass 83F DN15*	Endress+Hauser	*SSC*
(4)	Acoustic attenuation	Based on ADM (1 MHz, 2.27 m path length)	*Risonic*	Rittmeyer	*SSC*
(5)	Differential pressure	Pressure transmitters (u/s and d/s of penstock)	*2088, 1151*	Rosemount	*SSC*
(6)	Gravimetric	Bottle sampler with 24 bottles of 1 litre	*Isco 3700*	Teledyne Isco	*SSC*

The selected turbidimeter model (1) measures turbidity at a free-falling jet. No cleaning is required because its optical parts are not in contact with the sediment-laden water. This turbidimeter model has been mainly used for quality control in drinking water supply systems so far. Turbidity up to 4000 FNU (Formazine Nephelometric Units) is measured by light scattered at 90°.

With respect to LISST (2), a submersible all-round model without dilution chamber was used. With the inversion mode for so-called 'random shaped' particles [18], the instrument's nominal PSD range is 2 to 380 µm. Its optical path length was reduced from 50 to 5 mm by inserting the strongest available path reduction module (glass cylinder) to increase the upper limit of measureable *SSC*s.

The CFDM (3) contains two bent tubes with 8 mm inner diameter. The temperature is also measured and used in the internal data processing to compensate thermal expansion. The CFDM is factory-calibrated with respect to mass flow, density and temperature. The specified accuracy of the density measurement is ±0.5 g/l, which is a common specification [11].

3.2. Setup

The instruments (1), (2) and (6) of table 1 were installed in the valve chamber of HPP Fieschertal in June 2012. The valve chamber is located at the top of the penstock, downstream of a 2 km-long free-surface-flow storage tunnel (figure 1). In June 2013, the CFDM (3) was added. The ADM installation (4) and the pressure transmitters (5) have already been in place before the research project. The turbine water should contain only particles with less than 0.3 mm diameter because upstream gravel and sand traps are designed to exclude larger particles.

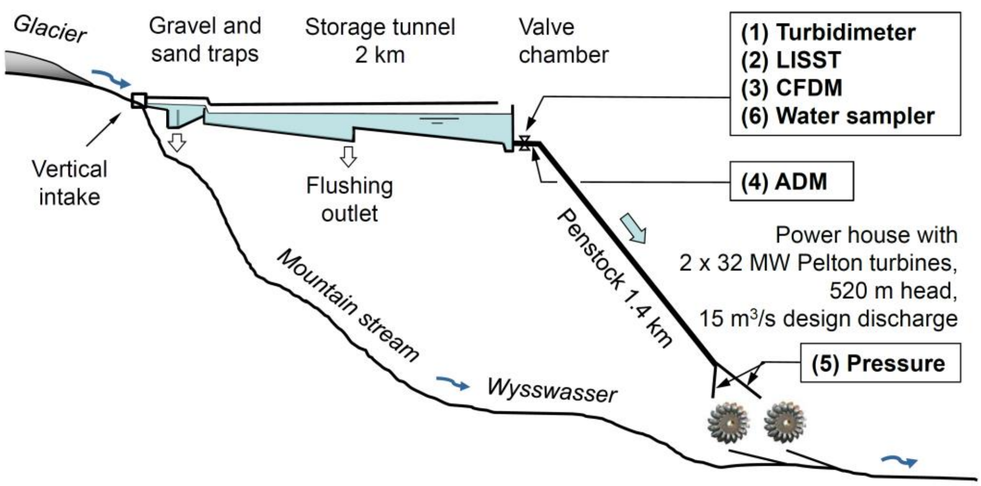

Figure 1. Schematic longitudinal profile of the HPP Fieschertal with the instrumentation for SSM; numbers refer to table 1.

The instruments (1) to (3) were fed with water from the penstock by a sampling pipe arrangement (figure 2). The discharges in the sampling pipes were regulated by ball valves at their outlets. The turbidimeter (1) requires a flow rate of only 0.06 to 0.12 l/s. In the main pipe, a minimum discharge of 0.15 l/s corresponding to a flow velocity ≥ 0.5 m/s was selected to prevent settling of particles in the ascending pipe. The discharge in the main pipe was up to 0.25 l/s at high water level in the tunnel.

At the measurement location, no air bubbles which would bias the measurements were observed in the water. No provision to prevent clogging of the CFDM was required because the sediment particles at the measuring location (≤ 0.3 mm) were much smaller than the internal diameter of the CFDM's measuring tubes (8 mm) and there was practically no floating debris. The CFDM was mounted vertically to reduce deposition of particles inside its measuring tubes.

The automatic bottle sampler (6) was controlled from a measurement computer in the valve chamber using an auxiliary software developed at VAW/ETH Zürich. Water samples of 0.5 l were pumped from the bucket (figure 2) every three days, or more frequently if the trigger signal exceeded certain threshold values. In 2012, turbidity was used as trigger signal. Since the installation of the CFDM in 2013, the mixture density has been used instead (generally better indicator for high *SSC*).

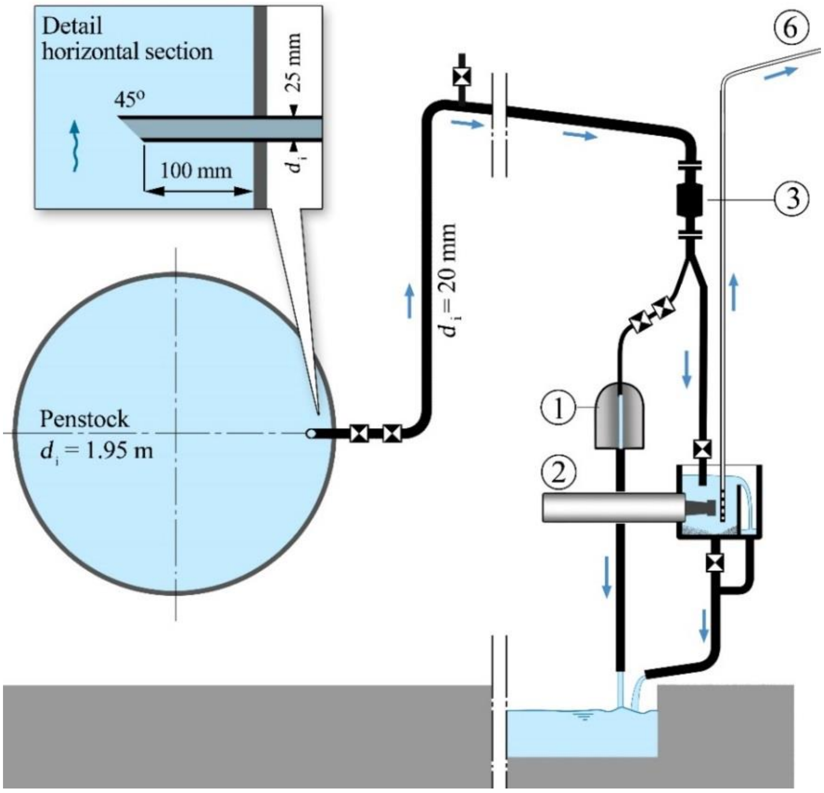

Figure 2. Vertical section of the setup for SSM in the valve chamber of HPP Fieschertal; numbers refer to table 1.

4. Methods

4.1. Data acquisition and laboratory work

The outputs of the turbidimeter (turbidity), of the CFDM (density, flow rate and temperature) and of the ADM (amplitudes of the forward scattered signals), as well as the head water level, the discharge in the penstock, the pressures upstream of the turbines and the electric outputs of the generators were recorded every second. The LISST was set to execute one burst per minute (10 measurements at 1 Hz followed by a break of 50 s). The optical parts of the LISST in contact with the water were manually cleaned every month on average. In the power house, the pipes between the penstock and the pressure sensors upstream of the turbines were flushed periodically. The instruments were used with their factory calibrations. From the 1 Hz data, minute-by-minute averages were calculated.

From the water samples, the *SSC*s were determined in the laboratory by gravimetrical analysis which included the following steps: weighing of sample, evaporation of water, weighing of dried residue, and calculation of *SSC* by accounting for the concentration of dissolved minerals (≤ 0.08 g/l). These *SSC*s served as a basis to convert the instruments' outputs to *SSC* time series. These conversions can also be called 'field calibrations' in the wider sense of the word. In the following, these conversions are described for each measuring technique.

4.2. Conversion of turbidity and acoustic damping to SSC

In figure 3a, the gravimetrical *SSC*s from 46 bottle samples in 2013 (< 3 g/l) and the turbidity values measured at corresponding times are compared. Turbidity values were not always available because the small hose leading to the turbidimeter was sometimes clogged, especially at higher *SSC*s. The scatter of the points is attributed to mainly temporal PSD variations. A linear fit through the origin was selected because the turbidimeter was not affected by fouling which would result in a turbidity offset. The relation in figure 3a was used to convert the measured turbidity time series to *SSC*. The time series of acoustic damping was converted to *SSC* in the same way [4].

4.3. Conversion of LISST's volume concentrations to SSC

As a first step of LISST data treatment, the volume concentrations in the 32 size bins were plotted as a function of time and checked for plausibility. Besides the concentrations in size bins well within the LISST's size measuring range, there were also relatively high concentrations in size bins (i) close to the lower end of the size measuring range and (ii) sometimes towards its upper end.

Generally there were relatively high concentrations in bins no. 1 to 3 (1.9 to 3.1 µm) decreasing towards a local minimum in bin no. 4 (3.1 to 3.7 µm). Relatively high concentrations at the fine end of PSDs were also reported by [17] and [18]. These may be due to effects of small out-of-range particles or highly non-spherical particles. The concentrations in bins no. 1 to 3 were judged to be implausible and were thus discarded [17].

At the coarse end of the PSDs, the concentrations in the range of bins 25 to 32 (100 to 380 µm) gradually increased during some periods in late summer and autumn. Such concentrations were attributed to fouling and were also discarded [20]. By summing up the remaining plausible volume concentrations in all size bins at each time step, the time series of the total volume concentrations (*TVC*) was calculated.

The average solid density of the particle material ρ_s = 2.73 g/cm^3 was measured in the laboratory by a helium pycnometer at dried residues of twelve bottle samples. *TVC*s were multiplied by ρ_s to convert from volume to mass concentrations (*SSC*s). The resulting time series was denoted as SSC_{L0}.

In Figure 3b, the gravimetrical *SSC*s below 3 g/l obtained from 96 bottle samples in 2013 are compared to SSC_{L0} at corresponding times. With the assumptions that the measuring uncertainty of the gravimetrical *SSC*s and of the pycnometer density are negligible, it was concluded that the *SSC*s obtained from LISST with ρ_s are on average 71% higher than these from the bottle samples (linear fit). In the laboratory investigation with angular feldspar or flaky mica particles, considerable LISST concentration overestimations by factors of 1.38 or 8, respectively were quantified [17]. These were attributed to mainly effects of highly non-spherical particle shapes and to possibly flocculation of fine particles. The SSC_{L0} values were divided by 1.71 to compensate the overestimation.

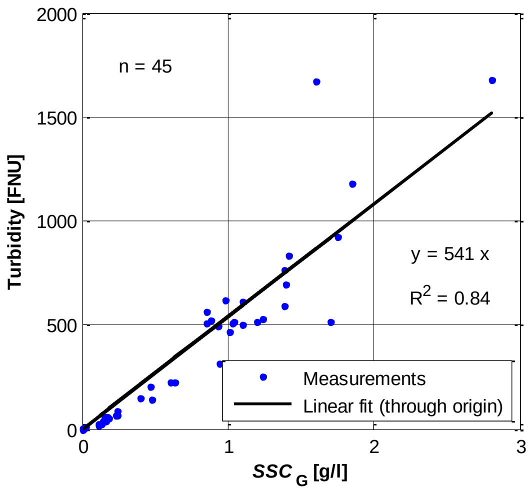

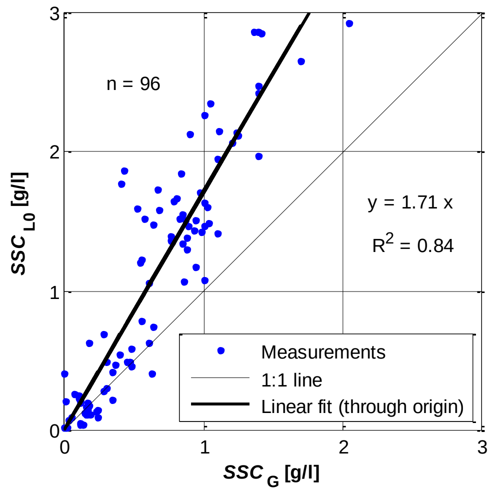

Figure 3. a) Turbidity, and **b)** SSC_{L0} obtained from LISST and the solid density of the particle material, both compared to gravimetrically determined reference *SSC*s (SSC_G, < 3 g/l) measured at the waterway of HPP Fieschertal in 2013.

Another way to obtain corrected *SSC*s from LISST, but without the need of pycnometer measurements, consists of the following steps: plot *TVC*s against gravimetrical *SSC*s at corresponding times, find a conversion factor by linear fitting through the origin and apply the factor to the *TVC*s. This factor has units of a density and was called 'apparent density' in [19]. In the present study, the apparent density is 1.60 g/cm^3 (= 2.73 g/cm^3 / 1.71). In [19], an average apparent density of 1.24 g/cm^3 was found for sediment particles in river waters, which was also considerably lower than ρ_s.

4.4. Conversion of CFDM's mixture density to SSC

The *SSC*s from the CFDM, denoted as SSC_C, were calculated from both measured time series of the mixture density $\rho_m(t)$ and the water temperature $T(t)$ using equation (1) [20]:

$$SSC_C = \frac{\rho_m(t) - \rho_w(T(t))}{1 - \frac{\rho_w(T(t))}{\rho_s}} + K(t) \quad \approx \quad 1.6\ [\rho_m(t) - \rho_w(T(t))] + K(t) \qquad (1)$$

The clear water density ρ_w was calculated as a function of the temperature $T(t)$. From the pycnometer measurements, ρ_s was taken as a constant. A site-specific and seasonally variable minor offset $K(t)$ was determined by comparing the *SSC*s from CFDM with the gravimetrical *SSC*s. This corresponds to a periodic *in-situ* calibration. $K(t)$ compensates density offsets due to (i) dissolved chemical elements, (ii) variable biofilm and/or particle deposits inside the measuring tubes, and other factors [20]. The approximation shown on the right-hand side of equation (1) is based on ρ_s = 2.73 g/cm^3.

The water temperatures varied between 0.1 and 6 °C, leading to a variation of ρ_w < 0.13 g/l. According to equation 1, this corresponds to a SSC-variation < 0.21 g/l. In autumns 2013 and 2014 a gradual slight increase of the mixture density was measured, while *SSC* was expected to decline to zero towards the winter. This increase was attributed to the growth of a biofilm inside the measuring tubes [20] and corresponded to an *SSC* offset of ≤0.6 g/l. The density signal was de-trended based on the gravimetrical *SSC*s. With the periodic *in-situ* calibration, the expanded *SSC* measuring uncertainty (at 95% confidence level) was quantified as ±0.35 g/l based on measurements from 2014 [20].

4.5. Determination of SSCs by the pressure-based technique

*SSC*s were determined from pressure and further measurements according to the following steps:

- Discarding of temporarily implausible pressure measurements (e.g. due to complete or partial clogging of pipes between the penstock and the pressure transmitters or of the transmitters);
- Comparison of pressure and head water level measurements in periods of no flow and clear water, and minor correction of pressure data by applying a scaling factor close to 1;
- Determination of the head losses in the penstock as a function of the discharge and the operation mode (one or two turbines running), based on measurements (quadratic fits);
- Identification of quasi-steady state periods by checking for changes in the discharge;
- Calculation of the density of the sediment-water mixture in the penstock at every time step in quasi-steady state periods, based on head water level, discharge and pressure measurements and considering the head losses;
- Conversion of the mixture densities to *SSC*s as described in section 4.4.

5. Results

The performances of the measuring techniques and instruments were assessed by evaluating the *SSC* and PSD time series from the measurements during three years. Figure 4 shows an example of these time series with *SSC* results from the five techniques for continuous measurements and the discontinuous reference technique (bottle samples). The particle size d_x, obtained from LISST, stands for the diameter of graded particles, of which x % by mass are smaller. The following observations and interpretations are made:

- The CFDM measured *SSC*s up to 13 g/l. It is expected that also higher *SSC*s can be measured as long as the measuring tubes are not clogged. With the particles mainly in the size range of silt, no considerable underestimation of *SSC*s due to phase decoupling was observed in the field measurements.
- The corrected *SSC*s from LISST matched generally well with those from the CFDM. However, no LISST results were available above 4 to 5 g/l at d_{50} = 30 to 35 µm (d_{50} in the size range of coarse silt).
- The *SSC*s calculated from the turbidimeter and the single-frequency attenuation measurements were considerably lower than the *SSC*s from the other techniques mainly in periods of elevated *SSC*s and often after *SSC* peaks [15], when the particles were coarser than usual. The temporary underestimations are explained as follows: The *SSC*s from these techniques were determined using linear conversions based on $SSC_G < 3$ g/l. These conversions are correct for the usually prevailing relatively fine particles, but lead to *SSC* underestimation if the particles are coarser.
- The pressure-based technique yielded similar *SSC*s as the CFDM and a bottle sample (figure 4). The *SSC* from pressure was considered only above 2 g/l, because the measuring uncertainty was judged to be too high at lower *SSC*s. The deviations between the *SSC*s from pressure and from CFDM are mainly attributed to the different measurement volumes: while the CFDM measured *SSC*s in a small sampling pipe at the top of the penstock (point measurement), the *SSC* from pressure refers to the volume of the whole penstock, i.e. is averaged over 3500 m^3.

Further results on the *SSC* and PSD measurements at HPP Fieschertal in the years 2012 to 2014 are presented in [5].

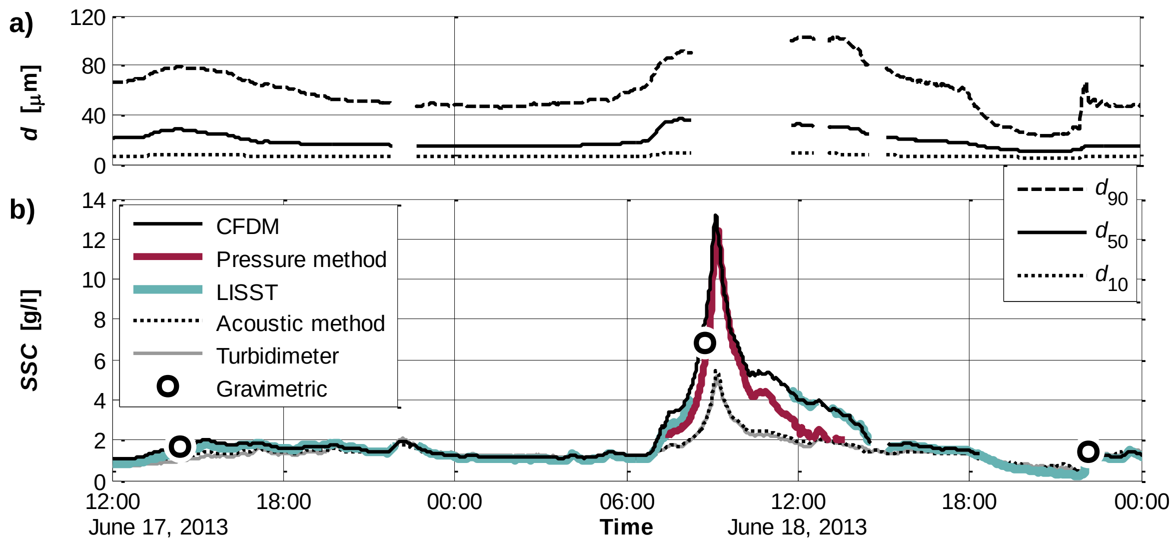

Figure 4. Examples of time series of **a)** particle sizes obtained from LISST and of **b)** *SSC*s from six techniques, measured in the valve chamber of HPP Fieschertal (modified from [6]).

6. Conclusions and Outlook

A turbidimeter, an all-round LISST instrument without dilution chamber, a CFDM, a single-frequency acoustic technique based on ADM, and pressure sensors were used to measure *SSC* at the waterway of an alpine HPP. In addition, PSDs were obtained from LISST. The SSC measuring performances of these instruments and techniques were assessed by comparison to also the gravimetrical technique.

With the **CFDM**, *SSC*s up to 13 g/l were measured without reaching the upper limit of the measuring range. Accounting for temperature variations and the seasonally variable density offset (by periodic field calibration based on gravimetric *SSC*s) contributed to reduce the *SSC* measuring uncertainty to ±0.35 g/l. Accepting a relative measuring uncertainty of approximately 20 %, the CFDM technique is thus suitable for *SSC*s ≥ 2 g/l. To further investigate the CFDM technique, systematic laboratory tests also with particles up to the size range of sand and at high *SSC*s are recommended.

Similarly, the **pressure**-based technique is suitable to measure *SSC*s ≥ 2 g/l at high- or medium head HPPs. This technique yields spatially well-averaged *SSC* measured directly in the penstock and has the advantage of using sensors which are already in place in many HPPs. The pressure technique has the drawbacks of (i) yielding no results during hydraulic transients (change of turbine flow rate leading to water hammer) and (ii) offering only a short pre-warning time for turbine switch-offs, because the sediment-laden water is already in the penstock if high *SSC*s are detected.

The *SSC*s obtained from the **LISST**'s plausible volume concentrations and the solid density of the particle material were on average 71 % higher than the gravimetric *SSC*s from bottle samples. With the LISST technique, an average particle shape has to be assumed in the calculation of the volume concentrations. In environments with highly non-spherical particles, as typically in mountainous regions, it is recommended to take bottle samples and to convert LISST volume concentrations to *SSC*s based on **gravimetrical** reference *SSC*s. Applying this method, effects of particle shapes and of particle density (including potential flocculation) on *SSC*s are compensated. The LISST with an optical path length of 5 mm and without dilution allowed measuring *SSC*s up to 5 g/l with d_{50} in the size range of coarse silt and with the shapes of the prevailing particles. Apart from the limited *SSC* measuring range, LISST offered the advantage of providing PSDs.

With the PSD results, temporary biases of *SSC*s obtained from **turbidimeters** and the single-frequency **acoustic** attenuation technique were explained as consequences of particle size variations. To reduce such *SSC* biases, the use of non-linear conversion functions is recommended, which consider (i) a potential correlation between d_{50} and *SSC*, and (ii) the potentially non-linear behavior of measuring systems at high *SSC*s. The practical advantages of the acoustic technique for sediment monitoring in HPPs based on ADM installations are highlighted in [4]. In contrast to turbidimeters and the single-frequency acoustic technique, the LISST, the CFDM and the pressure-based technique provided *SSC*s which were less or not affected by PSD variations.

The mentioned type of turbidimeter provided drift-free measurements without cleaning. For the LISST, manual cleaning every month was not frequent enough. Options to avoid fouling are to either use an auxiliary device to protect and clean the measuring window (a so-called '*bioblock*') or another type of LISST instrument with automatic cleaning. In the CFDM, fouling caused a gradual shift of *SSC*s by up to 0.6 g/l. Because frequent and rigorous cleaning inside the CFDM's measuring tubes is not practical in SSM applications, a correction based on gravimetric *SSC*s is recommended instead, if a high accuracy in SSC is required, e.g. to determine annual sediment loads. If a CFDM is solely used to warn of high turbine erosion potential, say above 5 or 10 g/l, no bottle sampling, laboratory analyses and field calibration are required, since small density offsets due to fouling are not relevant.

Based on these findings, a combination of a LISST instrument without a dilution chamber and a CFDM appears to be an economic option for SSM at HPPs, if *SSC* from a few mg/l to several 10 g/l of mainly silt is to be measured, and the lack of PSD data at high *SSC*s is accepted. In addition, automatic bottle sampling is highly recommended for calibration and validation of continuous indirect *SSC* measurements. The parallel use of several independent instruments based on different measuring techniques is seen as an advantage with respect to (i) the data coverage in environments with wide *SSC* and PSD ranges as well as (ii) the reliability of the measured values.

Acknowledgements
The support of the mentioned research project by swisselectric research, the Swiss Federal Office of Energy (SFOE), the HPP operator Gommerkraftwerke AG as well as the Swiss Competence Center for Energy Research - Supply of Electricity (SCCER-SoE) and the Research Fund of the Swiss Committee on Dams are gratefully acknowledged. Further thanks go to Endress+Hauser, Sigrist Photometers and Rittmeyer for lending measuring equipment as well as to all members of the project team for their contributions to the laboratory and field investigations.

References

[1] Wren D, Barkdoll B, Kuhnle R and Derrow R 2000. Field Techniques for Suspended-Sediment Measurement. *J. of Hydraul. Eng.* 126(2): 97–104

[2] Rai A K and Kumar A 2015. Continuous measurement of suspended sediment concentration: Technological advancement and future outlook. *Measurement* 76: 209–227

[3] Felix D, Albayrak I, Boes R M, Abgottspon A, Deschwanden F and Gruber P 2013. Measuring Suspended Sediment: Results of the first Year of the Case Study at HPP Fieschertal in the Swiss Alps. *Proc.* Hydro Conf., Innsbruck, Austria, paper no 18.03

[4] Gruber P, Felix D, Storti G, Lattuada M, Fleckenstein P and Deschwanden F 2016. Acoustic measuring techniques for suspended sediment. *Proc.* 28th IAHR Symposium on Hydraulic Machinery and Systems, Grenoble, France, IOP Conf. Series

[5] Felix D, Albayrak I, Abgottspon A and Boes R M 2016. Suspended sediment measurements and calculation of the particle load at HPP Fieschertal. *Proc.* 28th IAHR Symposium on Hydraulic Machinery and Systems, Grenoble, France, IOP Conf. Series

[6] Felix D, Albayrak I and Boes R M 2016. Continuous measurement of suspended sediment concentration: disussion of four techniqes. *Measurement* 89: 44-47

[7] Haimann M, Liedermann M, Lalk P and Habersack H 2014. An integrated suspended sediment transport monitoring and analysis concept. *J. of Sediment Research* 29(2): 135-148

[8] Downing J 2006. Twenty-five years with OBS sensors: The good, the bad, and the ugly. *Continental Shelf Research* 26(17–18): 2299-2318

[9] Agrawal Y C and Pottsmith H C 2000. Instruments for particle size and settling velocity observations in sediment transport. *Mar. Geol.* 168: 89-114

[10] Agrawal Y C, Mikkelsen O A, Pottsmith H C and Slade W H 2012. Turbine abrasion: one year's experience in real-time sediment monitoring at Hidroagoyan HPP, Ecuador. *Proc.* Hydro Conf., Bilbao, Spain: paper no. 14.08

[11] Kalotay P 1999. Density and viscosity monitoring systems using Coriolis flow meters. *ISA Transactions* 38: 303-310

[12] Bishwakarma M B and Støle H. 2008. Realtime sediment monitoring in hydro-power plants. *J. of Hydr. Research* 46(2): 282–288

[13] Basse N T 2014. A review of the theory of Coriolis flowmeter measurement errors due to entrained particles. *J. of Flow Measurement and Instrumentation* 37: 107-118

[14] Guerrero M, Szupiani R N and Latosinsky F 2013. Multi-frequency acoustics for suspended sediment studies: an application in the Parana River. *J. Hydraulic Research* 51(6): 696-707

[15] Felix D, Albayrak I and Boes R M 2015. Field measurements of suspended sediment using several methods. *E-proceedings* 36th IAHR World Congress, The Hague, The Netherlands

[16] Felix D, Albayrak I and Boes R M 2013. Monitoring of Suspended Sediment – Laboratory Tests and Case Study in the Swiss Alps. *Advances in River Sediment Research*, Fukuoka S, Nakagawa H, Sumi T and Zhang H (eds.). Taylor & Francis Group, London: 1757-1766

[17] Felix D, Albayrak I and Boes R M 2013. Laboratory investigation on measuring suspended sediment by portable laser diffractometer (LISST) focusing on particle shape. *Geo-marine Letters* 33(6) 485-498

[18] Agrawal Y C, Whitmire A, Mikkelsen O A and Pottsmith H C 2008. Light scattering by random shaped particles and consequences on measuring suspended sediments by laser diffraction. *J. of Geophysical Research* 113, C04023

[19] Czuba J A, Straub T D, Curran C A, Landers M N and Domanski M M 2015. Comparison of fluvial suspended-sediment concentrations and particle-size distributions measured with in-stream laser diffraction and in physical samples. *Water Resour. Res.* 51: 320–340

[20] Felix D, Albayrak I and Boes R M 2016. Combining in-situ laser diffraction (LISST) and vibrating tube densimetry to measure low and high suspended sediment concentrations. *Proc.* 13th Intl. Symposium on River Sedimentation, Stuttgart, Germany [accepted]

Suspended sediment measurements and calculation of the particle load at HPP Fieschertal

D Felix[1], I Albayrak[1], A Abgottspon[2] and R M Boes[1]

[1] Laboratory of Hydraulics, Hydrology and Glaciology (VAW), ETH Zürich, Hönggerbergring 26, CH-8093 Zurich, Switzerland

[2] Competence Center for Fluid Mechanics and Hydro Machines (CC FMHM), Hochschule Luzern (HSLU), Technikumstrasse 21, CH-6048 Horw, Switzerland

felix@vaw.baug.ethz.ch

Abstract. In the scope of a research project on hydro-abrasive erosion of Pelton turbines, a field study was conducted at the high-head HPP Fieschertal in Valais, Switzerland. The suspended sediment mass concentration (SSC) and particle size distribution (PSD) in the penstock have been continuously measured since 2012 using a combination of six measuring techniques. The SSC was on average 0.52 g/l and rose to 50 g/l in a major flood event in July 2012. The median particle size d_{50} was usually 15 µm, rising up to 100 µm when particles previously having settled in the headwater storage tunnel were re-suspended at low water levels. The annual suspended sediment loads (SSL) varied considerably depending on flood events. Moreover, so-called particle loads (PLs) according to the relevant guideline of the International Electrotechnical Commission (IEC 62364) were calculated using four relations between particle size and the relative abrasion potential. For the investigated HPP, the time series of the SSL and the PLs had generally similar shapes over the three years. The largest differences among the PLs were observed during re-suspension events when the particles were considerably coarser than usual. Further investigations on the effects of particle sizes on hydro-abrasive erosion of splitters and cut-outs of coated Pelton turbines are recommended.

1. Introduction

At high- and medium-head hydropower plants (HPPs) operated on sediment-laden rivers, turbine parts are subject to hydro-abrasive erosion. This causes high maintenance costs, and reduces turbine efficiency, electricity generation and revenues. As a basis for adequate countermeasures and optimizations in the design, operation and maintenance of such HPPs, the knowledge on hydro-abrasive erosion and its consequences needs to be improved. To this end, the Laboratory of Hydraulics, Hydrology and Glaciology (VAW) of ETH Zürich and the Competence Center for Fluid Mechanics and Hydro Machines (CC FMHM) of Hochschule Luzern, Switzerland, initiated an interdisciplinary research project.

In this project, the sediment load, the erosion of Pelton turbine runners and the efficiency changes have been measured and analyzed since 2012 at the high-head HPP Fieschertal in Valais, Switzerland. This run-of-river HPP with a free-surface flow storage tunnel has a design discharge of 15 m^3/s, a gross head of 520 m, and is equipped with two horizontal 32 MW Pelton turbines [1]. The water used in this HPP comes from a glaciated catchment and is known for high suspended sediment mass concentration (*SSC*) and abrasion potential.

This paper deals with the description and quantification of the suspended sediment load (*SSL*) and the so-called particle load (*PL*) at HPP Fieschertal in the years 2012 to 2014, whereas other parts of the project are treated in companion papers, e.g. [1] and [2]. The term *PL* has been introduced by IEC 62364 (2013) [3] and is explained in the present paper. After a description of the setup and the methods, selected results are presented and discussed. In particular, *SSL* and *PL* are analyzed and compared over the years and in selected events.

2. Measuring techniques, instruments and setup

The following instruments and measuring techniques were used for suspended sediment measurements:

(1) Turbidimeters;
(2) Laser in-situ Scattering and Transmissometry (LISST);
(3) Vibrating tube densimetry using a Coriolis Flow and Density Meter (CFDM);
(4) A single-frequency acoustic attenuation technique using a standard installation for acoustic discharge measurement (ADM) based on the acoustic transit time method;
(5) Pressure-based technique, i.e. the calculation of *SSC* based on static pressure, headwater level and discharge measurements in quasi-steady state conditions;
(6) An automatic water sampler.

The instruments (1) to (3) and (6) have been installed in the valve chamber at the top of the penstock. (1) to (3) are fed from the penstock by a sampling pipe. The measuring techniques (4) and (5) used pre-existing sensors. All instruments except the automatic water sampler are used for continuous real-time measurements of *SSC*. The automatic water sampler is used for discontinuous *SSC* reference measurements. The LISST technique additionally yields continuous real-time measurements of the particle size distribution (PSD) in the nominal range of 2 to 380 μm. Further information on the instruments and the measuring techniques as well as on the setup are given in [1] and [4].

3. Methods

3.1. Data acquisition

The outputs of the turbidimeters, the CFDM and the ADM were recorded simultaneously at 1 Hz. The LISST was programmed to perform one burst per minute. The optical instruments were cleaned every month on average. Water samples were pumped every three days or more frequently if the trigger signal, i.e. the density measured by the CFDM, exceeded certain threshold values. Furthermore, selected variables from the HPP's control system, such as headwater level, penstock discharge, pressures upstream of the turbines and electric power outputs were recorded at 1 Hz.

3.2. Laboratory analyses

SSCs were determined by gravimetrical analyses of 285 bottle samples collected in the years 2012 to 2014. The density, shape and mineralogical composition of the sediment particles were investigated in the laboratory on dried residues of selected bottle samples.

3.3. Data treatment

From the 1 Hz data, minute-by-minute average values were calculated. The outputs of the turbidimeters, the CFDM, the ADM and the LISST were converted to *SSC* time series based on the gravimetrically determined *SSC*s as described in [1] and [5]. In periods of SSC > 2 g/l, *SSC*s were calculated from the data of the HPP's control system using the pressure-based technique.

From the several *SSC* time series obtained from the various measuring techniques, a continuous *SSC* time series covering the years 2012 to 2014 was compiled, representing the best estimate of *SSC*. Based on data availability and investigations of the measuring uncertainties, preference was given to the *SSC*s from CFDM when the *SSC* was above 1 g/l. Otherwise, *SSC*s from LISST were taken. When no LISST data were available, *SSC*s obtained from turbidimeters or from the acoustic technique were used. *SSC*s from the pressure-based technique were included in the best estimate *SSC* time series only during a major flood event on July 2 and 3, 2012, when the CFDM had not been installed yet.

Based on the LISST data, the best estimate *SSC*s were split-up in five particle size classes with limits of 3, 20, 50, 100, 200 and 380 µm. Such *SSC*s are also called fraction-wise *SSC*s, because particles of given size classes are also called fractions. In addition, the time series of the median particle size d_{50} was calculated from the measurements. The d_x denotes the diameter of graded particles which is exceeded by *x* % of the particle mass.

3.4. Calculation of suspended sediment loads

The cumulative suspended sediment load $SSL(t)$ is the suspended sediment mass transported through the penstock or through a turbine since the start time t_0 (beginning of the observation period or of a single year) until the time $t > t_0$. *Q* denotes the discharge (volumetric flow rate) of the water-sediment mixture. The term '$Q_i \, SSC_i$' is the sediment transport rate (solid mass flux) which is integrated over time using equation (1). A constant time step of Δt = 1 minute was used; *i* denotes the time step number.

$$SSL(t) = \sum_{i=1}^{(t-t_0)/\Delta t} Q_i \, SSC_i \;\; \Delta t \quad = \Delta t \sum_{i=1}^{(t-t_0)/\Delta t} Q_i \, SSC_i \qquad \text{in [kg] or typically [t]} \qquad (1)$$

3.5. Calculation of particle loads according to IEC 62364

The concept of the so-called *PL* is described in [6] and in the IEC guideline [3]. The definition of *PL*(*t*) is recalled in equation (2). The dimensionless factors k_{hardness}, k_{shape} and k_{size} account for the effects of the particle hardness, shape and size, respectively, on the erosion. The *PL* reflects the erosion potential of the particles passing through a turbine as a function of time *t* since a certain start time t_0. In the model described in [3], *PL* is proportional to the erosion depth. In contrast to the *SSL* (equation 1), *PL* does not depend on the discharge.

$$PL(t) = \sum_{i=1}^{(t-t_0)/\Delta t} k_{\text{hardness},i} \;\; k_{\text{shape},i} \;\; k_{\text{size},i} \;\; SSC_i \;\; \Delta t \qquad \text{in [h * g/l] or [h * kg/m}^3\text{]} \qquad (2)$$

The factors k_{hardness} and k_{shape} were assumed to be constant over time (properties of the catchment area). Therefore, these factors are placed in front of the sum in the rewritten equation (3). The product of $k_{size,i}$ and SSC_i in equation (2) was calculated at each time step with the second sum in equation (3) based on the fraction-wise *SSC*s in five particle size classes (*j* = 1 to 5) and the factors $k_{\text{size},j}$. These factors reflect the relative erosion potential (*REP*) of the particles in each size class, as described below. The term SSC_{ij} stands for the *SSC* in the size class *j* during the time step number *i*. According to [3], SSC_{ij} were set to zero when the respective turbine was not running (Q_{Turbine} = 0). In the calculation of the *SSL*s and *PL*s of each turbine, it was assumed that the *SSC* in a turbine corresponds to the *SSC* measured in the penstock.

$$PL(t) = \Delta t \;\; k_{\text{hardness}} \;\; k_{\text{shape}} \sum_{i=1}^{(t-t_0)/\Delta t} \sum_{j=1}^{5} k_{\text{size},j} \;\; SSC_{ij} \qquad \text{in [h * g/l] or [h * kg/m}^3\text{]} \qquad (3)$$

The *REP* of particles of various sizes depends on several factors such as turbine type, location inside the turbine, and size of the turbine. Four different relations between the *REP* and particle size available in the literature were used in the present study:

1) As a baseline case, k_{size} was set to 1, i.e. erosion would not depend on particle size (Fig. 1a).
2) According to Nozaki [7] and IEC [3] the *REP* increases linearly with particle size. Nozaki selected k_{size} = 1 at *d* = 50 µm. IEC suggests to take the numerical value of d_{50} in millimetres

as k_{size}, i.e. $k_{size} = 1$ at $d = 1000$ µm (Fig. 1b). In the present study, the definition by IEC was adopted for the linear type of relation between *REP* and particle size.

3) According to erosion tests in the laboratory with particle-laden turbulent flow in the gap between a rotating shaft and its housing [8], the effect of particle size on erosion was found to be non-linear ([9] published in [10], Fig. 1c).
4) According to more recent laboratory tests on Pelton splitters [11], particles larger than approx. 100 µm cause considerably more erosion than smaller particles (Fig. 1d). This was explained by the higher inertia of the larger particles contained in the jet causing them to impinge on the splitter, whereas smaller particles follow mainly the streamlines around the splitter [11].

The factors $k_{size,j}$ listed in table 1were determined from figure 1 as average values within each size class. Note that $k_{size,j}$ are not comparable across the various literature sources since they do not have a common basis.

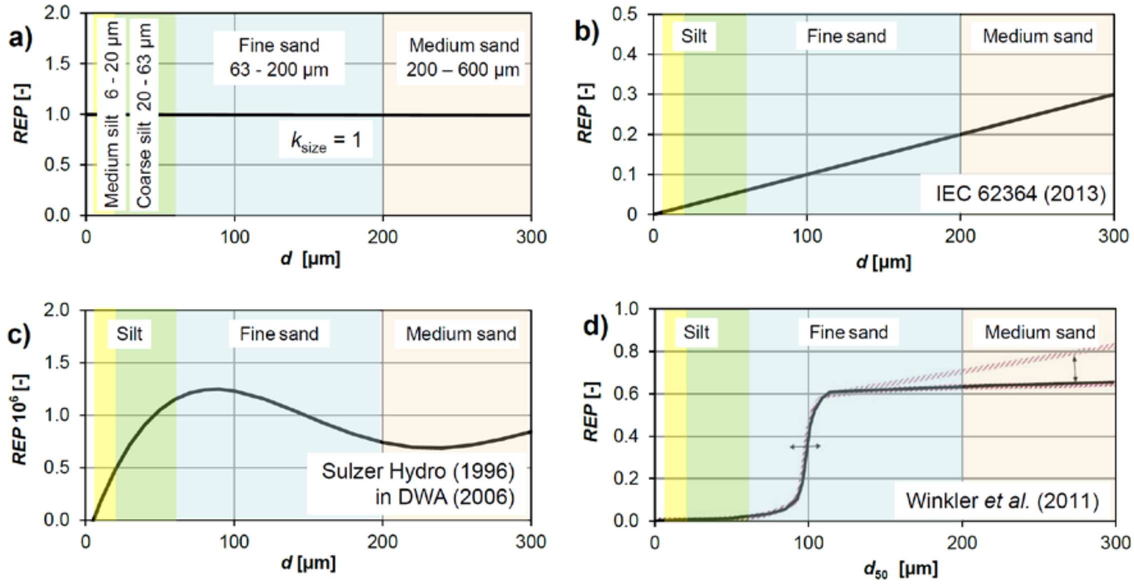

Figure 1. Relative erosion potential (*REP*) as a function of the particle diameter (d or d_{50}) according to four literature sources (a - d).

Table 1. *REP* of particles in five size classes ($k_{size,j}$) according to the relations in figure 1.

Literature source	$k_{size,j}$ [-]				
Particle size class j [-]	1	2	3	4	5
Range of particle diameters [µm]	3 - 20	20 - 50	50 - 100	100 - 200	200 - 380
a) Baseline case: constant	1.00	1.00	1.00	1.00	1.00
b) According to IEC 62364 (2013): linear	0.01	0.04	0.08	0.15	0.29
c) According to Sulzer Hydro (1996) / 10^6	0.21	0.79	1.20	0.99	0.81
d) According to Winkler et al. (2011)	0.01	0.02	0.08	0.60	0.70

4. Results and discussion

4.1. Density, hardness and shape of the particles

According to measurements with a Helium pycnometer on dried residues of twelve bottle samples, the solid density of the particle material is $\rho_s = 2.73$ g/cm^3. Rietveld X-ray diffraction analyses on three samples indicated the following mineralogical composition (by mass): 30 to 40 % Quartz (Mohs hardness 7), approximately 40 % Feldspars, Epidote and Hornblende (Mohs hardness 5.5 to 7), and the rest are softer minerals with Mohs hardness < 3, mostly mica (Muscovite, Biotite and Chlorite). The soft particles (sheet silicates) tend to be flaky, the hard particles have generally angular shapes (Fig. 2).

These results were used to determine the values of $k_{hardness}$ and k_{shape} based on literature. For $k_{hardness}$, IEC [3] suggests to take the mass fraction of the minerals which are harder than the turbine material. Because the usual base material for runners (martensitic stainless steel with 13% Cr and 4% Ni) has a Mohs hardness of 4.5, $k_{hardness}$ = 0.75 was obtained. For k_{shape}, Nozaki [7] proposed values of 0.75, 1.0 and 1.25 for rounded, angular and sharp-edged particles, respectively. IEC [3] suggests to take rounded particles as the reference (k_{shape} = 1) and proposes k_{shape} = 2 for angular particles. With the hard particles being angular, k_{shape} was set to 2 according to IEC. The product of these two factors is thus:

$$k_{hardness} * k_{shape} = 0.75 * 2 = 1.5$$

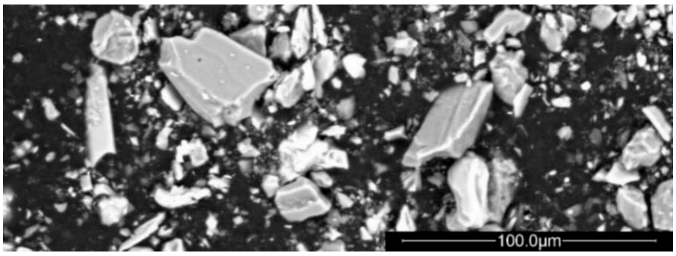

Figure 2.
Suspended sediment particles from the water sampled in the valve chamber of HPP Fieschertal (scanning electron microscope picture, ETH Zürich).

4.2. SSC, PSD and SSLs

The results of the measurements showed that the *SSC* and the *PSD* vary sometimes considerably and quickly. While the average *SSC* in the years 2012 to 2014 was 0.52 g/l, *SSC* peaks exceeding 5 g/l occurred several times a year (figure 3a). During the flood event on July 2 and 3, 2012, with an estimated return period of 20 years, the SSC rose up to 50 g/l.

The median particle diameter d_{50} was usually about 15 µm (in the range of medium silt) and increased occasionally to up to 100 µm (in the range of fine sand). The main reason for temporarily coarser particles in the turbine water is the operation of the headwater storage tunnel, i.e. a 2 km long free surface flow tunnel located between the intake and the inlet to the penstock: When the water level in the tunnel is high, relatively large and heavy particles settle preferentially. At low water level, the flow velocity and the bottom shear stress in the tunnel are considerably higher and previously settled particles are re-suspended [12]. The drawdowns of the water level in the storage tunnel led not only to higher d_{50} but also to higher *SSC*s (in the range of 10 g/l) when there were sediment deposits in the tunnel. A weak positive correlation between *SSC* and d_{50} was found. A reason for the low degree of correlation is the operation of the relatively small headwater storage leading to grain sorting.

The curves of the cumulative SSL in figure 3a show that sediment is mainly transported from mid of April to October, which is called the sediment season. The annual *SSL*s of the three years differ considerably, with the one in 2012 being the highest mainly due the major flood event in July. In all three years, 55 % of the sediment particles transported through the penstock were in the size range of fine and medium silt (≤ 20 µm), about 30 % were coarse silt (20 - 63 µm) and about 15 % were mainly fine sand (figure 3b). In 2012 the percentages of coarser particles were slightly higher than those in the other two years in which no major flood event occurred.

Figure 4b shows time series of *SSC* and cumulative *SSL* in the penstock from July 1 to 6, 2012. On July 2 and 3, the mentioned major flood event occurred; two days later a relatively high amount of sediment was re-suspended from the invert of the storage tunnel when the headwater level in the tunnel was drawn down for the first time after the flood (figure 4a). In these two events, the two highest *SSC* peaks during the three years of the study occurred and the cumulative *SSL* increased considerably in relatively short periods. Such periods are particularly important with respect to turbine wear.

During the flood event, about 17 000 t of sediment were transported through both turbines. This corresponds to 16 % of the annual *SSL* in 2012, or 33 % of the annual *SSL* in a year without any major flood (average of 2013 and 2014). During the first and largest re-suspension event after the flood, another 4000 t of sediments passed both turbines, corresponding to 4 % of the annual *SSL* in 2012.

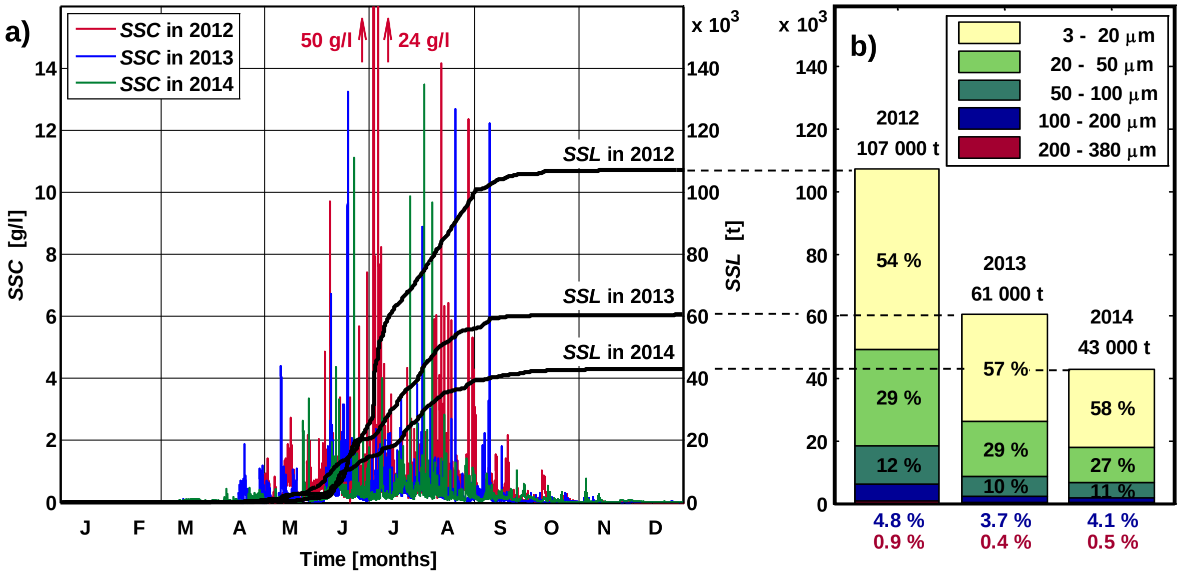

Figure 3. a) Time series of suspended sediment concentration *SSC* and cumulative sediment loads *SSL* in the penstock of HPP Fieschertal in 2012 to 2014 and **b)** annual *SSL*s by particle size classes.

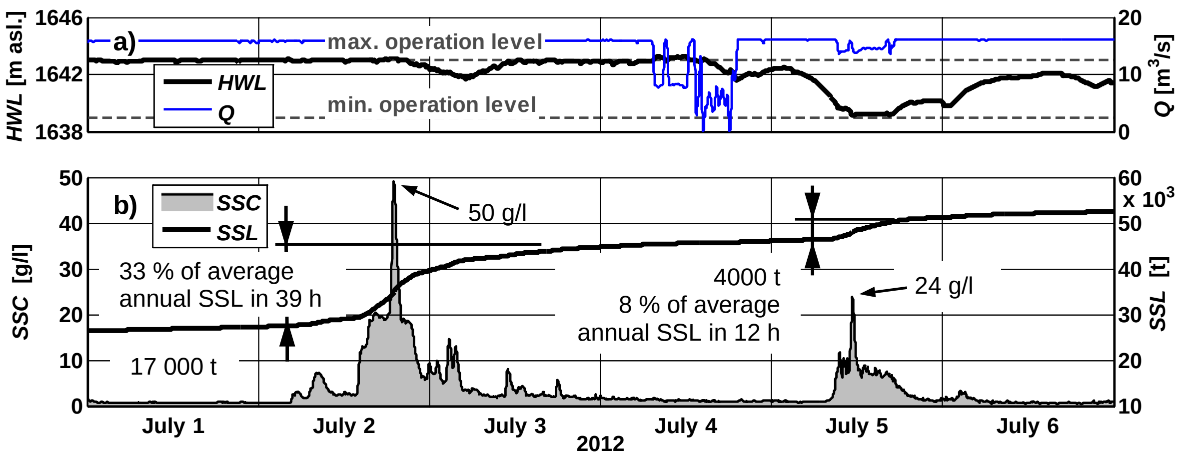

Figure 4. Time series of **a)** head water level *HWL* and discharge *Q* as well as **b)** best estimate suspended sediment concentration *SSC* and cumulative suspended sediment load *SSL* (since January 1, 2012) in the penstock at the beginning of July 2012.

Figure 5 shows the cumulative *SSL* for each turbine (called machine group, MG) as a function of the annual operating hours in the years 2012 to 2014. For MG 1, the annual *SSL* in 2012 was more than twice as high as in the other two years. The annual *SSL* of MG 2 in 2012 was smaller than that of MG 1, because MG 2 was out of operation from May 23 until June 22 (approx. 30 days) due to a problem at its transmission line while MG 1 was running almost permanently at full load. In 2013 and 2014 the annual *SSL*s were similar for both MGs.

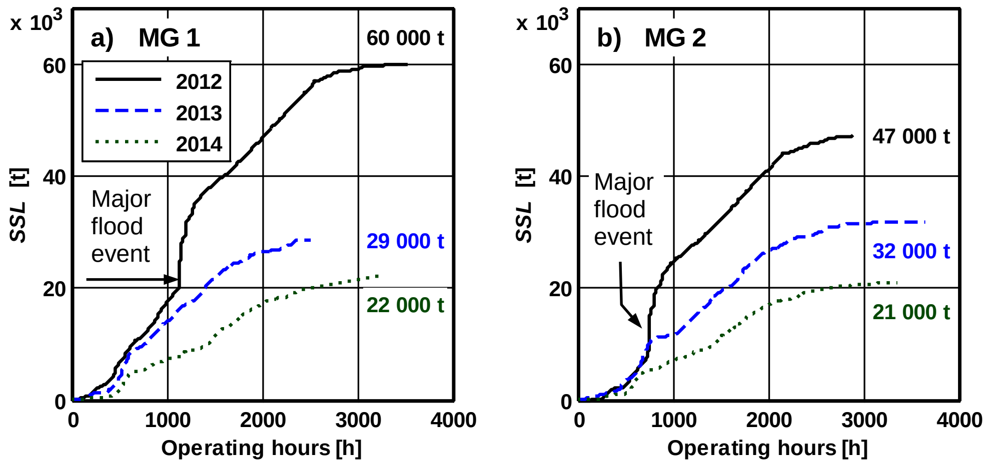

Figure 5. Suspended sediment loads *SSL*s for each machine group (MG) as a function of the annual operating hours in the years 2012 to 2014.

4.3. Particle loads according to IEC 62364

In figure 6, the *PL* with k_{size} = 1 and the cumulative *SSL* are shown for MG 1 as a function of the operating hours. The scaling of the vertical axes was adjusted to allow for a visual comparison of the two curves. The shapes of the two curves are quite similar. Comparing equations (1) and (3) with $k_{size} = 1$ yields that the curves would have exactly the same shape if either (i) the discharge Q was constant when $SSC > 0$, or (ii) if $SSC = 0$ (horizontal parts of the curves). One of the two conditions is often met due to the following reasons: (i) the HPP is generally operated at full load during the summer months when the *SSC* is high; and (ii) when the HPP is operated at partial load, the *SSC* is often low or tends to zero (in winter). The largest deviation between the two curves shown in figure 6 is observed in the second half of 2012. In the months after the flood, relatively high *SSC*s due to re-suspension in the storage tunnel occurred while the turbines were operated at partial load.

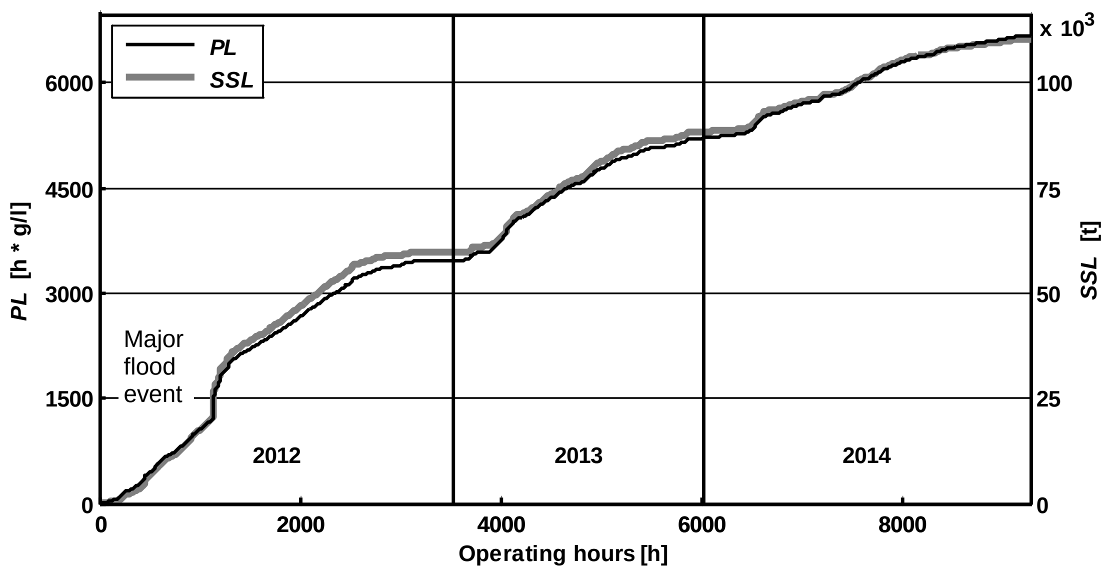

Figure 6. Particle load *PL* with k_{size} = 1 and cumulative suspended sediment load *SSL* of MG 1 as a function of the operating hours (since January 1, 2012).

In figure 7, the *PL*s of MG 1 calculated based on each of the four sets of the k_{size}-values from table 1 are shown, again as a function of the operating hours. To allow for a comparison of the shape of the curves, the *PL*s were normalized by their total values over the three analyzed years. As in figure 6, it is again observed that the four curves have generally quite similar shapes. The largest differences among the four curves are seen between the curve calculated with k_{size} according to Winkler et al. (2011) and the curve with k_{size} = 1. The main deviations between these two curves are observed (i) during and after the major flood event in 2012, (ii) in the months of late summer, and (iii) in the months of spring to early summer. The *PL* based on k_{sizes} according to Winkler et al. (2011) was higher than the *PL* with k_{size} = 1 in the cases (i) and (ii), whereas it was the other way round in case (iii). These deviations result from the high *REP* of particles above some 100 µm and the low *REP* of the normally prevailing finer particles. In cases (i) and (ii), the particles in the turbine water were generally coarser than normally due to the flood and re-suspension events. In case (iii) the particles were generally finer than normally. This is attributed to the phenomenon that relatively fine particles, which had been eroded at the glacier bed during winter, are washed-out from the glacier by the melt-water in early summer.

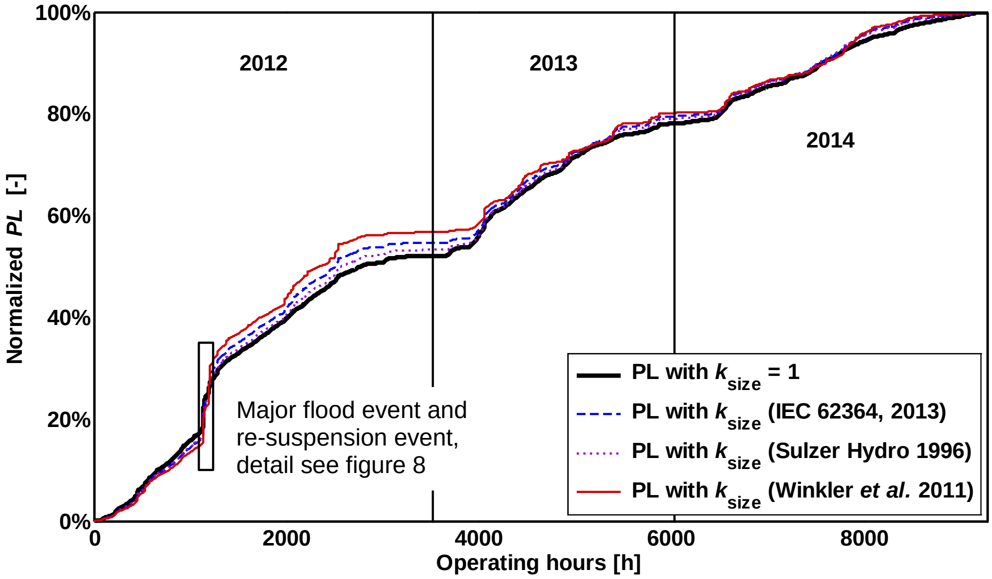

Figure 7. Normalized PLs of MG 1 calculated with four sets of k_{size}-values as a function of the operating hours from 2012 to 2014.

Figure 8 shows the time series of the normalized *PL*s during the first six days of July 2012. The time range is the same as in figure 4, including the major flood event and the first re-suspension event after the flood. The normalized *PL* calculated with k_{size} = 1 increased during these two events by 6 % and 2 %, respectively. The increase during the re-suspension event was thus one third of that during the flood event. With k_{size} according to Winkler et al. (2011) however, the increase in normalized *PL* during the re-suspension event was as high as that during the flood event (7 %). The *PL* calculated based on k_{size} according to Winkler et al. (2011) means that the approximately 4000 tons of mainly fine sand (mainly 63 - 200 µm) which passed the turbines during the re-suspension event (temporarily at part load) had a similar erosion potential as the considerably higher mass of finer particles (17 000 tons of mainly silt, 2 - 63 µm) during the flood event. The increases in normalized *PL*s during the re-suspension event calculated according to IEC (2013) and Sulzer Hydro (1996) show a higher erosion potential than with k_{size} = 1, too. The time series of *SSC*, *SSL* and *PL*s indicate that this and further re-suspension events after the flood caused considerable erosion in addition to the erosion during the flood itself.

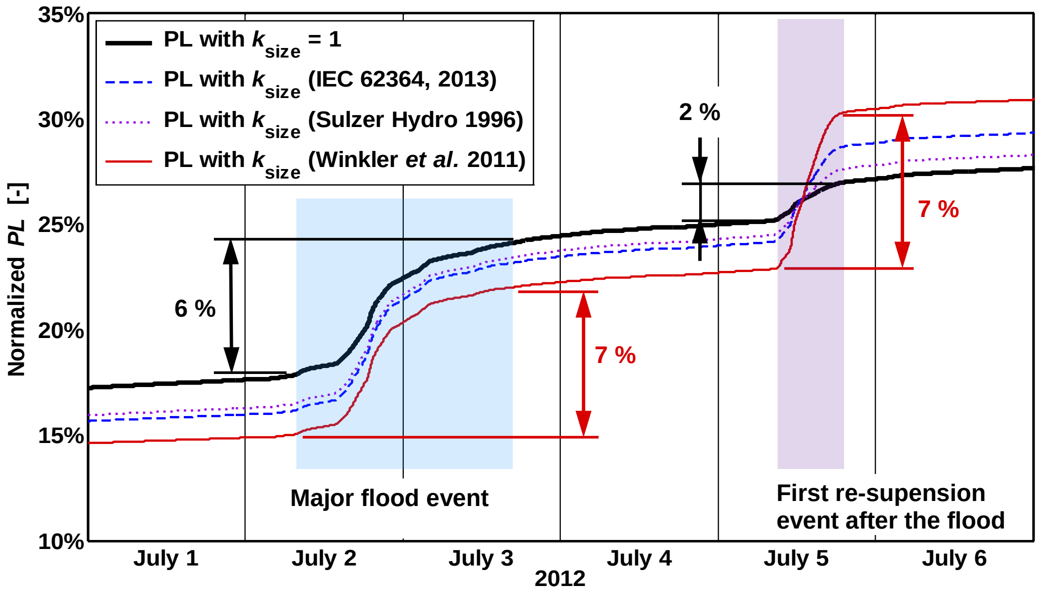

Figure 8. Detail of figure 7 in the beginning of July 2012.

5. Conclusions

SSC and PSD were measured at the waterway of the high-head HPP Fieschertal with a resolution of 1 minute during three years using an innovative combination of measuring techniques which – to the knowledge of the authors – has not been used before at any HPP.

The results of the measurements showed that *SSC* and PSD varied sometimes considerably, quickly and quite independently (weak correlation). In a major flood event in the beginning of July 2012, the *SSC* rose up to 50 g/l. The average *SSC* was 0.52 g/l and the d_{50} was normally about 15 µm. Coarser particles (up to 100 µm) were transported through the penstock and the turbines when the water level in the headwater storage tunnel was lowered (grain sorting due to re-suspension). High *SSC*s occurred due to such operational reasons or due to intense rain.

*SSL*s were calculated from the measured *SSC*s and discharges. The annual *SSL*s varied considerably from year to year, depending on flood events. The use of the LISST technology allowed quantifying the *SSC* and the *SSL* by size classes (fraction-wise).

In addition to the widely used *SSL*s, also *PL*s according to the recently introduced IEC guideline 62364 [3] were calculated using four sets of k_{size}-values. These factors reflect the relative erosion potential of particles of various sizes according to available literature. For the investigated HPP, the curves of the cumulative *SSL* and the *PL*s had generally quite similar shapes over three years. The *PL* curves deviated from the *SSL* curve mainly during partial load operation at relatively high *SSC*s. As expected from the k_{size}-factors, the largest differences among the calculated *PL*s were observed between k_{size} according to Winkler et al. (2011) and k_{size} = 1, mainly in periods when the particles were coarser than usual. The *PL* calculated with k_{size} according to Winkler et al. (2011) in the first re-supension event after the major flood in 2012 was as high as during the flood event: 4000 tons of mainly fine sand (i.e. mainly in the size range of 63 to 200 µm) led to the same *PL* as 17 000 tons of mainly silt (i.e. mainly between 2 to 63 µm).

6. Outlook

Further investigations regarding the effect of particle size on hydro-abrasive erosion especially at splitters and cut-outs of coated Pelton turbines are recommended. Laboratory investigations offer the advantages that parameters can be varied systematically and independently, and frequent erosion measurements are possible. For feasibility reasons, however, flow conditions and geometrical relations in laboratory tests deviate from prototypes, raising questions on the transferability of laboratory results to prototype conditions (upscaling). Therefore, also further field investigations with detailed measurements at HPPs are highly recommended to enlarge the set of prototype data and to provide a basis for comparison with laboratory investigations and numerical simulations.

Acknowledgements
The support of the mentioned research project by swisselectric research, the Swiss Federal Office of Energy (SFOE), the HPP operator Gommerkraftwerke AG as well as the Swiss Competence Center for Energy Research - Supply of Electricity (SCCER-SoE) and the Research Fund of the Swiss Committee on Dams are gratefully acknowledged. Further thanks go to Endress+Hauser, Sigrist Photometers and Rittmeyer for lending measuring equipment as well as to all members of the project team for their contributions.

References

[1] Felix D, Albayrak I, Abgottspon A and Boes R M 2016. Real-time measurements of suspended sediment concentration and particle size using five techniques. *Proc.* 28th IAHR Symposium on Hydraulic Machinery and Systems, Grenoble, France, IOP Conf. Series
[2] Abgottspon A, Staubli T and Felix D 2016. Erosion of Pelton buckets and changes in turbine efficiency measured in the HPP Fieschertal. *Proc.* 28th IAHR Symposium on Hydraulic Machinery and Systems, Grenoble, France, IOP Conf. Series
[3] IEC 62364 2013. Guide for dealing with hydro-abrasive erosion in Kaplan, Francis, and Pelton turbines. Edition 1.0, *International Electrotechnical Commission* (IEC), Geneva, Switzerland
[4] Felix D, Albayrak I, Boes R M, Abgottspon A, Deschwanden F and Gruber P 2013. Measuring Suspended Sediment: Results of the first Year of the Case Study at HPP Fieschertal in the Swiss Alps. *Proc.* Hydro Conf., Innsbruck, Austria, paper no 18.03
[5] Felix D, Albayrak I and Boes R M 2013. Laboratory investigation on measuring suspended sediment by portable laser diffractometer (LISST) focusing on particle shape. *Geo-marine Letters* 33(6): 485-498
[6] Winkler K, Dekumbis R and Wedmark A 2010. Finding a way to estimate the amount of abrasion. *Proc.* Hydro Conf., Lisbon, Portugal
[7] Nozaki T 1990. Estimation of repair cycle of turbine due to abrasion caused by suspended sand and determination of desilting basin capacity. *Report*, Japan International Cooperation Agency, Tokyo
[8] Grein H and Krause M 1994. Research and Prevention of Hydroabrasive Wear. *Proc.* 17th IAHR Symposium on Hydraulic Machinery, Beijing, China
[9] Sulzer Hydro 1996. Ein semi-empirisches Abrasionsmodell zur Vorhersage von hydro-abrasivem Verschleiss an X5 CrNi 13/4 Stahl (A semi-empirical abrasion model for the prediction of hydro-abrasive wear at X5 CrNi 13/4 steel). Report STT.TB94.020 (in German)
[10] DWA 2006 Entlandung von Stauräumen (Removal of reservoir sediments). Deutsche Vereinigung für Wasserwirtschaft, Abwasser und Abfall e.V., Hennef, Germany (in German).
[11] Winkler K, Dekumbis R, Rentschler M, Parkinson E and Garcin H 2011. Understanding hydro-abrasive erosion. *Proc.* Hydro Conf. Prague, Czech Republic
[12] Felix D, Albayrak I and Boes R M 2014. Variation des Feinsedimentgehalts im Triebwasser infolge Speicherstollenbewirtschaftung (Variation of suspended sediment load in turbine water due to operation of a storage tunnel). In Boes R M (ed.), *VAW-Mitteilung* 227, ETH Zurich, Switzerland: 183-193 (in German)

Hydro-abrasive erosion on coated Pelton runners: Partial calibration of the IEC model based on measurements in HPP Fieschertal

D Felix[1], A Abgottspon[2], I Albayrak[1] and R M Boes[1]

[1] Laboratory of Hydraulics, Hydrology and Glaciology (VAW), ETH Zürich, Hönggerbergring 26, CH-8093 Zurich, Switzerland

[2] Competence Center for Fluid Mechanics and Hydro Machines (CC FMHM), Hochschule Luzern (HSLU), Technikumstrasse 21, CH-6048 Horw, Switzerland

felix@vaw.baug.ethz.ch

Abstract. At medium- and high-head hydropower plants (HPPs) on sediment-laden rivers, hydro-abrasive erosion on hydraulic turbines is a major economic issue. For optimization of such HPPs, there is an interest in equations to predict erosion depths. Such a semi-empirical equation suitable for engineering practice is proposed in the relevant guideline of the International Electrotechnical Commission (IEC 62364). However, for Pelton turbines no numerical values of the model's calibration parameters have been available yet.

In the scope of a research project at the high-head HPP Fieschertal, Switzerland, the particle load and the erosion on the buckets of two hard-coated 32 MW-Pelton runners have been measured since 2012. Based on three years of field data, the numerical values of a group of calibration parameters of the IEC erosion model were determined for five application cases: (i) reduction of splitter height, (ii) increase of splitter width and (iii) increase of cut-out depth due to erosion of mainly base material, as well as erosion of coating on (iv) the splitter crests and (v) inside the buckets. Further laboratory and field investigations are recommended to quantify the effects of individual parameters as well as to improve, generalize and validate erosion models for uncoated and coated Pelton turbines.

1. Introduction

At medium- and high-head hydropower plants (HPPs) operated on sediment-laden rivers, turbine parts are subject to hydro-abrasive erosion. This causes high maintenance costs, and reduces turbine efficiency, electricity generation and revenues. As a basis for adequate countermeasures and optimizations in the design, operation and maintenance of such HPPs, the knowledge on hydro-abrasive erosion and its consequences needs to be improved. To this end, the Laboratory of Hydraulics, Hydrology and Glaciology (VAW) of ETH Zürich and the Competence Center for Fluid Mechanics and Hydro Machines (CC FMHM) of Hochschule Luzern, Switzerland, initiated an interdisciplinary research project.

In this project, sediment load, erosion on Pelton turbine runners and turbine efficiency changes have been measured and analyzed since 2012 at the high-head HPP Fieschertal in Valais, Switzerland. This run-of-river HPP with a design discharge of 15 m^3/s and a gross head of 520 m is equipped with two horizontal 32 MW Pelton turbines [1]. The water used in this HPP originates from a glaciated catchment and is known for relatively high suspended sediment concentration (*SSC*), i.e. *SSC* = 0.5 g/l on average, rising several times a year above 5 g/l. The injectors and the inner sides of the runner buckets are hard-coated with thermally sprayed tungsten carbide in a cobalt-chrome-matrix (WC-CoCr). The coating contributes to reduce the extent of erosion, but does not fully prevent the erosion of the base material. In each winter, damaged splitters and cut-outs are rounded by grinding if required and these zones are re-coated on-site. The Suspended Sediment Loads (*SSL*) and the so-called Particle Loads (*PL*) of the turbines in this HPP in the years 2012 to 2014 were quantified and presented in [2]. The turbine erosion in the corresponding period was also quantified and is treated in [3].

The present paper deals with the application of an equation to predict erosion depth, i.e. a semi-empirical erosion model, proposed by the relevant guideline of the International Electrotechnical Commission (IEC 62364, Edition 1, 2013) [4]. Frist, the processes causing hydro-abrasive erosion and the IEC model are described with focus on Pelton turbines. Then the model is applied to the data set of the HPP Fieschertal and the numerical values of a group of previously unknown model parameters are determined for five application cases to calibrate the model as far as possible. Finally, the results are discussed and recommendations on improvements of erosion prediction models for uncoated and coated Pelton turbines are given.

2. Hydro-abrasive erosion

2.1. Terminology and erosion mechanisms

Hydro-abrasion is a process causing material removal from a surface by the action of solid particles contained in flowing water (three-phase system). It is also described as a gradual alteration in state and shape of surfaces in contact with a particle-laden flow [5]. Hydro-abrasion is one of several processes causing erosion. In the field of hydro machines, also the combined terms ‘abrasive erosion’ [5] or ‘hydro-abrasive erosion’ are used [4]. The latter term is adopted in the present study.

Commonly, two erosion mechanisms are distinguished, mainly depending on the angle of attack α, i.e. the angle between the trajectories of the approaching particles and the surface (figure 1a) [6] [7]:

- Cutting of surface material due to sliding or impingement of particles at low α (‘cutting erosion’)
- Repeated plastic deformation of surface material and/or crack formation due to particle impacts at higher α, leading to breaking loose of material pieces (‘deformation erosion’)

For ductile materials, the erosion rate is usually highest between $\alpha \approx 20°$ and 40° (figure 1b). For brittle materials however, the erosion rate is highest at $\alpha \approx 90°$ and decreases pronouncedly with smaller α [6] [7]. While steel is typically ductile, hard-coatings (cermets) show brittle behaviour.

As a consequence of surface shape degradation due to hydro-abrasive erosion, cavitation may occur, which in turn may increase erosion (synergistic effect [4]). This complex interaction is not covered in the IEC erosion model [4] and is beyond the scope of the present study.

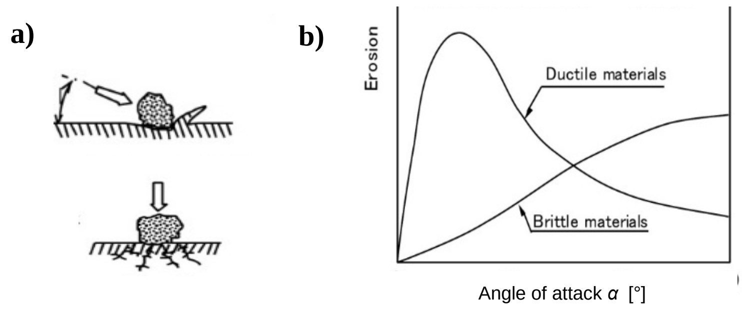

Figure 1. Schematic representations of **a)** two erosion mechanisms and **b)** typical erosion rates as a function of the angle of attack α for ductile and brittle materials, respectively [8].

2.2. Typical conditions in Pelton turbines

In the turbine water of high-head HPPs, the mineral particles are typically smaller than 300 µm, because coarser particles are mostly excluded by upstream reservoirs or sand traps. Typically, most particles are in the size range of silt (2 - 63 µm); particles in the size range of fine or medium sand are less frequent. The particles in the turbine water are generally transported in suspension and their velocity is similar to the flow velocity.

The highest velocities and accelerations occur in high-head Pelton turbines: for instance, at a head of 500 m, the relative velocity of the particle-laden flow in relation to turbine parts is 100 m/s at injectors (nozzles) and 50 m/s in a runner bucket. During the redirection of the flow in the two halves of a Pelton bucket for example, the acceleration normal to the bucket surface corresponds to typically several 10 000 times the gravitational acceleration. Such acceleration normal to the main flow direction drives particles generally outwards, leading to higher *SSC* close to convex surfaces, higher impingement rate and sliding of particles. The erosion inside Pelton buckets is due to the first mechanism mentioned above [9]. The second mechanism occurs typically on the splitter crests and the leading edges in the cut-outs, where α is high. These zones of Pelton buckets are particularly prone to erosion.

2.3. Erosion prediction

Many equations for the prediction of erosion have been developed since decades based on analytical considerations and laboratory tests, and numerical simulation methods have been increasingly used [10]. A major difficulty is to link the processes at the microscopic level to macroscopic models [11]. For engineering applications, there is an interest in easily applicable equations. Such semi-empirical equations comprise typically some calibration parameters and are limited to specific applications.

3. IEC erosion model for hydraulic turbines

3.1. Equation for the erosion rate

A working group of IEC formulated a concept for the modeling of hydro-abrasive erosion on hydraulic turbines for applied engineering purposes [12]. This concept and general design recommendations have been published in the IEC guideline 62364 [4]. It gives a factorized equation for the absolute erosion rate, considering the following parameters:

$$\frac{\Delta d_{\mathrm{e}}}{\Delta t} = \frac{K_{\mathrm{f}}}{RS^{p}} K_{\mathrm{m}}\, w^{x}\, SSC\; k_{\mathrm{size}}\, k_{\mathrm{shape}}\, k_{\mathrm{hardness}} \qquad \text{[mm/h]} \qquad (1)$$

where

- Δt — Exposure period [h];
- Δd_{e} — Depth of erosion during Δt [mm];
- K_{f} — Coefficient reflecting the flow pattern, i.e. angle of attack and turbulence intensity [dimensions as resulting from calibration], intended to be constant for each turbine component, see note 1 below;
- RS — Reference size of a turbine [m]; for Francis turbines RS = runner diameter D, for Pelton turbines RS = inner bucket width B;
- p — Exponent [-], a constant for each turbine component, for consideration of curvature-dependent effects, see note 1 below;
- K_{m} — Coefficient for the material at the surface of a turbine part [-], $K_{\mathrm{m}} = 1$ for martensitic stainless steel with 13% Cr and 4% Ni; $K_{\mathrm{m}} < 1$ for coating material;
- w — Characteristic relative velocity between the flow (or the particles) and the turbine part [m/s];
- x — Exponent [-], IEC suggests 3.4, literature values range between 2 and 4, see section 4.2.
- SSC — Suspended sediment mass concentration [g/l] = [kg/m^3], for Pelton $SSC = 0$ if no flow;
- k_{size} — Coefficient for particle size [-], IEC suggests to take the numerical value of d_{50} in [mm], d_{50} is the median size of graded particles which is not exceeded by 50% of the particle mass;
- k_{shape} — Coefficient for particle shape [-], IEC suggests $k_{\mathrm{shape}} = 1$ for rounded or 2 for angular;
- k_{hardness} — Coefficient for particle hardness with respect to the hardness of the surface material [-], IEC suggest to take the mass fraction of particles harder than the surface material.

Note 1: Numerical values for K_{f} and p are given in IEC for five locations (parts) within uncoated Francis turbines. These values resulted from a statistical evaluation of field data of up to seven HPPs, mainly in China. For Pelton turbines, no such values are given in IEC due to scarcity of field data.

3.2. Integration over time and the concept of Particle Load (PL)
To obtain the erosion depth Δd_e over a time interval Δt, equation (1) is multiplied by Δt. The erosion depths in the time intervals since the start time t_0 until the time t are summed up to obtain the cumulated erosion depth $d_e(t)$ as follows:

$$d_e(t) = \frac{K_f}{RS^p} K_m w^x \underbrace{\sum_{i=1}^{(t-t_0)/\Delta t} SSC_i \; k_{\text{size},i} \, k_{\text{shape},i} \, k_{\text{hardness},i} \, \Delta t}_{= PL(t)} \qquad \text{[mm]} \qquad (2)$$

The time step number is denoted as i. The parameters K_f, RS, p, K_m, w and x are constant or are assumed to be constant. The integral of the particle-related factors over the exposure period is called 'particle load' (PL). $PL(t)$ reflects the cumulated erosion potential of the particles passing through a turbine as a function of t since t_0. PL has units of [h · g/l] = [h · kg/m^3]. In contrast to SSL, the PL is not a function of the discharge and does not depend on the turbine's size. In equations (1) and (2), the erosion depth is modelled to be proportional to SSC and the exposure time. Thus, the same erosion depth is expected when a turbine runs e.g. for 1000 h at 0.5 g/l or for 100 h at 5 g/l (with the same particle properties), and the PL is the same in both cases.

3.3. Adaptation of the PL for Pelton runners
In contrast to reaction turbines or injectors of Pelton turbines, the erosion on a Pelton bucket takes place during only a part of the operation time (intermittent process). The erosion on a bucket decreases proportionally to the number of buckets z_2 because of the shorter exposure time per bucket. On the contrary, the erosion increases approximately proportional to the number of injectors (nozzles) z_0 because more buckets are simultaneously in contact with the sediment-laden water. The effects of z_0 and z_2 on the erosion rate or depth are stated in [13] (published in [14]) and are included in the so-called 'reference model' for Pelton turbines in the guideline [4]. To account for these effects, an adapted PL is introduced here:

PL for Pelton buckets $$PL_b = \frac{z_0}{z_2} PL \qquad \text{[h · g/l] = [h · kg/m}^3\text{]} \qquad (3)$$

The use of PL_b allows meaningful comparisons of the erosion potential on buckets between Pelton turbines with different numbers of nozzles and buckets.

4. Application and partial calibration of the IEC erosion model

4.1. Available erosion data and geometrical definitions
From the erosion measurements on the two machine groups (MGs) of the HPP Fieschertal, the following data are available from the years 2012 to 2014: (i) geometrical changes (in the range of mm) at the splitter crests and at the leading edges of the cut-outs of the runner buckets, where the coating was locally or systematically removed during sediment seasons with medium or high SSL (figure 2), and (ii) slight reductions of coating thicknesses (in the range of 10 µm) inside the buckets. The erosion on the nozzles was not monitored.

To quantify the erosion on the splitter crests and on the leading edges of the cut-outs, the geometrical definitions shown in figure 3 were introduced. The width s of an eroded splitter can easily be measured (e.g. with a ruler) if the splitter is flat on top and has sharp edges. The selected definition of s using the slopes of tangents [15] allows to determine s also if the splitter crest is unevenly eroded or rounded (e.g. due to grinding). The splitter width s is considered as an important indicator of the erosion status of a runner [16] [17]. The values of s and h are the maximum values along the splitter of a bucket. The cut-out depth d is the maximum value within the cut-outs of a bucket.

From the repeated measurements of these quantities at buckets no. 1 and 2 of each runner [3], the reduction of splitter height Δh, increase of splitter width Δs and increase of cut-out depth Δd were determined for each runner and each sediment season.

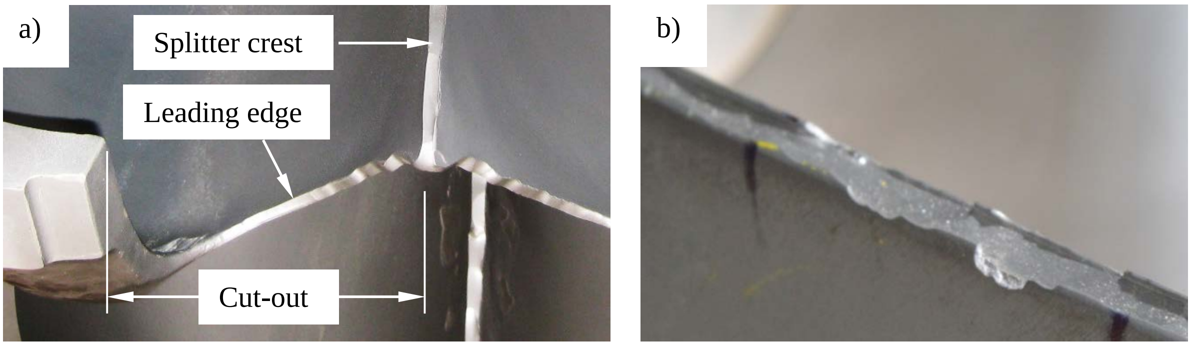

Figure 2. Examples of local erosion on hard-coated Pelton runners in the HPP Fieschertal: **a)** at splitter crests and leading edges of cut-outs (MG 2, August 08, 2012) and **b)** detail of eroded splitter with exposed base material on the crest (MG 2, November 15, 2013); the buckets were fully coated at the beginnings of the sediment seasons (pictures: VAW, ETH Zürich).

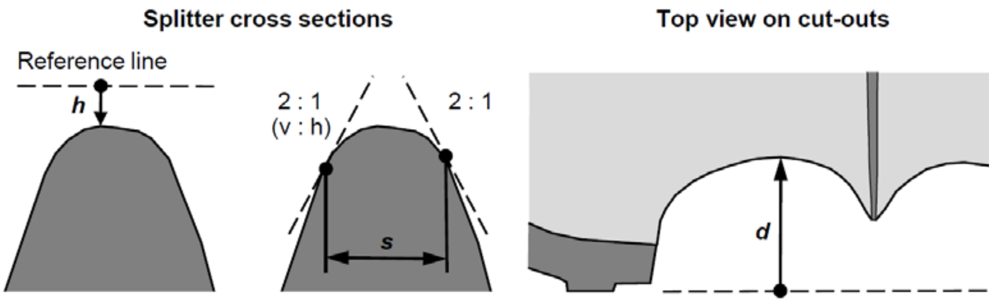

Figure 3. Geometrical definitions of h, s and d (modified from [15] and [3]).

4.2. Known values of model parameters

As a preparation for the application of the described erosion model, known parameter values are summarized in this section.

In Pelton turbines, the jet velocity and thus the relative velocity at the injector is $w_{\mathrm{inj}} = (2gh_{\mathrm{n}})^{0.5}$ where h_{n} is the net head and g is the gravitational acceleration. For the HPP Fieschertal, the net head varies between 499 and 515 m. With the time-averaged net head of 510 m, $w_{\mathrm{inj}} \approx 100$ m/s. The relative velocity w between the jet and the buckets is half of the jet velocity, thus $w = 50$ m/s.

IEC suggests a velocity exponent of $x = 3.4$ without specifying the turbine type and indicates a range between 2 and 4. For Pelton splitters, $2.8 \leq x \leq 3$ was found in laboratory tests [18]. In the present study, $x = 3$ was adopted, corresponding to [13] and other studies. Thus $w^x = 125'000$ $\mathrm{m^3/s^3}$.

Each turbine of HPP Fieschertal has two injectors ($z_0 = 2$) and each runner has 20 buckets ($z_2 = 20$) with an inner width $B = RS = 0.65$ m.

The $PL(t)$ for each turbine (MG) were determined based on the operating hours and the measured time series of the SSC and the median particle size d_{50}. To do so, k_{size} was determined as a function of the actual d_{50}, as described in the definition of the variables of equation (1). The coefficient k_{size} is a linear function of d_{50} with $k_{\mathrm{size}} = 1$ at $d_{50} = 1000$ µm. For HPP Fieschertal, the temporal average of the k_{size}-values during the three years was 0.033. The coefficients $k_{\mathrm{hardness}} = 0.75$ and $k_{\mathrm{shape}} = 2$ were assumed to be constant over time (properties of the catchment area) [2].

The PL obtained with k_{size} according to IEC used in the present paper are on temporal average 30 times smaller than the PL obtained with $k_{\mathrm{size}} = 1$ also reported in [2]. This recalls that the definition of $k_{\mathrm{size}} = f\,(d_{50})$ is important for the determination of the PL.

4.3. Identification of unknown parameters

For the application of equation (2) at Pelton buckets, PL was replaced by PL_b according to equation (3). For HPP Fieschertal, the PL_b-values are ten times smaller than the PL-values because of z_0 / z_2 = 0.1. The parameters d_e, w^x, PL_b and RS are known. K_m is known for the base material (K_m = 1 by definition), but is unknown for the coating. In order to obtain an equation applicable to erosion of coating and/or base material, K_m was treated as a generally unknown parameter. K_f and p are unknown. The equation was solved for the unknown parameters. This group of parameters was denoted as C:

$$\frac{K_f}{RS^p} K_m = \frac{d_e(t)}{w^x\, PL_b(t)} \qquad \text{with } C = \frac{K_f}{RS^p} K_m \quad \text{(definition)} \tag{4}$$

for HPP Fieschertal

$$C = \frac{1}{125\,000} \frac{d_e(t)}{PL_b(t)} \qquad [\text{mm} / (\text{h} \cdot \text{g/l} \cdot \text{m}^3/\text{s}^3)] \tag{5}$$

4.4. Model application cases

In the following, the erosion model in the form of equation (5) is applied to the following cases:

i. Decrease of splitter height Δh
ii. Increase of splitter width Δs
iii. Increase of cut-out depth Δd
iv. Decrease of coating thickness inside the buckets Δc
v. Decrease of coating thickness on the splitter crests (Δh within the coating)

The IEC model was developed for the estimation of erosion depths on plane or moderately curved surfaces, as in case (iv). Applying such a model to geometrical changes at splitter crests or in cut-outs, as in the other four cases, corresponds to an extension of the original range of application, but is considered to be useful in practice. Δh, Δd and Δc are erosion depths because they are measured approximately in the directions of the erosion. However, Δs is not an erosion depth but a geometrical quantity depending on Δh, the cross-sectional shape of the splitter and the initial splitter width.

4.5. Geometrical changes due to erosion at splitters and cut-outs

The Δh, Δs and Δd obtained from the measurements are shown in figures 4a, b and c, respectively, as a function of the PL_b. Approximate SSL per turbine, as determined in [2], are also indicated on the top axes for comparison. It has been shown in [2] for the HPP Fieschertal that PL and SSL are approximately proportional over longer time spans such as at least one year. The absolute values of the geometrical changes are given on the left ordinates, whereas the relative geometrical changes (normalized with the inner bucket width B = 0.65 m) are given on the right ordinates of figures 4a, b and c. In 2014, the PL_b of both MGs were almost the same and no significant geometrical changes were measured (circular markers on top of each other). The data points in figures 4a, b and c show a similar pattern, indicating a systematic dependency of Δh, Δs and Δd on PL_b.

To determine the C-values in equation (5) for each of the three cases (d_e = Δh, Δs or Δd), linear least squares regressions were made on the data points shown in figure 4. In a first step, linear relations passing through the origins of the axes (denoted as 'Fit type 1') were selected, shown with dashed lines. The obtained C- and the R^2-values are listed in the second column of table 1.

The investigated buckets were fully coated at the beginnings of the seasons (either factory coating or on-site re-coating). According to figure 4, the systematic erosion of base material at the splitter crests and the leading edges of the cut-outs began only after a certain PL_b. This threshold value was denoted as $PL_{b,0}$. The erosion process at the splitters and the leading edges of cut-outs can thus be divided in two stages: erosion of (1) mainly coating material and (2) mainly base material at a higher rate. According to unconstrained linear fits (denoted as 'Fit type 2', solid lines), the second stage of erosion began after $PL_{b,0} \approx 4.1$ [h · g/l]. These lines fit significantly better to the data, i.e. the R^2 are higher than those of the constrained fits. The C-values resulting from the unconstrained fits are also listed in table 1. Note that these C-values refer to only the second stage of erosion, i.e. to $PL_{b,2} = PL_b - PL_{b,0}$. The C-value for Δs is less than half of that for Δh due to geometrical reasons (the flanks of the splitter are relatively steep). The C-values for Δd and Δh are similar.

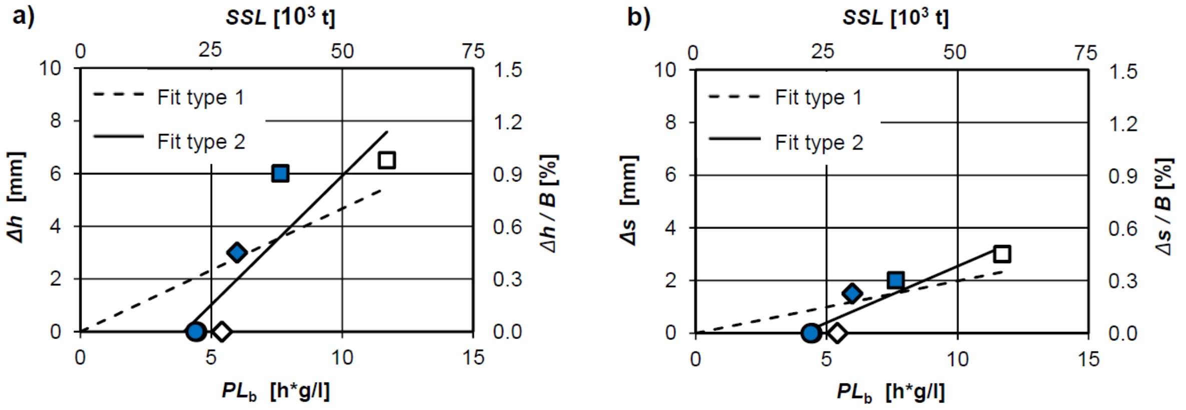

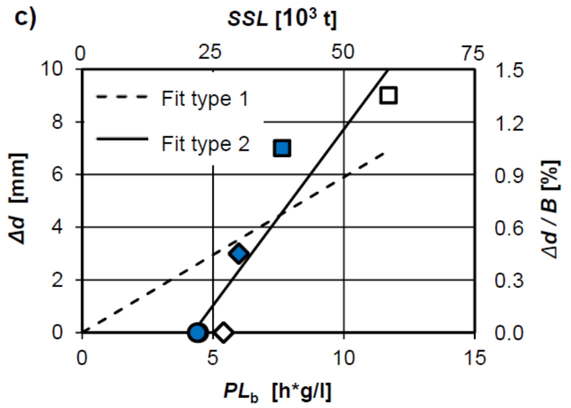

Figure 4.
a) Reduction of splitter height Δh,
b) increase of splitter width Δs and
c) increase of cut-out depth Δd
of the runner buckets of MG 1 (empty markers) and MG 2 (filled markers) of HPP Fieschertal in the sediment seasons 2012 (□), 2013 (◇) and 2014 (○) as a function of the particle load PL_b (with k_{size} = 0.033 on average, $k_{hardness}$ = 0.75, k_{shape} = 2, z_0 = 2, z_2 = 20) and approximate suspended sediment loads (*SSL*).

Table 1. Results of the fits between measured geometrical changes due to erosion and PL_b on Pelton buckets of HPP Fieschertal in the years 2012 to 2014; C and PL_b are defined in equations (4) and (3).

Application case (location in the Pelton bucket and measurement direction)	Erosion of coating and base material: Fit type 1 (dashed lines)	Distinguishing two stages of erosion (coating vs. base material): Fit type 2 (solid lines)	
	C [mm / (h · g/l · m³/s³)]	$PL_{b,0}$ [h · g/l]	C [mm / (h · g/l · m³/s³)]
Reduction of splitter height Δh	$3.7 \cdot 10^{-6}$ (R^2 = 0.54)	4.0	$7.8 \cdot 10^{-6}$ (R^2 = 0.78)
Increase in splitter width Δs	$1.6 \cdot 10^{-6}$ (R^2 = 0.58)	4.1	$3.4 \cdot 10^{-6}$ (R^2 = 0.86)
Increase in cut-out depth Δd	$4.7 \cdot 10^{-6}$ (R^2 = 0.56)	4.2	$10.7 \cdot 10^{-6}$ (R^2 = 0.87)

4.6. Erosion of the coating in the buckets

In contrast to the three previous application cases, the following two cases deal with the erosion of coating material only. The hardness of WC-CoCr-coatings (approx. 1200 HV) is similar to that of quartz (Mohs' hardness 7). In the water of HPP Fieschertal, no minerals harder than quartz were detected. According to the definition of the parameters in equation (1), this would lead to $k_{hardness}$ = 0 with respect to the coating and thus PL_b = 0. In order to keep non-zero PL_b-values and for comparability, the value of $k_{hardness}$ = 0.75 (determined with respect to the base material) was also used in cases with erosion of the coating material.

Regarding erosion of coating in the buckets, two data points are available from the detailed template-based measurements before and after the sediment seasons initiated in spring 2013: the coating thickness in the buckets of MG 1 was reduced by 10 µm and 4 µm in the sediment seasons 2013 and 2014, respectively [3]. These are average values over the surfaces inside buckets no. 1 and 2. With an uncertainty of ± 5 µm, the coating thickness reduction measured in 2014 lies within the band of uncertainty. From these two data points, the following approximate C-value was obtained:

Erosion of coating in buckets $C \approx 1 \cdot 10^{-8}$ [mm / (h · g/l · m³/s³)]

It should be noted that this value has a higher relative uncertainty than the C-values in section 4.5. However, the higher relative uncertainty is of no concern for practical application, because the erosion of the coating in the buckets in two years without a major flood was small and is not decisive for the times between overhauls.

4.7. Erosion of the coating on the splitter crests

The analysis in section 4.5 showed that the coating on the splitter crests was systematically eroded after a $PL_{b,0} \approx 4.1$ [h · g/l]. Note that this value is based on $k_{hardness} = 0.75$, as explained in the previous section. With the coating thickness meter used in this study [3], it was not possible to measure the coating thicknesses on the splitter crests for geometrical reasons. Assuming an initial coating thickness of 300 to 500 µm and a homogeneous and linear erosion on the splitter crest, the following approximate C-value results:

Erosion of coating on splitter crests $C \approx (0.6 \text{ to } 1) \cdot 10^{-6}$ [mm / (h · g/l · m³/s³)]

The C-value and the erosion rate of the coating on the splitter crests are thus about 60 to 100 times higher than in the buckets. This is mainly attributed to the effect of the angle of attack α on the erosion rate of brittle material, i.e. higher erosion at high α (figure 1).

5. Discussion

5.1. C-values

Various C-values were determined in the previous subsections for five different cases. C involves the parameters K_f, RS^p and K_m (equation 5). In the following, it is discussed whether it is possible to determine the values of some of these parameters based on the presented data set.

RS is known (0.65 m), but p is unknown. During the second stage of erosion, i.e. erosion of mainly base material, the coefficient for the properties of the eroded material is known by definition, $K_m = 1$. Thus, the values of the ratio K_f / RS^p are known for the cases (i) to (iii) during the erosion of the base material. From the presented data set, the exponent p, i.e. the effect of the turbine reference size RS on the erosion cannot be determined, because runners with only one size have been investigated.

Assuming that Δh, Δs and Δd do not significantly depend on RS, i.e. $p \approx 0$ and thus $RS^p \approx 1$, the K_f-values for the erosion of the base material correspond to the obtained C-values in the last column of table 1. Further measurements are required to investigate whether the slight difference in K_f for Δh and Δd is systematic (e.g. due to effects of the flow patterns and the profile shapes) or random, i.e. lies within the band of uncertainty.

The comparison of the C-values for erosion on the splitter crests in the base material (Δh in the second stage of erosion, $7.8 \cdot 10^{-6}$, table 1) and in the coating material (≈ 0.6 to $1 \cdot 10^{-6}$ in the same units) shows that the K_m-value for the coating is lower than that of the base material, as expected. The factor between the C-values of these two cases (both with high α) is about 10 (with the same $k_{hardness}$-values for both erosion of the coating and the base material).

Further measurements on buckets differing in size and with/without coating are required to further investigate the values of p, K_m and K_f for various cases.

5.2. Erosion of the coating in the buckets

During the years 2013 and 2014, the area-averaged erosion depths of the coating in the buckets (4 µm and 10 µm) were small compared to the initial coating thicknesses of 300 µm to 500 µm, and the erosion of coating material in the buckets was of no concern in these years.

In 2012 however, considerably more coating material was eroded in the buckets of the runner in MG 2: in the bottom region of some buckets, towards the bucket root, the coating was completely removed. In the vicinity of these zones, coating thicknesses of 50 µm to 100 µm were measured when the runner was taken out of operation after the major flood of July 2012 [3]. In the buckets of the runner in MG 1, however, no zones with totally eroded coating were observed after the major flood event, and the remaining coating thickness in the buckets was sufficient to use this runner for at least another three years. The considerable erosion inside the buckets of MG 2 in 2012 was probably related to the relatively wide and blunt splitters (s = 8 to 10 mm) which caused a disturbed flow field and could have induced cavitation as a secondary or combined damage mechanism. Local complete erosion of hard-coating in the bottom region of buckets was also observed in other studies [17].

6. Conclusions

The model for hydro-abrasive erosion proposed in the IEC guideline 62364 [4] with the concept of *PL* was summarized focusing on Pelton turbines. Based on sediment and erosion data acquired in the years 2012 to 2014 in the HPP Fieschertal, the numerical values C of a group of model calibration parameters were determined for five application cases: (i) reduction of splitter height Δh, (ii) increase of splitter width Δs, and (iii) increase of cut-out depth Δd mainly due to erosion of base material, as well as erosion of coating (iv) on the splitter crests and (v) inside the buckets.

Two stages of erosion at splitters and cut-outs were distinguished: Firstly the erosion of mainly coating, and secondly the erosion of mainly base material at a higher rate. The *PL* until the beginning of the second stage was quantified. C-values for Δh, Δs and Δd in the second stage were obtained from unconstrained linear fits. The C-values for the erosion of the coating on the splitters and inside the buckets confirm that the coating material has a much higher resistance to erosion than the base material. In particular, the C-value for the erosion of coating in the buckets is very low, proving that the coating is highly resistant to solid particle erosion if the angle of attack is low and there is no cavitation.

In field investigations, the parameters cannot be varied individually and systematically, and erosion depths cannot be measured frequently at most HPPs. The present study is based on three years of measurements in one HPP, i.e. the data set is limited and refers to a single bucket width (turbine size). Thus, it is not possible to determine the value of each model calibration parameter. However, with the definition of the C-value, it was possible to partly calibrate the erosion model and making it applicable. Care should be taken when applying the determined C-values to other HPPs, since the effects of some parameters have not been investigated yet, and the range of validity and the uncertainty of the calculated erosion depths are not yet quantified.

7. Outlook

In the described model, the factors k_{size}, K_{f} and p are the most challenging to quantify since they depend on many factors such as turbine type, location inside the turbine, flow pattern, angle of attack, radius of curvature and others. Further investigations by means of analytical considerations, laboratory tests, comprehensive measurements at further HPPs and numerical simulations are recommended. Additional laboratory and field data are required to (i) enlarge the data base especially for Pelton tubines, (ii) calibrate and validate semi-empirical equations and numerical models, (iii) extend and demonstrate the application range, and (iv) quantify the uncertainty of such models. For the further development of erosion models for uncoated and coated Pelton runners it is recommended to:

- Investigate the erosion processes of both the coating and the base material;
- Extend the models to four material phases: water, solid particles, base material and coating;
- Investigate the effect of turbine reference size (RS^p) and particle size (k_{size}) on erosion;
- Consider the effect of initial splitter width, in particular with respect to secondary damages;
- Investigate and consider non-linear effects in damage progression.

Acknowledgements

The support of the mentioned research project by swisselectric research, the Swiss Federal Office of Energy (SFOE), the HPP operator Gommerkraftwerke AG as well as the Swiss Competence Center for Energy Research - Supply of Electricity (SCCER-SoE) and the Research Fund of the Swiss Committee on Dams are gratefully acknowledged. Further thanks go to Endress+Hauser, Sigrist Photometers and Rittmeyer for lending measuring equipment as well as to all members of the project team for their contributions.

References

[1] Felix D, Albayrak I, Abgottspon A and Boes R M 2016. Real-time measurements of suspended sediment concentration and particle size using five techniques. Proc. 28th IAHR Symposium on Hydraulic Machinery and Systems, Grenoble, France, IOP Conf. Series

[2] Felix D, Albayrak I, Abgottspon A and Boes R M 2016. Suspended sediment measurements and calculation of the particle load at HPP Fieschertal. *Proc.* 28th IAHR Symposium on Hydraulic Machinery and Systems, Grenoble, France, IOP Conf. Series

[3] Abgottspon A, Staubli T and Felix D 2016. Erosion of Pelton buckets and changes in turbine efficiency measured in the HPP Fieschertal. *Proc.* 28th IAHR Symposium on Hydraulic Machinery and Systems, Grenoble, France, IOP Conf. Series

[4] IEC 62364 2013. Guide for dealing with hydro-abrasive erosion in Kaplan, Francis, and Pelton turbines. Edition 1.0, *International Electrotechnical Commission* (IEC) Geneva, Switzerland

[5] Duan C G and Karelin V Y (eds.) 2002. Abrasive Erosion & Corrosion of Hydraulic Machinery, *Book series on Hydraulic machinery*, Vol. 2. London: Imperial College Press

[6] Finnie I 1960. Erosion of surfaces by solid particles. *Wear* 1960(3): 87-103

[7] Bitter J G A 1963. A study of erosion phenomena, parts I and II. *Wear* 1963(6): 5-21, 169-190

[8] Matsumura M 2014. Erosion-Corrosion: An introduction to flow induced macro-cell corrosion. Bentham eBooks

[9] Neopane H P, Dahlhaug O G and Cervantes M 2011. Sediment Erosion in Hydraulic Turbines. *Global J. of Researches in Engineering, Mechanical and Mechanics Engineering* 11(6)

[10] Felix D, Albayrak I, Abgottspon A and Boes R M 2016. Hydro-abrasive erosion of hydraulic turbines caused by sediment – a century of research and development. *Proc.* 28th IAHR Symposium on Hydraulic Machinery and Systems, Grenoble, France, IOP Conf. Series

[11] Meng H C and Ludema K C 1995. Wear models and predictive equations: their form and content. *Wear* 181-183: 443–457

[12] Winkler K, Dekumbis R and Wedmark A 2010. Finding a way to estimate the amount of abrasion. *Proc.* Hydro Conference, Lisbon, Portugal

[13] Sulzer Hydro 1996. Ein semi-empirisches Abrasionsmodell zur Vorhersage von hydro-abrasivem Verschleiss an X5 CrNi 13/4 Stahl (A semi-empirical abrasion model for the prediction of hydro-abrasive wear on X5 CrNi 13/4 steel). *Report* STT.TB94.020 (in German)

[14] DWA 2006. Entlandung von Stauräumen (Removal of reservoir sediments). Deutsche Vereinigung für Wasserwirtschaft, Abwasser und Abfall e.V., Hennef, Germany (in German)

[15] Abgottspon A, Stern P, Staubli T, Felix D and Winkler K 2013. Measuring Turbine Abrasion and Efficiency Decrease: First Results of the Case Study at HPP Fieschertal. *Proc.* Hydro Conference, Innsbruck, Austria: paper 18.05

[16] Boes R 2009. Real-time monitoring of SSC and PSD in the headwater way of a high-head hydropower plant. *Proc.* 33rd IAHR Concress, Vancouver, Canada, 11026: 4037-4044

[17] Maldet R 2008. Pelton runner with high erosion caused by glacier sediment: assessment and measures. *Proc.* 15th Intl. Seminar on HPPs, Doujak E (ed.), Vienna, Austria: 639-646

[18] Winkler K, Dekumbis R, Rentschler M, Parkinson E and Garcin H 2011. Understanding hydro-abrasive erosion. *Proc*. Hydro Conference, Prague, Czech Republic

Optimization of hydropower plants with respect to fine sediment focusing on turbine switch-offs during floods

D Felix[1], I Albayrak[1], A Abgottspon[2] and R M Boes[1]

[1] Laboratory of Hydraulics, Hydrology and Glaciology (VAW), ETH Zürich, Hönggerbergring 26, CH-8093 Zurich, Switzerland

[2] Competence Center for Fluid Mechanics and Hydro Machines (CC FMHM), Hochschule Luzern (HSLU), Technikumstrasse 21, CH-6048 Horw, Switzerland

felix@vaw.baug.ethz.ch

Abstract. At medium- and high-head hydropower plants (HPPs) on sediment-laden rivers, hydro-abrasive erosion in turbines is an important economic issue. In HPPs with headwater storage, reservoir sedimentation is another problem related to fine sediment. On the one hand, turbine erosion is mitigated by reducing the sediment load in power waterways. On the other hand, reservoir sedimentation may be mitigated by conveying more fine sediment through power waterways to downstream river reaches. To optimize the operation of HPP schemes on the long-term, it is recommended to find a balance between these options based on real-time data using available monitoring techniques.

An operational measure to mitigate turbine erosion is to close intakes and switch-off turbines in periods of high suspended sediment concentration (SSC) and coarse particles, typically during floods. Prerequisites for such operation are (i) there is no obligation to generate electricity, (ii) real-time SSC measurements are available, and (iii) the value of the 'switch-off SSC' is known. In a case study at the high-head HPP Fieschertal, a switch-off SSC of 10 g/l was estimated. The economic analysis showed that it would have been clearly profitable to practice such a switch-off during the major flood in 2012 which had an SSC peak of 50 g/l.

1. Introduction

In the design and operation of hydropower plants (HPPs), handling of sediments is a major challenge. At medium- and high-head HPPs on sediment-laden rivers, hydro-abrasive erosion on hydraulic turbines is an important economic issue because it increases maintenance costs, and reduces turbine efficiency, electricity generation and hence revenues [1] [2] [3].

In HPPs with headwater storages, reservoir sedimentation is another problem related to sediments. The percentage of sediment which settles in a reservoir, i.e. the trap efficiency, depends mainly on the reservoir's storage volume compared to the mean volume of annual inflows, i.e. the capacity-inflow-ratio (CIR) [4]. The CIR reflects the mean residence time of the stored water. With high CIR, finer sediment particles settle. Reservoir sedimentation may have the following negative effects [4] [5]:

- Loss of active storage volume, and thus reduced ability to compensate in- and outflows for hydropower, irrigation, drinking water and flood retention;
- Increased turbine erosion because of higher SSCs and coarser particles in power waterways due to reduced trap efficiency of the reservoir;
- Reduced operational safety due to blockage of water intakes and dam outlets;

- Sediment deposits at the dam may compromise dam stability if not considered in the design;
- Lack of sediment in downstream river reaches, affecting the stability of river beds, banks and nearby infrastructures, as well as river morphology, ecology and habitats.

The loss of reservoir capacity due to sedimentation is estimated to be 0.8 % per year on worldwide average [6]. Because this is more than the increase of capacity due the construction of new reservoirs in recent years, the usable storage volume in reservoirs decreases worldwide [6] [7]. On the medium- and long-term, reservoir sedimentation may become economically more important than turbine erosion in some HPP schemes. Both turbine erosion and reservoir sedimentation are becoming more important for the following reasons:

- More sediment tends to be transported in rivers due to more intense precipitations as well as retreat of glaciers and permafrost (climate change);
- Additional HPPs are constructed on rivers with relatively high sediment loads;
- Public awareness and legal regulations regarding ecology and sustainability are increasing;
- Market situations may demand further economic and energetic optimization of HPPs.

This paper deals with measures to optimize the design and operation of HPPs at sediment-laden rivers. First, measures to cope with hydro-abrasive erosion and reservoir sedimentation are reviewed. The option of conveying fine sediment from reservoirs of low- or medium-head HPPs through the power waterways to downstream river reaches is highlighted. Then it is proposed to economically balance turbine erosion and reservoir sedimentation based on real-time sediment monitoring. In the second part of the paper, the option of temporary closing of intakes and pausing of turbine operation during floods is treated based on a case study at HPP Fieschertal, Switzerland, which was conducted in the scope of a research project [3] [8]. In particular, a relatively simple approach to estimate the so-called switch-off concentration is presented, i.e. the limit of suspended sediment concentration (SSC) above which the operation of a HPP is unprofitable. Finally, the economic benefit from such an operation regime is demonstrated in a scenario referring to a past major flood event.

2. Options to cope with hydro-abrasive erosion

2.1. Increasing the erosion resistance

One way to reduce hydro-abrasive erosion is to increase the erosion resistance of exposed parts. For hydraulic turbines, a martensitic stainless steel with 13 % chrome and 4 % nickel is mainly used [9]. Such steel has a Mohs hardness of 4.5 to 5, i.e. it can be eroded by harder mineral particles such as quartz and feldspar. Other steel grades and alloys with higher erosion resistance are used for e.g. welded hard-facing layers in Pelton buckets [10] or needles of Pelton injectors (e.g. steel-cobalt-alloys such as ‘stellite’).

Another option is to apply coatings on steel surfaces exposed to sediment-laden flow. Soft-coatings (based on polyurethane/epoxy resin) have been used in turbines at lower heads (e.g. Kaplan) [11]. In medium- and high-head turbines, thermally sprayed hard-coatings made of tungsten carbide, cobalt and chrome (WC-CoCr) have become state-of the art [1] [2] [11]. Such coatings are approximately as hard as quartz. They reduce the extent of erosion and increase the times between overhauls, but can still be damaged. Coated runners have generally a smaller initial efficiency than uncoated ones due to higher roughness and potentially different hydraulic profiles, but the loss of turbine efficiency is slower, resulting in higher revenues depending on site conditions [1].

2.2. Reduction of the sediment loading

Another approach to reduce hydro-abrasive erosion on turbines is to reduce the factors contributing to the sediment “loading”, i.e. the number of particles, their impact energy and angle of attack (mode of erosion). In the planning phase, a turbine can be designed to be less prone to hydro-abrasive erosion [9] [12]. To find a suitable combination of measures and a specific turbine design, turbine erosion needs to be addressed in an early stage of planning and meaningful sediment data are required [1] [2].

For existing HPPs, the head and the velocity inside the turbines cannot be generally reduced; and the hardness and shape of particles are properties of the river catchment.

The SSC and the median particle size can be reduced by investments in the design and construction of civil works and by suitable operation of HPPs. When the turbine water is not taken from a reservoir, one or several of the following facilities may serve for partial sediment exclusion:

- Sand traps [13], mostly in the form of long, open-air or subsurface settling basins, possibly preceded by a gravel trap. Various flushing systems are available. Typically, sediment particles with diameter > 0.3 mm are excluded; a smaller design particle size can be economically justified at high-head HPPs with hard and angular particles;
- Flushable intake areas, compensation basins/chambers or storage tunnels;
- Coanda-effect screens for intakes with low discharges (typically below a few m^3/s) and when typically grains with diameters > 0.5 or 1 mm are to be excluded;
- Hydro-cyclones in penstocks with moderate discharges (under development): according to numerical simulations, particles larger than 60 µm and some > 20 µm can be excluded [14].
- Additional sediment traps (often called 'rock traps') should be provided at HPPs with unlined waterways or with water adductions from simple intake structures into the power waterway.

The sediment load in power waterways and turbines can also be limited by temporary closing of intakes and pausing of turbine operation during floods or other events with high sediment load [1] [2] [15] [16] [17]. This operational measure is treated in detail in section 5. Hydro-abrasive erosion can also be reduced by avoiding part-load operation, because the amount of erosion per kWh is higher at part load than at full load [2].

Moreover, highly sediment-laden water may be released through Pelton turbines without erosion on the runner and without electricity generation when the jet deflectors are activated (as during an emergency closure). Such operation is an option for rare situations with very high SSCs, e.g. due to re-suspension of settled sediment, as may occur during the emptying of upstream storage facilities or dewatering of the power waterway.

3. Options to cope with reservoir sedimentation

3.1. Overview on countermeasures

There are many measures to mitigate reservoir sedimentation [4] [5] [6] [18] [19] [20] [21]. An overview of these measures is given in figure 1. Feasible measures depend also on the CIR. Because sediment input into reservoirs cannot be fully prevented, sediments have to be evacuated at the latest when the active storage volume is reduced to an unacceptable extent. Occasional restitution of sediment-laden water into the river at the dam toe (via dam outlets or by hydro-suction) may lead to high SSCs downstream of the dam [19]. To limit negative environmental impact, flushing operations are mostly combined with higher discharges and accompanying measures, and admissible SSCs have to be respected, depending on site conditions (e.g. [22]).

3.2. Sediment conveyance from reservoirs through power waterways

To mitigate reservoir sedimentation and to re-establish sediment continuity without causing high SSCs in the river downstream of the dam, fine sediments from reservoirs can be conveyed through power waterways and hence turbines to downstream river reaches [23]. Sediment particles from reservoirs can be transported into power waterways by (figure 1):

- Sluicing of sediment-laden water, possibly with the aid of jet-induced turbulence to hinder settling [23];
- Venting of turbidity currents, possibly requiring modifications of the intake and/or waterway [24];
- Re-mobilisation of settled fine sediment (often cohesive) by hydro-suction/pumping [25] [26], with the possibilities to control the area of sediment removal, the sediment transport rate and to exclude larger particles; or possibly by using air-bubbles [21].

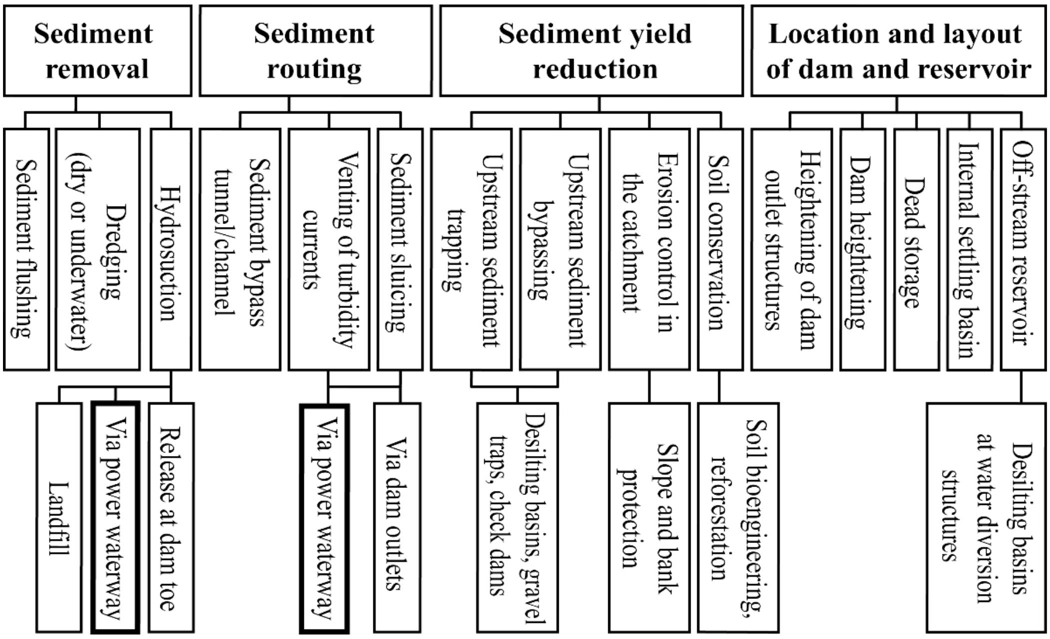

Figure 1. Overview on options to reduce reservoir sedimentation (modified from [5]).

With sediment conveyance from reservoirs through power waterways, the SSC in the river downstream of the HPP's water restitution point is relatively low, because the sediment is transported during long periods in a large volume of water. In the river reach between the dam and the HPP's water restitution point, i.e. in the residual flow reach, SSC is not increased. Other advantages are that no further transport, dewatering and land-based disposal of the sediment are required and no flushing water is lost for electricity generation. To limit turbine erosion, the following factors are favourable for this option of sediment handling:

- Low to medium head HPP, thus smaller flow velocities in the turbines;
- Relatively small particles (clay as well as fine and medium silt, ≤ 20 µm [21]);
- Low particle hardness (typically in catchment areas with sedimentary rocks);
- Suitable turbine design (e.g. seals, trunnions, cooling water system adapted to high SSCs).

Generally, sediment deposits close to intakes and dams are to be removed. In medium and large reservoirs, deposits in these zones consist typically of fine particles, because coarser sediment particles settle typically more upstream, in delta zones close to inflows. Because small particles cause less turbine erosion than larger particles at a given SSC [12] [27] [28], less erosion damage is expected from such fine sediment.

Sediment conveyance from reservoirs through power waterways was practiced e.g. in the three Francis HPPs listed in table 1. These HPPs have moderate heads and rather small reservoirs. Sediment particles (mainly silt) were transported by hydro-suction from the bottom of reservoirs in front of the intakes, where they were entrained into the power waterway and passed through the turbines. The admissible increases of SSC in the downstream river reaches were defined by environmental authorities as a function of the season and on the SSC in the rivers upstream of the restitution points (SSC_{us}). The hydro-suction units were controlled in function of the measured SSC_{us} or corresponding turbidity. In the second example in table 1, a more dynamic sediment mobilization regime was selected for environmental reasons. When the hydro-suction installation was operating at full capacity, i.e. removing 200 m^3 of sediment deposits per hour, the SSC in the turbine water was 1.4 g/l at design discharge. This is considerably lower than typical SSCs during reservoir flushing operations. The resulting downstream SSCs are similar to natural conditions before the construction of the HPPs on this river.

Table 1. Examples of HPPs, where fine sediments were removed from reservoirs by hydro-suction and conveyed through the power waterway to the downstream river reach.

HPP (river) and reservoir names, country	Gross head	Design discharge of turbines Q_d	Admissible increase of SSC in the downstream river reach	Admissible sediment return at Q_d
HPP Kubel (Sitter), Gübsensee, Switzerland [29]	97 m	16 m^3/s	0 in winter, 0.2 g/l otherwise	270 t/day
HPP Walgauwerk (Ill), Compensation basins Rodund, Austria [30]	162 m	68 m^3/s	0 if $SSC_{us} \leq 0.05$ g/l, 0.2 g/l if $0.05 < SSC_{us} < 0.2$ g/l, 1.5* SSC_{us} if $SSC_{us} \geq 0.2$ g/l	1170 t/day ≤ 4800 t/day
HPP Langenegg, Reservoir Bolgenach, Austria [21]	280 m	approx. 30 m^3/s	practiced restitutions of 0.02 g/l to 0.2 g/l (mainly at high natural Q) were below admissible SSCs	practiced ≤ 500 t/day (80 000 t/year)

4. Optimization of HPPs with respect to fine sediment

4.1. Balancing turbine erosion and reservoir sedimentation

It is proposed to balance the negative effects of fine sediments on HPPs, i.e. turbine erosion and reservoir sedimentation, by economical optimization considering the whole HPP scheme (civil structures and electro-mechanical equipment) over its lifetime.

The SSC in the power waterway can be partly controlled by operational decisions: The SSC can be increased to reduce reservoir sedimentation or can be limited to reduce turbine erosion (figure 2). The former can be achieved by transporting fine sediments in front of the power water intake as described in the previous section. The latter can be achieved by temporary closing of intakes and pausing of turbine operation during floods, as mentioned in section 2.2 and treated more in detail in section 5.

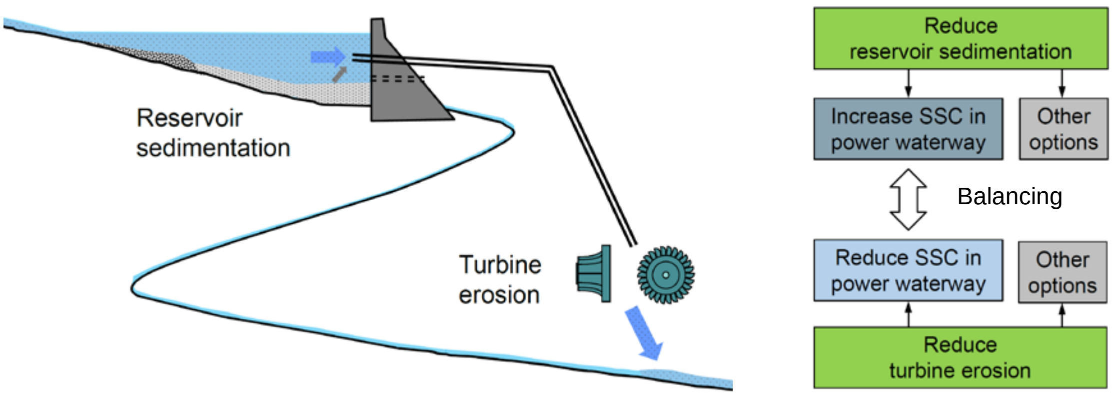

Figure 2. Economical balancing of reservoir sedimentation and turbine erosion at medium- and high-head storage HPPs by increasing or limiting the SSC in the power waterway.

4.2. Decision-making based on real-time data

For a few decades or years, various techniques and instruments (sensors) have been available for the continuous real-time monitoring of (i) sediment levels, SSCs and particle size distributions (PSD) as well as (ii) turbine efficiency ([31] [32] [33] [34] [35] [36] and [3]). It is recommended to make use of such monitoring data to optimize the operation of HPPs with respect to sediment and its consequences. In addition to real-time data, also hydro-meteorological forecasts may be considered in short-term operational decisions.

5. Option of turbine switch-offs at high SSCs

5.1. Temporary turbine switch-offs

SSC and PSD in the turbine water may vary considerably [8]. In a period with high SSC and potentially relatively coarse particles, the direct and consequential damages on turbines and other elements of HPPs may exceed the revenues from electricity sales in these periods. These damages include (i) the costs of repair works and replacement investments due to hydro-abrasive erosion, and (ii) losses of revenue due to reduced turbine efficiency or due to downtimes during revision works. If possible from the regulatory framework and production obligations, it is thus economical to close water intakes and to pause turbine operation when SSC and particle sizes exceed limit values. Since the effect of PSD on turbine erosion is not yet fully known, switch-off decisions are so far based on SSC. Engineers are thus faced to the task to determine the value of the so-called switch-off SSC.

5.2. Basic data and annual sediment-induced costs at HPP Fieschertal

To determine the switch-off SSC, data on the sediment load, turbine erosion, efficiency reductions, as well as the sediment-induced costs and electricity prices are required. In the frame of an interdisciplinary research project, such data were obtained for the high-head HPP Fieschertal in Valais, Switzerland. This HPP has a design discharge of 15 m^3/s, a gross head of 520 m and is equipped with two horizontal 32 MW Pelton turbines [1]. A storage tunnel (64 000 m^3) serves to compensate inter-daily variations of inflow and turbine discharge (no storage lake). Since the headwater storage is relatively small, the HPP is practically a run-of-river scheme.

The sediment load, turbine erosion and efficiency reductions in the years 2012 to 2014 are reported in [8] [3]. The average annual costs which are induced by the fine-sediment load transported through the turbines were estimated in table 2. For simplicity, the electricity price was assumed to be constant at 0.05 €/kWh (50 €/MWh). The annual costs in table 2 resulted from data on executed repair works and purchased turbine replacement parts as well as the estimated average annual probabilities of the individual cost elements. The annual costs induced by fine-sediment correspond to some percent of the value of the annual electricity generation and are thus economically relevant.

Table 2. Average annual costs induced by fine-sediment load at HPP Fieschertal (for whole HPP with two turbines, estimate based on data from 2012 to 2014).

Cost or loss item		10^3 €/year	Percentage of the value of the annual electricity
Costs of repairs and replacement parts		270	3.3 %
- Runners	180		
- Injectors and stationary turbine parts	60		
- Flushing system of sand trap	30		
Electricity generation losses		30	0.4 %
- Due to reduced efficiency	10		
- Due to downtime during runner exchange	20		
Total		300	3.7 %

5.3. Estimation of switch-off SSC at HPP Fieschertal

In the following, a simplified approach to estimate the switch-off SSC is proposed and illustrated by the example of HPP Fieschertal.

The long-term average annual load of fine sediment transported through both turbines was estimated as 50 000 tons. This is the average of the annual loads determined from the measurements in the years 2013 and 2014 [8]. For the sake of simplicity, it was assumed that the costs induced by the

fine sediment are proportional to its mass. With this assumption, specific sediment-induced costs resulted in 300 000 € per year / 50 000 tons per year = 6 €/ton = 0.006 €/kg.
With an average SSC of 0.5 g/l = 0.5 kg/m^3, the sediment-induced costs with respect to the water volume are 0.003 €/m^3. If the SSC rises for example to 10 g/l, the fine-sediment induced costs are also 20 times higher, i.e. 0.06 €/m^3.

For HPP Fieschertal, 1 m^3 water is equivalent to 1.2 kWh of electric energy. Thus, the sediment-induced costs with respect to electric energy is 0.003 €/m^3 / 1.2 kWh/m^3 = 0.0025 €/kWh at average SSC. When the SSC increases from 0.5 g/l to 10 g/l, the sediment-induced costs rise to 0.05 €/kWh, corresponding to the assumed electricity selling price. From this it is concluded that the operation of HPP Fieschertal is not profitable when SSC >10 g/l. This switch-off SSC is an approximate value since it resulted from a simplified linear approach and a relatively short data set (3 years). It is recommended to re-evaluate the assumptions and the approach when more data will be available.

5.4. Switch-off and switch-on procedure
The control system of HPP Fieschertal was programmed to issue a warning when the SSC measured at the top of the penstock exceeds 10 g/l for 15 minutes. Preliminary warnings are given from continuous turbidity measurements (i) in the river upstream of the intake and (ii) in the sand trap, offering both a prewarning time of about one hour (cross-section averaged flow time in the storage tunnel at full load at maximum operation level). If the SSC exceeds 10 g/l for 15 minutes, the staff member on duty has the competence to close the intake and to switch-off the HPP, considering the weather forecast and his observations.

Taking the HPP back to operation is associated with some effort, e.g. de-clogging of cooling water systems, flushing operations and checks. Therefore it was proposed to resume operation when SSC is considerably lower than 10 g/l, say 5 g/l, and when the flood is expected to end soon.

5.5. Switch-off scenario during the 2012 flood
These rules for turbine switch-off and restart were hypothetically applied to the situation of a major flood event which occurred in July 2012. This was the only flood event in the years 2012 to 2014, in which the switch-off criterion would have been met. The switch-off duration would have been 16 hours (figure 3).

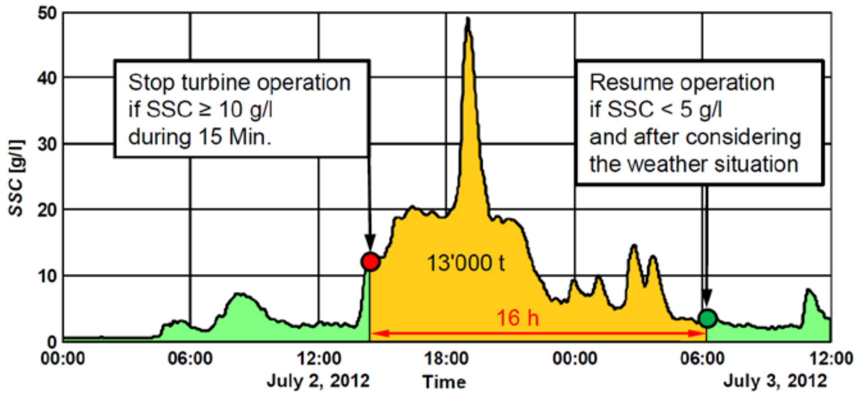

Figure 3. SSC time series in the turbine water of HPP Fieschertal during the major flood event of July 2012 [8] and switch-off scenario with the proposed rules.

During this time, 13 000 t of fine sediment were transported through the turbines (orange fill in figure 3). This corresponds to 12 % of the annual sediment load in 2012 or to 25 % of the sediment load in the other years without a major flood event (average of 2013 and 2014). The amount of sediment which entered the power waterway during these 16 h was higher than the sediment load of the turbines, because a part of the sediment entering the HPP system settled in the storage tunnel. These deposited sediments were occasionally re-suspended and transported through the turbines in the months after the flood. Thus, a sediment load of more than 13 000 t would have been prevented to enter the power waterway and to pass through the turbines if the intake had been closed during these 16 hours.

The economic potential of the switch-off scenario during this flood was evaluated and the result is summarized in table 3. This indicates that switching-off both turbines during the flood in July 2012 would have been clearly profitable, with a net benefit of roughly 200 000 €.

Table 3. Economic analysis (benefits vs. losses and costs) of the switch-off scenario at HPP Fieschertal during the major flood event in 2012 (for whole HPP with two turbines).

Benefits	€
Avoided repair costs because of less erosion (rough estimate)	200 000
Avoided generation loss because of less reduced efficiency	30 000
Avoided generation loss because of no runner exchange required	30 000
Total	260 000

Losses and costs	€
Generation loss during switch-off (2 * 32 MW * 16 h ≈ 1 GWh)	− 50 000
Potential penalty for non-compliance with the announced generation program	if applicable
Total (without potential penalty)	− 50 000

6. Conclusions

Measures to cope with turbine erosion and reservoir sedimentation were reviewed. To optimize HPP schemes with respect to fine sediment, a combined approach is required. This involves knowledge in engineering sciences (hydraulic, mechanical, material, civil and environmental) in combination with economic analysis.

Adequate solutions to mitigate reservoir sedimentation and turbine erosion depend on the site conditions, the layout and components of HPPs. Long-term measurements and documentation of sediment loads, turbine erosion, efficiency changes, maintenance actions and costs are highly recommended as a basis for economic and power production optimizations. To reduce reservoir sedimentation, conveying fine sediment through power waterways is an option for low- to medium-head storage HPPs if sediment particles are relatively small and soft, and SSCs are low. To mitigate turbine abrasion, temporary closing of intakes and turbine switch-offs in periods of high SSCs and coarse particles are economically interesting measures for medium- to high-head HPPs with no or only small headwater storages, if compliant with the regulatory framework and production obligations.

A relatively simple linear approach for the calculation of the switch-off SSC was proposed and a value of 10 g/l was obtained for HPP Fieschertal. If this switch-off SSC had been applied in the major flood in 2012, the shutdown duration would have been 16 hours and a net benefit of roughly 200 000 € would have resulted.

7. Outlook

As a basis for optimized design, operation and maintenance of HPPs, further knowledge on quantitative relations between sediment and turbine parameters, turbine erosion and efficiency reductions are required. Therefore, further field investigations with detailed measurements at HPPs are highly recommended to enlarge the set of prototype data and to provide a basis for comparison with laboratory investigations, numerical simulations and analytical considerations.

For some HPPs worldwide, a certain SSC-value is taken as switch-off criterion so far. However, a combination of SSC- and PSD-information would better account for the actual erosion potential. The effect of PSD on turbine erosion can be considered by defining a 'modified SSC' = SSC * k_{size}, as proposed by Nozaki [28]. The coefficient k_{size} reflects the relative abrasion potential of particles of various size classes. Then, a switch-off criterion referring to a modified SSC can be formulated and no additional criteria on limit particle sizes are required.

Acknowledgements
The support of the mentioned research project by swisselectric research, the Swiss Federal Office of Energy (SFOE), the HPP operator Gommerkraftwerke AG as well as the Swiss Competence Center for Energy Research - Supply of Electricity (SCCER-SoE) and the Research Fund of the Swiss Committee on Dams are gratefully acknowledged. Further thanks go to Endress+Hauser, Sigrist Photometers and Rittmeyer for lending measuring equipment as well as to all members of the project team for their contributions.

References

[1] Winkler K 2014. Hydro-abrasive erosion: problems and solutions. *Proc.* 27th IAHR Symposium on Hydraulic Machinery and Systems, Montreal, Canada. IOP Conf. Series 22 052022

[2] Wedmark A 2014. Living with particle abrasion. *Proc.* Hydro Conf., Cernobbio (Lake Como), Italy: paper no. 08.02

[3] Abgottspon A, Staubli T and Felix D 2016. Erosion of Pelton buckets and changes in turbine efficiency measured in the HPP Fieschertal. *Proc.* 28th IAHR Symposium on Hydraulic Machinery and Systems, Grenoble, France, IOP Conf. Series

[4] Morris G L and Fan J 1998. Reservoir sedimentation handbook. McGraw-Hill, New York

[5] Boes R M and Hagmann M 2015. Sedimentation countermeasures - examples from Switzerland. Proc. 1st Intl. Workshop on Sediment Bypass Tunnels, *VAW-Mitteilung 232* (Boes R M, ed.), ETH Zürich, Switzerland: 193-210

[6] ICOLD 2009. Sedimentation and sustainable use of reservoirs and river systems. *Bulletin* 147, International Commission on Large Dams (ICOLD), Paris, France

[7] Annandale G 2013. Quenching the thirst: sustainable water supply and climate change. Create-Space Independent Publishing Platform, North Charleston, South Carolina, USA.

[8] Felix D, Albayrak I, Abgottspon A and Boes R M 2016. Suspended sediment measurements and calculation of the particle load at HPP Fieschertal. *Proc.* 28th IAHR Symposium on Hydraulic Machinery and Systems, Grenoble, France, IOP Conf. Series

[9] IEC 62364 2013. Guide for dealing with hydro-abrasive erosion in Kaplan, Francis, and Pelton turbines. Edition 1.0, *International Electrotechnical Commission* (IEC) Geneva, Switzerland

[10] Maldet R 2008. Pelton runner with high erosion caused by glacier sediment: assessment and measures. *Proc.* 15th Intl. Seminar on HPPs, Doujak E (ed.), Vienna, Austria: 639-646

[11] Engelhardt M, Schneider C and Oechsle D 2001. Real scale performance of advanced erosion protection techniques on water turbines. In Kaushish S P and Naidu B S K (eds.), *Proc.* 2nd Intl. Conf. on Silting Problems in HPPs, Bangkok, Thailand: 168-175

[12] Naidu B S K 1999. Developing-Silt Consciousness in the minds of Hydro Power Engineers. In Varma C V J, Naidu B S K and Rao A R G (eds.), *Proc.* 1st Intl. Conf. on Silting Problems in HPPs, New Delhi, India (paper no. 1). Rotterdam/Brookfield: Balkema

[13] Ortmanns C 2006. Entsander von Wasserkraftanlagen (Sand traps of HPPs). *PhD thesis*, *VAW-Mitteilung 193* (Minor H E, ed.), ETH Zurich, Switzerland (in German)

[14] Doujak E and Götsch H 2010. Usage of an axial hydro cyclone as sediment seperator. *Proc.* 16th Intl. Seminar on Hydropower Plants, Doujak E (ed.), Vienna, Austria: 87-95

[15] Müller P and De Cesare G 2009. Sedimentation Problems in the Reservoirs of the KW Sarganserland – Venting of turbidity currents as the essential part of the solution. *Proc.* 23th ICOLD Congress, Q89 R21, Brasilia, Brazil

[16] Boes R M 2010. Kontinuierliche Messung von Schwebstoffkonzentration und –korngrössenverteilung im Triebwasser und Quantifizierung der Hydroabrasion an einer Peltonturbine (Continuous measurements of SSC and PSD in the turbine water and quantification of wear at a Pelton turbine). *Wasser Energie Luft,* 102(2), Switzerland: 101-107 (in German)

[17] Singh M, Banerjee J, Patel P L and Tiwari H 2013. Effect of silt erosion on Francis turbine: a case study of Maneri Bhali Stage-II, Uttarakhand, India. *ISH J. of Hydr. Eng.* 19(1): 1-10

[18] Sumi T 2005. Sediment flushing efficiency and selection of environmentally compatible reservoir sediment management measures, East Asia of ICOLD, *Proc.* Intl. Symposium on Sediment Management and Dams, 2nd EADC Symposium: 9-22

[19] ICOLD 1989. Sedimentation control of reservoirs. *Bulletin* 67, International Commission on Large Dams, Paris, France

[20] ICOLD 1999. Dealing with reservoir sedimentation. *Bulletin* 115, International Commission on Large Dams, Paris, France

[21] DWA 2006. Entlandung von Stauräumen (Removal of reservoir sediments). Deutsche Vereinigung für Wasserwirtschaft, Abwasser und Abfall e.V., Hennef, Germany (in German)

[22] BUWAL 1994. Ökologische Folgen von Stauraumspülungen (Ecological consequences of reservoir flushing). *Schriftenreihe Umwelt* no. 219; Bundesamt für Umwelt, Wald und Landschaft, Bern, Switzerland (in German).

[23] Jenzer Althaus J 2011. Sediment evacuation from reservoir through intakes by jet induced flow. *PhD thesis* no. 4927. Hydraulic Constructions Laboratory (LCH), Ecole Polytechnique Fédérale de Lausanne, Switzerland

[24] Lai J S, Lee F Z, Wu C H, Tan Y C and Sumi T 2015. Sediment bypass tunnels of the Shihmen Reservoir in Taiwan. Proc. 1st Intl. Workshop on Sediment Bypass Tunnels, *VAW-Mitteilung 232* (Boes R M, ed.), ETH Zürich, Switzerland: 55-70

[25] Schüttrumpf H and Detering M 2011. Innovative sediment handling to restore reservoir capacity. Dams and reservoirs under changing challenges, Schleiss A J and Boes R M (eds.), CRC Press: 345-352

[26] Jacobsen T and Jiménez A 2015. Recent experiences from sediment removal projects. *Proc.* Hydro Conf. Bordeaux, France

[27] Winkler K, Dekumbis R, Rentschler M, Parkinson E and Garcin H 2011. Understanding hydro-abrasive erosion. *Proc*. Hydro Conference, Prague, Czech Republic

[28] Nozaki T 1990. Estimation of repair cycle of turbine due to abrasion caused by suspended sand and determination of desilting basin capacity. *Report*, Japan International Cooperation Agency, Tokyo

[29] De Cesare G, Baumann R, Zuglian R and Binder F 2009. Sedimentausleitung aus dem Speicher Gübsensee über die Triebwasserleitung (Evacuation of fine sediment from the Gübsensee reservoir through the power waterway). *Wasser Energie Luft*, Switzerland 101(3): 203–206 (in German)

[30] Sollerer F and Matt P 2013. Sediment management of reservoirs – sediment discharge in dependence on the suspended load concentration in the run-off water. *Proc.* Hydro Conf. Innsbruck, Austria, paper no. 18.08

[31] Agrawal Y C and Pottsmith H C 2005. Turbine Erosion - lasers warn of abrasive sediments. *Proc*. Hydro Conference, Villach, Austria

[32] Bishwakarma M B and Støle H 2008. Realtime sediment monitoring in hydro-power plants. *J. of Hydr. Research* 46(2): 282–288

[33] Rai A K and Kumar A 2015. Continuous measurement of suspended sediment concentration: Technological advancement and future outlook. *Measurement* 76: 209–227

[34] Albayrak I, Felix D, Hagmann M and Boes R M 2015. Suspended Sediment and Bed Load Transport Monitoring Techniques. *Dresdner Wasserbauliche Mitteilungen* 53: 405-414

[35] Felix D, Albayrak I, Abgottspon A and Boes R M 2016. Real-time measurements of suspended sediment concentration and particle size using five techniques. *Proc.* 28th IAHR Symposium on Hydraulic Machinery and Systems, Grenoble, France, IOP Conf. Series

[36] Gruber P, Felix D, Storti G, Lattuada M, Fleckenstein P and Deschwanden F 2016. Acoustic measuring techniques for suspended sediment. *Proc.* 28th IAHR Symposium on Hydraulic Machinery and Systems, Grenoble, France, IOP Conf. Series

Measurement 89 (2016) 44–47

Contents lists available at ScienceDirect

Measurement

journal homepage: www.elsevier.com/locate/measurement

Continuous measurement of suspended sediment concentration: Discussion of four techniques

David Felix *, Ismail Albayrak, Robert M. Boes

Laboratory of Hydraulics, Hydrology and Glaciology (VAW), ETH Zurich, CH-8093 Zurich, Switzerland

ARTICLE INFO

Article history:
Received 23 January 2016
Received in revised form 21 March 2016
Accepted 29 March 2016
Available online 1 April 2016

Keywords:
Suspended sediment monitoring
Vibrating tube densimetry
LISST
Turbidimeter
Acoustic attenuation
Gravimetric

ABSTRACT

Continuous measurements of suspended sediment mass concentration (SSC) and particle size distribution (PSD) in surface waters and hydraulic schemes are of prime importance for the investigation and management of many fine-sediment related processes. In this paper, the performance of selected techniques and instruments for continuous SSC measurements is discussed based on results of a field study and a recent literature-review paper. SSCs measured with Laser In Situ-Scattering and Transmissometry (LISST) or vibrating tube densimetry were confirmed to be not or less biased by temporary PSD variations than SSCs obtained from turbidimeters or a single-frequency acoustic attenuation method. Vibrating tube densimetry allowed measurements of higher SSCs (e.g. 10 g/l) compared to the other investigated instruments. For the conversion of the instruments' outputs to SSC, i.e. calibration, and for validation, gravimetric analysis of bottle samples is recommended as reference.

1. Introduction

Measurements of SSC and PSD with high temporal resolution are important for a better understanding and management of fine-sediment related processes in rivers, reservoirs and hydraulic schemes. Therefore, there is a need for practical measuring systems, which cover relevant SSC and PSD ranges with an acceptable uncertainty and provide data preferably in real-time. An overview on measurement techniques for suspended sediment monitoring (SSM) is provided in [1], and more detailed descriptions and references to recent studies have been given in [2].

In the scope of an interdisciplinary research project on turbine abrasion [3], four indirect measuring techniques for continuous real-time measurements of SSC were experimentally investigated at the waterway of the hydroelectric power plant (HPP) Fieschertal in the Swiss Alps: turbidity measurement, single-frequency acoustic attenuation, LISST, and vibrating tube densimetry. Gravimetric analysis of bottle samples taken in parallel served as reference. These techniques were also partly treated in [1,2]. In the present contribution, complementary information on vibrating tube densimetry and the acoustic attenuation method are given, the setup and method of the field study are briefly described and the measuring performance of the instruments is discussed based on exemplary field data. Finally, the option of combining measuring techniques is highlighted and the conclusions drawn in [2] are discussed.

2. Measuring techniques and instruments

Turbidimetry and LISST have been reviewed in [2], and gravimetric analysis of bottle samples is well known. However, the literature contains only little information on vibrating-tube densimetry in the context of SSM, and the type of acoustic method used in this study is not widely known. Therefore, complementary information on the latter two techniques are given in the following.

2.1. Vibrating-tube densimetry

This measuring technique is used in 'Vibrating Tube Density Meters' (VTDMs, also called 'oscillating U-tubes') and in 'Coriolis Flow- and Density Meters' (CFDMs). The operation principles of these two types of instruments are e.g. described in [4,5], respectively. The density of a fluid flowing through a VTDM or a CFDM is measured based on the natural frequency of the measuring tubes, which drops as the mass in the tubes increases. VTDMs and especially CFDMs are common in the process industry, whereas they have been rarely used for in-situ SSM so far [6]. CFDMs are commercially available at roughly US$ 15 000. In many CFDM models, the temperature is also measured and thermal dilatation is compensated.

* Corresponding author.
E-mail address: felix@vaw.baug.ethz.ch (D. Felix).

http://dx.doi.org/10.1016/j.measurement.2016.03.066

The density measurements of VTDMs or CFDMs may be biased due to deposits, biofilm growth or abrasion inside the measuring tubes. With particulate fluids, i.e. fluids containing particles, CFDMs may underestimate the mixture density due to 'phase decoupling' [7] if the particles are large. The accuracy of the density measurement of the CFDM used in the authors' field study [3] is ±0.5 g/l according to the manufacturer, which is a common specification [5]. SSC is determined from the measured mixture density, the clear water density and the particle density which is assumed to be constant. Particle density can be determined from the dried residues of a few bottle samples using a pycnometer. The clear water density is calculated as a function of the measured temperature.

2.2. Single-frequency acoustic attenuation method

Ultrasonic signals are mostly used for SSM in connection with Acoustic Doppler Current Profilers (ADCPs), e.g. [8]. The use of ADCPs offers the advantage of obtaining spatially distributed SSCs in cross sections of water bodies. SSCs are inferred from backscattered signals and their correlation with gravimetrical SSCs from bottle samples. In the present study, a single-frequency acoustic method based on attenuation (forward scattering) was used. This method lends itself particularly well for SSM in rivers, canals and waterways where installations for acoustic discharge measurement (ADM) already exist. Like this, SSC can be monitored without additional sensors. ADM installations comprise acoustic transducers installed on both sides of acoustic paths crossing the flow section. For the determination of the flow velocity and the discharge, ultrasonic pulses are sent through the water. If the water contains sediment particles, the received signal is weaker due to attenuation [9]. Similarly to certain turbidimeters, this attenuation is correlated to SSC.

3. Field study set-up and method

In the study at HPP Fieschertal [3], the instruments No. 1 to 3 and 5 listed in Table 1 were installed in the valve chamber at the head of the penstock. For the acoustic method (No. 4), a pre-existing ADM installation with transducers inside the penstock was employed. The CFDM and the in-line turbidimeter were integrated in a sampling pipe fed with water from the penstock. At the outflow of the pipe, the measuring head of an all-round LISST instrument was accommodated in a bucket with an overfall and a bottom outlet. The partially opened bottom outlet allowed continuous sediment evacuation.

The water in this HPP comes from a highly glaciated catchment area and contains mainly silt particles. At the measuring location, the sediment particles are smaller than 0.3 mm, since coarser particles are removed by upstream gravel and sand traps. No air bubbles were observed in the sampling pipe during the study. Water samples were automatically pumped from the bucket every three days or more frequently in periods of high SSCs (triggered by CFDM density). From these samples, the SSCs were determined in the laboratory by gravimetrical analysis. These SSCs were taken as reference and served for the conversion of the instruments' outputs to SSC time series. These conversion functions can also be called field calibrations. In addition, PSDs were calculated from the LISST data in the range of 3–380 μm based on the assumption of so-called 'random shaped' particles [10].

4. Results and discussion

Out of three years of measurements, exemplary PSD and SSC time series during two summer days are shown in Fig. 1. The particle size d_x stands for the diameter of graded particles, of which x% by mass are smaller. The following comments on the measuring performance of the instruments are made:

1. The SSCs obtained from the instruments were similar if the particles were relatively fine ($d_{50} \approx 15$ μm), as during most of the time. In periods with larger particles transported, however, the turbidimeter and the acoustic method underestimated SSCs, due to effects of PSD variations which are not correlated to SSC. At sites with such highly dynamic sediment transport, SSCs obtained from turbidimeters or single-frequency acoustic methods may contain significant uncertainty. If PSD is constant (e.g. for wash load), or is highly correlated with SSC, these two methods may yield results with a good accuracy. With the LISST technique, changes in PSD are measured and accounted for in the calculation of SSC. With particles mainly in the size range of silt, no effect of PSD variations was observed on the SSC data obtained from the CFDM.
2. The SSCs from LISST and gravimetry are in good agreement because of the field calibration, which accounts for the particle density and compensates particle shape effects on LISST volume concentrations. Without field calibration, the SCCs would be overestimated by 70% on temporal average at this site. Considerable overestimations were also quantified in preliminary laboratory investigations with highly non-spherical particles [11].
3. The SSC sometimes exceeded the measuring range of the LISST instrument used in this study, as also indicated by Rai and Kumar [2] and the manufacturer. The upper limit of the SSC measuring range of a LISST instrument depends on its optical path length, the PSD and particle shapes [11]. The optical path length of the LISST instrument was reduced to 5 mm using the strongest available path reduction module, and a further reduction was not well feasible. Another type of LISST instrument, providing measurements at up to ten times higher SSC using sample dilution with clear water, was not affordable in the authors' study. Turbidimeters and the acoustic method were also not able to cover the whole range of SSCs occurring at the study site, i.e. up to 50 g/l in a major flood event. The CFDM, however, which was installed after that major flood, allowed measuring SSCs up to 13 g/l without reaching the upper limit of its measuring range (Fig. 1).

Table 1
Instruments for SSM in the valve chamber of HPP Fieschertal.

No.	Instrument description	Measuring technique	Instrument model	Instrument manufacturer	Instrument outputs	Derived parameters
1	Coriolis Flow- and Density Meter (CFDM)	Vibrating-tube densimetry	*Promass 83F DN15*	Endress + Hauser	Density, temperature	SSC
2	Standard LISST, with 90% path reduction	Laser diffraction (LISST)	*LISST-100X* (Type C)	Sequoia Scientific	Volume concentrations	SSC, PSD
3	In-line turbidimeter at free falling jet	Turbidity	*AquaScat*	Sigrist Photometer	Turbidity	SSC
4	SSC monitoring using ADM installation	Acoustic attenuation	*Risonic* (1 MHz)	Rittmeyer	Attenuation	SSC
5	Bottle sampler and weighing in laboratory	Gravimetric	*Isco 3700* (24 × 1 l)	Teledyne Isco	Filled bottles, SSC	–

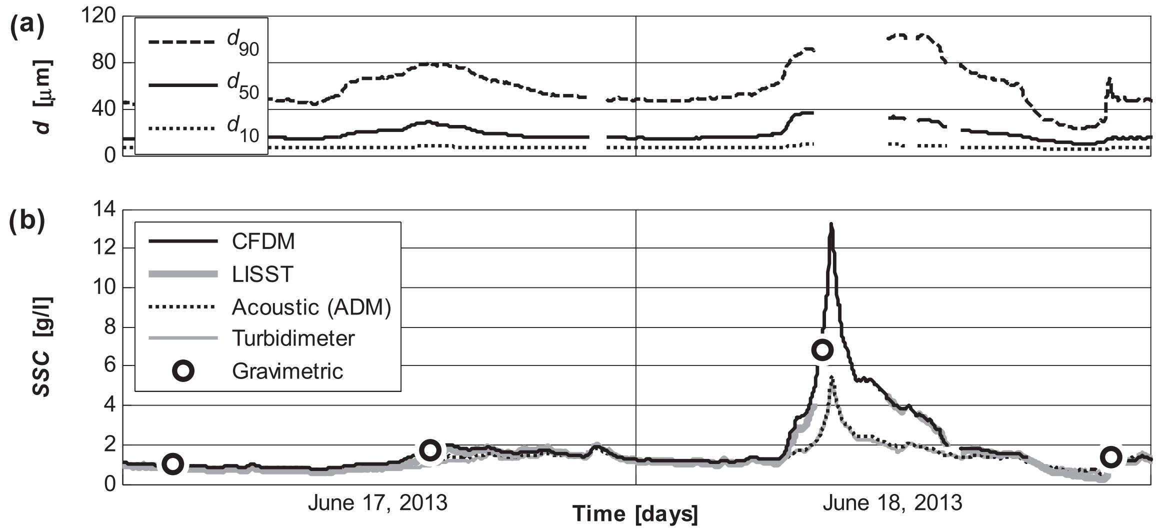

Fig. 1. Time series of (a) particle sizes measured by LISST, and (b) SSCs obtained from four continuous techniques compared to gravimetrically determined SSCs of bottle samples (reference).

From this field investigation it is concluded that the combination of a standard LISST instrument (without clear-water dilution) and a CFDM is an economical option to measure both low and high SSCs without temporary biases by PSD variations (in the size range of mainly silt), if the lack of PSD data at higher SSCs is acceptable. If only SSCs above 5 or 10 g/l are to be measured, e.g. to warn of high turbine abrasion potential, the use of a factory-calibrated CFDM is sufficient. Otherwise, when lower SSCs are also of interest, e.g. for the determination of annual sediment loads, the additional use of a LISST and bottle sampling for periodic in-situ calibration in parallel are recommended.

In [2] it was concluded from the literature review that acoustic techniques have a high development potential and presently a combination of LISST and holography seems to be the most promising option for SSM. The authors of the present paper are also aware of the development potential of acoustic methods and see the advantages of combining instruments employing different techniques, as also concluded by Wren et al. [1]. Such combinations (i) increase the data coverage in long-term measurements, (ii) allow for quality and accuracy assessment of measurement data by comparing the outputs of the instruments in overlapping measuring ranges, and (iii) may open new possibilities. However, no general recommendation on instrumentation can be given, as the selection of suitable measuring techniques and instrumentation depends on the specific application, i.e. the measuring task, site conditions and various constraints.

5. Conclusions and outlook

Based on [1,2] as well as the results and discussion above, it is recommended to consider the following aspects for the design of a SSM system:

- Ranges of SSC and particle sizes.
- Degree of correlation between SSC and median particle size.
- Acceptable measuring uncertainty and required reliability.
- Necessity to measure in-situ and non-intrusively, or possibility to measure on a sampling line.
- Accessibility of measuring sites and possibilities for data and sample transfer.
- Costs of the instruments, their installation, integration, calibration, operation and maintenance.
- Cost and time of laboratory work and data treatment.
- Availability, skills and training of involved persons.

Further investigations are recommended to address the mentioned aspects in order to provide additional information to scientists and engineers working in the area of SSM. In particular, laboratory investigations of CFDMs are recommended to assess (i) effects of particle size (up to the size range of sand) on the measured mixture densities, and (ii) the upper limit of measurable SSCs.

Acknowledgements

The support of the mentioned research project by swisselectric research, the Swiss Federal Office of Energy (SFOE), the HPP operator Gommerkraftwerke AG and the Swiss Competence Center for Energy Research – Supply of Electricity (SCCER-SoE) are gratefully acknowledged. Further thanks go to Endress+Hauser, Sigrist Photometers and Rittmeyer for lending measuring equipment as well as to Hochschule Luzern and other project partners for the good collaboration.

References

[1] D.G. Wren, B.D. Barkdoll, R.A. Kuhnle, R.W. Derrow, Field techniques for suspended-sediment measurement, J. Hydraul. Eng. 126 (2) (2000) 97–104, http://dx.doi.org/10.1061/(ASCE)0733-9429(2000)126:2(97).

[2] A.K. Rai, A. Kumar, Continuous measurement of suspended sediment concentration: technological advancement and future outlook, Measurement 76 (2015) 209–227, http://dx.doi.org/10.1016/j.measurement.2015.08.013.

[3] D. Felix, I. Albayrak, R.M. Boes, Field measurements of suspended sediments using several methods, in: E-proceedings of the 36th IAHR World Congress, The Hague, The Netherlands, 2015. <https://www.iahr.org/site/cms/contentDocumentLibraryView.asp?chapter=42&category=344>.

[4] C.D. Holcomb, S.L. Outcalt, A theoretically-based calibration and evaluation procedure for vibrating-tube densimeters, Fluid Phase Equilib. 150–151 (1998) 815–827, http://dx.doi.org/10.1016/S0378-3812(98)00362-8.

[5] P. Kalotay, Density and viscosity monitoring systems using Coriolis flow meters, ISA Trans. 38 (1999) 303–310, http://dx.doi.org/10.1016/S0019-0578(99)00023-3.

[6] M.B. Bishwakarma, H. Støle, Realtime sediment monitoring in hydro-power plants, J. Hydraul. Res. 46 (2) (2008) 282–288, http://dx.doi.org/10.1080/00221686.2008.9521862.

[7] N.T. Basse, A review of the theory of Coriolis flowmeter measurement errors due to entrained particles, J. Flow Meas. Instrum. 37 (2014) 107–118, http://dx.doi.org/10.1016/j.flowmeasinst.2014.03.009.
[8] M. Guerrero, R.N. Szupiany, F. Latosinsky, Multi-frequency acoustic for suspended sediment studies: an application in the Parana River, J. Hydraul. Res. 51 (6) (2013) 696–707, http://dx.doi.org/10.1080/00221686.2013.849296.
[9] L.I. Costa, G. Storti, B. Lüscher, P. Gruber, T. Staubli, Influence of solid particle parameters on the sound speed and attenuation of pulses in ADM, J. Hydrol. Eng. 17 (10) (2012) 1084–1092, http://dx.doi.org/10.1061/(ASCE)HE.1943-5584.0000555.
[10] Y.C. Agrawal, A. Whitmire, O.A. Mikkelsen, H.C. Pottsmith, Light scattering by random shaped particles and consequences on measuring suspended sediments by laser diffraction, J. Geophys. Res. 113 (C4) (2008), http://dx.doi.org/10.1029/2007jc004403.
[11] D. Felix, I. Albayrak, R.M. Boes, Laboratory investigation on measuring suspended sediment by portable laser diffractometer (LISST) focusing on particle shape, Geo-mar. Lett. 33 (6) (2013) 485–498, http://dx.doi.org/10.1007/s00367-013-0343-1.

River Sedimentation – Wieprecht et al. (Eds)
© 2017 Taylor & Francis Group, London, ISBN 978-1-138-02945-3

Combining *in-situ* laser diffraction (LISST) and vibrating tube densimetry to measure low and high suspended sediment concentrations

D. Felix, I. Albayrak & R.M. Boes
Laboratory of Hydraulics, Hydrology and Glaciology (VAW), ETH Zürich, Switzerland

ABSTRACT: Real-time measurements of suspended sediment mass concentration (SSC) and particle size distribution (PSD) are of importance to improve the understanding and management of many fine-sediment related processes. In the field study at the HPP Fieschertal in the Swiss Alps, a turbidimeter, a Laser In-Situ Scattering and Transmissometry instrument (LISST), a Coriolis Flow and Density Meter (CFDM), and an automatic bottle sampler were used to continuously measure SSC and PSD. The performance of the instruments was assessed based on the measurements conducted in 2013 and 2014. While the SSC measuring range of the LISST with an optical path length of 5 mm (without dilution) was confirmed to be limited to about 1.5 g/l of medium silt, the CFDM allowed measuring higher SSCs of up to 13 g/l. In this paper, the measuring techniques, instruments, setup, methods for data treatment and selected results are presented. The combined use of a standard LISST instrument and a CFDM, supported by automatic bottle sampling, is recommended to measure a wide range of SSCs in silt-laden waters with relatively low uncertainty and cost.

1 INTRODUCTION

Erosion, transport and deposition of fine sediments in surface water systems and hydraulic schemes for hydropower and irrigation are economically and ecologically important. Fine sediment may cause abrasion on hydraulic machines, colmation on riverbeds or reservoir sedimentation. For a better understanding and management of fine-sediment related processes, field measurements of suspended sediment mass concentration (SSC) and particle size distribution (PSD) with high temporal resolution are required. In many applications, continuous real-time data are advantageous or even a requirement to support short-term decision making. To mitigate turbine abrasion, real-time measurements of high SSCs are of particular importance.

Although many techniques for discontinuous and continuous suspended sediment monitoring (SSM) are available and described in literature (Wren et al. 2000, Rai & Kumar 2015), it is not evident how to design a monitoring system capable of measuring SSC and PSD in relevant ranges with reasonable accuracy, reliability and cost.

This paper deals with the investigation of measuring techniques for SSM in the recent field study at the high-head hydropower plant (HPP) Fieschertal in the Swiss Alps (Felix et al. 2013a, 2015). The water used in this HPP comes from a glaciated catchment and contains mainly silt particles with an average SSC of 0.5 g/l, rising several times a year above 5 g/l. During a flood event in July 2012 with an estimated return period of 20 years, the SSC reached 50 g/l.

To measure SSC and PSD, the following instruments and techniques have been used in the HPP Fieschertal: (1) turbidimeters, (2) a single-frequency acoustic attenuation technique based on a standard acoustic discharge measurement (ADM) installation, (3) a 'Laser In-Situ Scattering and Transmissometry' instrument (LISST) without dilution chamber, (4) a Coriolis Flow and Density Meter (CFDM) and (5) an automatic bottle sampler. Further information on the acoustic technique and various turbidimeter models are given in Felix et al. (2013a, 2015).

This paper focuses on LISST and CFDM, which have been rarely used for SSM at HPPs. To the knowledge of the authors, they have not been used in combination so far. One turbidimeter and the automatic bottle sampler are also treated in this paper to make reference to widely used instrumentation. After the description of the measuring techniques, the instruments, setup, further developed methods for data treatment and selected results are presented and discussed with respect to the measuring performances of the instruments. Finally, recommendations on combined instrumentation for SSM in environments with high sediment dynamics are given.

2 MEASURING TECHNIQUES

2.1 *Turbidimeters*

Turbidimeters are inexpensive and widely used for SSM. Typically, turbidity readings are converted to SSCs based on gravimetrically determined SSCs from bottle samples (e.g. Haimann et al. 2014). The relation between turbidity and SSC depends on particle size, shape and color (e.g. Downing 2006). This is a major drawback when using turbidimeters in environments with temporarily varying particle properties.

2.2 *Laser diffraction (LISST)*

Portable LISST instruments measure both PSD and concentration *in-situ* (Agrawal & Pottsmith 2000) and are increasingly used for SSM in rivers, reservoirs and HPPs. In these instruments, a laser beam is sent through the water. The scattering (diffraction) at small angles (0.05 to 9°) and the attenuation caused by suspended particles are measured. From the light intensities, the particle volume concentrations in 32 logarithmically spaced size bins (bin volume concentrations, BVCs) are computed with the corresponding software. From the BVCs, the PSD and the total volume concentration (TVC) are determined. In contrast to e.g. turbidimeters, the sizes of the actually prevailing particles are considered in the SSC measurement.

LISST instruments allow measuring SSCs as low as some mg/l. The upper end of the SSC measuring range is given by a minimal optical transmittance. To measure higher SSCs, a model with a built-in chamber for automatic 1:10 dilution of the sample with clear water is available (Agrawal et al. 2012), but at relatively high cost.

2.3 *Vibrating tube densimetry and CFDMs*

Vibrating Tube Density Meters (VTDMs) or Coriolis Flow and Density Meters (CFDMs) provide continuous density measurements which can be converted to SSC, if the density difference between the sediment-laden water and the clear water is large enough, and the densities of the water and the sediment particles are known. VTDMs and CFDMs can be installed on sampling lines. The density measurement is based on the measuring tubes' natural frequency, which drops as the mass in the pipe increases (Holcomb & Outcalt 1998). In CFDMs, the mass flow is measured in addition, based on the Coriolis effect (Kalotay 1999).

VTDMs and CFDMs are common in the process industry while they have been rarely used for SSM (Bishwakarma & Støle 2008, Schneider et al. 2011).

Biofilm, particles and/or debris accumulation on the inner surfaces of the measuring tubes may cause overestimation of the density. Contrarily, CFDMs may underestimate the density due to erosion in the measuring tubes, or if the fluid contains coarse particles, which do not follow the oscillation of the measuring tubes. This effect is called 'phase decoupling' (Zhu 2009, Basse 2014) and is known to be more important with larger particles, but has not yet been experimentally quantified for sediment particles in water.

2.4 *Automatic bottle sampler*

For indirect SSC measurements, gravimetric analysis of bottle samples is necessary as a reference. In field studies with manual bottle sampling, higher SSCs are likely to be missed, because permanent presence of personnel at measuring locations is often not affordable and may be dangerous during flood events. The use of an automatic water sampler, triggered by SSC from an instrument for continuous SSM, contributes to obtain bottle samples also at rarely occurring higher SSCs.

3 INSTRUMENTS AND SETUP

3.1 *Setup and overview on instruments*

This paper focuses on the instruments for SSM listed in Table 1. They were installed in the valve chamber of HPP Fieschertal (Figs 1 and 2). At this location, the water contains particles with less than 0.3 mm diameter since coarser particles are removed by upstream gravel and sand traps.

The instruments were fed with water from the penstock by a hose with an internal diameter of 20 mm (Fig. 2a). The discharge in the hose was regulated by a ball valve at its outlet. The flow rate ranged between 0.15 and 0.25 l/s, resulting in a flow velocity above 0.5 m/s to prevent settling of particles in the hose. The turbidimeter requiring a flow rate of only 0.06 to 0.12 l/s was connected at a small hose branching off from the main hose. In the following, further information on the used instruments and their installation are given.

Table 1. Instruments used for SSM.

No.	Type	Model	Manufacturer
1	CFDM	*Promass 83F*	Endress + Hauser
2	Turbidimeter	*AquaScat*	Sigrist Photometer
3	LISST	*LISST-100X*	Sequoia Scientific
4	Bottle sampler	*Isco 3700*	Isco Teledyne

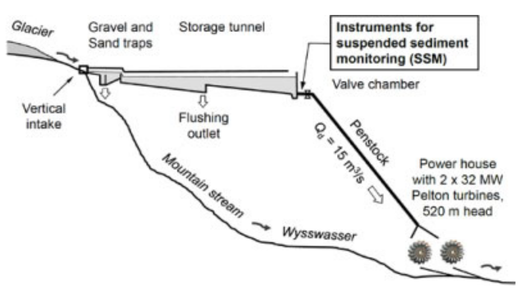

Figure 1. Schematic longitudinal profile of HPP Fieschertal with the location for SSM (after Felix et al. 2013a).

3.2 *Turbidimeter*

Among various turbidimeter models, an in-line turbidimeter measuring at a free-falling jet was used (item 2 in Table 1, Fig. 2c). So far, this model has been mainly used for quality control of drinking water. Turbidity is measured between 0 and 4000FNU (Formazine Nephelometric Units) by light scattered at 90°. This turbidimeter model has the advantage of not requiring any cleaning of its optical parts because they are not in contact with the water jet.

3.3 *In-situ Laser Diffractometer (LISST)*

A LISST-*100X*, i.e. an all-round model without dilution chamber, was used (item 3 in Table 1, Fig. 2c). The instrument has a nominal PSD measuring range of 2 to 380 μm with the inversion mode for so-called 'random shaped' particles (Agrawal et al. 2008, Sequoia 2011). To extend the range of measureable SSCs, its optical path length was reduced from 50 to 5 mm by inserting a glass cylinder. The LISST was installed looking sideward into a bucket with an overfall and a bottom outlet (Fig. 2c). The outlet was partially open to allow continuous sediment evacuation. The optical path of the LISST was positioned directly below the outlet of the sampling pipe.

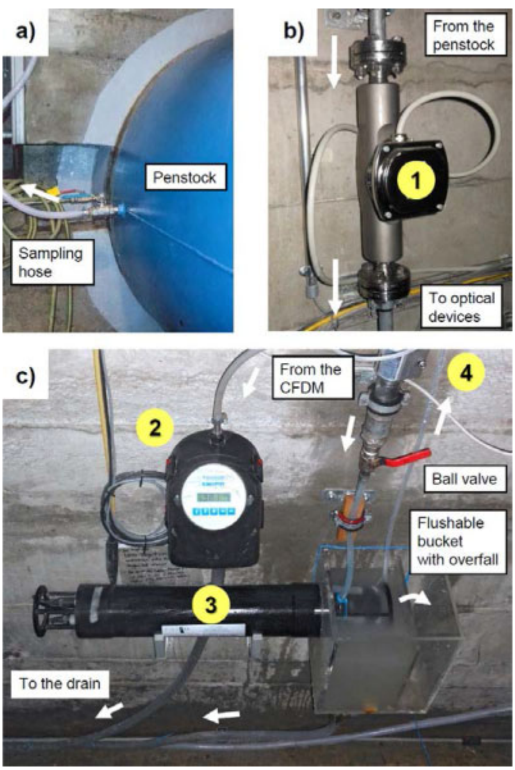

Figure 2. Sampling arrangement and setup of the instruments for SSM in the valve chamber of HPP Fieschertal; numbers refer to Table 1.

3.4 *Vibrating tube densimetry (CFDM)*

The CFDM (item 1 in Table 1, Fig. 2b) has two parallel bent measuring tubes inside the casing and DN15 connectors. It was mounted vertically to prevent deposition of particles in the measuring tubes. At the measurement location, no air bubbles which would bias the density measurements were observed in the water. The sediment particles at the measuring location (≤0.3 mm) were much smaller than the internal diameter of the measuring tubes (8 mm) and there was almost no floating debris. Therefore no provision to prevent blockage of the CFDM was required.

In the CFDM, temperature is also measured and used in the internal data processing to compensate thermal expansion. The CFDM is factory-calibrated with respect to density, flow rate and temperature. The specified accuracy of the density measurement is ±0.5 g/l (Endress + Hauser 2014), corresponding to 0.5 per mille of the density of water.

3.5 *Automatic bottle sampler*

An automatic bottle sampler (item 4 in Table 1) containing 24 bottles of 1 liter was used. The sampler was controlled from a measurement computer in the valve chamber using an auxiliary software developed at VAW. Water samples with a volume of 0.5 l were pumped from the LISST bucket (Fig. 2c).

4 METHODS

4.1 *Data acquisition and laboratory work*

The outputs of the CFDM and the turbidimeter were recorded every second, and minute-by-minute averages were calculated. The LISST was programmed to perform one burst per minute (10 measurements at 1 Hz followed by a break of 50 s). The optical parts of the LISST in contact with the water were manually cleaned every month on average. The real-time values of the mass flow rate measured by the CFDM were used to remotely detect a potential clogging of the sampling hose or the measuring tubes.

Furthermore, samples of the temporarily sediment-laden water were automatically taken every three days, or more frequently if the density measured by the CFDM exceeded certain threshold values, which were adapted over the seasons.

From these samples, the SSCs were determined in the laboratory by gravimetrical analysis, which involved the following steps: Weighing of samples, evaporation of the water (no filtration), weighing of the dried residues and calculation of the SSC by accounting for the concentration of dissolved minerals (≤0.08° g/l). These SSCs served as a basis to convert the outputs of the SSM instruments to SSC time series (field calibration). In the following, these conversions are described for each instrument.

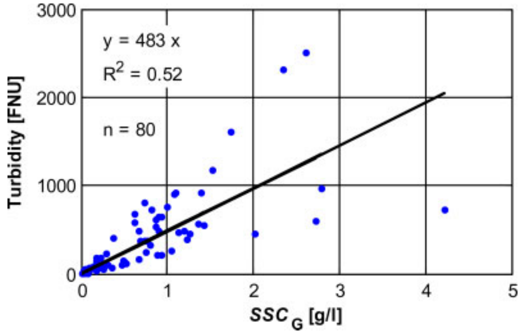

Figure 3. Turbidity measurements in the valve chamber of HPP Fieschertal compared to gravimetrically determined reference SSCs (SSC_G) in 2014 with linear fit.

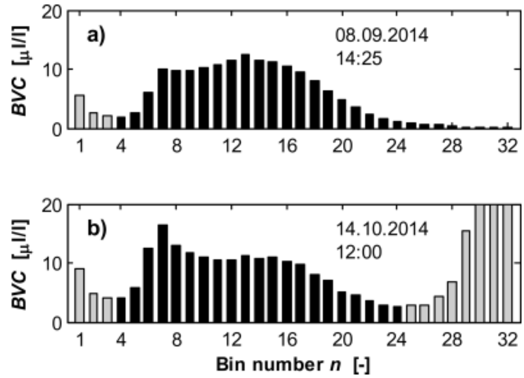

Figure 4. Examples of LISST volume concentrations in the 32 size bins (BVCs) at selected times; BVC's displayed in grey were discarded.

4.2 *Conversion of turbidity to SSC*

The gravimetrical SSCs from the bottle samples and turbidity values measured at corresponding times are compared in Figure 3. The relatively high degree of scattering is attributed to mainly temporal PSD variations, and possibly variations in particle densities and shapes. As the turbidimeter was not affected by fouling, a linear fit through the origin was selected. The relation in Figure 3 was used to convert the time series of measured turbidity to SSCs.

4.3 *Conversion of LISST TVCs to SSC*

Figure 4 shows two examples of BVCs, i.e. the volume concentrations obtained from LISST in the 32 size bins, at two selected times. This graphical representation corresponds to non-cumulative, volume- or mass based PSDs with logarithmically scaled size axis. Bin no. 1 corresponds to particle diameters between 1.9 and 2.1 µm, bin no. 32 to diameters between 322 and 380 µm.

As expected, there were in most time steps significant BVCs in size bins well within the LISST's size measuring range. However, there were also relatively high BVCs in size bins close to the lower end of the size measuring range and sometimes towards its upper end.

The BVCs in bins no. 1 to 3 decreased mostly to a local minimum in bin no. 4 (Fig. 4). Relatively high BVCs close to the lower end of the size measuring range were also reported by Agrawal et al. (2008), Andrews et al. (2011) and Felix et al. (2013b). Possible reasons for this are the presence of small out-of-range particles or non-spherical particle shapes. The BVCs in bins no. 1 to 3 (1.9 to 3.1 µm) were judged to be not realistic and were thus discarded.

In some periods there were also high BVCs towards the upper end of the size measuring range (Fig. 4b). High BVCs in these size bins occurred most often in late summer and autumn, increased over weeks, and were not present directly after cleaning of the LISST's measuring windows. Such BVCs were attributed to fouling, e.g. deposition of larger particles or flocs on the LISST's measuring windows. Hence, such BVCs in the range of bins 25 to 32 (100 to 380 µm) were removed if applicable.

After the calculation of the TVCs, i.e. the sum of all plausible BVCs at each time step, the TVCs were converted to SSC (mass concentration). In a first approach (Eq. 1), the TVCs were multiplied by the average solid density of the particle material $\rho_s = 2.73$ g/cm^3 which was measured in the laboratory by a helium pycnometer at the dried residues of twelve bottle samples:

$$SSC_{L0} = TVC \cdot \rho_s \tag{1}$$

The gravimetrical SSCs (<2 g/l) obtained from the bottle samples are compared to the values of SSC_{L0} at corresponding times in Figure 5. The measuring errors of the gravimetrical SSCs and the pycnometer density were assumed to be negligible. It is seen that LISST overestimated SSCs by 70% on average. This is similar to an overestimation of 68% found in an earlier period (03.06. to 10.10.2013) at the same study site (Felix et al. 2014). Considerable concentration overestimations by LISST were also quantified in earlier laboratory investigations and have been attributed to mainly effects of highly non-spherical particle shapes (Felix et al. 2013a, b). Another possible effect is flocculation, leading to particle densities below ρ_s. To compensate the overestimation, the SSC_{L0}-values were divided by 1.7, as determined in Figure 5. The corrected values were denoted as SSC_L.

A second approach to obtain SSC_L involves (i) plot TVCs against gravimetrical SSCs at corresponding times, (ii) find a conversion factor by linear fitting through the origin and (iii) apply the factor to the TVCs. This factor has units of a density. In the present study, it is 2.73 g/cm^3 / 1.7 = 1.61 g/cm^3. Czuba et al. (2015) called this factor 'apparent density', and in their study at U.S. rivers they found an average apparent density of 1.24 g/cm^3 with particles having $\rho_s = 2.56$ to 2.87 g/cm^3 and TVCs probably calculated from all size bins. As mentioned above, possible reasons

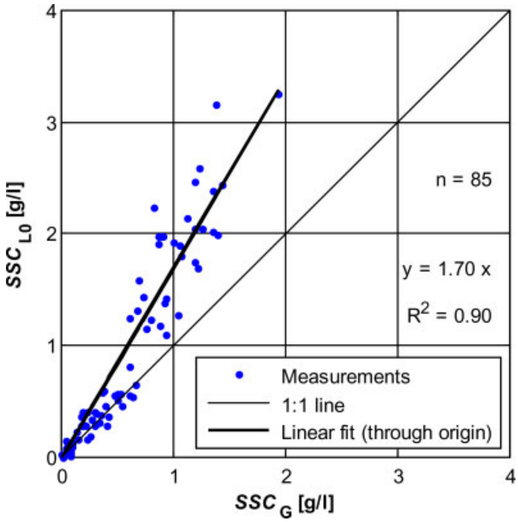

Figure 5. SSCs obtained from LISST in the valve chamber of HPP Fieschertal using the solid density of the particle material (SSC_{L0}) compared to gravimetrically determined reference SSCs (SSC_G); data from 2014 with $SSC_G < 2$ g/l.

for apparent densities lower than ρ_s are effects of non-spherical particle shapes on LISST concentration outputs and flocculation.

4.4 *Conversion of CFDM mixture density to SSC*

The SSCs from the CFDM (SSC_C) were calculated using Equation 2a, which was derived from a simple model containing a liquid and a solid phase, and using the definition of SSC (particle mass per unit of mixture volume). Equivalent equations are given in Morris & Fan (1998), Costa et al. (2012) and Endress + Hauser (2014).

$$SSC_C = \frac{\rho_m(t) - \rho_w(T(t))}{1 - \frac{\rho_w(T(t))}{\rho_s}} + K(t) \qquad \text{(2a)}$$

The time series of the mixture density $\rho_m(t)$ and of the temperature $T(t)$ were taken from the CFDM measurements. The clear water density ρ_w was calculated according to literature (Tanaka et al. 2001) as a function of the temperature $T(t)$. The solid density of the particle material, $\rho_s = 2.73$ g/cm^3 was taken from the pycnometer measurements as a constant.

A minor site-specific and seasonally variable offset $K(t)$ in Equation 2a was determined by comparing the SSCs from CFDM to the gravimetrical SSCs. This corresponds to a periodic *in-situ* calibration. *K(t)* compensates density offsets due to the following reasons:

- Difference in the concentration of dissolved chemical elements between the study site and the clear water in the used literature reference;

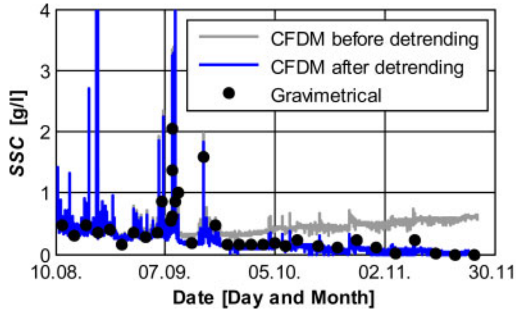

Figure 6. Time series of SSCs obtained from CFDM before (light grey) and after (dark blue) correction of fouling in autumn 2013 compared to the gravimetrical reference SSCs.

- Potential variable biofilm and/or particle deposits inside the measuring tubes;
- Potential differences between the conditions at the study site and at the calibration facility.

To show the principle of the conversion from mixture density to SSC, Equation 2a is simplified to Equation 2b using $\rho_s = 2.73$ g/cm^3 in the present study. The value of the denominator in Equation 2a is almost independent of temperature variations. Equation 2b shows that SSC is proportional to the 'excess density' $\rho_m(t) - \rho_w(T(t))$:

$$SSC_C \approx 1.6\ [\rho_m(t) - \rho_w(T(t))] + K(t) \qquad \text{(2b)}$$

At the study site, the water temperatures varied only between 0.1 and 6 °C. In this range, the effect of water temperature on the clear water density ρ_w is <0.13 g/l and thus <0.2 g/l on SSC (Eq. 2b).

In autumns 2013 and 2014 a progressive slight increase of the mixture density was measured while SSC was expected to tend to zero towards winter. Manual cleaning of the CFDM's measuring tubes with pipe cleaners in the winter seasons did not reveal visible fine-sediment deposits inside the tubes. The progressive slight increase of the mixture density was attributed to the growth of a biofilm inside the measuring tubes. Some microorganisms are able to grow also at low temperatures around 0°C (e.g. Margesin 2007). The trend in the measured mixture density correlated with the increased residence time and the temperature of the water in the storage tunnel in autumn and winter (low inflows).

Figure 6 shows time series of SSC obtained from CFDM before and after correction of fouling. The detrending was made based on the gravimetrical SSCs (also shown in Figure 6). The density offset correction in the years 2013 to 2014 corresponded to an SSC offset of $K = 0.6$ g/l.

No density bias due to abrasion inside the measuring tubes was detected after two years of operation. With the relatively low flow velocities in the measuring tubes (<2.5 m/s) in this application, abrasion is not expected to become a concern.

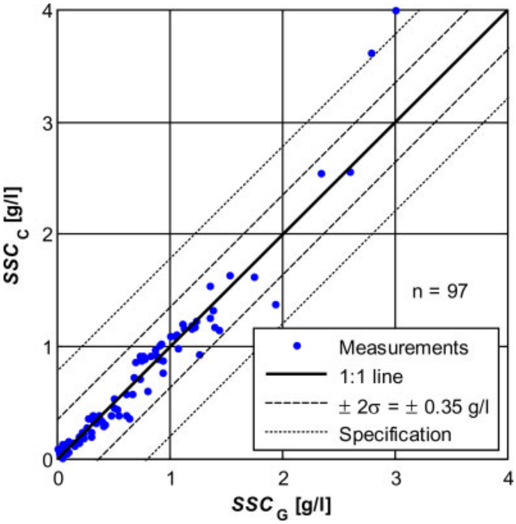

Figure 7. SSCs obtained from CFDM measurements in the valve chamber of HPP Fieschertal (SSC_C) compared to gravimetrically determined reference SSCs (SSC_G) in 2014.

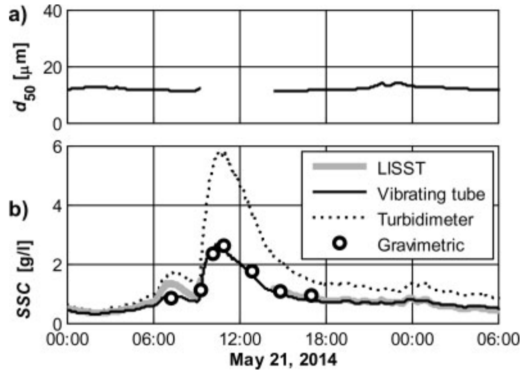

Figure 8. Time series of a) the median particle size d_{50} from LISST and of b) SSCs from various techniques measured in the valve chamber of HPP Fieschertal during approx. one day in spring 2014.

5 RESULTS AND DISCUSSION

5.1 *Measuring uncertainty of CFDM*

The SSC measuring uncertainty of the CFDM was assessed by comparing the SSCs from CFDM (SSC_C) and the gravimetrically determined SSCs (SSC_G) at corresponding times (Fig. 7). The points are the data from 2014 with a temporal gradient of $SSC_C < 0.1$ g/l per minute. At higher gradients, i.e. during sharper SSC peaks, the gravimetrical SSCs tended to be not representative. In the bucket from which the samples were pumped, sharp SSC peaks were probably dampened and delayed due to the mixing process.

The SSCs from CFDM and gravimetry were well correlated. The standard deviation of the differences between the SSCs from both techniques was $\sigma = 0.17$ g/l. Assuming that these differences are measuring errors of only the CFDM and that the errors are normally distributed, the expanded SSC measuring uncertainty of the CFDM (at 95% confidence level) was estimated to be $2\sigma = \pm 0.35$ g/l based on the data set. The larger deviations of the two points at $SSC_G \approx 3$ g/l might be a result of the above-mentioned effect of the mixing process in the bucket.

According to the operation principle of the CFDM and its specifications, the density measuring uncertainty in the considered range does not increase with SSC. At an SSC of 1 g/l for example, the relative measuring uncertainty is thus ±35% and at 10 g/l it is only 3.5%.

The accuracy of density measurement of ±0.5 g/l specified by the manufacturer of the CFDM corresponds to ±0.8 g/l with respect to SSC (Eq. 2b). The SSC measuring uncertainty of ±0.35 g/l determined from the field measurements is thus less than that specified by the manufacturer. The time-dependent adjustment of the density offset *K(t)*, i.e. the periodic in-situ calibration, contributed to reduce the SSC measuring uncertainty of the CFDM.

In the field measurements, no distinct particle size-dependent trend in the ratio between the SSCs from CFDM and gravimetry was apparent, indicating that phase decoupling was not a major issue with mostly silt (<63µm) and occasionally some fine sand (<200 µm) in the water.

5.2 *Comparison of the measuring performances of the instruments based on time series*

The measuring performances of the instruments for SSM were assessed at various SSCs and PSDs. Figures 8 and 9 show two typical examples of d_{50} and corresponding SSC time series out of two years of measurements. The median particle size d_{50}, obtained from LISST, stands for the diameter of graded particles of which 50% by mass are smaller.

In both examples, the SSCs from CFDM matched well with those from bottle samples between 1 and 7 g/l. The CFDM measured SSCs up to 13 g/l (Fig. 9). It is expected that also higher SSCs can be measured using a CFDM as long as the measuring tubes are not clogged.

The SSCs from LISST, after correction based on gravimetric SSCs, matched generally well with those from the CFDM. However, no LISST results were available above approx. 1.5 g/l at $d_{50} \approx 12$ µm (Fig. 8) or above approx. 5 g/l at $d_{50} = 30$ to 35 µm (Fig. 9). The upper limit of the SSC measuring range of a LISST depends on its optical path length, the PSD, the particle shapes and optionally on dilution (Sequoia 2008, Felix et al. 2013b).

The SSCs obtained from the turbidimeter strongly deviated from the other SSCs mainly in periods of higher SSCs and often after SSC peaks (Figs 8, 9). This was also observed at other SSC peaks (Felix et al. 2015). The deviations are attributed to mainly

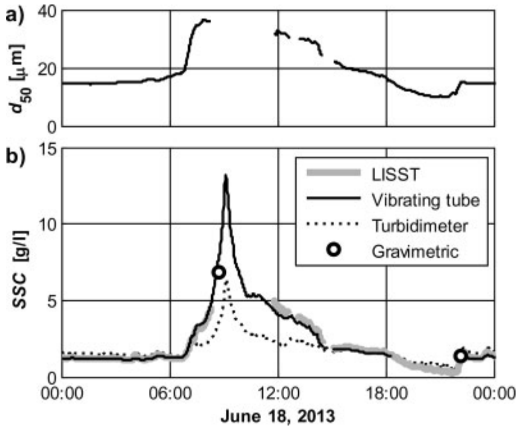

Figure 9. Time series of a) the median particle size d_{50} from LISST and of b) SSCs from various techniques, measured in the valve chamber of HPP Fieschertal during a summer day in 2013 (modified from Felix et al. 2016).

temporal variations in PSD. Because the SSCs from turbidimeters were calculated using the conversion (Fig. 3) which reflects the temporal average of the PSDs, the SSCs from turbidimeters were either too high (Fig. 8) or too low (Fig. 9) when the PSD was finer or coarser than the time-averaged PSD, respectively.

6 CONCLUSIONS

The SSC measuring performance of a turbidimeter, an all-round LISST instrument without dilution chamber and a CFDM were assessed *in-situ* at the waterway of an alpine HPP. The results of the measurements showed that SSC and PSD may vary considerably and quite independently.

With the CFDM, SSCs up to 13 g/l were measured without reaching the upper limit of the measuring range. The consideration of temperature variations and the periodic adjustment of the density offset based on gravimetric SSCs (periodic field calibration) contributed to reduce the SSC measuring uncertainty. The expanded SSC measuring uncertainty was quantified as ± 0.35 g/l. If a relative measuring uncertainty of 20% is accepted, the CFDM technique is suitable for SSCs above approx. 2 g/l.

The SSC_{L0} (calculated from the LISST's volume concentrations and the solid density of the particle material) were on average 70% higher than the gravimetric SSCs. It is recommended to convert LISST volume concentrations to SSCs based on gravimetrical SSCs. With this approach, the particle density is considered, potential effects of highly non-spherical particle shapes on LISST concentration outputs are compensated, and no pycnometer measurements are required. The LISST instrument with an optical path length of 5 mm and without dilution allowed measuring SSCs up to 1.5 or 5 g/l with d_{50} in the size range of medium or coarse silt, respectively. Apart from the drawback of the limited SSC measuring range, the LISST has the advantage of providing PSDs. With the PSD results, temporary biases of SSCs from turbidimeters were explained as consequences of PSD variations. If turbidimeters are used in dynamic sediment environments, where PSD variations are not well correlated to SSC, the obtained SSCs are temporarily biased. In contrast to turbidimeters, LISST and CFDM provided SSCs which were less or not affected by PSD variations.

With the used turbidimeter model measuring at a free-falling jet, the turbidity values had no drift. For the LISST, manual cleaning every month was not sufficient to prevent fouling in some periods of the year. The use of either an auxiliary device to protect and clean the measuring window (e.g. a so-called 'bioblock') or another type of LISST instrument would have been beneficial. In the CFDM, fouling caused a gradual shift of SSCs by up to 0.6 g/l. Since frequent and rigorous cleaning inside the CFDM's measuring tubes is not practical in SSM, a correction based on gravimetric SSCs is recommended instead.

If a CFDM is used at SSCs above 5 or 10 g/l, to warn of high turbine abrasion potential or for environmental monitoring during flushing of reservoirs, no frequent bottle sampling is required, since relatively small density offsets due to fouling are acceptable. It is still recommended to adjust the density offset of CFDMs in clear water conditions (zeroing), since this is only a small effort.

Based on these findings, a combination of a LISST instrument without dilution chamber and a CFDM appears to be a good option for SSM, if SSCs from a few mg/l to several 10 g/l of mainly silt are to be measured and the lack of PSD data at high SSCs can be accepted. With this combination, the costs for the measurements are judged to be relatively low in comparison to the large measurement range and good data quality. In addition, automatic bottle sampling is recommended for calibration and validation of the continuous SSC measurements.

7 OUTLOOK

Further evaluation of the field data is in progress. With respect to CFDMs, a laboratory investigation with particles ranging up to the size of sand is recommended to quantify the effect of particle size on the measured mixture densities. Together with measurements at high SSCs, this allows to quantify the range of applicability and the accuracy of CFDMs for SSM in various conditions.

ACKNOWLEDGEMENTS

The support by swisselectric research, the Swiss Federal Office of Energy (SFOE), the HPP operator Gommerkraftwerke AG and the Swiss Competence Center for Energy Research – Supply of Electricity

(SCCER-SoE) are gratefully acknowledged. Further thanks go to Endress + Hauser, Sigrist Photometers and Rittmeyer for lending measuring equipment as well as to Hochschule Luzern and the other project partners for the good collaboration.

REFERENCES

Agrawal, Y.C. & Pottsmith, H.C. 2000. Instruments for particle size and settling velocity observations in sediment transport, *Mar. Geol.* 168: 89–114.

Agrawal, Y.C., Whitmire, A., Mikkelsen, O.A. & Pottsmith, H.C. 2008. Light scattering by random shaped particles and consequences on measuring suspended sediments by laser diffraction, *J. of Geophysical Research* 113, C04023.

Agrawal, Y.C, Mikkelsen, O.A., Pottsmith, H.C. & Slade, W.H. 2012. Turbine abrasion: one year's experience in real-time sediment monitoring at Hidroagoyan HPP, Ecuador. *Proc. Hydro Conf.*, Bilbao, Spain: paper no. 14.08.

Andrews, S.W., Nover, D.M., Reuter, J.E. & Schladow, S.G. 2011. Limitations of laser diffraction for measuring fine particles in oligotropic systems: Pitfalls and potential solutions. *Water Resources Research*, 47.

Basse, N.T. 2014. A review of the theory of Coriolis flowmeter measurement errors due to entrained particles. *J. of Flow Measurement and Instrumentation* 37: 107–118.

Bishwakarma, M.B. & St/ole, H. 2008. Realtime sediment monitoring in hydro-power plants. *J. of Hydr. Research* 46(2): 282–288.

Costa, L.I., Storti, G., Lüscher, B., Gruber, P. & Staubli, T. 2012. Influence of solid particle parameters on the sound speed and attenuation of pulses in ADM, *J. of Hydrologic Eng*. 17(10): 1084–1092.

Czuba, J.A., Straub, T.D., Curran, C.A., Landers, M.N. & Domanski, M.M. 2015. Comparison of fluvial suspended-sediment concentrations and particle-size distributions measured with in-stream laser diffraction and in physical samples, *Water Resour. Res*. 51: 320–340.

Downing, J. 2006. Twenty-five years with OBS sensors: The good, the bad, and the ugly. *Continental Shelf Research* 26(17–18): 2299–2318.

Endress + Hauser. 2014. Coriolis flowmeter 'Proline Promass 80F, 83F'. *Technical information*. Endress+Hauser, Weil am Rhein, Germany.

Felix, D., Albayrak, I. & Boes, R.M. 2013a. Monitoring of Suspended Sediment – Laboratory Tests and Case Study in the Swiss Alps. In *Advances in River Sediment Research*, Fukuoka S., Nakagawa H., Sumi T., Zhang H. (eds.), Taylor & Francis Group, London: 1757–1766.

Felix, D., Albayrak, I. & Boes, R.M. 2013b. Laboratory investigation on measuring suspended sediment by portable laser diffractometer (LISST) focusing on particle shape. *Geo-marine Letters* 33(6): 485–498.

Felix, D., Albayrak, I. & Boes, R.M. 2014. Site-specific Conversion of Laser Diffractometer (LISST) Data to Suspended Sediment Mass Concentration (SSC). *Proc. Conference "Particles in Europe"*, Esbjerg, Denmark.

Felix, D., Albayrak, I. & Boes, R.M. 2015. Field measurements of suspended sediment using several methods. *E-proceedings,* 36^{th} IAHR World Congress, The Hague, The Netherlands.

Felix, D., Albayrak, I. & Boes, R.M. 2016. Continuous measurement of suspended sediment concentration: Discussion of four techniques, *Measurement* 89: 44–47.

Haimann, M., Liedermann, M., Lalk, P. & Habersack, H. 2014. An integrated suspended sediment transport monitoring and analysis concept. *J. of Sediment Research* 29(2): 135–148.

Holcomb, C.D. & Outcalt, S.L. 1998. A theoretically-based calibration and evaluation procedure for vibrating-tube densimeters. *Fluid Phase Equilibria* 150–151: 815–827.

Kalotay, P. 1999. Density and viscosity monitoring systems using Coriolis flow meters. *ISA Transactions* 38: 303–310.

Margesin, R. 2007. Alpine Microorganisms: Useful Tools for Low-Temperature Bioremediation. *Journal of Microbiology* 45(4): 281–285.

Morris, G.L. & Fan, J. 1998. Reservoir sedimentation handbook, McGraw-Hill, New York.

Rai, A.K. & Kumar, A. 2015. Continuous measurement of suspended sediment concentration: Technological advancement and future outlook. *Measurement* 76: 209–227.

Schneider, J., Harb, G., Klammer, G. & Fritz, H. 2011. New Application of a Density Probe for Determining the Suspended Sediment Concentration. *Proc. 34th IAHR Congress*, Brisbane, Australia.

Sequoia 2008. LISST concentration limits. Article dated August 29, 2008; Sequoia Scientific Inc., http://www.sequoiasci.com/article/lisst-concentration-limits/

Sequoia 2011. LISST bin sizes for inversions based on randomly shaped grains. Article dated March 18, 2011; Sequoia Scientific Inc., www.sequoiasci.com/article/lisst-bin-sizes-for-inversions-based-on-randomly-shaped-grains

Tanaka, M., Girard, G., Davis, R., Peuto, A., Bignell, N. 2001. Recommended table for the density of water between 0°C and 40°C based on recent experimental reports, *Metrologia* 38: 301–309.

Wren, D., Barkdoll, B., Kuhnle, R. & Derrow, R. 2000. Field Techniques for Suspended-Sediment Measurement. *J. of Hydraul. Eng.* 126(2): 97–104.

Zhu, H. 2009. Application of Coriolis Mass Flowmeters in Bubbly or Particulate Two-Phase Flows. *Diss.* University of Erlangen-Nuremberg, Germany; Shaker, Aachen.

Acoustic measuring techniques for suspended sediment

P Gruber[1], D Felix[2], G Storti[3], M Lattuada[4], P Fleckenstein[3] and F Deschwanden[1]

[1] Competence Center for Fluid Mechanics and Hydro Machines (CC FMHM), Hochschule Luzern (HSLU), Technikumstrasse 21, CH-6048 Horw, Switzerland
[2] Laboratory of Hydraulics, Hydrology and Glaciology (VAW), ETH Zürich, Hönggerberg-ring 26, CH-8093 Zurich, Switzerland
[3] Institute for Chemical and Bioengineering, ETH Zürich, Vladimir Prelog Weg 1-5/10, CH-8093 Zurich, Switzerland
[4] Adolphe Merkle Institute - Nanoparticles Self-Assembly, Université de Fribourg, Chemin des Verdiers 4, CH-1700 Fribourg, Switzerland; formerly at ETH Zürich[3]

peter.gruber@hslu.ch

Abstract. Acoustic signals can be used in various ways for suspended sediment monitoring. One possibility which lends itself particularly well in the context of hydropower plants (HPPs), is to use installations for acoustic discharge measurement (ADM). Such installations already exist at waterways of many HPPs. Similar to certain turbidimeters, the attenuation of the forward scattered signal travelling through the water-sediment mixture is correlated with suspended sediment concentration (SSC). This correlation can be based on reference SSCs, e.g. from gravimetric analyses of bottle samples. Without the need of additional sensors and practically maintenance-free, this method is used successfully in the HPP Fieschertal to warn the HPP operator of high SSC to prevent excessive turbine abrasion.

Acoustic methods and systems that allow for estimating both SSC and particle size distribution (PSD) are under development. The simultaneous determination of SSC and PSD is not possible using a single frequency. Therefore, multi-frequency approaches are investigated for generally scattered signals. When backscattered signals are used, a stronger frequency dependency can be exploited. However, the reliable simultaneous determination of particle size (and distribution) and concentration is still a major challenge due to a low signal-to-noise ratio and an ill-posed problem of estimating concentration and size from recorded signals. The optimal setup configuration (angles, frequencies) for such a system is not unique and further investigations are recommended.

1. Introduction

In various high- and medium head hydropower plants (HPP) worldwide, e.g. in the Alps, the Andes and the Himalayas, fine sediment particles (silt and fine sand) contained in the water poses at least temporarily a problem in terms of damaging turbines and other equipment due to abrasion. Typically, the mass concentration of suspended solids (SSC) covers a wide range, from less than 0.1 g/l to 10 g/l or occasionally even 100 g/l. To prevent excessive damage it is recommendable to close intakes and to shut down the turbines if SSC is higher than typically 1 to 10 g/l, depending on the HPP. Abrasion depends not only on the SSC but also on the particle size distribution (PSD). Therefore there is an interest to monitor both SSC and PSD continuously and in real-time.

SSC and PSD of sediment particles in water can be measured in many ways [Wren et al. 2000]. Wren et al. give a good survey of various methods with their advantages and disadvantages.

In the laboratory, SSC can be determined by weighing of the water-sediment samples and the dried residues after filtration or evaporation of the water from water samples. This gravimetrical method is still the reference. PSD can be measured in the laboratory by sieving (typically above 40 µm), sedimentation methods (hydrometer), laser diffraction and analysis of microscope images. However, no continuous real-time measurements are obtained from laboratory analyses.

For on-line SSC monitoring, two techniques are widely used: optical backscatter and optical transmission. The outputs of such turbidity meters (e.g. in Formazine Nephelometric Units FNU) need to be converted to SSC which depends unfortunately on particle size, shape and color. For on-line SSC and detailed PSD monitoring, Laser In-Situ Scattering and Transmissometry (LISST) devices have become available [Agrawal/Pottsmith 2000]. Felix reports on the application of a number of the mentioned and other methods for online SSC and PSD monitoring [Felix et al. 2013, Felix et al. 2016].

In two-phase suspension systems like silt-water mixtures, ultrasonic signal characteristics can also be used to obtain information about SSC and PSD. The advantages of the acoustic methods are: non-intrusive and rapid on-line measurements even under optically opaque conditions. On the other hand, air bubbles may strongly affect the measurements.

Acoustic techniques use the backscatter or forward scatter of pulsed acoustic bursts. Forward scattering can be exploited in installations for acoustic discharge measurement (ADM) based on the acoustic transit time (ATT) method. Such installations exist in many HPPs and can also be used – after a calibration – to estimate SSC or PSD, but not both [Costa et al. 2012].

In acoustic backscattering techniques, the intensity of the backscattered signal also depends on SSC, PSD and frequency. By using multiple frequencies (often with acoustic Doppler current profilers) basically both SSC and information about the PSD can be determined with little calibration [Thorne/Hanes 2002, Skripalle et al. 2012, Moore 2012, Thorne/Hurther 2014, Jourdin et al. 2014]. Most backscattering applications are reported from open waters like rivers, channels, lakes or seas. Problems still exist with the accuracy and repeatability of simultaneous SSC and PSD measurements.

The present paper deals with acoustic measuring techniques for SSC and PSD. First, physical models on the interaction of acoustic signals with solid particles in water which are suited for suspended sediment monitoring are described. A selection of models is presented, one for forward scattering and one for general scattering. Then SSC monitoring exploiting the attenuation of forward scattered signals as can be measured with ADM installations is presented. A comparison between the model prediction and measurements from a field study at HPP Fieschertal is shown and discussed. In a final section the opportunities for a simultaneous estimation of SSC and PSD by acoustic methods are presented.

2. Physical background

2.1. Overview on wavelength regimes and models

The scatter of acoustic signals at individual particles in motion is widely known and described in literature [e.g. Dukhin/Goetz 2002, Rossing 2007]. Theoretical models for determining the wave propagation speed and the attenuation of the sound wave as a function of particle concentration and size are derived from the interaction of the incoming sound wave with the particles (forward and backward scattering, absorption).

These models can be simplified by classification of different wavelength regimes dependent on the particle size (particle radius a) and the wavelength λ of the incoming sound wave. In figure 1 the boundaries of the three regimes are displayed in double logarithmic scales. In ADM applications the frequency lies for ATT installations typically between 200 kHz and 2 MHz and the particles' radius between 0.5 µm and 500 µm. This means that the models for the long wavelength regime (LWR) are applicable for most of the cases in the described context. In the LWR regime, visco-inertial and thermal effects dominate while in the SWR regime the scattering effect is dominant. In the intermediate IWR regime, all effects play a role and the most complex models must be applied.

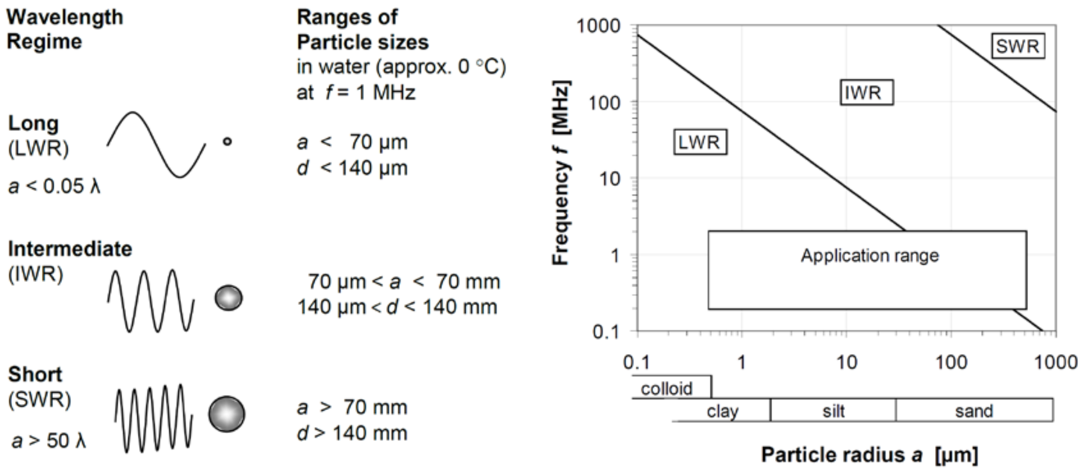

Figure 1: Identification of three simplified wavelength regimes (a = particle radius, λ = c/f) and their application ranges for solids in water (at 20°C), classification of particle sizes according to the Wentworth scale.

Models for only spherical particles were considered. There are two groups of models: The first group includes models based on the two-phase approach, such as the one developed by Atkinson and Kytömaa (AK) [Atkinson/Kytömaa 1992]. This model provides accurate relationships for the attenuation and the sound speed in a suspension, if the particles are not large compared to the sound wavelengths (LWR). However, it cannot be used to describe backscattering since the propagation and attenuation of sound waves is considered only in the forward direction. A similar model by Urick treats only the attenuation of the forward scattered wave but in a larger particle range [Urick 1967].

The second group of models considers the scattering behavior of individual particles by solving the equation of wave propagation inside and outside the particles. They can cover single scattering as well as multiple scattering (which is extremely challenging). This group of models includes those developped by Faran [Faran 1951], Epstein-Carhart-Allegra-Hawley (ECAH) [Epstein/Carhart 1953, Allegra/ Hawley 1972] and Hay and Mercer (HM) [Hay/Mercer 1985]. The advantage of these models is the accurate description of the scattering behavior of particles combined with the possibility to include elastic, viscous and thermal effects simultaneously. The three models differ only in the underlying approximations and will be discussed in more detail.

2.2. Attenuation and far field function

The Atkinson-Kytömaa (AK) model was chosen out of the first group as the appropriate model for the visco-inertial effects [Costa et al. 2012, Lüscher/Gruber 2010]. From the second group, the Faran model was chosen for the scattering effects [Fleckenstein et al. 2014]. Both models can be combined to model both effects. The more complicated models like ECAH and HM cover a greater range and take into account all major physical effects of acoustic wave interaction with a single spherical particle. The number of required model parameters however is very high for these models and not adequate for monitoring applications.

In the present application, the effect of the particles on the sound speed in the suspension is not exploited. The main quantities of interest are the attenuation and the far field function. The attenuation can be modelled for all physical effects while the far field function $|f_\infty|$ exists only in the models of the second group. In the range of interest, the far field function is similar for all examined models. Therefore, the model with the lowest complexity, i.e. Faran was chosen. For the application in connection with ADM installations, only the attenuation is of interest. For small values of $2\pi \cdot a/\lambda$ the Faran model underestimates strongly the attenuation while for large values of $2\pi \cdot a/\lambda$ the AK-model is underestimating the attenuation. In the present application, the long wavelength regime corresponding to small values of $2\pi \cdot a / \lambda$ is relevant. Thus the AK-model is used for the attenuation.

2.3. Attenuation and excess attenuation

The absorption of a plane acoustic wave in a two phase liquid–solid suspension is composed of three terms: the attenuation in water α_l, the attenuation of particles α_s and the attenuation due to the water-particle interaction, the so called excess attenuation α_{ex}:

$$\alpha = \varphi\alpha_s + (1-\varphi)\alpha_l + \alpha_{ex} \qquad \text{with } \varphi = \text{volume fraction of particle concentration [-]} \qquad (1)$$

As φ is usually small in the described application, equation (1) is approximated by $\alpha = \alpha_l + \alpha_{ex}$.

The acoustic signal emitted from the sensor propagates spherically and is reduced with increasing distance x from the transducer. As this is a pressure transducer, the amplitude A of the acoustic pulse in the far field is proportional to the acoustic pressure. α is normally expressed in Neper/m (Np/m) or dB/m (1 Np = 8.686 dB):

$$A = \frac{K_T}{x} e^{-\alpha x} = \frac{K_T}{x} e^{-\alpha_l x} e^{-\alpha_{ex} x} \qquad \varphi << 1 \qquad \text{with } K_T = \text{sensor constant} \qquad (2)$$

α depends very strongly on the frequency *f*. The attenuation increases basically with ~f^2 for $\varphi < 0.05$ (corresponding to SSC < 125 g/l) and the particle size range of interest in the described application. The dependency of the attenuation on the particle diameter is complicated. Comparisons have been done [Lüscher 2008] between Urick's and the AK-model. The agreement in the low diameter range is good, while for diameters larger than 100 μm the AK-model is no more valid and underestimates the attenuation (figure 2a). Urick's and the AK model show for small particle diameter (< 1 μm) an attenuation increase with ~d^2 and for medium size particles (1 μm < d < 100 μm) an attenuation decrease proportional to ~1/d, while for larger particles the attenuation increases with ~d^3 according to Urick's model. In the range of interest for the described application, the excess attenuation is practically proportional to SSC (figure 2b) and approximately proportional to ~1/d as mentioned above.

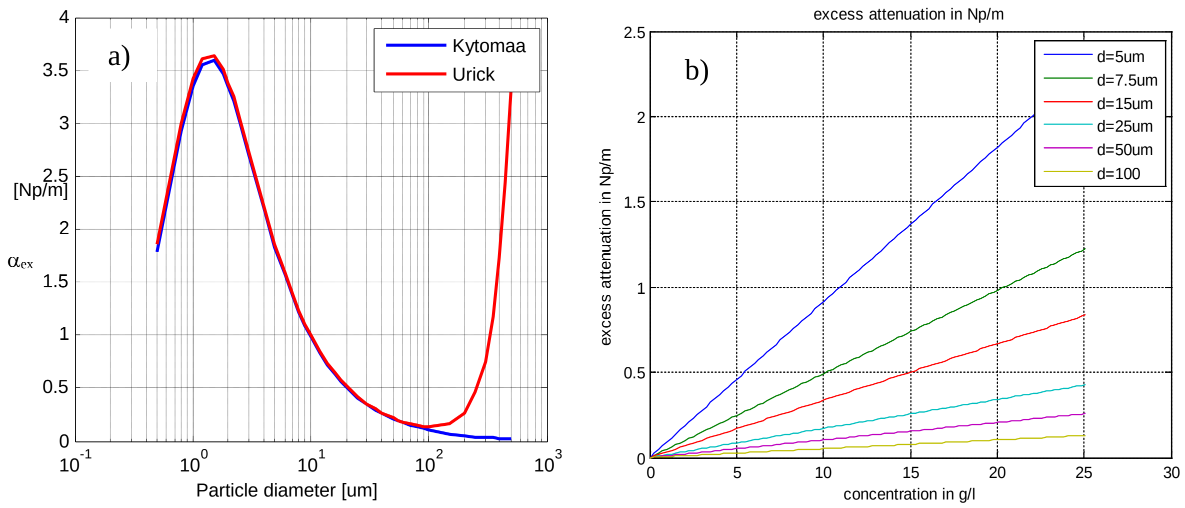

Figure 2. Excess attenuation α_{ex} for mineral particles ($\rho_s = 2500\, kg/m^3$, $c_s = 5000\, m/s$) at 1 MHz; **a)** for SSC = 20 g/l as function of particle diameter, **b)** as a function of SSC for various particle diameters (the smallest diameter d = 5 μm corresponds to the line with the steepest slope and vice versa).

Natural suspended sediment particles do not have a single size, i.e. they are not mono-disperse. For graded particles, it is not obvious to calculate the excess attenuation from the PSD. The naïve way of calculating a volume- or mass-averaged particle size and then using this diameter in a mono-disperse model is not accurate enough. For SSC ≤ 50 g/l as in this application, the following approach was used: For each diameter class of the PSD the excess attenuation is computed and added to obtain the excess attenuation of the particles of all sizes. Then, an equivalent average diameter is determined which leads to the same attenuation. This equivalent average diameter can then be used in mono-disperse models (AK, Urick).

2.4. Inferring SSC or average particle size from excess attenuation

The main problem when exploiting the forward scattering for sediment monitoring is that there exists an infinite number of combinations of SSC and particle diameter leading to the same excess attenuation (figure 3a). This means that the inverse problem does not have a unique solution. SSC can be calculated if the particle size is known, or the size can be calculated if SSC is known. Figure 3b shows the considerable influence of the actual particle diameter on the SSC if SSC is inferred from a measured excess attenuation and an assumed reference size. If the actual diameter is smaller than the reference, the SSC estimate is too high, and vice versa. The deviation of SSC is proportional to d_{ref}/d.

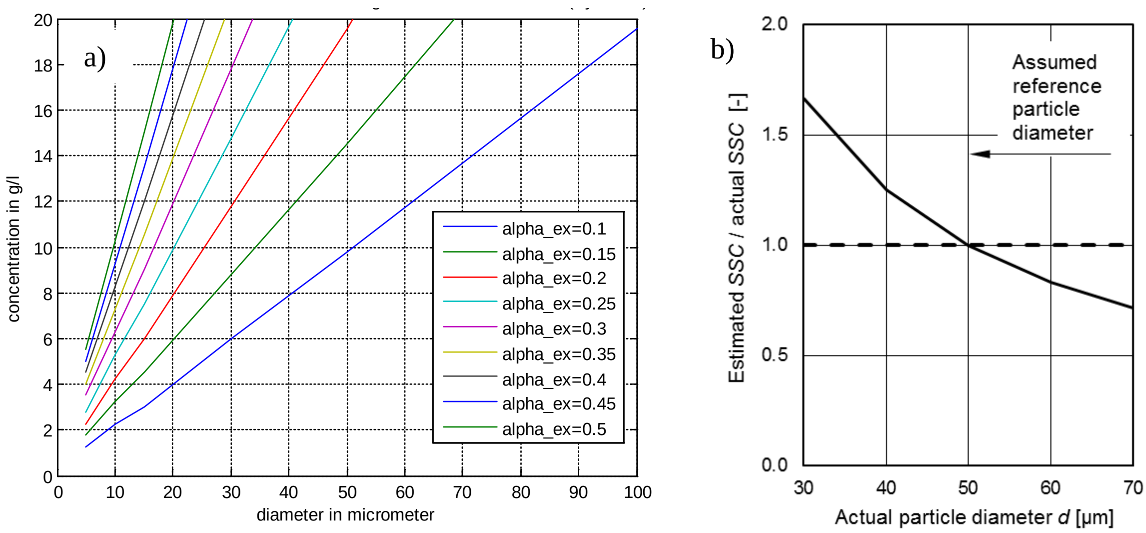

Figure 3. a) Pairs of particle diameter and SSC leading to the same excess attenuation (the highest value of α_{ex} corresponds to the line with the steepest slope and vice versa). **b)** Over- or under-estimation of SSC if the particle diameter differs from the assumed reference diameter; both diagrams calculated with the AK-model.

3. SSC Monitoring based on ADM installations

3.1. Acoustic discharge measurement

The multipath acoustic discharge measurement (ADM) based on the acoustic transit time (ATT) method is a well-established method for accurate discharge measurement especially in large conduits and channels. On each path between two transducers, the transit times of acoustic signals travelling in both directions are determined, from which the averaged axial path velocities are calculated. The discharge, i.e. the volumetric flow rate is calculated by integrating the path velocities over the area of the cross section.

The method allows to measure at a high temporal resolution not only the flow velocities of each path but also the sound speed *c* and the attenuation α of the acoustic pulses at all paths easily. The sent acoustic signal is characterized basically by its frequency, power (amplitude) and duration. The duration can be parameterized by the number of bursts. Normally ADM systems operate with a single frequency, typically at 500 kHz or 1 MHz. Beside the sound speed *c* and the attenuation α, the signal shape and the frequency content can also be analysed.

3.2. AK-model for SSC monitoring or field calibration

Figure 4a shows the principle way how the AK-model can be used for SSC monitoring. For given particle parameters (mainly diameter, shape and density as well as sound speed) an SSC can be obtained from the measured excess attenuation, as described in section 2.4. Information on particle size, shape and density can be obtained from laboratory analyses of bottle samples.

Another way besides the inverse use of the AK-model is to work with a field calibration: A relation between the attenuation and SSC is established by comparing gravimetrically determined SSCs and measured attenuations at corresponding times (figure 4b). This involves also some effort because bottle samples have to be collected and analyzed in the laboratory, but is relatively simple and includes all effects (e.g. also of non-spherical particle shapes which are difficult to parametrize).

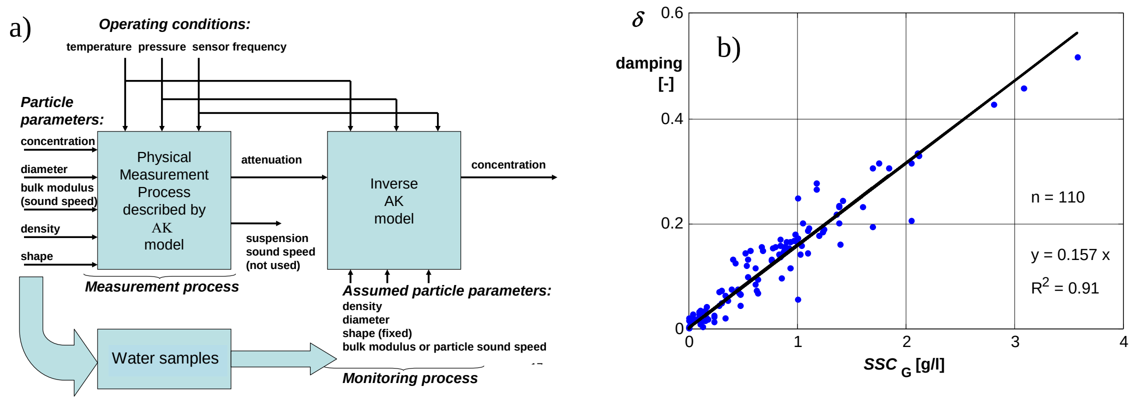

Figure 4. a) Application of the AK-model for SSC monitoring: The measured attenuation α_{ex} is post-processed in an inverse AK-model with assumed particle properties to obtain SSC. **b)** Damping of the acoustic signal δ (from single-frequency forward scatter method) as a function of the gravimetrically determined reference SSCs (SSC_G, below 4 g/l), measured in the waterway of the HPP Fieschertal in 2013, with a linear fit.

3.3. Field study: Setup and Methods

In an interdisciplinary research project on hydro-abrasive erosion on turbines of HPPs, SSC and PSD in the waterway of HPP Fieschertal in Valais, Switzerland, have been measured and analyzed since 2012 [Felix et al. 2013]. The water used in this HPP originates from a highly glaciated catchment and is known for relatively high SSC (approx. 0.5 g/l on average, 5 g/l exceeded several times a year). Among other measuring techniques, the method of acoustic single-frequency attenuation based on an ADM installation as described in section 3.1 has been employed [Felix et al. 2016]. A standard 4-path ADM installation with two measurement planes has already been existing at the top of the penstock (inner diameter 1.95 m). The path length is 2.27 m and the frequency of the signals is 1 MHz. The only modification which was required to use the existing ADM installation (*Risonic* from Rittmeyer) also for sediment monitoring was to define the amplitudes of the received signals at the four paths as additional outputs and to feed them in the data acquisition system.

For this ADM installation, equation (2) can be rewritten for a fixed distance of x = 2.27 m as follows:

$$A = K_{x=2.27\mathrm{m}}\, e^{-\delta} \qquad \text{where} \qquad K_{x=2.27\mathrm{m}} = \frac{K_T}{2.27\mathrm{m}} e^{-\alpha_l 2.27\mathrm{m}} \qquad \text{and} \qquad \delta = \alpha_{ex}\, 2.27\mathrm{m} \qquad (3)$$

The damping δ is a dimensionless quantity. Equation (3) for A was applied to two cases: first with clear water (A_0, $\delta = 0$) and then with an actual SSC and thus $\delta > 0$. The ratio of the amplitudes in the two cases is:

$$\frac{A}{A_0} = \frac{K_{x=2,27m}}{K_{x=2,27m}} \frac{e^{-\delta}}{1} = e^{-\delta} \tag{4}$$

A linearization of the exponential function (for $\delta << 1$) yields:

$$\frac{A}{A_0} \approx 1 - \delta \qquad \qquad \delta \approx 1 - \frac{A}{A_0} \tag{5}$$

The amplitudes of the signals were measured in Volts. The damping δ varies between 0 (clear water) to 1 (the sent signal does not reach the receiver on the other side of the acoustic path).

The value of A_0 was calculated from the recorded amplitude of the received signals in clear water conditions for each path. From the time series of the measured amplitudes A, the damping δ was calculated according to equation (5) for each path. Then the time series of plausible δ obtained from the various paths were averaged and filtered to reduce noise. The damping was correlated with gravimetrically determined reference SSCs from bottle samples (figure 4b). Reference SSCs were obtained from the weight of samples before and after evaporation of the water (no filtration) and by deducting the concentration of dissolved minerals (<0.08 g/l). For SSC below 4 g/l, a linear relation was obtained as predicted by the AK-model (figure 2b). The linear relation was applied to convert the time series of δ to SSC. For comparison, SSC was also determined from density measurements using a Coriolis Flow and Density Meter (CFDM) installed on a sampling pipe close to the ADM [Felix et al. 2016]. In addition, PSDs were measured using LISST.

3.4. Field study: Results and Discussion

Normally, the particles in the water were relatively fine, i.e. $d_{50} \approx 15$ μm (mainly medium silt). The d_{50} denotes the particle size which is not exceeded by 50 % of the particle mass (median particle size). Coarser particles up to $d_{50} = 100$ μm were present at higher SSCs of e.g. 10 g/l. However, high SSCs were not always associated with larger particles, also due to different reasons for high SSCs (flood vs. resuspension events).

The SSCs from the acoustic method corresponded generally well with the SSCs from gravimetry and CFDM (figure 5b). However, in periods with higher SSCs, the SSC from the acoustic method was considerably lower than the references. These temporary deviations are mainly attributed to the effect of particle size variations (figure 5a) on the acoustic damping as predicted by the AK-model. The applied conversion of δ to SSC (figure 4b) is mainly based on the usually prevailing small particles in the SSC range below 4 g/l and does not reflect the situations with temporarily coarser particles at higher SSCs. In the example of figures 5a and 5b, d_{50} measured by LISST increased in two events from 15 to 40 or 55 μm, respectively, leading to underestimations of the SSC from the acoustic method by a factor of 2 to 3.5. Because the correlation between SSC and d_{50} is quite weak at this study site, it is not possible to find a conversion from δ to SSC which would always yield unbiased SSCs. In situations with a higher degree of correlation between SSC and d_{50}, a non-linear conversion from δ to SSC could be applied compensating the undesired effects of d_{50}-variations on SSC.

Another reason for the underestimation of higher SSC with the acoustic method is the behaviour of the measuring system. While the relation between δ and SSC for a given particle type is approximately linear up to some g/l, it is nonlinear at higher SSC and approaches a saturation (figure 5b).

During a major flood event with an estimated return period of 20 years, high SSCs of up to 50 g/l occurred in the penstock of HPP Fieschertal [Felix et al. 2016]. The high SSC during the flood was also calculated using the pressure method (the CFDM has not yet been installed in 2012). In the pressure method, the effect of suspended sediment on the mixture density and on the pressure measured at the downstream end of the penstock is exploited [Felix et al. 2016]. The value of the peak

SSC of 50 g/l was verified by some bottle samples and Imhoff cone measurements during the event. Based on the data recorded during the event, the measuring performance of various devices for suspended sediment monitoring at high SSC was studied.

The upper limit of the typical measuring range of turbidity meters, i.e. 4000 FNU, indicated in figure 5b, was exceeded during several hours. However, a special type of turbidity meter (Optek TF16-N with flow cell F20), allowed measuring the turbidity during the whole event (figure 5b). This device measures NIR attenuation over an optical path of only 10 mm; turbidity is expressed in terms of concentration units CU. The time series of the acoustic damping is also shown in figure 5b. The scaling of the vertical axes was adjusted to facilitate a visual comparison. The acoustic damping during this event corresponded generally well to the turbidity, except for very high damping of $\delta > 0.95$, when the strength of the received signal tended to 0 ($\delta = 1$). In this event, the upper limit of the SSC measuring range of the acoustic system was between 15 and 20 g/l. This limit is not generally valid, since it depends on the particle properties, the power and the frequency of the sent acoustic signal, as well as the path length; as described by the AK-model.

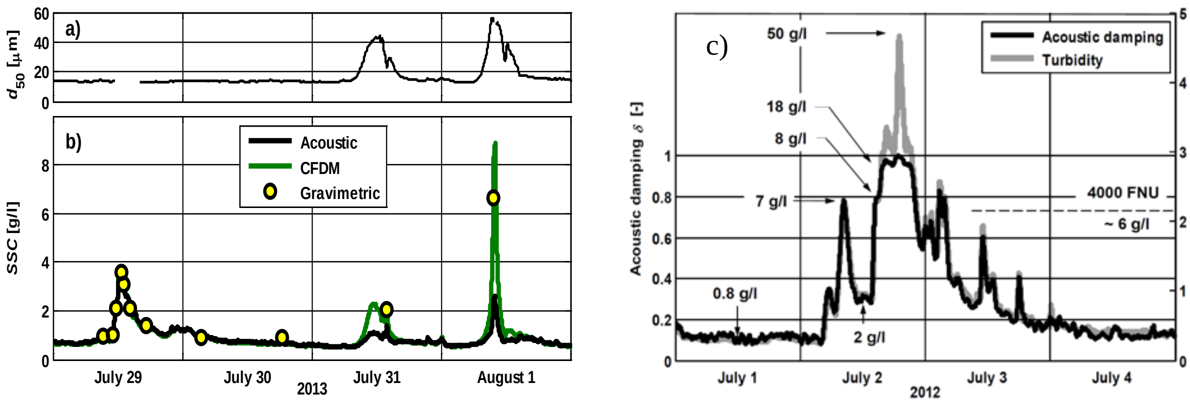

Figure 5. a) Time series of the median particle size d_{50} and **b)** corresponding SSC time series from the acoustic method (single-frequency forward scatter), from CFDM and from gravimetrical analysis of bottle samples, measured in the waterway of the HPP Fieschertal during four summer days. **c)** Time series of acoustic attenuation and turbidity measured at the same location during the major flood event in 2012 (modified from [Felix et al. 2012]).

4. Monitoring of SSC and PSD

Acoustic methods and systems which allow for estimating both SSC and PSD are under development and start becoming to be available commercially. The simultaneous determination of SSC and PSD is not possible using a single frequency. Therefore, multi-frequency approaches are investigated for generally scattered signals. When backscattered signals are used, a stronger frequency dependency can be exploited [Thorne/Hanes 2002, Moore 2012, Skripalle et al. 2012, Jourdin et al. 2014, Thorne/Hurther 2014, Deschwanden 2015]. However, the reliable simultaneous determination of particle size (and distribution) and concentration from generally backscattered signals, i.e. solving the inverse problem based on measurements, is a major challenge. For monitoring purposes, an accuracy of ±20 % for SSC and d_{50} would be sufficient. To the authors' knowledge, this goal has been achieved so far only for specific cases. The main problems are:

- the low signal-to-noise ratio requiring intensive averaging of the signals,
- the inversion problem is ill-posed, this means that a unique determination of SSC and PSD is difficult even under ideal conditions (no noise),
- the values of at least three parameters are to be determined simultaneously (SSC, d_{50} and a parameter for e.g. the width of the PSD).

The ill-posedness of the inversion problem can be reduced by finding

- an optimal set of sensors (frequency, bandwidth),
- an optimal installation configuration (angles, forward/backward combinations of sensors),
- a robust mathematical inversion and optimization method.

5. Conclusions

In the Fieschertal field study it was confirmed that the single-frequency acoustic method based on the acoustic discharge measurement (ADM) installation allows to measure SSC up to 15 g/l of mainly medium silt. The correlation between the attenuation of the acoustic signals and the SSC was established based on gravimetrical analysis of bottle samples. The attenuation of the forward scattered signals predicted by the AK-model was confirmed by the measurements. At low SSC, say below 0.5 g/l of silt, the signal-to-noise ratio is low requiring filtering and averaging of measurements, and optical methods may be more suitable. Above approx. 0.5 g/l of medium silt, the performance of the acoustic method is similar to widely used turbidity meters. The upper limit of the SSC measuring range of the acoustic method with the described setup is higher than the one of widely used turbidity meters. This acoustic method offers the advantage that no additional sensors are required in HPPs having similar ADM installations, the measurements are spatially well averaged (over the path length and optionally over several paths) and refer to the sediment-laden water directly in the waterway. Like this, there is no need for sampling pipe installations which require maintenance and may be prone to clogging or to potentially non-representative sampling. The field test confirmed that practically no maintenance is required, since acoustic systems are less sensitive to fouling than optical ones. Similarly to turbidity meters, the SSC obtained from this single-frequency acoustic attenuation method is biased by PSD variations if these are not correlated to SSC. Thus, the SSC measuring uncertainty is higher if the particle sizes are not well correlated to SSC.

The Faran model has been presented which allows to predict the backscattered signals in terms of SSC and PSD. Main output quantities of this model are the far field function and the attenuation. As the Faran model and the AK-model describe different physical effects for different application ranges, a combination of the two models is proposed. The simultaneous determination of SSC and PSD from measurements of forward- and backscattered acoustic signals at several frequencies remains a field for improvements.

Acknowledgements

The support of the Fieschertal field study by swisselectric research, the Swiss Federal Office of Energy (SFOE) and the HPP operator Gommerkraftwerke AG are gratefully acknowledged. Thanks go to Endress+Hauser, Sigrist Photometers and Rittmeyer for lending measuring equipment. Furthermore, the support by the Swiss Commission for technology and Innovation CTI in the two projects "Nr. 7947.2: Empfindlichkeit der akustischen Durchflussmessung auf Verschmutzung (Sensitivity of ADM to suspended sediment)" and "Nr. 13223.1 PFFLR-IW: Evaluation of forward and backward scattered acoustic signals to determine the flow and the particle, respectively bubble concentration in water", as well as the contributions of all project partners are acknowledged.

References

[Agrawal/Pottsmith 2000] Agrawal Y C and Pottsmith H C 2000. Instruments for Particle Size and Settling Velocity Observations in Sediment Transport, *Marine Geology* 168: 89-114

[Allegra/Hawley 1972] Allegra J R and Hawley S A 1972. Attenuation of sound in suspensions and emulsions: Theory and experiments, *J. Acoustical Society of America*, 51(5.2): 1545-1564

[Atkinson/Kytömaa 1992] Atkinson C M and Kytömaa H K 1992. Acoustic wave speed and attenuation in suspensions, *Int. J. Multiphase Flow* 18(4): 577–592

[Costa et al. 2012] Costa L I, Storti G, Lüscher B, Gruber P and Staubli T 2012. Influence of solid particle parameters on the sound speed and attenuation of pulses in ADM, *J. of Hydrologic Eng.* 17(10): 1084-1093

[Deschwanden 2015] Deschwanden F 2015. Evaluation of forward and backward scattered acoustic signals to determine the particle parameters in water, *Semester thesis*, HSLU Luzern, Switzerland (unpublished)

[Dukhin/Goetz 2002] Dukhin A S and Goetz P J 2002. *Ultrasound for characterizing colloids: Particle sizing, zeta potential, rheology*, Elsevier, Boston

[Epstein/Carhart 1953] Epstein P S and Carhart R R 1953. The absorption of sound in suspensions and emulsions, *J. Acoustical Society of America,* 25(3): 553-565

[Faran 1951] Faran Jr J J 1951. Sound scattering by solid cylinders and spheres, *J. Acoustical Society of America,* 23(4): 405-418

[Felix et al. 2012] Felix D, Albayrak I, Abgottspon A, Boes R M and Gruber P 2012. Suspended Sediment and Pelton Turbine Wear Monitoring: Experimental Investigation of various Optical and Acoustic Devices and Beginning of the Case Study at HPP Fieschertal. *Proc. 17th Intl. Seminar on Hydropower Plants*, Vienna, Austria: 483-494

[Felix et al. 2013] Felix D, Albayrak I, Boes R M, Abgottspon A, Deschwanden F and Gruber P 2013. Measuring Suspended Sediment: Results of the first Year of the Case Study at HPP Fieschertal in the Swiss Alps, *Proc. Hydro 2013,* Innsbruck, Austria, paper no 18.03

[Felix et al. 2016] Felix D, Albayrak I, Abgottspon A and Boes R M 2016. Real-time measurements of suspended sediment concentration and particle size using five techniques. *Proc. 28th IAHR Symposium on Hydraulic Machinery and Systems*, Grenoble, IOP Conf. Series

[Fleckenstein et al. 2014] Fleckenstein P, Deschwanden F, Storti G, Lattuada M and Gruber P 2014. Ultrasonic characterization of Silt Suspensions by Backscattering, *Proc. 9th Intl. Symposium on Ultrasonic Doppler methods for fluid mechanics & fluid engineering,* Strasbourg, France

[Hay/Mercer 1985] Hay A E and Mercer D G 1985. On the theory of sound scattering and viscous absorption in aqueous suspensions at medium and short wavelengths, *J. Acoustical Society of America,* 78(5): 1761-1771

[Jourdin et al. 2014] Jourdin F, Tessier C, Le Hir P, Verney R, Lunven M, Loyer S, Lusven A, Filipot J F and Lepesqueur J 2014. Dual-frequency ADCPs measuring turbidity, *Geo-Marine Letters* 34(4): 381–397

[Lüscher 2008] Lüscher B 2008. Abschlussbericht KTI-Projekt 7947.2: Empfindlichkeit der akustischen Durchflussmessung auf Verschmutzung (Sensitivity of ADM to suspended sediment, unpublished, in German)

[Lüscher/Gruber 2010] Lüscher B and Gruber P 2010. Silt monitoring via ultrasonic signal analysis, *Proc. IGHEM Conference*, Roorkee, India

[Moore 2012] Moore S A 2012. Monitoring flow and fluxes of suspended sediment in rivers using side- looking acoustic Doppler current profilers, *PhD thesis,* University of Grenoble, France

[Rossing 2007] Rossing T D 2007. *Handbook of Acoustics*, Springer, New York

[Skripalle et al. 2012] Skripalle J, Hies T, Liu Y and Nguyen H H 2012. Application of multi-frequency acoustics to estimate concentration of suspended sediments from Jurong lake Singapore, *Proc. 17th Intl. Seminar on Hydropower Plants,* Bauer C and Doujak E (eds.), Vienna, Austria: 725-737

[Thorne/Hanes 2002] Thorne P D and Hanes D M 2002. A review of acoustic measurement of small-scale sediment processes, *Continental Shelf Research*, 22(4): 603-632

[Thorne/Hurther 2014] Thorne P D and Hurther D 2014. An overview on the use of backscattered sound for measuring suspended particle size and concentration profiles in non-cohesive inorganic sediment transport studies, *Continental Shelf Research,* 73: 97–118

[Urick 1967] Urick R J 1967. *Principles of underwater sound for Engineers*, McGraw-Hill, New York

[Wren et al. 2000] Wren D, Barkdoll B, Kuhnle R and Derrow R 2000. Field Techniques for Suspended-Sediment Measurement, *J. of Hydraul. Eng*. 126(2): 97–104